

CONF-8005107

MARTIN MARIETTA ENERGY SYSTEMS LIBRARIES



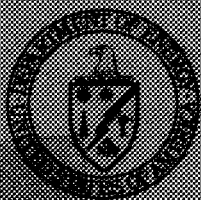
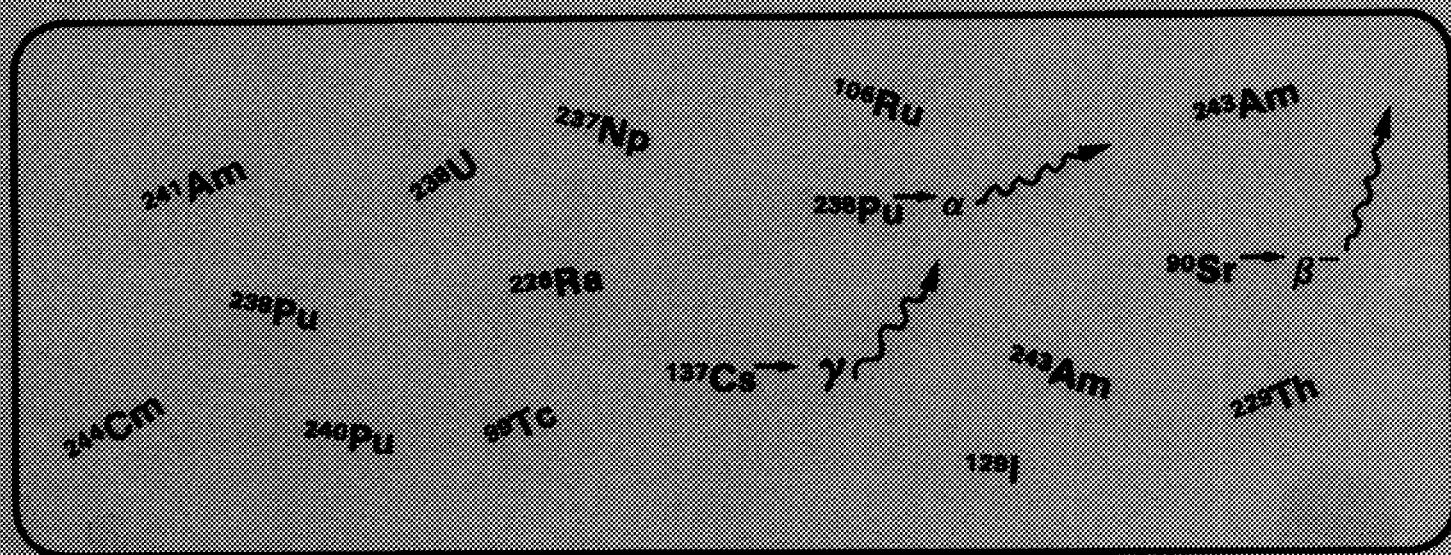
3 4456 0251323 3

Alternate Nuclear Waste Forms and Interactions in Geologic Media

Proceedings of a Workshop Summarizing Advanced Activities and Formulating Requirements for the Future

May 13-15, 1980
Gatlinburg, Tennessee

Published April 1981



Cosponsored by:
Oak Ridge National Laboratory
and
U.S. Department of Energy
Office of Energy Research
Division of Materials Sciences

OAK RIDGE NATIONAL LABORATORY
CENTRAL RESEARCH LIBRARY
CIRCULATION SECTION
4504N, ROOM 175

LIBRARY LOAN COPY

DO NOT TRANSFER TO ANOTHER PERSON

If you wish someone else to see this report, send its name with report and the library will arrange a loan.

U.S. GOVERNMENT PRINTING OFFICE: 1981

"This report was prepared as an account of work sponsored by the United States Government. Neither the United States nor the United States DOE, nor any of their employees, nor any of their contractors, subcontractors, or their employees, makes any warranty, express or implied, or assumes any legal liability or responsibility for the accuracy, completeness, or usefulness of any information, apparatus, product or process disclosed, or represents that its use would not infringe privately-owned rights."

Printed in the United States of America

Available from

National Technical Information Service
U.S. Department of Commerce
5285 Port Royal Road
Springfield, VA 22161

NTIS price codes

Printed Copy: \$20.00
Microfiche Copy: \$ 3.50

Alternate Nuclear Waste Forms and Interactions in Geologic Media

*Proceedings of a Workshop Summarizing Advanced
Activities and Formulating Requirements for the Future*

**May 13-15, 1980
Gatlinburg, Tennessee**

Published April 1981



**Cosponsored by:
Oak Ridge National Laboratory
Oak Ridge, TN 37830
and
U.S. Department of Energy
Office of Energy Research
Division of Materials Sciences
Washington, D.C. 20545**



3 4456 0251323 3

Editors:

L. A. Boatner

G. C. Battle, Jr.

Organizing Committee:

L. A. Boatner, ORNL, Chairman

M. M. Abraham, ORNL

E. H. Kobisk, ORNL

J. G. Moore, ORNL

M. C. Wittels, Division of Materials Sciences, USDOE

FOREWORD

In planning the Conference on Alternate Nuclear Waste Forms and Interactions in Geologic Media the intent and purpose was to organize a meeting that could simultaneously address several important goals - goals that, in retrospect, appear to be as ambitious now as they did prior to the actual realization of the conference in Gatlinburg, Tennessee, on the dates of May 13-15, 1980. The period of approximately two to two-and-one-half years preceding these dates had witnessed a series of significant events - events in the form of the publication of the results of some rather straightforward experiments. These results raised a serious fundamental question concerning the suitability of borosilicate glass for the primary containment of high-level nuclear waste in the environment of a deep geological repository. The raising of this initial question, in turn, led to a closer scrutiny of the pertinent characteristics of glass waste forms and to deep concerns that this approach might well have feet, in this case, not of clay - but of glass.

The ensuing controversy resulted in, among other things, the convening of a special committee by the National Academy of Sciences and, to appreciate fully the furor during this time, one has only to read the article entitled "Academy Squabbles over Radwaste Report" that appeared in the July 20, 1979, issue of Science Magazine on pages 287-289. More significantly, this controversy created a revival of interest in and research on primary waste forms that are alternatives to borosilicate glass. Hence, the context of "Alternate Nuclear Waste Forms," in the present case is that of nuclear waste forms which represent alternatives to encapsulation in borosilicate (or similar) glasses. This same controversy also led to a deeper appreciation of the need to consider not only the intrinsic chemical and physical characteristics of the waste form itself but how these properties might be modified by interactions associated with the immediate environment. Hence, the inclusion in the conference of topics related to "Interactions in Geologic Media."

The primary purposes of the conference on "Alternate Nuclear Waste Forms and Interactions in Geologic Media" were: First, to provide an opportunity for a review of the status of the research on some of the candidate alternative waste forms; second, to provide an opportunity for comparing the characteristics of alternate waste forms to those of glasses; and third, to stimulate increased interactions between those research groups that were engaged in a more basic approach to characterizing waste forms and those who were concerned with more applied aspects such as the processing of these materials. The motivating philosophy behind this "third purpose" of the conference was based on the idea that by operating from the soundest possible fundamental base for any of the candidate waste forms, hopefully any future unpleasant "surprise" - such as that alluded to earlier in the case of glass waste forms - could be avoided.

The conference was supported by the Oak Ridge National Laboratory and by The Division of Materials Sciences, Office of Basic Energy Sciences, USDOE.

The cooperation and participation of other groups supported by the U.S. Department of Energy were, of course, vital. Their complete cooperation is simply evidence of the desire that we all share - namely, the desire to provide the American people with a nuclear waste disposal system that can be deployed with the highest possible level of confidence in the safety and security of that system.

The papers and discussions contained in these proceedings were subjected to what the Editors felt was the minimum possible level of editorial tampering. The authors and participants, therefore, remain responsible for the content of their papers, questions, and comments, as well as for the style of presentation. The style of presentation, in fact, will be found to vary substantially from one paper to another. All of the oral presentations at the conference were recorded and the authors were furnished with typed transcriptions of their talks. Some authors edited these transcripts and others chose to prepare a separate version of their paper in the usual way. These two methods of producing a manuscript account for that portion of the disparity in style that could not normally be accounted for by the individual idiosyncrasies that, as authors, we all exhibit.

These proceedings have been prepared in the hope that they will provide a useful survey of activities for those entering the alternative waste form field while serving as a resource document for the veterans.

L. A. Boatner
Conference Chairman

ACKNOWLEDGMENTS

The conference chairman, the members of the organizing committee, and the editors of these proceedings are all indebted to a number of individuals who contributed substantially to the organization of the meeting in Gatlinburg and to the subsequent publication of the present document. Special thanks go to the authors and speakers, to Bonnie Reesor of the ORNL Conference Office and her staff, and to the staffs of the Photography, Graphic Arts, and Technical Publications Departments at ORNL. Special thanks also go to Anne M. Keesee, who transcribed all of the recordings of the oral presentations and performed a multitude of other tasks, and to Lazelle S. Tyler, who handled a heavy load of correspondence prior to the meeting and later retyped many of the manuscripts - all in addition to her regular secretarial duties. The assistance of M. M. Abraham, M. Rappaz, and J. O. Ramey in performing numerous tasks is also gratefully acknowledged.

CONTENTS

Foreword	iii
Acknowledgments	v
"Welcoming Remarks" Alex Zucker Oak Ridge National Laboratory	1
"Purpose and Objectives of the Workshop" Mark C. Wittels The Division of Materials Sciences USDOE	2
"The Application of Synroc to High-Level Defense Wastes" J. D. Tewhey, C. L. Hoenig, H. W. Newkirk, R. B. Rozsa, D. G. Coles, and F. J. Ryerson Lawrence Livermore National Laboratory	4
"On the Thermodynamic Stability and Kinetic Dissolution of Perovskite in Natural Waters" H. W. Nesbitt, G. M. Bancroft, W. S. Fyfe, S. Karkhanis, P. Melling, and A. Nishijima University of Western Ontario, Canada	25
"A Review of Ceramic Nuclear Waste Forms Through 1978" Gregory J. McCarthy North Dakota State University and Rustum Roy The Pennsylvania State University	37
"Hydrothermal Interaction of a Ceramic Waste Form with Basalt" B. E. Scheetz, S. Komarneni, D. K. Smith, and C. A. F. Anderson The Pennsylvania State University	44
"Probable Leaching Mechanisms for Spent Fuel" R. Wang and Y. B. Katayama Pacific Northwest Laboratories	58
"Short-Term Leaching Behavior of Waste Forms - A Potential Area for Improvement" Albert J. Machiels University of Illinois	70
"Radiation Damage in Natural Materials: Implications for Radioactive Waste Forms" Rodney C. Ewing The University of New Mexico	81

"Radiation Damage Studies on Natural and Synthetic Rock Salt" P. W. Levy and K. J. Swyler Brookhaven National Laboratory	100
"A Review of Heat Dissipation in Geologic Media" R. O. Pohl and J. W. Vandersande Cornell University	117
"Spent Fuel Resistance to Internally Produced Cladding Degradation" R. E. Einziger, D. A. Cantley, and J. C. Krogness Westinghouse Hanford Company and D. Stellrecht and V. Pasupathi Battelle Columbus Laboratories	135
"A Review of Research on Analogs of Monazite for the Isolation of Actinide Wastes" M. M. Abraham, L. A. Boatner, G. W. Beall, C. B. Finch, R. J. Floran, P. G. Huray, and M. Rappaz Oak Ridge National Laboratory	144
"The Application of EPR Spectroscopy to the Characterization of Crystalline Nuclear Waste Forms" M. Rappaz, L. A. Boatner, and M. M. Abraham Oak Ridge National Laboratory	170
"Hot and Cold Pressing of (La,Ce)PO ₄ -Based Nuclear Waste Forms" R. J. Floran, M. Rappaz, M. M. Abraham, and L. A. Boatner Oak Ridge National Laboratory	185
"A Survey of Concrete Waste Forms" J. G. Moore Oak Ridge National Laboratory	194
"Solidification of Nuclear Waste in Concrete" Hans Christensen ASEA-ATOM, Vasteras, Sweden	217
"Waste Form Characterization and Its Relationship to Transportation Accident Analysis" E. L. Wilmot and J. D. McClure Transportation Technology Center Sandia National Laboratories	229

"Sol-Gel Technology Applied to Alternative High-Level Waste Forms Development" P. Angelini, D. P. Stinton, J. S. Vavruska, A. J. Caputo, and W. J. Lackey Oak Ridge National Laboratory	242
"Chemically Vapor Deposited Coatings for Multibarrier Containment of Nuclear Wastes" J. M. Rusin and J. W. Shade Pacific Northwest Laboratory and R. W. Kidd and M. F. Browning Battelle Columbus Laboratories	248
"A Review of the Sorption of Actinides on Natural Minerals" G. W. Beall Radian Corporation	262
"Influence of Waste Solid on Nuclide Dispersal" M. G. Seitz and M. J. Steindler Argonne National Laboratory	287
"High Level Waste Fixation in Cermet Form" E. H. Kobisk, W. S. Aaron, T. C. Quinby, and D. W. Ramey Oak Ridge National Laboratory	297
"High-Silica Glass Matrix Process for High-Level Waste Solidification" Joseph H. Simmons and Pedro B. Macedo Catholic University	317
"A Review of Glass Ceramic Waste Forms" J. M. Rusin Pacific Northwest Laboratory	331
"Solid Radionuclide Waste Form Development in the United States" D. E. Gordon Waste Management Planning Division Savannah River Laboratories	355
"The Identification of Basic and Applied Research Needs in the Development of Radioactive Waste Forms - A Combined Presentation and Open Group Discussion" L. A. Boatner, ORNL, Chairman	369
Appendix A. Program	377
Appendix B. Attendees	382

WELCOMING REMARKS

Alex Zucker
Associate Director
Oak Ridge National Laboratory

Discussions of nuclear waste disposal are particularly appropriate to a multidisciplinary laboratory such as ORNL, since science and technology are closely linked in the nuclear waste field. If the discussions during this workshop can result in an agenda for research that will enhance our understanding of structures and chemical processes in nuclear waste forms and their interactions in geologic media, then real progress will be made toward making radioactive waste disposal safe and acceptable to the world at large.

I would like to suggest to you that the scientific aspects of the nuclear waste problem are really only half the battle. They are, in fact, the easy half. The most difficult part of the problem is to convince the country as a whole that scientists in this field are competent, that they do know how to dispose of nuclear waste, and that nuclear waste can be disposed of safely in many ways. The public at large must be convinced that the scientific community is a credible community: when statements are made they are based on fact and when the errors in our evaluations are considered, these too should be based on fact. It is important to show that nuclear waste is a problem that can be dealt with, as many other problems have been dealt with in a technologically advanced society, and that scientists are worthy of the public trust and that we, no more than others, want to risk our children and our children's children. The growing public mistrust of science and technology is probably the most serious problem that faces this country and is at the root of many of the things that we see happening in the world today. Nuclear waste is a symbol of this problem. I would like to urge those of you who are so inclined to consider seriously, while you are here, that the next conference might deal with such matters. You might consider a conference that includes not just your fellow scientists, but the nonscientific community as well. This must be done with some care, but the benefits could be very important. It is essential that the country regain an objective view of natural processes; and it is our duty as scientists to restore confidence in the validity of science.

PURPOSE AND OBJECTIVES OF THE WORKSHOP

Mark C. Wittels

Division of Materials Sciences
Office of Basic Energy Sciences
United States Department of Energy

I would like to begin by emphasizing that in my remarks today I am not functioning as a spokesman for the Office of Waste Management, and I will not be stating any official policy of the Department of Energy. I am, in fact, only going to act as an ombudsman and speak as an outsider. During the course of these opening remarks, you may hear some things that are controversial.

The purpose of the workshop is quite obvious. I believe that in the past year there have been some notable advances, and I think that this is a good time for an exchange of information among the scientists, the technologists, and the engineers in a multidisciplinary fashion. This may be one of the first times that such mixed disciplines including those studying the material nature of the waste form itself and those studying transport in geologic media have been brought together. I hope that as a result of this conference a few key problems will emerge that can be attacked in a cooperative way by scientists with very different disciplines. There is a tendency for too many isolated ongoing programs and too many individual projects continuing to grope for long periods of time.

At the conclusion of this conference we should ask ourselves a number of questions, and they should be serious questions that really drive to the heart of the waste program: Can reprocessing and separations be avoided? Our present policy of nonproliferation dictates a certain avenue of approach, but I think that, as scientists, we have to continue to ask ourselves, "Can we really accomplish this task without a separation of the radionuclides?" The adequacy of "standard" leaching tests as we presently understand them is highly questionable. I have read a lot of the publications in this field and very frankly, I am dismayed by the scores of tests that are made, for example, in quote "distilled water." This field needs to get down to a "real world" approach on standard leaching tests. One of the key elements that disturbed me recently was a scientific report by a group at Sandia, Albuquerque, in which they showed that leaching in brine was most seriously affected if magnesium impurities were present. We have to be very concerned about impurities, even in very minor amounts. Standards have to be set very critically.

I raise the question of multiple waste forms and their complexities. Again, because of some scientific results I have seen, I want to refer to microscopic observations. When one talks about a multiple waste form, whether it is polycrystalline, cermet, concrete, or glass,

as a scientist one has to be very careful about generalizing. If one looks at the scientific evidence microscopically in a multiphase system, one has the problem of grain boundaries. Do we really have the facilities, the spectroscopy, to look at systems on this scale and to make definitive statements?

Regarding the questions of analogs and limitations, I refer to the research efforts which substitute nonradioactive materials in order to conduct the research in an atmosphere which cannot handle radioactive material. I think this is necessary; this is done in universities; it should be continued. However, one must be very careful in drawing broad conclusions from these kinds of tests. These kinds of experiments can be very valuable if they are coupled with tests on similar systems which employ actual radioactive materials. We have already alluded to the question of policy limitations. We are limited by President Carter's nonproliferation policy. But, again I repeat, I think it is our duty to see the science as it really is. If we must come to the conclusion on a scientific and technological basis that wastes cannot be sequestered in one, solid, complex form without first separating them, I think that that fact should be honestly expressed.

Finally, I would like to comment on the question of scientific truth and the public perception that Alex Zucker referred to. This is a key issue. In the past year or two we have seen many public documents appear with a very high level of public acceptance. We see correspondence to the notable public literature - the New York Times - claims being made, counter-claims being made. It is time for scientists and technologists in this field to lower their profile. This is a very, very sensitive, difficult political problem, and I think the public would be well served if we pursue science and let the chips fall where they may, because credibility with the public will only decrease if we continue to hear public statements that are slightly shaded.

THE APPLICATION OF SYNROC TO HIGH-LEVEL DEFENSE WASTES

J. D. Tewhey, C. L. Hoenig, H. W. Newkirk,
R. B. Rozsa, D. G. Coles, and F. J. Ryerson

Lawrence Livermore National Laboratory, University of California
P.O. Box 808, Livermore, California 94550

ABSTRACT

The SYNROC method for immobilization of high-level nuclear reactor wastes is currently being applied to U.S. defense wastes in tank storage at Savannah River, South Carolina. The minerals zirconolite, perovskite, and hollandite are used in SYNROC D formulations to immobilize fission products and actinides that comprise up to 10% of defense waste sludges and coexisting solutions. Additional phases in SYNROC D are nepheline, the host phase for sodium; and spinel, the host for excess aluminum and iron.

Up to 70 wt% of calcined sludge can be incorporated with 30 wt% of SYNROC additives to produce a waste form consisting of 10% nepheline, 30% spinel, and approximately 20% each of the radioactive waste-bearing phases. Urea coprecipitation and spray drying/calcining methods have been used in the laboratory to produce homogeneous, reactive ceramic powders. Hot pressing and sintering at temperatures from 1000 to 1100°C result in waste form products with greater than 97% of theoretical density. Hot isostatic pressing has recently been implemented as a processing alternative.

Characterization of waste-form mineralogy has been done by means of XRD, SEM, and electron microprobe. Leaching of SYNROC D samples is currently being carried out. Assessment of radiation damage effects and physical properties of SYNROC D will commence in FY81.

INTRODUCTION

A considerable amount of research effort is currently being devoted to SYNROC applications for both commercial wastes and defense wastes. The focus of this presentation will be on high-level defense wastes, although I will be reviewing some of the work currently being done on civilian wastes. A synopsis of the presentation is as follows: First, I'll give an overview of SYNROC research as I know it. I will try to bring you up to date on SYNROC-related work in various universities and national laboratories. Second, I will present a brief overview of the nature of U.S. defense wastes. The major portion of the presentation will focus on the mineral waste form

development work being done at the Lawrence Livermore National Laboratory in the areas of powder preparation techniques, waste-form synthesis and characterization, leaching studies and, finally, some of our early thoughts on production technology schemes.

CURRENT SYNROC RESEARCH EFFORTS

SYNROC came on the scene in November, 1978, when it was introduced in a paper¹ by Professor A. E. Ringwood of the Australian National University. Ringwood's concept is a notable variation on the ceramic waste-form theme introduced earlier by Rustom Roy² and Gregory McCarthy³ at Pennsylvania State University. During the past two years, a considerable amount of research and development has been done on SYNROC, and I will briefly review some of those efforts (Table 1).

At the Australian Atomic Energy Commission, Keith Reeve and his colleagues have been conducting waste-form synthesis studies on SYNROC C (both hot pressing and sintering), leaching studies, and studies of radiation effects⁴. They are also working on production technology aspects of SYNROC, focusing on uniaxial hot pressing.

At Australian National University, Professor Ringwood and his colleagues are working on waste-form "optimization," i.e., they are experimenting with various modifications of the SYNROC C and SYNROC D⁵ formulations in order to get the best possible waste forms for commercial and defense applications. They are also doing radiation effects studies on natural zirconolite and perovskite and are thinking about various production technology schemes. Conceptual flow sheets for SYNROC processing are being evaluated, and I expect that a considerable effort will be devoted to that area of research during the next year. Professor Ringwood has recently published a paper which outlines his concept of a deep-hole waste repository⁶.

At Argonne National Laboratory, Chris Kennedy⁷ and Rich Arons are doing single-phase synthesis of hollandite, zirconolite, and perovskite as well as SYNROC C, and Kevin Flynn is doing leaching studies by means of neutron activation analysis. Bill Primak, who has been engaged in experimental research on radiation-effects in non-metallic inorganic solids for over three decades, will be involved in radiation damage studies of SYNROC phases.

At the Idaho Chemical Processing Plant (ICPP), they are looking at the potential application of SYNROC to some of their calcines, and have been doing waste-form synthesis, leaching, and characterization work.

At Los Alamos Scientific Laboratory, Frank Clinard's group is doing single-phase synthesis and radiation effects studies on the fluorite-type structures and zirconolite.

TABLE 1.
OVERVIEW OF CURRENT SYNROC RESEARCH

INSTITUTION	RESEARCH AREA
AUSTRALIAN ATOMIC ENERGY COMMISSION	WASTE FORM SYNTHESIS LEACHING RADIATION EFFECTS PRODUCTION TECHNOLOGY
AUSTRALIAN NATIONAL UNIVERSITY	WASTE FORM "OPTIMIZATION" RADIATION EFFECTS PRODUCTION TECHNOLOGY REPOSITORY DESIGN
ARGONNE NATIONAL LABORATORY	SINGLE PHASE SYNTHESIS LEACHING RADIATION EFFECTS
IDAHO CHEM. PROC. PLANT	WASTE FORM APPLICATION
LOS ALAMOS SCIENTIFIC LABORATORY	SINGLE PHASE SYNTHESIS RADIATION EFFECTS
NORTH CAROLINA STATE UNIVERSITY	RATE-CONTROLLED SINTERING CHARACTERIZATION LEACHING
OAK RIDGE NATIONAL LABORATORY	PRODUCTION TECHNOLOGY (SOL GEL) WASTE FORM SYNTHESIS CHARACTERIZATION (AUTORAD.)
SANDIA	TITANATE CERAMICS
BATTELLE (PNL)	WASTE FORM SYNTHESIS LEACHING RADIATION EFFECTS
UNIVERSITY OF WESTERN ONTARIO	PHASE STABILITY IN AQUEOUS SOLUTION
STATE UNIVERSITY OF NEW YORK AT STONY BROOK	MINERAL SYNTHESIS PHASE EQUILIBRIA
LAWRENCE LIVERMORE NATIONAL LABORATORY	WASTE FORM SYNTHESIS LEACHING RADIATION EFFECTS PRODUCTION TECHNOLOGY

At North Carolina State University, Hayne Palmour III and his colleagues⁸ are doing rate-control sintering, characterization of the sintered forms, and leaching studies.

At Oak Ridge National Laboratory, Jack Lackey, Pete Angelini, and Dave Stinton are doing production technology work in the application of sol gel techniques to SYNROC⁹. They are doing waste-form synthesis via the sol gel route and characterization of the waste forms by means of x-ray diffraction, microprobe analysis and autoradiography.

At Sandia Laboratories, they have been working on the titanate ceramic process for waste encapsulation for a number of years¹⁰. The phases that are produced from their titanate formulations are, in some cases, similar to the mineralogy of SYNROC. In addition to synthesis studies, they are also doing characterization of the microstructure, leaching studies and have been thinking about innovative ways to facilitate production technology. They are applying the titanate ceramic work to both commercial and defense wastes.

At Battelle Pacific Northwest Laboratories (PNL), they have done some early work in alternate waste-form synthesis and leaching, and more recently they have done radiation damage studies on synthesized zirconolite.

The University of Western Ontario personnel will present a paper at this symposium on the stability of perovskite in natural waters.

I have recently heard that Professor Don Lindsley, an experimental petrologist at SUNY, Stony Brook, will be doing phase equilibria work on SYNROC-type formulations.

Finally, at Lawrence Livermore National Laboratory, we are doing waste-form synthesis, characterization, and leaching. Production technology work is at the conceptual stage, and we are planning to study radiation effects in FY81. We have divided the effort into five tasks: waste form development and synthesis; characterization; stability assessment (leaching and radiation effects); ceramic processing; and production technology. We began our waste-form development work in July, 1979, and have progressed through the various SYNROC formulations during the past year. We began with SYNROC B (no radwaste), progressed to SYNROC C (the waste form for commercial radwaste applications), and are now working almost exclusively on SYNROC D (defense waste). A synopsis of the activities done in the five separate research and development areas under the LLNL program are given in Table 2.

U.S. DEFENSE WASTES

I will present a brief description of U.S. defense wastes for those who are not familiar with the particular characteristics of that

TABLE 2.
MINERAL WASTE FORM DEVELOPMENT PROJECT
AT
LAWRENCE LIVERMORE NATIONAL LABORATORY

WASTE FORM DEVELOPMENT	WASTE FORM CHARACTERIZATION	STABILITY ASSESSMENT	CERAMIC PROCESSING	PRODUCTION TECHNOLOGY
POWDER PREP	OPTICAL	ACCELERATED LEACH	PROCESS DEVELOPMENT	ENGINEERING ASSESSMENT
HOT PRESSING	XRD	CONTINUOUS FLOW LEACH	SCALE UP	ENGINEERING DEVELOPMENT
SINTERING	XRF	RADIATION EFFECTS	HOT CELL	QUALITY ASSURANCE OF THE WASTE FORM
HOT ISOSTATIC PRESSING	SEM	PHYSICAL PROPERTIES	TRACER LOADING	
PHASE EQUI-LIBRIA	MICROPROBE STEM	LEACH MECHANISMS	SYNROC C	

material. High-level defense wastes are generated by (1) the production of plutonium and tritium for nuclear weapons work at Hanford, Washington, and Savannah River, South Carolina, and (2) by processing of spent naval reactor fuels at the Idaho Chemical Processing Plant in Idaho Falls. Current inventories total approximately 76 million gallons. The distribution of wastes among the four storage sites is given in Table 3. Defense wastes, as it exists in tank storage, is made up of three components: sludge, salt cake, and supernatant liquid. The sludge and salt cake result from a process by which the acid waste stream from the nuclear fuel reprocessing cycle is neutralized with NaOH. The sludge is the focus of interest in the waste-form development work because all of the radionuclides, with the exception of cesium, are strongly partitioned into that material. The processing of the sludge results in the encapsulation of the actinides and most fission products. Cesium is strongly partitioned into the supernatant liquid which is processed in a separate line initially, but the cesium is ultimately incorporated with the other radwaste into a single waste form. The defense wastes at the Savannah River Plant are scheduled to be the first wastes processed for permanent storage. Hanford and the ICPP are currently in the process of evaluating the potential application of alternate waste forms to their diverse waste inventory.

Defense waste sludge is a formidable material with which to work. Physically, it is the color of axle grease, has the consistency of mayonnaise and consists of approximately 95% fluid and 5% solids.

TABLE 3.
CURRENT INVENTORIES OF U.S. DEFENSE WASTES

	10 ⁶ GALS	10 ⁶ CURIES	10 ⁶ GALS SLUDGE
HANFORD	50	540	11
SAVANNAH RIVER	22	570	3
IDAHO FALLS	3	85	*
WEST VALLEY	1	65	.03
	76	1.2x10 ⁹	14+

FOR COMPARATIVE PURPOSES, THE CURRENT INVENTORY OF U.S. COMMERCIAL WASTES (SPENT FUEL) IS 1.9x10⁹ CURIES.

*200 CU. YARDS OF ICPP WASTES EXIST AS DRY CALCINE POWDER.

Chemically, the material is diverse. Table 4A lists the major component compositions of specific tanks that have order-of-magnitude differences in iron, aluminum, uranium and others. Also listed is the composite or average composition for the total inventory. Minor element chemistry is also varied and diverse. A waste form that is to be applied to defense wastes must have the flexibility to incorporate the extreme differences in sludge composition.

TABLE 4A.
MAJOR COMPONENTS IN SIMULATED SRP WASTE CALCINES

Component	High Fe	Composite	High Al
Fe ₂ O ₃	53.17	36.13	5.32
Al ₂ O ₃	4.89	28.26	76.05
MnO ₂	3.56	9.94	4.37
U ₃ O ₈	12.34	3.26	1.28
CaO	3.62	2.69	0.35
NiO	9.08	4.47	0.78
SiO ₂	0.40	0.85	0.56
Na ₂ O	4.52	5.08	1.96
Na ₂ SO ₄	<0.50	0.93	<0.50
Ion-Siv IE-95*	8.82	8.93	9.33

*Mixture of CaAl₂Si₄O₁₂·6H₂O and (NaKCa)₃Al₃SiO₂₄·8H₂O

Strontium is the principal radionuclide in sludge, followed by cesium, ruthenium and europium. There is a minute amount of cesium in the sludge. The level of cesium in the supernatant liquid is equivalent to the strontium level in the sludge. Alpha activity level is quite low (Table 4B).

TABLE 4B.
RADIONUCLIDES IN WASHED, DRIED SLUDGES

	mCi/g			
	Tank 5	Tank 7	Tank 13	Tank 15
⁹⁰ Sr	74.7	27.0	15.5	25.6
¹⁴⁴ Ce	4.8	0.2	2.0	16.9
¹⁰⁶ Ru	2.7	1.4	0.4	1.7
¹⁵⁴ Eu	0.5	-	0.3	1.2
¹³⁷ Cs	1.3	1.3	0.3	0.1
Gross α	0.1	0.1	0.3	0.1

Source: Stone, J. A. et al, (1976), Sampling and Analysis of SRP High Level Wastes.
SR Publication DP-1399.

SYNROC MINERALOGY

The principal minerals in SYNROC formulations are titanates; hollandite ($\text{BaAl}_2\text{Ti}_6\text{O}_{16}$), zirconolite ($\text{CaZrTi}_2\text{O}_7$) and perovskite (CaTiO_3). All three are made up of Ti-O octahedra networks. In SYNROC D formulations, nepheline ($\text{NaAlSi}_3\text{O}_8$) and spinel ($\text{R}^{2+}\text{O}_3 \cdot \text{R}^{+}\text{O}$) are additional phases. Hollandite is the principal host for Cs in SYNROC, Sr goes into solid solution in perovskite and the rare earths and actinides are partitioned equally between perovskite and zirconolite. Uranium is partitioned into zirconolite (Fig. 1). The small amount of cesium that is present in the sludge enters into solid solution in nepheline. The theoretical density of SYNROC D formulations ranges from about 4.1 to 4.5 g/cc, depending on the spinel composition.

POWDER PREPARATION TECHNIQUES

Compositionally homogeneous and chemically reactive starting powders are necessary in order to sinter/hot press ceramics to full density at temperatures below the solidus. Three techniques have been used at LLNL to prepare reactive starting powders. The first technique is that of simply grinding and mixing oxides, hydroxides, and salts. The principle mode of mixing this material has been in a "vibro-energy" mill consisting of small alumina or zirconia pellets in

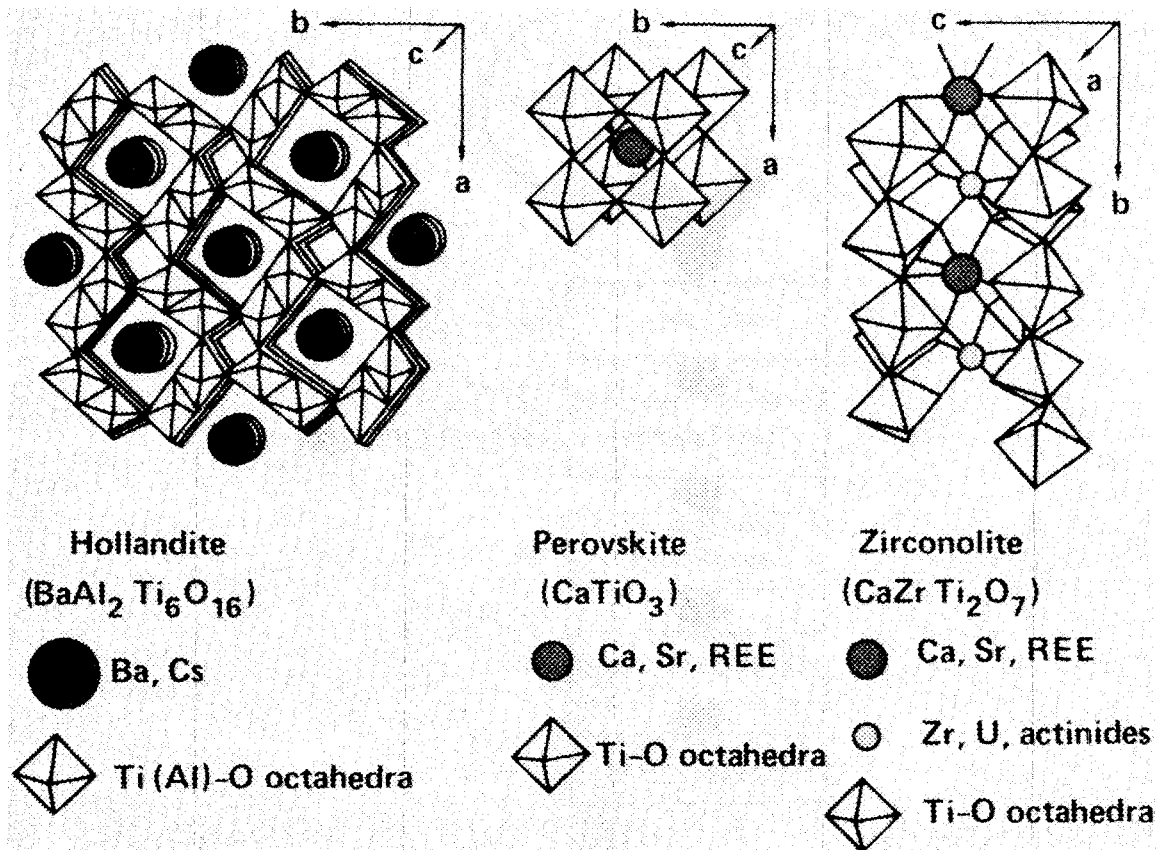
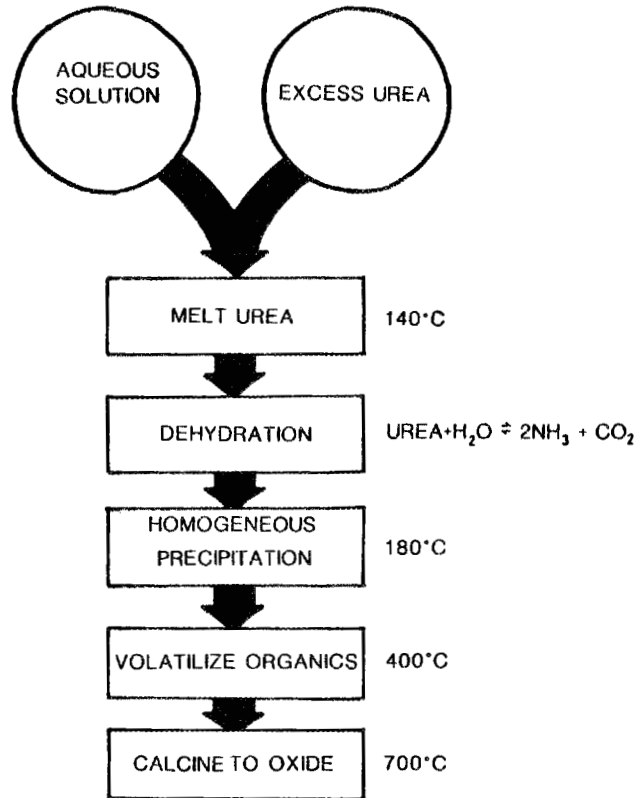


Fig. 1. The crystal structure and principal radwaste substitutions of SYNROC minerals.

a can containing a powder slurry. Vibratory motion causes the pellets to rub against one another and, in turn, grind and mix the powder.

We have made ample use of the urea coprecipitation technique developed by Tom Quinby¹¹ at ORNL. We have made about twenty-five different batches of starting material by means of the urea method. The principal advantage of the method is that homogeneous powders with very high surface areas are produced by the technique. The basis and mechanism of urea coprecipitation is given in diagrammatic form in Fig. 2.

The method we are currently using to do all of our powder preparation is spray drying (Fig. 3). Our reason for going to spray drying is that the process more closely simulates the production technology schemes that will be used in large-scale sludge processing. Powder properties have not been compromised for the sake of engineering simulation, however. The spray-dry technique has been found to produce very reactive powders. The highest temperature attained in the spray dryer is approximately 300°C, therefore batch calcining is done subsequent to drying.



(QUINBY, 1978, ORNL)

Fig. 2. Schematic representation of the methodology and processing temperature of the urea coprecipitation method for the production of ceramic powders.

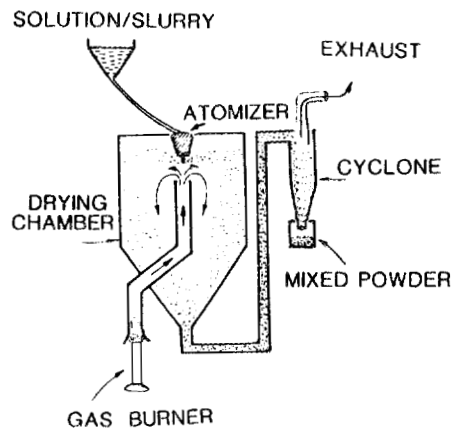


Fig. 3. Schematic of the laboratory-scale spray dryer used for the production of ceramic powders.

Reactive powders with high surface areas promote sintering at low temperatures and tend to produce dense, homogeneous ceramic end-products. The data in Fig. 4 represent measured surface areas for a variety of SYNROC powder preparations as a function of calcining temperature. It appears that sintering begins to take place when powders are heated to 600°C. X-ray diffraction data for a sample of SYNROC B powder calcined at temperatures between 600°C and 1000°C reveals that mineral phases begin to develop in the vicinity of 700°C (Fig. 5)¹². All of the principal SYNROC phases have been synthesized at 1000°C. Hot pressing or sintering to higher temperatures promotes grain growth and results in densification of the waste form. Optimum calcination temperatures for SYNROC formulations ranges from 650°C to 900°C.

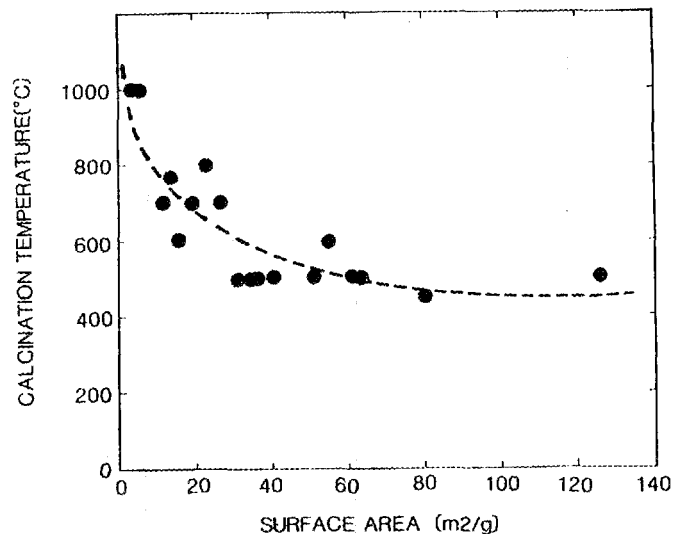


Fig. 4. Plot of measured surface area as a function of calcining temperature of SYNROC powder preparations made by urea coprecipitation and spray drying techniques.

WASTE-FORM SYNTHESIS

The experimental procedure for SYNROC waste-form synthesis is shown in Fig. 6. SYNROC D formulations contain up to 70 wt% sludge and 30 wt% SYNROC additives, i.e., the oxide components that bring about the desired phase assemblage. Defense waste sludges contain up to 10 wt% radwaste components, therefore, the maximum radwaste loading in SYNROC D is 7%. Cold pressing is a necessary step prior to sintering and hot isostatic pressing. Calcined powders go directly into the dies in the uniaxial hot-pressing operation.

Most of the waste-form synthesis work at LLNL has been done by uniaxial hot pressing, either in graphite dies or in metal (Ni or Fe) capsules (Fig. 7)¹³. The purpose of using the metal capsules (and

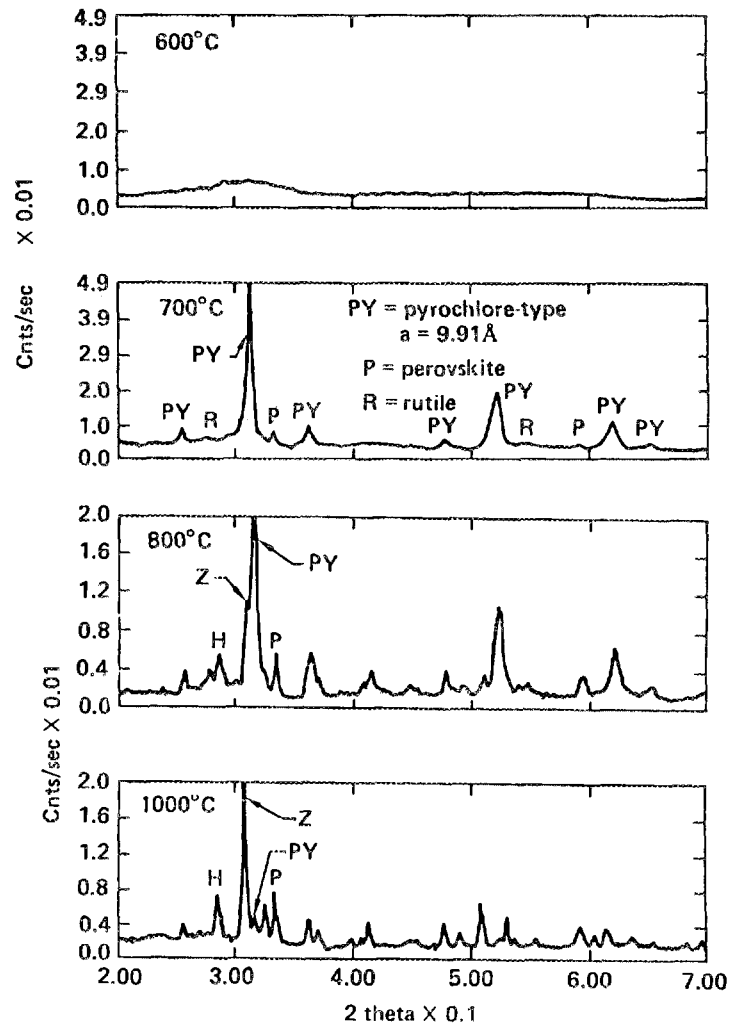


Fig. 5. X-ray diffraction patterns for a SYNROC B formulation as a function of calcining temperature. A pyrochlore-type phase forms at 700°C and has nearly disappeared at 1000°C. SYNROC phases are synthesized at 900°C. Powder was made by the urea coprecipitation method.

adding metal powder to the formulation) is to control the redox state during hot pressing. It is desirable on the basis of equilibria considerations, to have a ferric/ferrous ratio near unity and this is accomplished in the vicinity of the nickel-nickel oxide buffer; thus the use of capsules and metal powder. Differential thermal analysis indicates that the solidus for SYNROC D formulations with composite waste is near 1125°C. Hot-pressing parameter studies have been carried out at temperatures between 950°C and 1150°C (Fig. 8). Each data point in Fig. 8 represents the extent of densification that is attained at the end of a one-hour duration in the hot press. It is clear that SYNROC D formulations can be pressed to near theoretical density at temperatures as low as 1050°C. The SYNROC C data in Fig. 9 suggests that powders of a similar composition, but prepared by

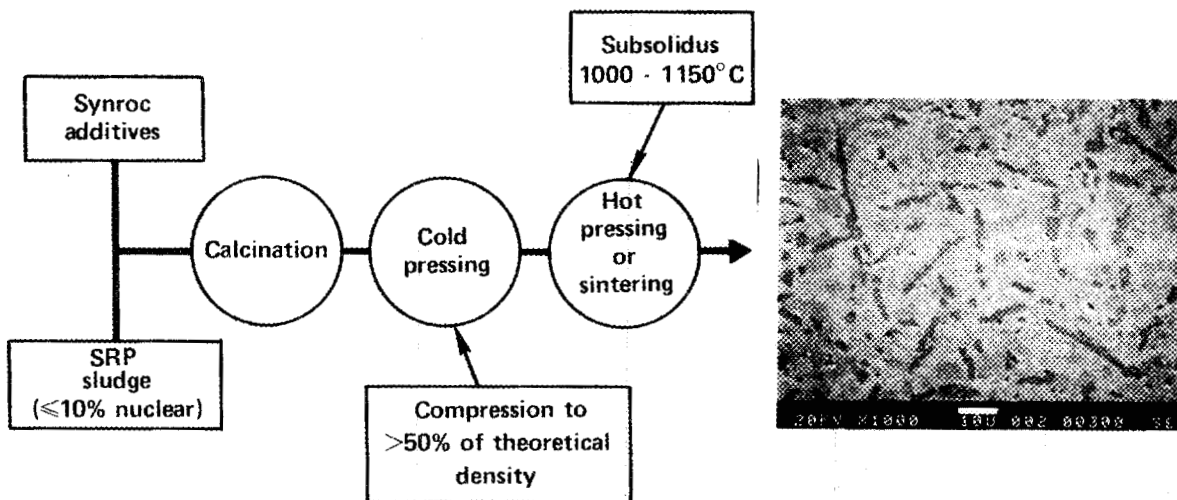


Fig. 6. Experimental procedure for the hot pressing/sintering of SYNROC D formulations with U.S. defense wastes. Bar on SEM photograph of microstructure is 10 µm.

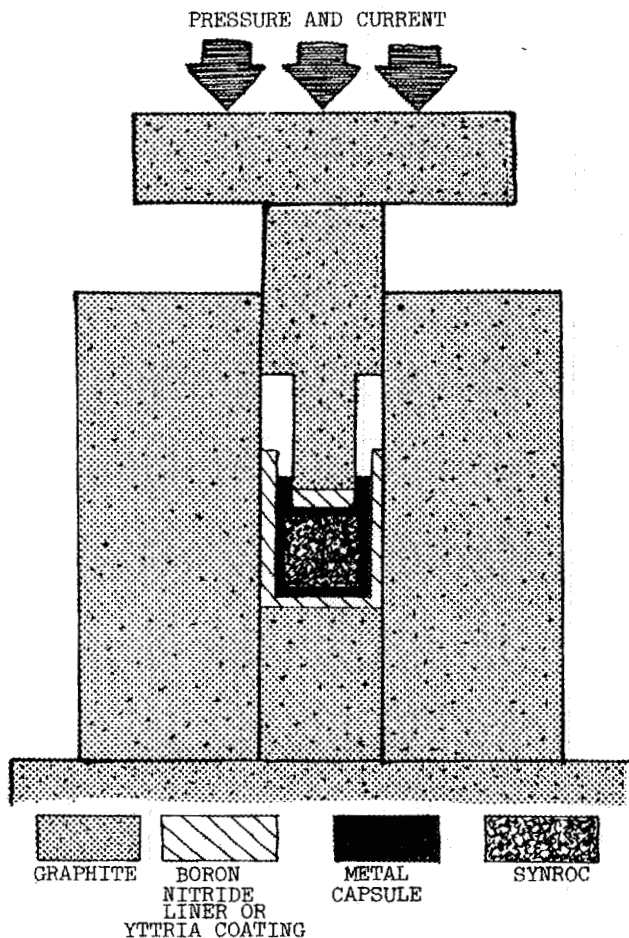


Fig. 7. Schematic of uniaxial resistance hot press for processing SYNROC D in metal capsules. The liner is not required when operating at temperatures below 1200°C.

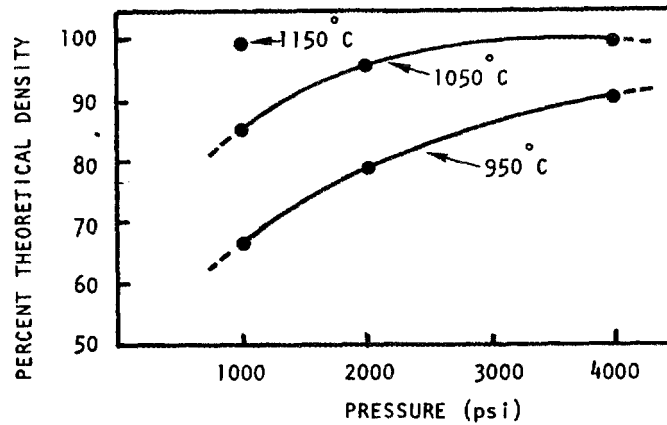


Fig. 8. Results of uniaxial hot pressing parameter study of SYNROC D formulation produced by means of urea coprecipitation. Each data point represents the extent of densification after one hour at temperature and pressure. The SYNROC D consists of 69 wt% simulated defense waste sludge (composite composition) and 31 wt% SYNROC additives.

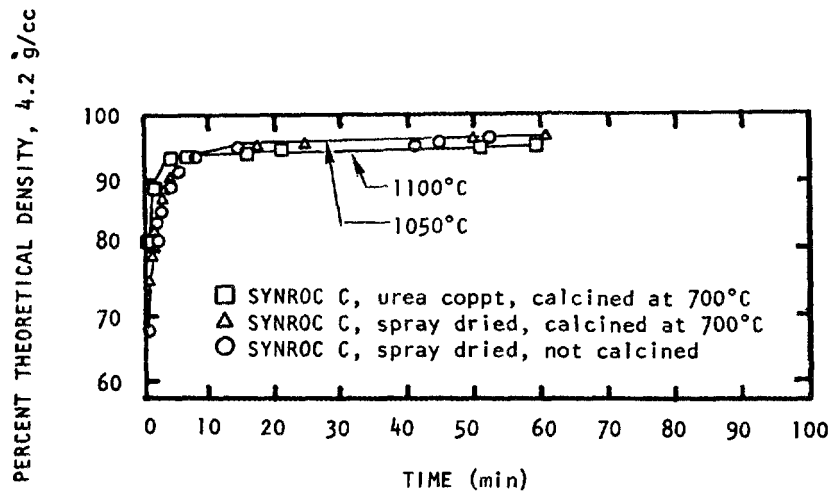


Fig. 9. Densification plots versus time for uniaxial hot pressing of SYNROC C formulations made by means of various powder preparation techniques.

means of different techniques, have similar densification characteristics during hot pressing. This is not a surprising result in that the urea coprecipitation and the spray drying techniques both produce powders with surface areas in excess of $100 \text{ m}^2/\text{gram}$.

PRODUCTION TECHNOLOGY

It was mentioned earlier that the sludge contains the bulk of the radwaste components of defense wastes and the supernatant liquid contains the cesium. The reference flow sheet for the processing of Savannah River Plant wastes¹⁴ defines a sludge-processing stream and a supernatant liquid-processing stream which merge so that all of the radwaste components are eventually encapsulated in the same waste form (Fig. 10). The specific makeup of SYNROC D is determined on the basis of the radwaste and inert components present in defense wastes. A SYNROC formulation based on SRP composite sludge is given in Table 5. The cesium host, hollandite, is presynthesized and added to SYNROC D calcine prior to hot pressing of the composite form.

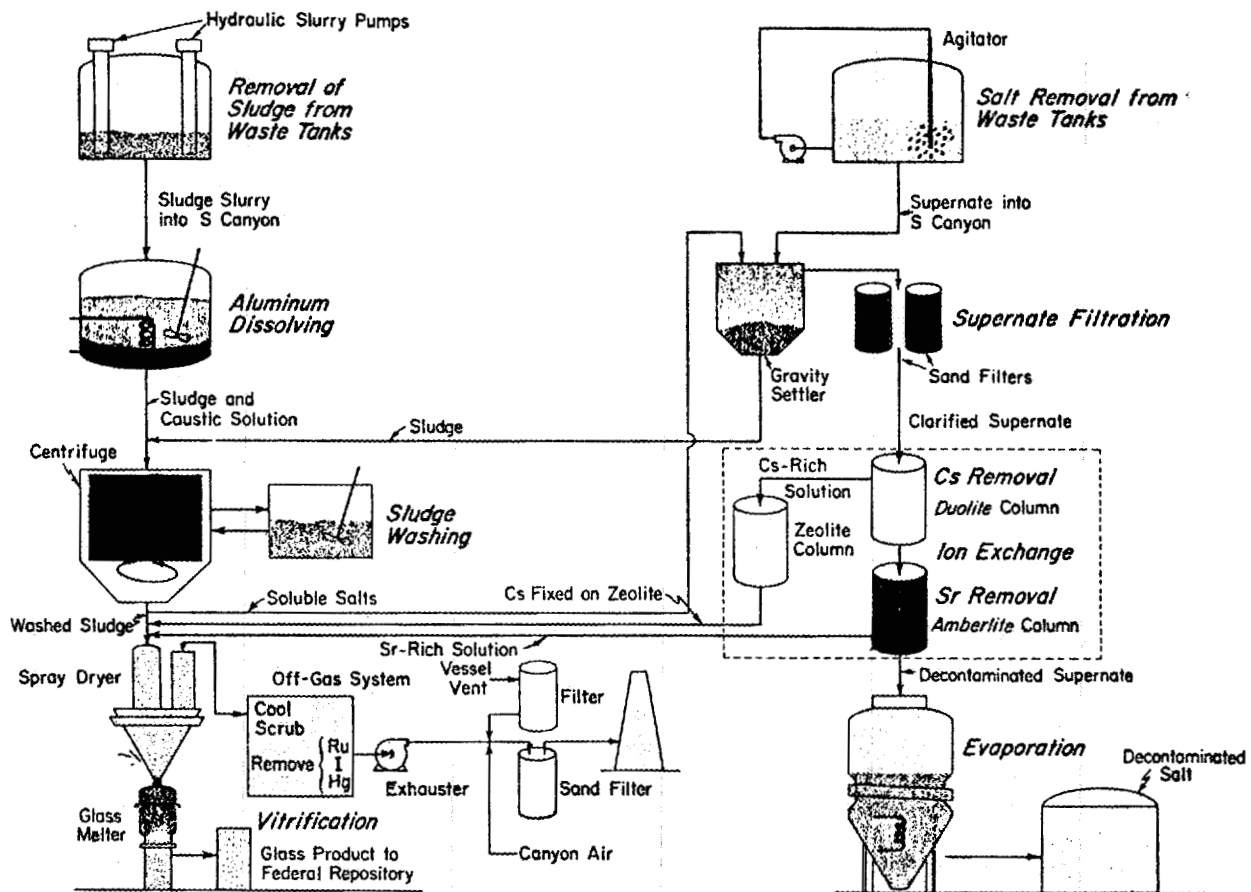


Fig. 10. Reference flowsheet for the processing of Savannah River Plant high-level defense wastes.

A conceptual flow sheet for uniaxial hot pressing of SYNROC D is shown in Fig. 11. The important aspects of the flowsheet are as follows: (1) the SYNROC additives are prepared outside of the hotcell, (2) a spray calciner or, alternatively, a spray dryer coupled with a

TABLE 5.
 SYNROC D COMPOSITION FOR SRP COMPOSITE SLUDGE

	Sludge Calcine	SYNROC Additives
SiO ₂	0.6	7.5
TiO ₂		15.0
ZrO ₂		4.0
UO ₂	2.3	
Al ₂ O ₃	21.2	
Fe ₂ O ₃	27.1	
MnO	6.1	
NiO	3.4	
CaO	2.0	4.9
SrO	0.7	
Gd ₂ O ₃	0.7	
CeO ₂	<u>0.7</u>	<u>.</u>
TOTAL (wt%)	68.6	31.4

rotary kiln are potential processes for the mechanism for decomposition of sludge and additives, and (3) a presynthesized Cs-bearing waste form is added prior to hot pressing. Fig. 12 depicts the type of "stacking" experiments that have been carried out at LLNL. Another alternate method that is currently being investigated represents a variation of the process presented in Fig. 12. Instead of hot pressing to final density, the successive disks in the stack are "warm" pressed in order to achieve a high initial density. The capsule would subsequently be hot isostatic pressed to full density. A large research effort in the area of large scale processing will be done at LLNL during FY81.

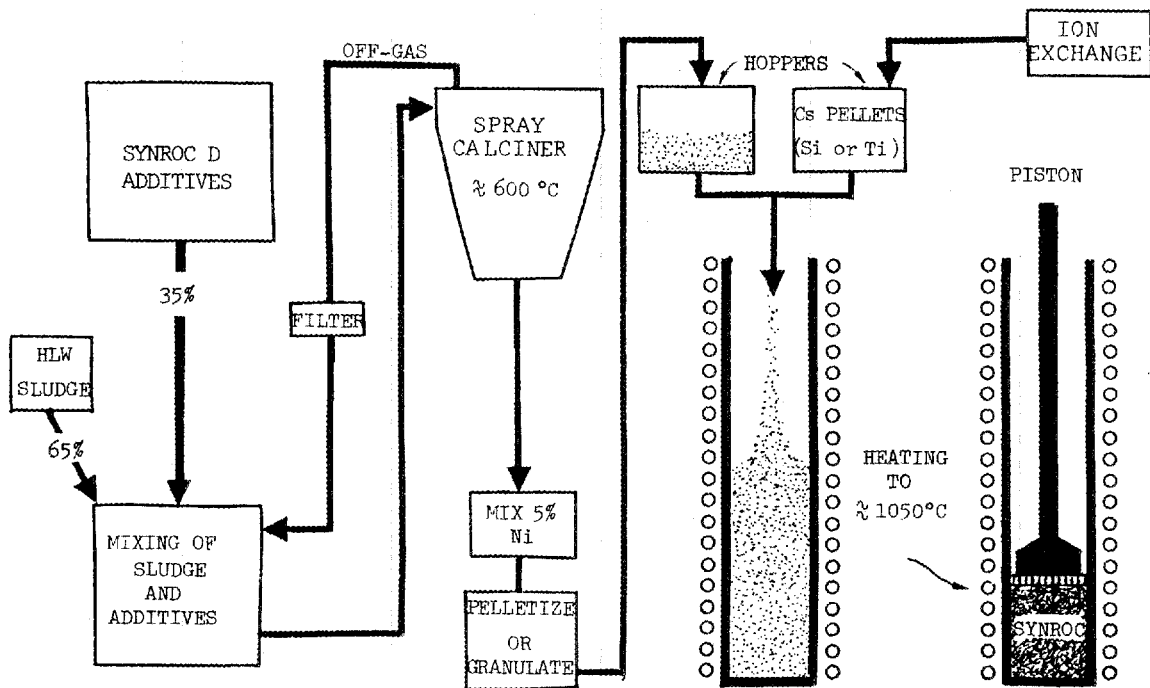


Fig. 11. Conceptual flowsheet for SYNROC processing utilizing uniaxial hot pressing.

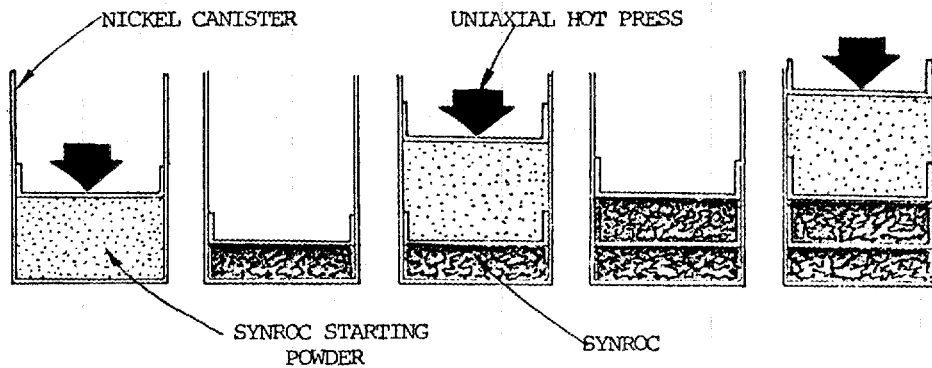


Fig. 12. The sequence depicts the hot pressing steps in the production of a "stacked" monolith of a ceramic waste form.

LEACHING

In consideration of the manner in which SYNROC D will be formulated, the leaching data is presented in terms of the respective host materials. The data presented in Table 6 represents the components of the SYNROC D matrix, i.e., the radwaste incorporated in perovskite, zirconolite and the small amount of cesium present in nepheline. The data in Fig. 13 represents the leaching characteristics of single phase Cs-bearing hollandite¹⁵. The leaching characteristics of the combined products are currently undergoing evaluation and will be available in early FY81.

TABLE 6.
LEACHING RESULTS FOR SYNROC D WITH Cs HOLLANDITE ADDITION

Leaching conditions:
300°C, 1kb, 1 day, distilled water.
Results expressed in terms of g/SYNROC/cm² · day.

Al	5.9 x 10 ⁻⁷
Ca	9.0 x 10 ⁻⁹
Ce	ND
Fe	3.2 x 10 ⁻⁹
Mn	7.9 x 10 ⁻¹¹
Na	3.8 x 10 ⁻⁵
Ni	ND
Si	9.0 x 10 ⁻⁸
Sr	ND
Ti	1.2 x 10 ⁻¹⁰
U	ND
ZR	ND
Cs	8.2 x 10 ⁻⁶
Gd	ND

Two types of leaching studies are currently being done at LLNL. Scoping or reconnaissance studies are being done in a static mode in Teflon containers at temperatures ranging from 75°C to 150°C for short periods of time. This method is in accordance with recommendations of the Materials Characterization Center (MCC) at PNL. More comprehensive studies are being done by means of the continuous flow leaching system at 25°C and 75°C for periods up to two months (Fig. 14). The duration of the continuous flow experiments has been limited by the sensitivity of analytical techniques used on the leachates. Tracer doping of SYNROC samples will be done in FY81 in order to increase analytical sensitivity.

DISCUSSION

POHL: I understood, from the introduction, that there is a great variety of chemical compositions in the Savannah River sludges. The conceptual flow sheet that you showed at the end did not seem to take that into consideration. Are you planning to make one grand mixture and then use that, or do you plan to use different mixing ratios and processes for the different compositions to be determined as you start going from one tank to the next tank?

TEWHEY: The experimental work we have conducted thus far has focused on the composite sludge composition. I have an extra slide (Fig. 15)

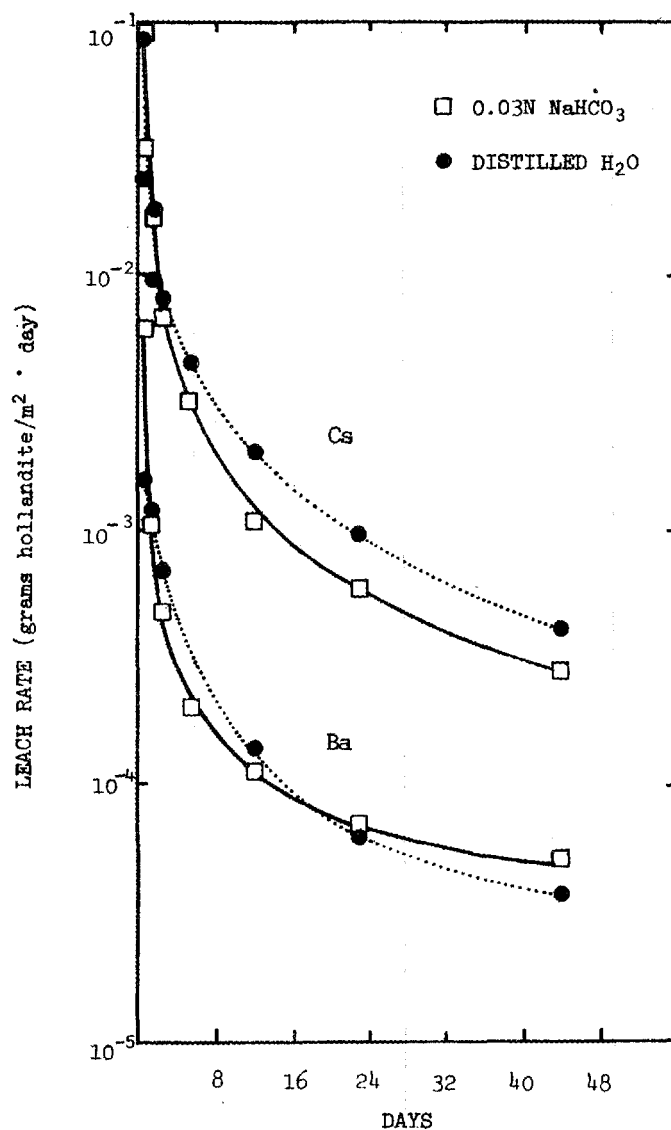


Fig. 13. Leaching rate versus time for Cs-bearing hollandite in the continuous-flow leaching system. Leaching temperatures were 25°C and 75°C, flow rate was 30 ml/day and leach solutions were distilled water and a 0.03N NaHCO₃ solution. Except for the earliest samples, no temperature effect on leach rate was noticed.

which depicts the phase equilibria for SYNROC D for three sludge compositions in terms of the three principal components, Al₂O₃, FeO, and TiO₂. The principal phases in the SYNROC D matrix; perovskite, zirconolite, nepheline and spinel are plotted in terms of their composition with respect to aluminum, iron and titanium. Note that the composition of the zirconolite, perovskite and nepheline show very little variation from one bulk composition to another. On the other hand, the composition of the spinel phase, which comprises up to 50

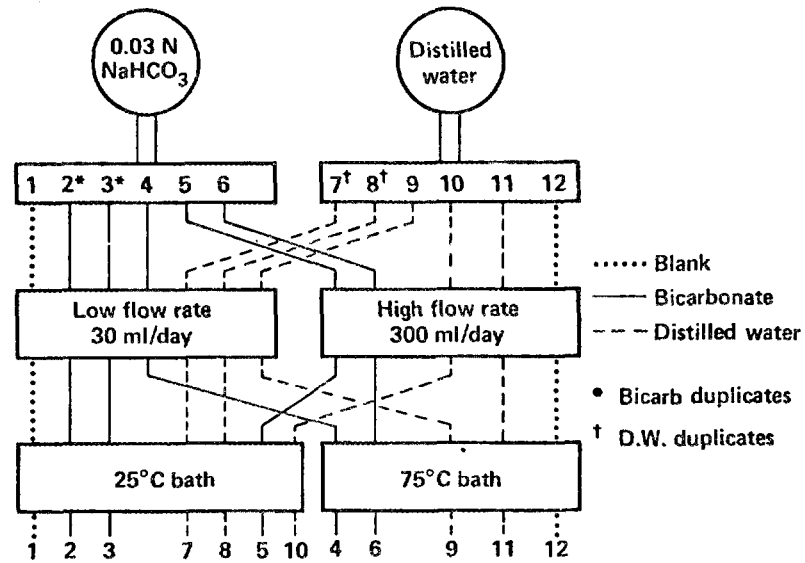


Fig. 14. Diagram of the continuous-flow leaching system as set up for leaching of SYNROC samples.

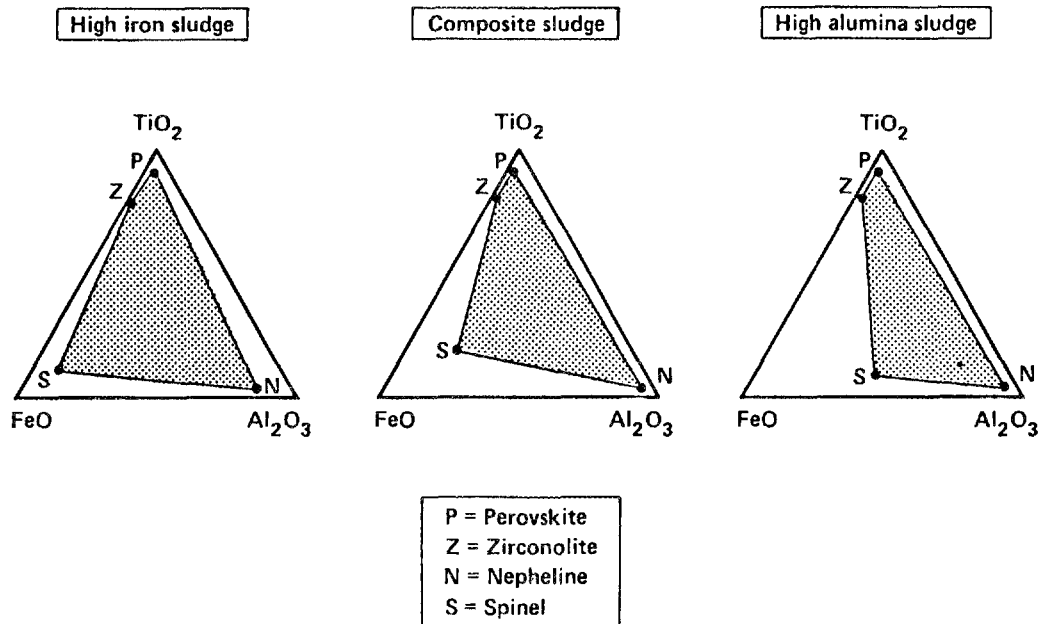


Fig. 15. Phase compositions for minerals in SYNROC D for three sludge compositions. Spinel (S) shows evidence of being a "forgiving" phase, i.e., the composition varies significantly with bulk composition.

wt% of the waste form, varies considerably in the three ternary diagrams. Spinel is the "forgiving" phase in SYNROC D, that is, the additive stream does not have to be "fine-tuned" for each sludge composition. We predict that an additive stream that is variable within narrow limits will be adequate to produce the desired SYNROC assemblage in the three sludge compositions. The considerable differences in sludge composition will influence the spinel composition, which will vary from being Al-rich to Fe-rich.

WITTELS: In the graphs you showed on leaching, the leach rate of hollandite tends to reduce as a factor of time. What did you measure, and what is the physical picture you ascribe to this decrease? I do not have a physical picture of why this rate should decrease so dramatically, if you have a through-flow system.

TEWHEY: Our method of analysis in the continuous-flow leaching experiments is to measure the composition of the leachate subsequent to it being in contact with the waste form. Samples are collected downstream from the sample holder and analyzed by means of XRF, ICP or INAA. The initial high leach rate is probably due to the material leached from surfaces and grain boundaries.

The leach rate that we are trying to determine is the rate that is measured thirty or forty days after the experiment starts. Up to now, we have had to stop our continuous-flow experiments prior to the time when the leach rate are expected to level out. Tracer loading of SYNROC samples will enable us to carry out longer leach experiments and to determine whether the leach rate levels off in the 10^{-9} or 10^{-10} region of the plot.

REFERENCES

1. Ringwood, A. E. (1978), Safe Disposal of High-Level Nuclear Reactor Wastes: A New Strategy. Australian National University Press, Canberra, Pp. 1-64.
2. Roy, R. (1975) Ceramic Science of Nuclear Waste Fixation (Abs). American Ceramic Society Bulletin, 54, 459.
3. McCarthy, G. J. and Davidson, M. T. (1975) Ceramic Nuclear Waste Forms: Crystal Chemistry and Phase Formation. American Ceramic Society Bulletin, 54, 728.
4. Reeve, K. D. and Woolfrey, J. L. (1980), Accelerated Irradiation Testing of SYNROC Using Fast Neutrons: First Results on Barium Hollandite, Perovskite and Undoped SYNROC B. Journal Australian Ceramic Society, 16, 1.
5. Ringwood, A. E., Kesson, S. E., Ware, N. G., Hibberson, W. O. and Major, A. (1979), The SYNROC Process: A Geochemical Approach to Nuclear Waste Immobilization. Geochemical Journal, 13, 141.

6. Ringwood, A. E. (1980), Safe Disposal of High-Level Radioactive Wastes. Res. School of Earth Sciences, Australian National University Pub. 1438.
7. Kennedy, C. R., Arons, R. M., Poeppel, R. B., Laskiewicz, R. A., Flynn, K. F. and Jones, D. J. (1980), Leachabilities of Component Phases of SYNROC B Containing Simulated Nuclear Fission Products. American Ceramic Society Bulletin, 59, 394.
8. Solomah, A. G., Hare, T. M. and Palmour, H. III (1980), Demonstration of the Feasibility of Subsolidus Sintering of Radwaste-Containing SYNROC B Composition. Nuclear Technology, in press.
9. Angelini, P., Stinton, D. P., Carpenter, R. W., Vavruska, J. S. and Lackey, W. J. (1980), Phase Identification and Partitioning of Elements in Sol-Gel-Derived SYNROC. American Ceramic Society Bulletin, 59, 394.
10. Dosch, R. G. (1979), Ceramic Forms for Nuclear Waste, in Radioactive Waste in Geologic Storage, S. Fried, ed. American Chemical Society Symposium Series 100.
11. Quinby, T. C. (1978), Method of Producing Homogeneous Mixed Metal Oxides and Metal-Metal Oxide Mixtures. U.S. Patent Application No. 787,128.
12. Smith, G. S. (1980), X-ray Diffraction Studies of SYNROC Waste Forms, American Ceramic Society Bulletin, 59, 394.
13. Hoenig, C. L. and Otto R. (1980), Hot Pressing and Sintering Studies of Ceramic Waste Forms for U.S. Defense wastes. American Ceramic Society Bulletin, 59, 394.
14. Stone, J. A., Goforth, S. T., Jr., and Smith, P. K. (1979), Preliminary Evaluations of Alternate Forms for Immobilization of Savannah River Plant High-Level Waste. Savannah River Laboratory DP-1545.
15. Coles, D. G., and Bazan, F. (1980), Continuous-Flow Leaching Studies of Crushed and Cored SYNROC. Journal of Nuclear Technology, in press.

ON THE THERMODYNAMIC STABILITY AND KINETIC DISSOLUTION
OF PEROVSKITE IN NATURAL WATERS

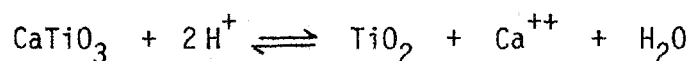
H. W. Nesbitt, G. M. Bancroft,* W. S. Fyfe, S. Karkhanis,
P. Melling, and A. Nishijima

Centre for Chemical Physics and Department of Geology
University of Western Ontario, London, Canada

ABSTRACT

Ringwood and coworkers have recently proposed using titanates and zirconates as hosts for nuclear waste in the Synroc B process. Three minerals are used as hosts: perovskite (CaTiO_3), Ba-hollandite ($\text{BaAl}_2\text{Ti}_6\text{O}_{16}$), and zirconolite ($\text{CaZrTi}_2\text{O}_7$). The Synroc philosophy relies heavily on geological and geochemical observations in selecting stable host minerals. Although it has been recognized that the Synroc minerals are not thermodynamically compatible with siliceous rocks, the minerals are considered to be thermodynamically stable in the presence of water, and it has been reported that these minerals are kinetically stable under high-temperature (up to 900°C) hydrothermal conditions.

We have made detailed thermodynamic calculations and leach tests which demonstrate: first, that perovskite is thermodynamically unstable in all known natural waters; and second, that perovskite leaches at a significant rate even at 100°C . Using data from Robie et al. and Helgeson, it is apparent that CaTiO_3 is not thermodynamically stable at any reasonable P_{CO_2} and a SiO_2 values. For example, for the reaction:



ΔG° is -25.0 kcal (-104.4 kJ) and -23.4 kcal at 25°C and 300°C respectively. At neutral pH, the Ca^{++} concentrations required to stabilize CaTiO_3 are $\sim 10^9$ ppm and ~ 100 ppm at 25°C and 300°C respectively. Similarly, CaTiO_3 is unstable with respect to CaCO_3 and TiO_2 at all P_{CO_2} values found in natural waters.

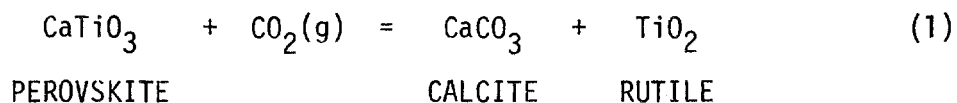
We have performed hydrothermal leach tests on natural and synthetic perovskite and perovskite analogues between 100°C and 300°C . Weight losses and solution concentrations were monitored. For an ~ 110 mg natural perovskite sample leached at 300°C for three weeks, the weight loss was ~ 600 ug, while 480 ug of Ca^{++} was leached into solution. The ratio of these two values is consistent with the above reaction taking place.

*Speaker

Somewhat surprisingly from a kinetic point of view, the leach rates for this single crystal and synthetic $MTiO_3$ samples at $100^\circ C$ ($M = Ca, Sr, Ba$) are comparable to, or larger than, those at $300^\circ C$ for the same sample. This observation is compatible with the thermodynamic calculations; the perovskite becomes less stable at lower temperatures. The results reported previously in the literature also show that perovskite is kinetically unstable in the presence of common silicates. Our results show that perovskite may be no more stable than siliceous glasses, such as rhyolite, which have been studied previously. Geologic evidence from common alkaline rocks also indicates that hollandite and zirconolite probably will not survive in common rock matrices.

As we have heard previously, perovskite is one of the important components in the Synroc¹ scheme. It is also the simplest mineral in that scheme. It seemed to us important to do some fundamental thermodynamic and kinetic work in order to look at the stability of perovskite both in rock matrices and in natural waters. Perovskite is a beautiful candidate for examining especially the thermodynamics: the thermodynamic properties of perovskite and reaction products are known; and there are some simple reactions which can be written for the decomposition of perovskite, both in rock matrices and in natural waters. I want to look very briefly at some of our thermodynamic calculations in the natural water area using known data,^{2,3} and then at some of our leach data on perovskite between 100 and $300^\circ C$. We hope to point out the relevance of the thermodynamics in the resulting leach tests.

We will begin by considering three very simple reactions of perovskite which could and do take place in natural waters. The first reaction that we will consider is perovskite plus CO_2 in water, going to calcite plus rutile:



The equilibrium constant for pure solids can be expressed:

$$\text{LOG } K_{\text{rxn}} = -\text{Log } (P_{CO_2}) \quad (2)$$

We can obtain the values of ΔG° for this reaction for a wide range of temperatures and establish an equilibrium constant, which is a function of the partial pressure of CO_2 . We now look at the stability diagram for this reaction (Fig. 1). The coordinates are the log of the CO_2 pressure vs the reciprocal of temperature. Celsius temperatures are given along the top. The solid line represents the equilibrium values for P_{CO_2} . Above the line, perovskite plus CO_2 will be thermodynamically

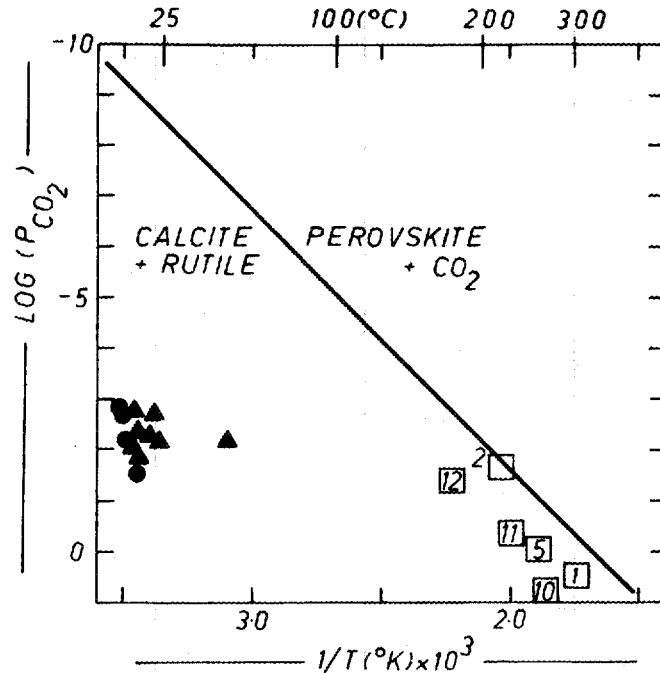
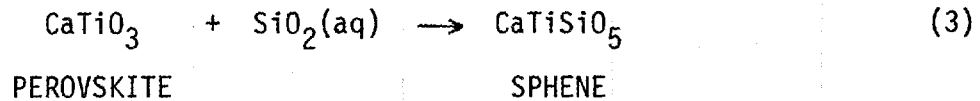


Fig. 1. Plot of $\log P_{\text{CO}_2}$ vs $1/T$ for reaction (1). P_{CO_2} , T values are plotted for near-surface ground waters from limestones (triangles), ultramafic rocks (circles), and hydrothermal solutions (squares).

stable; below the line, calcite plus rutile will be thermodynamically stable. We have plotted here the partial pressures of CO_2 in a number of different natural waters. Those in the vicinity of 200 to 300°C are from hydrothermal solutions. Those at low temperatures are from limestones and ultramafic rocks. We could also put high silica here. More common igneous rocks, such as granite, would also plot well in this region. Figure 1 indicates that the partial pressure of CO_2 in natural waters is generally too high to stabilize perovskite in this reaction.

The second reaction that we want to consider is perovskite plus silica, going to sphene; this is probably the most important reaction in any aqueous system:



$$\text{LOG } K_{\text{rxn}} = -\text{LOG} (\text{SiO}_{2\text{aq}}) \quad (4)$$

Again we obtain the ΔG° values for this as a function of temperature and establish an equilibrium constant, which is in the ideal case, a function of the SiO_2 concentration in aqueous solution. A stability diagram for this reaction is shown in Fig. 2. The coordinates are the log of the aqueous

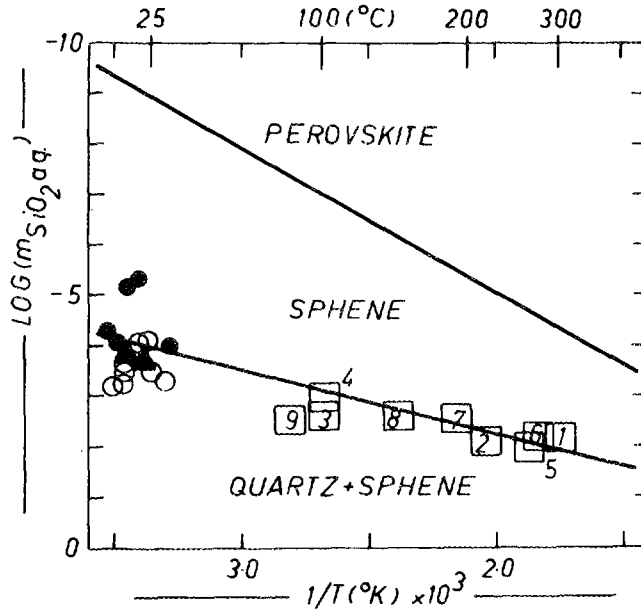
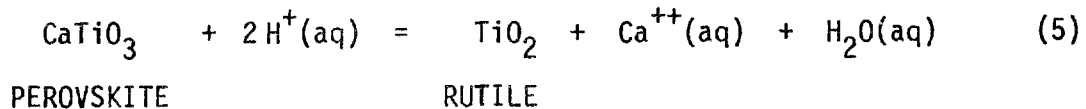


Fig. 2. Plot of $\log m_{\text{SiO}_2(\text{aq})}$ vs $1/T$ for reaction (3). The m_{SiO_2} , T values are plotted for ground waters emanating from dunites and peridotites (filled circles), and serpentinites (empty circles), limestones (triangles), and hydrothermal waters (squares). These all plot very close to the lower solid line representing solutions saturated with quartz.

silica concentration vs the reciprocal of temperature. Again, Celsius temperatures are given at the top. The upper line indicates the equilibrium concentrations of $\text{SiO}_2(\text{aqueous})$. Perovskite is stable at lower SiO_2 concentrations (above the line); sphene is stable at higher SiO_2 concentrations (below the line). The lower line in this figure actually gives the solubilities of quartz in natural waters. We have plotted the SiO_2 concentrations in various natural waters. Here, again, we have hydrothermal waters at high temperatures and limestones, peridotites and serpentines at low temperatures. Again, the silica concentration in all natural waters is far too high to stabilize perovskite thermodynamically.

The third reaction, which could also occur in natural waters, and which is perhaps more applicable to laboratory work which we have carried out, is the simple reaction perovskite plus acid going to rutile plus calcium ions plus H_2O ; that is presumably what is happening in most of our leach tests:



$$\text{LOG } K_{\text{rxn}} = \text{LOG}[\text{Ca}^{++}/(\text{H}^+)^2] \quad (6)$$

Again, we can calculate the values for ΔG° as a function of temperature and establish an equilibrium constant, which in this case is a function of the calcium ion concentration divided by the square of the hydrogen ion concentration. If we combine this reaction and the preceding one (the silica reaction), we can plot a stability diagram (Fig. 3). The coordinates are the log of (calcium ion concentration over the square of hydrogen ion concentration) vs the log of the aqueous silica concentration. The stability field for perovskite is in the block at upper left; sphene is stable above the diagonal line; rutile is stable below the diagonal line. Here, we have plotted points for evaporate and limestone deposits, and known data for silica, calcium, and pH data. Data for igneous rocks plot in this general area. Once again, in all known natural waters the concentrations of the aqueous species are not sufficient to stabilize perovskite. We conclude that, with the exception of some very high partial pressures of CO_2 in geothermal waters in the first reaction, perovskite is thermodynamically unstable in all natural waters.

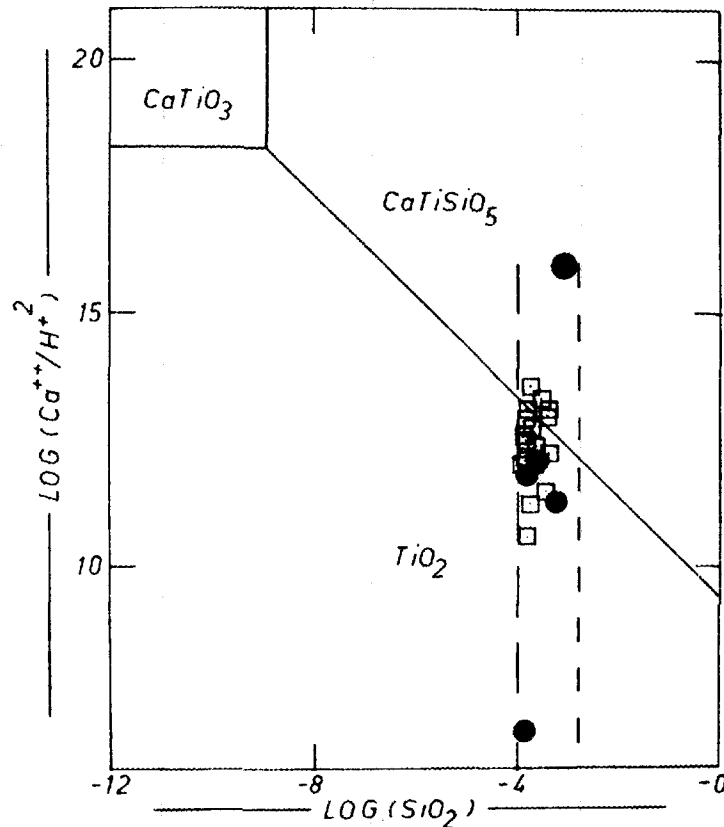


Fig. 3. Plot of $\log [a_{\text{Ca}^{++}}/a_{\text{H}^{+}}^2]$ vs $\log a_{\text{SiO}_2(\text{aq})}$ combining reactions (3) and (5) at 25°C . Solution compositions are plotted for basalts and gabbros (squares) and for rhyolites and granites (circles). The equilibrium line delineating the stability fields of sphene and rutile is obtained by subtracting the $\log k$ values of reactions (3) and (5).

Experimental data⁴ shows that the perovskite is unstable in the presence of siliceous minerals. This data summarizes the thermodynamics, but we all know that glasses that are being studied are thermodynamically unstable. What does this have to say, anyway, about the kinetics of dissolution of perovskites, or any mineral phase? We have to look at the kinetics and see whether the thermodynamics is of any relevance whatsoever.

We will now look at some of the laboratory tests that we have done. Considering the reaction in Table 1, perovskite plus acid, going to calcium ions plus rutile, the first set of experiments that we did were on a natural crystal of perovskite from Magnet Cove, Arkansas. In the initial experiment, we heated the crystal in 60 ml of water in an autoclave at 300°C for three weeks. The experimental weight loss was 600 ug, and the amount of calcium ion released, as found by atomic absorption, was 484 ug. If we take a 600 ug weight loss, then the theoretical amount of calcium ion in solution would be 430 ug based on that equation. Therefore, weight loss and the calcium ion released are reasonably consistent for that particular reaction taking place. The leach rate in Table 1 is not based on congruent dissolution, but is based solely on Ca⁺⁺ leached into solution. The leach rate at 300°C based on the calcium ion released, is about $2.8 \times 10^{-5} \text{ g cm}^{-2} \text{ day}^{-1}$. Other experiments that John Tewhey has described and that we have done, show that the leach rate does drop off dramatically with time, so most of this leaching is probably taking place within a day or so. We then repolished that crystal, and did experiments at 100°C, and the leach rates are about $1.9 \times 10^{-5} \text{ g cm}^{-2} \text{ day}^{-1}$, comparable to that at 300°C. The pH of the solution is between 6 and 7.

Table 1. Leaching of CaTiO₃ Single Crystal at 300°C^a

CaTiO ₃ + 2H ⁺ → Ca ⁺⁺ (aq) + TiO ₂ + H ₂ O(l)		
	Experimental	Theoretical
Weight loss, ug	600	---
Ca ⁺⁺ released, ug	484 ^b	430

^aSingle crystal (100 plane) from Magnet Cove, Arkansas. Weight ~120 mg. Surface area ~0.8 cm². Leach time, 3 weeks.

^bLeach rate (Ca⁺⁺) = $2.8 \times 10^{-5} \text{ g cm}^{-2} \text{ day}^{-1}$ (300°C)
 $1.9 \times 10^{-5} \text{ g cm}^{-2} \text{ day}^{-1}$ (100°C)

We then synthesized some strontium and barium titanates from the oxides and they were hot pressed. (These were prepared by Dr. S. Shin in the Japanese National Chemical Laboratory for Industry.) These weigh about 0.5 g, the nominal surface areas are about 2 cm² and the leach rates are given at 100, 200 and 300°C in Table 2. These were leached beginning like the single-crystal, at a pH of 6. The solutions were analyzed for strontium and barium after one week. These leach rates are based on strontium and the barium in solution; again, they are not corrected for congruent dissolution. We repeated this for a second week. They were

Table 2. Leach Rates of Perovskite Analogues^a
(g cm⁻² day⁻¹, Sr⁺⁺ or Ba⁺⁺)

Compound	T(°C)	Leach Rate	
		First Week	Second Week
SrTiO ₃	100	3.2 x 10 ⁻⁵	1.1 x 10 ⁻⁵
	200	6.0 x 10 ⁻⁶	2.7 x 10 ⁻⁶
	300	4.3 x 10 ⁻⁶	2.5 x 10 ⁻⁶
BaTiO ₃	100	3.5 x 10 ⁻⁵	3.0 x 10 ⁻⁵
	200	7.9 x 10 ⁻⁶	7.9 x 10 ⁻⁶
	300	< 3 x 10 ⁻⁶	< 3 x 10 ⁻⁶

^aSamples prepared from mixed oxides, heated at 1200° for 24 hours in air, and hot pressed into discs. Nominal surface areas ~2 cm².

rescraped between these two tests to refresh the surface; otherwise we would get a very much lower leach rate in the second week. Perhaps the important point here is that the leach rate at 100°C is, if anything, higher than that at 300°C. There is a general increase in all of these results from 300 to 200 and from 200 to 100°C.

We will not discuss our powder perovskite results, but they are compatible with the general idea that the leach rates do not change very much

on going from 100 to 300°C; I think this is qualitatively consistent, at least, with what John Tewhey has said previously.

Now this is very different from results obtained for glasses; I present, for comparison, Table 3, which contains results of work that we have done under very similar static hydrothermal conditions. The main comparison that should be made is between a natural volcanic glass, rhyolite, which we have studied in some detail,⁵ and the titanates of calcium, strontium, and barium. Rhyolite is a very stable natural volcanic glass; leach rates generally are an order of magnitude lower than that for sodium borosilicates. All of these results are from tests on disc-like material of usually around a few hundred milligrams with usually 10 ml of water in the autoclave. The leach rate for rhyolite is typical of glasses, and it increases dramatically with temperature, usually by a least an order of magnitude with each 100°; whereas the leach rates of perovskite and its strontium and barium analogs do not change substantially with temperature. You can see that at 300° the leach rates of the titanates are much, much lower than that of even a very stable glass, but at 100° they are, in fact, very comparable. The set of rhyolite values at three temperatures are based on congruent dissolution. The lower value for rhyolite is really more comparable with the ones for the titanates, because this is based on sodium in solution. We would be very interested in seeing

Table 3. Leach Rates of Glasses and Titanates
(g cm⁻² day⁻¹)

	100°C	200°C	300°C
Na borosilicates(a)	3.5 x 10 ⁻⁴		
Rhyolite(a)	3.5 x 10 ⁻⁵	3.2 x 10 ⁻⁴	1.3 x 10 ⁻³
(b)	3.0 x 10 ⁻⁶		
CaTiO ₃ (c)	1.9 x 10 ⁻⁵	---	2.8 x 10 ⁻⁵
SrTiO ₃ (c)	3.2 x 10 ⁻⁵	6.0 x 10 ⁻⁶	4.3 x 10 ⁻⁶
BaTiO ₃ (c)	3.5 x 10 ⁻⁵	7.9 x 10 ⁻⁶	< 4 x 10 ⁻⁶

(a) Based on weight loss.

(b) Based on Na in solution.

(c) Based on M⁺⁺ (M⁺⁺ : Ca⁺⁺, Sr⁺⁺, Ba⁺⁺) in solution.

whether results reported by John Tewhey show that the leach rates for the titanates again remain reasonably constant as you go down to lower temperatures. Now, why does the leach rate stay fairly constant with temperature? Well, we believe that this can be rationalized using the thermodynamics. Let us refer to the last reaction that was considered in eq. (5). The equilibrium concentration of calcium ions for that reaction at 300° is approached in the leach tests. We are within an order of magnitude of the equilibrium concentrations that we have calculated: and as equilibrium is approached, the leach rates are going to go down. On the other hand, at 100° the equilibrium calcium ion concentration is many orders of magnitude higher, and there is a large initial driving force to the leach rate at 100° and lower temperatures, because the equilibrium concentrations are extremely high.

To conclude, it is important to look at the thermodynamics of minerals that are being studied, and hopefully glasses as well, although the latter is of course very much more difficult. It is very difficult to get appropriate information on glasses, but I think that in the future at least the thermodynamics provides, a basis for discussion, which will be extremely important in nuclear waste disposal risk assessments.

Acknowledgements: We are very grateful to AECL (Canada) for financial support

DISCUSSION

J. TEWHEY: How did you characterize your perovskite from Magnet Cove, Arkansas, and how did you characterize the material that had been hot pressed in Japan?

BANCROFT: The Magnet Cove, Arkansas material has been characterized by x-ray diffraction and by probe measurements. It contains some very small inclusions, but, other than that, it appears to be pure. The strontium and barium substances have been characterized again by x-ray diffraction and by probe measurements. Of course, the general difficulty, as you well know, is that very small impurities can lead to very high initial leach rates; but the fact that we have leached, for example, the strontium and barium substances for three weeks in a row, getting very similar results indicates that the substances were pure and were not leaching out, say, an oxide.

SAME QUESTIONER: How did you characterize your surface areas?

BANCROFT: Just the nominal surface areas from measuring the outside of each disc.

SAME QUESTIONER: Were these fully dense disks?

BANCROFT: No. That is an important point. We have not checked how close to theoretical density those are. Those leach rates might well be higher than you would get with a fully dense material. (The density is over 90% of the theoretical).

J.H. SIMMONS: In looking at the high temperature leach rate, you are saying that basically the solution is saturating in calcium ions, and therefore the leach rate goes down in the case of the titanates.

BANCROFT: Right.

SIMMONS: What is the likelihood that this represents a real waste form burial condition?

BANCROFT: It probably does not. It depends, of course, on the particular flow rate in the repository. If you are refreshing the surface all the time, that would tend to increase the leach rate, but, of course, you probably have a buildup of a TiO_2 surface, which is preventing further leaching. I think that certainly the tests that we have done and the tests that I have heard about would indicate indeed that the leach rate drops off dramatically with time, whether or not you do a flow test or a static test.

SIMMONS: But it seems that you are biasing your results by saturating the solution. If you took a larger volume solution, you might have much higher leach rates. Is that what you are saying?

BANCROFT: I think that is true.

UNIDENTIFIED SPEAKER: There is calcium in ground water.

BANCROFT: Right. There are plenty of calcium ions in ground water; ~100 ppm. So, even with the concentrations we are talking about, we are within an order of magnitude of typical ground water concentrations.

SIMMONS: Thank you. The only thing I would like to convey is that we should be very careful in comparing the various materials under different conditions; for example, glasses in sealed systems and crystals in sealed systems. Sometimes there are certain mechanisms which tend to bias the results towards one material or the other; whereas, if you change the conditions (for example, put a lot of silica in solution), [things could be different]

BANCROFT: Obviously. I think with the equipment that we have, we have standardized as well as we could, to the same kind of bombs, the same volume of solution; but, certainly, there are still difficulties with that as you have pointed out.

UNIDENTIFIED QUESTIONER: In your theoretical calculation, do you take into account any activation energies, or are you assuming those as zero.

BANCROFT: We are just looking at the free energies of formation in each case - and not considering any sort of activation energy.

SAME QUESTIONER: Would not that be the most important thermodynamic property to consider?

BANCROFT: No. It is irrelevant.

SAME QUESTIONER: Not irrelevant in the hydrogen-oxygen reaction.

BANCROFT: Let's try to separate the thermodynamics and the kinetics. You're talking about the kinetics, rather than the thermodynamics. The activation energy is not a thermodynamic quantity. It is a kinetic quantity. It has nothing to do with the thermodynamics and never will have.

G. McCARTHY: I am very pleased to see this work presented. We have been waiting for it for years. I have actually wanted to do some of it myself, but never got around to it. Two quick ones on the thermodynamic data base, again. How much do you trust the ΔG° values? They are subject to great error, and they change as a function of time, sometimes completely changing the sign of the free energy. Secondly, in your abstract, you mention anatase, and yet your calculations are based on rutile; so do you feel you are approaching equilibrium the calculations apply?

BANCROFT: Perhaps I could ask Dr. Nesbitt that, He has done the calculations.

NESBITT: The studies that have been done on the solubility of rutile and anatase in isothermal experiments suggest that they are not greatly different in their calculated free energy; perhaps of the order of one Kcal in 200 kcal. I forgot the number at higher temperature; but at 25°, the free energy for one of the reactions discussed is -25 kcal – very negative.

BANCROFT: That's in the third reaction. In the perovskite plus proton reaction. In fact, in the first calculations that you did Wayne, using previous numbers, the ΔG was considerably more positive than that. But you are absolutely right that you can get changes, depending on what numbers are used in that particular reaction, by more than 10 kJ (2 kcal). But the free energies for most of those reactions are close to -100 kJ. They are really extremely negative. So, it would take very large changes in those numbers to dramatically alter, I think, the conclusion.

UNIDENTIFIED QUESTIONER: How do you get from 25 kJ in the abstract to 100 kJ?

BANCROFT: By the way, there is an error in the abstract. It should be 25 kcal rather than 25 kilojoules. There is very little change in going from 100 to 300°C. But because of the temperature in the $\Delta G^\circ = -RT \log K$ expression, K changes quite dramatically with temperature, even though ΔG° does not.

REFERENCES

1. A.E. Ringwood, S.E. Kesson, N.G. Ware, W.O. Hibbertson, and A. Major, *Geochemical Journal*, 13, 141-165, (1979).
2. R.A. Robie, B.S. Hemingway and J.R. Fisher, *U.S.G.S. Bull.*, 1452, 456 p. (1978).
3. H.C. Helgeson, *Amer. Jour. Sci.*, 267, 729-804, (1969).
4. R.D. Schuiling and B.W. Vink, 31, 2399-2411, (1967).
5. S.N. Karkhanis, G.M. Bancroft, W.S. Fyfe and J.D. Brown, *Nature* 284, 435-437 (1980).

A REVIEW OF CERAMIC NUCLEAR WASTE FORMS THROUGH 1978

Gregory J. McCarthy

Departments of Chemistry and Geology
North Dakota State University
Fargo, ND 58105

and

Rustum Roy

Materials Research Laboratory
The Pennsylvania State University
University Park, PA 16802

A popular textbook defines CERAMICS as "solid articles composed in large part of inorganic nonmetallic materials".¹ Thus, the term CERAMICS is broad enough to include virtually every solid nuclear waste form, from "salt cake" to hot pressed mineral-modeled forms. However, as has come to be the conventional usage in nuclear waste management, we will define ceramics as the largely crystalline materials designed as alternatives to the mostly noncrystalline vitreous or melt-formed products (glasses, glass-ceramics, sintered glass-ceramics). Another class of legitimate ceramics, cement and concrete forms, will not be treated in this review. The reader is referred to papers by D.M. Roy² and J.G. Moore in this workshop for reviews of these nuclear waste ceramics.

It is noteworthy that the solid defense high level wastes (salt cake, CsCl, SrF₂, ICPP calcine) are also ceramic nuclear waste forms. Vast experience has been gained in processing these hot ceramic forms. However, because they are unconsolidated and/or highly soluble in water, these forms are not usually considered to be suitable for final disposal and they also will not be considered further here.

An historical listing of the remaining classes of ceramic nuclear waste forms is given in Table I. Many people are surprised to learn that the desirability of solidification of high level nuclear waste into crystalline, mineral-modeled, ceramics or ceramic matrices was recognized nearly three decades ago. The objective of this short paper is to present a summary of these early, and not well known, studies through 1978. For the latest developments since then, the reader can consult the annual volumes of Scientific Basis for Nuclear Waste Management, the proceedings of the symposia of the same name held by the Materials Research Society in November of each year and published by Plenum Press.

We find in a 1953 overview article on nuclear waste disposal by L.P. Hatch,³ the suggestion that wastes be sorbed and fixed on minerals, especially clays and zeolites. A 1962 patent disclosure by Arrance⁹ describes one way in which this may be accomplished, namely through

TABLE I

Ceramic Nuclear Waste Forms -- An Historical Perspective

Year and Reference	Ceramic Nuclear Waste Forms	Sites and Principal Investigators
1953 [3]	Suggested Mineral-Modeled Ceramics	L.P. Hatch Brookhaven
1961 [4]	Radionuclides in Fluorophlogopite; Ceramic Coating, Hot Pressing	E.J. Evans AECL Chalk River
1962 [5]	Radionuclides in "Ceramic Sponge" Ceramic Coating	F.C. Arrance
1972 [6]	Radionuclides in Phosphates; Fusion Casting	J.L. McElroy J.E. Mendel Battelle Northwest
1972 [7]	Radionuclides in Silicate Minerals; STOPPER Process, Aqueous Silicate Process	G.S. Barney, L.E. Brownell, L.L. Ames, M.J. Kupfer, R.E. Isaacson, Hanford
1973 [8]	Ceramic Matrix Encapsulation, Gel Precursors, Hot Pressing	G.J. McCarthy Penn State University
1975 [9]	Ceramic Matrix Formed by Hot Pressing; Titanate Ion Exchange Process	R.G. Dosch, J.K. Johnstone, R.L. Schwoebel Sandia Albuquerque
1975 [10]	Radionuclides in an Assemblage of Mineral-Modeled Crystalline Phases; Liquid Phase Mixing; Hot Pressing or Conventional Ceramic Processing	G.J. McCarthy R. Roy Penn State University
1978 [11]	Radionuclides in an Assemblage of Mineral-Modeled Crystalline Phases; Fusion Casting (Later, Hot Pressing)	A.E. Ringwood Australian National University
1978 [12]	Ceramic Matrix Formed by Hot Pressing; Titanate Ion Exchange Process	T. Westermark, S. Forberg, H. Larker Sweden

absorption of liquid waste into a partially fired but porous ceramic rich in clay, followed by drying and sealing the porosity by sintering with some vitrification to give a consolidated ceramic.

In a remarkable foretaste of later developments, E.J. Evans and coworkers at AECL, Chalk River described in 1961 the fixation of small amounts of nuclear waste Cs and Sr in fluorophlogopite, $\text{KMg}_3\text{AlSi}_3\text{O}_{10}\text{F}_2$, processed the ceramic by hot pressing and formed an additional coating of nonradioactive ceramic to provide for greater leaching resistance. Solid solution stabilization in synthetic minerals, hot pressing and coatings figure prominently in today's waste forms R & D.

During the waste solidification Engineering Prototypes program carried out in the U.S. during the late 1960's, one of the waste forms evaluated was a fusion cast (poured from a melt) phosphate ceramic. It was processed remotely and contained radioactivity levels appropriate for power plant high level waste.⁶

A group of workers at the then Atlantic Richfield Hanford Company studied several means of converting their defense wastes into a mineral form using a very low temperature hydrothermal process.⁷ In one scheme, clays were added to a salt cake solution to make a nitrate analog of the feldspathoid mineral cancrinite, $\text{Na}_7\text{Al}_6\text{Si}_6\text{O}_{24}(\text{NO}_3) \cdot 2 \text{H}_2\text{O}$. At a rather early date Isaacson and Brownell⁷ of this group discussed several of the concepts which were to be applied in later work on mineral-modeled ceramics:

- On Pu Hosts: "Plutonium silicate is a structural analog of zircon, ZrSiO_4 , with... extremely low solubility... for a qualitative understanding of degree of solubility of plutonium silicate, one might refer to the presence of zircon and thorite in beach and river sands".
- On a Cs Host: "Cesium is highly soluble and volatile in most of its chemical forms; however, pollucite... is highly stable in neutral or basic chemical environments".
- On Sr Hosts: "Strontium also forms a number of aluminosilicates, one of which is a... feldspar... have very low solubilities and are stable at high temperatures".
- On Stability: "The silicate and aluminosilicate product forms are essentially inert and unreactive with most geologic materials. Exceptions would include hydrothermal solutions..."

An "encapsulation strategy" is one option for utilizing high stability ceramics/synthetic minerals in nuclear waste forms. Radionuclides form in highly dispersed, and not necessarily insoluble, phases in the ceramic matrix. The design effort is focussed on the dispersal of radionuclides and the elimination of any open porosity. This strategy was originated by McCarthy in the early 1970's and was later applied to matrix encapsulation of commercial high level waste calcine in collaboration with

Battelle Northwest. Of the numerous ceramic matrices investigated, forms of SiO_2 (α -quartz, amorphous from a LUDOX precursor) and consolidation by hot pressing gave the best combination of densification, thermal stability and leaching resistance in products having 20-30% waste calcine loading.⁸ This encapsulation strategy, optionally combined with additional design of insoluble, compatible radionuclide host phases, is ideally suited to defense waste sludge solidification where only traces of radionuclides are present and the bulk of the sludge consists of ceramic precursors. It is being utilized in the tailored ceramics R & D program of Rockwell International and Penn State University. In the mid-1970's, workers at Sandia Laboratories applied this strategy and processing to the consolidation of products prepared by sorption of high level liquid waste ions on titanate gel.⁹ The finished ceramic consisted of mineral-like titanates and oxides in a matrix of the rutile form of TiO_2 . A similar process and product were independently developed in Sweden.¹² The originator, T. Westermarck, has also discussed the encapsulation strategy and the exceptional stability of rutile as a ceramic matrix.¹²

In 1973 when we initiated research on ceramics as alternatives to vitrified waste forms, the US waste management policy was to solidify commercial waste and store it above ground in Retrievable Surface Storage Facilities. Because of waste volume considerations, high loading and thermal stability at a continuous 600-800°C centerline temperature were important design considerations. Realizing that the dilution necessary for ceramic encapsulation forms was too great for this application, we returned to earlier studies on mineral modeled ceramics consisting of compatible oxide, silicate, phosphate and aluminosilicate phase assemblages that would also be the radionuclide hosts. After establishing the framework for producing mineral-modeled ceramics (selection of compatible leach resistant phase assemblages, solution mixing of waste plus additives, consolidation by established ceramic processing¹⁰ during 1974, the Penn State/Battelle Northwest group developed specific formulations tailored for maximum waste loading and demonstrated these through the cold engineering scale.¹³⁻¹⁶ Fully radioactive demonstrations of several of these formulations (often called "supercalcine-ceramics") are scheduled at Battelle Northwest in the coming months.

At the Australian National University, a group headed by A.E. Ringwood introduced during 1978-1979 several quite different formulations of mineral-modeled ceramics (termed "synrocs" by their originator) that are characterized by substantially lower waste loadings.¹⁷⁻¹⁹ Table II compares the "mineralogies" of specific versions of these tailored ceramics designed for low-sodium commercial wastes.

This brings us to the pivotal year of 1978 when the Department of Energy initiated a major expansion of R and D on ceramic waste forms. It is hoped that this brief review will provide the reader with a historical perspective in which to interpret the many papers and reports now appearing on ceramic nuclear waste forms.

TABLE II

Radwaste Incorporation in Mineral-Modeled Ceramics

	Structure Type and Nominal Composition	Hazardous Radwaste Elements Incorporated ^a	
Current Supercalcine ceramics (SPC 2, 4-type)	MONAZITE LnPO_4	Ln^b , U, Th (TRU) ^c	
	APATITE $\text{Ca}_2\text{Ln}_8(\text{SiO}_4)_6\text{O}_2$	Ln, Sr, Cm, (Am)	
	FLUORITE $(\text{U}, \text{Ln}, \text{Zr})\text{O}_{2+x}$ $(\text{Zr}, \text{Ln}, \text{U})\text{O}_{2+x}$	Ln, U, Th, Cm, (TRU)	
	POLLUCITE $\text{CsAlSi}_2\text{O}_6$	Cs	
	SCHEELITE SrMoO_4	Sr	
	RUTILE RuO_2	Ru	
	Current Synrock (type B)	HOLLANDITE $\text{BaAl}_2\text{Ti}_6\text{O}_{16}$	Cs, Ru
		ZIRCONOLITE $\text{CaZrTi}_2\text{O}_7$	U, Ln, Sr, (TRU)
		PEROVSKITE CaTiO_3	Sr, U, (Ln, TRU)

^aElements in parentheses are inferred from crystal chemical principles.

^bLn = Rare earths La, Ce, Pr, Nd, Pm, Sm, Eu, Gd, Y.

^cTRU = Transuranic elements: Np, Pu, Am, Cm.

ACKNOWLEDGMENTS

We are pleased to acknowledge the support of our nuclear waste ceramics program by the National Science Foundation (1971-1973) and the Department of Energy and its predecessors through Battelle Northwest (1973-1979) and Rockwell Energy Systems Group (1979-).

DISCUSSION

UNIDENTIFIED QUESTIONER: I have a question which I am sure you have thought about. What happens in pollucite when the cesium decays to barium?

McCARTHY: I mention this in every talk; I just never got to it in this one. I do not know. I certainly expect a major structural change, and I think you would too. Half of the cesium that crystallizes in pollucite just by taking the waste alone is radioactive; the other half is nonradioactive. Therefore, half of the cesium is going to go to barium, ultimately. An experiment has been conducted; I do not know if the results are out yet, because the products were so highly radioactive.

REFERENCES

1. W.D. Kingery, H.K. Bowen and D.R. Uhlmann, Introduction to Ceramics, Wiley-Interscience (1976).
2. D.M. Roy, "Cement Based Nuclear Waste Solidification Forms", in High-Level Radioactive Solid Waste Forms, L.A. Casey, Ed., NUREG/CP-0005, pp. 481-509, December 1978.
3. L.P. Hatch, "Ultimate Disposal of Radioactive Wastes", *Am. Scientist* 410-421, July 1953.
4. E.J. Evans, "Process of Containing and Fixing Fission Products", U.S. Patent 3,000,072 (1961).
5. F.C. Arrance, "Method of Disposing of Radioactive Wastes and Resultant Product", U.S. Patent 3,093,539 (1962).
6. J.L. McElroy and J.E. Mendel, BNWL-1666 (1972).
7. R.E. Isaacson and L.E. Brownell, Ultimate Storage of Radioactive Wastes in Terrestrial Environments, Management of Radioactive Wastes from Fuel Reprocessing, OECD Proceedings, Paris, 953-986 (1972).
8. (a) G.J. McCarthy, Quartz-Matrix Isolation of Radioactive Wastes, *J. Mat. Sci.*, 8, 1358 (1973).
(b) G.J. McCarthy and M.T. Davidson, "Ceramic Nuclear Waste Forms: II, Ceramic-Waste Composite Prepared by Hot Pressing", *Am. Ceram. Soc. Bull.* 55, 190-194 (1976).

9. R.L. Schwoebel, Stabilization of High Level Waste in Ceramic Form, (Abstract) Am. Ceram. Soc. Bull., 54, 459 (1975).
10. (a) G.J. McCarthy and M.T. Davidson, Ceramic Nuclear Waste Forms: I. Crystal Chemistry and Phase Formation, Am. Ceram. Soc. Bull., 54, 728 (1975).
(b) R. Roy, Ceramic Science of Nuclear Waste Fixation (Abstract), Am. Ceram. Soc. Bull. 54, 459 (1975); and Rational Molecular Engineering of Ceramic Materials, J. Amer. Chem. Soc., 60, 350 (1977).
11. A.E. Ringwood, Safe Disposal of High Level Nuclear Reactor Wastes: A New Strategy, Australian National Univ. Press (1978).
12. S. Forberg, T. Westermark, H. Larker, and B. Widell, Synthetic Rutile Microencapsulation: A Radioactive Waste Solidification Systems Resulting in an Extremely Stable Product, Scientific Basis for Nuclear Waste Management, Ed. G.J. McCarthy, Plenum, NY, p. 201 (1979).
13. G.J. McCarthy, High Level Waste Ceramics: Materials Considerations, Process Simulation and Product Characterization, Nucl. Technol., 32: 92 (1977).
14. G.J. McCarthy, W.B. White, and D.E. Pfoertsch, Synthesis of Nuclear Waste Monazites, Ideal Actinide Hosts for Geologic Disposal, Mater. Res. Bull., 13: 1239 (1978).
15. J.M. Rusin, M.F. Browning, and G.J. McCarthy, Development of Multi-barrier Nuclear Waste Forms, Scientific Basis for Nuclear Waste Management, G.J. McCarthy (Ed.), pp. 169-180, Plenum Press, NY, 1979.
16. G.J. McCarthy, J.G. Pepin, D.E. Pfoertsch and D.E. Clarke, "Crystal Chemistry of the Synthetic Minerals in Current Supercalcine-Ceramics", in Ceramics in Nuclear Waste Management, T.D. Chikalla and J.E. Mendel (Eds.), DOE-CONF-790420, pp. 315-319 (1979).
17. A.E. Ringwood and S.E. Kesson, "Immobilization of High-Level Wastes in Synroc Titanate Ceramics", ibid., pp. 174-178.
18. A.E. Ringwood, et. al., "Immobilization of High-Level Nuclear Reactor Wastes in Synroc", Nature, 278, 219 (1979).
19. A.E. Ringwood, et. al., The SYNROC Process: A Geochemical Approach to Nuclear Waste Immobilization, Geochemical Journal, 13, 141-165 (1979).

HYDROTHERMAL INTERACTION OF A CERAMIC WASTE FORM WITH BASALT

B.E. Scheetz,* S. Komarneni, D.K. Smith** and C.A.F. Anderson**

The Pennsylvania State University, Materials Research Laboratory
University Park, PA 16802

ABSTRACT

The behavior of crystalline supercalcine-ceramic in the presence of basalt was investigated under mild hydrothermal conditions at 100, 200, and 300°C with a pressure of 300 bars. Both the solid phases and solution concentrations of the interaction products of basalt and supercalcine-ceramic were characterized.

At 100°C, no alteration products could be detected in experiments involving supercalcine-ceramic and basalt. The solution analyses for elements specific to the supercalcine-ceramic did not indicate any significant differences between the treatments with and without basalt, suggesting little or no interaction between basalt and supercalcine-ceramic at this temperature.

At 300°C, several solid alteration/interaction products were identified. These products included two phases, pollucite and scheelite, originally incorporated into the ceramic formulation but which reformed with different bulk chemical compositions. In addition, isolated crystals of unidentified K (\pm Ba) aluminosilicate phases were observed. Solution analyses of these runs did not indicate any significant differences between the treatments of supercalcine-ceramic with and without basalt, except that the Sr concentration decreased in the presence of basalt. Similar behavior was noted earlier, when basalt and SrZrO₃ experiments were conducted.

Alteration products and solution concentrations at 200°C lie intermediate between the 100° and 300°C results.

INTRODUCTION

Ceramic waste forms for the immobilization of high level commercial and defense wastes currently are underdeveloped at many research institutions. The chemistry of these second generation waste forms is

*Speaker. Forward all information to this author.

**Department of Geosciences, The Pennsylvania State University, University Park, PA 16802.

intrinsic to the philosophy developed by the individual research institutes. They include titanate-based system¹, mixed titanate phases², and mixed oxides³. The latter approach was the first to recognize mutual compatibility and thermodynamic stability of crystalline phases in a waste form as contrasted to the vitreous waste forms that had received extensive development over the last two decades.

The stability of the vitreous waste form was evaluated^{4,5} alone and in the presence of basalt⁶ at conditions of elevated temperature and pressure that would have been anticipated in a deep geological repository. These studies have demonstrated that the vitreous waste form readily alters.

The objective of this study is to determine the stability of supercalcine waste form in a basalt repository.

EXPERIMENTAL

Materials

Two formulations of the tailored crystalline ceramic were studied. These formulations are designated as SPC-2 and SPC-4. They differ principally in the relative amounts of rare earth elements (REE) in the formulations (Table 1). The effects of the different ratios of REE are

TABLE 1
Chemical Compositions of Tailored Crystalline Ceramics

element	SPC-2	SPC-4
Al	2.35	2.4
Ba	2.18	2.22
Ca	3.53	1.49
Ce	13.24	4.29
Cr	0.37	0.37
Cs	4.21	4.30
Fe	3.28	3.35
Gd	0.76	14.40
La	7.67	1.17
Mo	5.35	5.47
Na	0.14	0.15
Nd	5.17	11.50
Ni	0.17	0.18
P	1.82	1.86
Rb	0.50	0.52
Si	8.89	8.22
Sr	2.42	3.58
Zr	5.68	5.79

second order, that is the phase assemblages are not affected by the different REE ratios but only the relative sizes of the unit cells of the individual model phases in both assemblages (Table 2).

The basalt chosen for these studies represents a generic basalt, a United States Geological Survey (USGS) international standard, BCR-1⁷ (Table 3).

Hydrothermal Experiments

The solids chosen for these experiments were fragments that passed a 6-mesh sieve and were retained on a 10 mesh sieve. The mass of the individual charges ranged from 30 to 50 mg. In the mixed basalt/waste form experiments equal masses of rock and waste were used. The solids were weighed into a gold capsule and a ten to one ratio of deionized water to total solids was added. The gold capsules were welded to prevent transfer of matter into or out of the capsule. These capsules were then placed into cold seal vessels and pressurized to 300 bars or 30 MPa at 100°, 200°, and 300°C for up to four months of hydrothermal treatment.

After completion of the hydrothermal treatment, the pressure vessel was quenched and the capsules were removed and opened for analysis. The contents of the capsules were rinsed into volumetric flasks and diluted to 25 ml with deionized water. These solutions were then filtered to remove the solid phases for characterization. The solutions were analyzed by a combination of atomic emission and atomic absorption spectroscopy. Detection limits for this experimental design were typically 0.1 ppm. The solid phases were examined by scanning electron microscopy.

RESULTS AND DISCUSSION

The stability of the individual solid components of these experiments will be discussed in turn. The combination of rock/waste form will then be examined for the possible presence of synergistic effects.

Basalt

Basalt mineralogy is dominated by the presence of plagioclase feldspar, augitic pyroxene, minor amounts of olivine, ilvospinel-magnetite and an x-ray amorphous glassy phase. The glassy component of some of these Columbia River basalts flow over 40 vol/o⁹. The glassy component of the basaltic phase assemblage is the least stable under the test conditions and readily dissolved. The hydrothermal stability of basalt treated under identical conditions was reported⁸. Figure 1 is an SEM image of the surface of a disc of basalt that was altered under hydrothermal conditions. The lath like grains represent the resistant feldspar, the lighter gray grains with the rinds are pyroxene, the white equant grains are the ilvospinel-magnetite phase. Irregular intergranular voids represent the dissolved glassy groundmass material.

TABLE 2

Crystal Chemistry of Major Supercalcine-Ceramic Phases.^d

nominal composition	structure type	code	EDXS ^a chemistry	SPC-2 ^b	SPC-4 ^b
(Ca,Sr) ₂ RE ₈ (SiO ₄) ₆ O ₂	apatite (P6 ₃ /m)	A _{ss}	major: Si, Ca, RE (Gd, Nd > La > Ce > Pr > Y) minor: Sr, Zr, [Al] ^c	a _o = 9.558(4) ^e c _o = 7.032(16) v _o = 566.4 ^f	a _o = 9.497(4) c _o = 6.976(4) v _o = 544.9
REPO ₄	monazite (P2 ₁ /n)	M _{ss}	major: P, RE (Nd, Gd > La > Pr)	a = 6.820(8) b _o = 7.050(8) c _o = 6.499(8) β _o = 103.53(10) v = 303.8	a = 6.749(4) b _o = 6.971(4) c _o = 6.432(4) β _o = 103.96(10) v = 293.7
(U,Ce,Zr,RE)O _{2±x}	fluorite (Fm3m)	F _{ss}	major: U, Zr, RE (Gd > Ce > Y, Sm)	a _o = 5.342(3) v _o = 152.4	a _o = 5.190(3) v _o = 139.8
(Cs,Rb,Na)AlSi ₂ O ₆	pollucite (Ia3d)	P	major: Cs, Al, Si minor: [Ca], [Fe]	a = 13.640(4) v _o = 2537	a _o = 13.643(4) v _o = 2539
(Zr,Ce)O _{2±x}	tetragonal distorted fluorite	T _{ss}			
(Ca,Sr,Ba)MoO ₄	scheelite (I4 ₁ /a)	S _{ss}	major: Mo, Ca, Sr, [Ba]	a _o = 5.31(2) c _o = 11.83(3) v _o = 333	a _o = 5.378(4) c _o = 11.999(8) v _o = 347.1
(Fe,Cr) ₂ O ₃	corundum	(Fe ₂ O ₃) _{ss}	major: Fe minor: Cr		
(Ni,Fe)(Fe,Cr) ₂ O ₄	spinel	SP _{ss}	major: Fe minor: Ni, [Cr]		
RuO ₂	rutile	RuO ₂	major: Ru		

^aEnergy dispersive x-ray spectrometry.^bFinal report COO-2510-15, Advanced Waste Form.^c[] around an element indicates that it was not observed in the particular phase in every supercalcine-ceramic.^dAfter (3).^ea_o, b_o, c_o reported in Å.^fv reported in Å³.

TABLE 3
Bulk Chemical Composition
of USGS Basalt, BCR-1.

	USGS-BCR-1
major and minor constituents (%)	
SiO ₂	54.50
Al ₂ O ₃	13.61
Fe ₂ O ₃	3.68
FeO	8.80
MgO	3.46
CaO	6.92
Na ₂ O	3.27
K ₂ O ⁺	1.70
H ₂ O ⁻	0.77
H ₂ O	0.80
TiO ₂	2.20
P ₂ O ₅	0.36
MnO	0.18
CO ₂	0.03
SUM	100.28
Total Fe as Fe ₂ O ₃	13.16
selected trace elements	
Ba	675 ppm
Sr	330 ppm

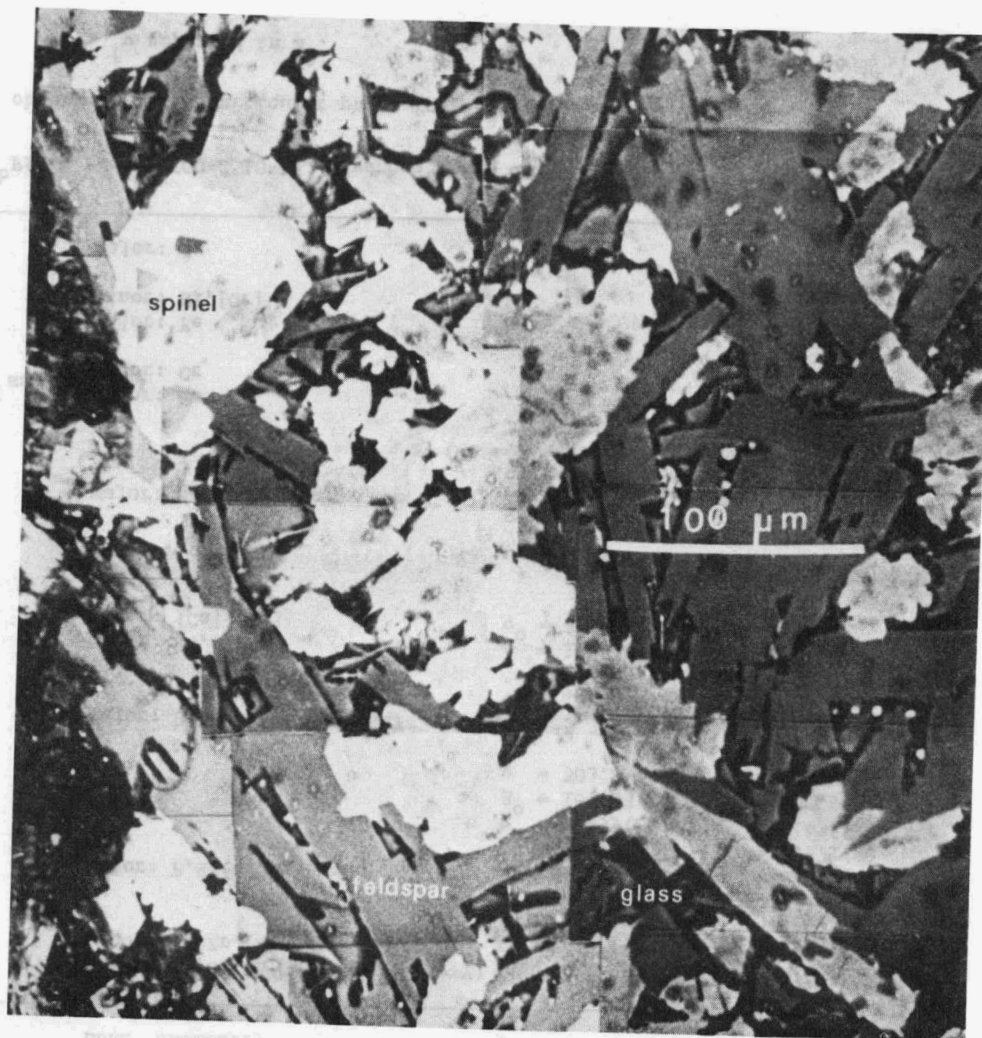


Fig. 1. SEM image of the etched surface of a hydrothermally altered Columbia River basalt.

after (7).

In the extended hydrothermal treatment experiments, the dominant alteration product of the basalt is an iron-rich smectite, nontronite (Figure 2). Very seldom were zeolitic phases observed. The results of the analysis of the hydrothermal solution will be presented in conjunction with the waste/rock experiments.

Tailored Crystalline Ceramics

The formulations for the tailored ceramic used in these studies contained approximately 70 wt/o waste loading. The chemical analyses of the solution in contact with the quenched samples for 100°, 200°, and 300°C experiments are presented in Table 4. Both the percentage of the available inventory detected in solution and the concentrations of the solution in µg/ml are presented for a series of one month experiments. A clear temperature dependence can be seen in these data; most notable is the total removal of sodium into solution along with 6% of Rb at 300°C. The release of Na and Rb into solution may be related to the recrystallization of pollucite excluding Na and Rb ions from its structure.

Characterization of the bulk chemistry of this material revealed only subtle enhancement in the diffraction pattern (peak sharpening) of pollucite and slight shifts in the peak location of the scheelite-structure phase. Detailed characterization with the aid of scanning electron microscope identified the occurrence of two classes of alteration.

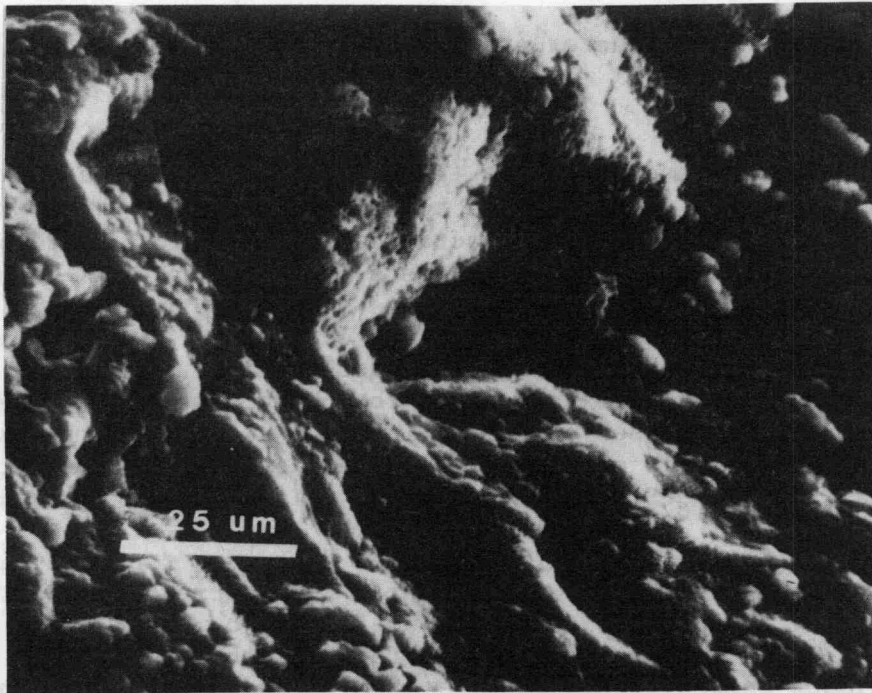


Fig. 2. SEM image of the extensive smectite formation on altering basalt.

TABLE 4

Average Concentration and Percentage of Element in Solution
(10:1 deionized water to SPC-4 supercalcine)

element	100°C*		200°C		300°C	
	µg/ml	%	µg/ml	%	µg/ml	%
Cs	12±1	0.3	7±1	0.2	22±5	0.5
Rb	<5	--	<5	--	35±5	6.2
Na	9±1	6.1	31±5	20.9	300±10	100
Sr	1.9±0.1	0.05	<0.2	--	2.4±0.1	0.07
Ba	<0.5	--	<0.5	--	5.9±1	0.26
Ca	4±1	0.27	--	--	8±1	0.5
Mo	15±1	0.3	61±5	1.1	520±10	9.5
Si	19±1	0.17	164±5	1.46	290±5	2.6
Al	2±1	0.08	4±1	0.17	9±1	0.38
Fe	<0.5	--	<0.5	--	<0.5	--
Cr	<0.5	--	3.9±0.1	1.4	0.4±0.1	0.12
Ni	1.5±0.1	0.4	17±1	5.0	0.3±0.1	0.19
Nd	3.4±0.1	0.03	<0.5	--	<0.5	--
La	<0.5	--	<0.5	--	<0.5	--
Zr	<0.5	--	<0.5	--	<0.5	--

*All experiments conducted at 30 MPa.
Duration 1 month.

Both pollucite and powellite (the mineral name for CaMoO_4 with the scheelite structure) were observed to have reformed as large euhedral crystals on the surface of the reacted ceramic. The presence of these phases on the exterior surfaces suggests that the crystals formed as a result of a transport of the appropriate ions from the ceramic into solution and then precipitated. In both cases, the precipitated crystals possess a bulk chemical composition that differs from the composition that was initially tailored into the phase assemblage. Semiquantitative chemical analyses of the pollucite phase that formed suggests that the Al:Si ratio is more nearly 1:3, analogous to the defect analcime¹⁰ $(\text{Na}_{0.67})(\text{Al}_{0.67}\text{Si}_{2.33})\text{O}_6$, than the initial Al:Si ratio of 1:2.

The powellite, $(\text{Ca},\text{Sr},\text{Ba})\text{MoO}_4$ phase, that were typically identified represent a Sr-substituted powellite or a Ba-substituted powellite, very rarely are Ca- or Ba-substituted Sr-powellites formed. Figure 3 represents a series of schematic phase diagrams for the powellite $(\text{Ca},\text{Sr},\text{Ba})\text{MoO}_4$ composition. At $T_1 = 1200^\circ\text{C}$, the diagram is dominated by a large single phase region with a two phase miscibility gap between the Ca and Ba components extending toward the Sr component. The open circle in this figure represents the bulk chemical composition of powellite in

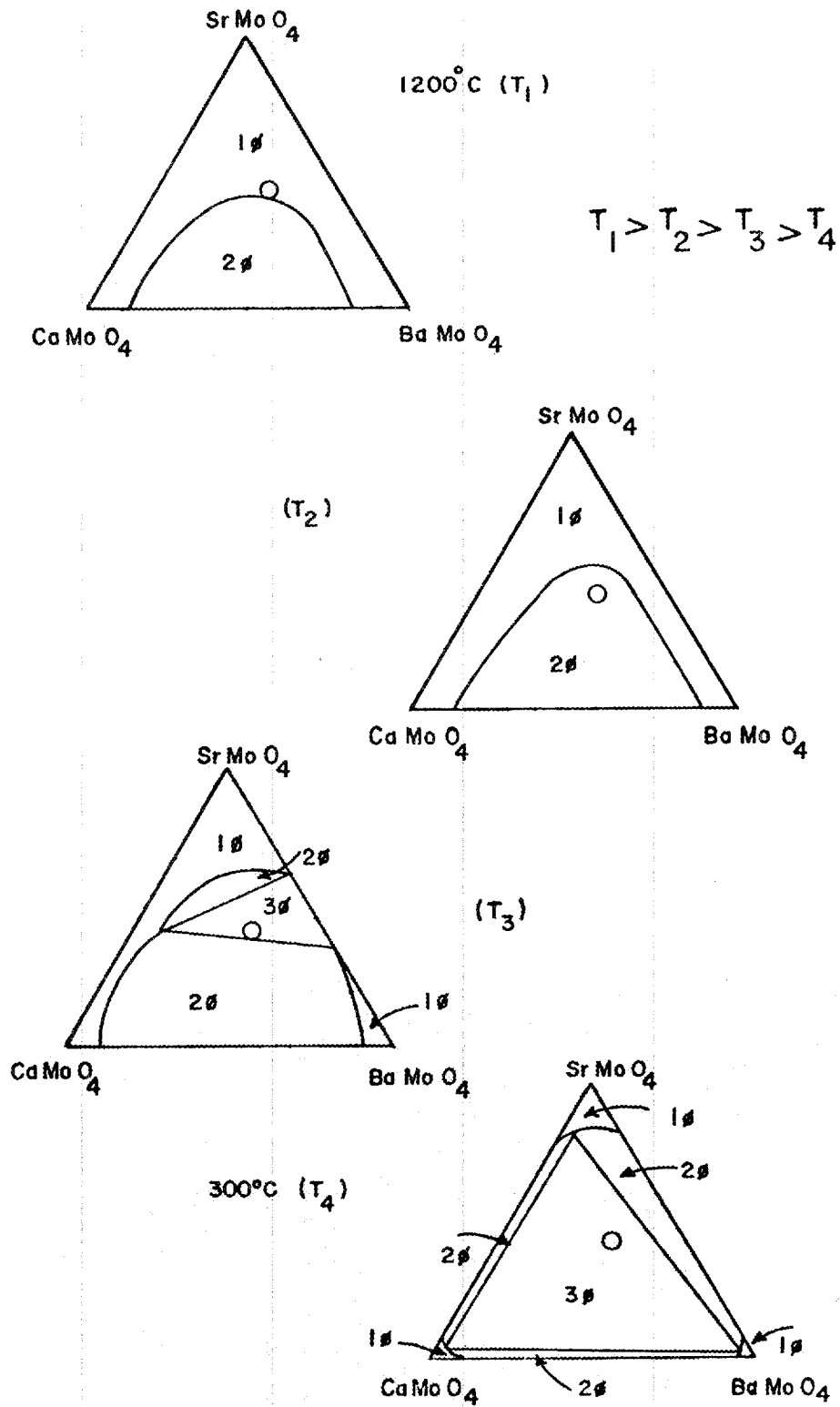


Fig. 3. Schematic phase relationship for scheelite-structure phase as a function of temperature.

the tailored ceramic. At successively lower temperatures the two phase region is enlarged and includes the bulk chemical composition of the powellite in the ceramic and ultimately it is intersected by a three phase region. At $T_4 = 300^\circ\text{C}$, the temperature of the hydrothermal treatment, an extensive three phase region exists with now only limited solid solution regions adjoining each apex.

In this model, the dissolution of the powellite phase is driven by the instability of the bulk phase assemblage at the reduced temperature of hydrothermal treatment. The data in Table 4 suggest that congruent dissolution of the powellites has not occurred.

It is noteworthy to mention at this point that the phases chosen as model phases in this waste form exhibit extreme compatibility as evidenced by the reformation of the same structural phases from solution but with different bulk chemical compositions.

The second class of alteration products from these experiments represented by the formation of "new" phases that were not tailored into the original phase assemblage. A hydrated calcium silicate, truscotite, and a Ba-aluminosilicate, wellsite, were identified (Figure 4). The preparation of the tailored ceramic waste form does not, in fact produce 100% crystalline phases. It has been reported that as much as 5

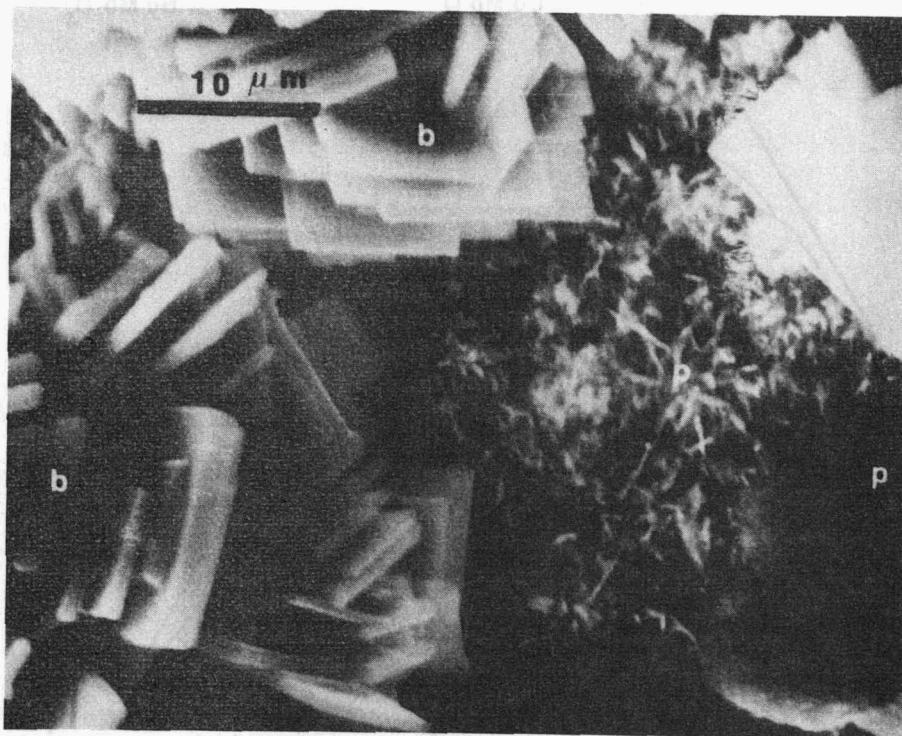


Fig. 4. SEM image of euhedral crystals of Ba-aluminosilicate phase formed as the hydrothermal alteration product of SPC-2. (B = Ba-aluminosilicate, wellsite; P = pollucite.)

wt/o of the waste form is composed of an amorphous aluminosilicate phase that contains varying amounts of alkaline earth elements¹¹. It is entirely possible that the formation of truscottite vs. wellsite is controlled by this variable composition.

Tailored Ceramic/Basalt

Tables 5 and 6 present the results of the analyses of two representative data sets at 100° and 300°C respectively. From these data no synergistic effects that would suggest enhanced dissolution of either the basalt or the waste form are observed. The percentage of sodium in solution in the presence of basalt appears to be suppressed. This low concentration, however, is a result of the mode of calculation which for the waste/rock reaction included the combined totals of available sodium in both materials.

Characterization of the solid experimental charges in the waste/rock runs typically reveals only those phases that were previously discussed when basalt or the waste form alone was treated in deionized water. One euhedral crystalline phase was recognized on the altered basalt that contained a bulk qualitative chemistry similar to K, Ba-aluminosilicate, perhaps representing minor barium substitution into the orthoclase component of the altering plagioclase feldspars.

TABLE 5

Concentration and Percentage of Elements in Solution at 100°C^a.
1:10 solid to deionized water

element	BCR-1		SPC-2		BCR-1 + SPC-2	
	BD 271		CD 274		BCD 268	
	µg/ml	%	µg/ml	%	µg/ml	%
Cs	---	--	10±1	0.2	<0.5	--
Rb	---	--	4±1	0.7	2±1	0.8
Na	6±1	0.3	<0.5	--	11±1	0.9
Sr	1±1	2.1	6±1	0.3	4±1	0.3
Ba	<0.5	--	<0.5	--	<0.5	--
Ca	40±5	0.8	65±5	1.8	70±5	1.7
Mo	---	--	14±1	0.3	11±1	0.4
Si	210±5	0.8	45±5	0.5	110±5	0.6

^aP = 300 bars; t = 4 months.

^bAl, Fe, Cr, Ni, Nd, La, Ce, Gd, Zr, and P were not detected in solution.

TABLE 6

Concentration and Percentage of Elements in Solution at 300°C^a.

element ^b	BCR-1		SPC-2		BCR-1 + SPC-2	
	BD 260		CD 263		BCD 257	
	µg/ml	%	µg/ml	%	µg/ml	%
Cs	--	--	14±1	0.3	9±1	0.4
Rb	--	--	4±1	0.9	<0.5	--
Na	70±5	2.8	120±5	85	95±5	7.5
Sr	<0.2	--	11±1	0.5	1±2	0.1
Ba	<0.5	--	<0.5	--	<0.5	--
Ca	25±5	0.5	25±5	0.8	25±5	0.5
Mo	<0.5	--	20±1	0.4	13±1	0.5
Si	310±10	1.2	370±10	4.1	430±10	2.5

^aP = 300 bars; t = 4 months; solid to deionized water ratio = 1:10.

^bAl, Fe, Cr, Ni, Nd, La, Ce, Gd, Zr, and P were not detected in solutions.

CONCLUSION

The hydrothermal stability of the tailored ceramic waste forms SPC-2 and SPC-4 have been demonstrated for the extremes of dispersed temperature and pressure. Table 7 represents a summary of the stability of the individual components of the tailored ceramic. Apatite, monazite, fluorite, corundum and spinel structure types do not appear to undergo alteration under the experimental condition of this study. Pollucite and scheelite structure types on the other hand have been identified to exhibit a dissolution/transport/reprecipitation behavior. The appearance of "new" alteration phases has been correlated to the existence of appreciable amounts of noncrystalline solids that have been formed during the fabrication of the tailored ceramic.

Finally, the alteration of the ceramic waste form appears for the most part to occur independently of the presence of basalt. Because none of the alteration products observed for the ceramic involved a redox couple, it is not surprising that the basalt plays an inert role in these experiments.

ACKNOWLEDGEMENT

This research was sponsored by a contract from the Department of Energy to Rockwell Hanford Operations DE-AC06-77RL-010301 and through subcontract SA-918 and SA-923.

TABLE 7

Stability of Supercalcine-Ceramic under
Hydrothermal* Conditions.

Structure type	Results
Apatite - A _{ss}	No apparent reaction.
Monazite - M _{ss}	No apparent reaction.
Fluorite - F _{ss}	No apparent reaction.
Pollucite - P	Dissociation releases Na to solution and reforms as defect pollucite $(\text{Cs})_{0.67}(\text{Al}_{0.67}\text{Si}_{2.33})\text{O}_6$
Scheelite - S _{ss}	Dissociation releases Ca and/or Ba to solution and reforms as two individual scheelite phases (Sr substituted Ca and Cr substituted Ba molybdates)
Corundum	No apparent reaction.
Spinel - SP _{ss}	No apparent reaction.

*Temperature 300°C; pressure 30 MPa; experimental duration four months.

DISCUSSION

POHL: I may have missed it when you said which basalt you were using in these experiments. I think you started out describing two different basalts; could you repeat what these basalts are, and did I hear correctly that one of them has a 40% amorphous content? In your leaching experiments, which ones did you use and was there any effect of this much larger glass concentration?

SCHEETZ: What I showed you was the BCR-1, which, of course, is the USGS standard. We have used, in parallel experiments, an additional basalt, DDH-3, from a drill hole on the Hanford reservation. The work that I reported here in the body of the talk was done with the BCR-1, which has a lower glass content; I am not sure exactly what the figure is on that. The DDH-3 (the Hanford basalt) can contain up to 40% glass. I cannot recall offhand the numbers for the differences in the two. There are slight, but not remarkable, differences.

UNIDENTIFIED QUESTIONER: I know you are interested in flow-through systems for leaching. Have you done any work or do anticipate doing any work in which you leach and take things out and precipitate them downstream where you have made nonsaturated or more dilute solutions?

SCHEETZ: Yes. We have done three experiments to date. One of them has been with that other waste form, the amorphous one. We have completed the data on supercalcine ceramic, a variation of the SPC-2 that contains uranium (you notice uranium on my solution analyses was conspicuously absent). Also, we have completed one run (that was terminated prematurely) with a flow-through apparatus, in which we brought deionized water into a basalt environment at temperature, flowed the water over the basalt environment onto glass (PNL 7668), and flowed it down to a column of the salt in a thermal gradient, and then of course, collected the water. So these things are in progress.

UNIDENTIFIED QUESTIONER: And are you analyzing your solution? .

SCHEETZ: We are analyzing the solutions taken at various time segments. I cannot quote the data exactly, but, for instance, the boron in the glass is only about 5% higher in the flow-through than it is in the static closed system.

REFERENCES

1. Johnstone, J.K., T.J. Headley, P.F. Hlava, and D.V. Stohl, "Characterization of a Titanate Based Ceramic for High Level Nuclear Waste Solidification," Scientific Basis for Nuclear Waste Management, Vol. 1. Ed. G.J. McCarthy. Plenum Press, NY (1979).
2. Ringwood, A.E., S.E. Kesson, N.G. Ware, W. Hibberson, and A. Major, "Immobilization of High Level Nuclear Reactor Wastes in SYNROC," Nature 278, 219 (1979).
3. McCarthy, G.J., "Advanced Waste Forms Research and Development: Final Report for the Period October 1, 1978 to September 30, 1979," COO-2190-15, Battelle Pacific Northwest Laboratories, Richland, WA (August 1979).
4. McCarthy, G.J., W.B. White, R. Roy, B.E. Scheetz, S. Komarneni, D.K. Smith, and D.M. Roy, "Interactions Between Nuclear Wastes and Surrounding Rocks," Nature 273, 216 (1978).
5. McCarthy, G.J., B.E. Scheetz, S. Komarneni, D.K. Smith, and W.B. White, "Hydrothermal Stability of Simulated Radioactive Waste Glass," Solid State Chemistry: A Contemporary Overview. Advances in Chemistry Series, American Chemical Society, Washington, DC (in press).
6. Scheetz, B.E., S. Komarneni, D.K. Smith, C.A.F. Anderson, S.D. Atkinson, and G.J. McCarthy, "Hydrothermal Interaction of Simulated

Nuclear Waste Glass in the Presence of Basalts," Scientific Basis for Nuclear Waste Management, Vol. 2. Ed. C.J. Northrup, Jr. Plenum Press, NY (in press).

7. Flanagan, F.J., "1972 Values for International Geochemical Reference Samples," *Geochim. Cosmochim. Acta* 37 (1973).
8. Barnes, M., and B.E. Scheetz, "Laboratory Alteration of a Columbia River Basalt by Hot Groundwater: New Applications to Deep Geological Disposal of Nuclear Waste," Geological Society of America, San Diego, CA (November 5-8, 1979).
9. McCarthy, G.J., and B.E. Scheetz, "High-Level Waste-Basalt Interactions. Annual Progress Report for the Period February 1, 1977 to September 30, 1977," RHO-BWI-C-2, Rockwell Hanford Operations, Richland, WA (May 1978).
10. Clark, D., S. Ueda, and M. Koizumi, "Crystallization of Analcime Solid Solutions from Aqueous Solutions," *Am. Min.* 64, 1 and 2 (1979).
11. McCarthy, G.J., J.G. Pepin, D.E. Pfoertsch, and D.R. Clarke, "Crystal Chemistry of the Synthetic Minerals in Current Supercalcine-Ceramics," *Ceramics in Nuclear Waste Management*. Ed. T.D. Chikalla and J.E. Mendel. American Ceramic Society Annual Meeting (April 30-May 2, 1979).

PROBABLE LEACHING MECHANISMS FOR SPENT FUEL

R. Wang and Y. B. Katayama

Pacific Northwest Laboratory*
Richland, Washington 99352

ABSTRACT

Current U.S. nuclear policies have suspended the reprocessing of spent fuel, and the Interagency Review Group has suggested consideration of spent fuel as a waste form suitable for placement in a repository. At the Pacific Northwest Laboratory, researchers in the Waste/Rock Interaction Technology Program are studying spent fuel as a possible waste form for the Office of Nuclear Waste Isolation. This paper presents probable leaching mechanisms for spent fuel and discusses current progress in identifying and understanding the leaching process.

Long-term leach tests have been producing safety assessment leach data for the last five years. During the past year, experiments were begun to study the complex leaching mechanism of spent fuel. The initial work in this investigation was done with UO_2 , which provided the most information possible on the behavior of the spent-fuel matrix without encountering the very high radiation levels associated with spent fuel. Both single-crystal and polycrystalline UO_2 samples were used for this study, and techniques applicable to remote experimentation in a hot cell are being developed. The effects of radiation are being studied in terms of radiolysis of water and surface activation of the UO_2 . Dissolution behavior and kinetics of UO_2 were also investigated by electrochemical measurement techniques.² These data will be correlated with those acquired when spent fuel is tested in a hot cell.

Oxidation effects represent a major area of concern in evaluating the stability of spent fuel. Dissolution of UO_2 is greatly increased in an oxidizing solution because the dissolution is then controlled by the formation of hexavalent uranium. In solutions containing very low oxygen levels (i.e., reducing solutions), oxidation-induced dissolution may be possible via a previously oxidized surface, through exposure to air during storage, or by local oxidants such as O_2 and H_2O_2 produced from radiolysis of water and radiation-activated UO_2 surfaces. The

*Operated by Battelle Memorial Institute for the U.S. Department of Energy.

effects of oxidation not only increase the dissolution rate, but could lead to the disintegration of spent fuel into fine fragments.

Research is in progress to identify and understand these probable leaching mechanisms for spent fuel. At this point it appears that the oxidation process caused by radiation may be a problem if spent fuel becomes an alternative waste form.

Spent fuel itself has been considered as a waste form in the United States, Canada, and in Sweden. In Pacific Northwest Laboratory's Waste/Rock Interaction Technology Program we have been studying the leaching behavior of spent-fuel wastes for the last five years. The purpose of this study is to acquire an understanding of the leaching behavior so that we can eventually develop models that will enable us to predict leaching behavior for long-term storage of spent fuel in repository environments. However, when we do different types of experiments it turns out that the leaching behavior also differs. After comparing notes with other laboratories doing similar studies, we feel it is essential to study spent-fuel leaching mechanisms, because they sometimes vary considerably--depending on the type of experiment and the condition under which it is done. What we present here is our tentative progress in understanding the leaching mechanisms for spent fuel through the study of UO_2 , the matrix material. Eventually, we want to extend the scope of this work and apply what we have learned to spent-fuel studies.

When we look at spent fuel as a waste form, we find that we are restricted to the spent fuel itself as it comes out of the reactor, and we must deal with the microstructure resulting from the thermal history of that spent fuel. Structural and microstructural features that affect leaching are shown in Fig. 1, which also lists several ways in which we study leaching, oxidation, and radiation effects. We need to know what happens if the leaching starts at the surface of grains and subgrains of UO_2 ; what the roles of the grain boundary, microcracks, and pores are in the spent fuel when it interacts with a leaching solution; what the effects of surface segregation and solid solutions are; and finally, what the effects of radiation are on the various factors of leaching behavior. In order to study all of these, we have undertaken the examination of different aspects of spent-fuel leaching mechanisms by using UO_2 . We are studying oxidation and dissolution behavior of single-crystal UO_2 surfaces. We study polycrystalline UO_2 pellets in order to determine the effects of grain boundaries, microcracks and pores. Also, we plan to dope polycrystalline UO_2 pellets to study surface segregation and solid-solution effects, and, most importantly, we would like to study the radiation effects on single-crystal as well as polycrystalline UO_2 in order to see which radiation effects would be worth considering. In tandem with these studies, we are going to characterize the surface and the leaching behavior of the spent fuel.

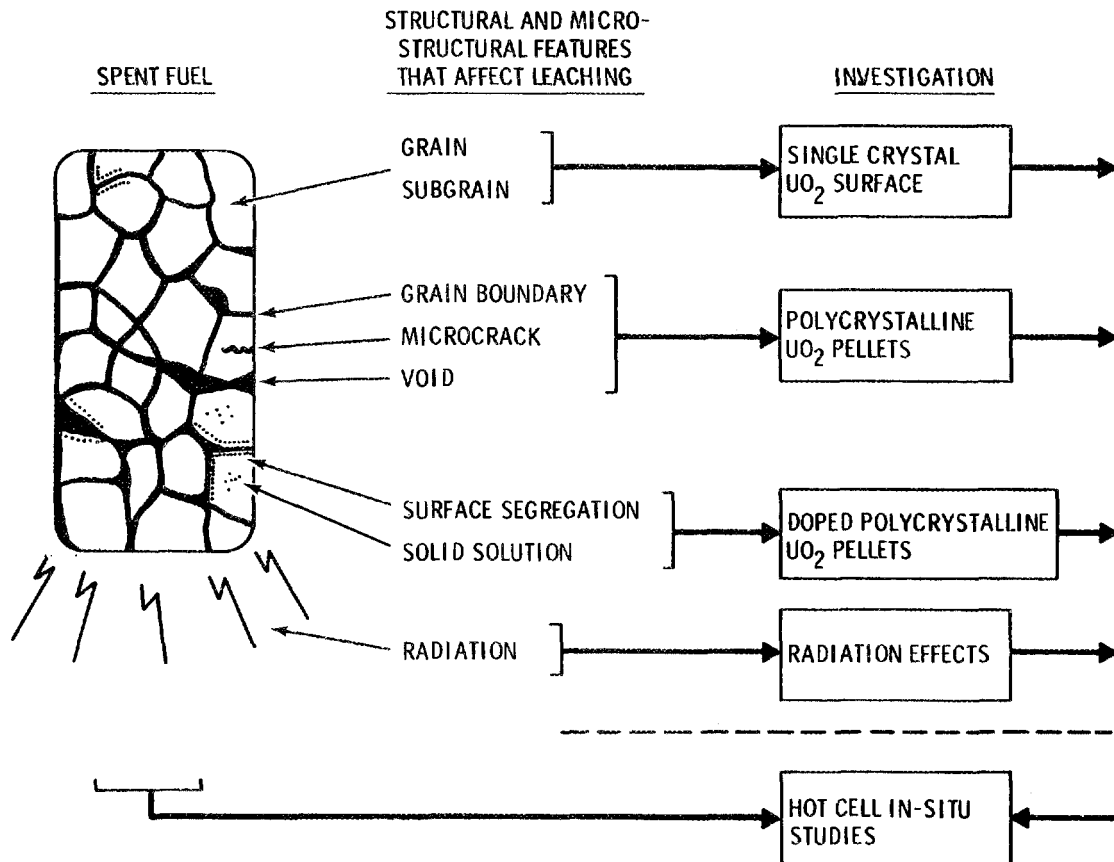


Fig. 1. PNL spent fuel oxidation and leaching studies.

The single-crystal surface studies summarized below have shown that oxidation of UO₂ is the main cause of increased leaching:

- Oxidation and dissolution
 - air oxidation
 - solution oxidation and dissolution
 - electrochemical oxidation and dissolution
- Experiments
 - air oxidation--Lang topography, Auger and SEM
 - solution oxidation--autoclave experiments and H₂O₂
 - electrochemical oxidation--H₂O, NaHCO₃, NaCl, and H₂O₂

We have consequently begun studying oxidation and dissolution--air oxidation (which may happen during the storage of spent fuel) and solution oxidation-dissolution (in which the solution contains an oxidizing agent). At the same time we are studying electrochemical dissolution, which will enable us to continuously monitor the oxidation and leaching mechanisms and the rate during the leaching steps. In our experiments involving air oxidation, we study the surface behavior of UO₂, as well

as its lattice behavior. In solution-oxidation work, we use autoclave experiments, and, for extreme oxidizing conditions, we examine the effects of incremental additions of hydrogen peroxide. At the same time, we study electrochemical oxidation using several leachants and H_2O_2 .

Figure 2 summarizes autoclave studies at both 75 and 150°C with 220-ppm pressurized oxygen in solutions. For three types of solution--deionized water, sodium bicarbonate, and WIPP B brine--we see relatively high leaching rates. The sodium carbonate has a very steady, relatively high leaching rate, while both water and brine show bigger changes in leach rate with time and are about 1 to 3 orders of magnitude lower.

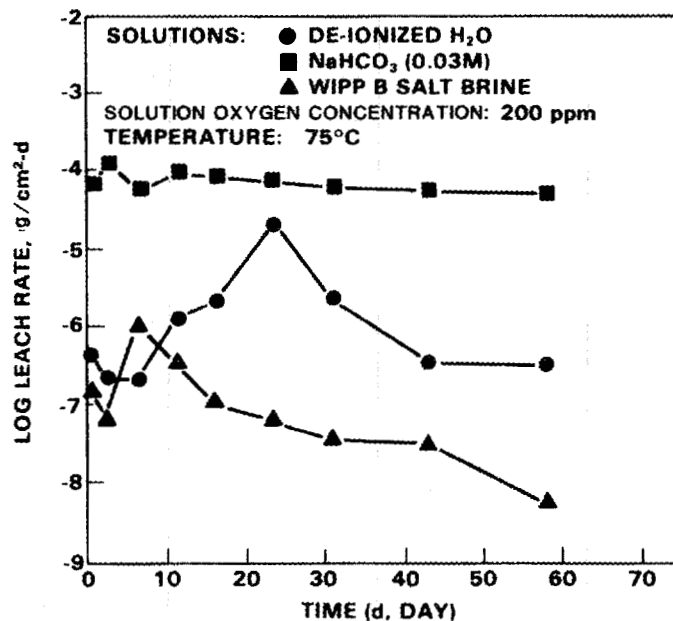


Fig. 2. Incremental leach rate vs time for single crystal UO_2 .

Typical behavior of the UO_2 single-crystal surface under potentiodynamic polarization, which is electrochemical dissolution, is shown in Fig. 3. Here we plot the potential versus the current. With this method, we can very quickly get accurate data from the initial stage of dissolution and can compare sodium bicarbonate, brine, and deionized water results.

In the radiation effects studies outlined below we are examining the radiolysis of water and radiation-induced surface activation of the UO_2 .

- Effects
 - radiolysis of water
 - surface activation

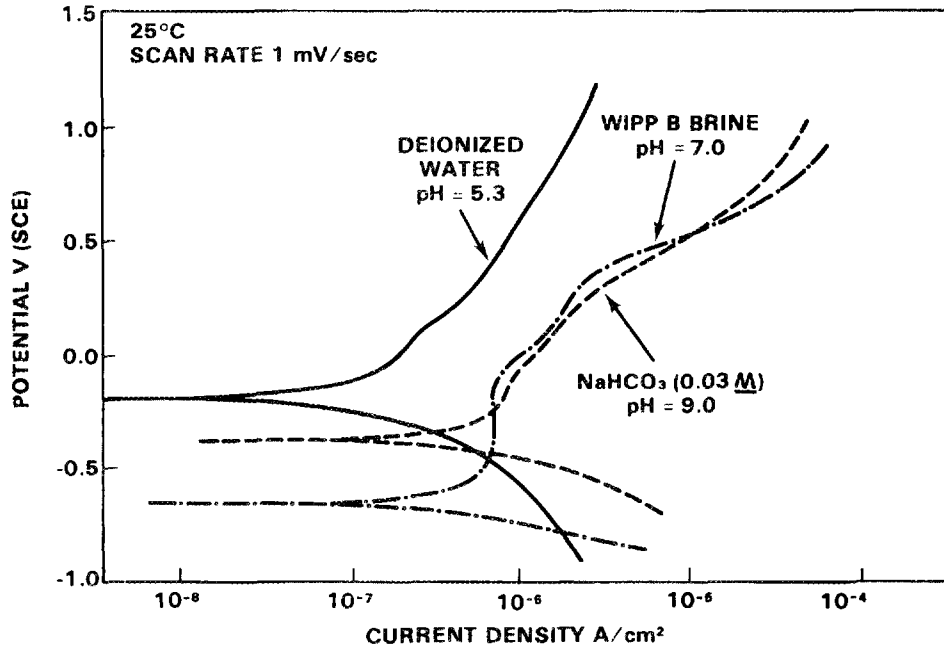


Fig. 3. Potentiodynamic polarization of single crystal UO_2 surface.

- Experiments

- gamma-ray-induced static dissolution
- gamma-ray-induced electrochemical dissolution
- photo-induced dissolution (ultraviolet radiation)

These experiments will enable us to understand which radiation effects are applicable.

An example of the influence of radiation effects on leaching is shown in Fig. 4. In IAEA uranium leaching tests after 467 days (this is a spent fuel), we find that the deionized water has a much greater dissolution rate than either sodium bicarbonate or sodium chloride, and we know that for the other studies, deionized water has a lower leach rate--probably between those for brine and sodium chloride. We monitored pH (Table 1) and it turns out that the pH of the deionized water, which was 6.55 at the beginning of the test, dropped to 4.33 after 400 days. The rest of the leaching solutions have smaller pH changes, but deionized water has the largest change. The radiation oxidized the nitrogen in the air and formed nitric acid in our solution, thus reducing the pH of the deionized water. Based on the solubility of $UO_3 \cdot 2H_2O$, shown in Fig. 5, the concentration of uranium in solution increases as the pH drops. Similarly, we have also seen the pH drop in water without uranium in solution as a result of radiation.

Another kind of radiation effect is caused by radiolysis of water. We have seen these effects in computer calculations by Burns and Moore,¹ based on the kinetics of different reactions and activation energies.

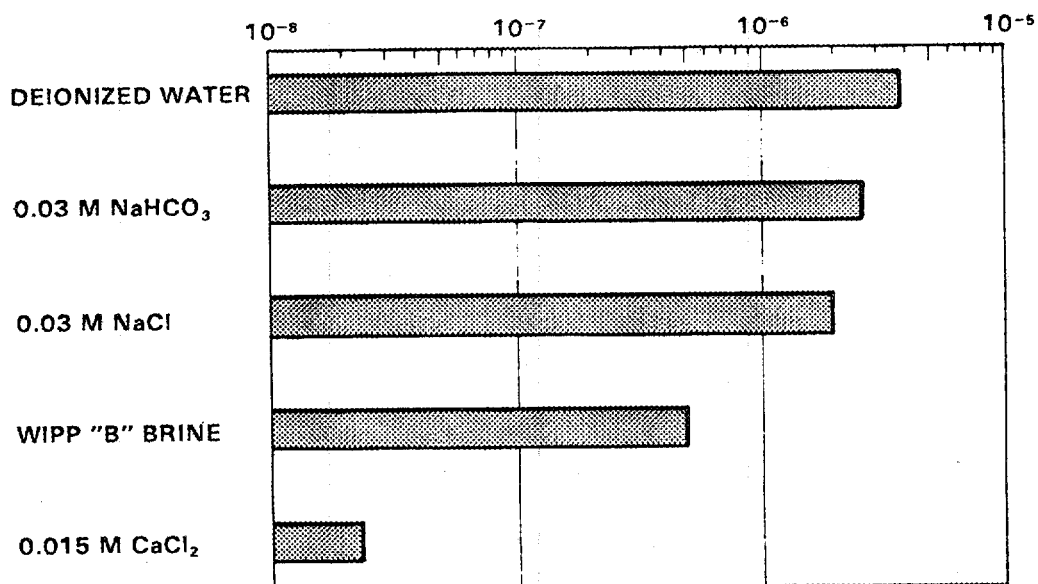


Fig. 4. IAEA uranium leach rates for spent fuel after 467 days at 25°C.

Table 1. Changes in pH During IAEA Leach Tests

Solution Type	Beginning pH	Final pH	pH Change During Test
NaHCO ₃ (0.03 M)	8.45	8.84	+0.39
WIPP B	6.53	5.60	-0.93
CaCl ₂ (0.015 M)	6.25	5.19	-1.06
NaCl (0.03 M)	6.43	4.91	-1.52
Deionized Water	6.55	4.33	-2.22

In Fig. 6 the concentrations of various species produced by radiolysis of water are plotted as a function of time. Hydrogen, oxygen and hydrogen peroxide were formed within 1 s and reached steady-state concentrations after 1 to 10 s. The important thing here is that approximately equal amounts of hydrogen peroxide and oxygen have been formed, which is equivalent to about 0.3 ppm.

We also wanted to determine the effects of hydrogen peroxide. We know that UO₂ is very vulnerable to oxidation, so we have undertaken an oxidation study based on hydrogen peroxide. Figure 7a shows, for reference, what happens in deionized water without hydrogen peroxide; we applied a voltage of 0.5 V, for 64 h and the UO₂ surface was etched. But as Fig. 7b shows, when we have 500-ppm hydrogen peroxide added to

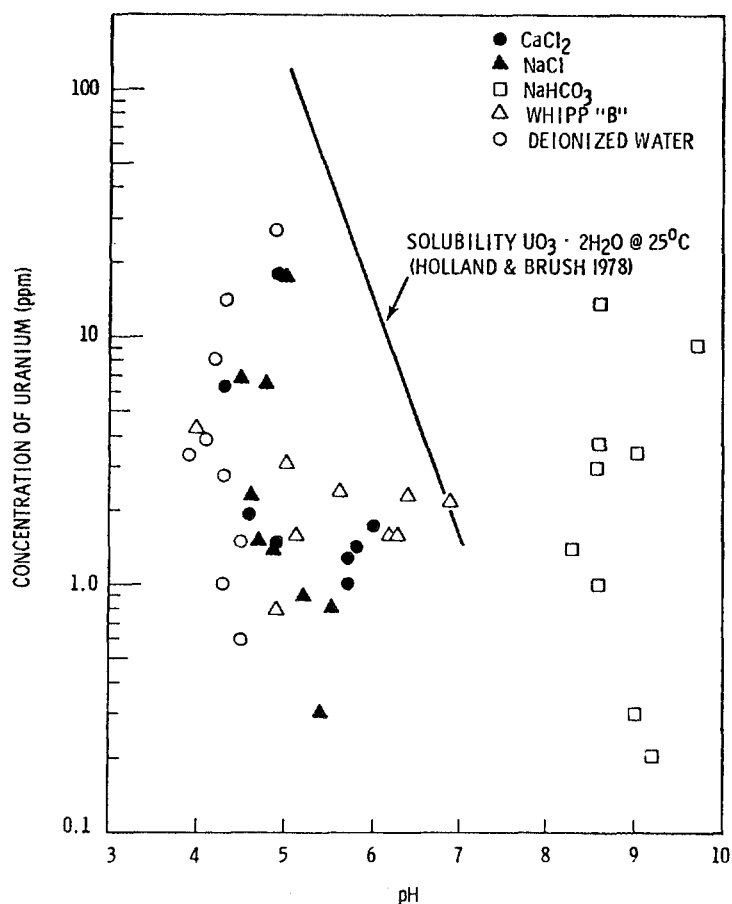


Fig. 5. Uranium concentration in water as function of pH.

the solution we see a 5- μ m-thick film which is UO_3 -hydrate. The film apparently cracks when the samples are removed from the solution for SEM analysis. The UO_3 -hydrate film may affect the leaching of UO_2 in this case.

The electronic properties of uranium oxides are also relevant to radiation effects. Uranium oxides are semiconductors and different uranium oxides have different ranges of resistivity (Fig. 8, Table 2). The conduction type can be n-type or p-type and the activation energy for extrinsic conduction is very low. In the case of n-type uranium oxides, probable surface reactions induced by radiation are shown in Fig. 9. The radiation will cause an electron to move from the valence band to the conduction band and leave a hole in the valence band. The hole may take part in three types of reaction. First, the hole will probably cause direct oxidation; U^{4+} will be oxidized into U^{6+} , which has a higher solubility. Second, the hole may cause anodic dissolution; UO_2 may act as an anode, react with holes and aqueous solution, and move directly into the solution. Third, oxidation of water is possible, which will produce hydrogen peroxide at the surface. The importance of

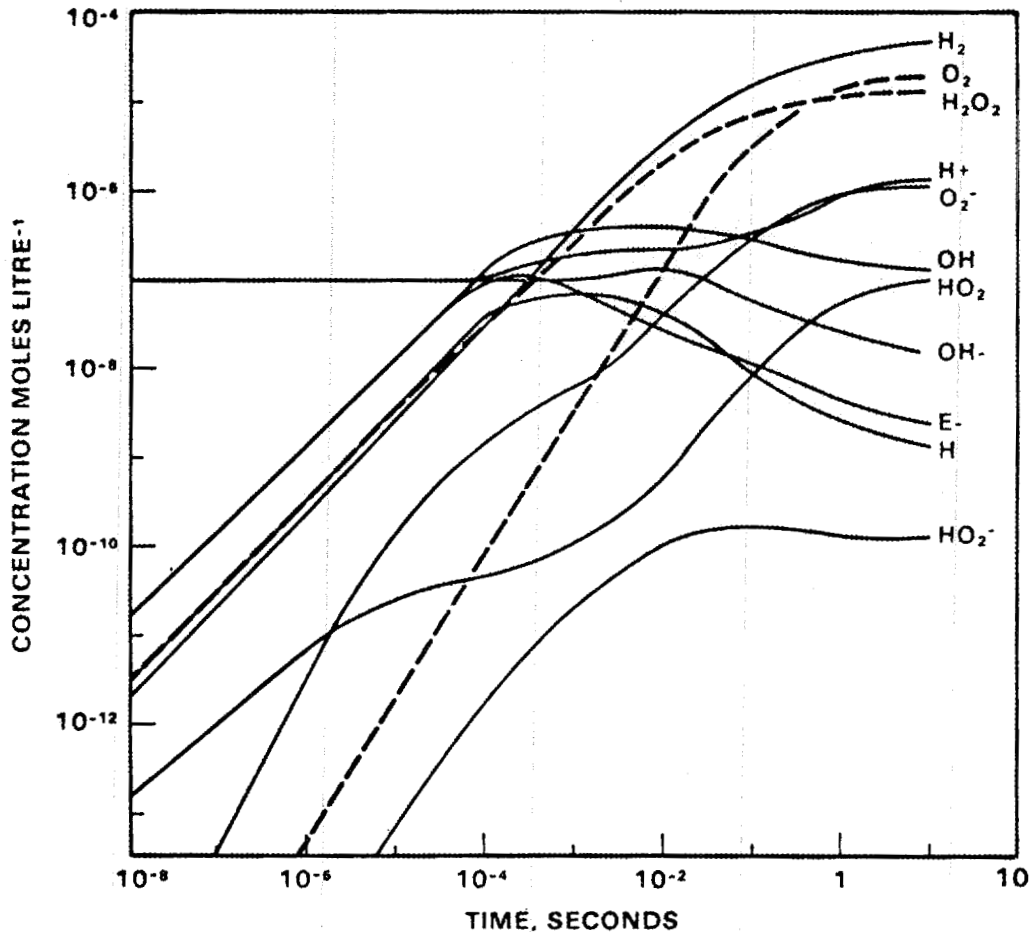


Fig. 6. $\beta\gamma$ Radiolysis (5 W g^{-1}) of water at 25°C^1 .

these radiation-induced surface reactions and the radiolysis of water is that while we may think we have a reducing environment for UO_2 , the radiation near the surface will actually put the surface into an oxidized state, which will make data interpretation difficult.

It is useful to apply the data gained through our UO_2 -based surface studies to work in hot cells, where we can drive *in situ*, spent-fuel measurements as summarized below:

- Spent fuel
 - high-burnup
 - low-burnup
 - oxidized fuels
- Techniques
 - electrochemical measurements-leaching kinetics
 - acoustic emission measurements--microstructure variations
 - spectroelectrochemical measurements--surface film structure and chemistry
 - polarography--solution chemistry

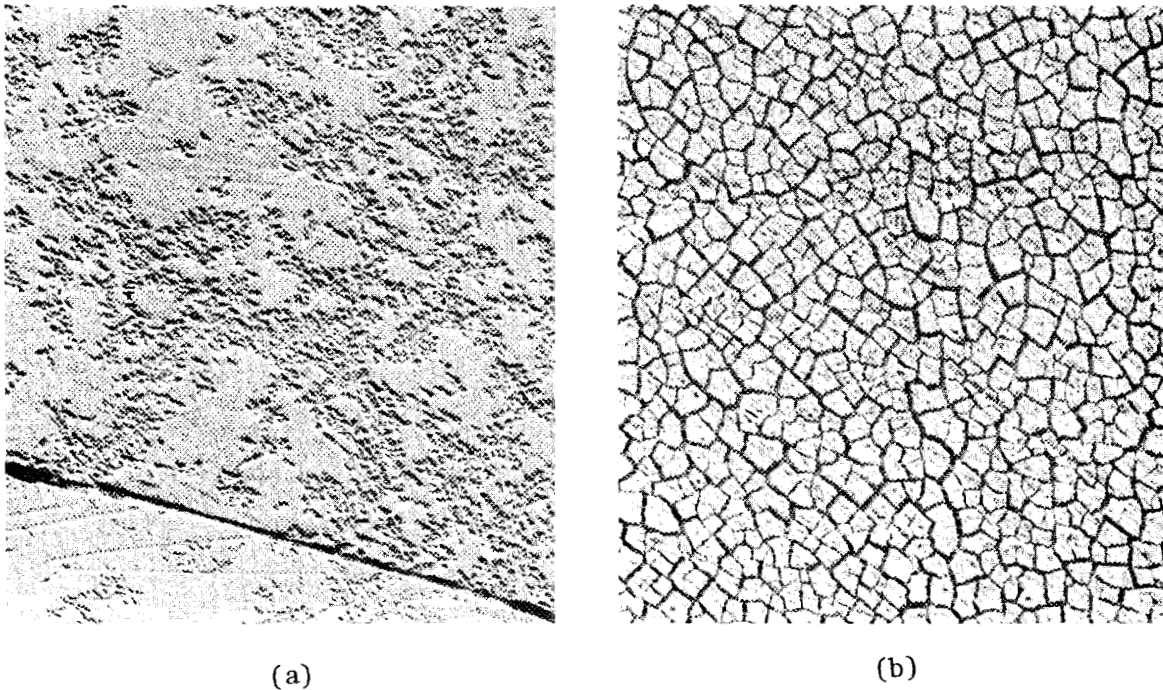


Fig. 7. A single crystal UO_2 surface after electrochemical oxidation dissolution in deionized water for 64 hr (a) and in deionized water of 500 ppm H_2O_2 for 26 hr (b). Voltage: 0.5 V (SCE). SEM micrographs 400X.

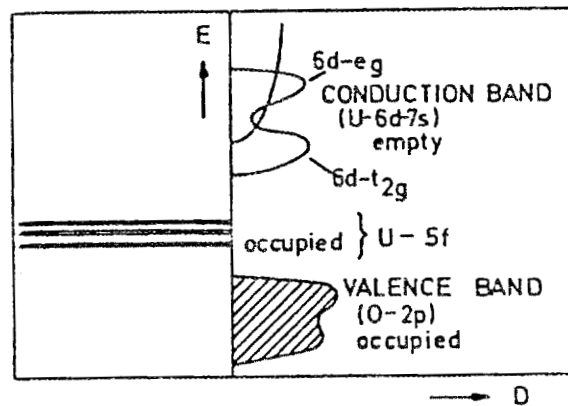
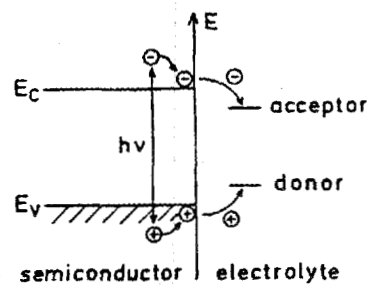


Fig. 8. Suggested band model for UO_2 .²

As indicated before, there are different types of spent fuel, depending on the microstructure and thermal history. We are now engaged in electrochemical measurements of leaching kinetics in the hot cell. We will monitor acoustic emission measurements for microstructural variations, such as formation of cracks and opening of voids. The surface of the material can be spectroelectrochemically measured for chemical composition as well as for structure. The concentration of the radionuclides

Table 2. Electronic Properties of Uranium Oxides²

Oxide	Resistivity ohm-cm	Conduction Type	Activation Energy for Extrinsic Cond., eV
UO _{2-x}	10 ⁴ - 10 ⁷	n	1.2
UO ₂	10 ³ - 10 ⁶	p	0.2
UO _{2+x}	10 ³ - 10 ⁷	p	0.1 - 0.4
U ₄ O ₉	10 ² - 10 ⁷	n	0.2 - 0.9
U ₃ O ₈	10 ³ - 10 ⁴	n	0.2 - 0.5
PuO _{2-x}	10 ² - 10 ¹¹	p	0.2 - 1.8



1. Direct Oxidation
 $U^{4+} + 2p^+ \rightarrow U^{6+}$
2. Anodic Dissolution
 $UO_2 + 6p^+ + Aq. \rightarrow U^{6+} Aq. + O_2$
3. Oxidation of Water
 $2(OH)^- + 2p^+ \rightarrow H_2O_2$

Radiation-Induced Redox Reactions at A
Semiconductor-Electrolyte Interface.

Fig. 9. Probable surface reactions induced by radiation.

in the solution can be measured by polarography. With these techniques, all of the measurements on spent fuel can be monitored continuously from outside the hot cells.

In conclusion, our studies have thus far depended upon the use of accelerating conditions in an effort to search for possible mechanisms of spent-fuel leaching. Of course, these studies are based on UO₂; for spent fuel the situation may be much more complicated. But, if we do not identify the leaching mechanisms for UO₂ it will be very difficult to search for the spent-fuel mechanisms. Our determination of probable leaching mechanisms is as follows:

- Increased dissolution of UO₂ resulting from oxidation to the U⁶⁺ state.

- Oxidation of UO_2 and precipitation of uranyl hydrate films by H_2O_2 (about 100 times more effective than dissolved O_2).
- Radiation-induced formation of H_2O_2 and O_2 by radiolysis of water and radiation-induced surface activation of UO_2 .
- Rapid oxidation of UO_2 single crystals and pellets (produces microcracks and causes disintegration).

As this list shows, we have found that increased dissolution of UO_2 results from its oxidation to the U^{6+} state. If we can maintain the U^{4+} state, the dissolution will be much lower. Oxidation of UO_2 by hydrogen peroxide is about 100 times more effective than is oxidation by dissolved oxygen in equivalent molar concentration. This is based on a recent paper given by Hiskey.³ Hydrogen peroxide may be formed by radiolysis of water and radiation-induced surface activation of UO_2 . This is a very interesting area, and we are concentrating on the identification of different aspects of radiolysis.

Finally, a rapid oxidation of UO_2 single crystals and pellets will produce microcracks and cause disintegration. We have used a high concentration of hydrogen peroxide (3000 ppm, for example) and have seen the UO_2 crystal literally shatter. It is important for us to understand these possible leaching mechanisms in order to construct the total picture of spent fuels.

DISCUSSION

WITTELS: Since you selected UO_2 as a model system, would you also consider measurements on the cladding that remains with the fuel?

WANG: We are considering it, because we think that the cladding, in association with the fuel, will produce an electrolytic cell, and that cell may change the mechanism of leaching. But first we have to understand the basic spent-fuel leaching mechanism in more breadth and depth.

WITTELS: Do you actually have crystals that can be resolved by Lang topography?

WANG: Yes. We have a large quantity of single-crystal UO_2 . I think that it is a benefit of this program. We perform solution oxidation and investigate the surface by Lang topography. Of course, once the surface film has been formed, we cannot see it. In air oxidation studies, the Lang topography gives a very interesting lattice parameter which cannot be measured by powder x-ray diffraction. It is a very sensitive tool for precise lattice measurements. We have some interesting data that we are still analyzing because we cannot explain the behavior of this lattice parameter.

HOWITT: Do you have any idea of the dislocation densities in the UO₂ single crystal?

WANG: We have not looked at the dislocation density because it must be very high, according to reflection Lang topography. We do see that there are many subgrains in our material. The subgrains turn out to be very interesting. When we solution-oxidized the UO₂, the subgrains seemed to open up a little. Later, after we substantially oxidized, the subgrains closed a little, meaning that we have identified sponge-like areas that the oxygen goes through in the subgrain.

BOATNER: Do you think it is possible that the effect of radiation in changing the solution chemistry may turn out to be much more important than the effect of radiation in producing structural damage and changing the solid-state chemistry of the waste form?

WANG: I think both are important. So far, we cannot control the radiation effects in the solid state--especially for spent fuel. We must work with what there is. Also, we think that we can study the radiation effects in the solution and the solution chemistry by electrochemical methods.

REFERENCES

1. W. G. Burns and P. B. Moore, *Radiation Effects* 30, 233-242 (1976).
2. Manes and Naegele, p. 361 in *Plutonium and other Actinides*, Eds., Bland and Lindner, North Holland Publishing Co. (1976).
3. J. B. Hiskey, "Hydrogen Peroxide Leaching of Chromium Oxide in Carbonate Solutions," *Symposium on Hydrogen Peroxide*, ASM, (1980).

SHORT-TERM LEACHING BEHAVIOR OF WASTE FORMS
A POTENTIAL AREA FOR IMPROVEMENT

Albert J. Machiels

University of Illinois
Urbana, Illinois 61801

ABSTRACT

In order to be able to predict the potential impact of nuclear wastes buried under specified conditions, nuclide migration must be modeled. This requires the following to be known as accurately as possible: the probable radioactivity release rates from the primary waste form to the groundwater in the repository (the source term), and the groundwater flow rates and the retention capacity of the geologic formations the water passes through (the transport term). The source term is strongly dependent upon the choice of the waste form, while the transport term is not.

Since glass waste forms have been the object of considerable research and development, they can be considered as standards against which alternate waste forms can be evaluated. A review of the available leach rate data for several glass waste forms reveals that, frequently, abnormally high leach rates are observed during the initial period of contact between the water and the waste, under both laboratory and field-testing conditions.

In an on-going field test at Chalk River, the leach rates decreased by nearly three orders of magnitude over about ten years. Attempts to fit the data points by assuming a model in which the basic governing mechanism is a diffusion-controlled process usually result in one of the following situations: the long-term leach rates are overestimated when a good fit of the initial leach rates is achieved, or the initial leach rates are underestimated when a good fit of the long-term leach rates is realized.

An overall good fit, however, can be obtained by assuming that another process is responsible for the high leach rates corresponding to short burial times. The total leach rate is then obtained by adding the two curves representing the contributions of the short- and long-term controlling mechanisms. Modeling efforts have shown that a second diffusion process or a surface process could be responsible for the short-term leaching behavior.

It is important to note that by extrapolating the leach rates to burial times long enough for all initial radioactivity to decay, 90% of the radioactivity eventually released in the environment is contributed by the controlling short-term mechanism.

Given the potential impact of the processes governing short-term leaching behavior, the likelihood of their occurrence has to be addressed when alternate waste forms are considered, because they can be determining as far as the source term in nuclide migration is concerned.

Disposal of nuclear wastes, as presently planned, is to be by burial in geologic repositories. Although the envisioned burial depths are generally great, it is accepted that at some time groundwater will come in contact with the waste form. Therefore, in order to be able to evaluate the impact of wastes buried under specified conditions, one has to know, as accurately as possible: the source term, meaning the probably release rates of radioactivity from the waste form to the water; and the transport term, meaning the flow conditions of the groundwater and the retention capabilities of the formations the water flows through. Of the source and transport terms, only the source term is strongly influenced by the choice of the waste form. Therefore, our attention will be focused on the leaching behavior and, more specifically, the short-term leaching behavior of the waste form. First, I would like to quickly review some well-known features of leaching, and then I would like to talk about a few of my observations.

The concept of leach rates tries to quantify the rate at which water attacks the matrix of a given waste form. If we perform an experiment during which water or aqueous solution is put in contact with a material containing some waste, we can obtain the following expression for the leach rate, $L(t)$, which is a function of time:

$$L(t) = \frac{aW}{AST} \quad (\text{g/cm}^2 \cdot \text{day})$$

where

- a = amount of a specified nuclide leached during the test duration, T,
- A = amount of the specific nuclide initially present in the test specimen,
- S = geometrical surface area of test specimen for glass (but might be surface area determined by some method such as BET for porous material),
- W = weight of test specimen,
- T = duration of test.

As has been discussed several times already this morning, one can distinguish between congruent dissolution and selective leaching. Congruent dissolution means that the relative concentrations of the various components of the waste form in the leachate are the same as in the solid waste form. Obviously, for selective leaching, this condition is not realized. Therefore, experimentalists striving for completeness specify a leach rate by giving the numerical rate and also specifying that the rate is based on the leaching behavior of the specific nuclide (or nuclides) which was monitored. Many test results are also reported in terms of cumulative leaching, which can be expressed as the integral over time of the leach rate:

$$\int_{t_i}^{t_f} L(t) dt \quad (\text{g/cm}^2)$$

It is also well known that, based on a few studies which have been made on simple glasses with leach rates high enough to be conveniently tested and monitored, cumulative leaching is very often expressed as $Q(t) = \alpha\sqrt{t} + \beta t$, where t is time, and α and β are constants. That means that if we have some curve representing the cumulative leaching such as that in the upper half of Fig. 1, we can decompose this total curve into two components, one linearly dependent on time, and the other varying as the square root of time. Similarly, if leach rate is expressed as $L(t) = (\alpha/2\sqrt{t}) + \beta$, the leach rate curve in the lower half of Fig. 1 can be decomposed into two curves, one a function of $1/\sqrt{t}$, and the other representing by the constant β . Generally, as you can see from Fig. 1, during the early stage of leaching, the dominant contribution is from the curve dependent on \sqrt{t} (or $1/\sqrt{t}$); but after some time the contribution from the other process takes over and becomes more important.

Two fundamental processes have been recognized: network dissolution and diffusion. Network dissolution gives cumulative leaching proportional to the first power of time. In the diffusion process, hydrogen ions of the water exchange for some of the sodium in the glass. The diffusion process can be obtained by using the two Fick's laws, which involve the use of a diffusion coefficient. When this diffusion coefficient is low enough, the time involved short enough, and the initial distribution of the activity in the sample uniform, then diffusion gives cumulative leaching proportional to the square root of time. Under some conditions, like a nonuniform distribution of the waste in the sample, the time dependence can be different. Usually, only the initial behavior of the diffusive process, assuming initial uniform distribution, gives the square root of time dependence.

We have been interested recently in the modeling of leaching, because a very large number of results are available now and some trends are clear although there is a large scatter in the magnitude of the various reported results. The hope is that by looking at some of those

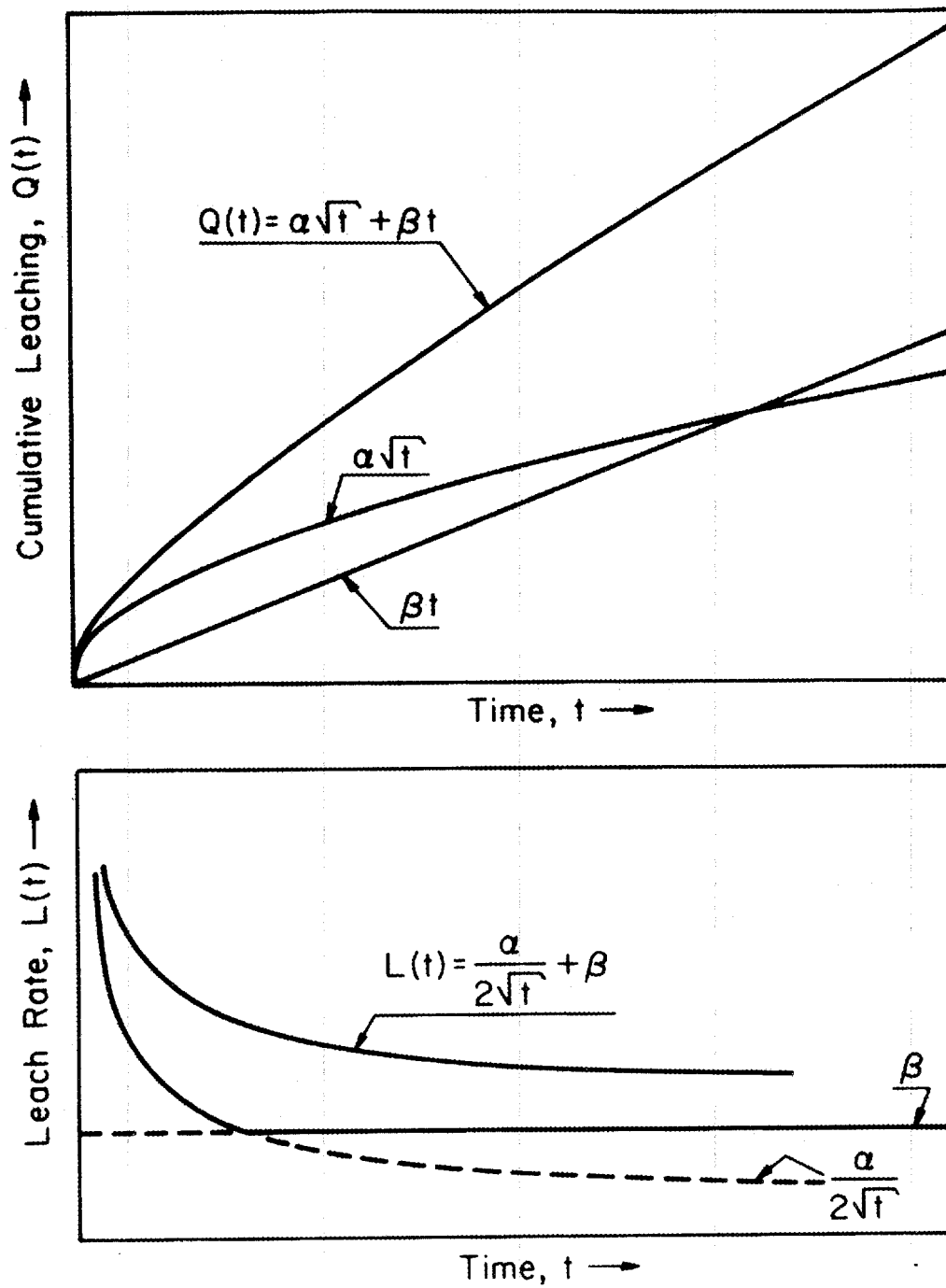


Fig. 1. Cumulative leaching and leach rate vs time.

trends, one should be able to explain them with a fairly small number of fundamental processes. Then, looking at all the possible processes which could yield a given behavior, it is hoped that one can devise specific experiments which test one model at a time, and pinpoint eventually the processes responsible for the leaching behavior of a waste form.

Modeling, itself, involves the choice of at least three parameters: (1) a geometry, (2) an initial distribution of the activity in the sample, and (3) some boundary condition at the interface between water and waste form. Examples of modeling attempts which have been published are the work of Bell,¹ published in 1971, and the work of Godbee and Joy,² published in 1974. A more recent example is the work of Wiley,³ published in 1979. There are also additional descriptions from the Catholic University of America and The Pennsylvania State University, for example, which are more complex than those of Bell and Wiley and which, because of their complexity, have not been developed into strict mathematical formulations. Bell's work assumes a one-region diffusion and no network dissolution; Wiley's work is a combination of these two; some of the other works assume multi-region diffusion (several regions in the waste form which are governed by diffusion) and also network dissolution.

We have looked at the available leach rate data, and we have concentrated our modeling effort on one experiment⁴ being conducted at Chalk River in Canada, which is, the test that is closest to an actual field test. Twenty-two blocks of aluminosilicate glasses containing about 1000 curies of miscellaneous fission products were buried without any canister or other barrier around them; for about 18 years the radioactivity released in the environment was monitored (Fig. 2). A feature which is not uncommon is the drastic reduction in leach rates, from fairly high values at the beginning of the experiment to extremely low values after a few years. In Fig. 2, there is a decrease of about three orders of magnitude in about 10 years.

We have developed a mathematical model designed to explain the behavior in Fig. 2. The model is treated in some detail in ref. 5. Some of its salient features are presented here. The blocks buried by the Canadians were hemispherical (about 14 cm in diameter), so we adopted the hemispherical geometry and the notations shown in Fig. 3. The mathematical formulation of the model is:

$$\frac{\partial C}{\partial t} = D \nabla^2 C - \lambda C$$

where

C = ⁹⁰Sr atomic concentration,
 D = diffusion coefficient (= constant),
 ∇^2 = Laplacian operator,
 λ = ⁹⁰Sr decay constant,
 t = time.

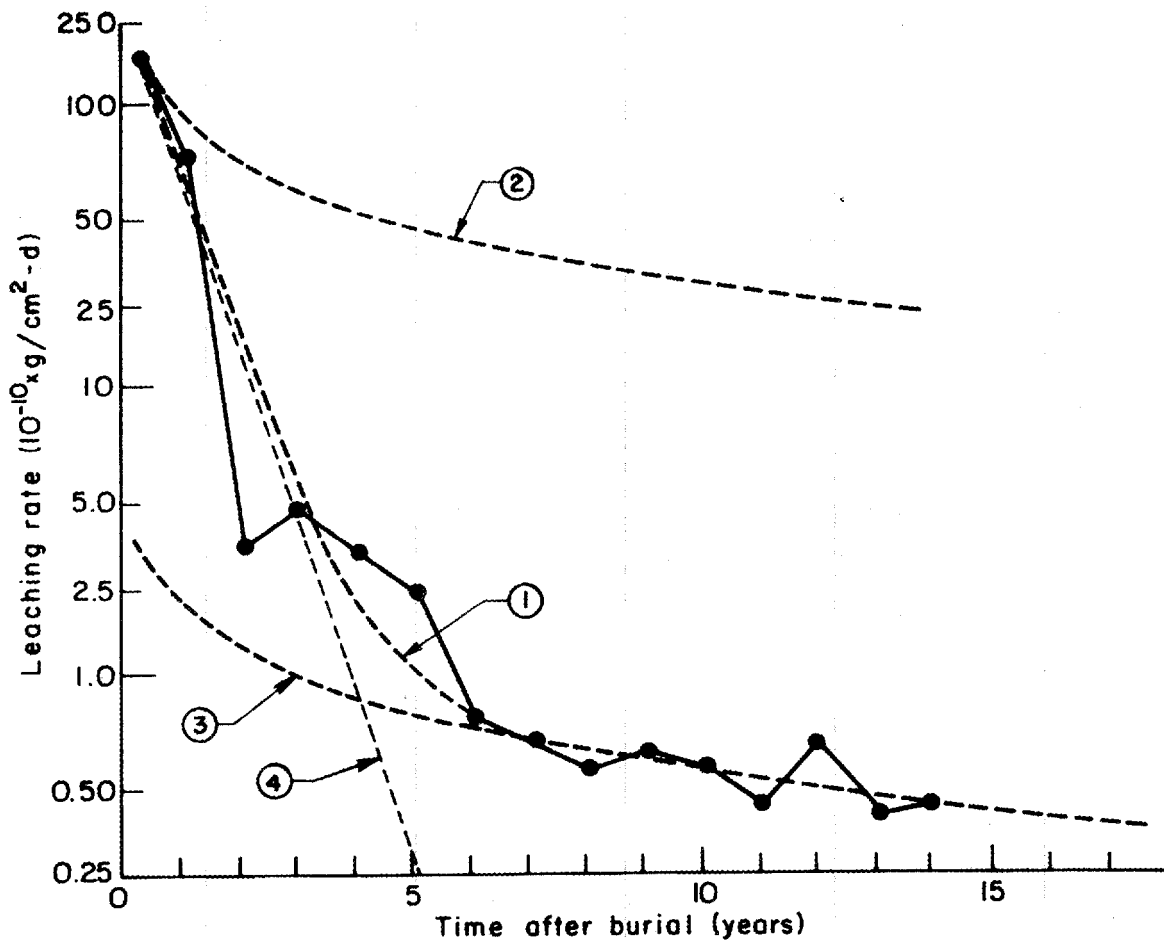


Fig. 2. Experimental and theoretical leach rates for the Chalk River field test.

By using Fick's law and correcting for the decay, in order to obtain the radioactivity released into the environment, we can solve this equation as a function of position in the hemisphere, polar angle, and time:

$$C = C(r, \theta, t).$$

This gives the concentration of waste in the hemispherical block. We can impose the following boundary conditions:

$$\begin{aligned} C(0, \theta, t) &\text{ remains finite,} \\ C(r, \pi/2, t) &\text{ remains finite and } = 0, \\ C(R, \theta, t) &= 0. \end{aligned}$$

The water contacting the waste maintains a zero concentration at the surface of the block.

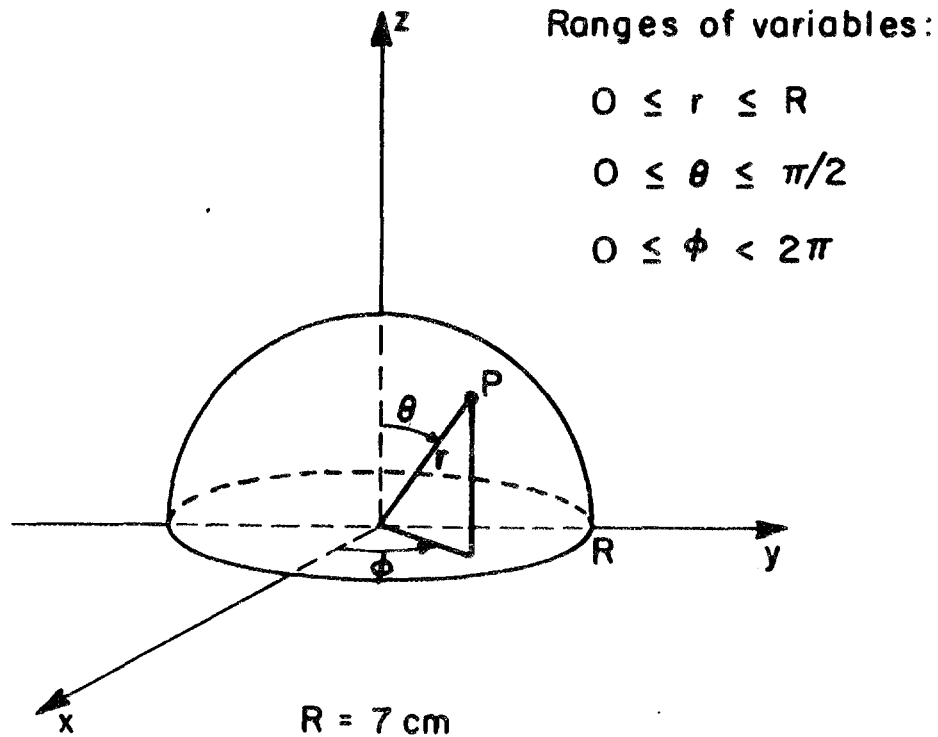


Fig. 3. Hemispherical geometry.

The initial concentration is:

$$C(r, \theta, 0) = 2C_0 \cos \theta$$

We intentionally did not assume a uniform initial concentration. We simply took an initial concentration which is independent of the radius but which is a function of the polar angle. The reason for doing so, was to simplify the mathematical handling.

In deriving the equation for the leach rate, we have multiplied by the surface area, so that the leach rate is expressed as ^{90}Sr atoms released per year. The leach rate is given by:

$$L(t) = 16 \text{ DRC}_0 \exp(-\lambda t) \left\{ \sum_{i=1}^* G_i \exp \left[-D \left(\frac{a_i}{R} \right)^2 t \right] + \frac{R}{8} \sqrt{\frac{\pi}{Dt}} \cdot \text{erfc} \left(\sqrt{\lambda t} \right) \right\}.$$

For λ small enough and D small, $L(t)$ behaves as $1/\sqrt{t}$ as $t \rightarrow 0$; this yields the classical behavior; when the diffusion coefficient is small enough, the second term dominates. For λ small enough and D large, $L(t)$ behaves as $\exp(-Dt/R^2)$; the exponential terms are dominant, so we have, more or less, an exponential dependence upon time.

Referring again to the experimental behavior shown in Fig. 2, we tried to fit the experimental points with our mathematical formulation.

When we tried to fit the initial release rates (curve 2), the model predicted longer-term leach rates which were much higher than the actual longer-term leach rates. On the contrary, when we tried to fit the longer-term results (curve 3), the predicted initial leach rates were much lower than they should have been. The model, which included only a single diffusion process, failed to fit the experimental results. Therefore, instead of using only one diffusion process to describe the behavior of the ^{90}Sr atoms, we assumed that a second diffusion process was responsible for the initial leach rates. We could get a very good overall fit by fitting the initial leach rates with the second diffusion process (curve 4), fitting the longer-term leach rates with the first diffusion process (curve 3), and combining curves 4 and 3 to obtain curve 1, the total leach rate.

This is mathematical handling, and eventually we have to try to justify why it works. (You know that when something works you can always find justification for it.) We concluded that, if describing the total behavior of this curve in terms of two diffusion coefficients has any physical meaning, it is because two types of sites are available in the glass, which means two types of bonding for the ^{90}Sr in the glass; some of the ^{90}Sr would be strongly bound and would be leached out very slowly, but some would be weakly bound and leached out more rapidly. The latter could occur if one would be far from the ideal formulation for the glass, because the glass matrix would not adequately incorporate all of the ^{90}Sr . If we look back at the expression for the leach rate, $L(t)$ (the last equation), we see that for the sites which involve weak bonding, the release rate roughly follows an exponential behavior.

An exponential behavior can also be explained by a chemical rate process. If there are any nonhomogeneities on the specimen surface which are significantly more leachable, and if the leach rate of the ^{90}Sr on the surface can be expressed as equal to a rate constant, k , multiplied by the number, N_s , of ^{90}Sr atoms belonging to nonhomogeneities on the surface, $-dN_s/dt = kN_s$, there would also be exponential decay:

$$-\frac{dN_s}{dt} = kN_s,0e^{-kt}$$

Therefore, there are two possibilities to account for the experimental behavior. By adding to the slow diffusion term a contribution which is more rapid: either some ^{90}Sr which is diffusing rapidly, or some chemical process which is responsible for releasing during the initial period of time, some strontium ^{90}Sr into the water.

It is important to note that when the leach rates are extrapolated to a time long enough for decay of all initial radioactivity to take place, assuming that leaching will proceed as expected, about 90% of the radioactivity which will be eventually released will be released during the initial period of time (Fig. 4). Therefore, the initial leaching behavior is very important. However, if we assume that this mechanism is not quite

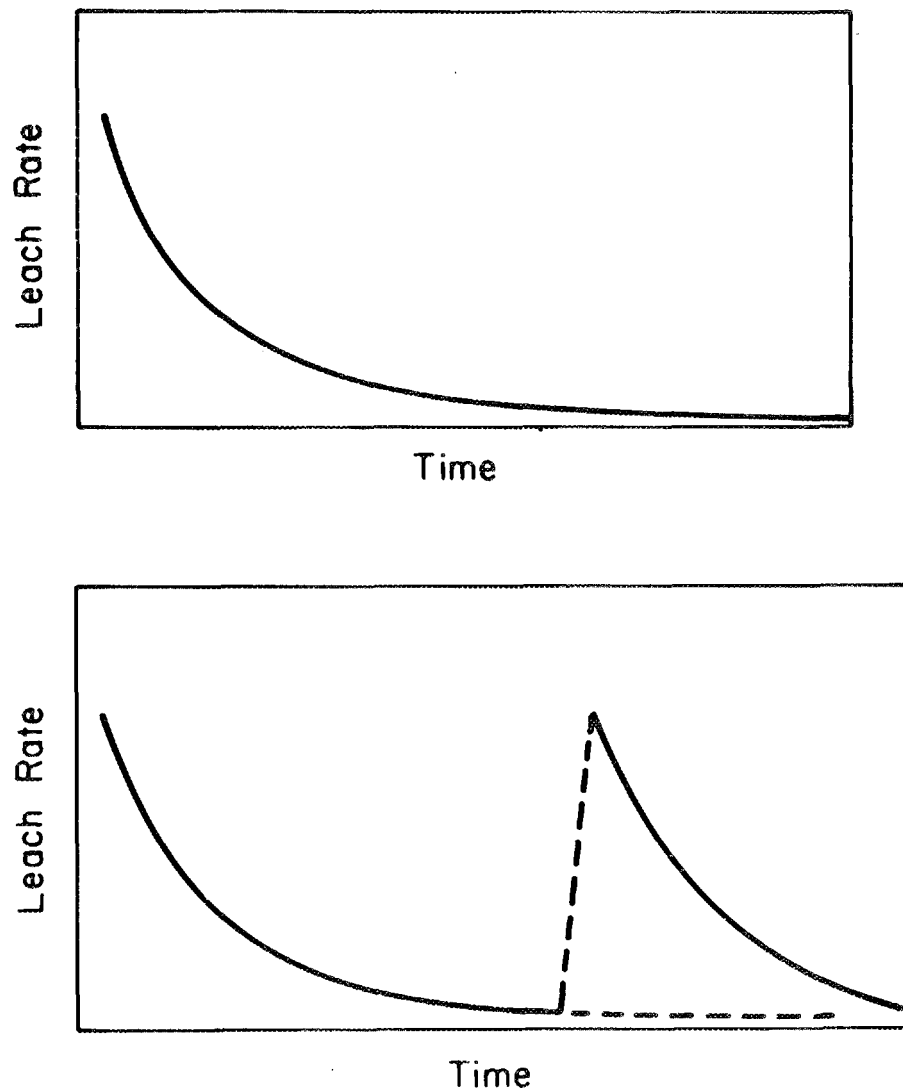


Fig. 4. Extrapolation of leach rates.

correct, and that the nonhomogeneities are not only present at the surface but also inside the sample, we can postulate that, as the glass degrades some new homogeneities are exposed and another sharp rise in leach rate occurs (lower half of Fig. 4).

In conclusion, the short term leaching behavior may be very important. The short-term leaching behavior can be explained in terms of a number of possibilities, such as incomplete fixation of waste or non-ideal formulation of the waste form, or surface contamination (during preparation of the sample or by interaction with the crucible or the canister). It seems that that could be an area for improvement for either glasses or alternate waste forms; but it appears, after hearing some of the arguments this morning, that this is a problem we may have to live with for any type of waste form under consideration.

DISCUSSION

RUSIN: I am not familiar with the field tests. I was just curious as to how it was guaranteed that they were actually sampling all the material that was being leached out of the glass.

MACHIELS: The details can be found in Ref. 4. Twenty-two blocks were buried 12 feet in the ground, exposed to the groundwater under the water table. A probe, located about 1-1/2 feet from the sample, gave fairly decent information about the water which was flowing by the block.

RUSIN: So it is being done in alluvium, or gravels, or...

MACHIELS: It is done in impermeable sand. This is a feature we like, because that means the water is saturated with silica and, therefore, some of the network dissolution process is unlikely to be occurring at a very high rate.

BOATNER: Why couldn't you explain these results by the idea that, after a certain length of time, a gel layer is formed at the surface of the block, and that this then inhibits any further leaching of the material and essentially changes the effect of the diffusion process?

MACHIELS: There are two answers to this question. In general, when you go through a mathematical description, you see that any diffusion process acts as a flywheel, so that you never get drastic variations in the release rate, assuming a particular diffusion process. What you have to assume is a different value for the diffusion coefficient; then you can induce drastic changes. This is one reason. The second reason is that the Canadians have looked at those blocks after 18 years; alterations that they have seen in the glass involve about 10 to 20 Å at the most. That means that the glass was not significantly altered in order to give a drastic change in the diffusion behavior of the species.

BOATNER: In these tests, movement of the groundwater was probably very slow, I assume, so that this is like an unstirred leaching experiment.

MACHIELS: That's right. But at least the water is flowing.

UNIDENTIFIED QUESTIONER: Couldn't you explain your curves by a constant speed of dissolution and a proper partition of the impurities in the sample, like a surface segregation, so it will leach more in the beginning and less as a function of time, because the impurities would be segregated on the surface mainly?

MACHIELS: Yes. This is possible. At the beginning there is segregation of a part of the ^{90}Sr on the surface, and this would be leached. This is modeled by the chemical process. And then, on top of that, there is the diffusion process which brings ^{90}Sr atoms to the surface.

UNIDENTIFIED QUESTIONER: I would like to know if you have thought about the possibility that there is a buildup of strontium concentration in the water right outside the surface, and how would that affect your diffusion equation? You know, if your boundary condition at the surface does not go to zero.

MACHIELS: Yes, it is a possible effect that we have not looked at yet. Basically, as long as you assume that there is steady concentration at the surface, it does not matter whether it is zero or constant, one gets the behavior which has been described in the paper. To obtain the observed effect one would have to assume a concentration at the surface which was initially low and then would increase. This is definitely something which could give the sharp variation.

REFERENCES

1. M. J. Bell, "An Analysis of the Diffusion of Radioactivity from Encapsulated Wastes," ORNL-TM-3232 (1971).
2. H. W. Godbee and D. S. Joy, "Assessment of the Loss of Radioactive Isotopes from Waste Solids to the Environment, Part I: Background and Theory," ORNL-TM-4333 (1974).
3. J. R. Wiley, Nucl. Technol. 43, 268 (1979).
4. W. F. Merritt, Nucl. Technol. 32, 88 (1977).
5. C. Pescatore and A. J. Machiels, Trans. Am. Nucl. Soc. 33, 416 (1979).

RADIATION DAMAGE IN NATURAL MATERIALS:
IMPLICATIONS FOR RADIOACTIVE WASTE FORMS

Rodney C. Ewing

Department of Geology, University of New Mexico
Albuquerque, New Mexico 87131

ABSTRACT

The long-term effect of radiation damage on waste forms, either crystalline or glass, is a factor in the evaluation of the "integrity" of waste disposal mediums. Natural analogs, such as metamict minerals, provide one approach for the evaluation of radiation damage effects that might be observed in crystalline waste forms, such as supercalcline or synroc.

Metamict minerals are a special class of amorphous materials which were initially crystalline. Although the mechanism for the loss of crystallinity in these minerals (mostly actinide-containing oxides and silicates) is not clearly understood, damage caused by alpha particles and recoil nuclei is critical to the metamictization process. The study of metamict minerals allows the evaluation of long-term radiation damage effects, particularly changes in physical and chemical properties such as microfracturing, hydrothermal alteration, and solubility. In addition, structures susceptible to metamictization share some common properties: (1) complex compositions, (2) some degree of covalent bonding, instead of being ionic close-packed MO_x structures, and (3) channels or interstitial voids which may^x accommodate displaced atoms or absorbed water. On the basis of these empirical criteria, minerals such as pollucite, sodalite, nepheline and leucite warrant careful scrutiny as potential waste form phases. Phases with the monazite or fluorite structures are excellent candidates.

The essential questions that remain to be clearly answered are: (1) What are the structural controls on radiation damage? (2) What is the structure of the metamict state? and (3) What is the effect of metamictization on critical properties, such as leachability? As regards the selection of waste forms, all radiation damage effects can be mitigated by simply lowering the waste loading.

This work was in part supported by the U.S. Department of Energy under Contract EY-76-C-06-1830 by Battelle Pacific Northwest Laboratory.

Radiation damage in natural materials manifests itself in a number of ways, such as the formation of fission tracks, pleochroic halos, and metamict minerals. For this presentation, I want to confine myself to comments on metamict minerals, although some of the other effects that I have mentioned may be important, and I want to take advantage of the informality of the workshop to review what is known about the metamict state, discuss its applicability to the evaluation of radiation damage in crystalline waste forms, and, finally, make some comments on present thoughts concerning radiation damage in crystalline phases and its effects on leachability.

First, a little bit of history. The term metamict was first defined in 1893 by Broegger¹ as one of three classes of amorphous materials. Metamict minerals were considered to be materials which were initially crystalline, but which by some process, had been converted to the amorphous state. The initial crystallinity was evidenced by well-formed crystal faces. Of course, at that time, Broegger made no statement that the "amorphous" state was the result of radiation damage. It was not until 1914 that Hamberg² suggested that the metamict state was due to alpha damage, generated by uranium and thorium atoms that were constituents in the crystalline lattice.

Of course, today we have a slightly clearer view of radiation damage effects. Gamma and beta radiation, although quite penetrating, have the primary effect of ionization of atoms, and this will have little effect on the structural properties of the material. Transmutation effects, associated with beta decay, such as the transmutation of cesium to barium, may be important because of changes in the size and charge of cations in particular crystallographic sites. But the really important effects are the effects of the short-range particles, the alpha particles, and they present, I think, the greatest structural difficulties. A high-velocity alpha particle dissipates energy by excitation of electrons or ionization, and as it slows down it displaces atoms by collision, say 100 to 1000 displacement events per alpha particle. Even more important are the displacements caused by the recoiling parent nucleus. In addition, energy is released in the form of heat, so that thermal spikes are formed along the track of the alpha particle. The alpha damage, the recoil damage, and the thermal spike all have the potential of causing structural damage in the material; and if we look, for example, at reprocessed nuclear fuel wastes, the cumulative³ alpha dose is something on the order of 10^{18} alpha particles per cm^3 during the first 100 years, one quarter of this dose occurring during the first 10 years. So, I think we have to be concerned about the structural damage that may occur in crystalline waste forms, and as a footnote I should mention that we would also expect structural damage in a glass.

Let me list the properties of metamict minerals as they are described by mineralogists, and as they have been studied in the past few years. Metamict minerals are optically isotropic; they may be in part anisotropic but the anisotropy decreases with increasing metamictization. This becomes quite obvious when we look at the decrease

in birefringence with increasing degree of radiation damage. Metamict minerals lack cleavage; they have a characteristic conchoidal fracture. Some metamict minerals are pyrogonomic; that is, as they are annealed they are recrystallized and they may glow incandescently as the exothermic recrystallization reactions release heat. With metamict minerals, the crystalline structure can be reconstituted on heating, but this usually produces a polycrystalline phase assemblage, and that polycrystalline phase assemblage can consist of phases that do not include the original premetamict phase. Metamict minerals, of course, contain uranium and thorium, but the interesting thing is that the concentrations can often be quite low; concentrations as low as fractions of one weight percent of uranium and thorium have caused certain minerals to become completely metamict. Metamict minerals are "amorphous" to x-ray diffraction. With increasing degree of radiation damage we see a broadening of diffraction maxima, a decrease in intensity, and a shift to lower values of 2θ . This, of course, is correlated with an expansion of unit cell parameters and, therefore, a decrease in the density. This volume change results in numerous microfractures. We often see pervasive alteration; the alteration is of various types, perhaps hydrothermal, perhaps weathering, but the alteration is concentrated along the microfractures. I will show you some photomicrographs of this shortly. Some phases occur in both the metamict and non-metamict state, where we can reconstruct what the structure must have been before metamictization; and, of course, the crystalline structures are those which have low concentrations of uranium and thorium. Finally, there are certain compositions (dimorphs or polymorphs) that have several structural possibilities, in which one of the structures seems to be susceptible to radiation damage; so we see, and I will have some examples of this, clear evidence for structural controls on the degree of radiation damage.

The essential question with metamict minerals is whether or not it is desirable to use them as natural analogues for radiation damage. There are some entries in the plus column. First, metamict minerals provide us with a long-term experiment, which has taken place over millions of years, and gives us information that allows us to validate short-term laboratory simulations of radiation damage. A second advantage of looking at natural analogues is that this is the type of evidence that the general public is likely to be able to understand and accept; this is a point that Ringwood has made many times. Finally, the study of metamict minerals, particularly the study of structures that are susceptible to radiation damage, gives us an empirical list of the structures that might be good or poor candidates for isolating radionuclides.

There are, however, a number of limitations. First, among these, is the fact that the effects we see in the natural analogues include not only the radiation damage effects but later geologic effects, such as hydrothermal alteration and surface weathering; it is sometimes difficult to sort these out. Another important limitation, that I will discuss in more detail later, is the fact that the radiation damage effects in these natural materials can be annealed so that we cannot

simply calculate the total alpha dose received by a material, examine its crystallinity, and say that its properties are the end result of a certain alpha dose. We are also limited by the fact that there are usually important compositional and structural differences between the natural analogues and the crystalline radioactive waste form. Also, the natural materials experience radiation damage in a different way from the way in which, I think, the crystalline waste form phases will experience radiation damage. For the natural materials, uranium and thorium are the source of the radiation damage. If you think back to the structural pictures of the three phases for synroc, the cations are located in voids and surrounded by a cage of edge sharing titanium octahedra. However, in a waste form phase, that cage of titanium octahedra will also include radionuclides, such as technetium, substituting for the titanium; therefore, the sum total of the radiation damage effects in the crystalline waste forms is bound to be different from the effects that we see in the natural materials. Finally, we always have to remember the question of the effect of dose rate and annealing rate on the material.

For this review I want to look at single phase, zircon ($ZrSiO_4$) and to show you what data is available in the literature, some of the limitations, particularly of using natural analogues. I have selected zircons because they are the most studied. Zircons are used by geologists in uranium-lead dating. Geologists have been very interested in alteration effects in zircons and radiation damage effects. In the middle 1950's, geologists considered radiation damage in minerals as a potential age-dating technique, so there were several fine studies that attempted to relate total alpha dose and the age of the material to the degree of metamictization. And then, finally, zircons are by far the simplest of the metamict structures that are available for study, so that there is some possibility of understanding exactly what is going on.

Zircon ($ZrSiO_4$) is essentially tetragonal (space group $I4_1/amd$); lattice parameters⁴ are $a = 6.60$ Å and $c = 5.98$ Å. As I indicated earlier for metamict materials, there are changes in density³ with increasing metamictization. The density decreases from 4.65 g/cm³ for crystalline zircon to 3.95 g/cm³ for metamict zircon. Zircon contains up to 3 weight percent (U, Th) O_2 . The classic study of³ zircon, I think, is still the 1955 study of² Holland and Gottfried, in which they were attempting to use the degree of radiation damage as an age-dating technique. They determined the total alpha dose on gem quality zircons from Ceylon and related it to changes in the physical and structural properties of the material. I would like to go through some of their data. Figure 1 shows changes in refractive index and in density as¹⁶ a function of radiation damage (in terms of total alpha dose of 10^{16} alpha particles per milligram, which will be denoted here as alphas/mg). As has often been observed, but not as nicely documented as it is in this figure, there is both a decrease in refractive index and a decrease in the density of material with increasing dose. The important thing to keep in mind¹⁶ is that the magic number in terms of total alpha dose is about 10^{16} alphas/mg, where we reach saturation. They completed a powder diffraction study

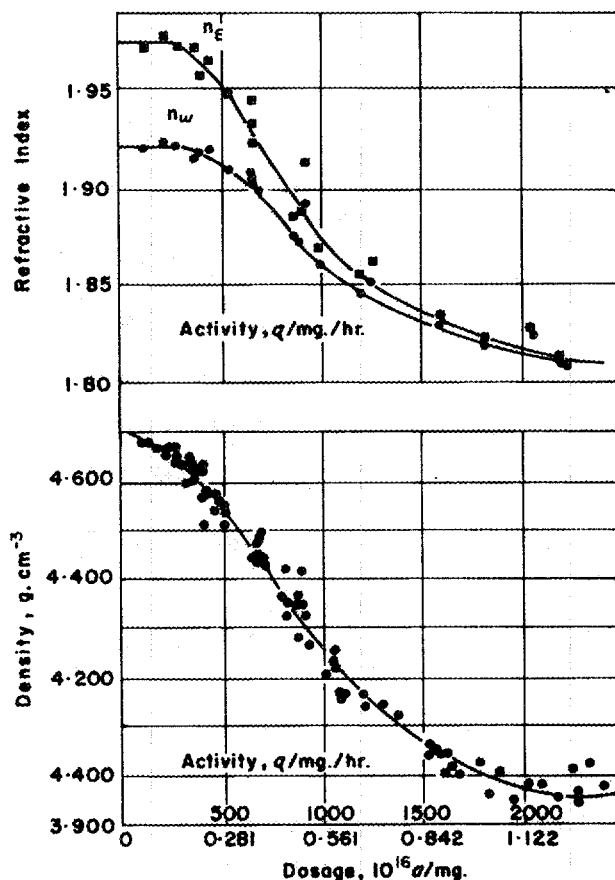


Fig. 1: Refractive indices and density of Ceylon zircons as a function of total alpha dosage³.

of the material and showed (Fig. 2) that with increasing dose there are decreases in peak intensity, broadening of the peak, and a shift to lower values of 2θ . From the powder data they were able to refine the unit cell parameters. The unit cell parameter increases, reaching saturation at a little less than 10^{15} alphas/mg; and the c unit cell parameter increases with saturation reached at about the same dose. Now, one of the interesting things is that the rate of change in the unit cell parameters was not isotropic. For a dose less than 2.3×10^{15} alphas/mg, c was expanding faster than a ; and at doses of greater than 2.3×10^{15} alphas/mg, a began to expand faster than c . So we have a structure in which volume changes may be as high as 10 percent, flexing at different rates, at different times, in different directions.

This type of study is really excellent for our purposes, because, when we have the complete range of doses, we can come to an understanding of exactly what the saturated dose is; in this case I would suggest 10^{16} alphas/mg as the dose required to reach saturation. But to indicate how far off you can be if you just go to the geologic record and pick up a single zircon, I reviewed the literature, and I

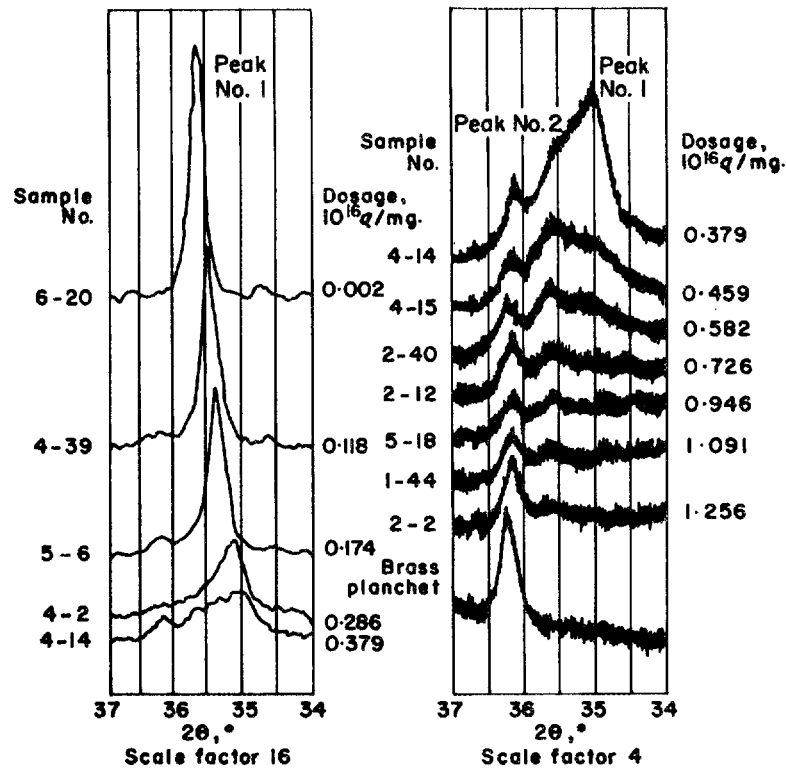


Fig. 2: The reflection of x-rays from the (112) planes of Ceylon zircon with increasing alpha dose³.

was able to find zircons with doses of 10^{14} or 10^{15} alphas/mg which were completely metamict and, conversely, other zircons with a total dose of, say, 9×10^{18} alphas/mg which were completely crystalline. So the warning is that you can find examples of just about anything in the geologic literature; and the difficulty, of course, in coming to the right figure is calculating the total alpha dose and then being sure that your zircon has not been annealed by some more recent thermal event.

Another study, which was a follow-up of the work of Holland and Gottfried, was a study by Burcell and McClaren,⁴ in which they looked at zircons in which the doses varied from 10^{14} alphas/mg to in excess of 10^{16} alphas/mg. An interesting result was that for the metamict zircon, with the dose of 10^{16} alphas/mg, using transmission electron microscopy and transmission electron diffraction, they found a pattern which is essentially that of a single crystal; and they interpreted this as indicating that the totally metamict zircon consisted of crystallites with a diameter of perhaps 100 Å and slightly misoriented; a very different picture from that proposed by others for the structure of the metamict state. I show this with some hesitation, because I have to mention that a paper now in review, written by Roy and Vance, takes issue with exactly this figure and suggests that this is an artifact and that, in fact, this material is not amorphous. I

have included it because the results of Burcell and McClaren are in excellent agreement with a study by Sommerauer⁵ in Zurich, in which he also used transmission electron microscopy to study metamict zircons. The picture he presents is more complicated; there are several different crystalline phases, as well as regions that are amorphous, and the proportion of crystalline phases to the amorphous area changes with increasing radiation dose, but he has crystallites, and they are approximately of the same dimension. Figure 3 summarizes radiation damage effects on zircon, subject to the reservation that perhaps the particles in the microfractured material are crystallites. This is one of the main issues in work on metamictization.

CHANGES IN PHYSICAL PROPERTIES OF ZIRCON		
PROPERTY	HIGH ZIRCON	METAMICT ZIRCON
DENSITY (gm/cc)	4.65	3.90
REFRACTIVE INDEX:		
No	1.92	1.82 (ISOTROPIC)
Ne	1.98	
No-Ne	.06	
ALPHA DOSAGE (α/mg)	LESS THAN 10 ¹⁵	MORE THAN 10 ¹⁶
EXTENSIVE MICROFRACTURING ?	NO	YES
DIFFRACTION OF X-RAYS ?	YES	NO, BECAUSE "PARTICLE SIZE LINE BROADENING?"

Fig. 3: Summary of the changes in the physical properties of zircon with metamictization.

In the interest of time, I will not review all the literature on zircons. I will simply mention that there is a considerable amount of literature, particularly using infrared spectroscopy to determine whether this process of metamictization is one in which the radiation damage accumulates in a progressive way until the metamict state is reached, or whether it represents a series of discontinuous steps that form crystallites and different crystalline phases and perhaps ends with a very finely crystalline assemblage of say, SiO₂ and ZrO₂ in the case of zircon.

There are three very important studies which I will just mention, that can be related to the work of Holland and Gottfried. There are ion bombardment experiments on zircons which have used argon and krypton ions in the energy range of 1 to 3.5 MeV, and induced the metamict state at a dose of 2×10^{15} ions per cm².⁶ There are fast-neutron bombardment experiments which have also induced the metamict state. There is the work of Vance and Boland in which they have induced the metamict state in zircon powders using fission fragment damage of activated uranium impurities in the zircon. They found that it requires approximately 10^{16} fission events per cm² to transform the zircon to the metamict state. Or, another way to look at it, it takes about 10^4 more alpha particles to do the same amount of

damage. These types of experiments are very important, because it is the ion bombardment, the fast-neutron irradiations, and the fission fragment damage experiments that will probably be conducted on candidate crystalline waste forms, and the fact that we have such a detailed study of radiation damage in natural zircons allows us to relate the laboratory simulations to the long-term experiments.

Another question related to metamictization is that of alteration. This is essentially a question of whether there is an increase in solubility or leachability as a function of radiation damage. An increase in leachability might be due to increased surface area, it might be due to microfracturing, or it might be due to chemical degradation (actually breaking the originally crystalline material into other components). If we consider the ambiguity and controversies surrounding leach data and then add radiation damage as another variable, I think that we have a complicated situation, and one in which there is really no data that allows us to come to any straightforward conclusion. What I would like to do is review some of the data that has been cited in various studies and comment on the limitations to some of the conclusions.

One item that is often cited is that metamict zircons are used in uranium-lead age dating, and that the ability to get dates from these metamict zircons means that the uranium-lead systematics have not been disturbed. This ignores the fact that most uranium-lead dates are discordant. Also, the discordant dates are usually thought of as being caused by loss of lead. I am not sure that the retentivity of lead is the most important aspect of the retention of radionuclides; and natural zircons are fairly inhomogeneous, so it is difficult to assess exactly what has been lost.⁹ Another study that has been cited is a study by Pidgeon and others⁹ in which metamict zircons (one of the zircons was from Holland and Gottfried's study) were subjected to hydrothermal conditions - 500°C, 1000 bars and 2 molal sodium chloride solution. Under these conditions there was no loss of uranium, thorium, or lead, and the system appeared to be closed. There are two points that I would make. One is that the conditions of this experiment are conditions in which you would expect very little loss of uranium; Eh, pH, total carbonate concentration, and temperature have a tremendous effect on the mobility of uranium, so I think this one zircon and one hydrothermal solution is hardly evidence for low leachability of metamict zircons. Also, I would point to the concluding paragraph of Pidgeon and others, which says that this is only a single data point and cannot be used to generalize as to the long-term retentivity for uranium, thorium, and lead in zircon.

Another aspect of the alteration of zircons has been the argument over the loss of silica. Annealed metamict zircons often have a powder pattern which can be indexed in terms of $ZrSiO_4$ plus ZrO_2 , indicating loss of silica. There are reports of ZrO_2 pseudomorphs after zircon. Finally referring to Fig. 4, which is data from Mumpston and Roy¹⁰, if we plot the compositions of natural zircons and thorites and if there is no loss of silica, they should lie along the line of equimolar

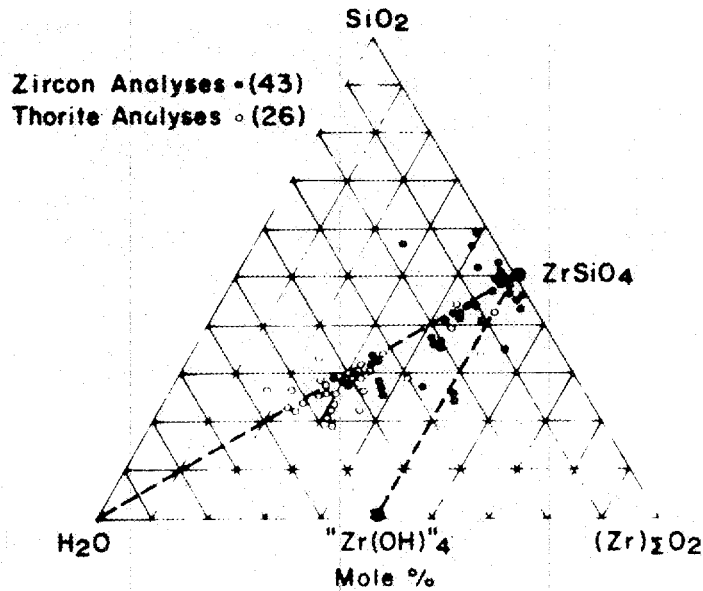


Fig. 4: Compositions of natural zircons and thorites plotted on a molecular basis¹⁰.

concentrations of SiO₂ and (Zr)_ΣO₂; I will simply point out there are quite a number of natural zircons which are silica-deficient.

Another approach is that of Krogh¹¹. Krogh uses zircons for age dating and is interested in understanding alteration effects. He has looked at etching features on natural zircons which were mixtures of crystalline material and altered metamict material. His etchant is fairly extreme, it is dilute hydrofluoric acid, so this does not represent the conditions in a repository. Nonetheless, I think, the differential effect is quite obvious; that is, the crystalline material stands as resistant ridges and the altered and metamict material is easily removed (Fig. 5). There is a differential effect; how important it is remains to be evaluated. Fleischer¹² has shown that recoil nuclei can be removed by differential etching of a surface along the track of the recoil nucleus. He points out that this has obvious implications for waste forms, and it is interesting that he finds the same effect in volcanic glasses and in crystalline materials: feldspars, quartz, and muscovites. Citing this array of evidence, I am led to the feeling that we really cannot say what the final result of radiation damage will be on the solubility or leachability of a material.

I will end this part of the discussion by addressing one other point that is sometimes raised. Certain workers have maintained that the fact that metamict minerals exist at all is testimony to their long-term stability. Although I have shown these slides at several meetings, I think it is instructive to look at what these things that are surviving actually look like, and I am not particularly encouraged. Figure 6 is an autoradiograph of a metamict

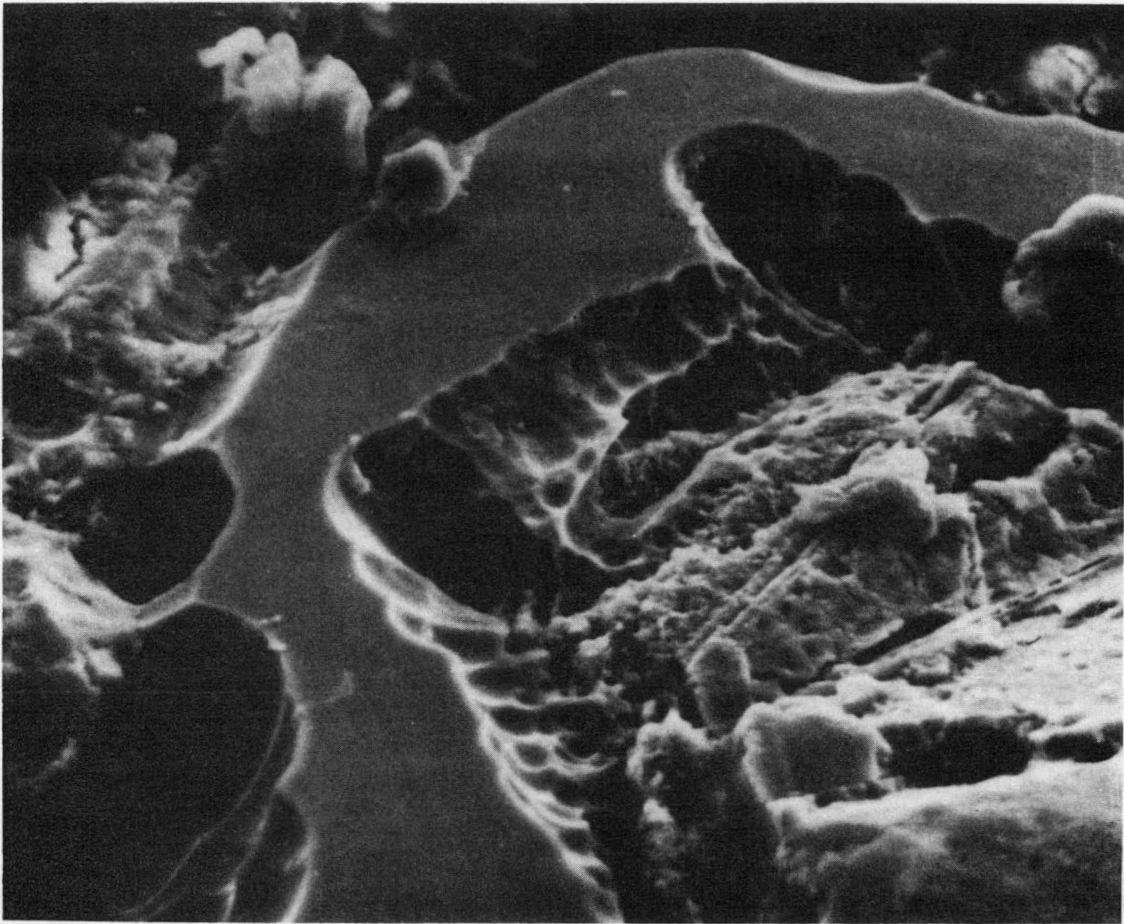


Fig. 5: Scanning electron photomicrograph of zircon grain etched with 48% HF¹¹.

niobium-tantalum-titanium oxide. The light areas show extensive leaching of uranium and thorium along the microfractures, so you get some idea of how fractured this type of material can be. Figure 7 shows a single crystal of a metamict Nb-Ta-Ti oxide. The yellow area is the altered area. There are four magnifications, but I think you can see, the extensive microfracturing and the pervasive alteration that cuts across the material. Certainly, these radiation-damaged materials exist at the surface, but they do not exist in a pristine state that would indicate that they are suitable for waste forms. Also, we have recrystallization effects. Figure 8 shows a spherulite growing in an isotropic, metamict matrix. The spherulite is about 80 microns across. A microlite crystal is shown in Fig. 9; I have chosen it because its structure is related to that of zirconolite. It is completely metamict, fractured, and very much altered. So, these things are complicated as they exist on the surface of the earth, and there is ample evidence to suggest that they have been altered.

Leaving the question of alteration, I would like to say a little about the common structural properties of metamict minerals. If we

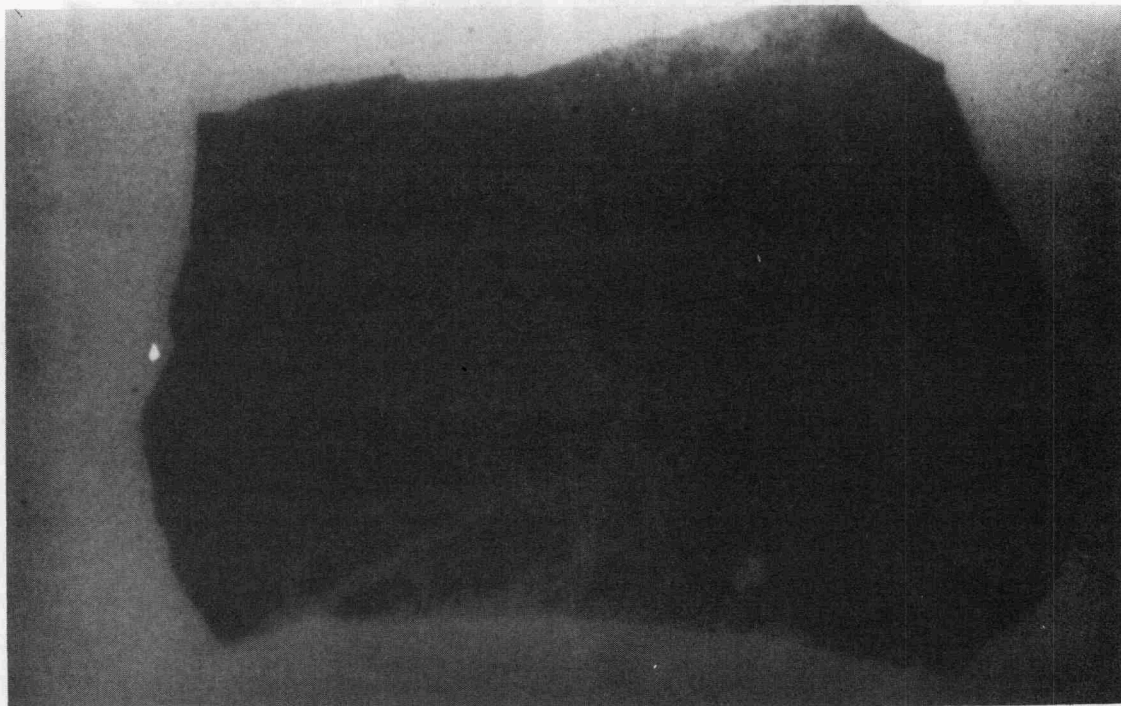


Fig. 6: Autoradiograph of metamict, complex Nb-Ta-Ti oxide showing numerous fractures with differential leaching along the fractures. The specimen is approximately 2.8 cms across.

look at the structures that suffer the radiation damage, can we make any generalizations? They have a number of common properties. One such property is that they have complex compositions and stoichiometries. This is particularly true in the niobium-tantalum-titanium oxides, and we would expect the same to be true in say, a titanate assemblage. The complex structures depend in part on the A-site cations. One way to look at it is that the structure that is formed depends on the average ionic radius of the A-site cations. This has been documented by Burcell¹³ in a recent paper in *Acta Crystallographica*, in which he looked at structural discontinuities in rutile and hollandite structures and showed the effect of variations in the cation compositions.

Another common property of metamict structures is that they exhibit mixed bonding, covalent and ionic. It is most important to observe that the bonds are quite directional¹⁴; and this is in keeping with the criteria of Naguib and Kelley¹⁴, in which ion bombardment results show that amorphization occurs for materials with an ionicity of less than 0.47. Their temperature ratio criteria and heat of atomization criteria are less easily applied to metamict minerals.

A third common property of metamict minerals, which has been pointed out by several people, among them Rustum Roy, is that the

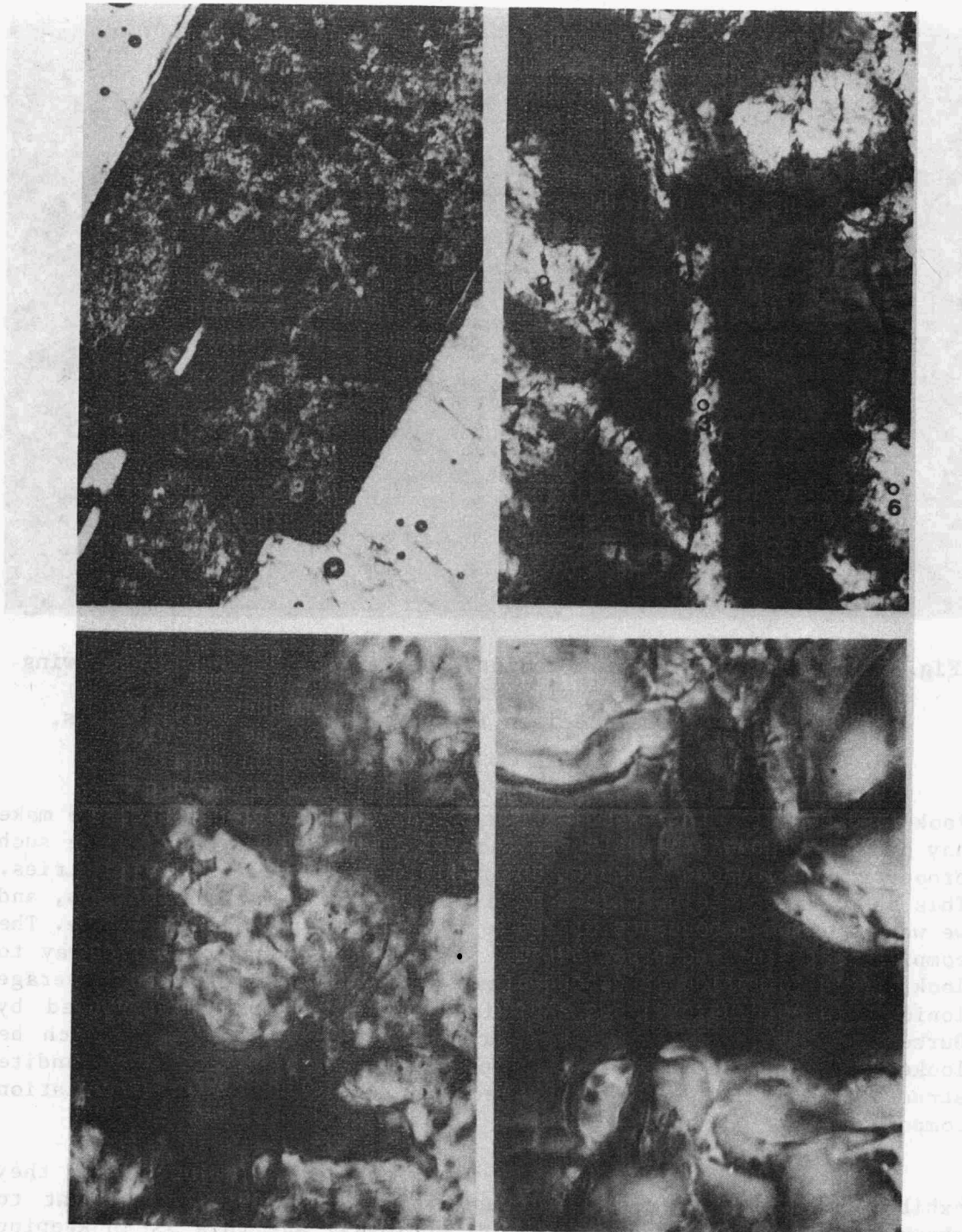


Fig. 7: Photomicrographs of blomstrandine (complex Nb-Ta-Ti oxide) showing microfractures and alteration (lighter areas). Scale: upper left, 1 cm = 150 microns; upper right, 1 cm = 40 microns; lower left, 1 cm = 15 microns; lower right, 1 cm = 6 microns.

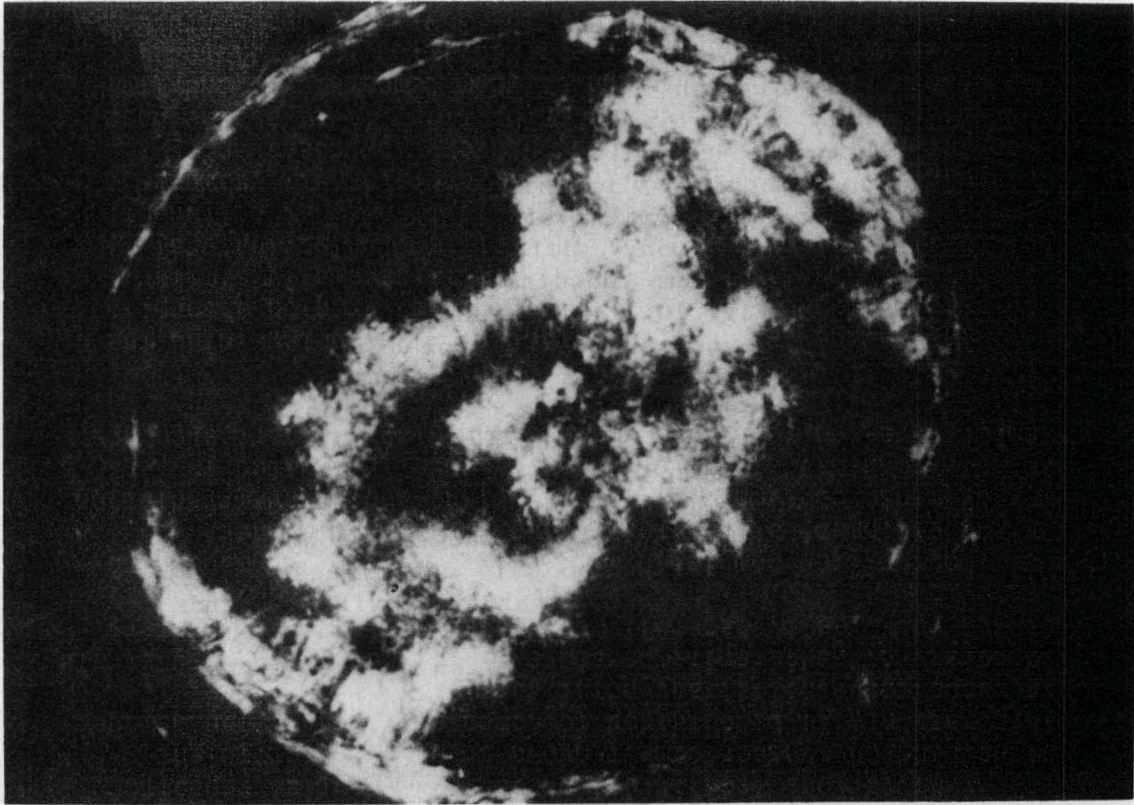


Fig. 8: Rare-earth fersmite spherulite in matrix of metamict polycrase viewed in transmitted light under crossed polars. The spherulite is approximately 80 micrometers in diameter¹⁵.



Fig. 9: Microfractures in a partially metamict microlite in transmitted light. The long axis of the print = 1.07 mm.

structures contain large cavities which can accommodate recoil nuclei or impurities, such as molecular water. The best examples of this are the thorium silicate dimorphs, monoclinic huttonite and tetragonal thorite. These ThSiO_4 dimorphs are quite interesting, because thorite is usually completely or partially metamict and is isostructural with zircon. Whereas huttonite has only been recognized in the crystalline state, and is isostructural with monazite, one of, I think, the premier candidates for the isolation of actinides. So here we have two different structures with very different behaviors in terms of radiation damage. The thorium coordination polyhedra for these two structures are shown in Fig. 10. The thorite structure has four apical oxygens which are at the corners of silicon-oxygen tetrahedra; down the *c* axis, the thorium coordination polyhedra are joined together by edge-sharing silicon-oxygen tetrahedra. The huttonite structure is similar, except that another silicon-oxygen tetrahedron has been squeezed in, so that the coordination number for huttonite is 9, as opposed to 8 for thorite. If we take a different view of the structure (Fig. 11) and look at the effect of the change in coordination number, we see large connected cavities, about 14 cubic angstroms in volume, in the thorite structure, and we see that the cavities do not exist in the huttonite structure. If we look at other structures that seem to be susceptible to radiation damage, we often find that they also have large structural cavities.

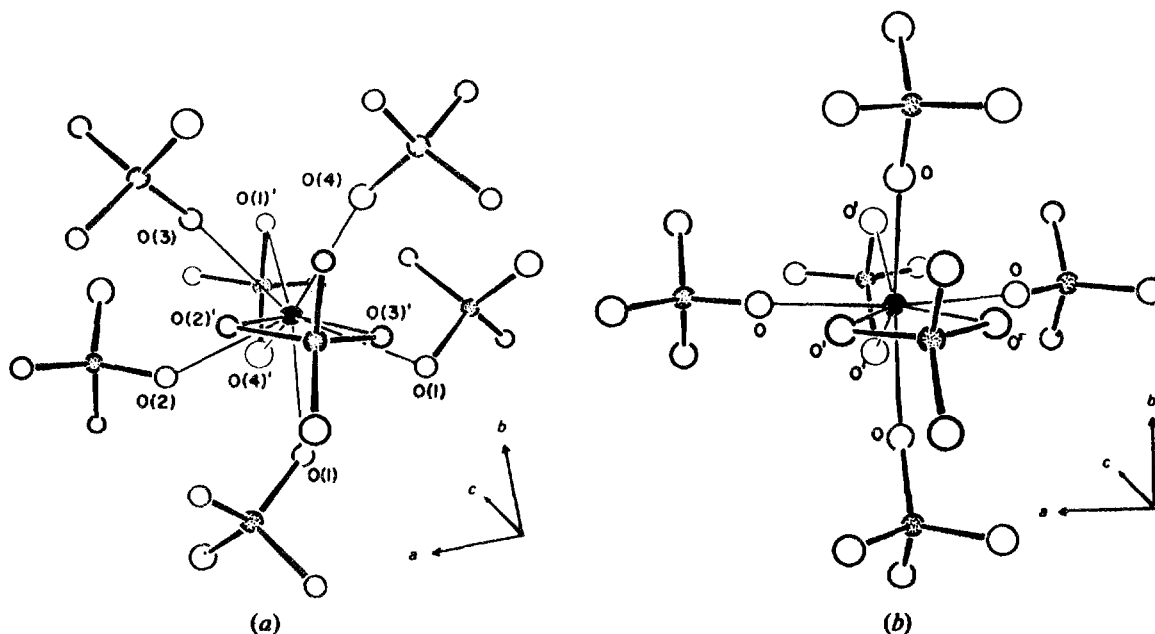


Fig. 10: The environments in (a) huttonite and (b) thorite. Open circles are oxygens, gray circles are silicon, and black ellipsoids are thorium. Axial and equatorial oxygen atoms have primed and unprimed labels, respectively¹⁶.

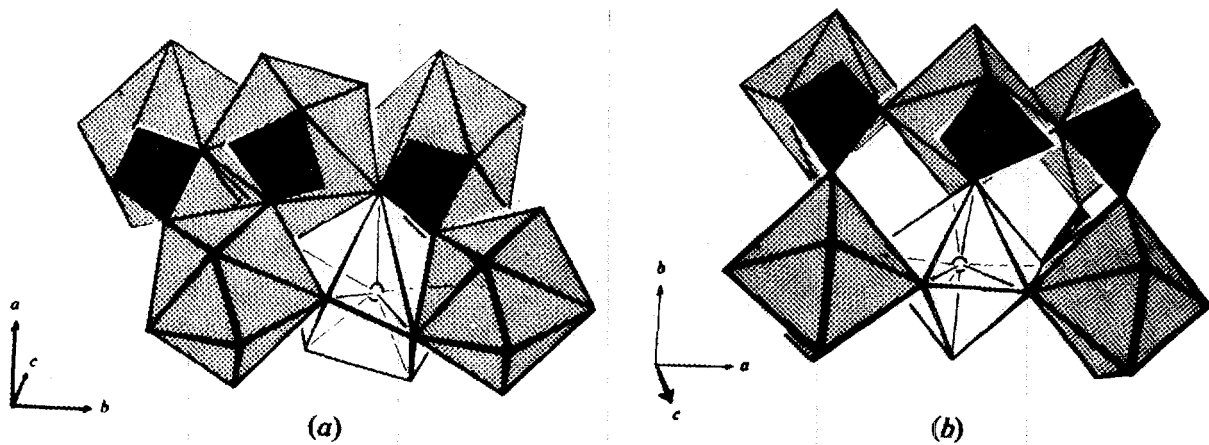


Fig. 11: Perspective polyhedral representation of the (a) huttonite, and (b) thorite structures. Darker tetrahedra are SiO_4 groups and lighter polyhedra are (a) ThO_9 and (b) ThO_8 groups⁴¹⁶.

A final generalization that I would like to make about metamict structures, if you would allow me to make the grossest possible generalization based on the data in the literature, is that I think the best value for the dose at which we expect to see metamictization would be approximately 10^{16} alphas/mg.

Commenting on these general properties, I would make the following point. The two desirable features of crystalline phases that will be used to isolate radionuclides are that (1) they have large voids into which we can put atoms, molecules, etc. (e.g. the hollandite structure), and (2) they are able to tolerate complex compositions, so that all of the waste nuclides may be placed in a limited number of structures. These two properties may, however, be features that make a structure more susceptible to radiation damage.

I would like to review some of the radiation damage experiments that have been reported or are in progress and make some brief comments on their limitations. First, I have already mentioned this, but it should be emphasized, we always have to keep in mind that the sum total of the radiation damage effects in the crystalline waste form will certainly be different from the radiation damage that occurs in a natural material, simply because of the types of radionuclides present in the structure. With that in mind, let me mention some of the approaches.

One approach has been to go to the rock record and collect the material that is a structural analogue to the waste form phase, calculate its total alpha dose, and x-ray it to see how crystalline it is. The difficulty here is that the material may have been annealed by some later process, so you have to demonstrate - and I would say that this is very difficult - that the total dose that we calculate has actually passed through the material that you are evaluating. Related to collecting a sample, calculating its total alpha dose and x-raying

it, we always have to compare the results of that study with laboratory experiments, or else I think that we are not presenting a clear picture of the process and effects. An example I can cite is a study of loparite, which is a cerium-niobium oxide with a perovskite structure (perovskite is CaTiO_3). Natural crystals of loparite have been studied, and the calculated alpha dose is 10^{18} alphas/mg. X-ray diffraction studies indicate that the material is still crystalline, so it looks good. The sample was annealed at 1200°C , and the structure contracted slightly. If the change in volume is converted to a change in density, the calculated change in density was 1.7 percent. If all of that change was due to radiation damage and accounted for all radiation-induced density change in the sample, that would be the maximum volume change expected for that particular dose. The 1.7 percent calculated density is then pointed to as evidence for the fact that volume changes will not be important. What I would simply point out is that if you go to another perovskite structure for which we have laboratory evidence, curium-aluminum oxide (CmAlO_3), there are experiments in which this perovskite structure has been doped with Cm-244, and the changes in density and unit cell parameters were measured as a function of dose. For essentially the same dose the density change was 6.5 percent. So, there are discrepancies. In addition, there are neutron bombardment experiments on an array of perovskite structures - a barium-titanium oxide, a potassium-niobium oxide, and a lead-titanium oxide. These experiments show that the fast neutron irradiation can stabilize higher-temperature cubic phases. This is all by way of pointing out that the natural material will not give us the final answer, that in any radiation damage process we can expect to have not only volume changes, but perhaps the stabilization of other crystalline structures and the associated volume changes.

Another approach is isotopic analysis in which a sample is collected, dated, and the date compared to the date that we expect, and I think that concordant dates based on isotopic evidence are persuasive evidence. I am quite impressed by efforts to use isotopic studies to indicate that a crystalline material is a closed system, but I would have to emphasize that, in demonstrating a closed system, we are dealing with a fairly restricted set of elements. We have to be able to assure the public that this work applies to the nuclides that are to be isolated. I would also like to mention that we always have to be concerned with the question of dose rate, and I think that no one has really addressed that question at all.

In summary, I would say that there are some critical questions that remain unanswered, and I would list four: (1) We do not know the structure of the metamict state. (2) We do not know the end result of radiation damage. (3) We do not know why some structures are more susceptible to radiation damage than others. (4) We do not know the effect of metamictization on critical waste form properties, particularly leachability. So, I would say that there is room for a lot of basic science that will be directly applicable to the evaluation of crystalline waste forms. As a last thought on this question of metamictization and leachability, I would guess - and it is only a

guess - that the variation of leachability between different phases in a crystalline phase assemblage will be greater than the variation caused by radiation damage in any single phase. If that guess is correct, that would relegate radiation damage to a second-order effect in terms of research priorities on crystalline waste forms.

DISCUSSION

UNIDENTIFIED QUESTIONER: What are some typical annealing temperatures, and what is the effect of the presence of water on annealing?

EWING: In general, annealing experiments are not conducted in the presence of water, so I cannot answer very specifically. I would say that it would have the effect of lowering the annealing temperature. In mineralogic studies of metamict minerals, if we look at the DTA curves as we heat them there is a loss of absorbed water in the range of 200 - 300°C and crystallization beginning at probably no lower than 400 - 450°C and continuing up to 900 - 1100°C. For silicate structures, referring to the work of Hurley when he was trying to use radiation damage in silicates as an age dating technique, the thing that put the skids under that whole project was that the radiation damage was so small and the natural annealing rate was so high that essentially none of the radiation damage was preserved.

UNIDENTIFIED QUESTIONER: I would like to disagree with you on something. Metamictization, as you showed in some of your slides, will evidently cause a large amount of microfracture, and since we know that this accumulation of leach sites will be proportional to the exposed surface area, if all of this is exposed to a solution, there could be changes of several orders of magnitude.

EWING: Two points: If you are thinking about the slides you have to realize that you are falling prey to the problem that there are lots of things that have happened to the samples since they were damaged, hydrothermal alteration being an important one for the ones that have come from pegmatite. So, certainly not everything that you see there is the result of radiation damage. The second point I would make is that the way I arrived at that guess, and it certainly could be wrong, is if you just look at a rock, which is a polycrystalline phase assemblage, the difference in the solubilities of those phases, as expressed by either their absence or presence, seems to be greater than differences I see in a single array of metamict minerals. So, it is just speculation.

HOWITT: There has been a great deal of work done on metamictization of quartz by radiolysis techniques, and I think your early statement that one can ignore the gamma dose and the electron dose is perhaps a little optimistic.

EWING: Right, and I would also add to that comment that there have been reports of changes in leach rates in a crystalline phase after it

has been put into a gamma field (someone else will have to speak of this - I just have the bare outline of the details.) If it is put into a gamma field and then immediately leached, there is an increase in the leachability; and if the leaching experiment is done in a gamma field, there is an increase in the leachability.

REFERENCES

1. Broegger, W. C. Amorf. Salmonsens Store Illustrede Konversation slexikon, 1, 742-742 (1893).
2. Hamberg, A. Die Radiaktiven Substanzen und die Geologische Forschung. Geol. For. Forh., 36, 31-96 (1914).
3. Holland, H. D. and Gottfried, D. The Effect of Nuclear Radiation on the Structure of Zircon. Acta. Cryst., 8, 291-300 (1955)
4. Bursill, L. A. and A. C. McLaren, Transmission Electron Microscope Study of Natural Radiation Damage in Zircon. Phys. Status Solidi, 13, 331-336 (1966)
5. Sommerauer, J. Die Chemisch-Physikalische Stabilität Natürlicher Zirkone und. Ihr U-(Th)-Ph System. Ph.D. Dissertation, Eidgenössischen Technischen Hochschule Zuerich (1976)
6. Cartz, L. and R. Fournelle. Metamict Zircon Formed by Heavy Ion Bombardment. Radiation Effects, 41, 211-217 (1979)
7. Crawford, J. H. and Wittels, M. C. A Review of Investigations of Radiation Effects in Covalent and Ionic Crystals. Radiation Effects, 8, 654-656 (1964)
8. Vance, E. R. and J. N. Boland. Fission Fragment Damage in Zircon Radiation Effects, 26, 135-139 (1975)
9. Pidgeon, R. T., J. O'Neill and L. Silver. Uranium and Lead Isotopic Stability in a Metamict Zircon under Experimental Hydrothermal Conditions. Science, 154, 1538-1540 (1966)
10. Mumpton, F. A. and Roy, R. Hydrothermal Stability Studies of the Zircon - Thorite Group Geochim. Cosmochim. Acta, 21, 217-238 (1961).
11. Krogh, T. E. and Davis, G. L. Alteration in Zircons and Differential Dissolution of Altered and Metamict Zircon, Annual Report of the Director of the Geophysical Laboratory, Carnegie Institution, 619-623 (1975)

12. Fleischer, R. L. Isotopic Disequilibrium of Uranium: Alpha-Recoil Damage and Preferential Solution Effects, Science, 207, 979-981.
13. Bursill, L. A. Structural Relationships between α -Gallia, Rutile, Hollandite, Psilomelane, Ramsdellite, and Gallium Titanate Type Structures. Acta Cryst., B35, 530-538 (1979)
14. Naguib, H. M. and R. Kelley. Criteria for Bombardment - Induced Structural Changes in Non-Metallic Solids, Radiation Effects, 25, 1-12 (1975).
15. Ewing, R. C. Spherulite Recrystallization of Metamict Polycrase, Science, 184, 561-562 (1974)
16. Taylor, M. and R. C. Ewing The Crystal Structures of the ThSiO_4 Polymorphs: Huttonite and Thorite, Acta Crystallographica, B34, 1074-1079 (1978)

RADIATION DAMAGE STUDIES ON NATURAL AND SYNTHETIC ROCK SALT*

P. W. Levy and K. J. Swyler

Brookhaven National Laboratory
Upton, New York 11973

ABSTRACT

Radiation damage studies are being made on natural rock salt from various localities, including potential repository sites, and on synthetic melt-grown crystals. Sufficient information will be obtained to compute the radiation damage in repository salt at any point as a function of time, temperature, canister temperature and radiation levels, strain in the rock, salt, backfill materials, and other parameters.

Most of the completed measurements have been made with unique equipment at BNL for making optical and other measurements on samples before, during, and after irradiation with 1- to 3-MeV electrons. Samples are irradiated in temperature-controlled chambers containing an inert exchange gas.

The damage is readily characterized by determining the radiation-induced F-center, colloid, and V-region absorption. Damage in synthetic and natural salt is generally similar, but the damage formation kinetics differ. Also, natural samples from various localities exhibit somewhat different damage properties. In both natural and synthetic samples, F-center absorption is observed at very low doses and increases monotonically to a "saturation" level as the dose increases. The level is high at room temperature, and it decreases monotonically as the irradiation temperature is increased. It is negligible in the 300-350°C temperature region. At temperatures where sodium metal colloid particles are formed, the colloid absorption vs. dose curves contain both induction and rapid growth regions. The onset of rapid colloid growth occurs as the F-center curves reach saturation. Colloid growth curves follow a $(\text{time})^n$, or $(\text{dose})^n$, behavior. The growth rate is low or zero at 100°C, has a maximum at 150-175°C, and is negligible near 250°C. Plastically deforming samples prior to irradiation reduces the induction period; it is negligible after a 10 to 12% deformation.

*Research supported by the Department of Energy Office of Nuclear Waste Isolation, operated by Battelle Institute, Columbus, Ohio, and the Department of Energy Division of Basic Energy Sciences, under contract DE-AC02-76CH00016.

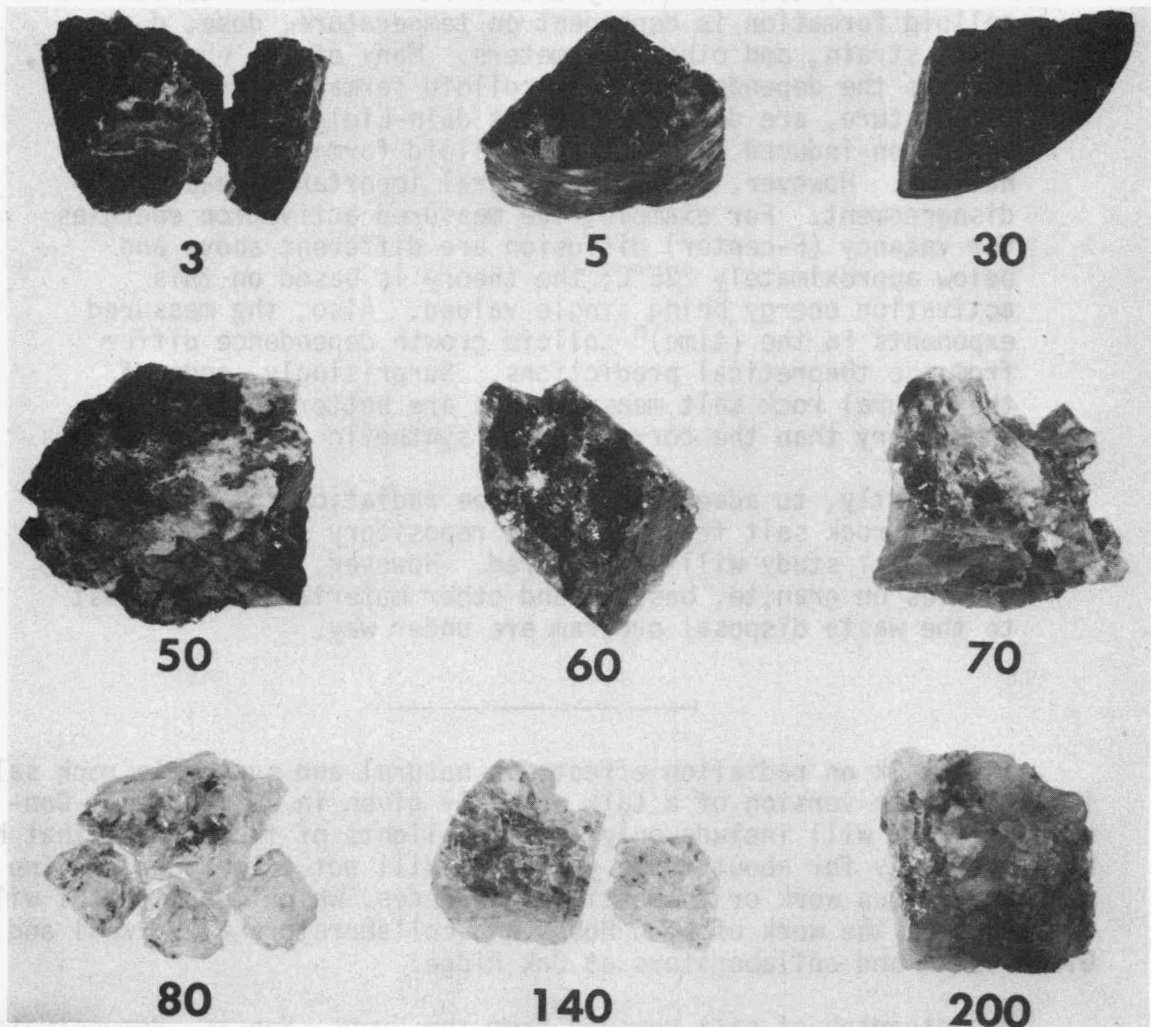
In both natural and synthetic samples, the F-center and colloid formation is dependent on temperature, dose, dose rate, strain, and other parameters. Many of the observations, such as the dependence of the colloid formation rate on temperature, are described by the Jain-Lidiard theory for radiation-induced F-center and colloid formation in alkali halides. However, there are several important areas of disagreement. For example, the measured activation energies for vacancy (F-center) diffusion are different above and below approximately 225°C; the theory is based on this activation energy being single valued. Also, the measured exponents in the (time)ⁿ colloid growth dependence differ from the theoretical predictions. Surprisingly, some of the natural rock salt measurements are better described by the theory than the corresponding synthetic salt measurements.

Lastly, to adequately describe radiation damage in natural rock salt from potential repository sites, appreciable additional study will be required. However, radiation damage studies on granite, basalt, and other materials of interest to the waste disposal program are under way.

This talk on radiation effects in natural and synthetic rock salt is a 15-minute version of a talk normally given in 40 minutes. Consequently, it will include only the high-lights of the studies that have been under way for about three years. I will not attempt to outline any of the previous work or to mention references, which means that I will not describe the work of Lynn Hobbs and collaborators at Harwell and Glenn Jenks and collaborators at Oak Ridge.

A photograph of salt removed from the Lyons, Kansas, demonstration project after the fuel element had been removed is shown in Fig. 1. I will sketch the changes which this rock salt undergoes as it is irradiated. Salt which was about 200 cm from the fuel element, and received a dose about 10^4 to 10^5 R, is quite normal, although slightly colored. Salt which was about 3 cm from the fuel element, and received a dose between 10^7 and 10^8 R, is quite brittle and has all of the characteristics of severely radiation damaged NaCl.

All of the measurements which I am going to describe have been made with the unique equipment, shown schematically in Fig. 2, for making optical and other radiation damage measurements during irradiation with 1-3 MeV electrons. Basically, this is a 13-meter-long spectrophotometer, which measures absorption and luminescence in a sample while it is being irradiated with electrons. Only optical absorption data will be given in this talk although all of the samples emit strong luminescence. Figure 3 shows the irradiation chamber. It contains fused silica windows to permit the spectrophotometer light to enter one side and come out the other. Electrons enter and leave through thin Havar



**APPROXIMATE DISTANCE
FROM FUEL ELEMENT, cm.**

Figure 1. Samples of rock salt, removed from the Lyons, Kansas, demonstration project, after irradiation by a fuel element. The sample which was 200 cm from the fuel element received a dose of 10^4 to 10^5 R; the sample at 3 cm a dose of 10^7 to 10^8 R.

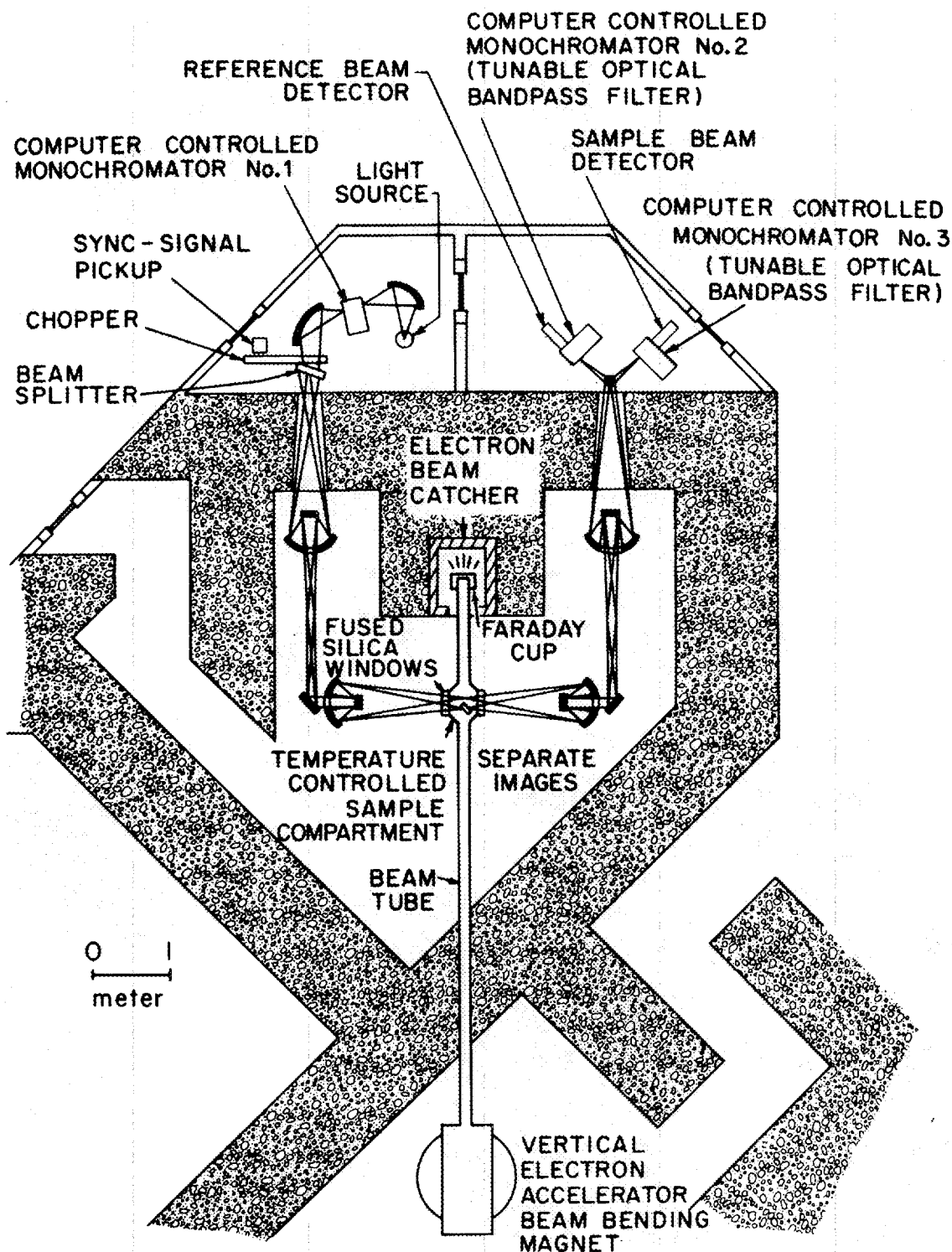


Figure 2. Equipment for making optical absorption, luminescence and other measurements on samples while they are being irradiated with 1 to 3 MeV electrons.

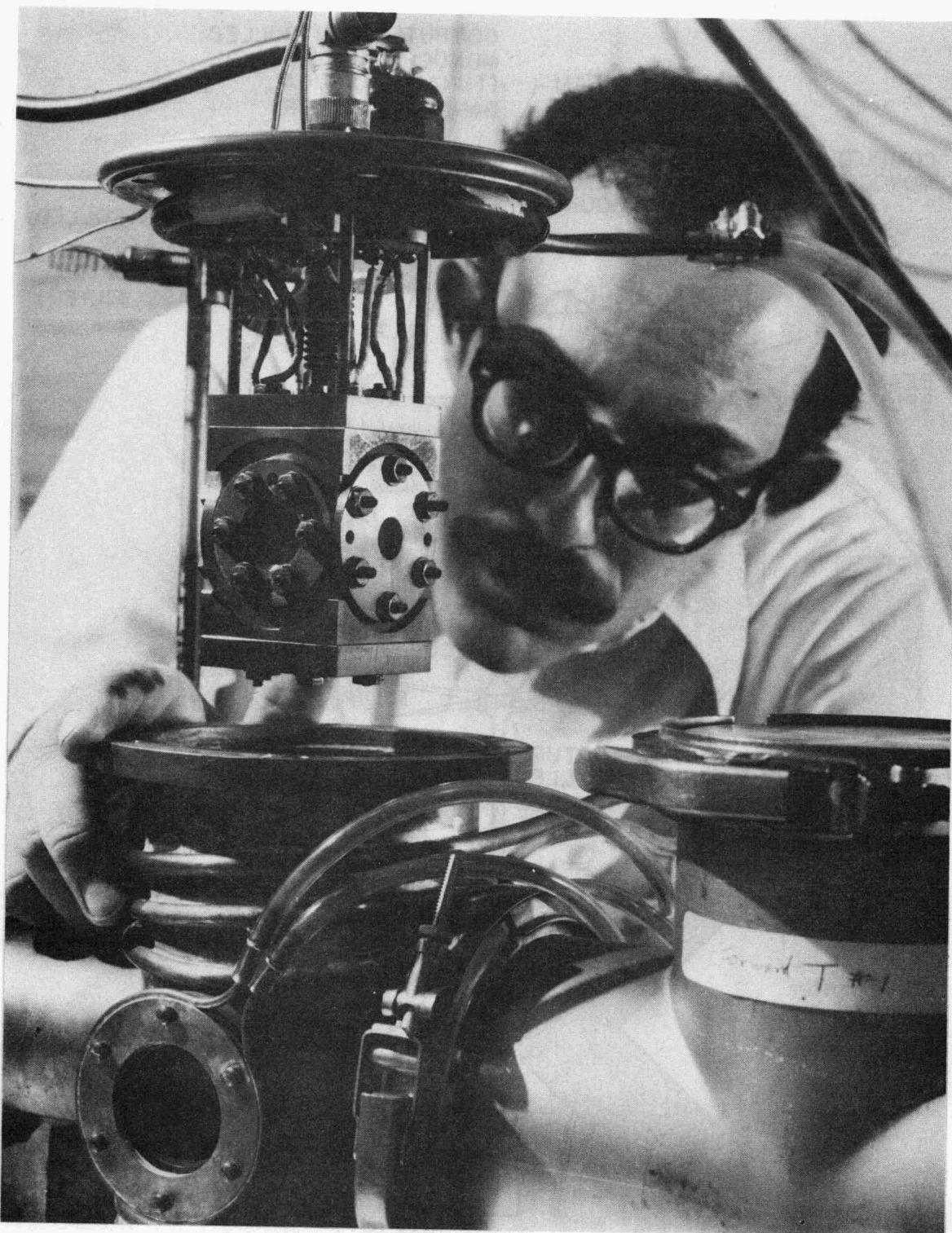


Figure 3. The irradiation chamber used for optical measurements on samples during electron irradiation. The chamber contains an inert exchange gas and the temperature is controlled electronically.

windows. Figure 3 also shows my chief collaborator, Karl Swyler, who has now left our group to join a new Division at Brookhaven supported by the Nuclear Regulatory Commission. Figure 4 shows a number of things. First, it illustrates some of the types of measurements we make. The optical absorption in the sample is shown as a function of photon energy. (3.0 eV is roughly equivalent to 400 nm, and 1.5 eV is roughly equivalent to 800 nm.) Each one of these curves represents a measured absorption spectrum. The numbers represent each of a series of different measurements. We can make one measurement every 40 sec while the sample is being irradiated with electrons. Most measurements reported were made at a dose rate of 1.2×10^8 rad/hr.

The basic phenomenology of radiation effects in both natural and synthetic rock salt is illustrated by Fig. 4. The absorption that corresponds to the F-center band is a measure of the number of negative ion vacancies induced in the crystal as a function of dose. The absorption band marked "colloid" represents the nucleation and growth of colloidal particles of sodium metal. Colloid formation does not occur, in this data, until the F center, or the negative ion vacancy, concentration has reached a saturation level. For larger doses the intensity increases quite rapidly. In other words, it is described by a classical nucleation and growth curve. The F-center absorption is

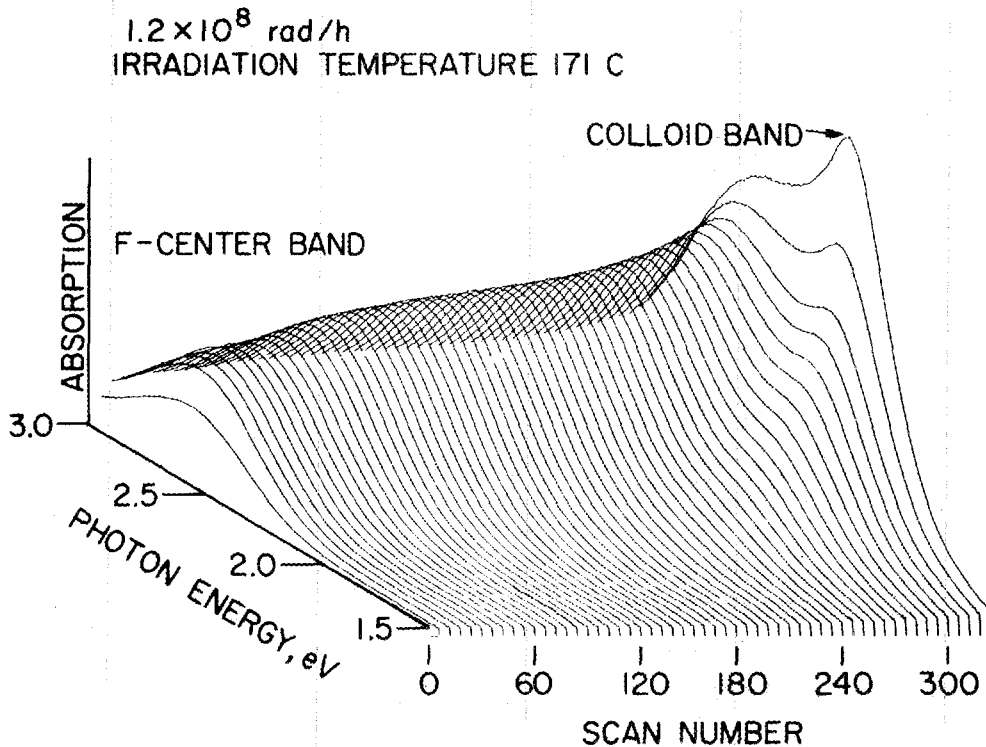


Figure 4. Spectra recorded during irradiation showing the F-center growth and the nucleation and growth of colloids in synthetic NaCl. Spectra can be recorded as often as every 40 sec (90 per hour). Not all recorded spectra are shown.

superimposed on the colloid absorption and vice-versa. We have developed a procedure for separating these two bands. Later, data on the size of the radiation induced colloid particles will be given which was obtained by fitting resolved colloid band spectra with a modified version of Mie theory.

The remainder of the talk will illustrate how the growth of the F-center and colloid bands depend on a number of parameters. Figure 5 shows typical F-center growth in natural rock salt from Drill Hole AEC-8. This hole is very close to the WIPP site, which is AEC-9. This figure illustrates one principal feature. As the radiation progresses the F-centers increase to a saturation value and as the irradiation temperature increases this saturation value decreases.

Figure 6 shows, again for AEC-8 (these data and the data shown in Fig. 5 were developed from the same measurements), the growth of the colloid band as a function of irradiation time. The nucleation and growth character is quite apparent.

Among the questions we are investigating is the following: Do natural rock salt samples from different localities develop radiation damage at different rates, or are they in some other way different? Figure 7 is what I could call an honest plot. It shows the F-center formation in two samples from the WIPP area, one from Alt Aussee in Austria, and one from Lyons. If I were to show you only the low dose part of the figure, the differences would appear very large. There are differences in the rock salt from different localities, but all

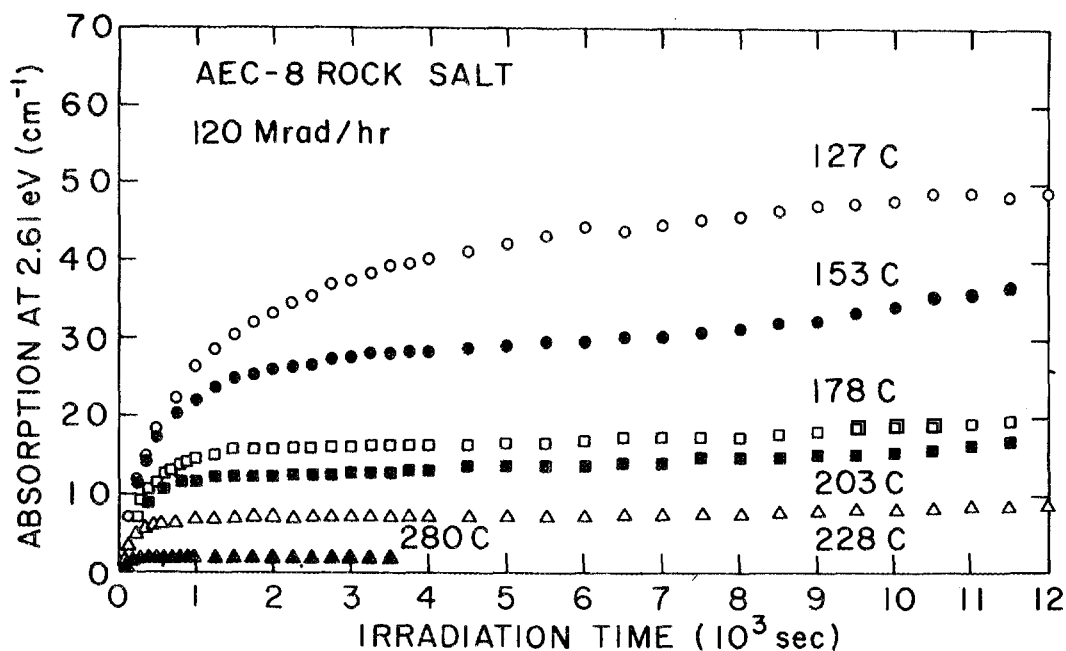


Figure 5. Typical F-center growth in natural rock salt at the indicated temperatures. This data, and that in Fig. 6, has not been corrected for F and colloid band overlap.

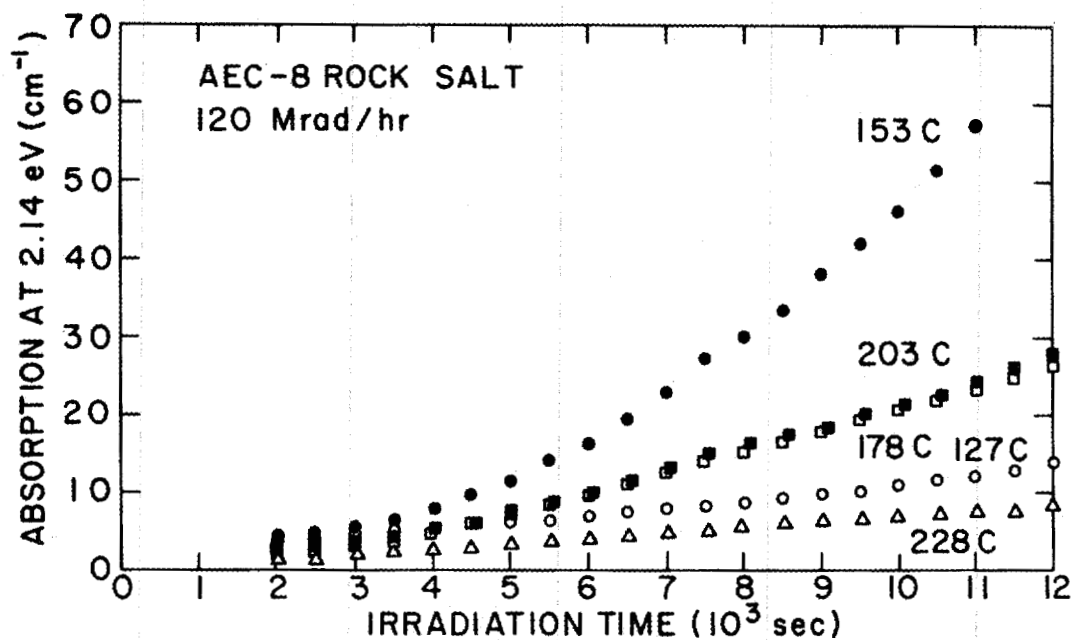


Figure 6. Typical nucleation and growth curves for colloid absorption in the same sample, and recorded at the same time, as used for Fig. 5. Note that the maximum colloid formation rate occurs around 150°C.

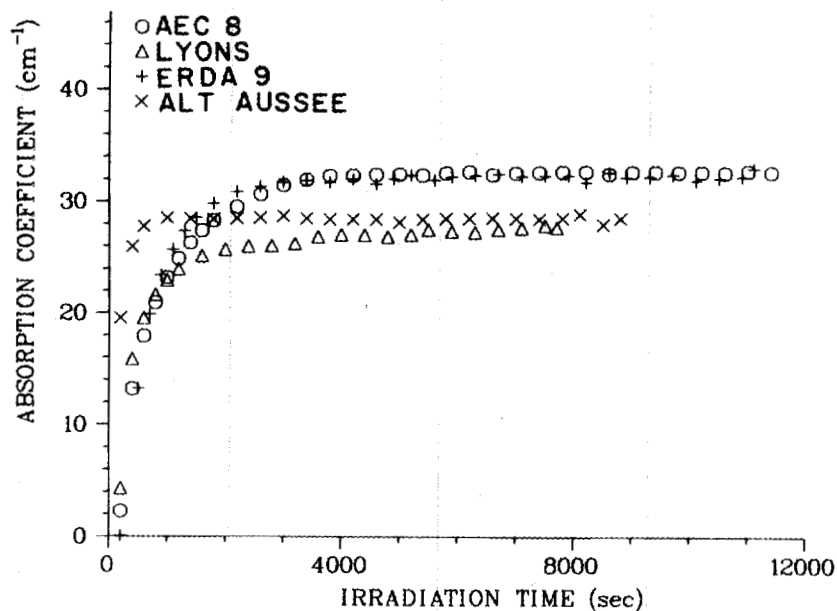


Figure 7. Typical F-center growth, at 150°C, in natural rock salt from several localities. This data has been corrected for F and colloid band overlap.

exhibit the basic saturation-type growth curve. Figure 8 shows the colloid growth in synthetic sodium chloride. It is included to illustrate the strong temperature dependence of the colloid growth in synthetic rock salt. We do not yet have equally detailed data for natural rock salt. Figure 9 shows comparable colloid growth data for the four natural rock salt samples for which F-center data were shown in Fig. 7. Again, the colloid growth behavior is the same in the sense that these curves are quite linear, at least at long irradiation times on this log-log plot. In other words, all of the colloid growth data follows a $(\text{time})^n$ or $(\text{dose})^n$ type behavior. I mentioned before that we were able to obtain information on the colloid properties by analyzing the shape of the colloid absorption band. The data in Fig. 10, for synthetic sodium chloride, shows just what you would expect. Namely, there is a strong temperature dependence; also, we observe colloids at the smallest colloid radius which we can detect and as the irradiation progresses the colloid radii increase. At very large doses the colloid absorption is too large to measure with the present equipment.

One of the reasons for showing Figure 10 was to provide a background for Figure 11, which shows colloid formation in natural rock salt. This demonstrates one of the principal ways, we have discovered, in which natural rock salt differs from synthetic rock salt. At the lowest dose producing colloids, a given colloid radius is obtained. As the irradiation continues, usually with a very rapid increase in colloid absorption, the colloid absorption band shape does not change. This

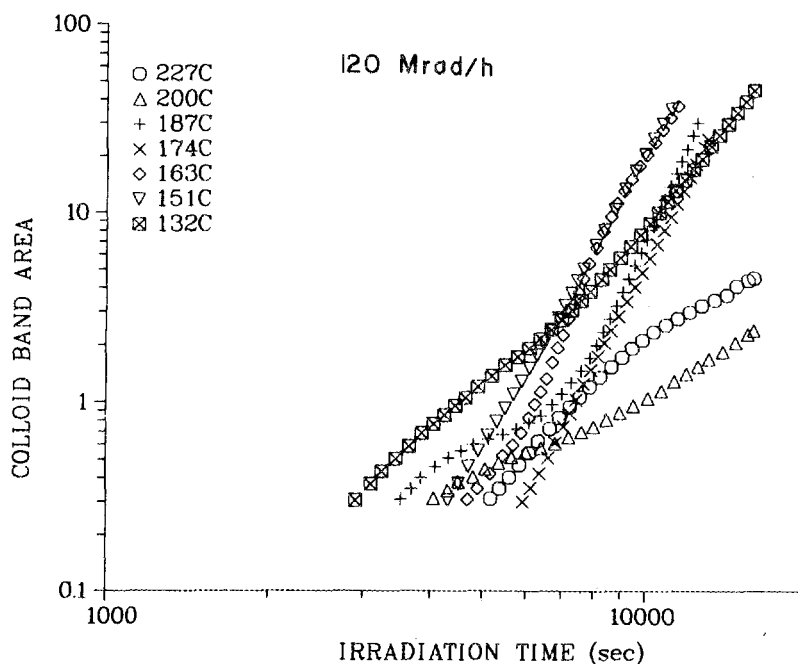


Figure 8. Typical colloid band growth in synthetic NaCl, recorded at various temperatures, and plotted on a log-log plot. At high irradiation times these curves are well described by a t^n relation.

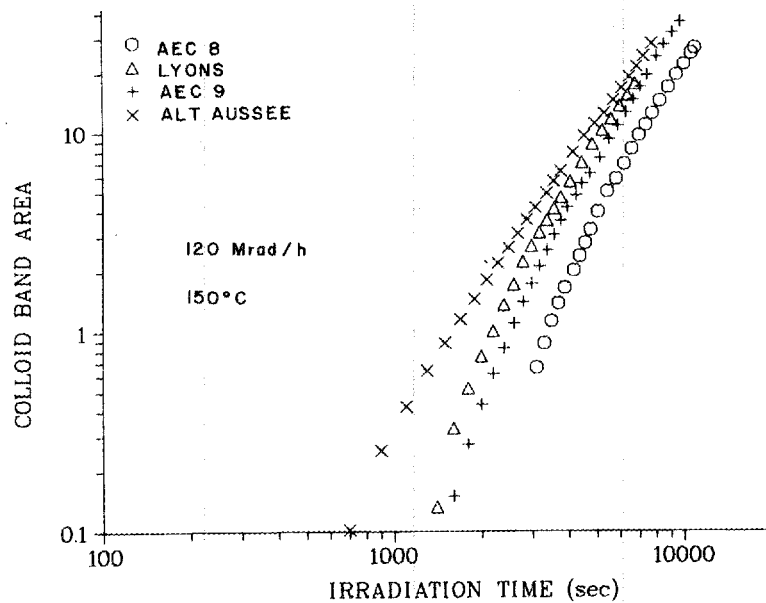


Figure 9. Typical colloid band growth, at 150°C, in natural rock salt recorded at the same time, and on the same sample, as used for Fig. 7. At large irradiation times these curves are well fitted by a t^n relation.

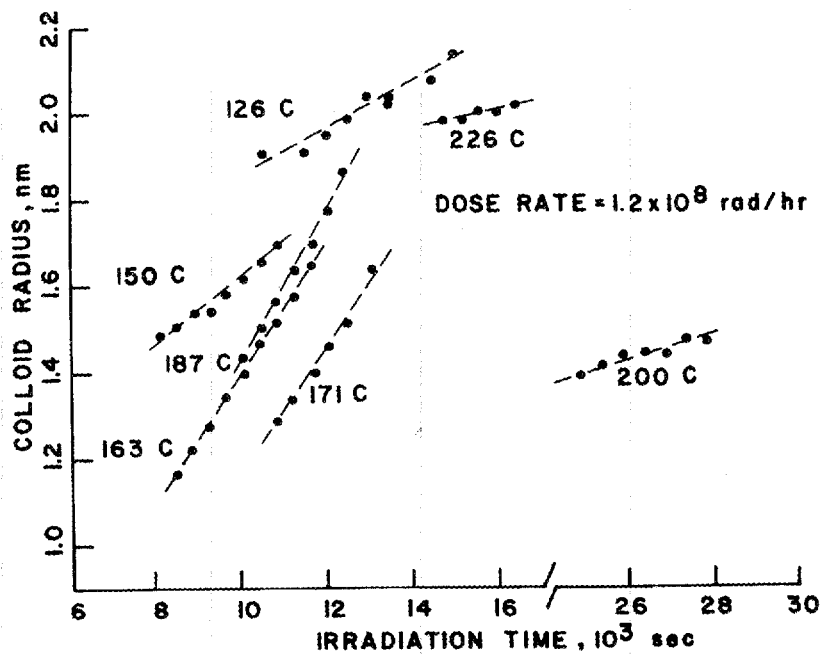


Figure 10. Colloid radius vs. irradiation time for synthetic NaCl irradiated at various temperatures. The colloid radius increases with increasing dose.

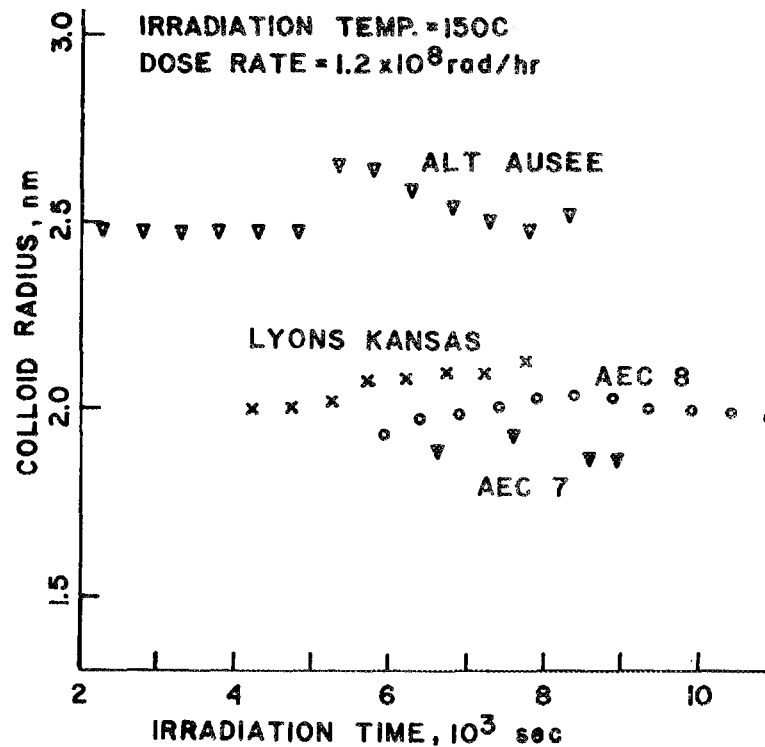


Figure 11. Colloid radius vs. irradiation times in various natural rock salt samples. The colloid radius does not increase with dose. However, the total colloid absorption, i.e. number of colloid particles, is increasing rapidly.

means that, as far as our measurements show, the colloids which appear suddenly at a given dose have a fixed radius; and, as the number of colloid particles continues to increase quite rapidly, the colloid particles do not appear to increase in radius.

The data shown in Fig. 12, which has been observed numerous times, is included to demonstrate how colloid growth depends on strain. This figure shows colloid formation in AEC-8 rock salt which has not been subjected to any strain in the laboratory. By comparing this data with similar data for synthetic samples, which presumably are unstrained, or natural samples which presumably have had the strain removed by heating, it appears that this sample contains 3 or 4% natural strain. This type of data can be the basis of a method for mapping out the natural strain in a salt repository. Clearly, the effect of strain on colloid formation is very pronounced. As the strain is increased, the colloid formation induction period decreases and at large strains is essentially zero. Those of you who have worked with classical nucleation and growth phenomena are familiar with the fact that this type of behavior can be explained in two ways: Either there is a very large increase in the rate of nucleation processes or alternatively, something has happened to obviate or remove the nucleation step.

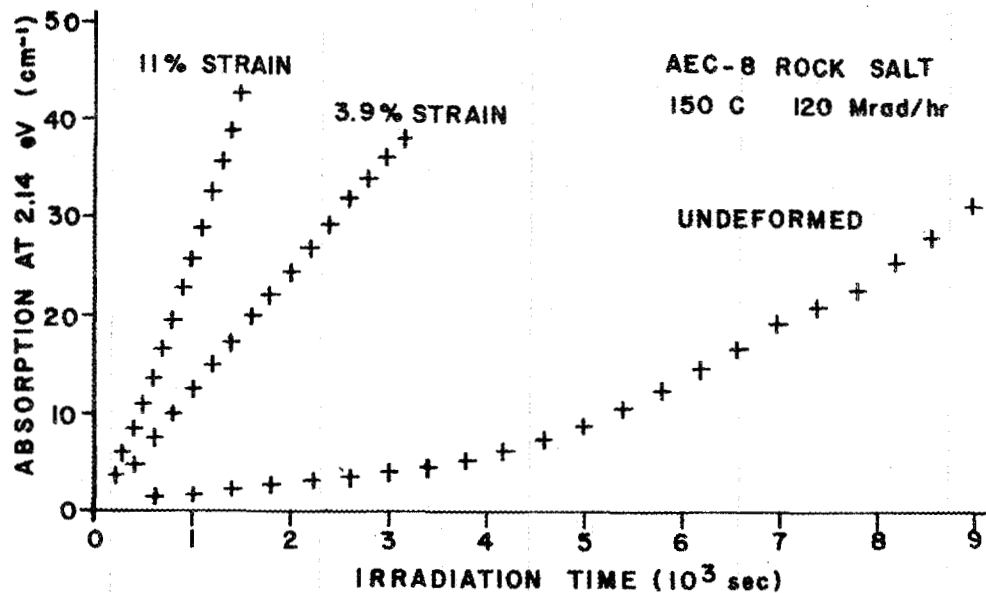


Figure 12. Influence of strain, applied prior to irradiation, on the colloid formation rate. The sample marked "undeformed" contains 3 or 4 percent "natural" strain.

I want to discuss briefly the correspondence between these measurements and a theory proposed by Jain and Lidiard [Phil. Mag. 35, 245-290 (1977)]. On the basis of data obtained by electron microscope work, primarily at Harwell, Alan Lidiard and a graduate student, Uma Jain, developed a theory for colloid formation in natural rock salt. I should really say for any rock salt, but it seems to apply better for natural rock salt than for synthetic rock salt. There is simply not time to do more than sketch how this works. I have chosen to do this by showing, in Fig. 13, a little of their theory for F-center formation. Basically, they write down conservation equations for the F-center formation as well as the corresponding interstitial center formation. The F-centers are formed by radiation, lost at dislocations and colloids, and lost by F- and H-center recombination. There are corresponding terms for the interstitial centers. The word equations in the top half of Fig. 13 are expressed mathematically in the middle of the figure. The solution of these equations is obtained by making a number of approximations. The most important of these is the absence of nucleation processes. Their theory starts with the assumption that the colloids are nucleated. The equation they obtain for the F-center growth curve is unique: it is of a typical saturating exponential curve but to the square root power.

Figure 14 shows F-center formation in synthetic rock salt. It is very similar to curves for natural rock salt (Fig. 5); but it is included to point out that many of the growth curves contain structure in the low dose region. It is qualitatively impossible for the Jain-Lidiard expression to fit this type of data. In other words, many of the synthetic rock salt growth curves cannot be fitted by an expression of this type. However, Fig. 15 shows a fit of the Jain-Lidiard expression

Jain-Lidiard Theory of Radiation Induced

F Center and Colloid Growth in NaCl*

$$\frac{d}{dt} \begin{pmatrix} \text{F} \\ \text{center} \\ \text{conc.} \end{pmatrix} = \begin{pmatrix} \text{F center formation} \\ \text{by radiation and} \\ \text{diffusion from colloids} \end{pmatrix} - \begin{pmatrix} \text{F center capture} \\ \text{by dislocations} \\ \text{and colloids} \end{pmatrix} - \begin{pmatrix} \text{F and H} \\ \text{center} \\ \text{recombination} \end{pmatrix}$$

$$\frac{d}{dt} \begin{pmatrix} \text{H} \\ \text{center} \\ \text{conc.} \end{pmatrix} = \begin{pmatrix} \text{H center formation} \\ \text{by radiation and} \\ \text{diffusion from colloids} \end{pmatrix} - \begin{pmatrix} \text{H center capture} \\ \text{by dislocations} \\ \text{and colloids} \end{pmatrix} - \begin{pmatrix} \text{F and H} \\ \text{center} \\ \text{recombination} \end{pmatrix}$$

$$\frac{dC_F}{dt} = K' - K_1 C_F - K_2 C_F C_H$$

$$\frac{dC_H}{dt} = K - K_3 C_H - K_2 C_F C_H$$

Assuming that interstitials quickly reach equilibrium,

i.e. $\frac{dC_H}{dt} = 0$ and making several approximations

$$C_F = C_F^{\text{saturation}} [1 - \exp(-2K_1 t)]^{1/2}$$

*Phil. Mag. 35, 245-290 (1977).

Figure 13. A "sketch" of the F-center portion of the Jain-Lidiard theory of F-center and colloid growth in NaCl.

to natural rock salt data. The agreement is very good. Note that we have plotted the square of the F-center concentration to include the square root dependence. There is some systematic fluctuation in this curve which is an artifact of the F-center colloid-band resolution procedure. These fluctuations are exaggerated because of the nature of the plot.

Table 1 contains a list of various predictions of the Jain-Lidiard theory. First, they predict a monotonic increase of F-centers to a saturation level. This occurs in both the synthetic sodium chloride and in the natural rock salt data. It is predicted that the F-center saturation level is independent of crystal source (type) and strain. In both materials a (dose rate)^{1/2} dependence (which I have not shown

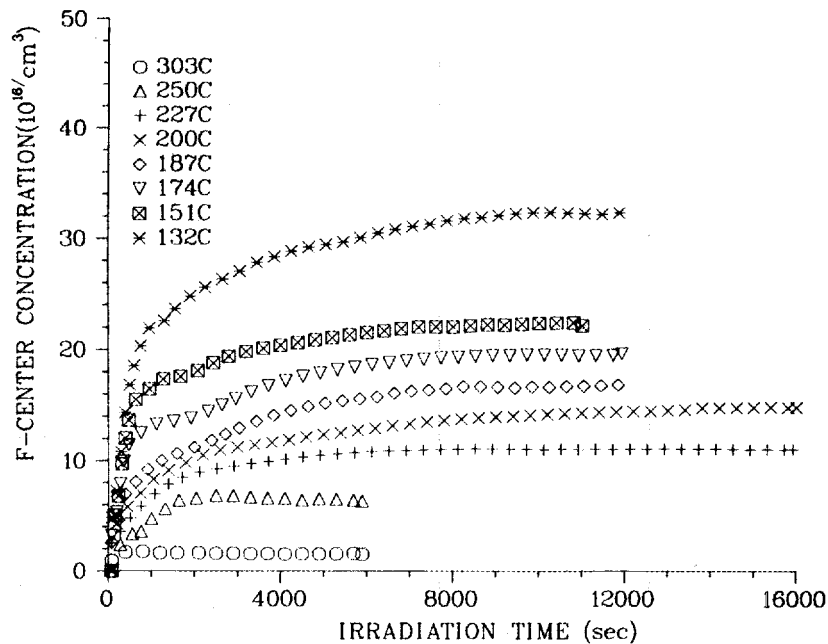


Figure 14. F-center growth in synthetic NaCl at various temperatures. Note the "structure" in some of the curves at low irradiation times. This is not in accord with the Jain-Lidiard theory.

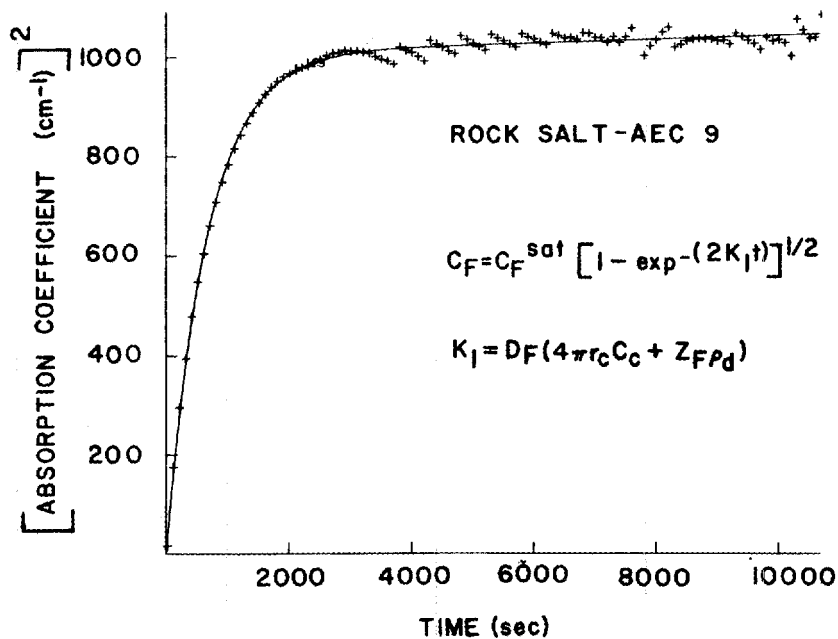


Figure 15. A comparison of the Jain-Lidiard theory with F-center growth in natural rock salt. The discontinuities are an artifact introduced by the procedure for separating the overlapping F and colloid bands.

TABLE 1
SELECTED COMPARISONS WITH JAIN-LIDIARD THEORY

Theory	Synthetic NaCl	Natural Rock Salt
F-centers increase monotonically to a "saturation" level	observed	observed
F-saturation level independent of crystal source and strain	observed	observed
F-saturation level varies as (dose rate) ^{1/2}	observed	observed
Activation energy obtained from F-center saturation single valued and ≈0.4 eV	0.2 eV observed below ≈250C and 0.9 eV above ≈250C	0.3 eV observed below ≈225C and roughly 0.9 eV above ≈225
Colloid formation in a restricted temp. range	observed	observed
Colloid formation not observed at low dose rate	not studied	not studied
Colloid induction period dependent on dislocation density	observed: induction period reduced by prior strain	observed: induction period reduced by prior strain
Colloid formation rate in the t ² to t ^{3/2} range	t ⁴ to t ⁵ observed in unstrained crystals, t ^{1.2} to t ^{2.3} observed in highly strained crystals	t ^{1.7} to t ^{2.1} observed in crystals not additionally strained

data for) is observed. However, there is a fundamental disagreement regarding activation energies for F-center diffusion. These can be obtained from the measured F-center saturation levels. The theory is based on a single activation energy of 0.4 eV for F-center diffusion. We obtain two activation energies, one below 250 or 225°C, and another above. Neither of them agree with the 0.4 eV, and this disagreement occurs both in the synthetic rock salt and the natural rock salt. There is one point which I did not emphasize as strongly as I should have. In the curve showing colloid growth at different temperatures, the colloid growth was low at low temperatures, went to a maximum, and then dropped to a low value. This is in accord with theory. They also predict that colloid formation will not be observed at low dose rates. This we have not studied in detail. However, I do not believe that we are going to agree with that prediction. Another prediction, the colloid induction period is dependent on dislocation density. Clearly, this is observed.

There is another point on which theory and measurement do not agree. The theory predicts that the colloid formation rate at long irradiation times will follow a t^2 to the $t^{3/2}$ dependence. We observe a t^4 to t^5 dependence in unstrained crystals and a $t^{1.2}$ to $t^{2.3}$ dependence in highly strained synthetic crystals; a $t^{1.7}$ to $t^{2.1}$ dependence is observed in natural crystals. These dependences are quite important if you want to predict the amount of colloidal sodium formed in repository rock salt as a function of time after it has been exposed to radiation from a waste canister.

Outlined above are some of the studies that we have made on natural and synthetic rock salt. A lot has been learned about the radiation damage processes in natural and synthetic rock salt. However, clearly the job has not been finished. For example, we do not know if the radiation damage in natural rock salt from one locality differs appreciably from that in salt from other localities. Finally, we do not have the information needed to determine the dose rate dependence. There is evidence that the damage increases, on a unit dose basis, as the dose rate decreases. The dose rate dependence could be one of the most important factors controlling the damage formed in an actual repository.

The work on rock salt has been going on for almost three years. Similar projects are being started on other materials. Primarily, these are minerals from other waste disposal sites under consideration, namely, granite and basalt. Hopefully, we will find one or more granite or basalt mineral that can be studied in sufficient detail to provide all of the information needed for both repository selection and design. Also, this information should be useful for other purposes, such as the selection or design of waste forms.

DISCUSSION

BOATNER: I noticed in the graph where you compared the colloid formation rates for strained and unstrained crystals, that in the unstrained crystals the curves start out with a low or mild slope and then begin to increase in slope. Surely the formation of colloids in the crystal itself must increase the overall average strain in the crystal, I would think. Can that be used to account for the corresponding increase that you see later in the slope of the curve?

LEVY: One of the things I did not discuss in detail was the process by which colloids are formed. The process is believed to be the diffusion of vacancies to the colloid nuclei. This leaves behind sodium atoms on the original crystal lattice sites, and one finds that sodium on original lattice sites has a lattice constant which is approximately 11% larger than that of metallic sodium. So one would not think it would be exerting much of a strain on the lattice. If it does exert any kind of a strain at all, it would be some sort of a tension due to the fact that the colloid particle would actually be smaller than the space that it is supposed to occupy.

POHL: What maximum sodium metal fraction do you expect in the sodium chloride after it has received something of the order of 10^{10} rads, which is what we would get right next to one of the old-fashioned model waste canisters? Where does all the chlorine go?

LEVY: Thanks for mentioning the chlorine. I really intended to say that that is one of the principal scientific questions which we have not solved. We do not know for sure where the chlorine goes. The people at Harwell would like to think that the chlorine forms some sort of platelike or sheetlike arrangement, accompanying dislocation climb. We do not have any evidence for that from our studies. There is some electron microscope evidence for it, but it is not very clear.

As to the sodium metal fraction, if I simply extrapolate the data to the dose expected adjacent to the canisters, and try to be very pessimistic, I obtain something like 1% colloid. If I want to be extremely pessimistic I can make it 10%. If I want to be real optimistic from the point of view of minimizing the colloid formation, then it is in the range of 0.01% to 1%. I have answered your question this way because I want to emphasize that we do not have the ability to predict these levels accurately at the present time. One of the principal reasons for this is that we do not have sufficiently good dose rate data.

ABRAHAM: What happens if you try to anneal out the colors and F-centers and then try to do the irradiation again? Is there reversibility?

LEVY: Consider the case when we irradiate a sample in our apparatus, see the colloids form and then turn the beam off. Usually, there is appreciably F-center decay immediately. The colloids decay much more slowly. Next raise the temperature 50° . This will cause a very large reduction in the observed colloid concentration. When we turn the beam on again, we get an immediate, very rapid restoration of the colloid concentration. In fact, repeated cycles of the process I have just described appear to have the same effect as straining the crystal. In other words, turning the beam on and off or cycling the temperature would appear to, in some way, create nuclei or enhance the nuclei formation rate for colloids. Again, this is an area which I probably could have included in my list of things we do not understand. Also, there are exceedingly interesting transient effects associated with these processes. I think one thing is clear: We are dealing with a diffusing entity which is present only during irradiation, in addition to the diffusing entities which are present when the irradiation is not present.

A REVIEW OF HEAT DISSIPATION IN GEOLOGIC MEDIA*

R. O. Pohl and J. W. Vandersande**

Laboratory of Atomic and Solid State Physics
Cornell University, Ithaca, New York 14853, USA

ABSTRACT

Existing data on the thermal conductivity of various rocks, e.g., rocksalt, granite, basalt, etc., will be critically reviewed, with the objective of determining the likely range of conductivity to be expected in a geologic repository.

Research carried out at Cornell on the thermal conductivity of rocksalt from different sources, and from different horizons at the WIPP site in New Mexico will be described, as well as the search for the influence of ionizing radiation and of heat treatment.

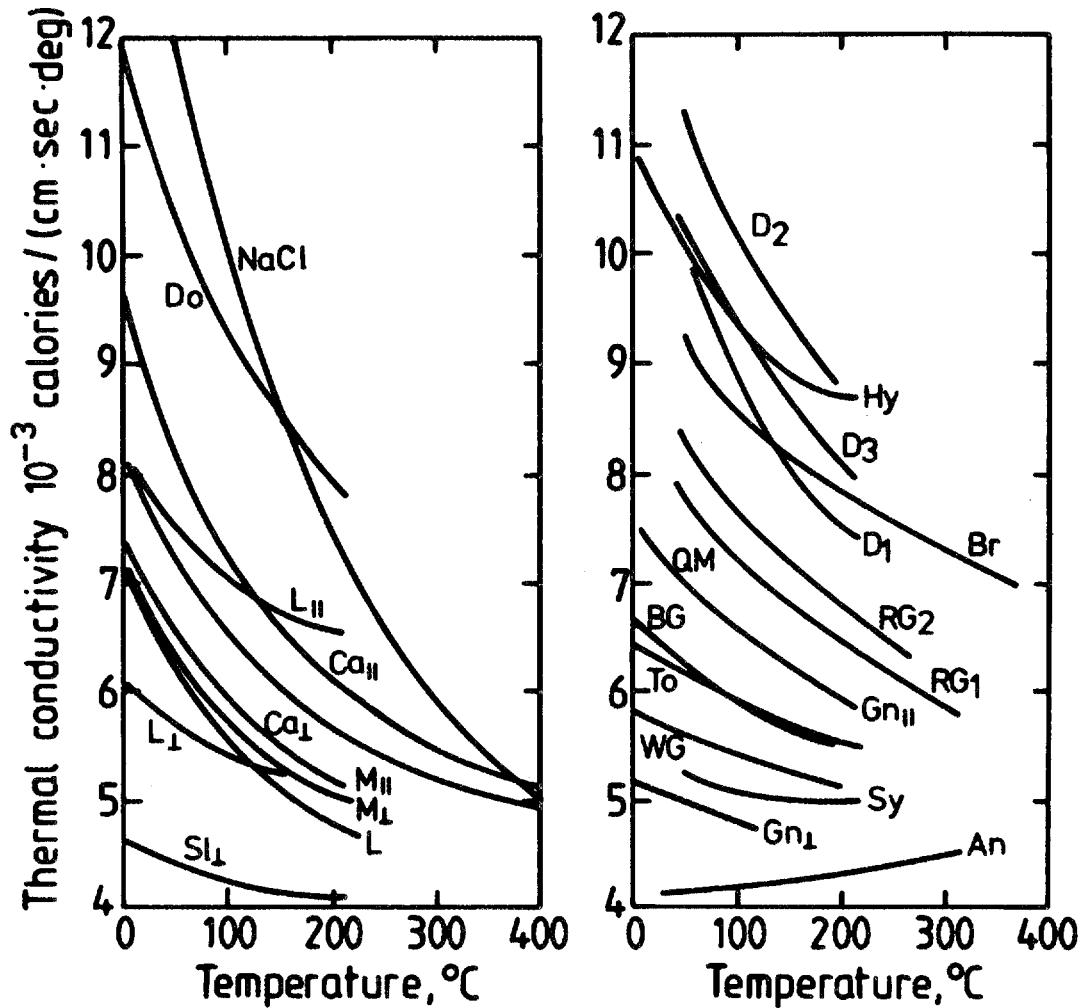
A few examples chosen from previously published calculations of expected temperature profiles will be presented; the considerable discrepancies demonstrate the need for more reliable calculations and for sensitivity analyses.

The temperature in the near-field as well as in the far-field of a repository is probably the most important single parameter concerning the safe disposal of high-level waste. The temperature rise for a given thermal loading is determined by two quantities, the specific heat, which is fairly independent of temperature as well as of the material of the host rock, and the thermal conductivity, which is quite dependent on the material as well as on the temperature, as we shall see in the course of this lecture. It is, therefore, very important to know the thermal conductivity of the rock in which the repository is located. A great amount of work has been done studying the thermal conductivity of a variety of rocks. Fig. 1 shows an example of the range of conductivities observed. It is taken from a paper by Birch and Clark.¹

The variations in conductivity are perhaps not very large by the standards of a solid state physicist, who is usually interested only in orders of magnitude. However, in the case of nuclear waste disposal we must realize that for a given waste loading in a repository, the temperature increase in the vicinity of the heat source will double when the

*Work supported by the USNRC, Contract No. NRC-04-78-261.

**Permanent address: Physics Department, University of the Witwatersrand, Johannesburg, South Africa.



Sl_⊥ Slate, Penn., ⊥ bed-plane.
 L_⊥ Limestone, Penn., ⊥ bed-plane.
 L_∥ Limestone, Penn., ∥ bed-plane.
 L Limestone, Solenhofen.
 M_⊥ Marble, Vermont, ⊥ bed-plane.
 M_∥ Marble, Vermont, ∥ bed-plane.
 Ca_⊥ Calcite, single crystal, ⊥ optic-axis.
 Ca_∥ Calcite, single crystal, ∥ optic-axis.
 Do_∥ Dolomite, Penn.
 NaCl Halite
 An Anorthosite, Quebec.
 Gn_⊥ Gneiss, Pelham, ⊥ bed-plane.
 Gn_∥ Gneiss, Pelham, ∥ bed-plane.

Sy Syenite, Ontario.
 WG Westerly Granite.
 To Tonalite, Calif.
 BG Barre Granite.
 QM Quartz monzonite, Calif.
 RG₁ Rockport Granite 1.
 RG₂ Rockport Granite 2.
 Br₁ Bronzite.
 Hy Hypersthene.
 D₁ Dunite 1.
 D₂ Dunite 2.
 D₃ Dunite 3

Fig. 1. Thermal conductivity of a variety of rocks, after Birch and Clark, ref. 1.

conductivity is halved. Put another way: For a certain maximum permissible temperature rise, the area over which the waste must be spread is inversely proportional to the conductivity of the repository medium. Consequently, a precise knowledge of the conductivity is of considerable economic importance.

One of the great attractions of rock salt is that it has a fairly high thermal conductivity (Fig. 1). Granite, on the other hand, has a lower one, and the conductivity of basalt is lower yet. However, it is important to realize that even for a given type of rock a wide range of conductivities has been found. In anticipation of one of the major points to be made in this lecture, let me tell you that it is possible in some type of rock salt containing the proper kind of impurities to find a thermal conductivity that is even lower than that of basalt.

I refer again to Fig 1, which contains conductivity measurements for several types of granites. At room temperature (300 K), the conductivity of Rockport granite exceeds that of Westerly granite by 50%. This raises the following question: How can we predict what the thermal conductivity in a given repository is going to be, and how can we, in particular, determine that without having to measure the thermal conductivity of every piece of granite that we would like to drill into? To answer this question, we first have to understand what causes the wide spread in thermal conductivity for the different rocks shown in Fig. 1.

In my talk I will spend the first part giving you a brief review of some solid state physics aspects of thermal conductivity in materials in general; then I will talk about a review of the thermal conductivity of a variety of different granites, basalts, and rock salts.

I begin by showing you the thermal conductivity of several high-purity, nearly perfect crystalline solids, lithium fluoride, α -quartz, and cesium iodide (Fig. 2). You see that the thermal conductivity of these solids increases with decreasing temperature, goes over a maximum, and then decreases. The reason for this is the following: Heat in electrical insulators is carried by elastic waves. In the quantum picture they are called phonons. These phonons travel with the speed of sound from the heat source to the heat sink.

As they propagate, they get scattered, either by other phonons - that is the density fluctuations in the lattice resultant from the heat - or by lattice defects. In perfect, crystalline solids the only scattering mechanism is the scattering of phonons by other phonons. However, their number decreases exponentially as the temperature decreases and therefore the thermal conductivity rises rather steeply. Why, then, doesn't it approach infinity at even lower temperature? The answer is that the ultimate limitation of the phonon mean free path (i.e. the distance between collisions) is the surface of the crystal. In other words, if we had samples of infinite extent, their thermal conductivity would keep on increasing, but for experimental reasons one usually uses samples of the order of a few millimeters in diameter, and so what happens is that

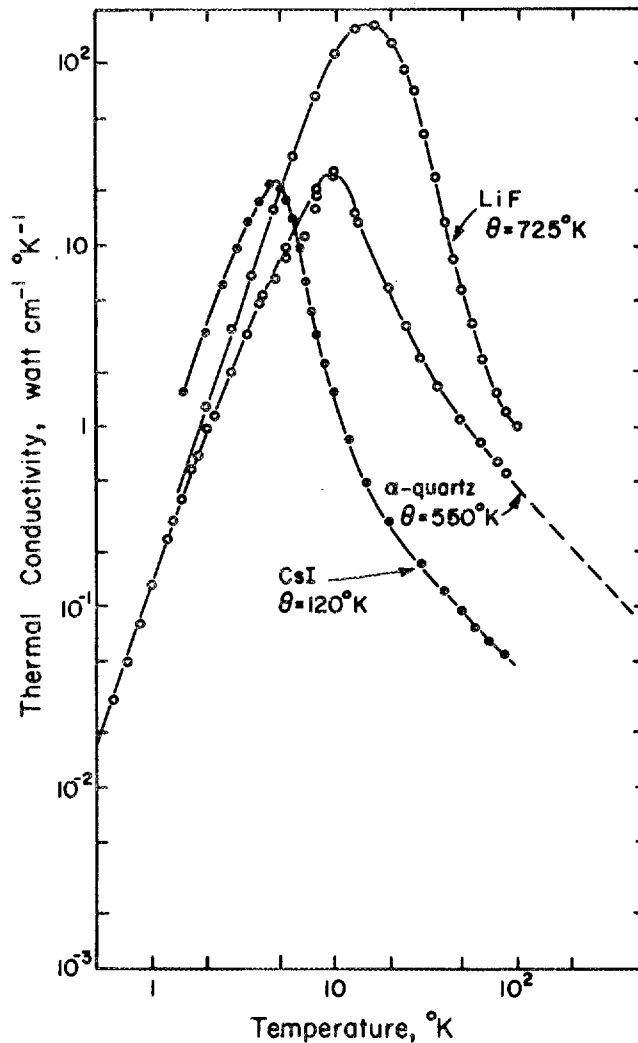


Fig. 2. Thermal conductivity of high purity, synthetic single crystals.
 θ : Debye temperature.

the phonons are being scattered by these crystal surfaces, which limits their mean free path. Then why does that scattering decrease the thermal conductivity, as evidenced in Fig. 2? It decreases the thermal conductivity because the number of phonons which can carry the heat will decrease as the heat capacity decreases. The heat capacity, as you know, varies at low temperatures in proportion to the third power of the temperature; therefore, below the conductivity maxima the curves in Fig. 2 all vary approximately as the third power of the temperature.

Now I would like to present a few examples of what happens when such pure crystals are not all that pure any more because of some intentional or unintentional impurities.

Figure 3 shows a comparison of a natural and of several man-made single crystals of rocksalt (NaCl).² Above 40 K, their conductivities

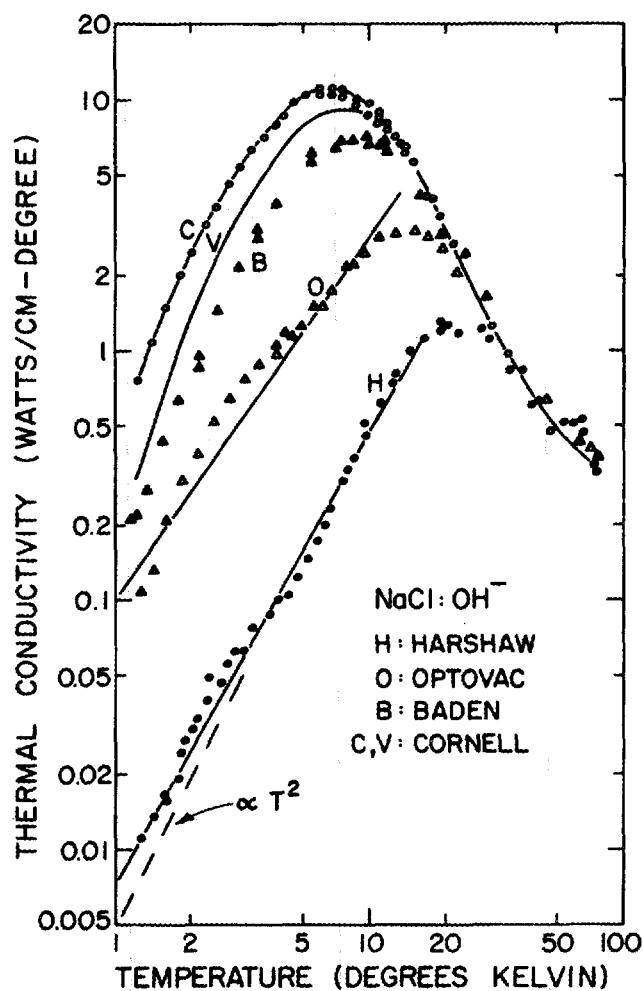


Fig. 3. Thermal conductivity of a pure and almost perfect natural single crystal NaCl (B, from Baden, Germany) and of several synthetic single crystals of NaCl. The commercial samples, labeled H and O, contain OH⁻-ions substituting for Cl⁻ in $\sim 0.1\%$ concentrations. In samples C and V, these impurities had been largely removed. After Klein, ref. 2.

are quite similar, while at lower temperatures, their conductivities differ by several orders of magnitude. We now know that trace amounts of OH⁻-ions substituting for Cl⁻-ions are responsible for this decrease in the conductivity. The phonons are scattered by the molecular ions which can perform almost free rotational motions in the crystal lattice.

Another example of what happens to the thermal conductivity in impure crystals is demonstrated in NaCl containing different concentrations of bromine ions³ (Fig. 4). The lowest curve has been measured on a sample containing approximately 1% NaBr, i.e. 1% of the chlorine ions have been replaced by bromine ions. One sees that the thermal conductivity is not depressed as much at low temperatures as it is in Fig. 3, but the

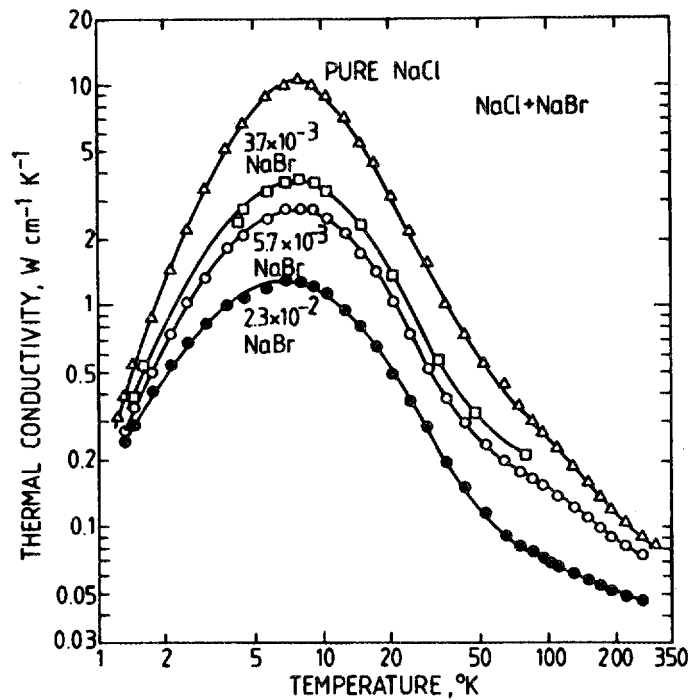


Fig. 4. Thermal conductivity of single crystal synthetic NaCl doped with NaBr. Concentrations in mole fractions. After Caldwell and Klein, ref. 3.

effect begins to spill over into the high temperature region. The thermal conductivity is depressed most strongly in the neighborhood of 80 K. This is another resonance scattering phenomenon. You can visualize this as follows: The heavy bromine ion, which replaces the chlorine ion, changes the vibrational spectrum of the host lattice in such a way that, in the simplest form, one can say that the bromine ion oscillates back and forth relative to the surrounding NaCl lattice, in the same way that a cork floating on water will bob up and down when hit by a wave. The strongest phonon scattering occurs in the temperature range in which the heat is carried predominantly by thermal waves whose frequencies are close to the resonant frequency of the bromine oscillation, which happens to be around 80 K.

In the next example, we consider a solid of SiO_2 which is so highly disordered that every atom has been displaced from its original lattice site. Such a material is called amorphous or glassy. In Fig. 5, it is shown that the thermal conductivity has now been greatly lowered in the amorphous sample, all the way up to 500 K ($\sim 200^\circ\text{C}$).⁴ You also notice how the thermal conductivity near room temperature keeps increasing with increasing temperature while the conductivity of the crystalline quartz is decreasing. In the amorphous phase, the low temperature peak observed in crystals has been replaced by a plateau. The power law of the conductivity below the plateau represents a great puzzle for solid state physicists, but in this talk I will confine myself to a discussion of the

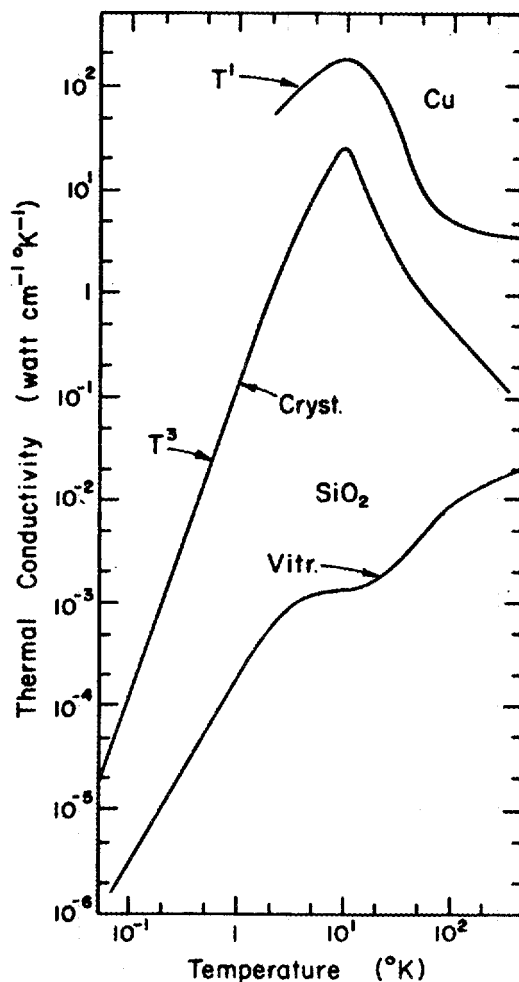


Fig. 5. Thermal conductivity of crystalline and of amorphous SiO_2 . After Zeller and Pohl, ref. 4. Note for comparison the large contribution to the heat transport by the free electrons in a metal, copper.

conductivity at higher temperatures. I begin by presenting the data shown in Fig. 5 in a different form; this requires a brief introduction: I have mentioned previously the picture of the heat being carried by individual particles of elastic energy, phonons, traveling with the speed of sound, v . The connection between the thermal conductivity, Λ , and the phonon mean free path $\bar{\lambda}$, i.e. the average distance traveled by the phonons between collisions, can be written as follows:

$$\Lambda = (1/3) C_V v \rho \bar{\lambda} \quad (1)$$

where C_V is the specific heat of the material and ρ its mass density. With C_V , ρ , and v known, we can use eq. (1) to determine $\bar{\lambda}$ from the experimental data shown in Fig. 5. The results are plotted in Fig. 6. In the crystalline sample, the phonon mean free path at very low temperatures is of the order of 1 cm. This is the sample diameter that I mentioned

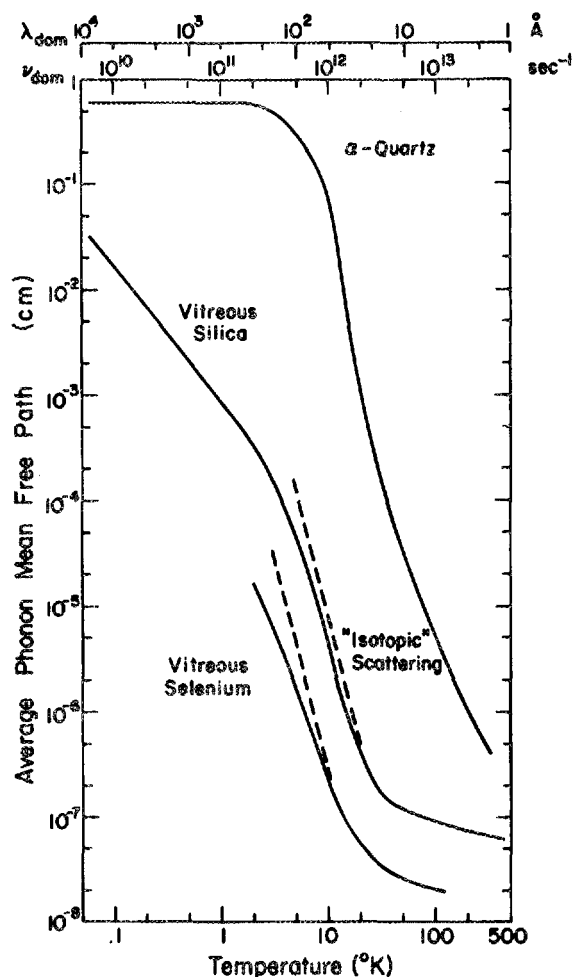


Fig. 6. Phonon mean free path, $\bar{\lambda}$, as discussed in the text, for crystalline and amorphous SiO_2 , and also for selenium, ref. 4. The dominant phonon frequencies ν_{dom} and wavelengths λ_{dom} characterize the phonons which, in the Debye approximation, carry most of the heat at a given temperature. For details see ref. 4.

earlier. As the temperature increases, however, at around 10 K the mean free path drops off rapidly as the result of collisions of phonons with other phonons. In the glass, the thermal conductivity is lower, even at the lowest temperatures, and hence, the mean free path is also lower than in the crystal. In the temperature range around 10 K, the phonon mean free path begins to drop off quite rapidly, almost as the fourth power of the temperature, as shown by the dashed line in Fig. 6. Also shown in Fig. 6 is a behavior that is similar to that found in another glass, selenium. In fact, the glassy thermal conductivity shown in Fig. 5, and the mean free path shown in Fig. 6, are characteristic of all amorphous solids (if they are electrical insulators).⁴ The decrease of the phonon mean free path with the fourth power of T:

$$\bar{\lambda} \propto T^{-4} \quad (2)$$

results from the same physical phenomenon that makes the sky appear to be blue. It is called Rayleigh scattering. In the amorphous solid, the phonons are scattered by the random fluctuations of mass density and force constants which were frozen into the glass as it solidified. This Rayleigh scattering increases as the wavelengths of the thermal waves decrease, and since the wavelengths of these waves decrease as the temperature increases, the mean free path of the phonons decreases with increasing temperature, exactly as expressed in Eq. (2). (In the Rayleigh scattering of light waves, the shorter (blue) waves of the sun light are scattered more strongly by the mass density fluctuations in the atmosphere than the red ones, and hence the sky appears blue.) Above approximately 100 K, the phonon mean free path appears to level off at a value of a few Å ($\text{Å} = 10^{-8}$ cm). The interpretation is that a phonon mean free path cannot be smaller than the interatomic spacing which is typically a few Å. In this limit, the concept of an elastic wave traveling through the solid ceases to be a meaningful description of the heat flow. A more appropriate picture is that of the elastic energy propagating in a random walk from one atom to a neighboring one. In other words, one atom will oscillate, perhaps one period only, and then kick the next one, and so on. This results in a diffusion of the heat via some kind of a Brownian motion. The thermal conductivity will now be determined by the frequency of oscillations and the interatomic spacing. This is the conclusion that we are reaching by looking at the high temperature behavior of the phonon mean free path in very heavily disordered, amorphous solids. It is difficult to imagine how heat can propagate more slowly through a solid than with this random walk. Thus we further conclude that the conductivity observed in amorphous SiO_2 represents a lower limit of the thermal conductivity in any Si-O lattice. This is one of the major conclusions of our discussion so far, and is one to which we will return.

After this introduction into the physics of heat transport in ordered and in disordered solids we now turn to the discussion of natural rocks. Our goal is to understand the origin of the wide range of thermal conductivities observed in rocks, and to predict lower limits of the conductivities that might be encountered in a geologic formation.

Figure 7 shows measurements on two rocks between 500 K (223°C) and 0.3 K, compared with data obtained on crystalline and amorphous, chemically pure SiO_2 . The granite sample (actually quartz monzonite) was taken from the Climax stock at the Nevada test site, while the basalt sample originated at the Hanford Reservation, and is slightly porous ($\rho = 2.6$ g/cm³ vs 3 g/cm³ for non-porous basalt). At low temperatures, below a few degrees Kelvin, the conductivity is described by a power law ($\Lambda \propto T^n$), the exponent ($n \sim 2.5$) being intermediate between the one found in pure single crystals ($n = 3$) and in glasses ($n \sim 1.9$). We believe that in rocks, phonon scattering by internal surfaces or grain boundaries is the cause for the power law behavior, but we will not pursue this subject further in this talk. At high temperatures, starting at around 100 K (-173°C), the conductivities of both rocks appear to approach that of amorphous silica. In Fig. 8 the mean free paths determined with the help of Eq. (1) show the same behavior: Near the upper end of our measuring

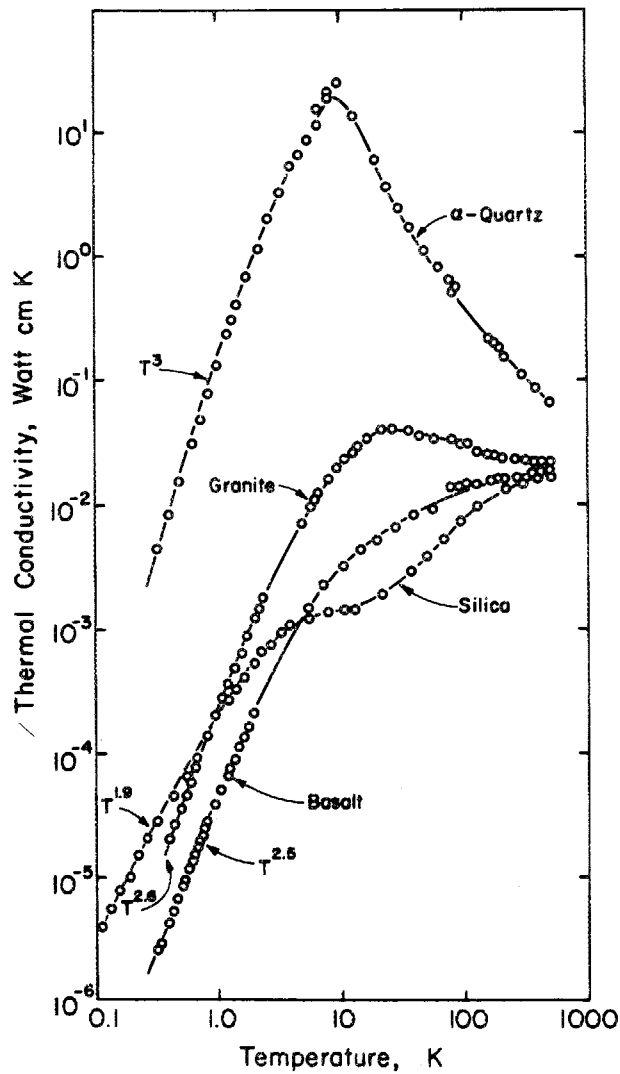


Fig. 7. Thermal conductivity of a sample of granite (quartz monzonite, Climax stock) and basalt (Hanford), with that of quartz and silica.

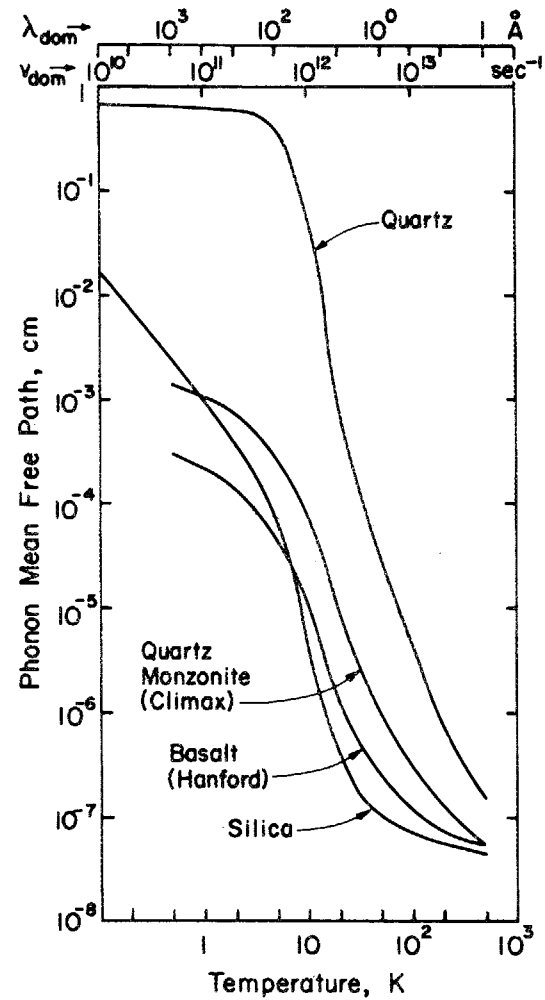


Fig. 8. Phonon mean free path of quartz monzonite and of basalt, derived from data presented in Fig. 7, with the use of Eq. (1).

range (200°C), the mean free paths in the rocks seem to merge with those of silica. In the temperature range between 10 and 100 K, the phonon mean free paths in the rocks decrease rapidly with increasing temperature, suggesting a Rayleigh scattering. We conclude that the disorder in these natural rocks causes a Rayleigh-type scattering mechanism, which is not quite as strong as in the fully disordered amorphous solid; above a few hundred degrees Kelvin, however, the phonon mean free path approaches the same limiting value as in silica, a few Angstroms. We conclude that in the temperature range of interest in this lecture, near and above room temperature, the heat is transported by the same random walk process discussed earlier for amorphous solids. (By looking at the mean free path for pure crystalline quartz in Fig. 8, it appears that this regime of heat transport will not be reached below 1000 K, i.e. it appears that the phonon picture remains valid up to that temperature.)

We had argued earlier that the thermal conductivity of amorphous silica represented a lower limit for a Si-O lattice. Our observations on the two rock samples, shown in Figs. 7 and 8 appear to confirm this argument, although the chemical composition of these rocks differs from that of SiO₂; nevertheless, the atomic masses and interatomic spacings and binding forces are reasonably close to those in SiO₂, and these are the only important quantities involved in this picture of heat transport. Figure 9 summarizes the conductivities of a variety of silica based rocks between 1 and 500 K. The solid lines between 300 and 500 K were taken from the paper by Birch and Clark;¹ A stands for anorthite, Ga for gabbro, Gr for granite, and Q for quartz (D and S stand for dolomite and rock salt, non-silica based rocks). Our own measurements below 100 K confirm the picture of silica as having a limiting thermal conductivity: Eleana shale and tuff, both from the Nevada test site, basalt and granite (same data as the ones shown in Fig. 7), labradorite, and gabbro, all have conductivities which are larger, or close to that of silica. The presence of internal surfaces appears to be important below 10 K, but is ignored in this lecture. The conductivities of anhydrite, dolomite, and of a heavily α -radiation damaged niobate-tantalate metamict mineral, studied by Ewing⁵ and labeled R-13 by him, are unimportant for the present discussion.

Figures 10 and 11 summarize all of the measurements of the thermal conductivity of granite and basalt from a variety of sources.^{1,6-11} As is to be expected, the thermal conductivity of granitic rocks covers a fairly wide range, even if the samples come from the same drill hole, as was the case in Izett's study.⁷ Our own data are close to the lower limit of the conductivity range, although Morgan and West⁸ have observed an even lower conductivity on one of their samples. A similar spread of the conductivity is observed in basalts. We conclude that the atomic disorder responsible for the Rayleigh scattering is different in different rocks, as one should expect. It is interesting, however, that no conductivity lower than that of amorphous silica has been observed in these rocks, which provides further confirmation for our claim that the conductivity of silica represents something of a lower limit for silicate based rocks.

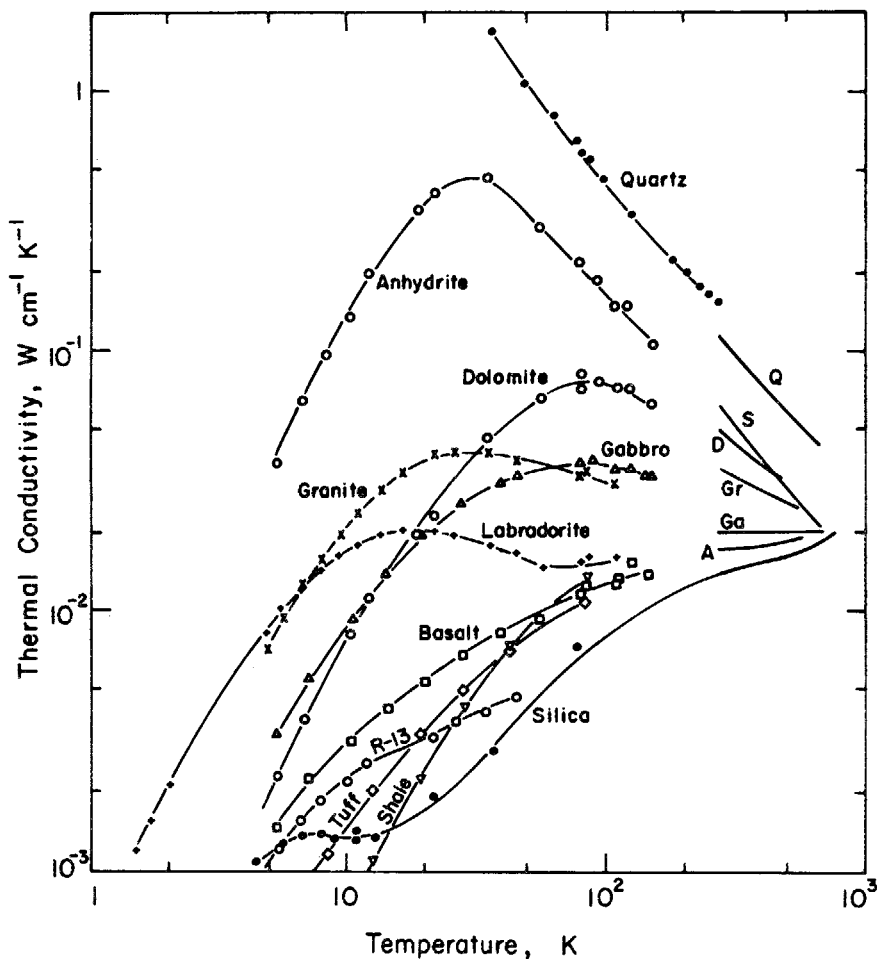


Fig. 9. Thermal conductivity of several rocks. Data above 300°K after Birch and Clark, ref. 1. A: Anorthosite; Ga: Gabbro; Gr: Granite; Q: Quartz; D: Dolomite; R: Rock salt.

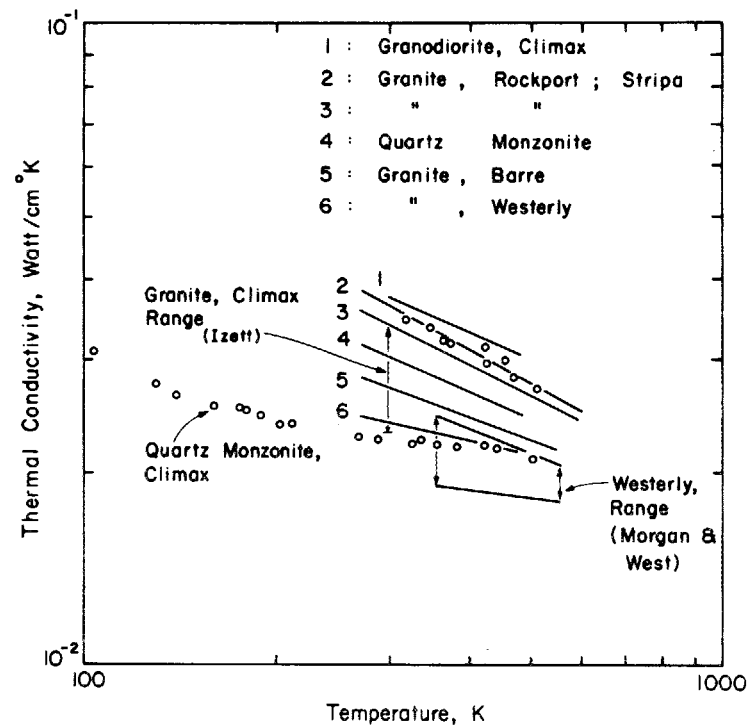


Fig. 10. Summary of thermal conductivity of granite from a variety of sources. Curves 2 through 6, ref. 1; curve 1 and open circles close to curve 2, Climax granodiorite and Stripa granite, ref. 6; double arrow labeled Izett, range of room temperature data from one drill hole into the Climax stock, ref. 7; Westerly range, ref. 8; lower set of data points, present investigation.

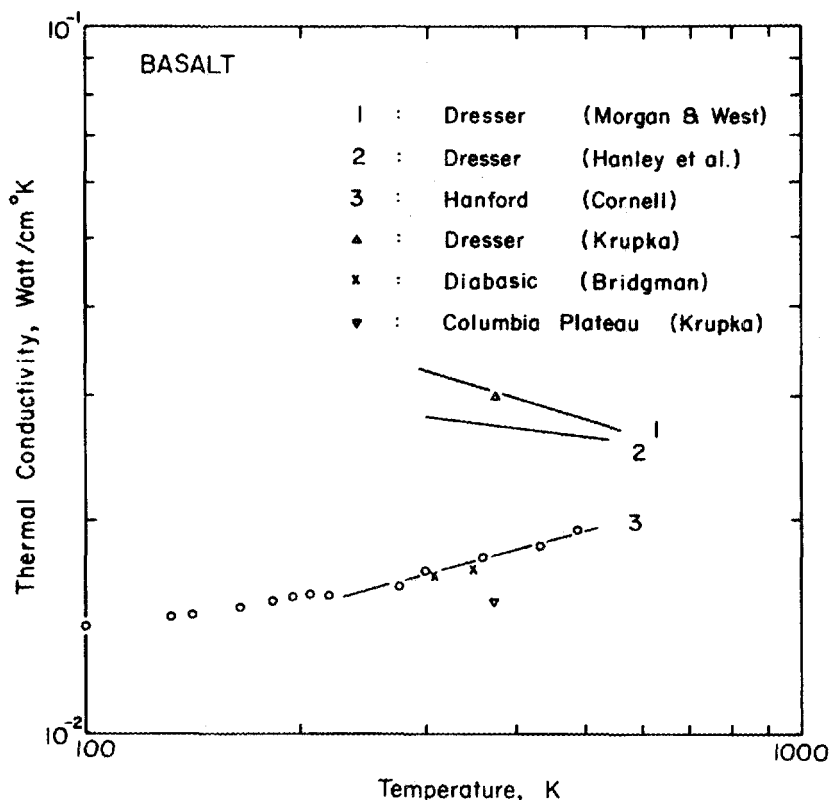


Fig. 11. Summary of thermal conductivity of basalt from different sources. Dresser basalt: Morgan and West, ref. 8; Hanley et al, ref. 9; Krupka, ref. 10; two data points for diabasic rock after Bridgman, ref. 11; one point labeled "Columbia Plateau" after ref. 10; data points and line 3 drawn through them: present investigation.

We now turn to the discussion of a different kind of rock, namely rock salt. We have seen previously (Fig. 4) that the right kind of doping even with relatively small concentrations can affect the conductivity of single crystals of NaCl even at room temperature. Figure 12 summarizes previously published data on purified NaCl¹² and on natural rock salt.^{1,13,14} Again, the spread in conductivity is significant. The lower range of the Louisiana dome salt lies below that of granite, although still above that of basalt. It is worth mentioning that in most calculations of temperature profiles in nuclear waste repositories the conductivity of reasonably pure, single crystal natural rock salt (i.e. curve 2 in Fig. 12) has been used. This can lead to a sizable underestimate of the actual temperature increase under certain conditions.

At Cornell University, we have started to explore the range of conductivity that can be expected in natural rock salt, and the effect of ionizing radiation on the conductivity. Figure 13 shows preliminary results, obtained on samples from a drill core at the WIPP site in New Mexico. This drill core section has been labeled WIPP No. 10 by Sweet and McCreight at Sandia Laboratories, who have studied a variety of drill

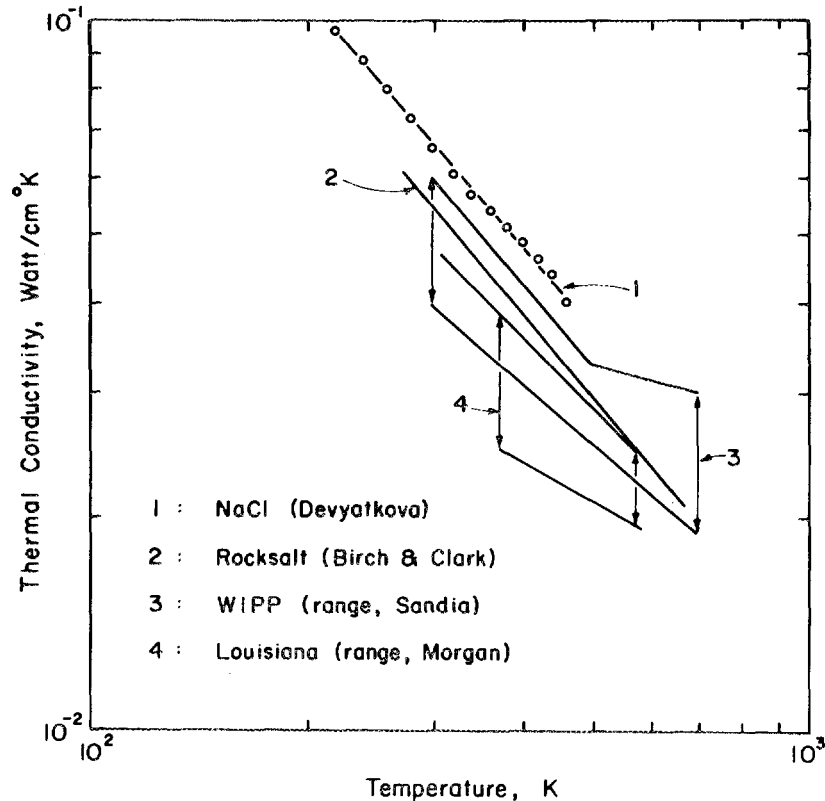


Fig. 12. Thermal conductivity of rock salt. 1: Synthetic, high purity NaCl, ref. 12; 2: ref. 1; double arrows, labeled "3": ref. 13; double arrows labeled "4" Louisiana, ref. 14.

cores at the WIPP site.¹³ The section of the core from which we cut our samples contained an estimated 10 to 20 wt% of polyhalite ($K_2SO_4 \cdot MgSO_4 \cdot 2CaSO_4 \cdot 2H_2O$). Before irradiation in a Co-60 gamma cell, the salt portions were black, while the polyhalite inclusions appeared unchanged in color. After exposure to 10^{10} rad at $150^\circ C$, the salt portions were black, while the polyhalite inclusions appeared unchanged in color. We first measured the irradiated samples (solid circles in Fig. 13), and found remarkable variations from sample to sample. It appears that the conductivity decreases with increasing polyhalite concentration. Of particular importance is the fact that conductivities lower than those observed in granite, basalt, or even in silica were observed in two of the rock salt samples. We had argued earlier in this lecture that the conductivity of silica represents a lower limit for all rocks in which SiO_2 is a major constituent. It is, however, unlikely that the lower limit of the conductivity in highly disordered rock salt could be considerably lower than that of silica, because of the longer period of oscillation of its ions (i.e. its smaller restrahl frequency). Amorphous NaCl does not exist, but Slack¹⁴ has estimated the lower limit of the conductivity in the case that the thermal energy diffuses from atom to atom. He found a limit of 5×10^{-3} Watt $cm^{-1} \text{ } ^\circ K^{-1}$ (above room temperature), three times lower than the conductivity predicted (and observed) in amorphous SiO_2 .

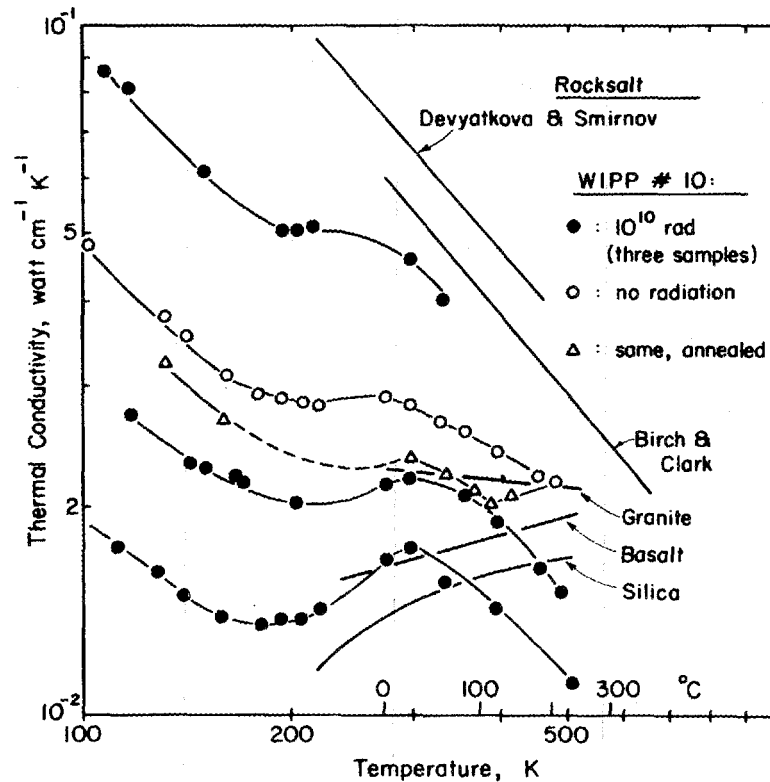


Fig. 13. Thermal conductivity of high purity synthetic NaCl, Devyatkova and Smirnov, ref. 12. Pure natural rock salt, ref. 1. All other data: Natural polycrystalline rock salt from the Waste Isolation Pilot Project, core taken at the drill hole AEC # 8, at a depth of 1995.6 ft. Pieces taken from the section labeled WIPP No. 10 in ref. 13. Solid circles: measured on three sections of a piece 5 cm long irradiated to 10^{10} rad at $\sim 150^\circ\text{C}$. The data shown with open circles were obtained on a different piece which had not been irradiated. The open triangles were obtained after thermal treatment as described in the text.

None of the irradiated samples had been studied prior to the irradiation and, therefore, no conclusion can be drawn as to the effect of the radiation damage. However, when we measured an unirradiated sample (open symbols in Fig. 13), we observed irreversible decreases of the conductivity after thermal cycling below and above room temperature. The open triangles were obtained after the sample had been cycled in vacuum first to a temperature of 100 K, and subsequently annealed for one day at 200°C . However, even the lower curve does not represent a reproducible set of conductivity data. Further thermal cycling lowered the conductivity even more.

In the light of these observations, the data on the irradiated samples must be viewed with caution. During irradiation, the samples

were heated, which may have had a greater effect on the conductivity than the radiation itself. Furthermore, irreversibilities of the conductivity measured on the irradiated samples had also been observed, but had been ignored at that time.

Consequently, we have to be very cautious at this time in drawing conclusions from our studies on rock salt. The following points, however, can be made: In certain samples of natural, impure, rock salt, in which NaCl is the major constituent, conductivities as low or even lower than those of silica based rocks have been observed. An irreversible lowering of the conductivity subsequent to heat treatment has been observed. The effects of ionizing radiation and of impurities in the rock salt (polyhalite, water, etc.) have not been separated and must be further explored.

To summarize: The thermal conductivities of the silica based rocks, granite and basalt, show a wide spread in the temperature range of importance for nuclear waste disposal. We have presented evidence that the thermal conductivity of amorphous silica represents a lower limit for these rocks. This observation is important for an estimate of upper limit of temperature increase expected in a repository.

In certain rock salts, conductivities as low or even lower than in granite or basalt can occur. In this rock salt, irreversible decreases of the conductivity have occurred after heat treatment. In particular, the latter phenomenon must be studied in detail, before a temperature profile in a salt formation can be predicted.

DISCUSSION

LEVY: How does the lowest curve for the irradiated WIPP specimen (Fig. 13) compare with the curve for irradiated synthetic sodium chloride?

POHL: The thermal conductivity of such a sample, which you had irradiated for us, and which we subsequently irradiated to a cumulative dose of 3×10^9 rad was practically unaltered from that of pure NaCl above 50°K. At lower temperatures, large decreases were seen (the conductivity of irradiated NaCl is qualitatively similar to that of OH⁻ containing NaCl, see Fig. 3).

LEVY: Irrespective of the radiation data, what I really would like to know is how does that curve which you have on the graph compare to a curve for synthetic sodium chloride?

POHL: They are within a few percent, 10% or 20%, I think, is the maximum for the purest NaCl ever produced. (Note added in proof: I believe that this question referred to a comparison of the conductivity of unirradiated synthetic and of natural, almost perfect single crystals of NaCl. Figure 3 shows such a comparison. The two uppermost curves in Fig. 13, labeled Deviatkova and Smirnov (synthetic) and Birch and Clark (natural) differ by 20%.)

LEVY: Maybe it is worthwhile to mention then that the large crystals, such as I think you have from Baden, are referred to by many geologists as recrystallized salt, and they are really not at all typical of the normal bedded salt, and some of them are exceedingly pure. So it does not surprise me that if you have large crystals from a natural source that they are going to resemble rather closely some of the high-purity synthetic salts.

POHL: And vice versa.

UNIDENTIFIED QUESTIONER: I am from the Nevada program and in that program we are looking at thermal properties of some of the argillaceous rocks, like the ones that we sent you, and I just wanted to make a comment that at least in those rock types the conductivity is also very sensitive to the degree of water saturation, and you can change it by a factor of two, even at ambient temperature, depending on whether it is fully saturated or fully dehydrated, and I was just curious if your experiments were run under controlled saturation conditions?

POHL: They were not. It is certainly possible that water has something to do with the irreversibility that I have referred to. After having measured the thermal conductivity of the WIPP No. 10 rock salt to 100 K you warm up to room temperature and find the conductivity to have dropped by another 30 or 40%. That could certainly be the effect of water, which we have discovered the hard way. But we do not know.

UNIDENTIFIED QUESTIONER: In the temperature range of 300°C, I guess this is about the maximum of what your experiments have been going?

POHL: 200°C.

UNIDENTIFIED QUESTIONER: Is the heat transfer by radiation important in natural rocks? In other words, by photon transmission rather than phonon transmission?

POHL: I do not think so, simply because other people have said that it is not, but I have not thought about it myself. Perhaps I could say this, that as far as the phonon mean free path goes, there is no inflection. When I plotted the mean free path for amorphous silica, it dropped off as T^4 and then leveled off (see Fig. 8). If there were a photon contribution (which, of course, shouldn't be blamed on the phonon mean free path), you would expect an upturn of the mean free path. As I said, I have glanced at papers in which discussions of radiative heat transfer were made and in which it was concluded that at these temperatures there is no problem.

LAPPIN: Are there any porosity effects on thermal conductivity of these materials? Because pores can scatter phonons and, as we know, influence the thermal conductivity sometimes.

POHL: I do not think that is very likely because of the enormously short mean free path that we are dealing with. Not unless we have cracks that go almost all the way through the crystal, one crack after the other, so that the sample becomes effectively longer. They have to be real cracks, not just grain boundaries. I do not think that in view of the enormously strong phonon scattering observed in our rocks that one can expect much.

This is one of the points I was trying to make. I think that we really have to look on the microscopic scale. The scattering is just too enormous to be produced by a few of these macroscopic defects. (Note added in proof: This answer was only partially correct. Dr. Lappin has observed lower thermal conductivities in porous samples of tuff. Since the pores are essentially empty, they cannot contribute to the heat transfer, and they also increase the path length for the diffusion of the heat. On the other hand, their effectiveness as individual scattering centers is probably negligible, in comparison to the $\sim 10 \text{ \AA}$ mean free path observed in the bulk of the disordered rocks).

REFERENCES

1. F. Birch and H. Clark, *Am. J. Science* 238, 529 (1940).
2. M. V. Klein, *Phys. Rev.* 122, 1393 (1961).
3. R. F. Caldwell and M. V. Klein, *Phys. Rev.* 158, 851 (1967).
4. R. C. Zeller and R. O. Pohl, *Phys. Rev. B* 4, 2029 (1971).
5. R. C. Ewing and A. J. Ehlmann, *Can. Mineral.* 13, 1 (1975).
6. H. R. Pratt et al., Terratek, Inc., Salt Lake City, Utah, Rept. TR-77-92 (Oct. 1977) and TR-78-47 (Aug. 1978).
7. G. A. Izett, U.S. Geological Survey Rept. TEM-836-C (1960), Interim Report, Part C, Physical Properties.
8. M. T. Morgan and G. A. West, Oak Ridge National Laboratory, Oak Ridge, TN, Rept. ORNL-TM-7052 (Jan. 1980).
9. E. J. Hanley, D. P. De Witt, and R. E. Taylor, *Proc. Symp. on Thermo-physical Properties*, Vol. 7, p. 386 (1977), and E. J. Hanley, D. P. De Witt, and R. F. Roy, *Eng. Geology (Amsterdam)* 12, 31 (1978).
10. M. C. Krupka, Los Alamos Laboratories, Rept. LA-5540-MC (1974).
11. P. W. Bridgman, *Am. J. Science* 7, 81 (1924).
12. E. D. Devyatkova and I. A. Smirnov, *Sov. Phys.-Solid State* 4, 1445 (1963).
13. J. M. Sweet and J. E. McCreight, SAND-79-1665 (March 19, 1980).
14. M. T. Morgan, Oak Ridge National Laboratory, Oak Ridge, TN, Rept. ORNL/TM-6809 (June 1979).
15. G. A. Slack, *Solid State Physics* 34, 1 (1979), Academic Press, New York, H. Ehrenreich et al., eds.

SPENT FUEL RESISTANCE TO INTERNALLY PRODUCED CLADDING DEGRADATION

R. E. Einziger, D. A. Cantley, and J. C. Krogness

Westinghouse Hanford Company
Richland, Washington

and

D. E. Stellrecht and V. Pasupathi

Battelle Columbus Laboratories
Columbus, Ohio

ABSTRACT

Spent fuel as a waste form for geologic disposal is currently being studied by the Office of Nuclear Waste Isolation. Its nuclear and criticality characteristics are understood and technology exists for handling, transporting, and packaging of the fuel. Although the cladding of these rods provides a significant barrier to migration of fuel and fission products during its storage, it may degrade due to external corrosion and a number of internal mechanisms. This report describes work which was undertaken to identify and study the internal cladding degradation mechanisms.

At expected repository temperatures ($< 370^{\circ}\text{C}$) and nominal rod internal pressures (~ 2.8 MPa), the degradation processes are too slow for laboratory study. Since all the identified degradation mechanisms are temperature dependent, initial tests were conducted at elevated temperatures to obtain results in a shorter period of time. Whole unmodified PWR rods were tested so that the rod internal environmental conditions, and thus any possible breach mechanisms, would not be changed by the test procedures.

Three high temperature tests were conducted on Turkey Point PWR fuel with the parameters shown in the table. The test at 482°C was stopped when the 515°C test exceeded the expected stress rupture breach time; an examination was conducted to validate parameters used in the lifetime calculations. Profilometry indicated that there was more cladding creep than had been expected, which caused the internal rod pressure to drop 46% resulting in a drop in the hoop stress of 31%. This was confirmed by puncturing the rods. There was no additional gas release from the fuel pellets or axial fission product migration. The eddy current technique revealed no new cladding cracks being formed during the test.

Temp(°C)	Expected 1st Breach (h)	Blackburn's Breach Time (h)	Hours Operated
402	1.8×10^4	0.5	4.6×10^3
515	2.4×10^3	0.045	7.8×10^3
571	20	7×10^{-4}	6.7×10^2

Without breach, the actual mechanism of degradation cannot be determined, but these data do allow us to evaluate the extent to which the stress-rupture mechanism might operate. Blackburn's¹ formulation is presently being used to set maximum allowable storage temperatures. A comparison shows Blackburn's formulation to be conservative in time by a factor of 10^5 at 515°C and 104 at 482°C (see Table). Due to the cladding creep at elevated test temperatures, the time to rupture is significantly increased.

Below 340°C, the radiation damage will not anneal out during storage as it did in these tests. Although the response of other mechanical properties such as ultimate and yield strength indicates that irradiation damage should increase the cladding strength, the response of the stress rupture properties at these temperatures must be determined. Also the condition of these Turkey Point rods must be compared to the general population of spent fuel rods to determine if these tests are applicable to spent fuel assemblies available for disposal. Before the results of this investigation can be applied to the lower anticipated storage temperatures, these points must be resolved.

INTRODUCTION

Current U.S. nuclear policy precludes reprocessing of spent fuel to recover unused fissile material. Consequently, unmodified spent fuel is being studied by the Office of Nuclear Waste Isolation (ONWI) as a final waste form for geologic disposal. The intact cladding and pellets of this waste form would prevent migration of potentially harmful radionuclei in a geologic repository. The cladding, however, may degrade during disposal due to exterior corrosion or in response to fuel rod internal conditions at disposal temperatures. Blackburn¹ identified and evaluated a number of potential degradation mechanisms. These include mechanical overload, stress rupture, stress corrosion cracking, rapid fracture of flawed cladding, internal hydriding and cladding oxidation. After evaluation, he concluded that stress rupture and stress corrosion cracking were the most likely mechanisms to be operative. Since both of these phenomena are thermally activated, it should be possible to preclude degradation by limiting the maximum temperature during disposal. Blackburn estimated a maximum permissible isothermal temperature for 100 year storage at 321°C. This temperature,

however, is dependent on the validity of his underlying assumptions which involve the failure mechanism, the cladding material properties, and the cladding physical condition.

Obviously, direct verification of this temperature limit at expected repository operating conditions cannot be made in a laboratory time frame, but requires that either Blackburn's assumptions be validated or that they be shown to be conservative. To accomplish this purpose, a testing program was established to identify and evaluate internally induced fuel rod degradation mechanisms. Since all the apparent degradation mechanisms are temperature dependent, initial verification tests were conducted at elevated temperatures to obtain results in a short period of time. The primary objectives of these tests were to determine potential mechanisms leading to cladding breach and to improve and validate the basis for the maximum allowable cladding temperature for safe geologic disposal. This paper discusses the results of the first series of tests conducted for this purpose.

TEST PROCEDURES

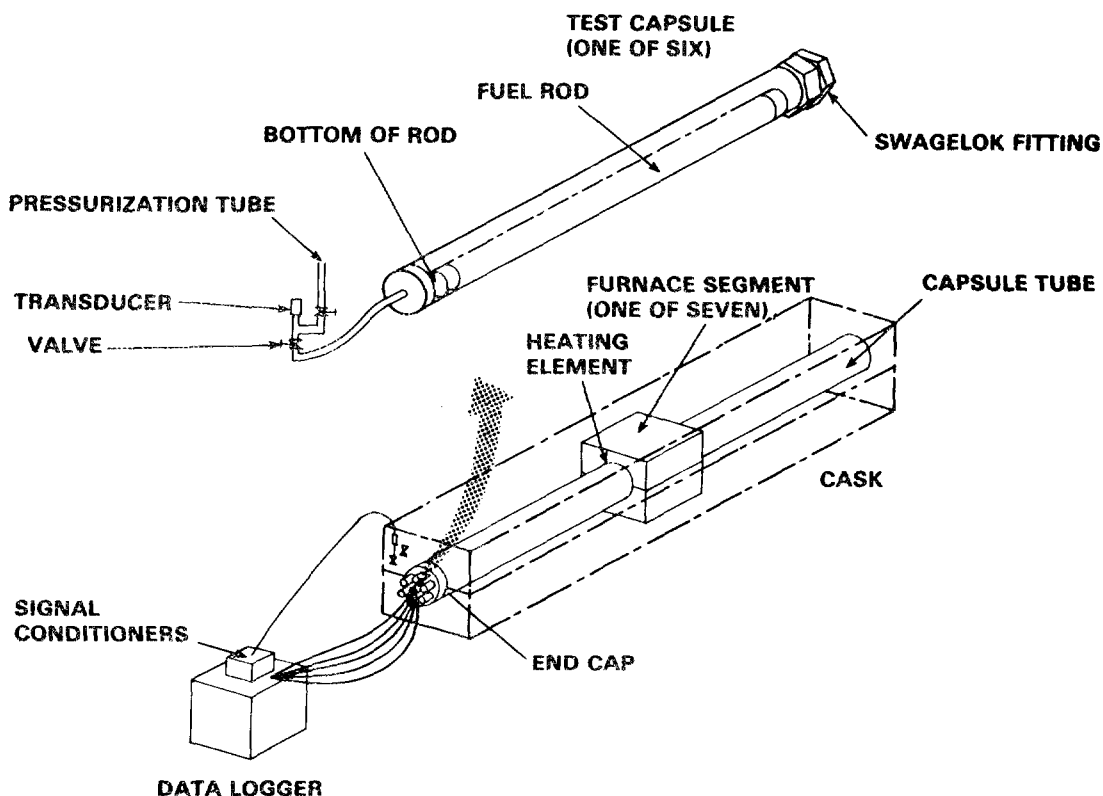
Both tests contain six unmodified Westinghouse designed prepressurized PWR rods from Turkey Point Unit 3. Whole, intact fuel rods were used to ensure that the performance and breach mode obtained were real consequences of rod properties and internal conditions and not the consequence of artifacts resulting from sample preparation. Pertinent characteristics of the rods are summarized in Table 1. Each rod was nondestructively examined before the test to determine length, diameter, surface condition, axial fission product distribution, and any internal or external cracks that were detectable by the eddy current technique. In addition, companion rods from the same fuel assembly were destructively examined to determine rod internal pressure, fission gas content, exterior surface oxidation and fuel cladding corrosion.

Table 1. Characteristics of Fuel Rods Used
in the Whole Rod Tests

Westinghouse prepressurized PWR rods from Turkey Point Unit 3
2 cycles near core center with $\sim 28,000$ MWd/MTu BU
3-2/3 years in H ₂ O pool prior to testing
Cold worked Zircaloy-4 cladding with 10.7 mm OD and 0.62 mm wall
2.6% enriched UO ₂

The details of the test apparatus² are schematically shown in Fig. 1. Each furnace is housed within a steel-lined lead-filled shield to provide the proper personnel biological protection. It has seven independently controlled heat zones. The axial temperature distribution is measured with chromel-alumel thermocouples. Each furnace contains a test rig capable of holding six individually encapsulated fuel rods. The present tests each contain three rods encapsulated in helium and three rods encapsulated in air. The capsule pressure, initially near 0.14 MPa at operating temperature was continuously monitored with a pressure transducer to detect rod breach.

The rods were initially brought to temperature over a 340-hour period during the summer of 1979 and then ran continuously except for minor shutdowns due to power outages prior to the interim examination recently conducted. The intent of these tests was to run until breach occurred, and then to conduct examinations to verify the breach mechanism. Analyses using unirradiated stress rupture properties,¹ the MATPRO creep equation,³ and estimates of rod internal pressures based on examination of companion rods were made to estimate breach times. Results of these analyses are shown in Table 2. For the test at 510°C and 571°C, the time of expected first breach was considerably exceeded



HEDL 8004-249.8

Fig. 1. High-temperature whole rod test apparatus detailing the furnace construction and rod encapsulation.

Table 2. Operating Conditions, Expected Breach Times, and Status of the High-Temperature Tests

Test	Temperature (°C)	Expected 1st Breach (h)	Hours Operated	Status
2a	482	1×10^4	4.6×10^3	stopped
1	510	2.4×10^3	7.8×10^3	continuing
2b	571	20	6.7×10^2	stopped

with no breaches. To investigate why the breach time had not been predicted, an interim examination was performed on the test at 482°C prior to the time of expected first breach.

RESULTS AND DISCUSSIONS

After shutdown of the test at 482°C, the cover gas surrounding the fuel rods in the capsules was analyzed for xenon and krypton to see if there had been any small undetected leaks. Two of the rods were then removed, visually inspected, profilometered, eddy current and gamma scanned and punctured for fission gas analysis.

No outstanding differences were noticed between the pre-test and post-test visual examinations. This was expected since the visual examination would only reveal very gross changes in the rod condition. The eddy current examination showed no indication of any crack formation during the test, but the limit of detection of the eddy current technique for an inner wall crack is about 15% of the wall thickness and tends to be somewhat qualitative. There was no detectable change in the gamma activity profile which indicates that there was no axial transport of ^{137}Cs or other fission products. There were no detectable length changes of the rods during the test indicating a 2:1 biaxial stress state which was consistent with the calculation assumptions.

Comparison of pre- and post-test profilometry revealed between 1.5 and 2% cladding creep. In addition to the creep, the cladding showed a significant reduction in ovality and ridging. Rod puncturing, gas analysis, and internal void volume determinations revealed an increased final internal void volume, as would be expected due to the significant cladding creep, but the total amount of gas in the rods and the volume of fission gas in the rods remained the same as before the test started. Except for an increase in the water content of the internal gas, the composition of the gas remained approximately constant indicating no apparent fission gas release during the test. These results also show that the cladding stress dropped 31% during the course of the test.

The single most significant observation is the unexpectedly high cladding creep. This was a factor of 6 higher than predicted by the MATPRO creep equation³ used in the original analysis and largely explains the lack of breach as predicted by calculations. The difference between the measured creep strain and the creep strain predicted by the MATPRO equation results either because the MATPRO equation is not suitable for the test conditions or the hoop stress in the rods was higher than calculated. This calculated stress was determined using nominal diameters and wall thicknesses and an internal pressure of approximately 6.9 MPa. The actual stress could be higher if the actual cladding diameter was larger, the wall was thinner, or the pressure higher than used in the calculation. In actuality, when all these variations are assessed, the calculations were done at approximately 92% of the actual stress, which implies that the problem lies with the creep equation.

Figure 2 is a plot of expected time to breach based on the stress rupture mechanism as a function of constant operating temperatures determined by a number of different methods. Blackburn's method,¹ which was used to develop the temperature limit, uses a fixed room temperature internal pressure of 8 MPa and a stress rupture correlation which is 2/3 of the lower 95% confidence interval for unirradiated stress rup-

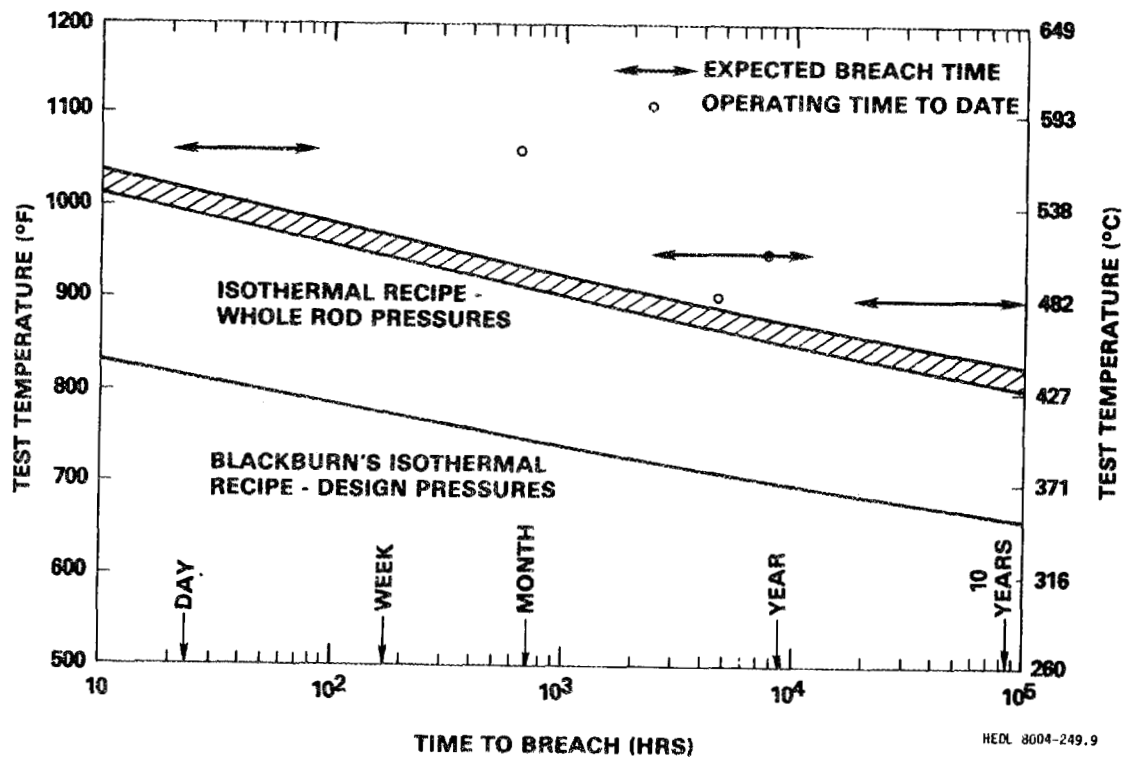


Fig. 2. Fuel rod predicted time to breach as a function of operating temperature based on the stress rupture mechanism determined by a number of different formulations.

ture properties. The design lifetimes resulting from this formulation are shown as the bottom line in this figure. Using the same formulation as Blackburn, except using the actual pressure range determined from the companion rods, one gets a range of breach times indicated by the cross hatched region. Neither of these calculations takes into account the cladding creep and subsequent reduction in hoop stress that was observed. If one goes further and uses the nominal expected internal pressures, the \pm 95% confidence band on stress rupture properties, and allows creep as calculated by the MATPRO equation, the predicted breach times are indicated by the arrowed bands. If the measured creep rate predicted by Merckx creep equation⁴ is factored into the calculation of lifetimes, then breach is not expected within a reasonable laboratory time frame via a stress rupture mechanism. For all three tests, the predicted design recipe breach time using nominal pressures and indicated by the cross hatch region is exceeded. With respect to the breach time, Blackburn's isothermal formulation is conservative by factors of at least approximately 10^6 at 571°C, 10^5 at 510°C, and 10^4 at 482°C, as determined by comparing predictions with operating experience and recognizing that no breaches have occurred.

It is significant to note, however, that these tests were conducted at temperatures which were above the temperature where in-reactor radiation damage quickly anneals.⁵ This means that the material condition of the cladding and test temperatures may be significantly different than at anticipated geologic disposal temperatures where the damage may never be completely annealed. Based on comparisons with other post irradiation mechanical properties such as ultimate and yield strength⁶ which show that the strength increases and ductility decreases, one can hypothesize that compared to unirradiated material, the irradiated material should have a longer time to stress rupture since it is stronger, but the breach should come at a lower strain. While this appears to be a favorable situation from the point of view of disposal, it must be confirmed by testing.

CONCLUSIONS

These tests were conducted over a narrow temperature range considerably above anticipated disposal conditions and utilized only one set of rods from a single reactor. Therefore, the extent to which these results apply to disposal conditions for the entire population of fuel rods which would be subject to disposal is uncertain. With these qualifications, the following conclusions are made relative to the results of these particular tests. The measured cladding strain was sufficiently large so that failure mechanism verification by inducing breaches in unmodified rods heated to elevated temperatures for short periods of time does not appear to be practical based on a stress rupture mechanism. At the elevated test temperatures, however, Blackburn's formulation based on stress rupture gives very conservative estimates of breach times. In addition to the high cladding strain, the fuel exhibited no additional gas release or axial fission product migration at 482°C. The nondestructive examination gave no additional indication of internal deterioration of the fuel rod.

ACKNOWLEDGMENTS

The authors wish to thank Mr. Robert B. Davis for conducting the pretest examinations, Mr. David M. Bosi for the creep analysis, and Ms. LaDonna M. Hendricks for typing the manuscript.

DISCUSSION

POHL: You referred on several occasions to fission gas trapped inside the fuel rods. I was wondering what other volatile fission products would be available for this kind of volatilization. What is the fraction of the cesium that could join in the pressure buildup?

EINZIGER: Generally the tests have shown, and the literature has shown, that the fraction of fission products that is released from the fuel is essentially the same as the fraction of gas that is released from the fuel, and the volatiles that would be of most importance are iodine, and, to some extent, bromine. While cesium is volatile, there is not enough of it to cause a substantial pressure until we get above the boiling point, which we never reach.

POHL: My question really is - what fraction of the cesium has escaped during reactor operation from the fracturing fuel elements but is still contained in the cladding? What fraction of the cesium - 1%? 0.1%?

EINZIGER: In general, for prepressurized PWR fuel rods approximately 1% of the fission products is released during reactor operation. For BWR fuel rods, as much as 20% has been measured. There is some work going on now in this area, since there are indications that, as you increase the burnup of the fuel rod, you are going to have a rapid, accelerated release of fission gas and fission products. Since the current plans are to try to bring the burnup of the fuel up to as much as 50 or 60 gigawatt-days per metric ton, this is a concern - not only from the point of view of releasing the gas; it also releases additional fission products which could possibly add to making stress corrosion cracking the primary mechanism.

REFERENCES

1. L. D. Blackburn, D. G. Farwick, S. R. Fields, L. A. James, R. A. Moen, "Maximum Allowable Temperature for Storage of Spent Nuclear Reactor Fuel - An Interim Report," HEDL-TME 78-37 UC-70, May 1978.
2. D. E. Stellrecht, V. Pasupathi, J. C. Krogness, "Elevated Temperature Testing of Spent Nuclear Fuel Rods," to be published in ANS Transactions for 1980 Annual Meeting, June 8-13, 1980.
3. D. L. Hagrman and G. A. Reymann, Ed., "MATPRO - Version 10, A Handbook of Materials Properties for Use in the Analysis of Light Water Reactor Fuel Rod Behavior," February 1979, NUREG/CR-0497, TREE-1280.

4. K. R. Merckx, "Calculational Procedures for Determining Creep Collapse of LWR Fuel Rods," Nucl. Eng. and Design 31, 95-101 (1974).
5. G. J. C. Carpenter and J. F. Watters, "Irradiation Damage Recovery in Some Zirconium Alloys," Zirconium in Nuclear Applications, ASM STP 551, 1973, pp. 400-514.
6. G. M. Bain and T. P. Papazoglou, "Hot Cell Examination of Creep Collapse and Irradiation Growth Specimens - End of Cycle 2" LRC-4733-7, August 1979.

A REVIEW OF RESEARCH ON ANALOGS OF MONAZITE FOR THE
ISOLATION OF ACTINIDE WASTES

M.M. Abraham, L.A. Boatner, G.W. Beall,* C.B. Finch,[†] R.J. Floran,^{††}
P.G. Huray,* and M. Rappaz

Solid State Division, Oak Ridge National Laboratory**
Oak Ridge, Tennessee 37830

ABSTRACT

The lanthanide orthophosphates (LnPO_4) are being investigated as a means of primary containment for high-level actinide wastes. Lanthanum orthophosphate and orthophosphates of the first half of the lanthanide transition series (i.e., Ce through Gd) are analogs of the mineral monazite. The known long-term (10^9 yr) stability of this mineral under a variety of geological conditions, its ability to incorporate the naturally occurring actinides Th and U, and its apparent resistance to α -particle-induced radiation damage indicate that the analogous lanthanide orthophosphates could well represent ideal hosts for the immobilization of transuranic actinide wastes.

A flux technique has been used to grow single crystals of every lanthanide orthophosphate (except PmPO_4) as well as ScPO_4 and YPO_4 , and these crystals have been employed in a variety of x-ray, electron paramagnetic resonance, Mössbauer, radiation damage, and chemical stability studies. A redetermination of the monazite crystal structure was carried out using a flux-grown crystal of pure CePO_4 and the structure was found to be monoclinic (space group $P2_1/n$) with $a = 6.777 \text{ \AA}$, $b = 6.993 \text{ \AA}$, $c = 6.445 \text{ \AA}$, and $\beta = 103.5^\circ$. Each cerium atom is coordinated with nine oxygen atoms.

Single crystals of uranium-doped LaPO_4 were grown from an oxide mixture containing 10 wt.% $^{238}\text{UO}_2$. The optical absorption spectra show that the uranium impurity is present in these crystals in the tetravalent state. Crystals of LaPO_4 doped with 1.0 wt.% $^{241}\text{Am}_2\text{O}_3$ have been grown, and the optical spectra show that americium is incorporated in the LaPO_4 host in the trivalent state. Other actinide-doped crystals that have been grown and investigated include materials grown from oxide mixtures of 90 wt.% La_2O_3 with 10 wt.% $^{242}\text{Pu}_2\text{O}_3$ and 99.3 wt.% La_2O_3 with 0.7 wt.% $^{246}\text{Cm}_2\text{O}_3$. The 4+ valence state was also observed for plutonium in the LaPO_4 host.

*Chemistry Division, ORNL; [†]Metals and Ceramics Division, ORNL;

^{††}Environmental Sciences Division, ORNL

**Operated by Union Carbide Corporation under contract W-7405-eng-26 with the U.S. Department of Energy.

Leach tests of the orthophosphate crystals resulted in IAEA leach indices that were smaller than those reported for grouts or borosilicate glasses by a factor of 16 for CePO_4 in 4 M NaCl at 200°C and 250 psi, and a factor of 295 for $\text{La}(\text{Am})\text{PO}_4$ in distilled water at 200°C and 250 psi. These results are particularly promising since the leaching studies on the glasses and grouts were conducted at room temperature and atmospheric pressure.

Although the flux growth process represents a reliable method for obtaining single-crystal specimens for leach tests and other research investigations, it is not thought to be a practical method for processing actual waste material. The method of precipitation in molten urea does, however, represent a promising technique for the practical synthesis of actinide-containing rare-earth orthophosphates. The phosphate particle size can be controlled in this process, and consolidation via hot pressing of powders with a suitably small particle size has resulted in bodies with 97% of the theoretical density. Examination of suitably doped precipitated powders using electron paramagnetic resonance has shown that rare-earth impurities occupy identical sites in both the single crystals and the urea-precipitated material.

The present results lend support to the concept of employing lanthanide orthophosphates for the containment of α -active wastes and have provided new insight into the properties of these combined materials as well as information on the practical processing of such systems.

This research effort is directed toward identifying new radioactive waste forms that could be superior to glass. The primary interest in the current work is in actinide containment which involves long-term isolation. This containment must be secure under a variety of conditions, many of which have been discussed at this workshop and elsewhere.

Figure 1 provides an illustration of the length of time required to contain the actinide elements as well as other long-lived isotopes generally found in the fission products. It can be seen that ^{137}Cs and ^{90}Sr are only important up to about 1000 yr, as is ^{244}Cm . Americium-241 and ^{240}Pu are of considerable importance up to about 5000 yr; and ^{243}Am and ^{239}Pu are significant up to 20,000 or 30,000 yr. It should be noted that even though ^{226}Ra and ^{229}Th begin to appear after about 10,000 yr, the summation (Σ) curve of relative biological hazard remains more than 3 orders of magnitude lower than it was at 100 yr. From the actinide half-lives noted above it is apparent that times on the order of 1000 to 10,000 yr must be considered as a minimum waste form stability period.

The approach taken in the present work consists of an evaluation of the lanthanide orthophosphates that are analogs of the mineral monazite.^{1,2}

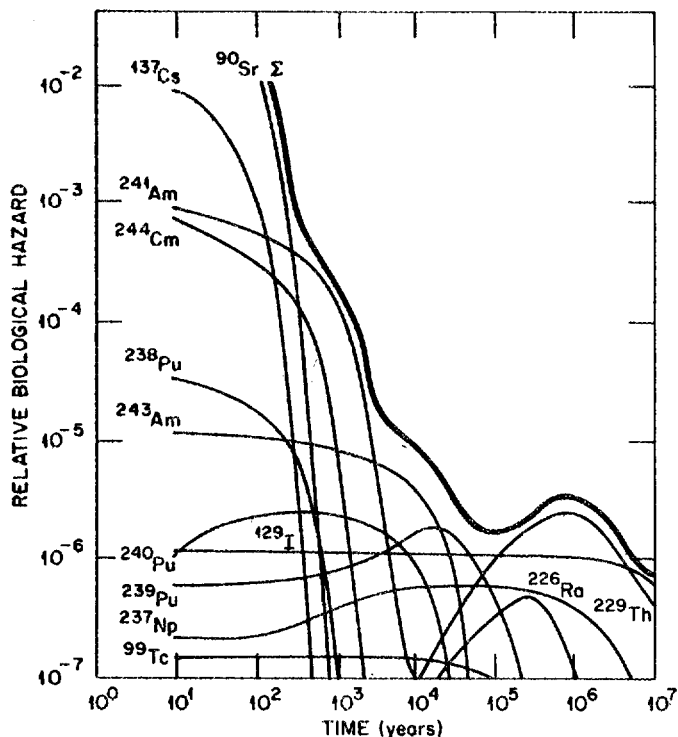


Fig. 1. The relative biological hazard of radioactive nuclei as a function of time. After several hundred years the dominant hazard is represented by various actinide isotopes.

Analogous of monazite were chosen for a number of reasons. First, monazite is a natural mineral that is one billion years old in some cases. Also, it is a major natural source of thorium and uranium and incorporates large percentages of these elements. The ages of two particular monazite sands (Fig. 2) are roughly two billion years for a Brazilian specimen and a half billion years for sands from Normandy, France. There are other deposits in Africa and India that are equally as old. Figure 3 shows some representative chemical compositions of monazites from Italy, Ceylon, California, and North Carolina. As can be seen, the monazite from Italy contains 15 wt.% uranium oxide and 11 wt.% thorium oxide, and the specimen from Ceylon contains 14 wt.% thorium oxide. The lanthanide oxides and P_2O_5 obviously make up the preponderance of these monazites, but other oxides are present as well.

One very interesting fact regarding monazite, in addition to its age and natural actinide loadings, is that it always occurs in the crystalline state in nature (Fig. 4). The radiation from uranium or thorium in natural monazite does not appear to change the monazite crystal into an amorphous state. This represents an additional reason for investigating monazite for the purposes of waste isolation. Another point illustrated in Fig. 4 is that monazite appears to be much more resistant to the loss of uranium or thorium than other minerals.

SOURCE	AGE (years)	REFERENCE AND COMMENTS
BRAZIL	~ 2,000,000,000	O. H. LEONARDOS, JR. ECON. GEOL. 69, 1126 (1974) – INITIAL FORMATION OCCURRED DURING THE ARCHEAN (PRE-CAMBRIAN PERIOD)
NORMANDY	570,000,000	PAUL PASTEELS,* ECLOGAE GEOL. HELV. 63, 231 (1970). FORMED DURING THE UPPER PRE-CAMBRIAN PERIOD. DATED BY $^{207}\text{Pb}/^{206}\text{Pb}$ RATIOS.

***THE RADIOMETRIC $^{207}\text{Pb}/^{206}\text{Pb}$ AGE IS GENERALLY CONSIDERED AS THE MOST RELIABLE AGE INDICATION FOR URANIUM BEARING MINERALS.**

THE FORMATION OF THE NORMANDY MONAZITE PREDATES THE EARLIEST EVIDENCE FOR THE EXISTENCE OF BIRDS, MAMMALS, AND FLOWERING PLANTS BY OVER 400 MILLION YEARS.

Fig. 2. The geological age of monazite ores found in Brazil and Normandy.

MINERAL SOURCE	UO ₂ (wt %)	ThO ₂ (wt %)	COMBINED		P ₂ O ₅ (wt %)
			LANTHANIDE OXIDES (wt %)	OTHER OXIDES (wt %)	
PIONA, ITALY ¹	15.64	11.34	35.24	6.76	31.02
RATUNAPURA, ² CEYLON	0.10	14.32	53.51	5.03	26.84
SAN MATEO, ³ CALIFORNIA (BEACH SANDS)	6.95	4.22	N. D.	N. D.	N. D.
BURKE COUNTY ⁴ N. C.	0	6.49	62.26	1.97	29.28

¹C. M. GRAMACCIOLI AND T. V. SEGALSTAD, AM. MINER. 63, 757-761 (1978).

²T. KATO, MIN. JOURN. (JAPAN) 2, 224 (1958).

³C. O. HUTTON, GEOL. SOC. OF AM. BULL. 62, 1518 (1951).

⁴S. L. PENFIELD, AM. JOUR. SCI., 3d SER. 24, 252 (1882).

N.D. – NOT DETERMINED.

Fig. 3. The chemical composition of natural monazites from various deposits. This mineral is obviously capable of incorporating relatively large amounts of thorium and uranium.

- METAMICTIZATION: RADIATION INDUCED CHANGES IN THE STRUCTURE AND ORDER OF CRYSTALLINE MATERIALS. CHANGES CRYSTALLINE MATERIAL INTO AN AMORPHOUS STATE
 - "THERE ARE MINERALS THAT MAINTAIN THEIR STRUCTURES AGAINST RELATIVELY HIGH α -PARTICLE FLUXES - R. C. EWING, AM. MINERAL 60, 728 (1975)
 - "... MONAZITE IS FOUND ONLY IN THE CRYSTALLINE STATE." - R. C. EWING, ERDA CONF. 770102, 139-146 (1977).
- MOBILITY OF URANIUM AND THORIUM IN MONAZITE: "THE STABILITY OF MINERALS WITH RESPECT TO DIFFUSION OF URANIUM AND THORIUM DIMINISHES IN THE FOLLOWING ORDER: MONAZITE, URANINITE, ORTHITE, PYROCHLORE, ZIRCON, SPHENE, AND VIKITE." - S. L. MIRKINA, VOPROSY GEOKHROLOGII I IZOTORNOJ GEOLOGII, 106-112 USSR (1976).

Fig. 4. Evidence for the resistance of monazite to natural α -particle induced radiation damage and for the relative stability of monazite with respect to the diffusion of uranium and thorium.

Table 1 lists the actinides that are of primary interest for the purposes of nuclear waste isolation. The second column in Table 1 lists the usual valence states that one finds for these elements. Unlike the rare earths, which are predominantly trivalent, it can be seen that the actinides may have more than one valence. The ionic radii of the various ions are posted in the third column. The rare earths exhibit an interesting behavior because in going from element 57, lanthanum, down to 71, lutetium, there is a contraction, so that the lanthanum ionic radius is larger than that of lutetium. The same effect occurs in the uranium, or actinide, series, but the changes do not correspond to those found for the lanthanides, i.e. curium does not have the same ionic radius as gadolinium, etc. When the lanthanides or actinides are substituted in a host lattice, the d^2 electrons (fourth column of Table 1) are usually removed, leaving only f electrons. For the case of trivalent uranium in a host lattice, there are three $5f$ electrons. Trivalent neptunium would probably have four $5f$ electrons, but in some cases other than f -electrons may be present.

One of the interesting features of the lanthanide orthophosphates is that there is more than one crystalline form (Table 2). Monazite is the monoclinic (high-temperature) form of lanthanum phosphate or cerium phosphate. If a crystal is grown at a temperature below 400°C, a low temperature hexagonal form will be produced. Above 400°C, the monoclinic form is obtained. The hexagonal form is metastable and once it has transformed from the hexagonal to the monoclinic form it cannot revert to the hexagonal structure. The monoclinic structure is therefore the stable form for the rare earths in the first half of the transition series. A tetragonal form characterizes the rare earths in the second half of the series.

Table 1. Properties of Actinides Contained in Radioactive Wastes

Element	Valence States	Ionic Radii (Å)	Electronic Configuration	Atomic Number
Th	4	0.95 (4+)	$6d^2 7s^2$	90
U	6,5,4,3	1.11 (3+) 0.97 (4+)	$5f^3 6d 7s^2$	92
Np	6,5,4,3	1.09 (3+) 0.95 (4+)	$5f^4 6d 7s^2$	93
Pu	6,5,4,3	1.07 (3+) 0.93 (4+)	$5f^6 7s^2$	94
Am	6,5,4,3,2*	1.06 (3+) 0.92 (4+)	$5f^7 7s^2$	95
Cm	3	-	$5f^7 6d 7s^2$	96

*Observed in solid solution.

Table 2. Crystalline Forms of Lanthanide Orthophosphates*

Compound	Structure			Transition temperature (°C)	Melting point (°C)
	Low-temp. form	Intermediate form	High-temp. form		
LaPO ₄	Hexagonal	-	Monoclinic	400	2300
NdPO ₄	Hexagonal	-	Monoclinic	450	2250
EuPO ₄	Hexagonal	-	Monoclinic	500	2200
GdPO ₄	Hexagonal	Monoclinic	Tetragonal	550	2200
TbPO ₄	Hexagonal	Monoclinic	Tetragonal	600	2150
DyPO ₄	Hexagonal	Monoclinic	Tetragonal	600	2150
ErPO ₄	-	-	Tetragonal	-	2150
YbPO ₄	-	-	Tetragonal	-	2150
YPO ₄	-	-	Tetragonal	-	2150

*I. A. Bondar' et al., Russian J. Inorg. Chem. 21, 1126 (1976).

Yttrium phosphate and scandium phosphate are also tetragonal systems. A low-temperature hexagonal form of $GdPO_4$, $TbPO_4$ or $DyPO_4$ can be obtained, and the quoted transition temperature for these three compounds listed in Table 2 is for the hexagonal-to-monoclinic transition temperature, and not for the monoclinic-to-tetragonal transition.

Single crystals of all of the lanthanide orthophosphates except $PmPO_4$ have been grown in the high-temperature form in our laboratory³ (Fig. 5). These crystals were grown in a platinum crucible using a lanthanum oxide - lead hydrogen phosphate mixture. This mixture is heated at $1360^\circ C$ for one day; H_2O is driven off and leaves lead pyrophosphate. The crucible is then slowly cooled at $1^\circ C-hr^{-1}$, to about 900° . The single crystals are entrained in a flux of lead pyrophosphate, and this flux is dissolved away with boiling nitric acid in order to free the crystals. Although it cannot be seen in Fig. 5, the erbium, holmium, and yttrium crystals are tetragonal, and the remaining specimens are monoclinic. The colors of these crystals are as follows: $CePO_4$ - black, $PrPO_4$ - green, $ErPO_4$ - pink, $NdPO_4$ - purple, $HoPO_4$ - orange, YPO_4 - yellow, and $EuPO_4$ and $LaPO_4$ are colorless.

ORNL PHOTO 3459-79

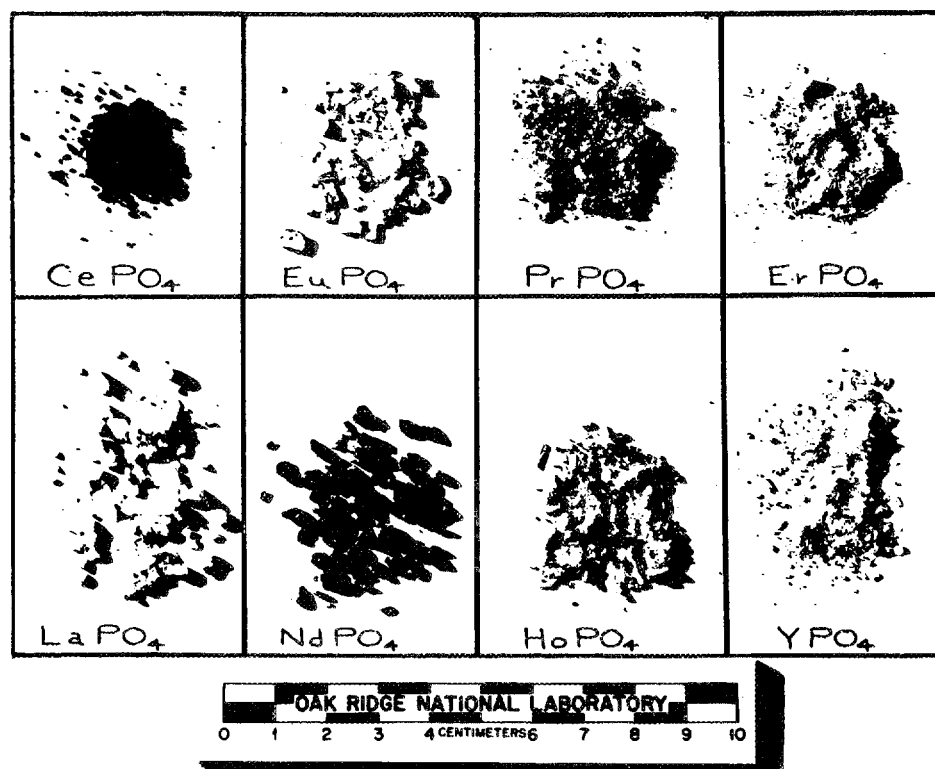


Fig. 5. Single crystals of various orthophosphates prepared by means of a flux technique. A $Pb_2P_2O_7$ flux is employed in the growth of these specimens.

X-ray powder diffraction and precession camera techniques were used to establish two different crystal habits for monazite crystals, as exemplified by the LaPO_4 and EuPO_4 crystals illustrated in Fig. 6. The b axis is the unique axis in these crystals and the a and c axes are perpendicular to the b axis. The a-c plane is perpendicular to the b axis, but the a axis and c axis are not at right angles to each other.

Figure 7 shows crystals of ^{241}Am in LaPO_4 with an $\sim 1\%$ Am_2O_3 doping. These crystals were grown in a glove box. The crystals are amber but

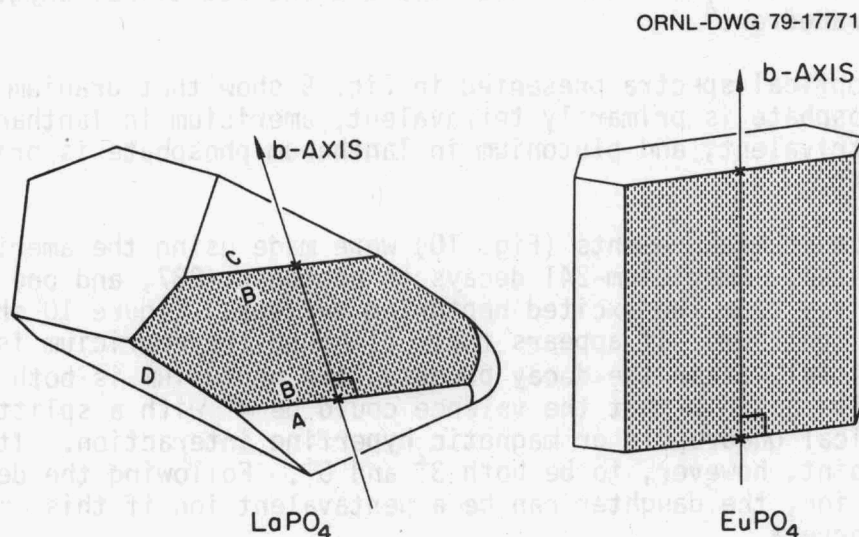


Fig. 6. Observed crystal habits of monazite-type (i.e., monoclinic) lanthanide orthophosphates.

ORNL PHOTO 3596-79

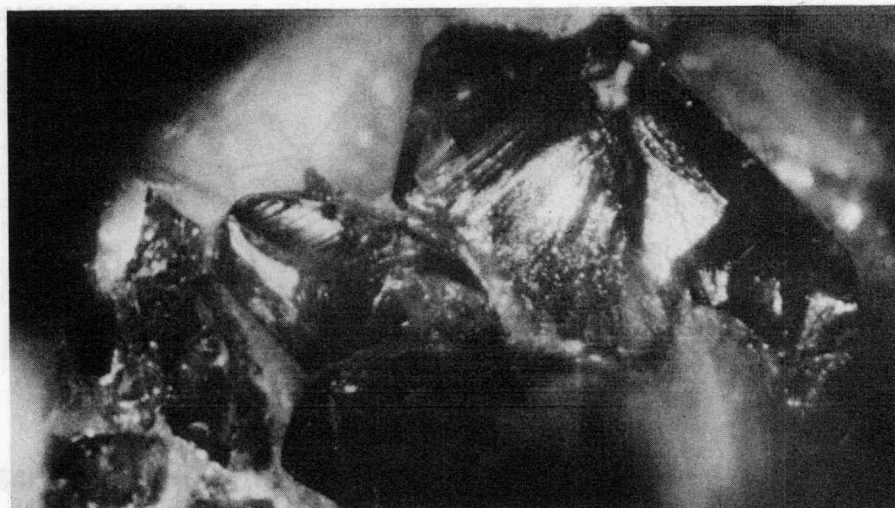


Fig. 7. Crystals of americium-doped lanthanum orthophosphate as seen through the glovebox window. The large crystal in the upper right hand portion of the photograph is approximately 6 mm in length.

this color is not directly due to the americium itself. Radiation damage arising from the americium α -decay in the crystal produces this brown coloration. These crystals will become completely clear at an annealing temperature of about 200 or 300°C, but at room temperature the color returns. This is merely a color center effect due to the production of point defects in the crystal.

Figure 8 illustrates the coordination around the cerium or lanthanum rare earth site. There are nine oxygens surrounding the rare earth ion. There are interpenetrating PO_4 tetrahedra and each site has 8 oxygens from four different tetrahedra and one additional oxygen from a fifth tetrahedron.⁴

The optical spectra presented in Fig. 9 show that uranium in lanthanum phosphate is primarily tetravalent, americium in lanthanum phosphate is trivalent, and plutonium in lanthanum phosphate is primarily tetravalent.

Mössbauer measurements (Fig. 10) were made using the americium-doped LaPO_4 crystal. Americium-241 decays to neptunium-237, and one observes the gamma ray from the excited neptunium nucleus. Figure 10 shows the gamma-ray spectrum. It appears that, although the americium is trivalent in the crystal, after the decay process, the neptunium is both 3^+ and 5^+ . It is still possible that the valence could be 4^+ with a splitting due to an electrical quadrupole or magnetic hyperfine interaction. It appears at this point, however, to be both 3^+ and 5^+ . Following the decay of a trivalent ion, the daughter can be a pentavalent ion if this interpretation is correct.

Figure 11 is an illustration of the monazite structure, showing four different lanthanide sites in the unit cell. An examination of the PO_4

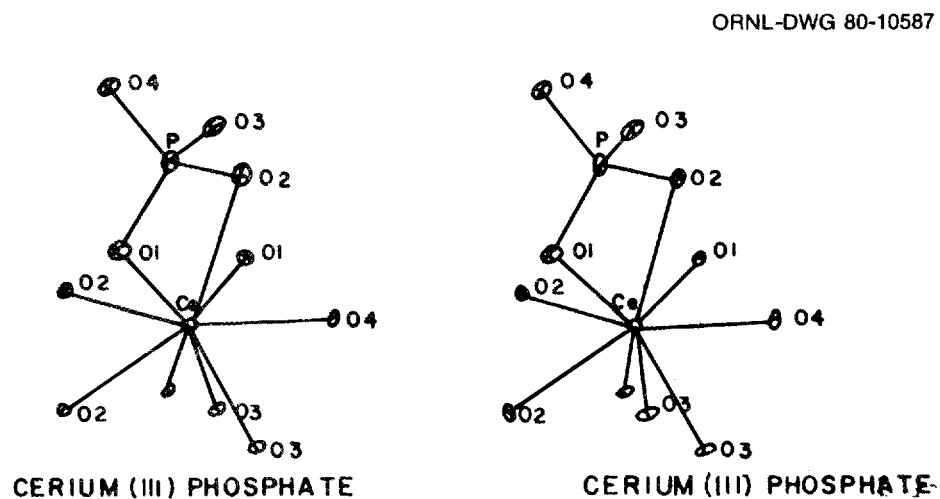


Fig. 8. Stereo projection of the local coordination around the cerium site in CePO_4 . The cerium ion is coordinated with 9 oxygens.

ORNL-DWG 80-10343.

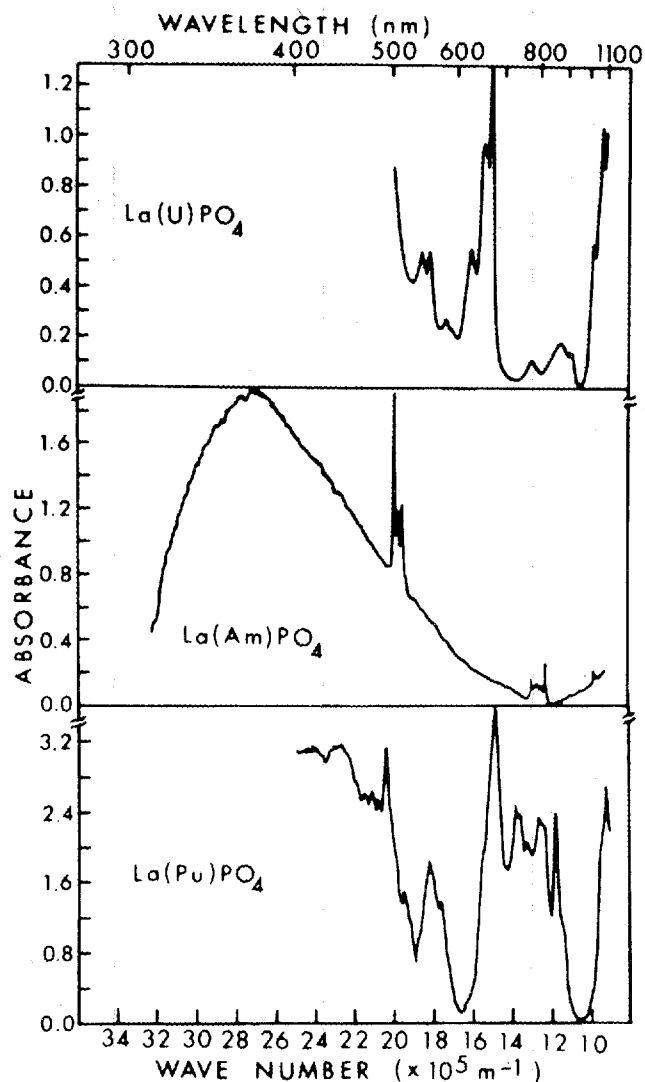


Fig. 9. Optical absorption spectra for uranium-doped lanthanum phosphate (upper trace), for americium-doped lanthanum phosphate (middle trace), and plutonium-doped lanthanum phosphate (lower trace).

tetrahedra shows that Ln_4 and Ln_1 are sites with inversion symmetry. Similarly, the Ln_2 and Ln_3 sites have inversion symmetry. In a magnetic resonance experiment the inversion symmetry prevents the magnetic field from distinguishing between Ln_4 and Ln_1 . Therefore, a magnetic resonance experiment would show two magnetically inequivalent spectra in the unit cell, with each spectrum representing two sites, 1 and 4 or 2 and 3. The two pairs of sites are actually equivalent, but their phase angles are different with respect to the magnetic field.

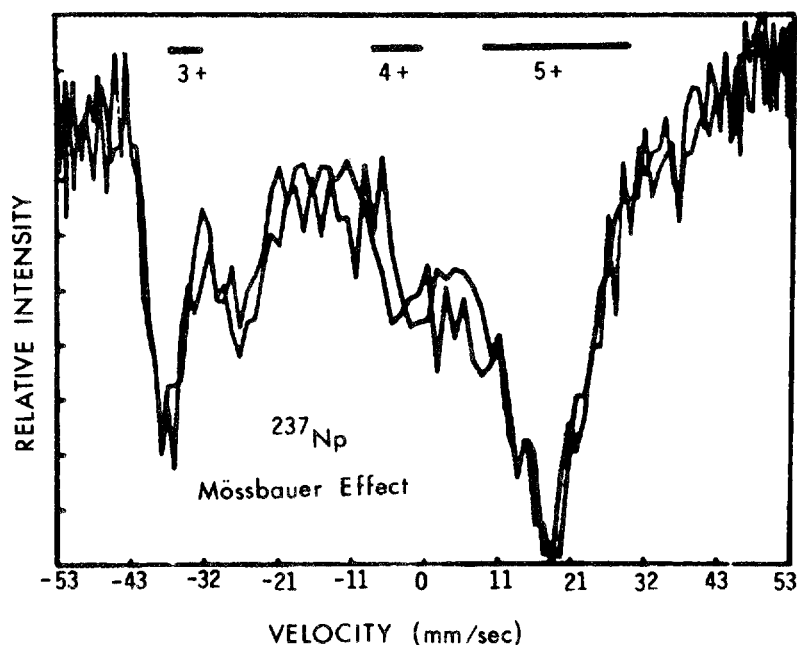


Fig. 10. Mössbauer spectrum of neptunium-doped lanthanum orthophosphate.

Figure 12 shows an electron paramagnetic resonance spectrum of a gadolinium-doped lanthanum orthophosphate crystal⁵ taken at 35 GHz and room temperature. The crystal is oriented with the b axis perpendicular to the magnetic field so that the magnetic field can be rotated in the a-c plane. In this case the two magnetically inequivalent pairs of sites always have equivalent orientations relative to the magnetic field. For gadolinium 3^+ seven allowed transitions occur between the eight crystal-field-split levels of the $8S_{7/2}$ ground state, and seven electron magnetic resonance lines are observed. In the present case these lines are doubly degenerate. If the rotation of the magnetic field is not in the a-c plane, the 7 lines will split into 14 lines. These lines provide information regarding the symmetry in the region surrounding the gadolinium ion, and using this information it is possible to determine that the gadolinium is in a substitutional lanthanum site.

Figure 13 shows an EPR powder pattern for the $\text{LaPO}_4:\text{Gd}^{3+}$ system. A powder pattern represents an average over all angles between the applied H-field and the crystal axes, and therefore, the extreme positions are observed as singularities. These "peaks" are essentially the zeros of derivatives. One can take the positions of singularities, i.e. shoulders and divergences in the average over all possible angles, and mark them on a bar diagram, and they are precisely the extreme positions of the EPR lines for the single crystal. This fact can be used to orient the single crystal if one does not know the axes. The extreme positions can be determined from the "powder" spectrum and then, by moving the

ORNL-DWG 79-17769R

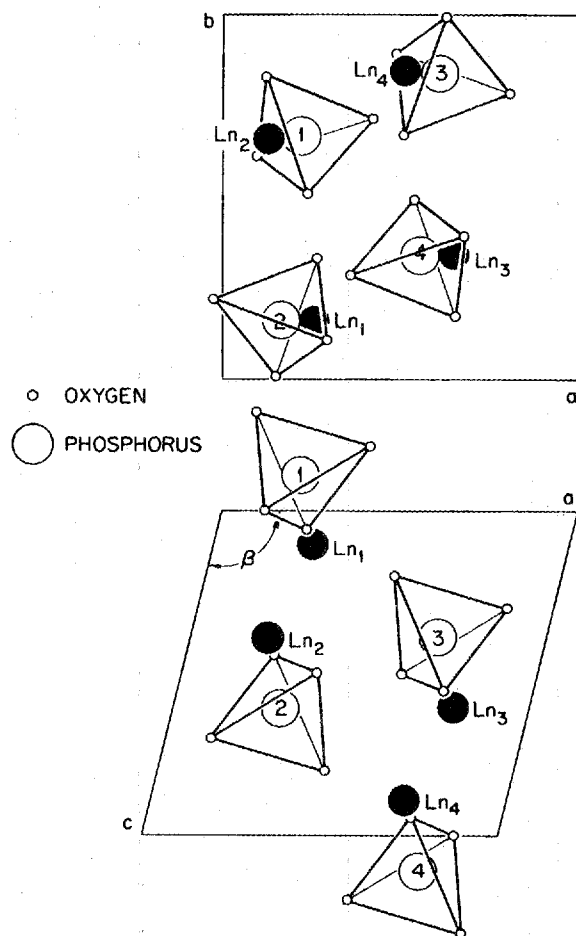


Fig. 11. Projections of the monazite crystal structure on the ac plane [(010) plane] and the ab plane [(001) plane]. The PO_4 tetrahedra and the Ln ions are arbitrarily labeled 1 to 4. It should be noted that in the monoclinic structure the axis perpendicular to the other two nonorthogonal axes is called the b axis (i.e., it is not termed the c axis).

ORNL-DWG 79-17781

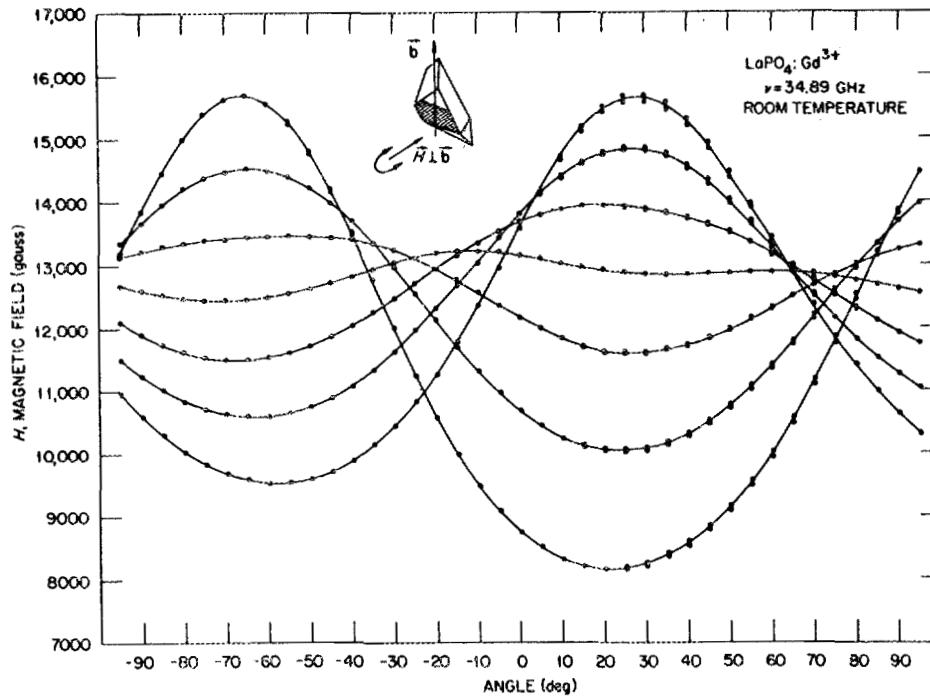


Fig. 12. Angular dependence of the EPR transitions for Gd^{3+} in an $LaPO_4$ single crystal when \vec{H} is rotated in the plane perpendicular to the b axis [i.e., in the (010) plane]. Each curve in this figure is doubly degenerate, but due to a small misalignment of the $LaPO_4$ crystal, a slight resolution of the superimposed lines is apparent at certain angles. This proves that the (010) plane is a plane of equivalence for two magnetically inequivalent, but otherwise equivalent, Gd^{3+} sites. This result is in agreement with the symmetry properties of the four different Ln sites contained in the unit cell of the monazite structure and with the occupation of predominantly Ln^{3+} sites by Gd^{3+} impurity ions.

ORNL-DWG 79-15615

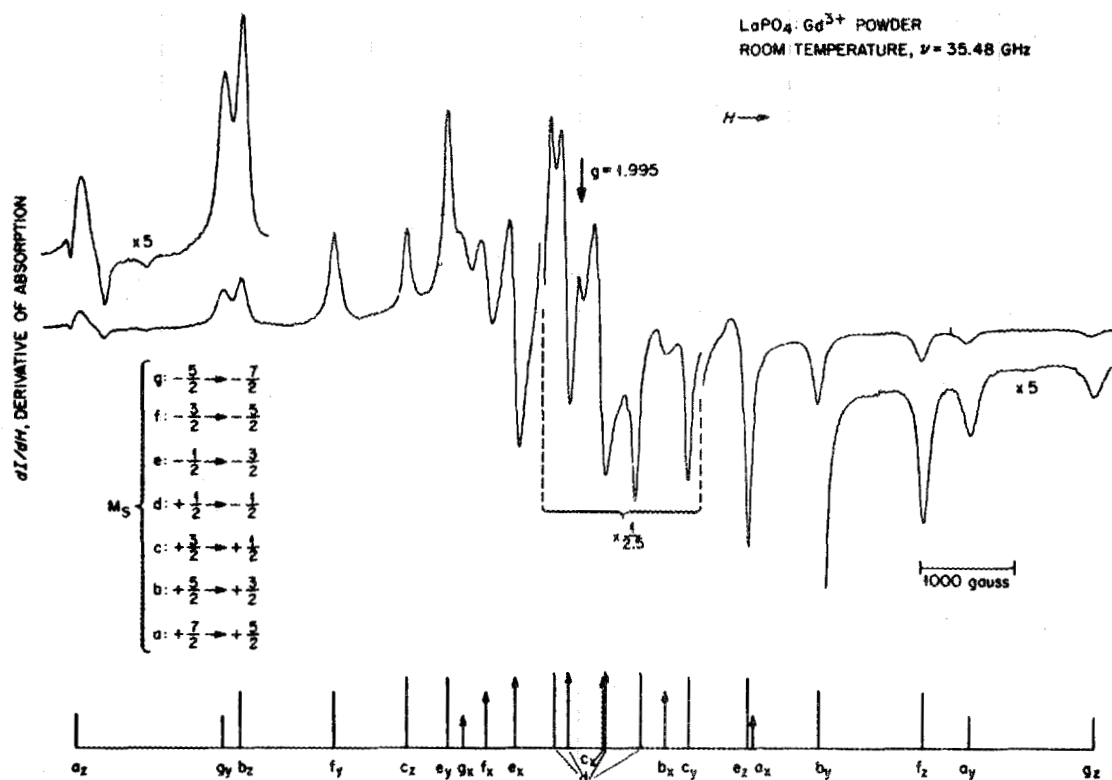


Fig. 13. EPR spectrum of LaPO₄:Gd³⁺ powder prepared using the technique of precipitation in molten urea. The seven allowed transitions $M_S \rightarrow (M_S - 1)$ are labeled with the letters a-g. The subscript x is used to identify the divergences whose magnetic field positions are identical to those of the corresponding single-crystal lines when \vec{H} is parallel to the principal electric field x axis. The y and z subscripts label the shoulders corresponding, respectively, to the relative and absolute extremes of the positions of the EPR single-crystal lines (i.e., the transitions observed with $\vec{H} \parallel y$ and $\vec{H} \parallel z$, respectively).

crystal in the magnetic field, it is possible to find the crystal field axes.

Figure 14 shows the spectrum for a tetragonal system.⁶ This is a much simpler case because there is only one magnetic site, and the magnetic resonance exhibits only one seven-line spectrum. The spectrum (a) is obtained for \vec{H} oriented along the tetragonal axis. Spectrum (b) is obtained for \vec{H} perpendicular to the tetragonal axis, and (c) is the EPR powder pattern. The seven extremes in spectrum (a) are aligned with

ORNL-DWG 79-15095

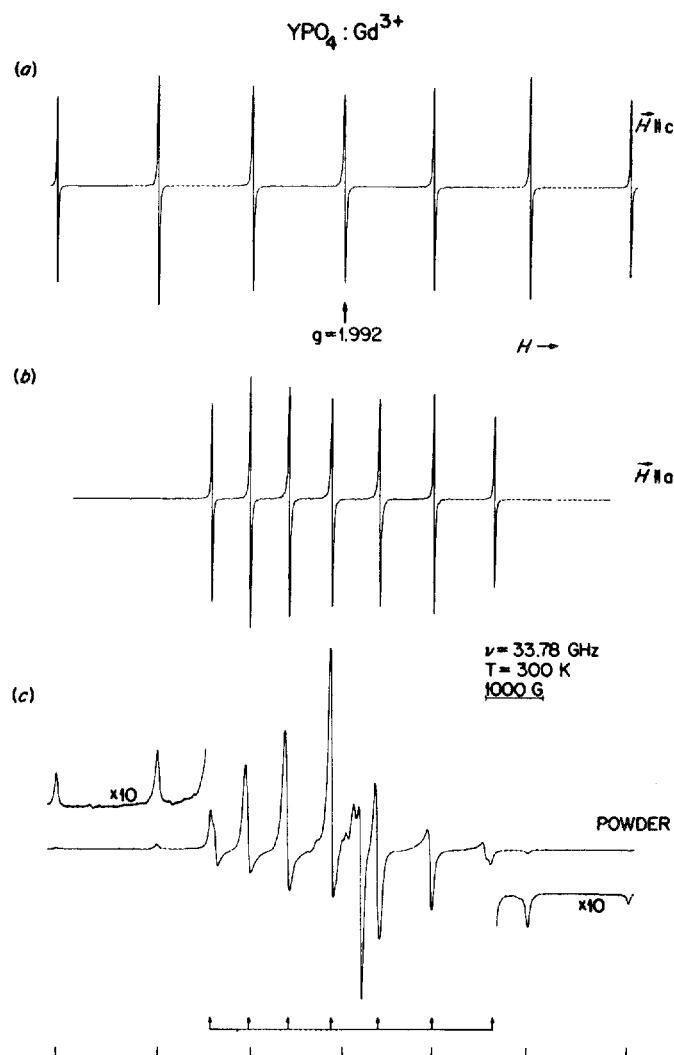


Fig. 14. EPR spectrum of Gd^{3+} in YPO_4 : (a) spectrum observed for a single crystal with $\vec{H} \parallel c$, (b) spectrum for a single crystal with $\vec{H} \parallel a$, and (c) spectrum of Gd^{3+} in a YPO_4 powder.

corresponding extremes in the powder spectrum (c), and the seven extremes in spectrum (b) are also aligned with corresponding extremes in spectrum (c). The bar diagram at the bottom of Fig. 14 represents those positions in the powder pattern that correspond precisely to \vec{H} parallel to the a and c directions of the single crystal.

For YPO_4 and LuPO_4 crystals that were grown in the lead-pyrophosphate flux, trivalent lead impurities were found in the crystals (Fig. 15). Lead is present in the flux as divalent lead, PbHPO_4 , but since yttrium and lutetium are trivalent, some constraint in the crystal forces the substitutional lead to become trivalent. A similar effect is found for rare earths in calcium fluoride. Even though the rare earth is normally trivalent, one can make trivalent rare earths divalent in calcium fluoride, because the divalent calcium site exerts an extra constraint on the rare earth. Pb^{3+} has a single 6s electron, and the wave function of a 6s electron is "spread out" and interacts with the neighboring ions. Figure 15 shows the hyperfine interaction for a single lead line. The lead spectrum shows a 1-4-6-4-1 hyperfine pattern representing an interaction with four neighbors, each of which has a nuclear spin of 1/2. The initial interpretation of this hyperfine structure was that the four neighbors were yttrium ions, because this hyperfine structure was not observed in lutetium phosphate. The lead line in lutetium was slightly broader, however, so it was not possible to determine whether this

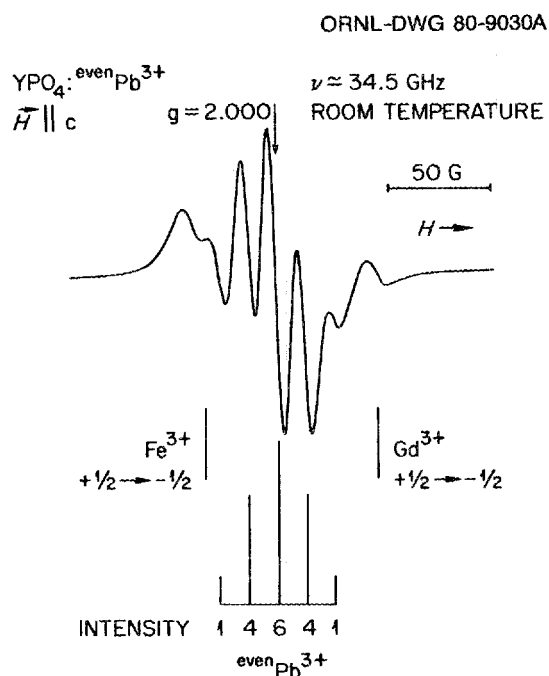


Fig. 15. EPR spectrum of Pb^{3+} in YPO_4 single crystal. The hyperfine structure indicates that there is an interaction with 4 equivalent $I = 1/2$ nuclei. ENDOR results determined that this interaction was due to the four second nearest ^{31}P neighbors.

structure was actually due to yttrium or to phosphorus. Both yttrium and phosphorus are 100% nuclear spin 1/2 nuclides. Double resonance experiments were used to demonstrate that the five-line hyperfine structure is due to the second-nearest-neighbor phosphorus ions. At liquid helium temperature, each of these five lines further splits into three lines. These are due to interactions with the two first-nearest-neighbor phosphorus ions, which have a smaller interaction than the second-nearest-neighbor phosphorus ions. This interesting effect also occurs in the alkali halides with F-centers, where the nearest-neighbor interaction is occasionally smaller than the next-nearest-neighbor interaction.

Lead has an isotope with 20% abundance, ^{207}Pb , that is characterized by a very large hyperfine value. Figure 16 is an energy-level diagram showing the levels for an ion with a nuclear spin 1/2 and an electronic spin 1/2. Transitions for the ^{207}Pb isotope were observed at X band (9 GHz), at K band (25 GHz), and at K_a band (35 GHz). The so-called "forbidden" lines were observed at X band, and at K_a band. By observing an allowed and a forbidden line at K_a band, it is possible to perform a unique measurement of the ^{207}Pb hyperfine constant. That is, $A = 35\sqrt{2}$, if the allowed transition is coincident with the forbidden transition.⁷ When the frequency is increased, one of these transitions (the allowed) will move toward higher magnetic fields. The other (forbidden) transition will move down in field with increasing frequency (Fig. 17). An

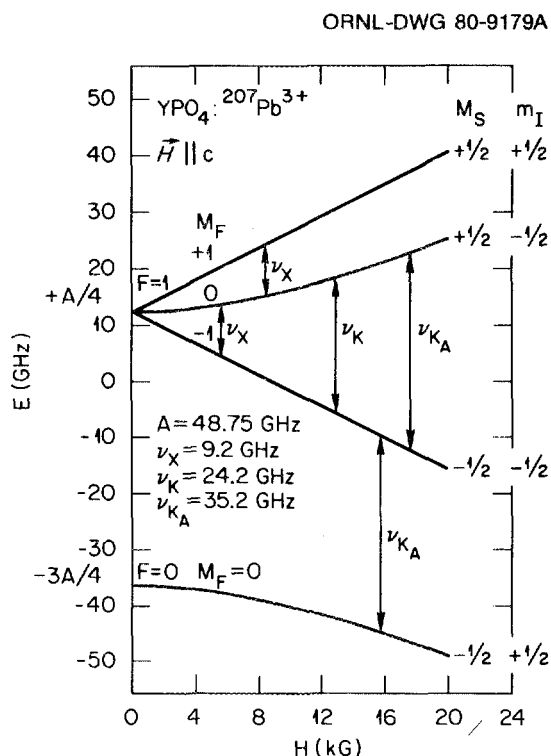


Fig. 16. Breit-Rabi diagram for ^{207}Pb ($I = 1/2$) in YPO_4 . The various transitions observed at different microwave frequencies are depicted.

ORNL-DWG 80-9036A

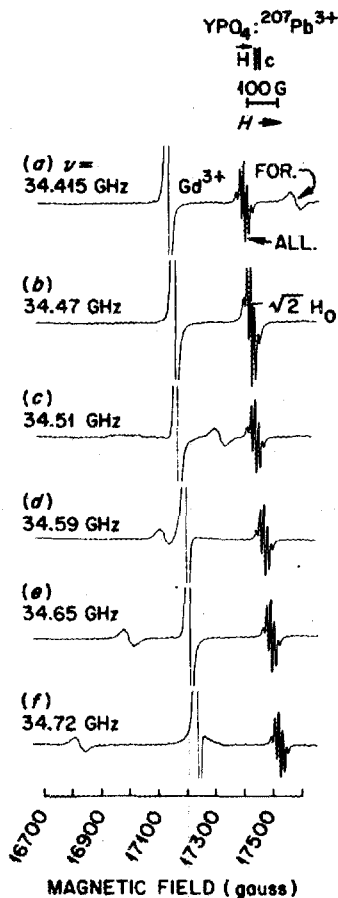


Fig. 17. EPR spectra showing $^{207}\text{Pb}^{3+}$ hyperfine lines (forbidden and allowed) in YPO₄. The spectra were obtained as a function of frequency, and the superposition of both the allowed and forbidden Pb hyperfine lines gives a measure of the hyperfine interaction through the relationship $A = 2^{1/2}H_0$.

allowed transition and a forbidden transition of the lead are noted in the figure. They are coincident at one point in Fig. 14. At this point, one can determine the magnitude of the hyperfine interaction without measuring the magnetic field.

A summary of the valence states observed in rare earth orthophosphates is given in Table 3. Divalent manganese has been seen along with a number of trivalent ions, some tetravalent ions, and some pentavalent ions. This does not imply that all of these valence states were seen in all of the orthophosphates. For instance, trivalent uranium has been identified only in the tetragonal orthophosphate at this point in time. In order to investigate the monoclinic structure with its two magnetically inequivalent spectra and identify a given impurity, it is necessary to describe every line that is observed. This is often

Table 3. Impurity Valence States Observed in the Rare-Earth Orthophosphates

2+	3+	4+	5+	
Mn [*]	Fe ^{*‡}	Yb [*]	U [†]	Np [‡]
	Ce [*]	Pb [*]	Np [‡]	Cr [*]
	Nd [*]	U [*]	Pu [†]	
	Gd [*]	Np ^{†‡}		
	Dy [*]	Am [†]		
	Er [*]	Cm [†]		

Detected by: ^{*}EPR[‡]Mössbauer[†]Optical Absorption

difficult when two different spectra are competing and it is convenient to examine the tetragonal crystals first and to use "labeled" isotopes. From the tetragonal crystals, one can obtain parameters that are useful in interpreting spectra of ions in the monoclinic hosts. ¹⁶⁷Er, ¹⁷³Yb, or ¹⁴³Nd have been used in this way to eliminate problems in identification. One has difficulty in identifying uranium because it is predominantly ²³⁸U, which has no nuclear spin. It would be preferable to investigate an isotope such as ²³⁵U or ²³³U.

In a research program dealing with the containment of radioactive wastes, studies using single crystals obviously represent a basic approach. Applied work is also currently underway. The method of Aaron et al.,⁸ involving urea co-precipitation, has been applied to the orthophosphates (Fig. 18). Starting with lanthanide oxide (in the case of cerium, cerium nitrate, which is easier to dissolve, is used) the oxide powder is dissolved in nitric acid and water and ammonium hydrogen phosphate is added in a stoichiometric amount. This forms the orthophosphate by metathesis. Urea is then added and heated. Following the intermediate step of low-temperature heating and subsequent high-temperature heating, an orthophosphate powder is obtained. This powder can then be either hot-pressed or cold-pressed and sintered.⁹ This procedure was first applied to a cerium compound and various amounts of urea were used. As shown in Table 4, in five samples the amounts of cerium nitrate, ammonium hydrogen phosphate, and nitric acid were invariant. The amount of water was also fixed, except for sample 1. Urea was added in differing amounts, from about 500 to 4,000 grams, in order to vary the mole ratio of urea to cerium. The apparent density of the powder

ORNL-DWG 79-19389

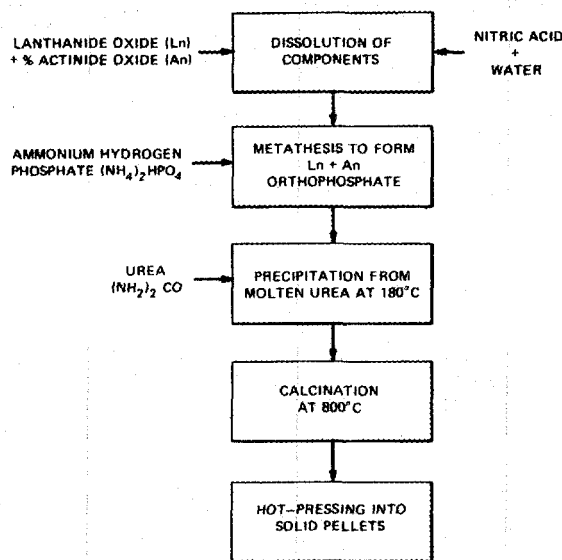


Fig. 18. Processing sequence for the conversion of lanthanide-actinide oxides into orthophosphates. Following the calcination at 800°C, compaction of the resulting powders via hot pressing can yield bodies with 97% of the theoretical density of the compound.

Table 4. Powder Preparation Constituents and Apparent Densities

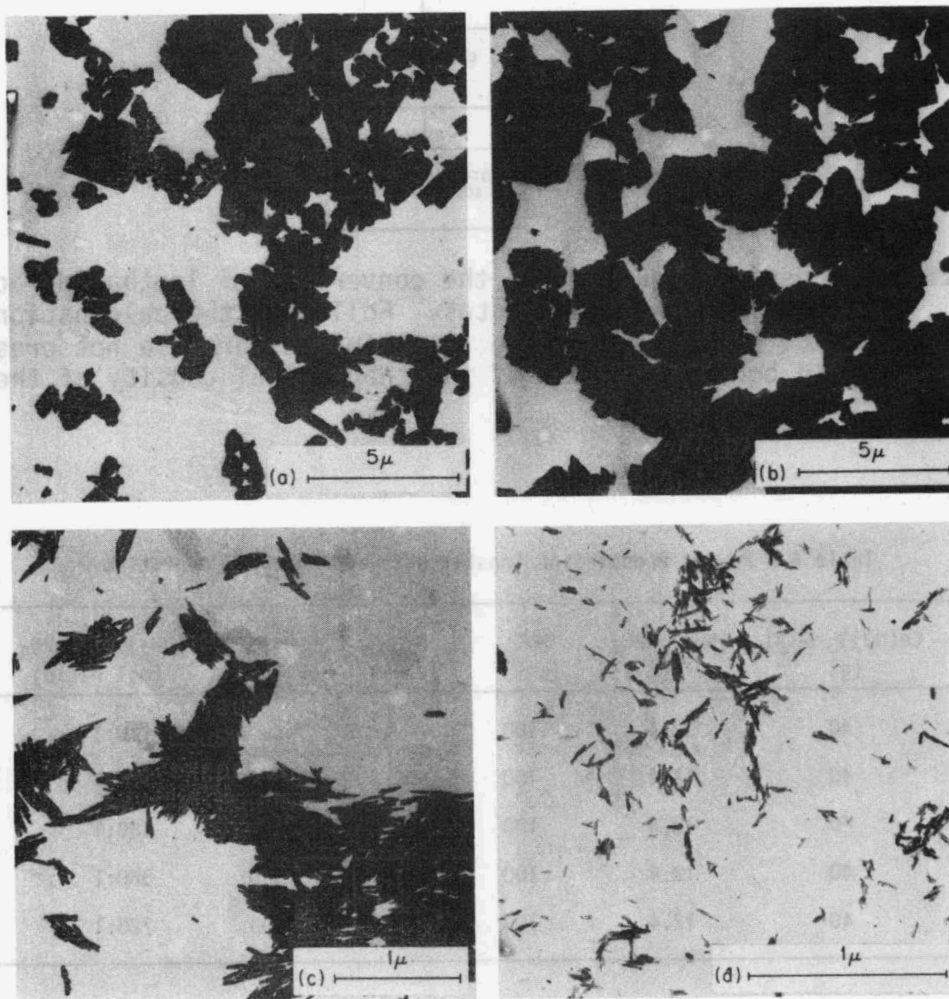
Sample	Ce(NO ₃) ₃ ·6H ₂ O (g)	(NH ₄) ₂ HPO ₄ (g)	HNO ₃ (cm ³)	H ₂ O (cm ³)	(NH ₂) ₂ CO (g)	(NH ₂) ₂ CO:CePO ₄ (mol ratio)	Apparent Density (g·cm ⁻³)
I	40	12.4	100	-	-	0:1	0.625
II	40	12.4	100	100	500	90:1	0.225
III	40	12.4	100	100	1000	180:1	0.122
IV	40	12.4	100	100	2000	360:1	0.033
V	40	12.4	100	100	4000	720:1	0.022

decreased as more urea was used. (Apparent density is a description of the "fineness" (particle size) of the powder.) Although a small particle size is desirable, the smaller particle sizes result in increased difficulty in hot-pressing or sintering.

To compare the crystal structure of these powders (and between powders and single crystals), mechanically ground single crystals were

employed along with powder that had been precipitated without urea, and powders precipitated with a 90:1 mole ratio and a 720:1 mole ratio of urea to phosphate. The corresponding x-ray powder patterns are typical of the monoclinic cerium phosphate structure. Transmission electron micrographs of the four samples are shown in Fig. 19. Note that the scale is 5 microns on (a) and (b) and 1 micron on (c) and (d) in Fig. 19. The urea apparently prevents an aggregation of the crystallites since, in the powder precipitated without urea, the crystallites

ORNL-DWG 79-19391

TRANSMISSION ELECTRON MICROGRAPHS OF CePO_4

- (a) MECHANICALLY GROUND SINGLE CRYSTALS
- (b) PRECIPITATED POWDER WITHOUT UREA
- (c) PRECIPITATED POWDER WITH UREA: $\text{CePO}_4=90:1$ MOLS
- (d) PRECIPITATED POWDER WITH UREA: $\text{CePO}_4=720:1$ MOLS

Fig. 19. Transmission electron micrographs comparing CePO_4 particles in powders precipitated with and without urea and particles obtained by mechanically grinding single crystals.

coagulate. The results of the x-ray broadening and transmission electron microscopy (TEM) measurements are listed in Table 5. It can be seen that the crystallite sizes are not very different in the various specimens. The sample designations in Table 5 are the same as those in Table 4, where the urea:cerium phosphate mole ratios were 0:1, 90:1, 180:1, 360:1, and 720:1 for samples I, II, III, IV, and V, respectively. The particles from mechanically ground single crystals are obviously larger than those in urea precipitated powders. The lengths of the precipitated particles decrease as more urea is used. The crystallite sizes are the same, but the particle size is smaller with increasing amounts of urea.

Table 6 shows the results of hot-pressing these powders for 1 hr at 4000 psi, at various temperatures. As can be seen, the density is about 5.1 or 5.2 g/cm³ which is roughly 95 to 97% of the theoretical density

Table 5. Crystallite Size Deduced from X-ray Broadening and Particle Size Obtained from TEM

Sample	200 Å	120 Å	012 Å	212 Å	Length Å	Width Å
I	284	290	364	284	~ 10,000	~ 10,000
II	294	268	364	304	1,400	200
III	270	246	336	290	1,200	160
IV	194	188	304	216	1,000	140
V	134	148	226	154	600	80
Ground crystal	> 2,500	> 2,500	> 2,500	> 2,500	~ 10,000	~ 10,000

Table 6. Hot Pressing Conditions and Densities for CePO₄ Compaction

Sample	Temperature (°C)	Density (g·cm ⁻³)	% of theoretical density
I	1000	3.87	73.7
I	1300	5.05	96.0
II	1000	3.96	75.3
II	1100	5.11	97.2
II	1300	5.08	96.6
III	1000	5.07	96.4
IV	1000	5.00	95.2
V	900	2.26	43.1
V	1000	4.01	76.3

Densities of the pellets shown are obtained after hot-pressing at 280 bars (4000 psi) for 1 hr.

when powders with an intermediate particle size are used. The smallest particle size resulted in a decrease in the density. With roughly constant conditions, there appears to be an optimum particle size for hot-pressing. Figure 20 is a photograph of typical pellets produced by this method.

ORNL PHOTO 3458-79



Fig. 20. Compacted pellets of CePO_4 .

Figure 21 shows the magnetic resonance spectrum observed for Gd^{3+} in cerium phosphate powder made as described above. The resonance parameters do not change appreciably in phosphates of the rare earths, lanthanum, cerium, praseodymium, neodymium, samarium, and europium. A comparison of Fig. 21 for $\text{CePO}_4:\text{Gd}^{3+}$ with Fig. 13 for $\text{LaPO}_4:\text{Gd}^{3+}$ shows that, because cerium phosphate has a magnetic ground state, the linewidths are slightly broader than in lanthanum phosphate, which has a diamagnetic ground state. Europium phosphate, which has a non-magnetic ground state, again shows sharp lines for the gadolinium spectra, while for neodymium or praseodymium phosphate, which have magnetic ground states, the linewidths are broader. The gadolinium is in essentially the same position in the lattice, however, and the powder and the single crystal are the same as far as the rare earth substitutional site is concerned.

In summary, the continuing research program for the lanthanide orthophosphates will consist of studies of actinides in tetragonal hosts in order to understand the more complicated monoclinic system. EPR, Mössbauer, optical absorption, and Raman techniques will continue to be employed in order to study the characteristics, stability, and leachability of these hosts, incorporating high-level radioactive wastes, which include the actinides as well as other radionuclides.

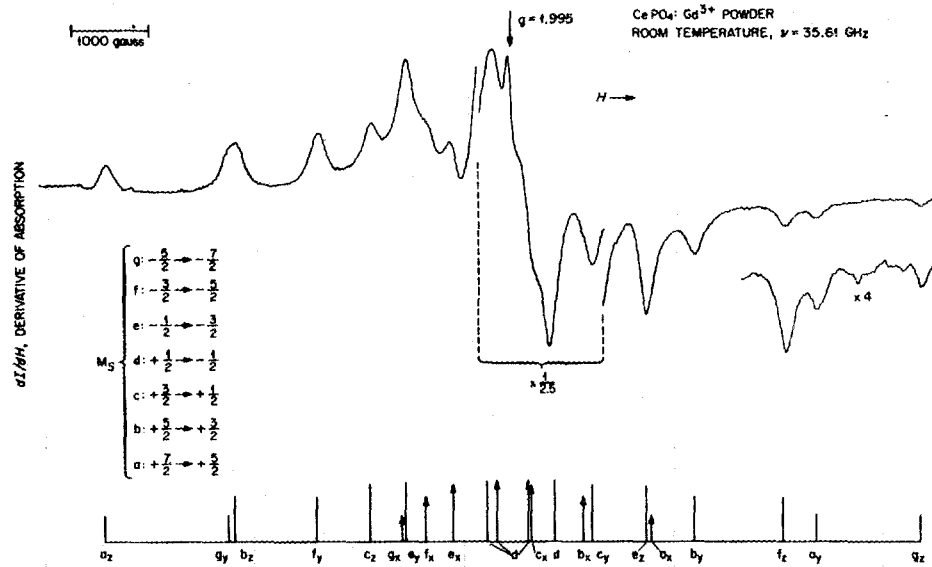


Fig. 21. EPR spectrum of a urea-precipitated powder of CePO₄:Gd³⁺. The x divergences are labeled with arrows, while the y and z shoulders are identified by bars at the bottom of the figure. The heights of both the shoulder bars and divergence arrows are drawn in proportion to the theoretical intensity of the corresponding EPR single-crystal transitions: i.e., 7:12:15:16:15:12:7 for the $M_S \rightarrow (M_S - 1)$ transitions with $M_S = \frac{7}{2}, \frac{5}{2}, \frac{3}{2}, \frac{1}{2}, -\frac{1}{2}, -\frac{3}{2}, -\frac{5}{2}, -\frac{7}{2}$, respectively.

DISCUSSION

UNIDENTIFIED QUESTIONER: If I heard you correctly, you said that you doped the lanthanum phosphate with 1% americium, and in a different experiment 10% uranium, but you did not mention the doping for plutonium.

ABRAHAM: The plutonium doping was 10 wt.% ²⁴²Pu₂O₃ added to the flux. We are not absolutely sure how much is in the single crystal.

SAME QUESTIONER: Where do you think the limits of doping are? How much loading can you put into this kind of crystalline matrix?

ABRAHAM: I do not think that there is any limit with the actinides. I believe that the pure actinide phosphate can be made.

JOHN A. STONE: Over the years, at Savannah River, we have looked at a great many neptunium- and americium-type Mössbauer spectroscopy experiments, and in particular, there are a number of source-type experiments such as the one you showed. It is not at all uncommon to find americium decaying into all sorts of valence states of neptunium, including the 5⁺

state, even though the americium may have started out in the 3^+ state. There is work reported, not only from us, but from workers in Israel, that demonstrates this.

Perhaps, another comment on this would be that the results of a source-type experiment really only shows you the valence state a few microseconds after the decay takes place; namely, the mean lifetime of the nuclear excited state. I think that it would be a very interesting experiment to dope the orthophosphates with neptunium and look at the absorber-type experiment. Have you done this, or do you have plans to do this?

ABRAHAM: We do plan to carry out experiments of this type.

UNIDENTIFIED QUESTIONER: In regard to the question on actinide loadings, Mr. Davis, at Penn State, is looking at the question of how much uranium and thorium (the actinides that he can handle) will go into the monazite structure. If the charge compensation with calcium is made on a one-to-one basis, it is a very simple exercise to make calcium-thorium phosphate without any rare earth in it at all. He mentioned that in Boston. It has not been a simple exercise to make calcium-uranium-IV phosphate, and the latest word is that there seems to be an oxygen fugacity range where it will form. At the reducing end, UO_2 drops out as a separate phase; at the oxidizing end, higher valence state uranium phosphates come out. We will have the final word on this in a paper at Boston.

ABRAHAM: Because the actinides have different valences, it would probably be difficult to make pure trivalent uranium phosphate, but I believe that trivalent curium phosphate could easily be made. If some Pb^{2+} is in the crystals, it acts as a valence compensator for tetravalent ions. Therefore, one can put a tetravalent ion in with a divalent ion to take care of two trivalent sites. We probably have a lot of Pb^{2+} lead in our tetravalent uranium crystal.

UNIDENTIFIED QUESTIONER: In theory, in crystal chemistry, you should have one Pb^{2+} for one U^{4+} .

ABRAHAM: Exactly. That is exactly what I am saying.

SAME QUESTIONER: But no data? No microprobes?

ABRAHAM: No, but measurements of this type are in progress.

ROBERT POHL: I have a question on the favorability of these crystals in groundwater solutions. Do you know what their etching characteristics are? I guess my reaction, looking at a phosphate, is that they are fairly highly soluble in acidic solutions.

ABRAHAM: In order to remove the phosphate crystals from the crystal growth flux, boiling concentrated nitric acid is used. The flux dissolves but the crystals remain. You have to boil them for weeks to remove the flux.

REFERENCES

1. L. A. Boatner, G. W. Beall, M. M. Abraham, C. B. Finch, P. G. Huray, and M. Rappaz, to be published in Scientific Basis for Nuclear Waste Management, Vol. II, C. J. Northrup (ed.), Plenum Press, 1980.
2. L. A. Boatner, G. W. Beall, M. M. Abraham, C. B. Finch, R. J. Floran, P. G. Huray, and M. Rappaz, to be published in the Proceedings of the International Symposium on the Management of Alpha-Contaminated Wastes, sponsored by the International Atomic Energy Agency and the Commission of the European Communities, Vienna, Austria, June 2-6, 1980.
3. R. S. Feigelson, *J. Am. Ceram. Soc.* 47, 257 (1964).
4. G. W. Beall, L. A. Boatner, D. F. Mullica, and W. O. Milligan, *J. Inorg. Nucl. Chem.* (in press).
5. M. Rappaz, M. M. Abraham, J. O. Ramey, and L. A. Boatner, *Phys Rev.* (in press).
6. M. Rappaz, L. A. Boatner, and M. M. Abraham, *J. Chem. Phys.* 73, 1095 (1980).
7. M. M. Abraham, L. A. Boatner, and M. Rappaz, *Phys. Rev. Lett.* 45, 839 (1980).
8. W. S. Aaron, T. C. Quinby, and E. H. Kobisk, "Cermet High Level Waste Forms," U.S. DOE Report ORNL/TM-6404, June 1978.
9. M. M. Abraham, L. A. Boatner, T. C. Quinby, D. K. Thomas, and M. Rappaz, *Radioactive Waste Management* (in press).

THE APPLICATION OF EPR SPECTROSCOPY TO THE CHARACTERIZATION
OF CRYSTALLINE NUCLEAR WASTE FORMS

M. Rappaz,* L. A. Boatner, and M. M. Abraham

Solid State Division, Oak Ridge National Laboratory**
Oak Ridge, Tennessee 37830

ABSTRACT

Electron paramagnetic resonance (EPR) spectroscopy is currently a well established technique that is frequently applied in materials science to the study of paramagnetic impurities and defects in solids. EPR spectroscopy is a very powerful, site-specific technique, and it is rather surprising that it has not been applied more extensively to the problem of characterizing alternative nuclear waste forms. The technique yields the maximum amount of information when applied to crystalline substances, and the recent increase in interest in ceramic waste forms and crystalline systems analogous to resistant natural minerals suggests that EPR spectroscopy can play a major role in characterizing primary containment media of this type.

The EPR spectrum of a paramagnetic impurity (e.g. Ce^{3+} , Am^{2+} , Gd^{3+} , Fe^{3+} ...) in a dielectric host crystal reflects the crystalline electric field created by the neighboring ions which surround the impurity. Therefore, the number of EPR transitions observed and their positions as a function of the strength and relative orientation of the applied magnetic field can be used to determine the valence state of the paramagnetic impurity, and the site(s) occupied by the impurity and can provide information regarding the local crystal structure.

The intensity of the EPR transitions for a given impurity ion is directly proportional to the number of such paramagnetic ions present in the sample, and this fact can be used to obtain information regarding the phase diagram of mixed host-impurity systems. For example, a comparison of the EPR spectra due to Gd^{3+} and Fe^{3+} ions in LuPO_4 has shown that Fe^{3+} impurities are not incorporated into LuPO_4 as easily as Gd^{3+} .

* Present address: Laboratoire de Physique Expérimentale, École Polytechnique Fédérale de Lausanne, 1007 Lausanne, Switzerland.

** Operated by Union Carbide Corporation for the U.S. Department of Energy under contract W-7405-eng-26.

Unlike the broadening of x-ray powder diffraction peaks, which primarily results from effects due to the size of crystallites that compose the powder, the linewidths of EPR transitions are mainly affected by the number of defects or impurities present in the structure. Accordingly, paramagnetic impurities can be used to monitor defects, and strains, such as those due to the presence of impurities of different ionic size or valence, or to radiation damage produced by actinide dopants.

In the preceding paper, entitled "A Review of Research in Analogs of Monazite for the Isolation of Actinide Wastes," the Electron Paramagnetic Resonance (EPR) spectra of Gd^{3+} and Pb^{3+} in monazite- and zircon-type orthophosphates were presented. The present paper reviews in more detail the contributions of EPR spectroscopy to the characterization of alternate nuclear waste forms in general, and to the characterization of crystalline waste forms in particular.

EPR is a spectroscopic technique¹ that deals with unpaired electrons, and thus far it has been applied to investigations of point defects, metals, free radicals and paramagnetic impurities. Although EPR spectroscopy can be a powerful tool for studying radiation-induced point defects in crystalline materials, the following discussion will focus mainly on paramagnetic impurities diluted in a dielectric host.² For such systems, the technique of EPR is similar to, and complements, high-resolution optical spectroscopy. EPR deals only with the ground state of the paramagnetic impurity, however, and therefore an external magnetic field is usually applied in order to lift the ground-state degeneracy. Transitions between the resulting magnetic-field-split Zeeman levels are then induced by photons whose frequency lies in the microwave region (i.e. 9 to 35 GHz for magnetic fields ranging between 3 and 12 kG). Since it is difficult to vary the microwave frequency in an EPR experiment, the energy difference corresponding to the various transitions is matched by varying the amplitude of the external magnetic field. Consequently, an EPR spectrum consists of one or more absorption lines whose number and magnetic-field positions will reflect: i) the type of impurity being studied, ii) the valence state of this impurity, and iii) the local crystal field symmetry at the impurity site (Fig. 1).

From Table 1, it is apparent that EPR spectra have been observed for most of the elements that are present in the composition of PW-4b nuclear waste. The second column of Table 1 lists the chemical valence states usually found for these elements in accordance with the periodic table. The third column lists the valence states for which an EPR spectrum has been reported in the literature.³ It should be noted that, for special cases such as La^{2+} , unusual valences induced by the crystal host and/or irradiation have been observed by EPR. With a few exceptions such as Gd^{3+} or Fe^{3+} , which are characterized respectively by a typical 7- or 5-fine-structure-line EPR spectrum, a clear identification of the paramagnetic impurity is usually made possible via a hyperfine interaction with the nucleus of one or more isotopes. A few examples of such spectra are given in Figs. 2-7.

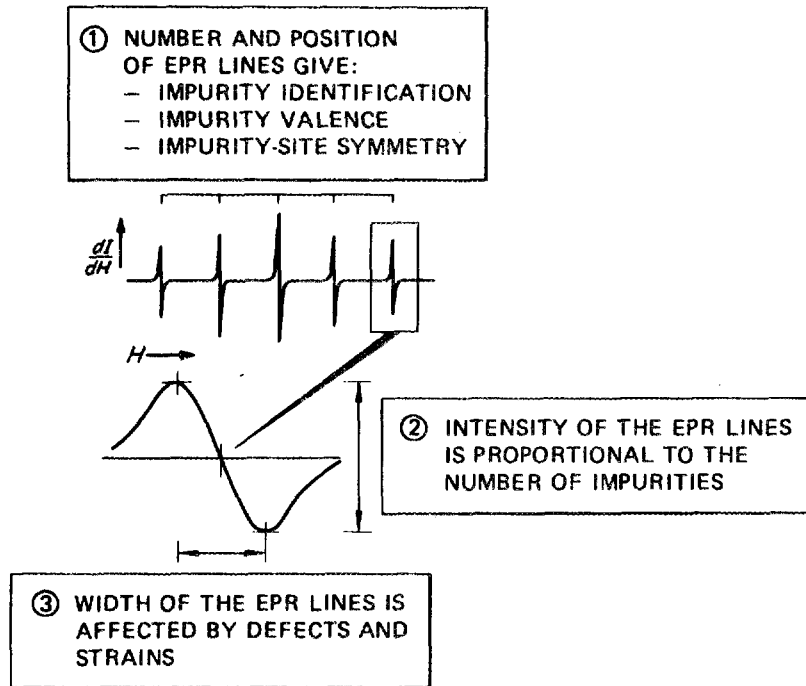


Fig. 1. The type of information that can be deduced from EPR spectroscopy.

Table 1. Elements in the composition of PW-4b nuclear waste, with their most common chemical valences and valence states for which an EPR spectrum has been reported (Ref. 3).

	MOL %	VALENCE	DETECTED BY EPR		MOL %	VALENCE	DETECTED BY EPR
La	26.4	+3	+2	Pd	4.1	+2, +4	+3
Ce		+3, +4	+3	Sr	3.5	+2	
Pr		+3, +4	+3	Ba	3.5	+2	
Nd		+3	+3, +4	Rb	1.3	+1	
Pm		+3	+3	U	1.4	+3 → +6	+3, +4, +5
Sm		+2, +3	+3	Th		+4	
Eu		+2, +3	+2	Np	0.2	+3 → +6	+4, +6
Gd		+3	+3	Pu		+3 → +6	+3, +6
Tb		+3, +4	+3, +4	Am		+3 → +6	+2, +4
Dy		+3	+3	Cm		+3	+3
Ho		+3	+2, +3	Fe	6.4	+2, +3	+1, +2, +3
Er		+3	+3	Na	1.0	+1	
Tm		+2, +3	+2	PO ₄	3.2		
Yb		+2, +3	+3	Tc		+7	+4
Lu	+3		Rh	9.0	+2, +3, +4	+2	
Zr	13.2	+4	Te		-2, +4, +6		
Mo	12.2	+6, +2	In		+3	+2	
Ru	7.6	+2, +3, +4 +6, +8	Ni		+2, +3	+1, +2, +3	
Cs	7.0	+1	Cr		+2, +3, +6	+3, +5 (+4) +1 (+2)	

ORNL-DWG 79-17776

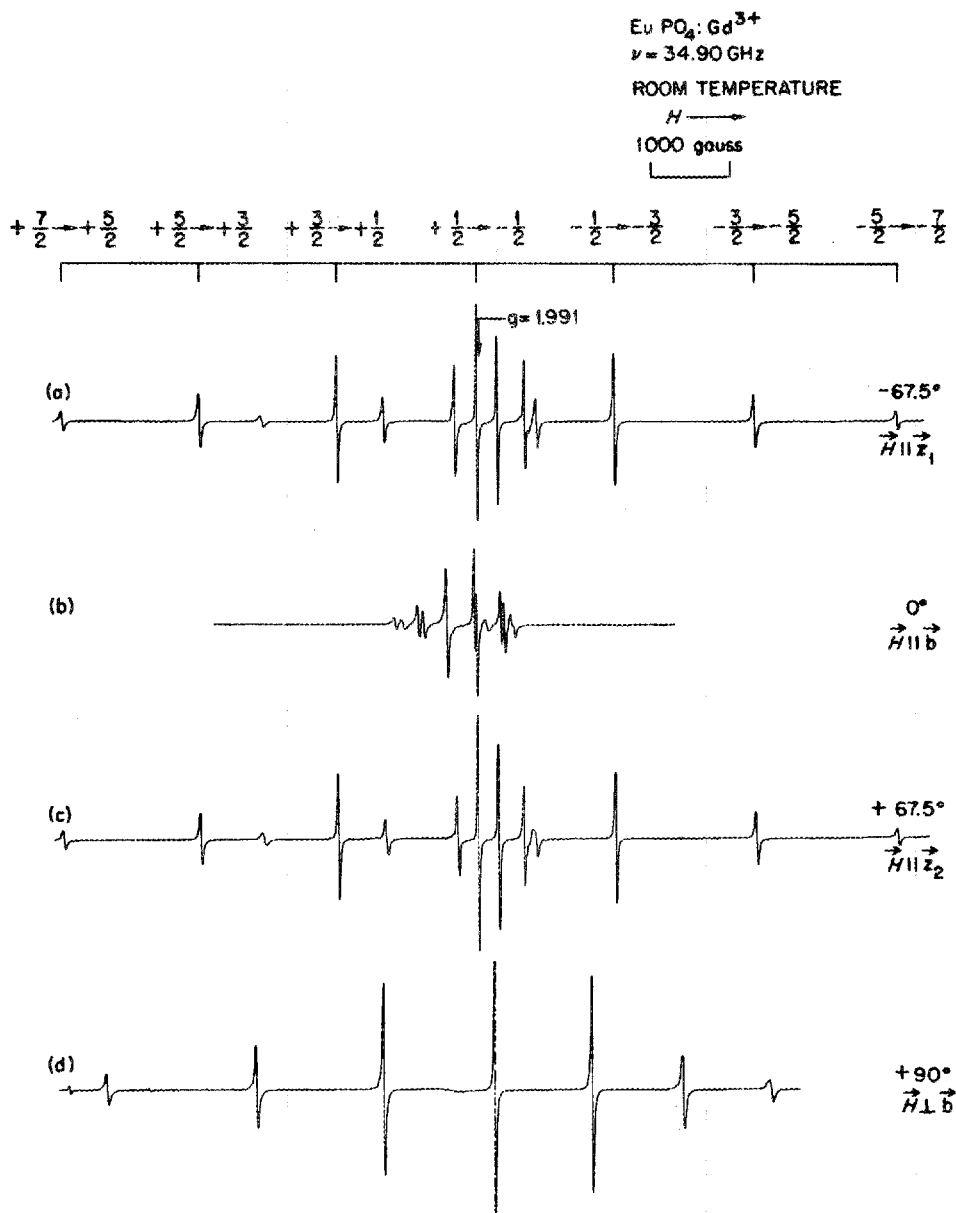
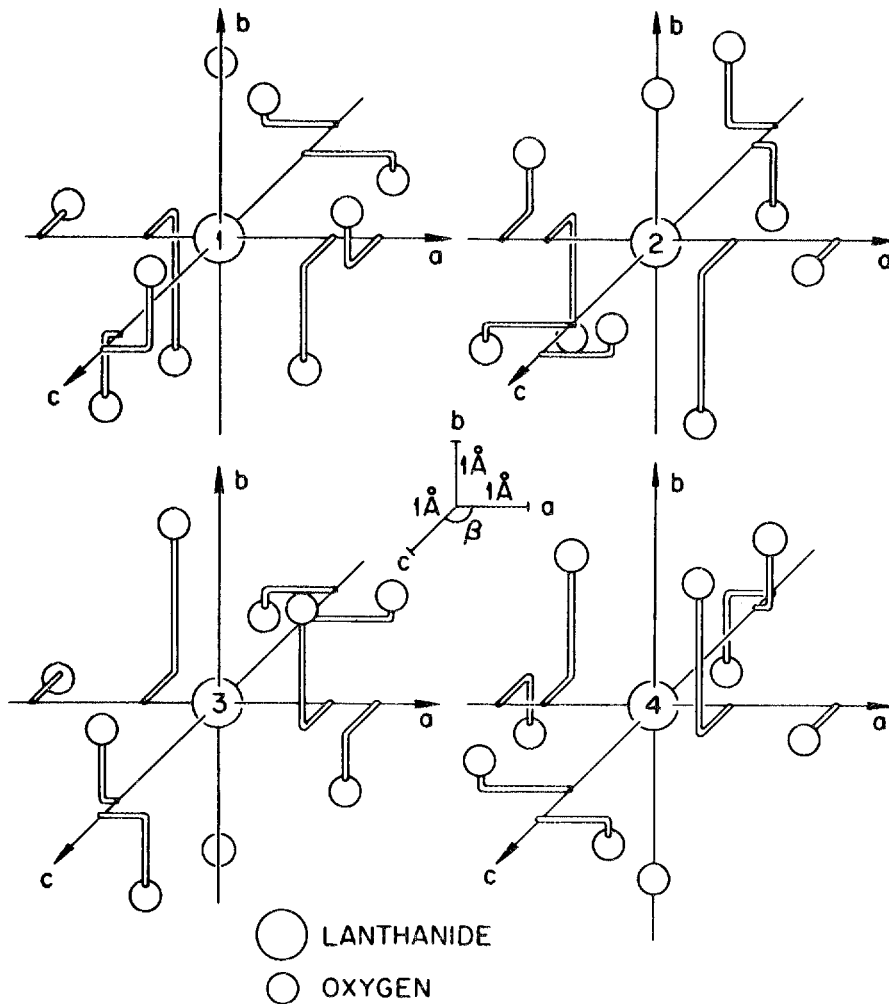


Fig. 2. EPR spectrum of Gd³⁺ in a monazite-type single crystal of EuPO₄. a) The magnetic field \vec{H} is applied parallel to the principal electric field z-axis of the magnetically equivalent sites (1,4) (see Fig. 3). The lines that are not labeled at the top of the figure correspond to Gd³⁺ ions which are in the sites (2,3). b) \vec{H} is parallel to the twofold-symmetry axis of the monoclinic structure, and the four sites are equivalent (i.e. only 7 degenerate lines are observed). c) \vec{H} is parallel to the z-axis of sites (2) and (3). The lines that were in the center of trace (a) are now extremes and are labeled at the top of the figure. d) \vec{H} is perpendicular to the b-axis and, therefore, only 7 doubly-degenerate lines are observed.



SITE	SYMMETRY OPERATION TO TRANSFORM (Ln_1 -SITE) \rightarrow (Ln_x -SITE)
Ln_2	180° ROTATION ABOUT THE b-AXIS
Ln_3	REFLECTION ABOUT THE (010) PLANE
Ln_4	INVERSION

Fig. 3. The four different rare-earth sites contained in the unit cell of the monazite structure, with their 9 oxygen nearest neighbors. These sites are equivalent from a crystallographic point of view since the symmetry operations listed at the bottom of this figure can transform any one given site into another.

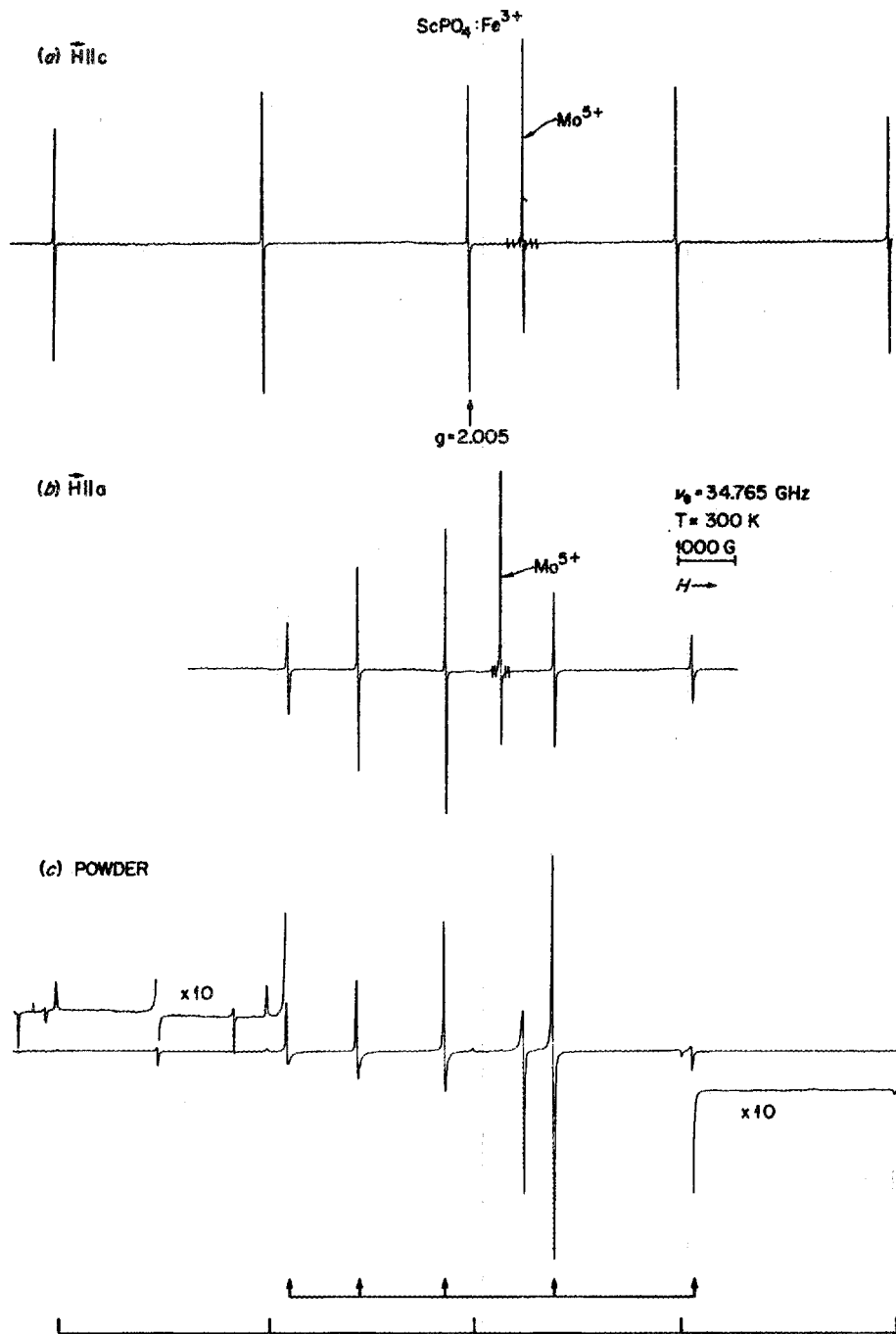


Fig. 4. EPR spectra of Fe³⁺ in a single crystal and a powder of zircon-structure ScPO₄. In (a) the magnetic field \vec{H} is parallel to the c-axis of the single crystal, while in (b) it is applied perpendicular to this axis (i.e. $\vec{H} \perp a$). c) The EPR spectrum obtained for the powder can be compared with traces (a) and (b).

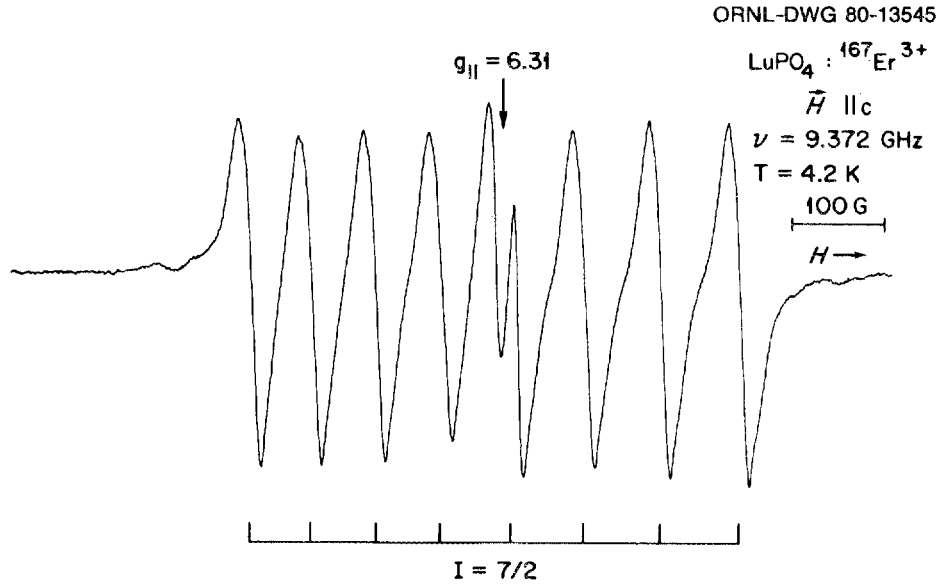


Fig. 5. EPR spectrum of ¹⁶⁷Er³⁺ in a single crystal of LuPO₄, exhibiting the 8 hyperfine-line structure due to the $I = 7/2$ nuclear spin of ¹⁶⁷Er. The magnetic field is applied parallel to the c-axis.

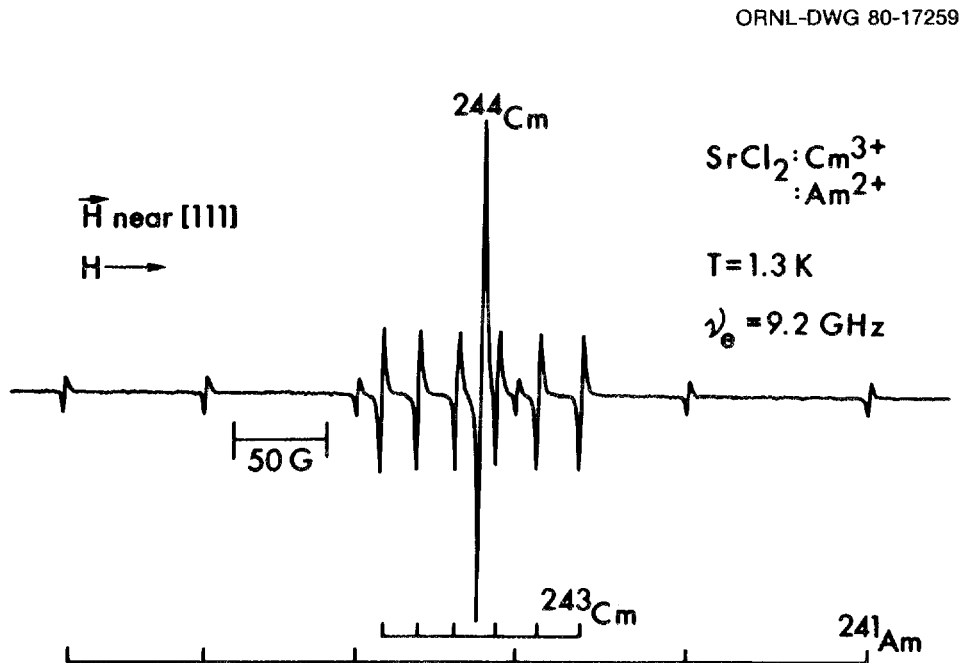


Fig. 6. EPR spectra of ²⁴³Cm³⁺, ²⁴⁴Cm³⁺ and ²⁴¹Am²⁺ in SrCl₂, when the magnetic field is applied parallel to a [111] axis of the cubic structure. (Ref. 7)

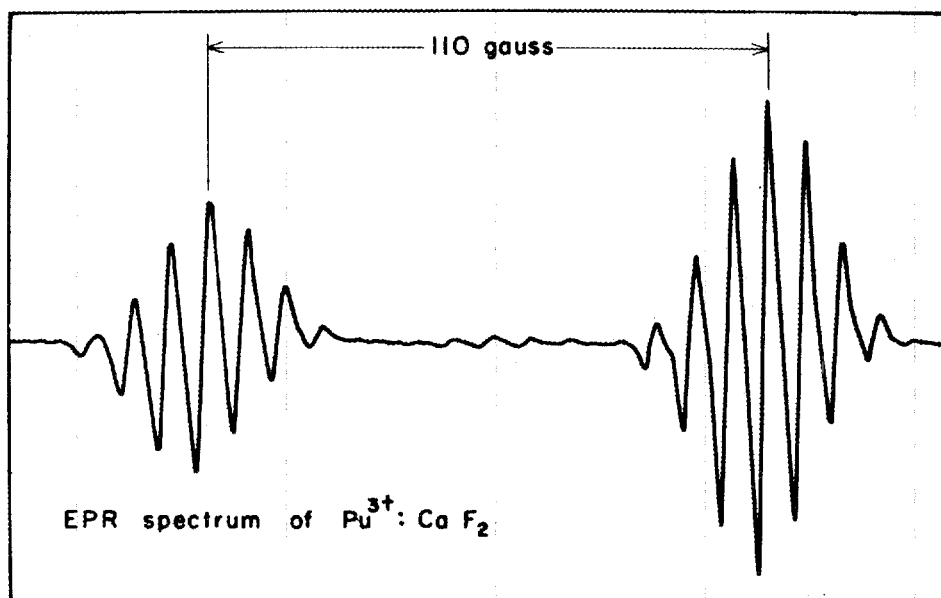


Fig. 7. EPR spectrum of $^{239}\text{Pu}^{3+}$ in CaF_2 , exhibiting, in addition to a 110 G hyperfine interaction due to the $I = 1/2$ nuclear spin of ^{239}Pu , superhyperfine interactions with the ($I = 1/2$) ^{19}F neighbor nuclei. (Ref. 8)

Figure 2 shows the EPR spectrum of Gd^{3+} in a monazite-type single crystal of EuPO_4 .⁴ As can be seen, this spectrum is composed of two sets of 7 lines, indicating that the Gd^{3+} impurities are in two sites. Since these lines can be brought to a position of equivalence, however, (i.e. only 7 degenerate lines are observed in trace (d) of Fig. 2), it is concluded that these two sites are only magnetically inequivalent, and are otherwise equivalent. These findings are in agreement with the statement that Gd^{3+} ions predominantly occupy rare-earth substitutional sites in the monazite structure, and with the description of the structure itself according to x-ray analysis. The monoclinic monazite structure contains four rare-earth sites in the unit cell (Fig. 3) but as a result of inversion symmetry, the sites labeled (1) and (4) on Fig. 3 are magnetically equivalent, as are sites (2) and (3). The symmetry operation that transforms these two sets of sites is a 180° -rotation along the b-axis of the monoclinic structure. Therefore, the four sites must be magnetically equivalent for either $H \parallel b$ or $H \perp b$, which is the case in Fig. 2 (spectra (b) and (d), respectively).

An additional example is provided by Figure 4, where the EPR spectra of Fe^{3+} in a single crystal and a powder of ScPO_4 are compared.⁵ From the 5-line spectrum, it can be concluded that Fe ions are in the 3+ valence state, and from the relative and absolute extremes of the EPR lines which occur when the magnetic field is applied along the a- and c-axes of the zircon structure, respectively, it is deduced that these impurities occupy the Sc site. A comparison with the powder spectrum shown at the bottom

of Fig. 4 indicates that Fe^{3+} ions occupy the same site in ScPO_4 powder prepared by coprecipitation in molten urea. Such a comparison demonstrates the ability of EPR to "follow" an impurity through complex physical- or chemical-process sequences. The extra line that is not labeled by an arrow or a bar at the bottom of Fig. 4 is due to an unintentional impurity. The large central line is due to an even isotope and is surrounded by 6 weak hyperfine lines characteristic of an odd isotope with a nuclear spin of 5/2. From the magnetic-field position of the central line and the magnetic-field separation of the hyperfine lines, this impurity can be identified as either Mo^{5+} (two odd isotopes ^{95}Mo and ^{97}Mo , both with $I = 5/2$ and natural abundances of 15.8% and 9.6%, respectively) or Zr^{3+} (only one odd isotope, ^{91}Zr , with $I = 5/2$ and a natural abundance of 11.2%). Although the EPR spectrum of Zr^{3+} has never been observed (see Table 1), the relative intensities of the six hyperfine lines compared with the central line seem to favor the presence of Zr^{3+} impurities. Further work is in progress for this system, but it has not been possible to reproduce this spectrum by intentional doping at the present time.

EPR spectra of rare-earths and actinides in solids can be clearly identified by using special enriched isotopes. Figure 5 shows the EPR spectrum of $^{167}\text{Er}^{3+}$ in LuPO_4 ,⁶ while Figure 6 represents the EPR spectrum of $^{243}\text{Cm}^{3+}$, $^{244}\text{Cm}^{3+}$, and $^{241}\text{Am}^{2+}$ in SrCl_2 .⁷ In Figure 7 the EPR spectrum of $^{239}\text{Pu}^{3+}$ in CaF_2 ⁸ exhibits, in addition to the hyperfine interaction with the $I = 1/2$ nuclear spin of ^{239}Pu , a superhyperfine interaction with the 8 nearest fluorine nuclei ($I = 1/2$). Such a hyperfine interaction with the neighbors is very useful in locating the paramagnetic impurity in the host lattice with a high degree of certainty.

As can be seen in Fig. 1, EPR spectroscopy can also provide useful information via the line intensity which is proportional to the number of paramagnetic impurities. Therefore, some indication of the nature of the phase diagram can be obtained. Figure 8 shows the EPR spectrum of Fe^{3+} in a single crystal and a powder of LuPO_4 . It must be specified, however, that the single crystal has been grown using a starting composition composed of Lu_2O_3 with 99.999% purity and 0.5 mol% of Fe_2O_3 . As can be seen, the intensities of the Fe^{3+} lines are comparable to those of Gd^{3+} , which is an undesirable impurity in this case. Accordingly, these findings indicate that either most of the Fe ions are in the divalent state or that most of the Fe ions remain in the lead flux used to grow the crystals, because the phase diagram of $(\text{Lu-Fe})\text{PO}_4$ is not favorable for the incorporation of a high Fe concentration at high temperature. Correlated Mössbauer experiments⁹ confirmed the second hypothesis, since Fe^{2+} was not detected by this technique. Similar conclusions can be reached by studying coprecipitated powders of Fe-doped LuPO_4 (Fig. 9). At thermodynamic equilibrium, a broad line is observed (see spectrum (a) at the top of Fig. 9) which, in correlation with the results of Mössbauer experiments, can be attributed to FePO_4 aggregates. The small features on each side of the broad line correspond to the fine-structure lines of those Fe^{3+} ions which are already in substitution in the LuPO_4 lattice. Heat treatment of the powder followed by a quench brings the system out of thermodynamic equilibrium and thereby increases the solubility limit of Fe ions in the LuPO_4 host. Spectrum (b), as presented at the bottom of Fig. 9, demonstrates this fact, i.e. following the quench, the $\text{LuPO}_4:\text{Fe}^{3+}$ signals are much more intense while the broad line due to FePO_4 aggregates has substantially decreased.

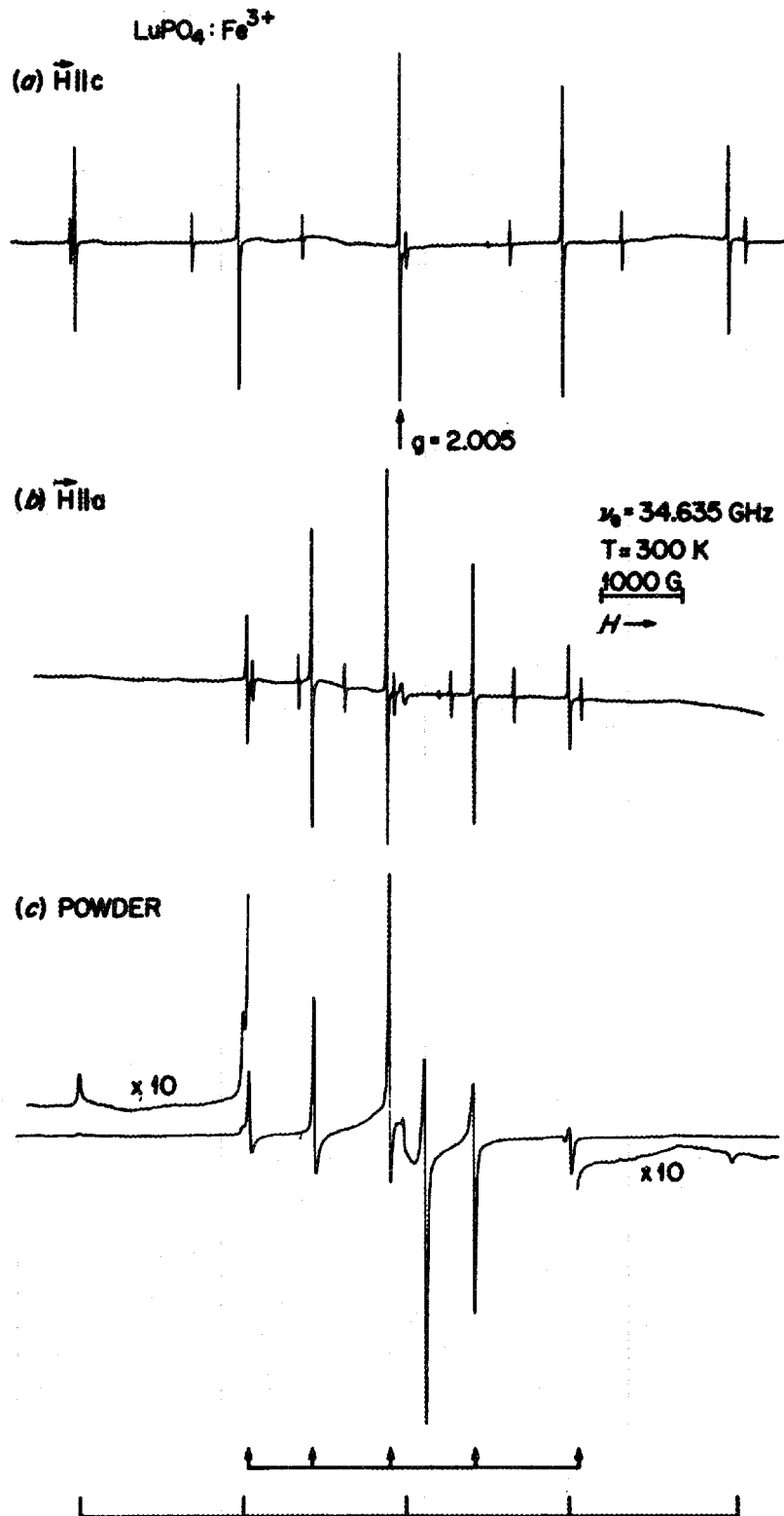


Fig. 8. EPR spectra of Fe^{3+} in a single-crystal and a powder of zircon-structure LuPO_4 . In (a), (b) \vec{H} is parallel to the c- and a-axes, respectively, of the single crystal, and in (c) the EPR spectrum of a precipitated powder is shown.

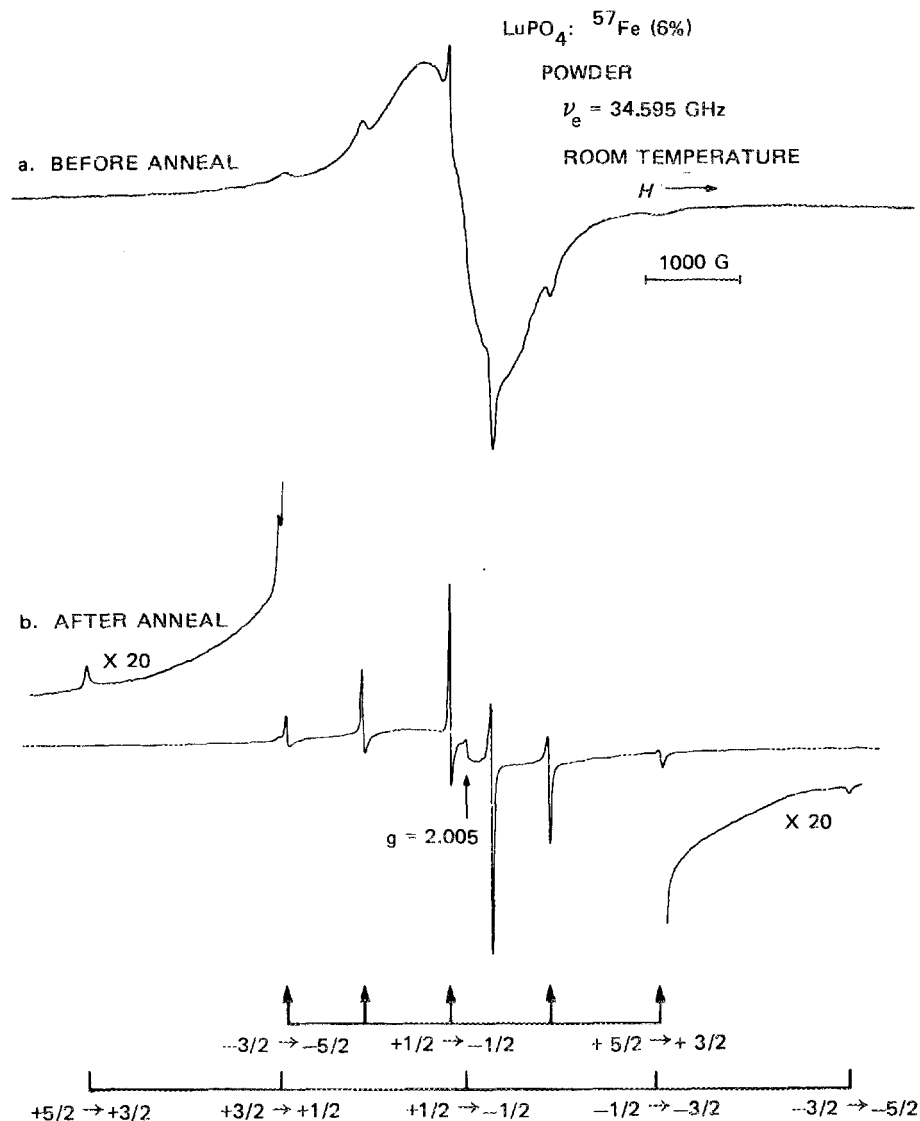


Fig. 9. EPR spectra of Fe^{3+} in a powder of LuPO_4 prepared by coprecipitation in molten urea:^{4,5} (a) as obtained after calcination at 800°C , and (b) after heating the powder in a torch and quenching. The broad line (a) is attributed to FePO_4 aggregates, while the lines identified at the bottom of the figure correspond to Fe^{3+} ions in substitutional sites in LuPO_4 .

Information that EPR spectroscopy can also provide in order to characterize nuclear waste forms is obtained from the linewidths of the different EPR transitions (Fig. 1). Since the linewidths are sensitive to defects and strains, paramagnetic impurities such as Gd^{3+} can be used to probe the "quality" of the host crystal structure. This technique offers some advantages over x-ray diffraction techniques, since any broadening of the diffraction peaks are screened by the intrinsic linewidths resulting from the instrument characteristics and the crystallite size. For example, single crystals of $LaPO_4$ have been grown with the addition of various amounts of PW-4b simulated waste, and the EPR spectra of Gd^{3+} in these samples have been compared with that obtained for a pure $LaPO_4$ single crystal. Such a comparison is shown in Fig. 10 for a mixed crystal grown from a starting composition of 5:1 by weight of La_2O_3 and PW-4b calcined waste. The magnetic field positions of the different Gd transitions are unchanged in the PW-4b doped samples, and, therefore, it can be concluded that the host still has the monazite structure characteristic of pure $LaPO_4$. The linewidths, however, are broader due to the other impurities that are in solid solution in the crystal. Figure 11 shows quantitatively the relationship between the average linewidth of two symmetric transitions and their magnetic field separation. The measurements were carried out for four different crystals and two different magnetic field orientations. Since the linewidth of the transitions is proportional to its magnetic field separation from the central line, it can be concluded that the line broadening is "inhomogeneous" (i.e. the line broadening is due to a distribution of line positions with this distribution resulting from a distribution of impurities in the crystal). It can be seen, however, that the amount of waste in solid solution in the crystal does not depend solely on the initial concentrations used for the crystal growth.

The sensitivity of the Gd linewidths to defects or strains is under current investigation as a means of detecting metamictization phenomena in orthophosphates. Mixed $Ln_{1-x}An_xPO_4$ crystals, where Ln is a rare earth and An an actinide, have been grown and EPR spectra of Gd^{3+} in these systems are of considerable interest for detecting radiation damage created by α -particles or α -recoil of the An ions.

In conclusion, I would like to mention the review article by Lynn Boatner and Marvin Abraham¹⁰ concerning the actinides in many crystals. I think this is very useful for the purpose of characterizing actinide nuclear waste forms.

DISCUSSION

BOATNER: I would just like to re-emphasize a couple of points from these two papers this morning, and I hope that you can see from these papers that in our program we have a two-pronged attack. One, is a very basic approach in which we are using what I think are some fairly sophisticated spectroscopic techniques to really investigate, on a microscopic basis, what is going on in these crystalline materials; exactly where a given impurity is and what is its valence state. In other words, we are really looking

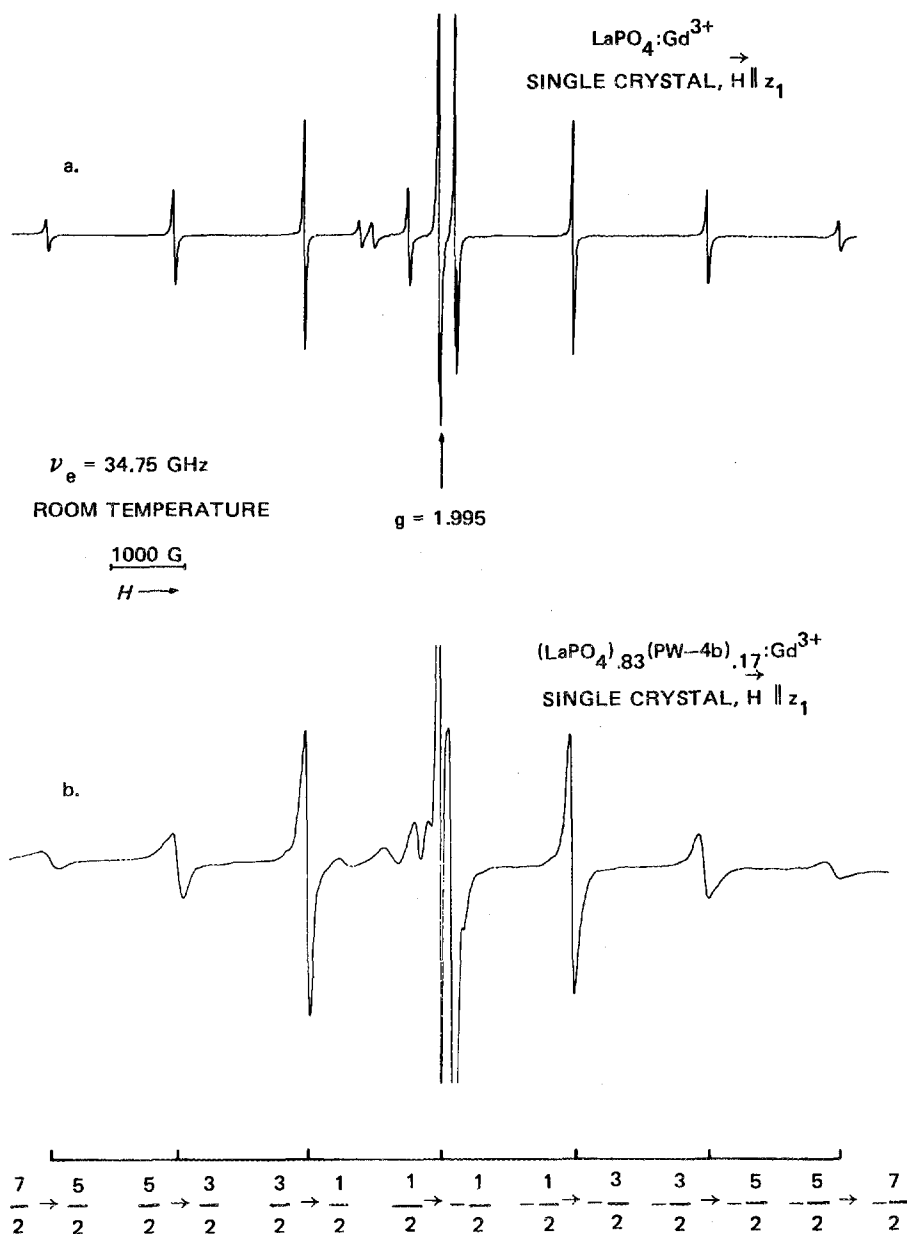
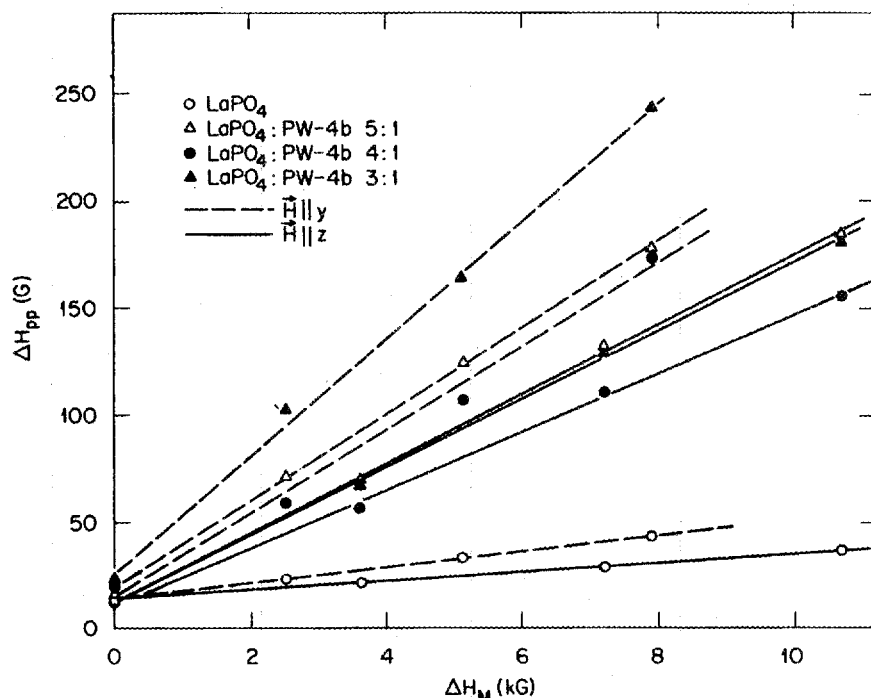


Fig. 10. EPR spectrum of Gd^{3+} in monazite-type LaPO_4 single crystals with H parallel to the principal electric field z -axis of one set of two magnetically-equivalent sites (i.e. (1,4) or (2,3) in Fig. 3). a) Pure single crystal, b) single crystal grown from a starting composition of 5:1 by weight La_2O_3 and PW-4b calcined simulated waste. The average linewidth ΔH_{pp} of two symmetric transitions, measured peak-to-peak on the first derivative spectrum, is reported in Fig. 11 as a function of the magnetic-field separation ΔH_M of these transitions.



Average Peak-to-Peak Linewidths ΔH_{pp} Versus Magnetic-Field Separations ΔH_M for the Symmetric Transitions $M \leftrightarrow M-1$ and $-M \leftrightarrow -M+1$ ($M = 7/2, 5/2, 3/2, 1/2$) of Gd^{3+} in Single Crystals of $LaPO_4$ Doped With Various Amounts of PW-4b Simulated Waste.

Fig. 11. The average linewidth ΔH_{pp} of two symmetric Gd^{3+} transitions (see Fig. 10) as a function of the magnetic field separation ΔH_M of these transitions is shown for different single crystals of $LaPO_4$ grown with various amounts of PW-4b simulated waste, and for two different orientations of the applied magnetic field ($\vec{H} \parallel z$ and $\vec{H} \parallel y$).

closely at the solid state chemistry of these materials, and we can use the magnetic resonance technique to follow things through both chemical and physical processes. That was brought out in the work on the cerium phosphate. You can look at the gadolinium spectrum in a single crystal that has been deliberately doped, then you can do something like the urea precipitation process, do physical processing at the end, and can use the spectroscopic technique to say that this impurity ion, after all of this, is in exactly the same place in exactly the same structure as in the single crystal. So you can follow what is going on through a fairly complicated chemical and physical process and, by means of this technique, you can say that in this process we have not created a crystalline form or polycrystalline form that is highly non-stoichiometric so that impurities have become associated with nearest-neighbor defects. That is, we have not really changed the solid state chemistry of the polycrystalline (e.g. hot-pressed) pellet relative to the single crystal.

REFERENCES

1. For an introduction to EPR, see for example: J. W. Orton, Electron Paramagnetic Resonance, Iliffe Books, Ltd., Pitman Press, 1968.
2. For a complete review of EPR of paramagnetic impurities in dielectrics see: A. Abragam and B. Bleaney, Electron Paramagnetic Resonance of Transition Ions, Oxford University Press, New York, 1970.
3. S. A. Al'Tshuler and B. M. Kozyrev, EPR in Compounds of Transition Elements, J. Wiley and Sons, New York, 1974.
4. M. Rappaz, M. M. Abraham, J. O. Ramey, and L. A. Boatner, Phys. Rev. B, in press.
5. M. Rappaz, L. A. Boatner, and M. M. Abraham, in preparation.
6. M. M. Abraham, L. A. Boatner, and M. Rappaz, in preparation.
7. M. M. Abraham, L. A. Boatner, C. B. Finch, R. W. Reynolds, and W. P. Unruh, Phys. Lett. 44A, 527 (1973).
8. W. Kolbe and N. Edelstein, Phys. Rev. B 4, 2869 (1971).
9. P. G. Huray, S. E. Nave, J. R. Paterson, M. B. Hoyt, L. A. Boatner, M. M. Abraham, and M. Rappaz, Symposium on Spectroscopy Applied to Inorganic Solids, American Chemical Society Meeting, New Orleans, 1980.
10. L. A. Boatner and M. M. Abraham, Rep. Prog. Phys. 41, 87-155 (1978).

HOT AND COLD PRESSING OF (La,Ce)PO₄-BASED
NUCLEAR WASTE FORMSR. J. Floran,^{*} M. Rappaz,[†] M. M. Abraham,[†] and L. A. Boatner[†]

^{*}Environmental Sciences Division, [†]Solid State Division
Oak Ridge National Laboratory**
Oak Ridge, Tennessee 37830

ABSTRACT

Synthetic analogs of the mineral monazite [(Ce,La,Ca,Th,U)(P,Si)O₄] are promising host phases for the isolation of actinide wastes. The favorable properties of this class of materials include (a) similar geochemical behavior of lanthanide and actinide elements which permits extensive ionic substitution within the monazite crystal structure, and (b) high resistance to weathering, hydrothermal alteration, and leaching by natural groundwaters or solutions. Synthetic LaPO₄ and CePO₄ crystals doped with varying amounts of transuranic elements have been grown in the laboratory and preliminary leaching studies confirm the highly resistant nature of these monazite-like phases. In the present investigation, the optimal conditions necessary to form high-density, simulated waste pellets from calcined LaPO₄ and CePO₄ powders have been examined. Pellets that are close to the theoretical density are necessary in order to minimize porosity and hence potential avenues along which fluid/waste interactions can take place.

Calcined powders prepared by a urea precipitation process were cold pressed and hot pressed under a range of controlled conditions to form coherent, cylindrical pellets. Changes in density were examined as a function of P, T, and duration of sintering. For cold-pressed pellets, a significant increase in density occurs during sintering between 1000°C and 1100°C. This increase is correlated with substantial grain coarsening of the pellet microstructure. A comparison of cold and hot pressing techniques suggests that, only after sintering, does the density of cold-pressed pellets approach (but not equal) that of the hot-pressed pellets. Densities > 90% of the theoretical value of 5.11 g/cm³ are easily attainable by hot pressing without sintering.

The significance of density differences on pellet stability will be investigated in future leaching studies. The apparent advantages of the higher densities achieved by hot pressing

**Operated by Union Carbide Corporation for the U.S. Department of Energy under contract W-7405-eng-26.

must be weighed against the increased technological/engineering complexities involved when working at sustained high temperatures in a remote environment. Thus the cold pressing technique may ultimately prove more practical for large-scale commercial operations.

INTRODUCTION

One of the most promising alternative nuclear waste forms currently under investigation for the isolation of actinide elements are synthetic analogs of the rare-earth orthophosphate mineral monazite.^{1,2} Natural monazites $[\text{Ce,La,Ca,Th,U}](\text{P,Si})\text{O}_4$ appear to be highly resistant to chemical alteration and radiation damage. However, much additional research will be required before monazite waste forms can be fully developed.³ In this paper, preliminary results obtained by cold and hot pressing synthetic monazite powders (LaPO_4 , CePO_4) into simulated waste pellets are presented. Emphasis is placed on the optimal conditions necessary to form high-density pellets and how these conditions correlate with changes in microstructure or petrographic texture.

METHOD

Synthetic monazite powders were prepared by precipitation in molten urea.⁴ Using a cold-pressing technique, calcined LaPO_4 powders were mixed with a small amount of binder consisting of steric acid plus acetone. The resultant mixtures were uniaxially compressed, typically for 15 minutes, at various pressures. In most instances this procedure resulted in the formation of coherent cylindrical pellets. The pellets were then sintered at temperatures ranging from 1000°C to 1300°C for time periods that varied between 8 and 160 hours. In the hot-pressing technique LaPO_4 and CePO_4 powders, without any binder, were formed into pellets at 1100°C and 275 bars. Portions of these pellets were then sintered at 1000°C or 1300°C, usually for 8 hours (see Table 1).

TABLE 1. TYPICAL CONDITIONS FOR MAKING PELLETS

COMPOSITION	COLD PRESSING	HOT PRESSING
	LaPO_4	LaPO_4 CePO_4
PRESSURE (bars)	340 680	275
TEMPERATURE OF SINTERING (°C)	1000 1100 1200 1300	1000 1300
TIME OF SINTERING (h)	8 80 160	8

RESULTS

Cold Pressing

Figure 1 illustrates the increases in density that occurred in response to variations in pressure (P), temperature of sintering (T_s), and duration of sintering (t_s) for cold-pressed pellets. Each of these parameters was compared with the other two variables held constant.

Figure 1a shows the effect of different pressures on the percent theoretical density. Only the two most common pressures are compared; at higher pressures, typically 1360 bars, the pellets frequently cracked and split into two or more fragments. Note that significant increases in density (up to 42%) occur as a result of sintering. Relatively high densities close to the theoretical value can be achieved at low pressures by a combination of cold pressing and sintering (e.g. samples 18 and 20). However, the magnitude of the increase at 340 and 680 bars is very similar.

A comparison of pellets that were sintered at different temperatures (T_s) reveals that a large increase in density occurs at 1100°C (Fig. 1b). This conspicuous jump in density between 1000°C and 1100°C correlates very nicely with a very large increase in pellet grain size (see Fig. 2). Note that above 1100°C no real increase in density is observed.

Density changes as a function of sintering time (t_s) are quite variable but increase for each pair of pellets with increasing time (Fig. 1c). Under appropriate conditions, densities of $\sim 90\%$ theoretical or greater can be achieved in as little as 8 hours; increasing t_s to 80 hours does not significantly increase the density.

In summary (Table 2) the present cold pressing experiments with LaPO_4 indicate that:

- (a) higher pressures result in higher densities, however no significant increases were noted above 340 bars;
- (b) higher temperatures yield higher densities but no significant increases in density were observed above 1100°C, and,
- (c) no major increase in density was recorded by sintering for more than 8 hours; optimal t_s may be considerably less than 8 hours and will certainly require further investigation.

With regard to hot pressing, the limited number of experiments conducted indicate that densities greater than 90% of the theoretical value were readily achieved at 1100°C; subsequent sintering does not significantly increase density. A comparison of the cold and hot pressing techniques suggests that only after sintering does the density of cold pressed pellets approach, but not equal, that of the hot pressed pellets.

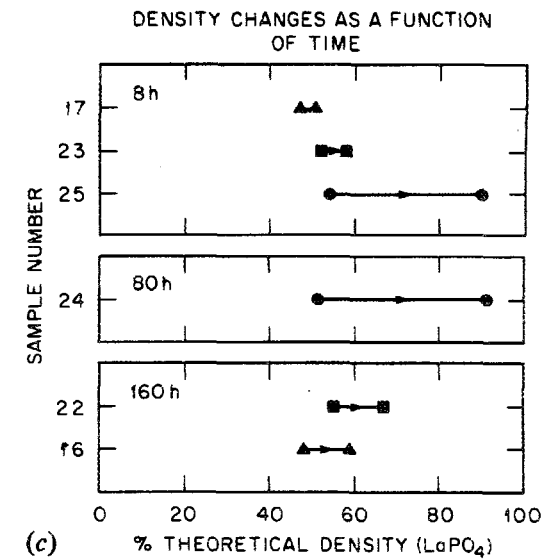
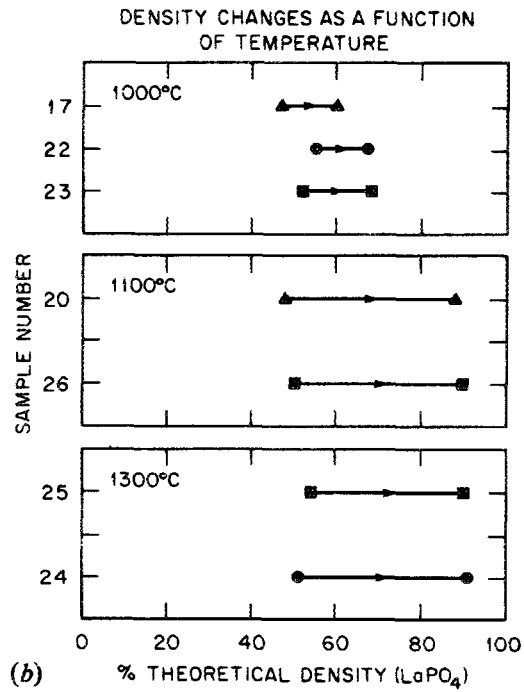
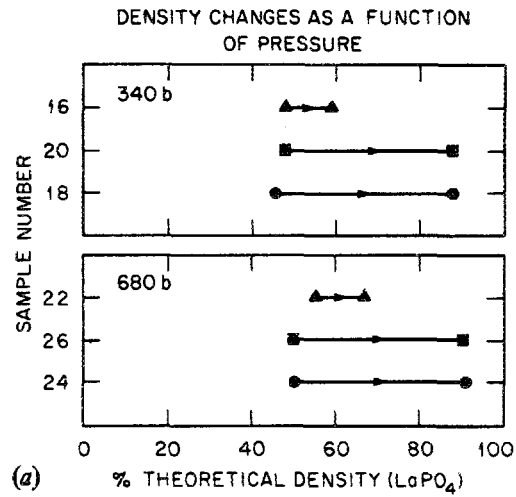
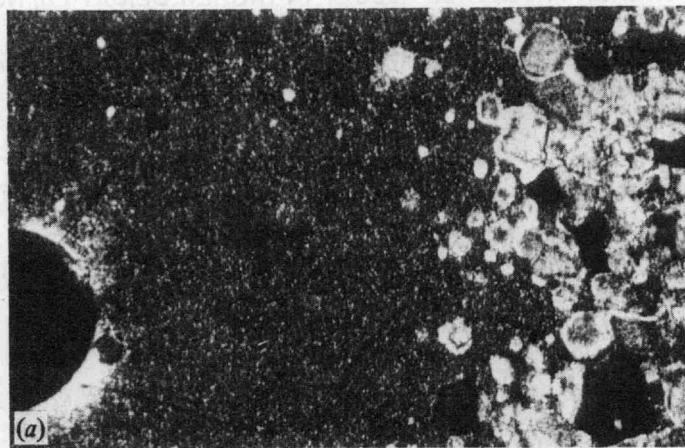


Fig. 1a-c. Density changes for cold-pressed pellets as a function of pressure, temperature, and duration of sintering. Arrows denote increases in density after sintering.

ORNL PHOTO 4619-80



ORNL PHOTO 1347-81

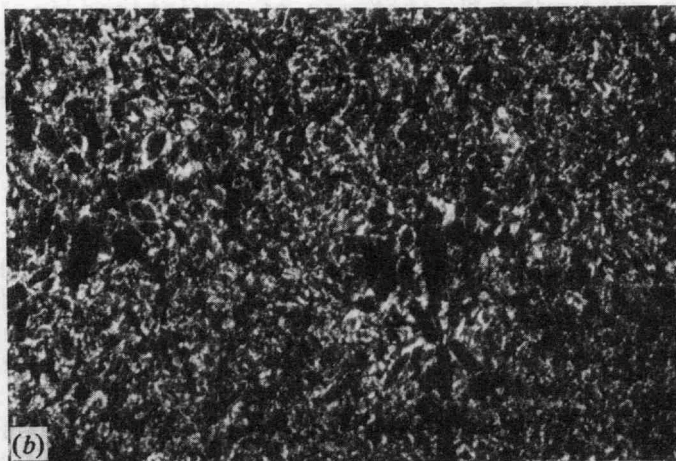


Fig. 2. Microstructure of cold-pressed pellets (LaPO_4).

a) Sample # 22, uniaxially pressed at 680 bars, sintered in air at 1000°C for 160 h; final density = 67%. Note extremely fine-grain size of matrix and irregular development of coarser nuclei of LaPO_4 . Rounded area at extreme left is a void. Scale: 0.85 mm across, doubly polarized light.

b) Sample # 26, uniaxially pressed at 680 bars, sintered in air at 1100°C for 8 h; final density $\approx 90\%$. Note relative homogeneity and coarse grain size of matrix compared to # 22. Scale: 0.85 mm across, doubly polarized light.

TABLE 2. SUMMARY OF RESULTS

COLD PRESSING

- HIGHER PRESSURES RESULT IN HIGHER DENSITIES; NO SIGNIFICANT INCREASE NOTED ABOVE 340 bars
- HIGHER TEMPERATURES YIELD HIGHER DENSITIES; NO SIGNIFICANT INCREASE ABOVE 1100°C
- OPTIMAL TIME OF SINTERING MAY BE LESS THAN 8h

HOT PRESSING

- DENSITIES > 90% OF THE THEORETICAL VALUE ARE READILY ACHIEVED AT 1100°C; SUBSEQUENT SINTERING DOES NOT SIGNIFICANTLY INCREASE DENSITY

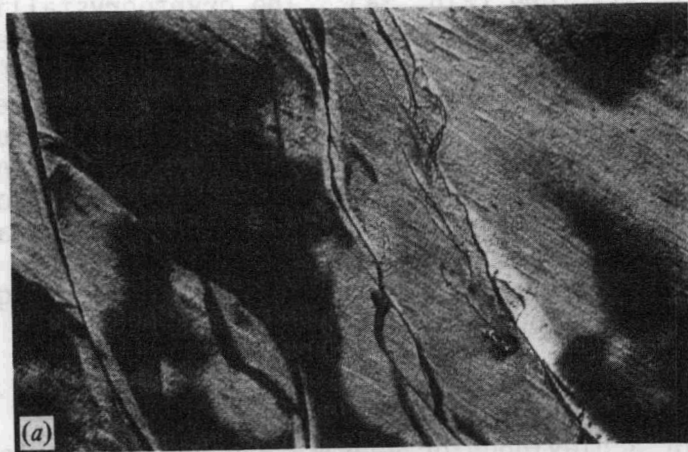
MICROSTRUCTURE

A microscopic investigation of the cold- and hot-pressed pellets was undertaken to determine the effects of variations in T, P, and t_s on the microstructure. A diversity of petrographic textures was produced (e.g. Figs. 2-3), depending on the conditions of formation. Variations in temperature, however, appeared to be the most influential parameter controlling textural development.

Cold-Pressed Pellets

Pellets sintered at 1000°C for varying lengths of time (24-160 h) tended to be extremely fine grained and texturally heterogeneous (Fig. 2a). Localized areas comprised of relatively coarse, rounded nuclei of LaPO_4 are randomly distributed throughout a cryptocrystalline matrix that is similar in appearance to cherty quartz. Rounded voids or vesicles typically associated with radial fractures are largely responsible for the relatively low densities of these pellets ($\sim 70\%$ theoretical density). The growth of coarse nuclei around these voids emphasizes the textural heterogeneity of these samples. In contrast, pellets that were formed under similar conditions but which were sintered at 1100°C for only 8 hours are considerably more dense ($\geq 90\%$ theoretical), coarser grained, and more homogeneous on a microscopic scale (Fig. 2b). A conspicuous coarsening in grain size occurs between 1000°C and 1100°C which correlates very nicely with a large increase in density (Fig. 1b). Although there is some variability in grain size, a typical pellet consists of well-formed elongate crystals arranged in a decussate texture. Individual crystals typically consist of a cloudy or turbid core surrounded by a transparent rim. The cause of the turbidity is uncertain but may be due to incomplete recrystallization of the originally submicron sized particles. Under high magnification, grain boundaries are observed to be very irregular - an indication that textural equilibrium has not quite been achieved.

ORNL PHOTO 4622-80



ORNL PHOTO 4623-80

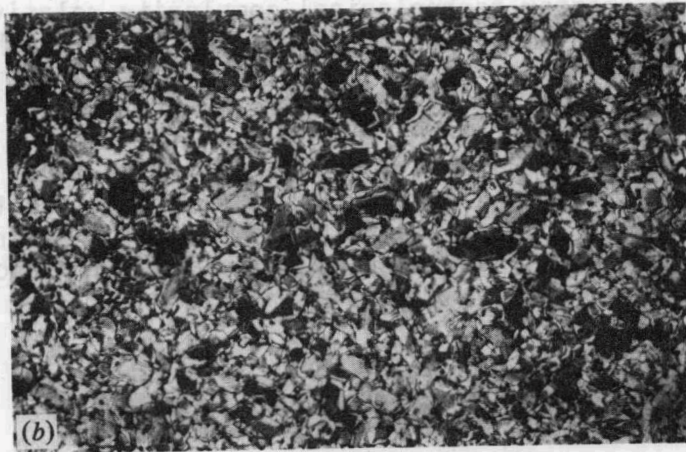


Fig. 3. Microstructure of hot-pressed pellets (CePO_4).

a) Sample #4627, uniaxially pressed in vacuum at 340 bars at 1000°C for 1 hr; not sintered. Entire mass consists of cryptocrystalline grains oriented in one direction (here, NW-SE). Dark areas are at positions of extinction indicative of strain. Note large fractures. Scale: 0.85 mm across, doubly polarized light.

b) Sample 4625, uniaxially pressed in vacuum at 1100°C at 340 bars for 1 hr, sintered in air at 1000°C for 8 h. Note well crystallized nature of grains and transparent nature of individual crystals. Scale: 0.85 mm across, doubly polarized light.

Hot-Pressed Pellets

Pellets that were hot pressed at or below 1000°C and not sintered are extremely fine grained, have a high porosity, and in many instances, are riddled with fracture (Fig. 3a). The cryptocrystalline fibers comprising the pellets exhibit a preferred orientation as well as considerable internal strain. In contrast, pellets formed at 1100°C and subsequently sintered at 1000°C for 8 hours have high densities ($\geq 90\%$ theoretical) and are well crystallized (Fig. 3b). The turbid cores that are characteristic of the cold-pressed pellets are not present. At high magnification, the grain boundaries were found to be straight or gently curved, and to form triple-boundary junctions approaching 120° angles. In general, individual grains are approximately equidimensional with an average grain size of $\sim 50 \mu$. These features suggest that textural equilibrium was approached.

CONCLUDING REMARKS

In terms of achieving high density and an acceptable microstructure both the hot- and cold-pressing techniques appear to be acceptable. Although hot pressing yields slightly better results, its advantages may be offset by its greater technological complexity relative to cold pressing. Both techniques should be used to investigate synthetic monazite waste forms. In addition, the feasibility of incorporating non-actinide elements into monazite-like phases should be examined.

If uranium and plutonium from commercial high-level wastes are re-processed or recycled, then it should be noted that the technology already exists so that the actinide elements can be separated from the fission products. In such an operation, monazite alone could readily accommodate the long-lived actinide elements.

DISCUSSION

HOWITT: It would appear, just generally from your micrographs, that you crossed the solidus line. Have you any idea which one?

FLORAN: Which phases are you talking about?

HOWITT: I am not sure, but your structures look very much like liquid-phase sintering. The moment you get above 1000°C, the microstructure changes rapidly.

FLORAN: The melting point of lanthanum phosphate is well over 2000°. Many of the grain boundaries of these samples display triple junctions, and this seems to be fairly good evidence of solid-state annealing rather than melting.

HOWITT: How do you get that almost step functional change in growth behavior of those phases?

FLORAN: Well, in terms of the microstructure, there is no indication of any melting taking place. When you get these triple junction boundaries, this seems to be a pretty good indication that you are dealing with solid state phenomena.

HOWITT: You can't trust the microstructure on this scale. You are approaching the resolution of optical microscopy. You are probably looking at boundaries that are one or two microns wide. The point is, you have a radical change here in microstructure as you go above 1000°C. You must have a change of growth mechanism.

MCCARTHY: The phase diagrams for a number of P₂O₅ systems are known, and you could easily have crossed a boundary in a sintering mechanism. I agree that this is liquid-phase sintering, but you need to go to higher resolution.

LEVY: From the economic geology point of view, what is the availability of lanthanum?

FLORAN: Lanthanum is relatively common. On the other hand, lutetium seems to be rare compared to lanthanum.

UNIDENTIFIED QUESTIONER: You would not use pure lanthanum; you would use unseparated oxides?

FLORAN: Right.

REFERENCES

1. Draft Environmental Impact Statement, "Management of Commercially Generated Radioactive Waste," DOE/EIS-0046-D, Washington (1979).
2. L. A. Boatner, G. W. Beall, M. M. Abraham, C. B. Finch, P. G. Huray, and M. Rappaz, "Monazite and other lanthanide orthophosphates as alternate actinide waste forms," The Scientific Basis for Nuclear Waste Management, Vol. II. Edited by C. J. Northrup, Plenum Press (1980), (in press).
3. R. J. Floran, M. M. Abraham, L. A. Boatner, and M. Rappaz, "Geologic stability of monazite and its bearing on the immobilization of actinide wastes," The Scientific Basis for Nuclear Waste Management, Vol. III (submitted for publication).
4. M. M. Abraham, L. A. Boatner, T. C. Quinby, D. K. Thomas, and M. Rappaz, "Preparation and compaction of synthetic monazite powders," Radioactive Waste Management (in press).

A SURVEY OF CONCRETE WASTE FORMS

J. G. Moore

Chemical Technology Division, Oak Ridge National Laboratory*
Oak Ridge, Tennessee 37830

ABSTRACT

The incorporation of radioactive waste in cement has been widely studied for many years. It has been routinely used at nuclear research and production sites for some types of nuclear waste for almost three decades and at power reactor plants for nearly two decades. Cement has many favorable characteristics that have contributed to its popularity. It is a readily available material and has not required complex and/or expensive equipment to solidify radioactive waste. The resulting solid products are noncombustible, strong, radiation resistant, and have reasonable chemical and thermal stability.

As knowledge increased on the possible dangers from radioactive waste, requirements for waste fixation became more stringent. A brief survey of some of the research efforts used to extend and improve cementitious waste hosts to meet these requirements is given in this paper. Selected data are presented from the rather extensive study of the applicability of concrete as a waste form for Savannah River defense waste and the use of polymer impregnation to reduce the leachability and improve the durability of such waste forms. Hot-pressed concretes that were developed as prospective host solids for high-level wastes are described.

Highlights are given from two decades of research on cementitious waste forms at Oak Ridge National Laboratory. The development of the hydrofracture process for the disposal of all locally generated radioactive waste led to a process for the disposal of I-129 and to the current research on the German *in-situ* solidification process for medium-level waste and the Oak Ridge FUETAP process for all classes of waste including commercial and defense high-level wastes. Finally, some of the more recent ORNL concepts are presented for the use of cement in the disposal of inorganic and biological sludges, waste inorganic salts, trash, and krypton.

*Operated by Union Carbide Corporation for the U.S. Department of Energy under contract W-7405-eng-26.

One of America's leading cement technologists, whenever he is asked to talk about concrete, always likes to preface the talk by saying: This is the one time man tried to play God, and succeeded. He made a rock! He took some lime (now cement), a little volcanic ash, some sand and gravel, and added a little water to it, stirred it up, waited awhile, and presto! He had a rock-like solid."

A very general definition of cement is simply an adhesive substance capable of uniting fragments or masses into a compact whole. That obviously covers a multitude of sins, but for the most part the present work will deal with Portland cement. This material is made by heating in a kiln a mixture of limestone and clay, which contains oxides of calcium, aluminum, iron, and silicon. The resulting clinker is pulverized to a fine powder. In the 1800's, the term "Portland" cement was applied to this material because it looked much like the Portland limestone that was quarried at Portland, England. These cements usually have a composition range similar to that shown in Table 1; i.e., the material is primarily calcium and silicon, with just a little aluminum in it plus some iron and manganese. These are the Portland cements, but high-alumina cements will also be mentioned in the following discussion. In the high-alumina cements both the calcium and aluminum content are quite high, ranging anywhere from about 36 to 42%. The silica content is quite low (usually 4-7%) and the material can contain as much as 20% iron.

Table 1. Composition of Portland Cement

Component	Wt %
CaO	60-67
SiO ₂	17-25
Al ₂ O ₃	3-8
Fe ₂ O ₃	0.5-6.0
MgO	0.2-1.3
Alkalis	0.2-1.3
SO ₃	1-3

Naturally, cement dates farther back than the 1800's. The Egyptians found that they could heat gypsum, mix it with water, and produce a mortar which could be used to unite slabs of stone. We normally

think that some of the monuments left by the Egyptians are just stone piled upon stone, but this is not true. There is a very thin layer of mortar between the stones of many of these monuments. The use of lime probably originated with the Greeks, but it was really the Romans who brought the use of lime to its height, and they took this knowledge throughout their vast empire. The Greeks found that if you took lime, mixed it with volcanic ash, ground it up, and added a little sand, you had a fantastic mortar. You could mix this with a little gravel and you had concrete. Concrete was born. They found that this mortar was so good that it could even resist fresh or salt water. It was a great material for building cisterns, aquaducts, walls, and many other structures. Pliny and Vitruvius, in the first century, give detailed instructions on how to make these cisterns and aquaducts.¹ For those who doubt the durability of cementitious material, let me remind you that some of them have endured for a long period of time. There are aquaducts and cisterns dating back as much as 3000 years.² They are still in use. While this is not the 10,000, or possibly more, years that we are looking for now, it is well on the way. The Pantheon is another example of the durability of concrete. It has a dome of solid concrete with a span of slightly over 142 ft. Two thousand years after its construction it is still standing. This brief introduction was necessary because it can serve to explain two things: One, why cement was considered so early as a means of fixing nuclear waste and, two, why it is so often maligned and dismissed as a useful host for these noxious compounds. Familiarity breeds contempt.

Concrete is currently being used and investigated for a variety of applications in the nuclear industry. Examples of this activity include: The polymer concrete, as developed about a decade ago at Brookhaven National Laboratory,³ The Savannah River Laboratory studies for the disposal of defense waste,⁴ the Penn State hot-pressed concrete,⁵ and the Federal Republic of Germany is currently working on an *in situ* solidification process.⁶ Nuclear applications of concrete at ORNL include the ORNL hydrofracture process,⁷ which has been used for a decade to dispose of all intermediate level wastes generated at the laboratory, a process for the disposal of iodine-129,⁸ and the development of FUETAP concrete,⁹ which is really nothing more than an autoclaved concrete.

The properties of concrete, of course, are well known. At least everyone thinks he knows the properties of concrete because he has built a patio, put up a post for a fence, laid some brick, etc. The basic characteristics of concrete can be summarized as follows: Concrete is inexpensive (amazingly so, if you ever see a concrete plant and see what goes into one) and is widely available. Most of the concrete processes involve relatively low temperatures. It is chemically quite stable. You will remember the previously mentioned cistern that has been used for three thousand years² with water over it, for those who fear water. The thermal stability of concrete is quite good, and it is quite radiation resistant.

Concrete has been used for low- and some intermediate-level wastes, from reactors for about 30 years.¹⁰ The material is usually used by

itself, but often it is mixed with vermiculite in the case of liquids, or with tuff. Concrete has already been used to dispose of everything from resins to evaporator bottoms, filter cartridges, sludges, and incinerator ash. Metallic materials have been placed in a large tank which was then filled with concrete. For the most part, these are very simple, low-temperature processes. So simple, for example, that in some of them the canister is simply filled with liquid waste and cement and a concrete block is added. The top of the canister is sealed and the canister is tumbled several times in order to mix the contents. Then it is set aside to solidify.

During the early 1970's, Peter Colombo and his group at Brookhaven decided to investigate concrete for the fixation of Savannah River defense waste.³ This waste has a low thermal activity (less than 0.01 W/l) and it seemed to be ideal for disposal in concrete. There was concern that the waste would leach because of the porosity of the concrete, so a simple but very effective idea was developed. A decision was made to try to fill up the pores in concrete with plastic and to use styrene for this purpose since it is noted for its high resistance to radiation. The waste was first mixed with cement and allowed to solidify at ambient temperatures. Then styrene monomer and a catalyst were poured over the surface of the concrete and allowed to soak in. After heating at a low temperature (50-70°C), a polymer-impregnated concrete body was formed (Fig. 1). The styrene formed a thin surface over the top of the material and in the surface pores.

ORNL-DWG 81-5866

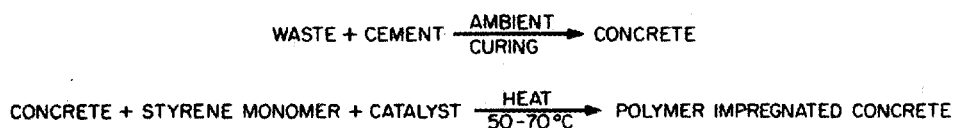


Fig. 1. Procedure for polymer-impregnated concrete.

Polymer-impregnated concrete had a number of favorable properties. The cesium and the strontium leachability was reduced by approximately two to three orders of magnitude. The compressive strength was approximately two to three times the strength of ordinary concrete (i.e., it had up to 20,000 psi compressive strength). This material was virtually completely resistant to freeze-thaw cycling, and the chemical resistance greatly improved. It was an excellent product. This material is not presently being used, or even considered, for Savannah River wastes, but a large glove-box scale version of the process is planned for operation at Mound Laboratory sometime during 1982 for the fixation of tritium.

Work on the fixation of Savannah River waste continued at the Savannah River Laboratory. This waste consists of an aqueous solution containing a sludge of the hydrous oxides of various metal ions, primarily iron and aluminum, with varying amounts of mercury and manganese.

The sludge contains most of the fission products, mainly ^{90}Sr . The supernate contains the soluble salts and most of the ^{137}Cs .

A very simplified schematic of the conceptual flowsheet for the head-end treatment is shown in Fig. 2. The supernate is separated from the sludge, and the cesium is eventually sorbed on a zeolite exchanger. The sludge is washed three times, then dried or lightly calcined at about 700°C . The wash water may be treated to remove the cesium. At this point, the cesium and sludge waste may be handled separately or together.

ORNL-DWG 81-5662

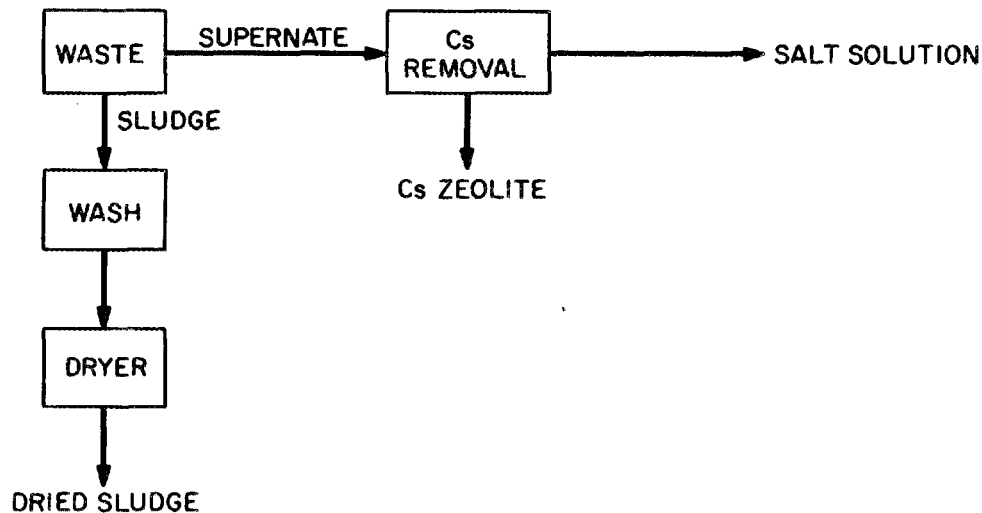


Fig. 2. Simplified conceptual flowsheet for the head-end treatment of SRP waste.

A detailed study was made to determine the applicability of simple concretes as a matrix for these wastes.⁴ A factorial experimental design was used to study 162 formulations of cement, simulated sludge, and water, plus 18 formulations with actual sludges. Different types and concentrations of sludge, cements, and water-to-cement ratios were used. The solids produced from each formulation were examined with respect to compressive strength, leachability, radiation stability, and thermal stability.

An example of the data from these investigations is illustrated in Fig. 3. This shows results from leach tests on concretes made with high alumina cement and containing 40 wt % actual sludge from tank 5. The sludge has high concentrations of iron, manganese, and uranium, so it should be reasonably representative of a Purex sludge. The compressive strength, even with a 40 wt % waste content, was something like 2000-3000 psi, which is quite ample. The leach rates decrease with time and are quite reasonable for the strontium and the α -active isotopes. The α -active material, in fact, was at the limit of detectability. The cesium

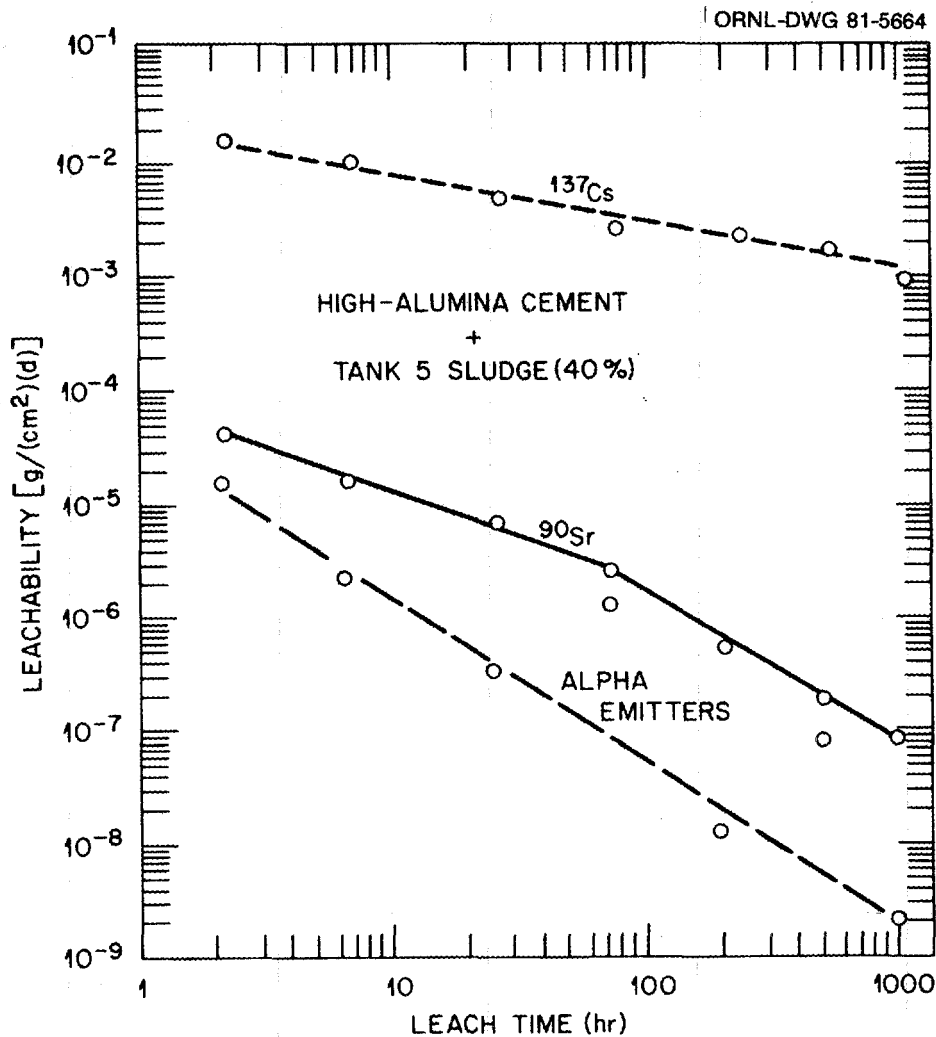


Fig. 3. Leach rates of concretes containing SRP sludge.

rates are not quite as good. However, if the cesium had been sorbed on zeolite, the leach rates would be much lower. Another interesting point concerning the strontium is that the strontium rate may be as much as two orders of magnitude less than the values found in tests with simulated waste. It is extremely difficult to simulate sludge wastes containing strontium.

The results of these investigations can be summarized as follows: High waste loadings (up to 40 wt %) could be achieved while maintaining adequate compressive strength (2000-3000 psi). The thermal stability was good. The material could be heated to 400°C for weeks. The radiation stability was good, up to $\sim 10^{10}$ rads, and no evidence was found for any adverse effects. In fact, the strontium leachability improved slightly when the material was irradiated. It did have a couple of unfavorable properties, however. The cesium leachability, as shown in Fig. 3, was quite high, but the solid was only a neat cement paste. The

leach rate would be improved if the cesium had been fixed on zeolite. With some sludge compositions it is possible to have flash set which would be difficult to handle in a plant. Although the concrete matrix remained intact and kept its strength after heating to 400°C, steam pressurization would occur because of the water content in the solid. This can be rectified, however, by heating the concrete to 150° for a few hours to remove the unbound water. In general, the data were quite encouraging, and, if a decision had not been made to go to glass, results from these studies could be used as a starting point for a program to produce improved concrete waste forms.

In the early 1970's, Della Roy and her group at Penn State started an investigation on the applicability of hot-pressed concrete in waste management.⁵ Attempts were made to make very dense, less permeable solids by using extremely low water-to-cement ratios and hot-pressing the resulting mixes. They used moderate temperatures (150-400°C) and pressures ranging from 25,000 to 100,000 psi. They investigated Portland cements, Types 1, 3, and 4, plus the calcium aluminate or high-alumina cements, Fondu and Secor 250. To determine the ability of these materials to fix radioactive waste, tests were made with four simulated waste compositions, one of which was quite high in sodium nitrate. The properties of the resulting small pellets (they were about one-half by one-half inch) were absolutely amazing.

Pellets were produced with porosities less than 2% and with compressive strengths of over 100,000 psi (Fig. 4). The concretes were so impermeable that they resisted corrosion even in concentrated hydrochloric acid, whereas ordinary concrete would disintegrate very rapidly. In tests using simulated wastes with a high nitrate concentration, a little sticky nitrate substance would exude out of the solid at the high pressures. With the calcine, however, they had no difficulty whatsoever, and even with 50 wt % calcine in the material, the tensile strength was as high as 2000 psi. This is as high as the compressive strength of many concretes. In addition, the nitrate-containing pellets were stable to 230°C. Pellets containing calcined waste were stable to over 700°C. The studies did not include many leaching experiments, but a small gain in weight was observed on placing the pellets in water, so there were additional hydrates being formed.

More research needs to be done on these hot-pressed concretes, in particular with the high alumina cement, because this cement forms concretes that are dense, strong, durable, thermally quite stable, and should have an increased resistance to leaching.

Americans are not the only ones looking at unique applications of cementitious material in radioactive waste management. Figure 5 shows an example from the Federal Republic of Germany for the disposal of medium-level waste.⁶ This activity level corresponds approximately to some of our defense wastes. In this concept, high-nitrate liquid wastes are converted into pellets using a dry cementitious mix based loosely on the ORNL hydrofracture mix. The pellets are shipped to the disposal site at a salt dome, where they are mixed with a neat cement paste (perhaps

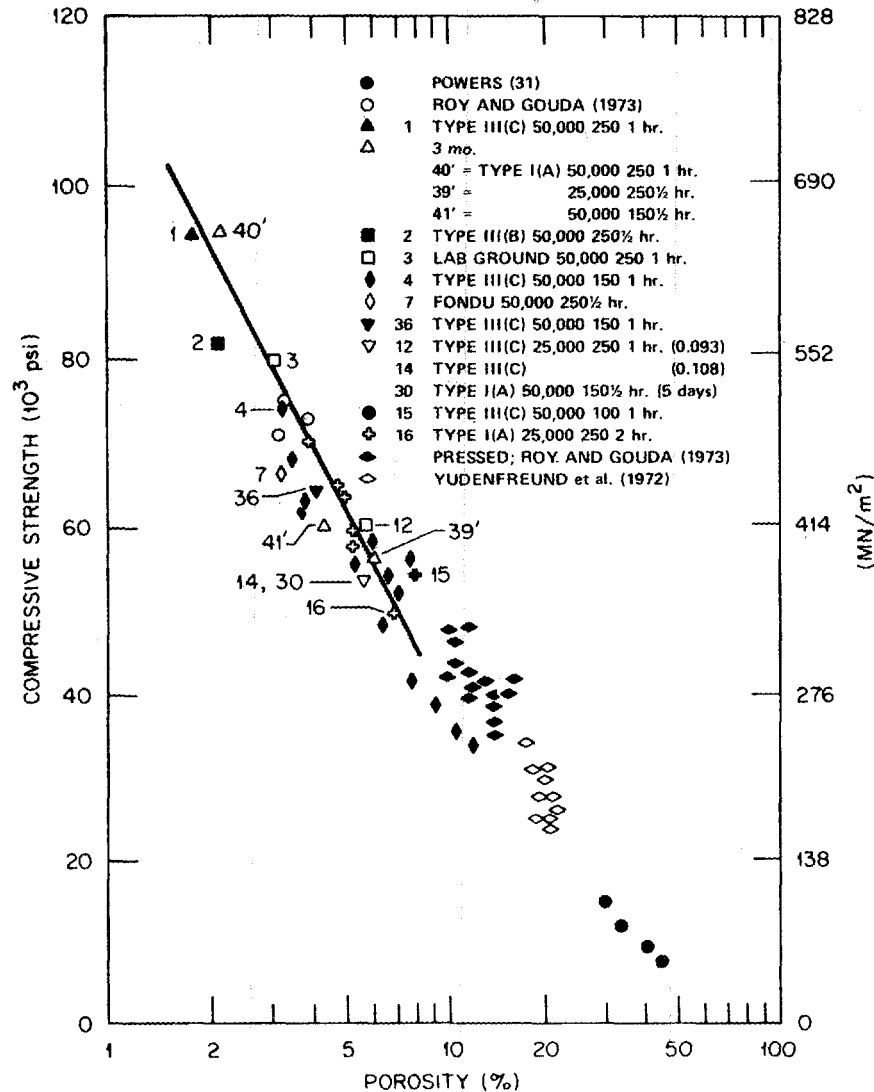


Fig. 4. Effect of porosity on compressive strength of hot-pressed concrete (after ref. 5).

even with tritiated paste), and pumped down into a large cavity. This cavity is 75,000 cubic meters and is large enough to accommodate all of the medium-level waste from a 1400-ton-per-year fuel reprocessing plant over a five-year period. During the course of this investigation, leach studies were performed with concretes containing various agents to fix the cesium. A German Bentonite clay has shown the best affinity for reducing the leachability of cesium. Strontium is fixed by adding barium silicate. The process has many interesting possibilities, and this year ORNL is starting a joint project with the F.R.G. to explore the possibilities of this concept.

Interest in cementitious materials at ORNL goes back to decades when the work was initiated on the Laboratory's intermediate level waste

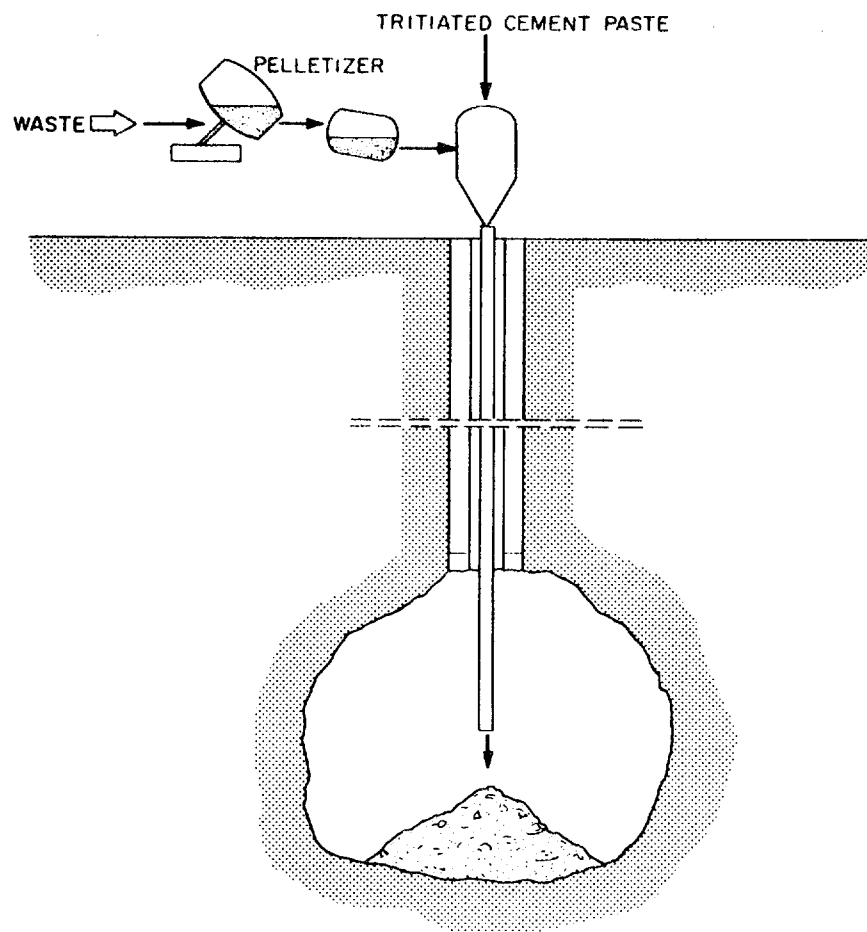


Fig. 5. Simplified schematic of the F.R.G. in-situ solidification process.

disposal facilities.¹ It was decided that one possibility for eliminating the ORNL intermediate level waste was by injection into the Conasauga shale bed formations that are located in the area. This investigation led to the hydrofracture process that is currently routinely used for the disposal of all of the ORNL intermediate level wastes. As shown in Table 2, this waste is a mixture of all the liquid waste produced in the laboratories, hot cells, and reactors at the Laboratory and even includes a small amount of organic material. After the liquid is collected, it is neutralized with sodium hydroxide and the supernate is concentrated by evaporation. Although the composition is different each time an injection is made, Table 2 represents an example of the type of waste involved. It is predominantly sodium nitrate (about 1 molar), with a high pH because of the sodium hydroxide addition. The major radioactive component is cesium-137, which is usually less than 1 curie/gal but would be acceptable as high as 20 curies/gal. A little strontium is in the liquid (≤ 0.1 curie/gal), but most of the strontium is precipitated out by sodium hydroxide. Approximately one millicurie/gal of ^{244}Cm is present.

Table 2. Composition and Properties of a Typical Waste Solution

Constituent	Concentration (g-mole/liter)
Na ⁺	1.78
NH ₄ ⁺	0.003
Al ³⁺	0.0074
NO ₃ ⁻	0.835
OH ⁻	0.18
Cl ⁻	0.093
CO ₃ ²⁻	0.255
SO ₄ ²⁻	0.094
Property	
pH	11.52
Density, g/ml	1.085

The liquid waste is blended with a dry mix at the injection site. The dry mix has the composition shown in Table 3. The cement is Type 1 Portland cement, and the fly ash is a low-calcium, low-carbon ash. Attapulgate 150 is a drilling clay that serves as a suspending agent and reduces the aqueous phase separation. The clay is added to adsorb cesium and thus reduces the cesium leach rate. In addition, a retarder is added to delay solidification so the grout will be pumpable for at least 8 to 10 hours. Tributyl phosphate (TBP) is added at the rate of 400 ppm to reduce foaming.

Figure 6 shows the ORNL hydrofracture disposal facility. The storage bins, where the dry mix is stored, are indicated along with the mixing tank, where the grout is formed by jet mixing with the dry mix. It is then forced 800-1000 feet under ground under pressure. The pressure causes the shale layers to fracture horizontally, and continued pumping produces a very thin pancake (about 1 cm thick) of radioactive grout between the shale layers. After a few hours the grout solidifies, fixing the radioactivity and completely removing it from man's environment. Thus far, approximately 600,000 curies of cesium and 50,000 curies of strontium have been injected.

Table 3. Composition of the Standard Hydrofracture Dry Mix

Constituent	Composition (wt %)
Cement	35.8
Fly ash	38.5
Attapulgite-150	15.3
Clay	7.7

ORNL-DWG 63-3830

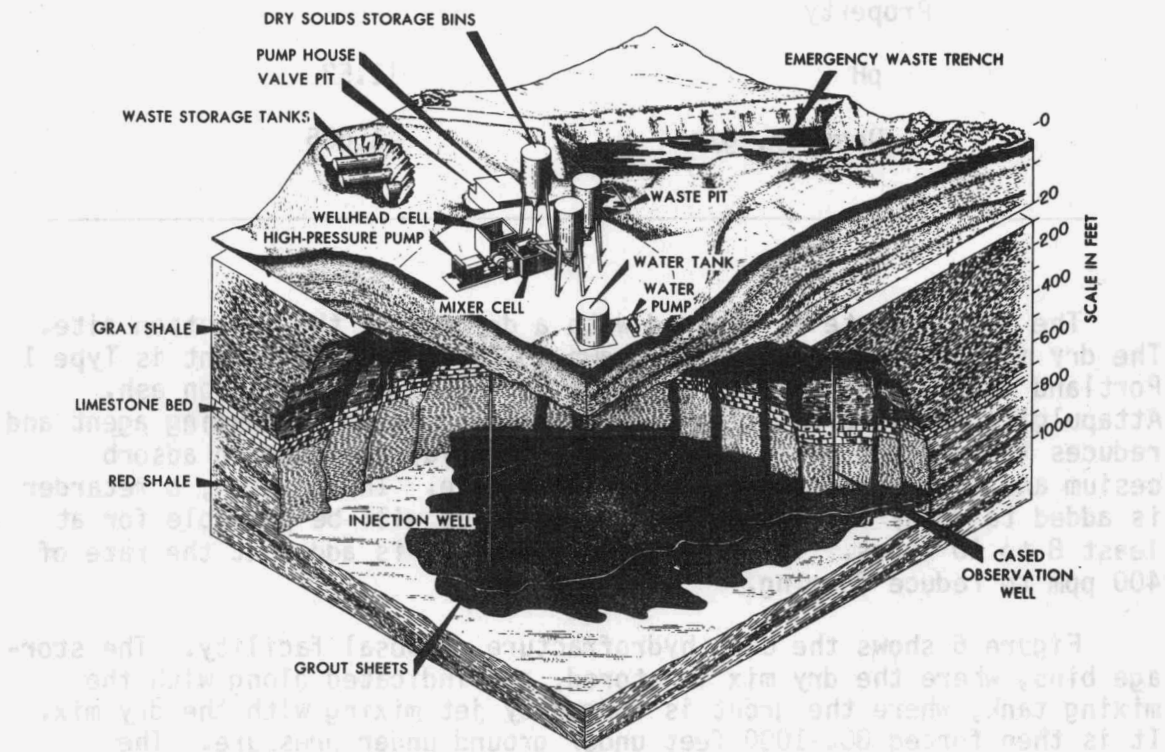


Fig. 6. ORNL hydrofracture disposal pilot plant.

Laboratory studies show that in the unlikely event that water ever penetrated this area (there is a geologic barrier that has been dry for millenia) the leach rates were quite low. In fact, the leachabilities of the nuclides cesium, strontium, and plutonium are essentially diffusion controlled. Figure 7 shows an example of a leach test in progress for 400 days, which was later extended for approximately two years. The straight-line relationship between the fraction leached and the square root of time indicates the leachability of cesium was essentially diffusion controlled. The leachability of cesium was comparable to that of borosilicate glass. Figure 8 compares the cesium leach rates from a hydrofracture grout containing Conasauga shale to retain the cesium with data from a borosilicate glass leach test.¹¹ The cesium diffusivity

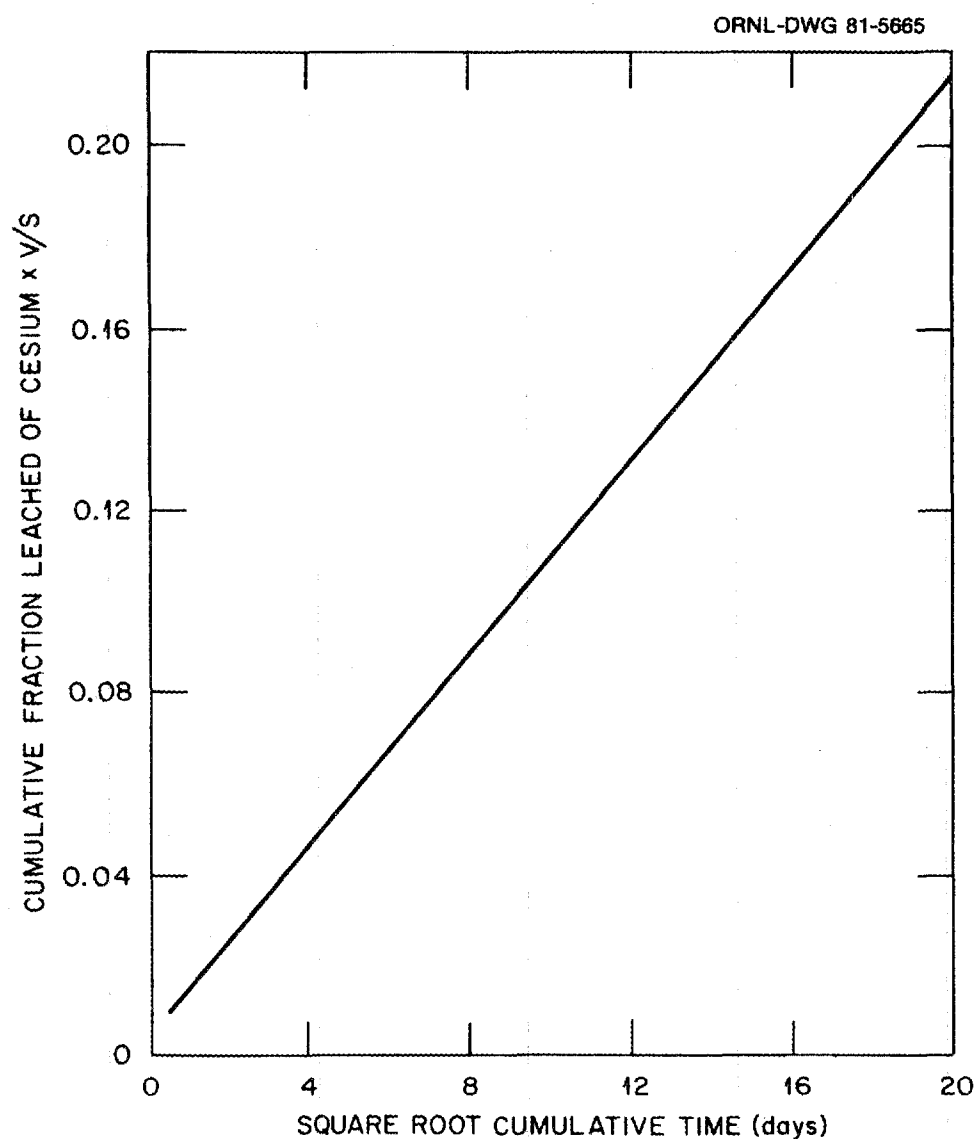


Fig. 7. The leachability of cesium from simulated hydrofracture grout into distilled water.

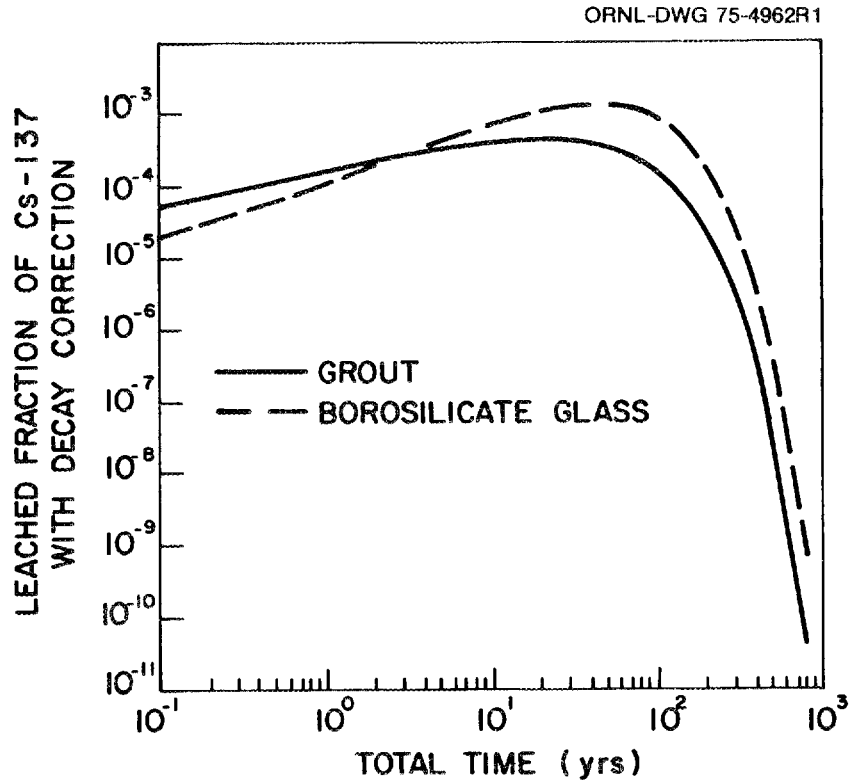


Fig. 8. Comparison of cesium leach rates from a hydrofracture grout containing Conasauga shale with those from a borosilicate glass.

from the grout was approximately 7×10^{-14} cm²/sec. The data show that at short times, a slightly smaller fraction of cesium is leached from the glass product than from the grout. At longer times, however, there is a reversal and there is less leaching from the grout than from the glass. These are obviously long extrapolations from short-term data. But it indicates that the leachability can be comparable to borosilicate glasses.

A new hydrofracture facility is being constructed at ORNL for the disposal of the radioactive sludge produced by the neutralization of liquid waste over the years. The sludge is currently stored in Gunit tanks, and, although the composition of the sludge in these tanks varies, the sludges are primarily iron and aluminum oxides (Table 4). Spot checks with actual sludge show that the sludge is almost like fine sand and settles very rapidly. Satisfactory hydrofracture grouts can be prepared using a dry mix that is simply cement and fly ash with a clay added to take care of the small amount of cesium that is included in the sludge (Table 5). Leach tests show that this material gives leach rates that are as good as or better than the standard hydrofracture grouts prepared from the liquid wastes.

The success of the shale fracturing process provided the impetus to start a generic investigation on the use of tailored concretes for radioactive waste management. Specific nuclides such as iodine, strontium,

Table 4. Composition of ORNL Waste Sludges

Cation*	Wt %
Iron	10-50
Aluminum	0-7
Lead	0-1
Chromium	0-1
Calcium	0-1.5

*Present as hydrated oxides and insoluble compounds combined with 0-30 wt % water-soluble material.

Table 5. Proposed Hydrofracture Dry Mix for Sludge Disposal

Component	Wt %
Cement	46
Fly ash	46
Clay	8

cesium, carbon, and tritium were considered along with low- and intermediate-level waste, actinide containing waste, and even high-level waste.

The first nuclide to be studied was iodine-129, which has a very low specific activity but a long half-life (1.6×10^7 yr). A series of laboratory tests showed that iodine may be immobilized in concrete as the readily prepared, insoluble compound, barium iodate.⁸ Leach studies were made using concretes containing 15 wt % iodine as barium iodate. Again, the leach rate was found to be diffusion controlled (Fig. 9). The iodine effective diffusivity into distilled water is approximately 1×10^{-10} cm²/sec. Thus from a full-size 200 lb drum, with all sides exposed to flowing distilled water for a year, approximately seven-tenths of one percent of the total iodine would be removed.

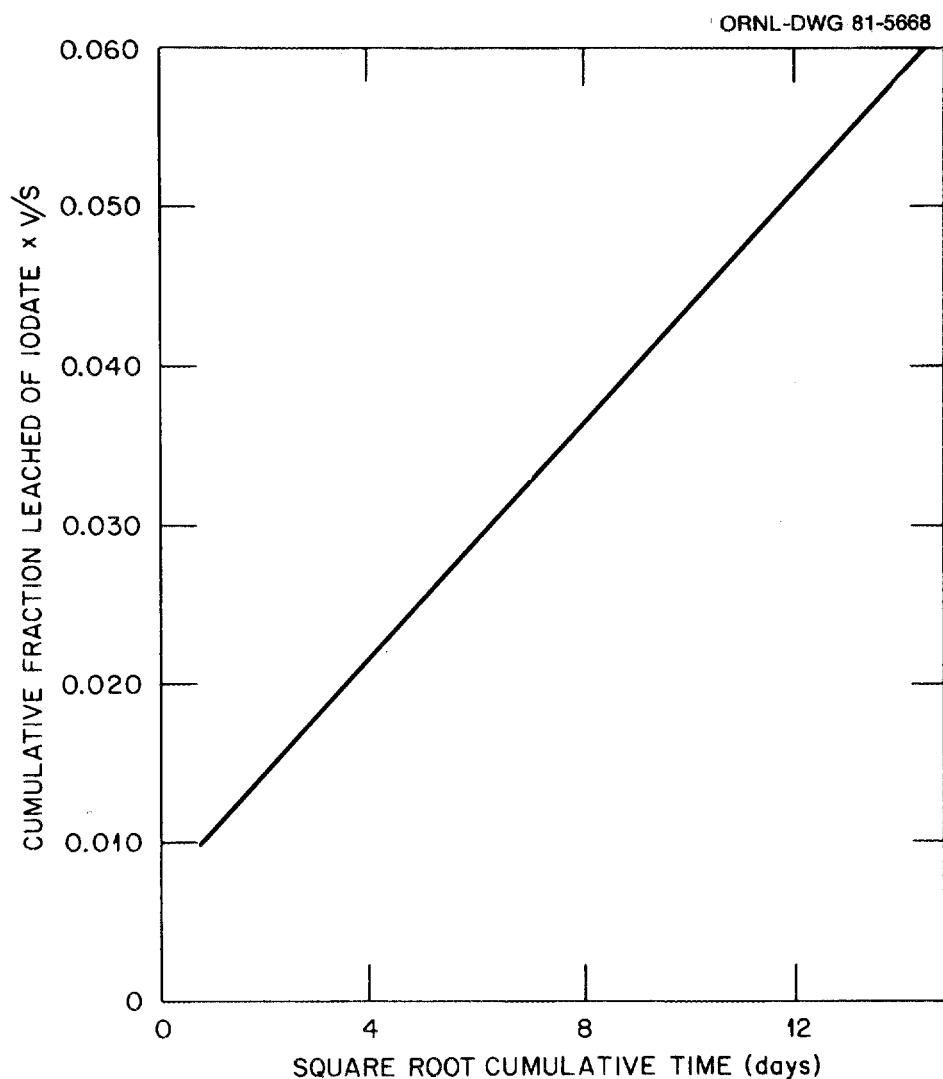


Fig. 9. The leachability of iodine into distilled water from concrete containing 15 wt % iodine as barium iodate.

A number of concrete formulations and leachants were examined. The composition of the leachant changed the diffusion coefficient by as much as four to five orders of magnitude (Table 6). In fact, in sea water and magnesium chloride the leachabilities were so low that it was difficult to measure them. One of the reasons for this was that a deposit, primarily of magnesium hydroxide, was building up on the concrete. The calcium hydroxide produced during the hydration process reacts with the magnesium to form a barrier on the surface. Under these alkaline conditions, an adsorption product forms with the magnesium as the iodine migrates to the surface. This is extremely insoluble material, and thus a low leach rate is obtained. It suggests that perhaps we should dump the material in the ocean. A calculation shows that the release rate would be so low that one would die from the iodine or from potassium-40 which is already in the ocean, long before we would ever get enough

Table 6. Effect of Leaching Composition on the Leachability of Iodine from Concrete^a

Leachant	D_e (cm ² /sec)
CO ₂ -Sat. H ₂ O	3.3 x 10 ⁻⁹
Dist. H ₂ O	1.2 x 10 ⁻¹⁰
Louisiana brine	9 x 10 ⁻¹¹
Sandia	4 x 10 ⁻¹¹
1500 ppm MgSO ₄	4 x 10 ⁻¹³
2500 ppm MgCl ₂	2 x 10 ⁻¹⁴
Sea water	4 x 10 ⁻¹⁴
Tap water	8 x 10 ⁻¹⁵

^a15 wt % I₂ as Ba(IO₃)₂, type I cement, water/cement (w/c) = 0.72, 28-day cure.

iodine-129.⁸ At any rate, it was found that iodine-129 could be segregated from man's environment using concrete.

The question now arises: Can concrete be used for high-level waste? The concept illustrated in Fig. 10 is one which we call the FUETAP approach. In this concept, the concrete is cured under autoclave conditions, i.e., formed under elevated temperature and pressure; it uses previous waste fixation studies^{4,5} as the starting point. A liquid waste or slurry is evaporated to obtain a desired concentration. It is known that concrete will accept large amounts of nitrate, but the upper limits are not known, so it may be necessary to add a denitration step to partially denitrate the material. In our studies, the assumption was made that we would start with a calcined material simulating the material that Hanford and Savannah River would obtain in their head-end process. This calcine is mixed with a cementitious material containing the necessary admixtures required to fix or hold the nuclides in question. The consistency is sufficiently liquid so that the material will flow into a canister. Good products are obtained at temperatures as low as 100°C, so the canister could also act as the autoclave. The canister is simply sealed. In the case of defense waste, one would have to apply heat, but for high-level waste it might even be possible to use the inherent heat of the waste. After 24 hours one would have the finished product, a

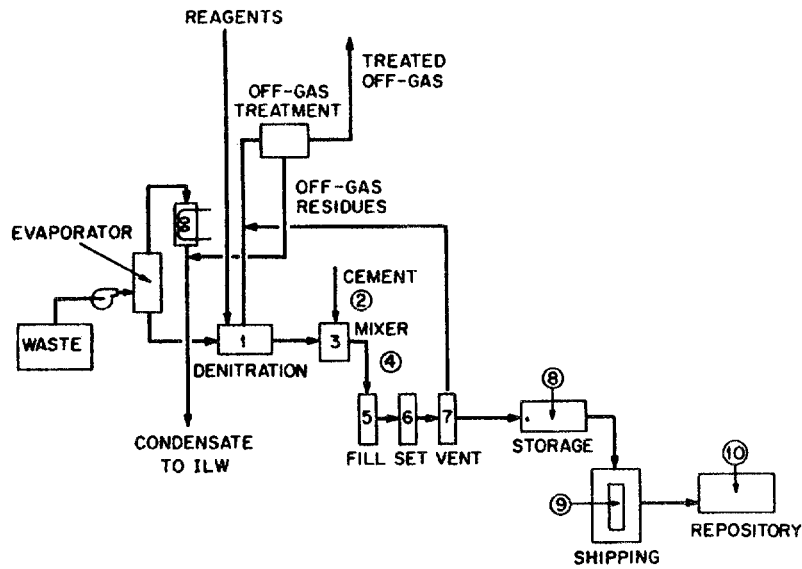


Fig. 10. Conceptual flowsheet for radioactive waste management using FUETAP concrete.

brick or ceramic like concrete. To eliminate the possibility of future pressurization due to steam or radiolysis we will remove the unbound water. The canister is vented and heated at 250° for twenty-four hours. This removes all of the unbound water and a small amount of the bound water. From there the product simply goes to storage, shipping, and finally to the repository.

As our laboratory studies progressed, a standard FUETAP formulation evolved (Table 7). The mixture contains Type I Portland cement and fly ash, with the ratio adjusted to maximize the compressive strength. Clay is present to lower the leachability of cesium. The mixture shown in Table 6 has only 15 wt % simulated solids, although we can go up to 25 wt %. Sand is added to improve the strength and the thermal conductivity. A water reducer is used to produce an almost liquid grout at a low water/cement ratio. The water concentration is very low; only 15 wt %. On curing this formulation for 24 h at 100°C and 0.1 MPa, compressive strengths of 60 MPa are obtained. These are solids that would fit the British code for high structure or the American code for high-strength concrete.

When the concrete is dried at 250°C for 24 hours, the unbound water is removed leaving about 2 wt % water in the solid. To determine what would happen on further heating, specimens were heated at 400° for 24 hours, and 900°C for 214 hours (Table 8). (For people who are new to the field, one must deal with the mythical shipping accident where the waste solid is submitted to very high temperatures for a half hour or so.) At 900°C it is difficult to determine how much water remains in the FUETAP, but a good estimate would be about 1%. The material was

Table 7. Standard FUETAP Formulation

Ingredient	Wt %
Cement	22
Fly ash	11
Clay	7.5
Simulated waste solids	15.0
Sand	27.75
Water	1.00
NO ₃	0.75
Water	15.0

Table 8. Dewatering of FUETAP Concrete

Temp. (°C)	Time (h)	Wt Lost (%)	Volatiles Lost* (%)	Water Remaining (~ wt %)
250	5	12.34	67	3.0
	24	13.08	71	2.2
	48	13.29	72	2.0
400	5	14.91	81	**
	24	15.08	82	**
900	24	16.97	92	**

* Initial grout made up to contain 15 wt % H₂O. Other mix ingredients normally lose 3.41% weight on heating 24 h at 900°C.

** Mass spec. indicates that decomposition of hydrates, nitrates, and carbonates occurs at temperatures \geq 400°C.

quite good after heating at 900°C. The sample did shrink, and there were a couple of microcracks. After all, it had lost quite a bit of water and some of the nitrate, but it still had a compressive strength of approximately 2000 psi. Additionally, it maintained its integrity when crushed. It merely cracked, creating essentially no fines whatsoever.

Since much of the water was removed to eliminate the danger from steam pressurization, the question arises: What happens with radiolytic gasification? It was found in some of the earlier studies that FUETAP concrete acts as an excellent catalyst to recombine oxygen and hydrogen. To verify this, some specimens were made which were doped with 0.6 mg of ^{244}Cm per g of concrete. These were placed in small containers, and the pressure was measured as a function of time. The results are shown in Table 9. For the control sample, which was cured at ambient conditions and was not dewatered, we calculated that the specimen was generating approximately 73 std cm^3/yr . For an earlier FUETAP concrete and the standard formulation, it is very difficult thus far to read the pressure. If we take the highest value, we are generating perhaps 4 std cm^3/yr .

Table 9. Gas Generation by Alpha Radiolysis of Concrete Containing ^{244}Cm (0.6 mg/g)

Specimen	Δ Pressure in 60 days (10^3 Pa)	Calculated Gas Generated (std cm^3/yr)
Control	215	73
FUETAP concrete	7-15	4
Standard FUETAP	8-16	4

Leachability results for the FUETAP material are shown in Table 10. We find again that the leachability is essentially diffusion controlled. Data are presented from studies with the original formulation and the standard formula mentioned earlier. The standard formula that we are now working with has cesium and plutonium leachabilities on the order of borosilicate glass. For the strontium it is higher than glass, however, Stone's⁴ observation that for the actual waste it is possible to improve the Sr leachability by one or two orders of magnitude should be remembered. Additionally, we are trying some old-fashioned chemical tricks which may tie up the strontium.

Table 10. Leachability of FUETAP Concrete

Cation	FUETAP Formula	Approximate Order of Effective Diffusivity, D_e , cm^2/sec		
		Demineralized Water	Spring Water	Sandia Brian
Cs	Original	10 ⁻¹¹	10 ⁻¹²	10 ⁻¹²
	Standard	10 ⁻¹⁴	10 ⁻¹⁴	10 ⁻¹²
Sr	Original	10 ⁻¹¹	10 ⁻¹⁰	10 ⁻¹¹
	Standard	10 ⁻¹⁰	10 ⁻¹¹	-
Pu	Original	-	10 ¹⁸	-

In summary, FUETAP appears to be an excellent host for defense wastes. The solid can be formed at a low temperature (e.g., at 100°C and 0.1 MPa) to yield a high-strength solid with compressive strengths $>$ 60 MPa. The thermal conductivity is excellent ($>$ 1W/(m.K)). The material has a reasonable density, 2 g/cm³. The waste loading runs 15 to 25 wt %, depending on whether or not we try to add the cesium zeolite to the sludge. With the cesium zeolite, the 15 wt % loading must be used. The material accepts a wide variety of wastes, and it tolerates nitrate. The plutonium and cesium leachabilities are extremely low, and the gasification from radiolysis is potentially very low. It is thermally stable to at least 900°C. All in all, it is a very reasonable product.

Are cementitious hosts a thing of the past? The best way to answer that is to look at some of the studies currently in progress. Della Roy is continuing her work on a pressed concrete and is getting some very interesting results. J. Doty, at Mound Laboratory, is looking at cold-pressed concrete as a means of fixing incinerator ash and gets an excellent product. Savannah River is evaluating concrete for the disposal of their salt cake, i.e., to make a saltcrete. Some people think that concrete will not accept much sodium nitrate. At ORNL we put in 60 wt % and got a pretty good waste form. Tritiated concrete work is going on at Mound Laboratory, in which they will dispose of tritium in concretes. There are many laboratories looking at better sorbents, natural as well as other inorganic exchangers, and better cements. At ORNL we are investigating ways to treat the defense waste liquids and sludges directly, in order to avoid a costly head-in process. We are looking at the TRU waste; it seems that concrete could be an ideal host in which to dispose

of TRU waste. We are even thinking of using cementitious mixtures for getting rid of trash, i.e., combustible material and cellulose. Concrete also seems to be an ideal material for the disposal of inorganic salts. One of the things that we will be trying fairly soon is taking barium carbonate with carbon-14 as the carbon part and making a concrete out of that. Finally, people are even thinking of putting krypton into hydrofracture grout. Since krypton has a fairly high solubility in water at elevated pressures, if we can dissolve it in our grout, and keep the pressure elevated until the grout is solidified, this might be a way to fix the krypton. So cement is definitely not dead. It is going strong and it offers a safe, economical means for the disposal of many types and levels of radioactive wastes.

DISCUSSION

HOWITT: What chemical compounds are formed in concrete? Do you have any idea of the specific compositions and in what ways the waste is fixed?

MOORE: You mean what are the chemical compounds that are formed that contain the radioactive nuclides? We do not know. Given enough research money, we would love to know where they are located. There has been quite a bit of work done on the various phases that are formed under different conditions. The condition that I am using right now, for example, in the FUETAP concrete is this: We are trying to get the silica-to-calcium ratio such that we would form a phase called tobermorite, which is quite stable, and it is hoped that this is what contains our radioactive material. But no, we have not been able to go into that as yet.

HOWITT: I am sorry, but the comment that I suppose one must automatically make is that they are funding you to pump it into the ground, but they are not funding you to find out what it is.

UNIDENTIFIED QUESTIONER: John, would you share with us what your ideas are for tying up strontium?

MOORE: I would rather not. I can say that we are trying the barium silicate approach of the Germans. I do not really like it too much, because they are using a large amount. The last time I talked with them, I think they were using 5 or 6%, which we consider to be just too much. I cannot say much more than that, because one of the men in the group has just had an idea, and I would like to see if it works first. He is going back to some very simple strontium chemistry, and it looks like it is improving the situation.

TAMURA: As far as cesium on these clays is concerned, I guess the work that we have done shows that the cesium goes into the particular lattice structure of the so-called zeolite silicate. In the case of zeolite, of course, it is a basal ion exchange reaction. With strontium, when you describe the use of fly ash, what we found was that, in the reaction in

cement where you get calcium silicate, one of the products is calcium hydroxide, which solidifies because the silicate takes the water away. When you do a leaching test, the calcium hydroxide is easily soluble. If you add fine-grained silicate, you minimize calcium hydroxide formation causing calcium-strontium silicates to form. That, I think, is basically the mechanism.

MOORE: Yes, but we do not have any very fancy work to show it. Clay is one of the things in this FUETAP; when we heat it to 250°C, clay people believe we could collapse the edges slightly, which could prevent cesium from coming out.

MARK WITTELS: You mentioned using barium iodate for the retention of iodine. Why can't you put the strontium in the barium iodate?

MOORE: That is one thing that some of our group have thought of using.

REFERENCES

1. F. M. Lea, The Chemistry of Cement and Concrete, 3rd ed., pp 3-7, Chemical Publishing Co. Inc., New York, 1971.
2. R. Malinowski, "Concretes and Mortars in Ancient Aqueducts," Concrete International, pp 66-76, January 1979.
3. P. Colombo, et al., Savannah River Laboratory Long-Term Waste Storage Program, Progress Reports 1-9, July 1973-April 1975.
4. J. A. Stone, Evaluation of Concrete as a Matrix for Solidification of Savannah River Plant Waste, DP-1448 (June 1977).
5. D. M. Roy and G. G. Gouda, "High Level Radioactive Waste Incorporation into Special Cements," Nucl. Technol. 40, 214-19 (September 1978).
6. G. Rudolph, "Chemical Investigations on Cementation of Radioactive Waste Products," KFK-Nachrichten Jahg. 11, p. 41, March 1979.
7. W. de Laguna, T. Tamura, H. O. Weeren, E. G. Struxness, W. C. McClain, and R. C. Sexton, Engineering Development of Hydraulic Fracturing as a Method for Permanent Disposal of Radioactive Wastes, ORNL-4259 (August 1968).
8. M. T. Morgan, J. G. Moore, H. E. Devaney, G. C. Rogers, C. Williams, and E. Newman, "The disposal of Iodine-129," Scientific Basis for Nuclear Waste Management, Vol. I, G. J. McCarthy (ed.), Plenum Press, New York, 1979, p. 453.

9. J. G. Moore, G. C. Rogers, J. H. Paehler, and H. E. Devaney, "FUETAP (Formed Under Elevated Temperatures and Pressures) Concretes as Hosts for Radioactive Wastes," Ceramics in Nuclear Waste Management, CONF-790420, 1979, p. 132.
10. A. H. Kibbey and H. W. Godbee, A Critical Review of Solid Radioactive Waste Practices at Nuclear Power Plants, ORNL-4924 (March 1974).
11. J. E. Mendel and J. L. McElroy, "Waste Solidification Program, Vol. 10, Evaluation of Solidified Products," BNWL-1966, Battelle Northwest Laboratories (July 1972).

SOLIDIFICATION OF NUCLEAR WASTE IN CONCRETE

Hans Christensen

Chemical Process Engineering
ASEA-ATOM
Västerås, Sweden

ABSTRACT

A summary is given of the operational experience gained from six years of concrete solidification in processing BWR and PWR medium-level radioactive waste. Parameters such as water resistance, crushing strength, waste distribution in the solidified cement gel, and leaching resistance have been examined.

INTRODUCTION

The cement solidification system to be described was originally designed to solidify low- and medium-level radioactive wastes from one BWR-unit. After two years of operation, the system was redesigned to raise the capacity and also to make it possible to solidify boric-acid-containing mixed-bed resins from one PWR unit.

The solidification process occurs in prefabricated concrete pre-forms with an external dimension of 1.2 x 1.2 x 1.2 m. Two standard wall thicknesses of 0.1 and 0.25 m have been used. After six years of operation, approximately 200 concrete moulds containing medium-level waste (bed resins) have been generated. An additional 400 moulds containing low-level waste (filter sludge) have also been produced. They have been stored in a humid atmosphere at temperatures between -20°C and 25°C (-4°F and 77°F) without any signs of deterioration or crack formation.

Core samples drilled from full scale solidified products show a homogeneous distribution of the waste (bed resins) in the cement gel. The crushing strength varies between 350-500 kg/cm² (5000-7000 psi). The leach rate of cesium from naked specimens containing BWR and PWR bed resins varies between 1.3×10^{-9} and 9×10^{-7} g/cm² · d depending on additives.

WASTE CATEGORIES, WASTE VOLUMES, AND SPECIFIC ACTIVITY

The waste categories and the waste volumes generated from one BWR- and one PWR-unit are given in Table 1. Also the annual production of concrete moulds, the waste volumes to be stored, and the surface dose rate on the moulds are given in Table 1.

Table 1. BWR and PWR Waste Categories and Annual Generated Waste Volumes

Category	Source	Spec. Act. Ci/m ³	Waste Volume m ³	No. of Concrete Containers	Surface ¹⁾ Dose Rate rem/h
Granular resins	Reactor water cleanup system	300	12	25 70	20 (0.1) 1 (0.25)
Powder resins	Pool water cleanup system	10	3	4	0.5-1 (0.1)
Powder resin	Condensate cleanup system	0.1	25	30	<0.1 (0.1)
Granular resin	Liquid waste system	1-10	5	10	0.1-1 (0.1)
Evaporator concentrate	Floor drain	0.1-1	No production during seven years		
<u>PRW-wastes²⁾</u>				<u>70-115</u>	
Granular resins	Primary systems	1000	10	60 120	4 (0.25) 2 (0.25)
Granular resins	Sec. systems	<0.1	15	20	<<0.1 (0.1)
				<u>80-140</u>	

1) Figures in parenthesis: Wall-thickness (in m) of concrete container.

2) PWR-wastes. H₃BO₃: 60 g/kg waste.

PRETREATMENT OF THE WASTE BEFORE SOLIDIFICATION

Water Content of the Waste

Powdered resins and filter sludge are partially dewatered by means of a Funda dewatering device (Fig. 1). The dry content of the sludge before solidification is 22-25% by weight. Granular resins are conveyed by means of an air lift from a storage tank to a dosage tank and then flushed to the solidification system by a given amount of water (Fig. 2). Granular resins constitute the waste category most likely to disturb the solidification process - mainly because of their swelling tendency and boric acid content. To obtain an acceptable solidified product, the water content of the resins must be well known so that a correct and acceptably low water-to-cement ratio ($w/c \leq 0.40$) can be obtained. Also the resin content of the solidified product is limited by the requirement of sufficient space between the granules. A three-component diagram for resins, water, and cement is shown in Fig. 3. The area of interest is that within the triangle AB_1C . Line one (I) in the diagram refers to the addition of transport water to the resins in an amount corresponding to about 16% of the resins. The waste volume corresponds to about 27% of the solidified product (point B_1). To meet the requirement of sufficient space between the granules, the maximum allowable amount of resins corresponds to about 32% of the solidified product (point B_2). Line two (II) refers to no addition of

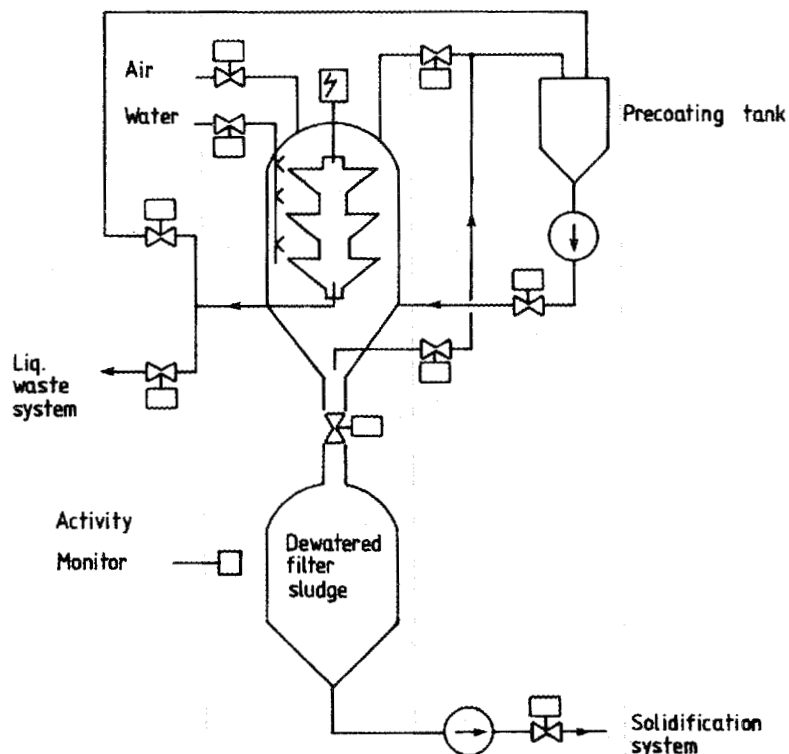


Fig. 1. Filter sludge dewatering equipment.

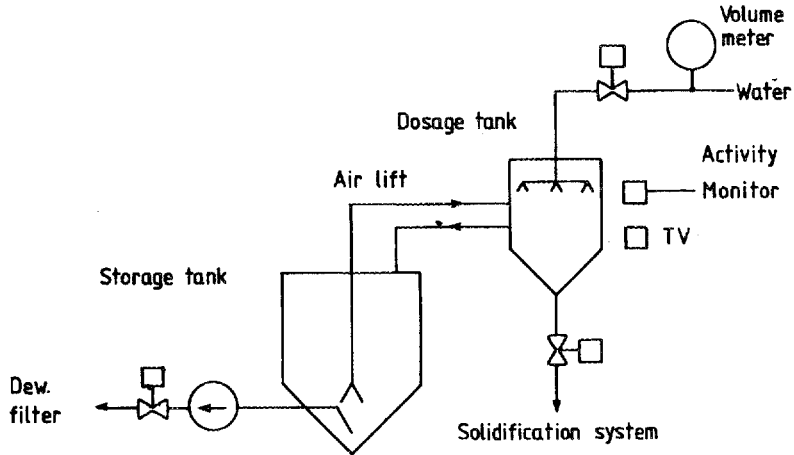


Fig. 2. Dosage equipment for granular resins.

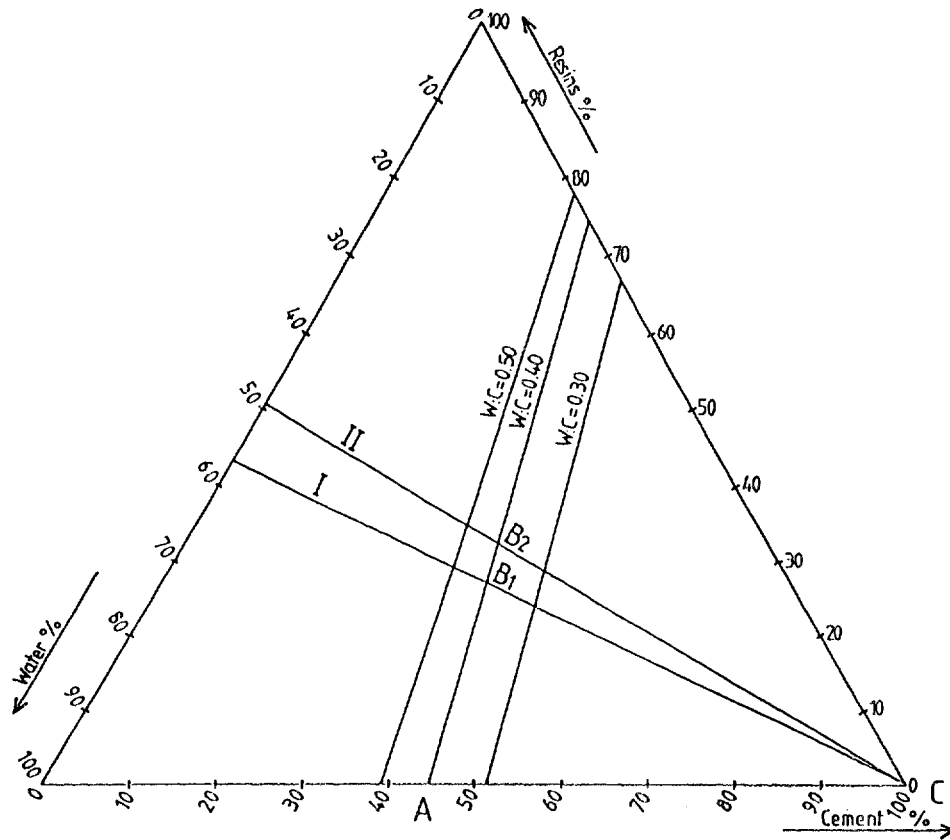


Fig. 3. Three component diagram of resin-water-cement. Percent by volume.

transport water to the resins. During six years of operation, full scale solidification has been achieved within the triangle AB_1C . By working within this area the operator has the possibility to correct mistakes. The chances for carrying out corrections within the triangle AB_2C are limited. To prevent water transport in the solidified products and to prevent swelling of the resins after solidification, liquid and solid chemicals are added before mixing the waste with cement. The permeability of the cement gel is reduced by adding an integral waterproofer.

Boric Acid Content of the Waste

As shown in Fig. 4, curve IV, boric acid is an excellent retarder of cement setting, holding up setting and hardening indefinitely¹. This effect of boric acid can be inhibited by adding a complexing agent. The amount to be added depends on the concentration of boric acid adsorbed on the resins.

For a resin-containing boric acid, placed in a water solution of OH^- ions and allowed to come to equilibrium, the selectivity coefficient K_B^{OH} for the reaction

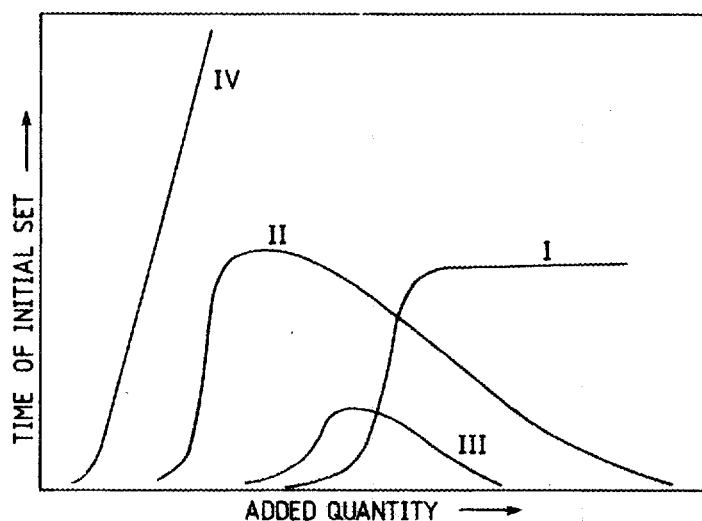


Fig. 4. Action of various retarders. Examples of salts in the different groups:

- I. $CaSO_4 \cdot 2 H_2O$
- II. $CaCl_2$
- III. Na_2CO_3
- IV. $Na_2B_4O_7$

is expressed by the equation

$$K_B^{OH} = \frac{[OH]_r \cdot [B]}{[B]_r \cdot [OH]} \quad \text{Eq. (2)}$$

$$K_B^{OH} = \text{Selectivity coefficient}$$

$$[OH]_r = \text{Concentration of } OH^- \text{ in the resin}$$

$$[OH] = \text{Concentration of } OH^- \text{ in solution}$$

$$[B]_r = \text{Concentration of boric acid in the resin}$$

$$[B] = \text{Concentration of boric acid in solution}$$

$$[C]_r = \text{Adsorption capacity of the anion exchange resin} \\ = [OH]_r + [B]_r$$

$$[] = \text{Concentration expressed in mol/l.}$$

The equations

$$[OH] = \frac{K_V}{[H]} \quad \text{Eq. (3)}$$

and

$$[H] = 10^{-pH} \quad \text{Eq. (4)}$$

are combined with Eq. (2) to yield the equation

$$\frac{[B]_r}{[C]_r - [B]_r} = \frac{[B] \cdot 10^{-pH}}{K_B^{OH} \cdot K_V} \quad \text{Eq. (5)}$$

Setting

$$A = \frac{[B] \cdot 10^{-pH}}{K_B^{OH} \cdot K_V}$$

$$\log A = \log [B] - pH - \log K_B^{OH} + 14 \quad \text{Eq. (6)}$$

In Fig. 5 experimental values of $\log K_B^{OH}$ are plotted against the pH-values of the liquid phase. By determining the value of $[B]$ and the pH-value of the liquid phase, the values of A and $[B]_r$ can be calculated:

$$[B]_r = \frac{A \cdot [C]_r}{(1 + A)}$$

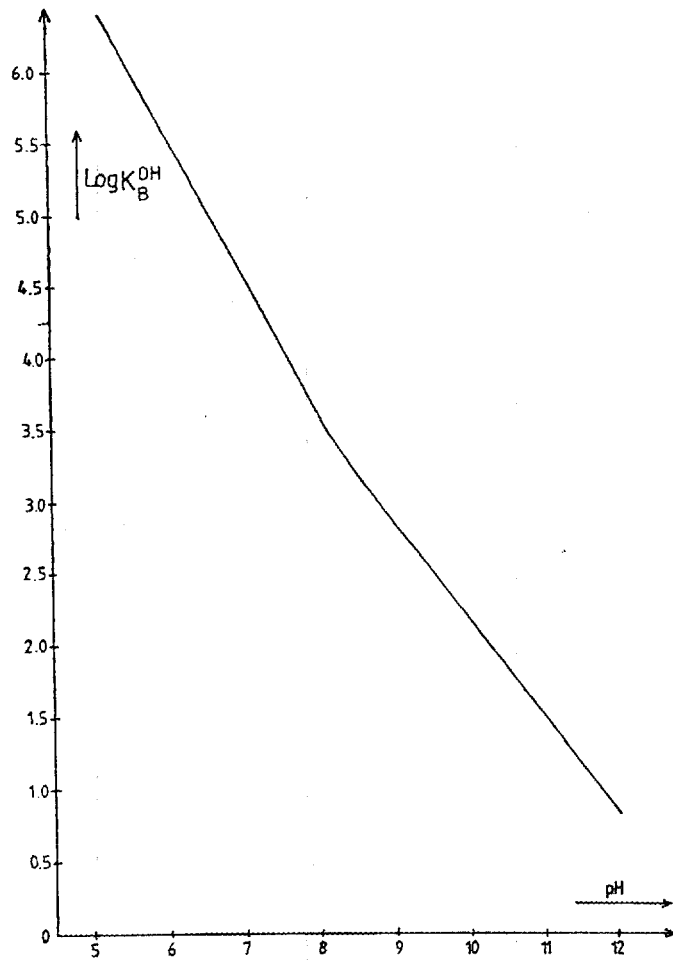


Fig. 5. Log of the selectivity - coefficient vs pH of the solution.

The Specific Activity of the Waste and the Surface Dose Rate on the Concrete Container

The two wall thicknesses of the prefabricated concrete preforms used are 0.1 m and 0.25 m, respectively. The wall thickness is chosen in each case to keep the surface dose rate of the mould to 1 rem/h which is the regulatory requirement in Sweden. The operator therefore has to know the activity level of the waste to be solidified. As shown in Fig. 6, the surface dose rate of moulds with varying thicknesses is plotted against the specific activity of the waste. It has been assumed that cement and additives dilute the waste to twice the original volume.

The use of concrete cubic preforms with a 0.25 m wall thickness and 1.2 m side length, admittedly increases the volume of waste to be stored and disposed of by a factor of 5. The assessment has been made

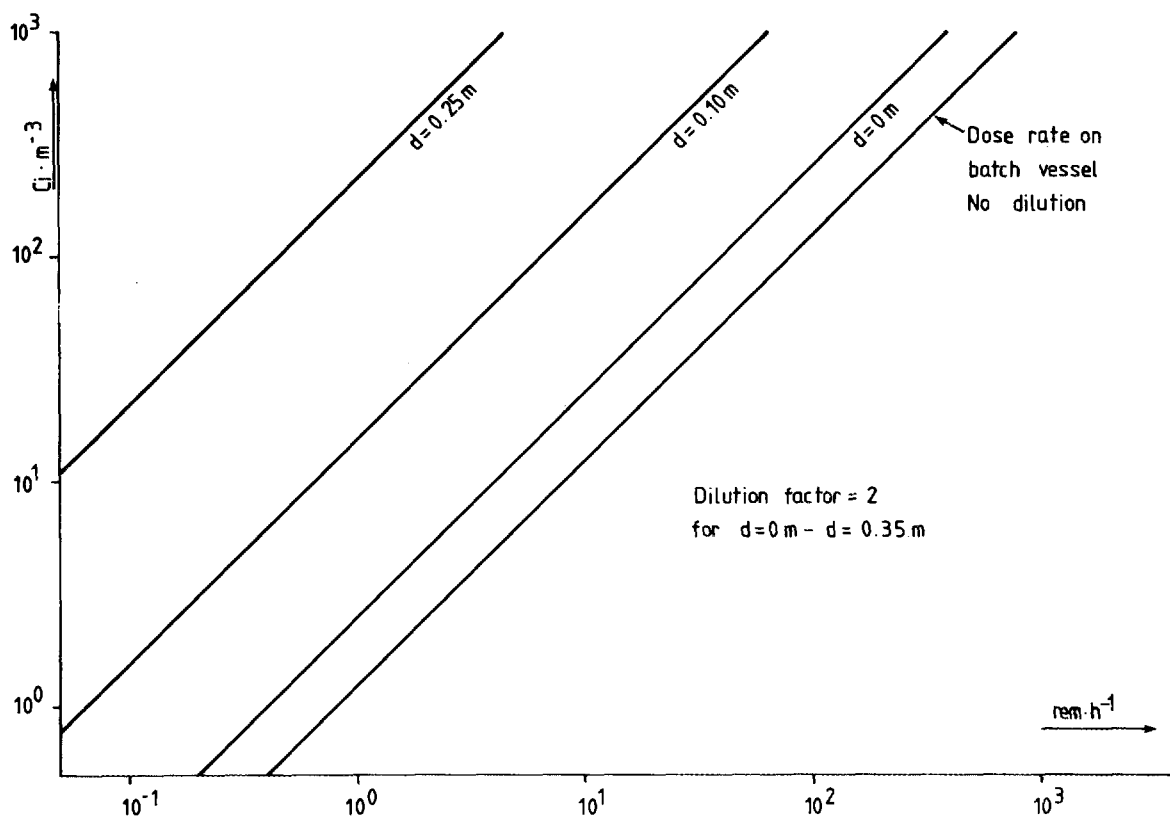


Fig. 6. Surface dose rate and activity concentration.

that this is a worthwhile penalty to accept. One achieves a waste product which is easily handled and transported and therefore suitable for storage at the site, awaiting final disposal in conjunction with plant decommissioning. However, it should be pointed out that the use of prefabricated moulds is, of course, not a prerequisite for applying a concrete solidification process as described here. Any type of "container" could be utilized if there are no requirements on either the container as a barrier to radioactivity escape or on the surface dose rate of the product to be stored and disposed of.

PLANT DESIGN AND SYSTEM OPERATION

A flow sheet of the system is shown in Fig. 7. The prefabricated concrete moulds are transferred to the solidification position by means of a programmed and remotely controlled transport vehicle. The moulds are filled with a closely controlled mixture of partially dewatered waste, additives, and cement. The mixture in the mould is homogenized with a remotely controlled mechanical stirrer. The stirrer is left in the solidified waste and serves as reinforcement. The process is supervised by means of weighing, radiation monitoring and closed circuit television. Special attention has been paid to the problem of cleaning the system after operation and to prevent airborne activity in the surrounding premises. When the filling and mixing operations are completed,

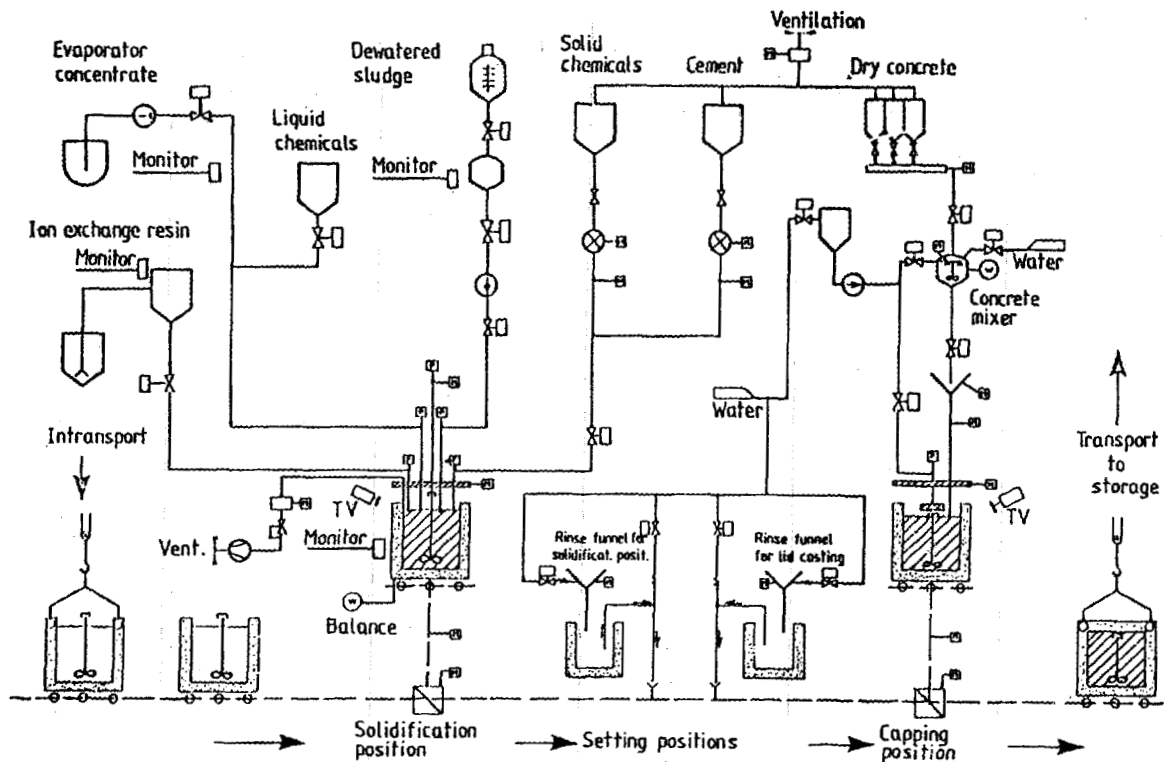


Fig. 7. Concrete solidification system.

the mould is transferred to the capping position. Here, a special type of dry concrete is mixed with a small volume of water and poured on top of the solidified waste in the concrete container. After setting of the concrete lid, the block is transferred to the site storage.

THE SOLIDIFIED PRODUCT

Core samples with a length of 1 m and a diameter of 0.1 m have been obtained from full scale solidified products. The core samples do not exhibit any change and do not show any tendency towards disintegration after being submerged in water for about two years. The crushing strength varies between 350-500 kg/cm² (5000-7000 psi). Concrete moulds split into two sections reveal a homogeneous distribution of the granules in the cement gel. After six years of operation, approximately 200 concrete moulds containing medium-level waste (bed resins) have been generated. An additional 400 moulds containing low-level waste (filter sludge) have also been produced. They have been stored in a humid atmosphere at temperatures between -20°C and 25°C (-4°F and 77°F) without any signs of deterioration or crack formation.

THE LEACHING RESISTANCE OF THE SOLIDIFIED WASTE

The leach rate of cesium from naked specimens containing simulated BWR and PWR bed resins contaminated with Cs-137 and nonradioactive CsCl as tracer has been determined after 50 days of leaching in tap water. The specimen contained exfoliated vermiculite to an amount of 1% and 2% and sodium zeolite to an amount of 2.5% and 5% of the cement weight. The reference specimens contained no additives except those necessary for the solidification process. The water-to-cement ratio was 0.35 and the volume and surface area of the specimens were 100 cm³ and 120 cm², respectively. The leaching water (200 cm³) was renewed once a day during the first 10 days, then every two days. The diffusion constants for cesium from the naked specimens were found to be 2.3×10^{-4} → 2.1×10^{-6} cm²/d depending on additives. Using these values, the diffusion of Cs-137 has been computed from waste solidified in moulds with a wall thickness of 0.1 m. The blocks were assumed to be submerged in water containing no cesium. The amount of cesium released from intact blocks is shown in Fig. 8, and the amount of cesium leached from concrete moulds split into two sections with a naked exposed area of 2 m² is shown in Fig. 9. In Table 2 the leach rate of cesium from solidified products described here is compared with the leach rate of alkali- and alkaline-earth elements from other matrices.

DISCUSSION

UNIDENTIFIED QUESTIONER: What is the maximum loading in curies that you can put into a cubic meter? You indicated a thousand. When you were doing the experimentation to choose that particular set of parameters, presumably you loaded the resins above and beyond that point, and placed them in concrete to see how they would withstand the radiation. How much radiation did you put on them?

CHRISTENSEN: We have been up to about 5000 curies per cubic meter of the PWR resin.

REFERENCES

1. F. M. Lea, The Chemistry of Cement and Concrete, Third Edition, Edward Arnold (Publishers) Ltd., London 1976.
2. J. G. Moore, H. W. Godbee, and A. H. Kibbey, "Leach Behaviour of Hydrofracture Grout Incorporating Radioactive Wastes, Nucl. Technol. 32, 39 (1977).

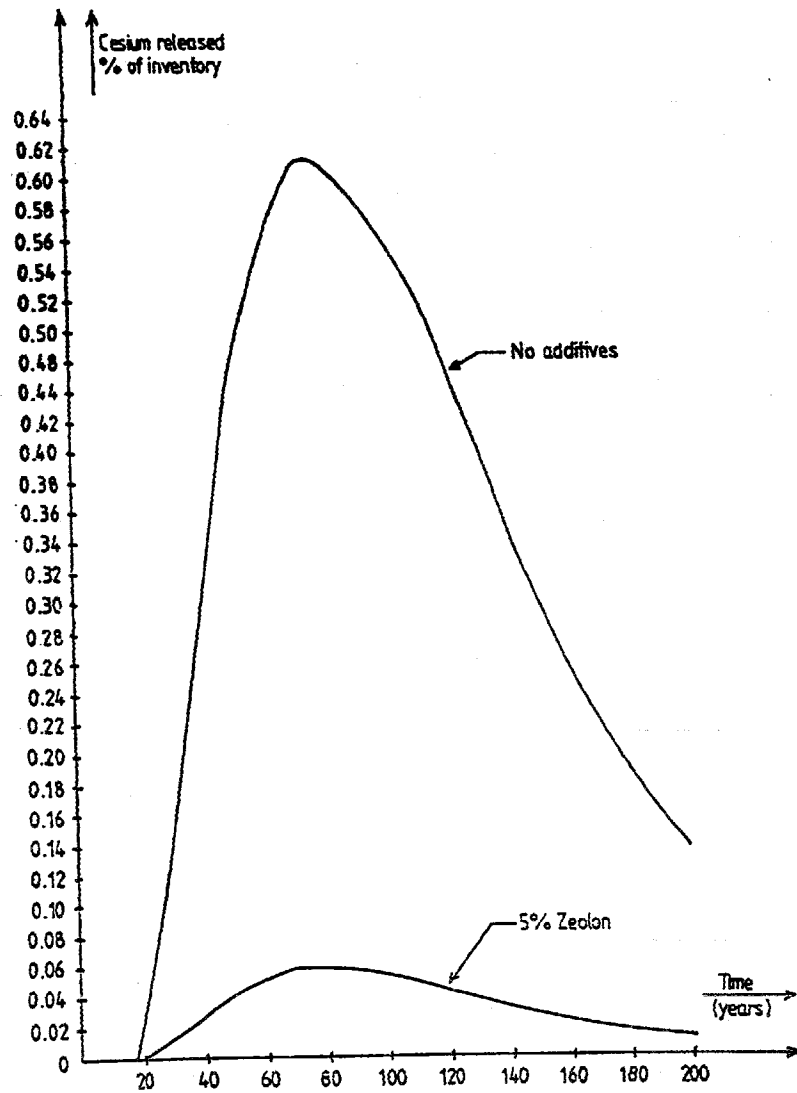


Fig. 8. Release of Cs-137 from intact moulds (0.1 m).

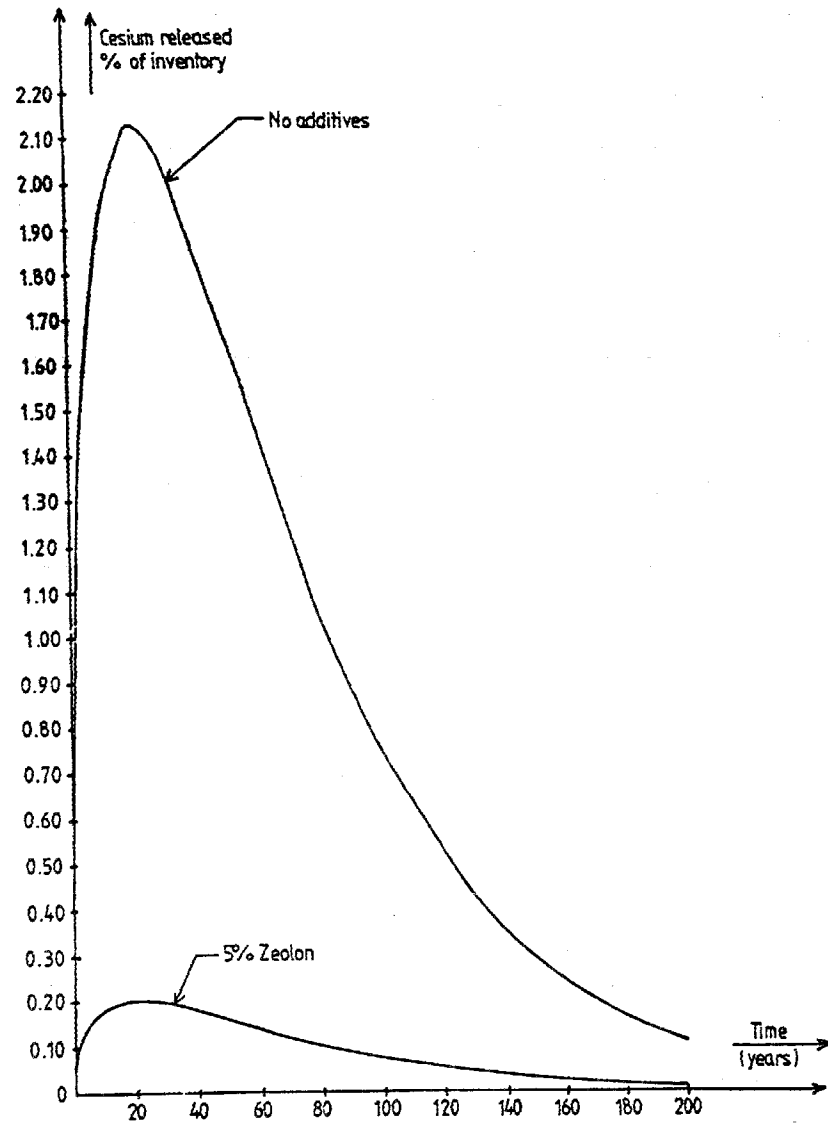


Fig. 9. Release of Cs-137 from concrete moulds split into two sections.

Table 2. Comparison of Cesium Leach Rates from Different Matrices

Waste Products	Leach rates g/(cm ² · d)	Reference
Calcines	$1 \times 10^{-1} \rightarrow 1 \times 10^0$	} 2
Ceramics: Phosphate Devitrified	$5 \times 10^{-5} \rightarrow 8 \times 10^{-3}$	
Phosphate Glass	$2 \times 10^{-4} \rightarrow 5 \times 10^{-3}$	
Glasses: Borosilicate	$8 \times 10^{-8} \rightarrow 4 \times 10^{-5}$	
Phosphate	$2 \times 10^{-8} \rightarrow 5 \times 10^{-5}$	
Aluminosilicate	$3 \times 10^{-8} \rightarrow 5 \times 10^{-7}$	
Bitumens:	$3 \times 10^{-7} \rightarrow 2 \times 10^{-4}$	
Cements:	$4 \times 10^{-6} \rightarrow 1 \times 10^{-1}$	
Grouts:	$5 \times 10^{-7} \rightarrow 8 \times 10^{-4}$	
Mixed bed resins (BWR- and PWR-primary resins) solidified in cement gel	$1 \times 10^{-9} \rightarrow 9 \times 10^{-7}$	

WASTE FORM CHARACTERIZATION AND ITS RELATIONSHIP TO TRANSPORTATION
ACCIDENT ANALYSIS*

E. L. Wilmot and J. D. McClure

TRANSPORTATION TECHNOLOGY CENTER
Sandia National Laboratories
Albuquerque, NM 87185

ABSTRACT

During the development and characterization of waste forms, an often overlooked consideration is the relationship between waste form criteria and environmental impacts associated with transporting waste material. The waste form influences the consequences predicted for potential transportation accidents calculated for environmental impact statements and is a critical factor for licensing packagings to be used for transporting waste. Consequently, when establishing criteria for waste forms to be used for final or interim storage, transportation requirements should be considered along with those related to processing and disposal.

The response of potential waste forms should be determined for extreme transportation environments that must be postulated for environmental impact analysis and also for hypothetical accident conditions to which packagings and contents must be subjected for licensing purposes. The best approach may be to test materials up to and beyond their failure point; such an approach would establish failure thresholds. Specification of what denotes failure would be defined by existing or proposed regulations or dictated by requirements developed from accident analysis. Responses to physical and thermal insults are the most important for licensing or analysis and need to be thoroughly characterized. Others in need of characterization might be responses to extreme chemical environments and to intense and prolonged radiation exposure. A complete characterization of waste-form responses would be desirable for environments that are considered extreme for transportation accidents but which may be typical for processing or disposal environments.

In addition, the characterizations that are performed must be completed in laboratory environments which can be readily correlated to accident environments and must be meaningfully conveyed to a transportation impact analyst. As an example, leaching data as commonly presented are not usable to the analyst and are

*Prepared by Sandia National Laboratories for the United States Department of Energy under contract DE-AC04-76DP00789.

obtained under conditions that are not directly applicable to conditions of most transportation accidents.

Transportation analysts are in need of data useful for calculating environmental impacts and for licensing of packagings. Future waste form development programs and associated decisions should consider the needs of transportation analysts.

During the development and characterization of nuclear waste forms, the relationship between waste form and environmental impacts associated with transporting nuclear waste is often overlooked. The waste form influences transportation-accident consequences calculated for environmental impact statements and is a critical factor for licensing packagings. Consequently, when establishing criteria for waste forms for final or interim storage, transportation requirements should be considered along with those related to processing and disposal.

In transporting nuclear waste, the packaging provides the safety, and no special vehicle safety requirements are required except for those routinely required for vehicles used to transport all hazardous materials. In this paper, a transportation package is defined as the packaging, the interior canister (or canisters) that holds the nuclear waste, and the nuclear waste, itself. An example of a conceptual package is given in Figure 1 for high level waste (HLW). Even though conceptual designs exist for HLW casks, none have actually been manufactured. The canisters are being developed and a design is shown in Figure 2. The design shown in the figure is for a single canister, but future designs may require double canisters (i.e., a canister within a canister). The HLW completes the package, but what its form will be is not as yet decided. However, for risk analyses that have been performed to date, borosilicate glass has been considered as the reference waste form. Its characteristics are considered as a reference or, in other words, the "minimum" acceptable. Transportation packages for other waste forms, including contact-handled and remotely-handled transuranics, generally have advanced only to the conceptual stage.

In order for nuclear waste to be transported, a package must be licensed for each waste form; the packaging for HLW, for example, will be specifically licensed for the HLW that will be carried in it. Very rigorous licensing requirements exist and involve a series of tests designed to produce package damage equivalent to that which might be expected for a very severe transportation accident. These test conditions are found in 10 CFR 71, Appendix B and are as follows:

Drop test - a 9 m drop onto an unyielding target

Puncture test - a 1 m drop onto a 15 cm diameter probe

Thermal test - 30-minute fire at 800°C

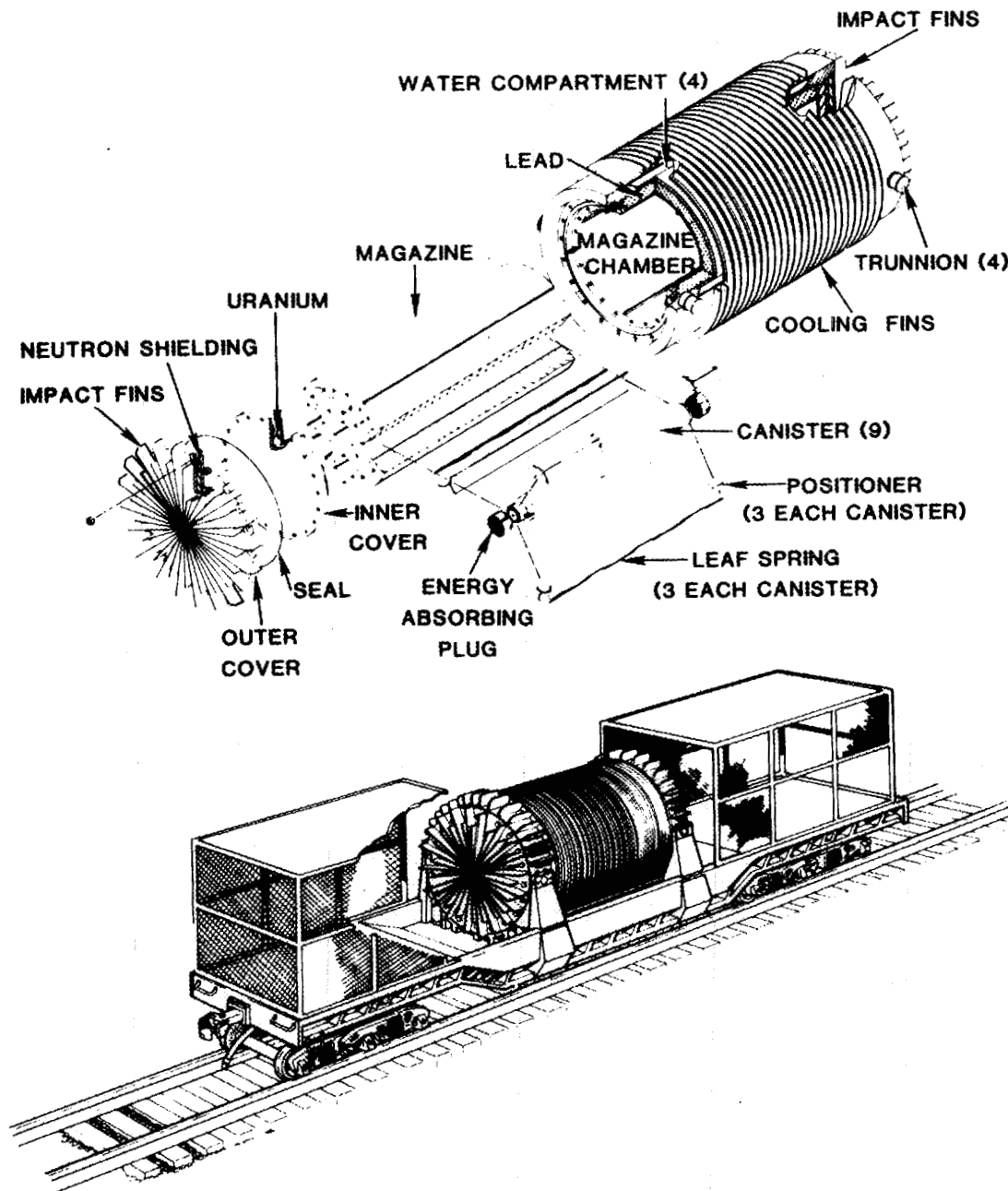


Fig. 1. Transportation package.

Water immersion - 8 hours in 1 m of water (for fissile materials only).

The package must be subjected to these conditions in sequence. If however, the canister inside the package contains more than 20 curies of plutonium, the canister might also be subjected to the same test conditions in order to satisfy the regulatory requirements for double containment. Survival as defined in the regulations means that no nuclear material

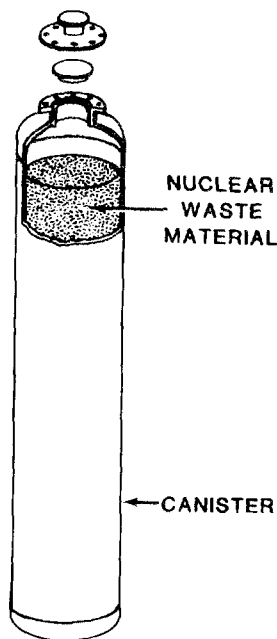


Fig. 2. Conceptual canister.

except gases or that material which is entrained in the coolant may be released to the environment, and the amount of released material can be no greater than certain prescribed limits.

Some very obvious characteristics of a transportable and "licenseable" nuclear waste form may be described. The waste form should be a solid that is in a non-dispersible form and that does not generate fines when impacted. The form should not be degraded by elevated temperatures, and any allowable degradation should not increase the quantity of fines. The waste form should not be volatile; chemical species should have vapor pressures that are low. In addition, the waste form should have good resistance to water leaching even for elevated water temperatures. All of these characteristics are necessary, not surprisingly, for reducing any impacts associated with a transportation accident.

Any project that requires the transport of nuclear material must determine in its environmental impact statement the impact of transporting that material. Unfortunately, as now written, NEPA regulations in 40 CFR 1502.22 require a worst-case analysis when data are impossible to obtain, are too expensive or are just not available. As a result, the accident environments that must be analyzed are, in reality, as unbounded as is the imagination of any concerned member of the public. For example, without any experimental data in the extra-regulatory range (beyond the regulatory test conditions in 10 CFR 71, Appendix B), there is no limit to the accident environments that must be considered. Consequently, the package would have to be tested beyond the regulatory test conditions in order to satisfy the data needs for environmental impact analyses.

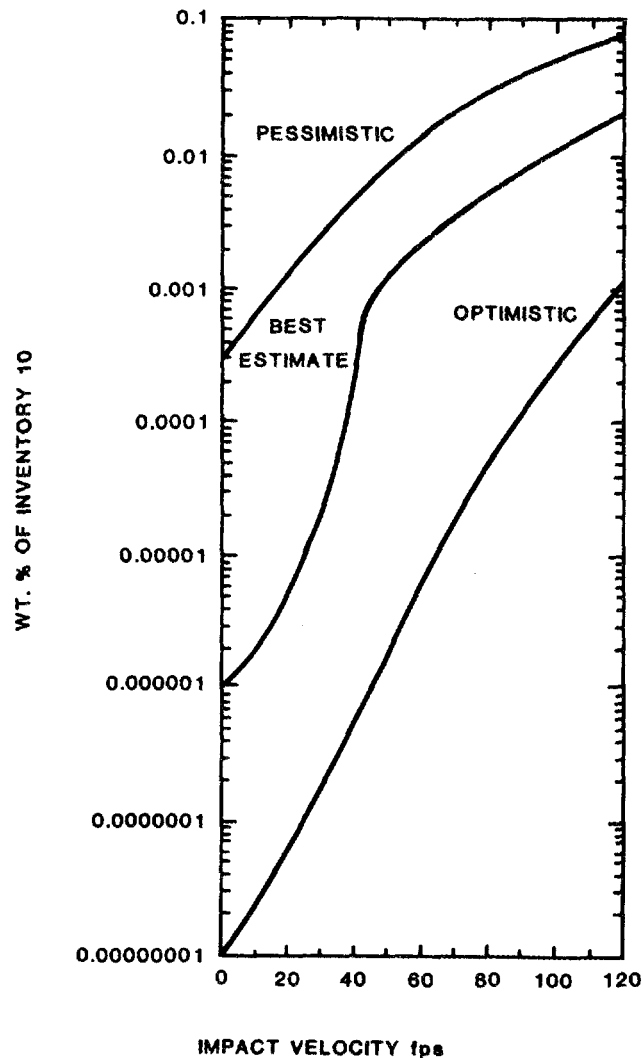
The regulations and the analytical needs of the risk analysis define environments that the package must be subjected to, but they do not define the environments actually seen by the canister or nuclear material. For this reason it is easiest to test the full scale package to the conditions prescribed and simply measure the waste form response. However, these full scale tests are very expensive and only a few tests could be performed. Another testing option, actually the preferred option when cost is considered, is to test the canister and its nuclear contents without the packaging. The cask is a protective barrier for the canister and the nuclear waste, but in this alternative, the amount of protection provided would have to be analytically predicted. The analytically determined cask response would then have to be used to estimate the environments to which a canister and its contents would be subjected. If nuclear material is tested without its canister or cask, both protective barriers have been removed so the amount of protection would have to be analytically predicted for both. The difficulty of accurately predicting the amount of protection offered by both barriers increases because computer analyses cannot accurately predict detailed canister response. Small samples of the nuclear material can be tested to provide some data, but the usefulness of this data is even more restricted because it is difficult to directly correlate to the package response and to scale material response. Small sample testing is the least desirable but is the most expedient and least costly option.

The preferred method for obtaining data would be to test the full scale package containing actual nuclear waste. The data obtained would be formatted as shown in Figures 3 through 5 for impact, volatility and leaching, respectively. However, a preferred unit of measure for leaching would be the fraction of material leached.

Very little data has been obtained for full scale package tests. Results of full scale tests performed to date which provide materials information are shown in Figures 6 through 9.³ These figures depict the results of full scale tests performed with a spent fuel packaging that contained fresh fuel. Figure 6 shows the condition of a spent fuel cask that has survived an impact of about 100 kph, and Figure 7 shows an end-on view of the unirradiated fuel within the cask. Figures 8 and 9 are closer examinations of that fuel assembly. This sort of testing provides invaluable data, but testing the package at full scale is nearly impossible because it is expensive; consequently, testing the canister and a surrogate nuclear waste is the most reasonable testing option.

In all testing options, a nonradioactive surrogate nuclear waste will probably have to be used. This, in turn, means that surrogate material will have to be qualified through a battery of comparative tests, which would ensure that the surrogate predictably behaves in a manner that can be correlated to the manner in which the nuclear waste behaves.

What then are the test data that are needed by the transportation risk analyst? Three environments are considered for analysis and the regulations; data are needed for physical, thermal and chemical environments. Physical and thermal environments are the most important because they are the most likely ones to be encountered in an accident. Of secondary importance is chemical because it is not likely to be encountered.



PREDICTION CURVES FOR SUB-10 μ FINES GENERATION

Fig. 3. Impact data (from BNWL-1903,¹ Fig. 39).

The data needed for each of the three environments are impact data (more specifically, the fraction of fines generated that are less than 10 microns mean aerodynamic diameter), data for response to thermal environments and leaching data. These data are generally not available for nuclear waste materials, but a few good references providing data are available. A very widely referenced work is BNWL-1903.¹ This study was carefully done and provides impact data for borosilicate glass in a canister. A figure taken from this reference is shown in Figure 3. This is a very good example of what kind of data is needed by a transportation risk analyst and is also a good example of how data should be presented. The abscissa in the figure is the impact velocity, which ranges well beyond the regulatory velocity for the package, and the ordinate is the weight percent of fines

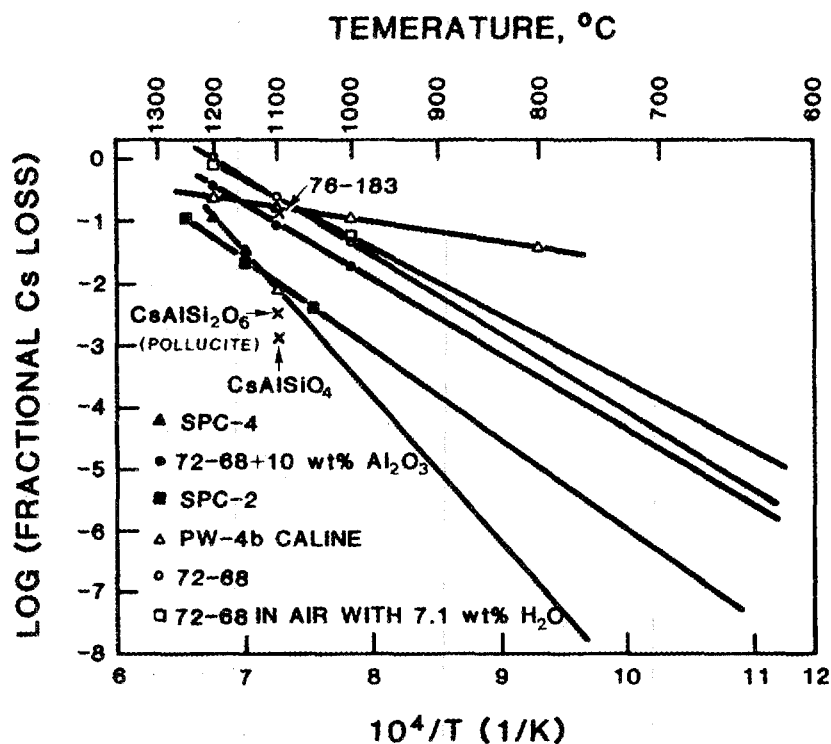
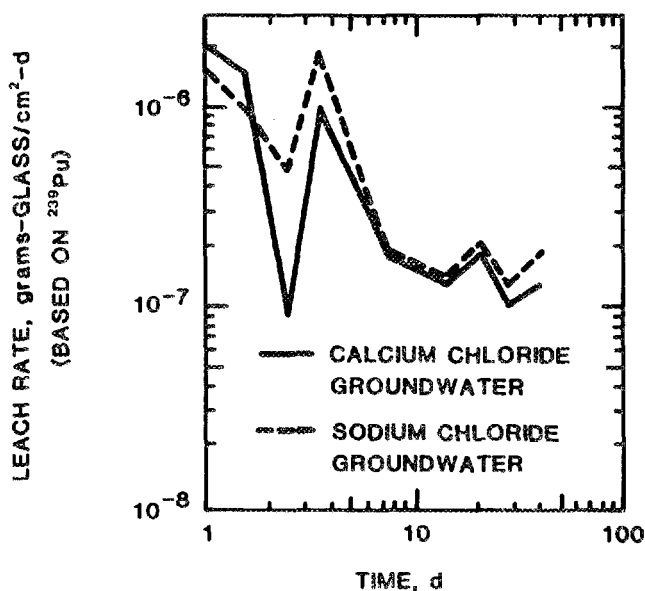


Fig. 4. Thermal data (vaporization) (from PNL-3060,² Fig. VIII.1).

generated by the impact. An example of data for volatilization is taken for cesium in the form of a thin sample of HLW and is shown in Figure 4.² The abscissa, in this case, is reciprocal temperature, and the ordinate is the fraction of the cesium inventory lost. An example of data for leaching is shown in Figure 5.² Here, the abscissa is the time and the ordinate is leach rate.

These are three examples of the best data presently available to the transportation risk analyst. Unfortunately, the application of much of the data is restricted because the experimental conditions used to produce the data do not relate to the sort of conditions produced in actual transportation accidents or in regulatory test conditions.

The recording format for data obtained from impact testing should be very similar to that shown in Figure 3. The weight percent fines generated should be plotted with corresponding impact velocity. Impact velocities should be considered through a range exceeding the failure threshold of the material. In addition, it would be helpful to perform the impact tests in a closed system where a material balance could be performed when material is released from its canister.



**LONG-TERM LEACH RATES IN
CaCl₂ AND NaCl SOLUTIONS**

Fig. 5. Chemical data (from PNL-3060,² Fig. VII.6).

The specifications for data obtained in a thermal environment would be nearly identical to Figure 4, shown earlier for volatilization, except that the data would be required for much shorter time periods (15 minutes to several hours). The temperature range over which data should be obtained is from a few hundred degrees Centigrade to around 1000°C. Since the amount of material volatilized is a function of nuclear-waste surface area, it would be preferable to take a canister used for an impact test and subject it to a thermal environment. The canister and its contents should be tested together to ensure that the role of the canister in preventing release is considered. As shown in Figure 4, the fractional loss of nuclides is the preferred recording option.

The leaching data are of secondary importance, but they are still of value. The existing leach data are difficult to use, are not generally standardized, are frequently obtained using small samples with a maximum surface area and are taken over very long periods of time. The most useful leaching data would be obtained from testing an impacted canister and its contents. The leaching should be done with "tap" or stream water since distilled water is particularly conservative for transport accident conditions. Of interest for transportation analysis is data that is obtained for very short time periods (hours to a day or two), and the data are only useful if presented as a fraction of the original inventory released. Leach rates are not as important as the fraction of inventory released in a specified period.

The "wish list" should not be particularly difficult to obtain, but it is vitally important that the nuclear waste be characterized according

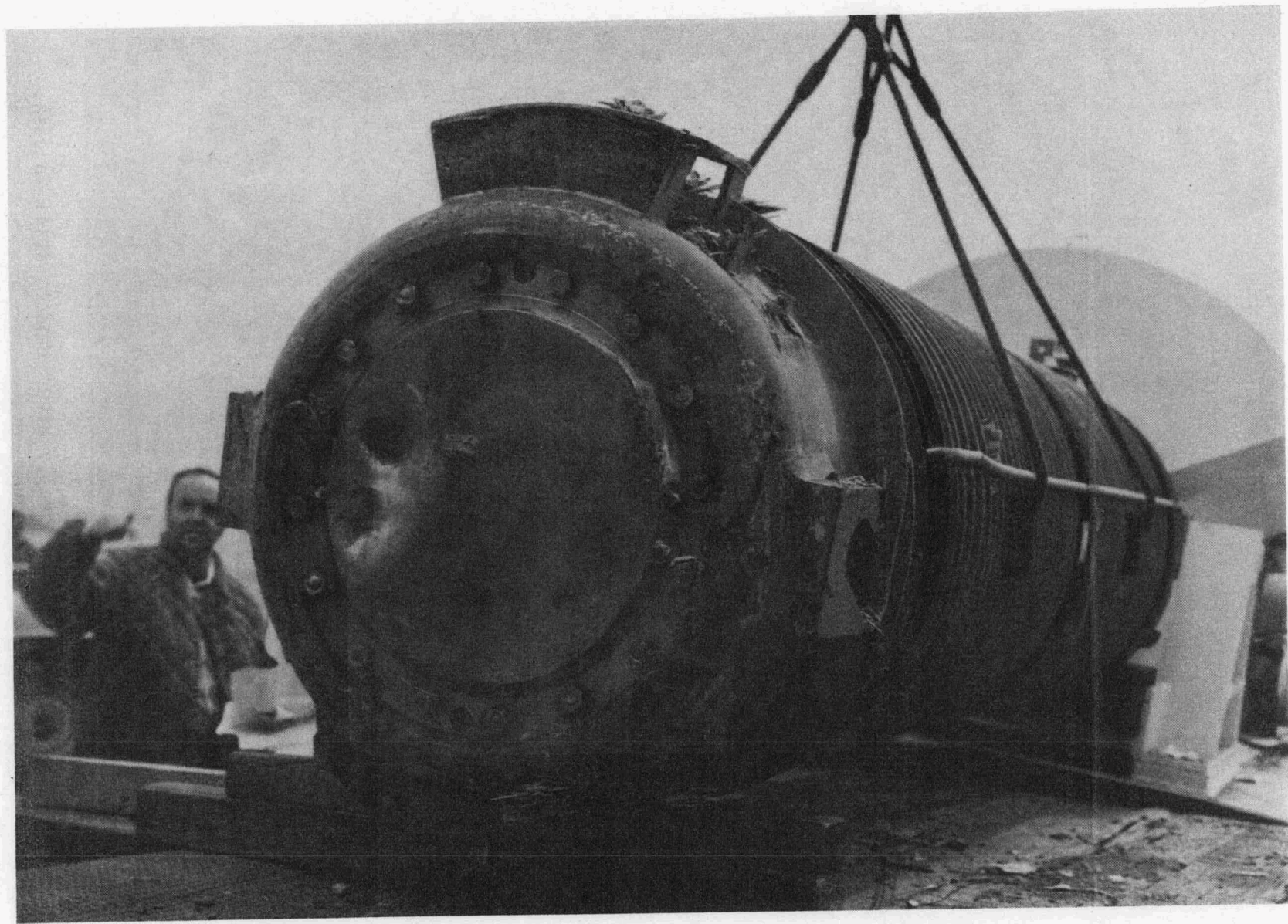


Fig. 6 Spent fuel cask after surviving 100-kph impact.

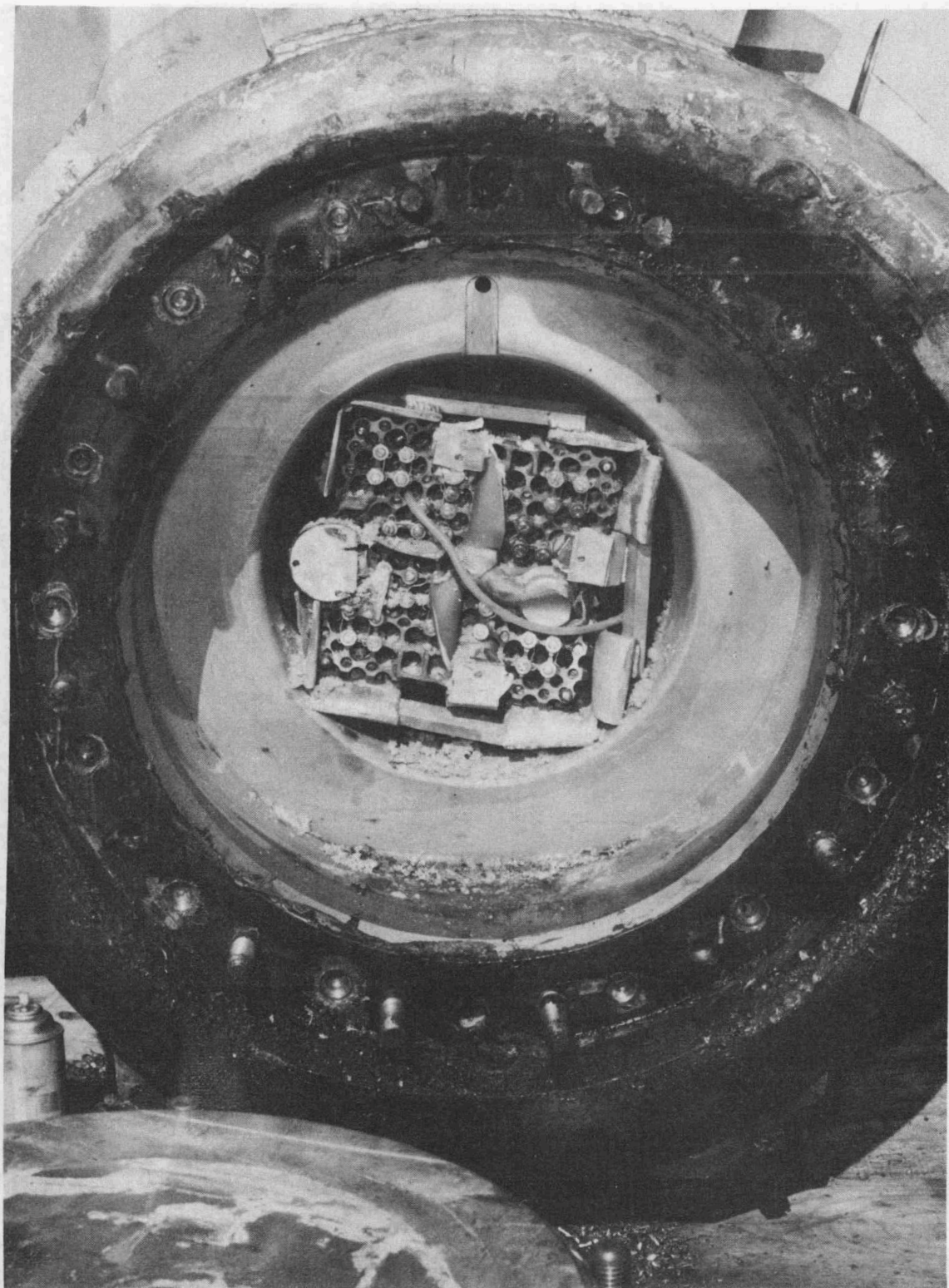


Fig. 7. Unirradiated fuel assembly after impact, still in cask.

Fig. 7. Unirradiated fuel assembly after impact, still in cask.

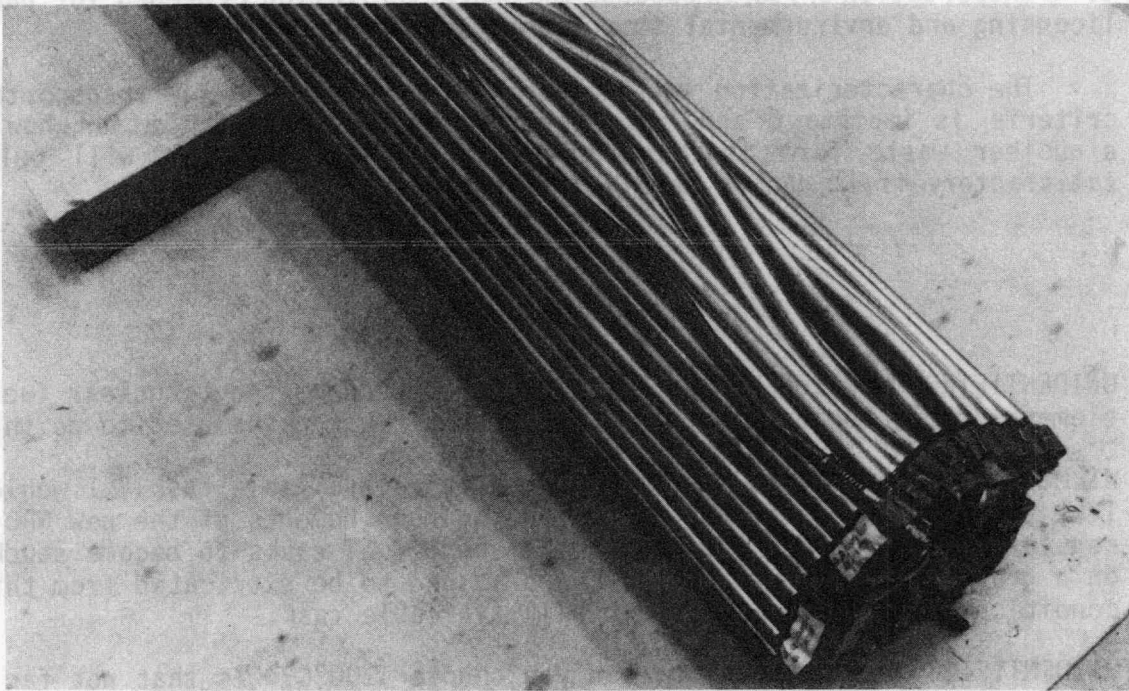


Fig. 8. Unirradiated fuel assembly after impact, out of cask.

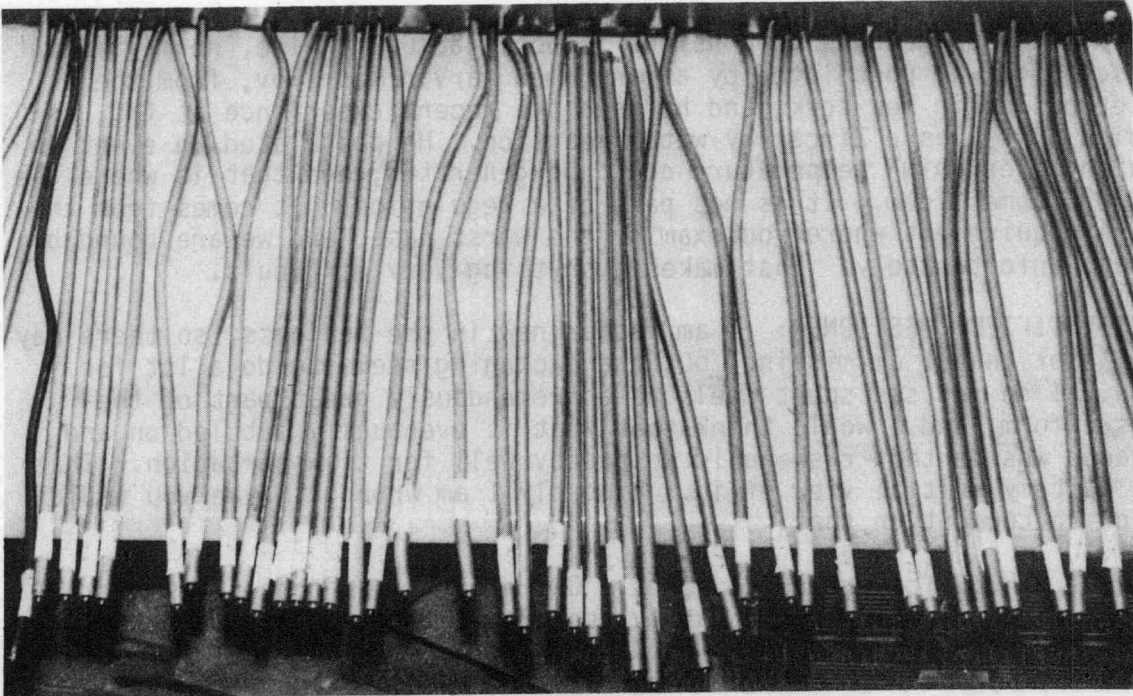


Fig. 9. Fuel assembly disassembled.

to transportation criteria because the characterization is needed for package licensing and environmental impact analyses.

The characterization of nuclear waste form based on transportation criteria is important and should not be overlooked. No matter how well a nuclear waste form is characterized for a repository, it will only be satisfactory if it can be safely transported.

DISCUSSION

UNIDENTIFIED QUESTIONER: Recently DOE shipped some spent nuclear fuel elements from Florida to Nevada. Was one of your casks used to do this?

WILMOT: No, this was a standard commercially available cask. I would like to point out that the strict routing requirements of the new NRC regulations caused the truck with the spent fuel casks to become stuck on a gravel road going up a hill, and it had to be extricated from this condition. But it was a commercially available cask.

UNIDENTIFIED QUESTIONER: Why did you choose 1200°C? Is that not far higher than the temperature that even someone who was trying to stop it could produce?

UNIDENTIFIED QUESTIONER: Is that part of an actual regulation? I have never seen such a high temperature before.

WILMOT: What we have to consider is about a 1000°C fire, normally, but a scenario was postulated by a man named Marvin Resnikov, from the Sierra Club in New York, and he used the recent experience at TMI, in which there was a Zircalloy-water reaction. He postulated an event in which a very high temperature could be generated, and that is where the 1200°C comes from. It is not part of a regulation. It comes from the NEPA requirement where you examine the worst case, and we are bound by that, unfortunately. That makes everything very difficult.

UNIDENTIFIED QUESTIONER: I am rather new in the business, so there may be a lot that I am missing, but the packaging seems to do a lot for you. I do not see spent fuels as a tremendously great part of the waste form, and I would think that what is eventually settled on and placed inside that cask would do pretty well for transportation. That is just my initial view of it. Probably I am wrong. Maybe you would want to comment on that.

WILMOT: No. You are quite right. Our attitude is that it is the package that really is the safety associated with nuclear transport. Unfortunately, when you get into the realm of environmental impact statements, and you start dealing with the public, then you have to be looking at the waste form as well, because they are very concerned that you may generate some powder and somehow it might leak out through a small crack or something. You still have to consider it, unfortunately.

UNIDENTIFIED QUESTIONER: Were you saying that the tests that you show on drop puncture, fire, and submersion are consecutive on the same canister, or parallel?

WILMOT: They are consecutive. It is a sequential test.

SAME QUESTIONER: You truly try? You smash it, then you drop it, then you burn it, and then you drown it?

WILMOT: That is right.

ANGELINI: What temperature for the inside of the cask is specified in the regulation?

WILMOT: That is part of the problem. We have no specification on the inside of the canister. We have a specification on the outside: 800°C. That is part of the licensing requirement on the outside of the cask.

HOWITT: If you ever do another one of those rather spectacular tests, instead of putting stainless steel rods inside you might want to put in strain gauges. You are probably much more interested in the behavior, or the stress conditions, inside the can than in the response of a single material. You may be able to retrieve some of that from your data, because there is a great deal of fracture toughness work that has gone on in stainless steel. I would suggest that you try to relate your work to some of the tabulated mechanical properties of materials, rather than take the approach of expecting people to do mechanical tests on nuclear waste forms.

WILMOT: That is a good suggestion, but the unfortunate problem is that it is difficult to monitor inside the can, simply because any perturbation of the cask itself may result in some sort of failure mechanism that would not be there unless you had perturbed the can. So there is a problem with actually monitoring inside the can.

REFERENCES

1. T. H. Smith and W. A. Ross, Impact Testing of Vitreous Simulated High-Level Waste in Canisters, BNWL-1903, Battelle Memorial Institute, Pacific Northwest Laboratories, Richland, WA, May 1975.
2. W. A. Ross and J. E. Mendel, Annual Report on the Development and Characterization of Solidified Forms for High-Level Wastes, PNL-3060, Battelle Memorial Institute, Pacific Northwest Laboratories, Richland, WA, December 1979.
3. R. M. Jefferson and H. Richard Yoshimura, Crash Testing of Nuclear Fuel Shipping Containers, SAND77-1462, Sandia National Laboratories, Albuquerque, NM, February 1978.

SOL-GEL TECHNOLOGY APPLIED TO ALTERNATIVE
HIGH-LEVEL WASTE FORMS DEVELOPMENT*P. Angelini, D. P. Stinton, J. S. Vavruska†
A. J. Caputo, and W. J. LackeyMetals and Ceramics Division
Oak Ridge National Laboratory
Oak Ridge, Tennessee 37830

Fixation of high-level and transuranium radioactive waste in glass or alternative ceramic forms requires remotely operable processes and equipment, and sol-gel technology developed for reactor fuel refabrication appears applicable.¹ The major steps in a typical (internal gelation) sol-gel process are shown in Fig. 1. Advantages of the sol-gel process are absence of dust, easy pneumatic transfer and sampling of either liquids or free-flowing solid microspheres,² excellent sinterability, and equipment amenable to remote operation because of mechanical simplicity.

Sol-gel processes have previously been applied to preparation of nuclear fuel, spherical catalyst, and structural ceramics. Remotely operable sol-gel processes³ and equipment for fabrication of recycle reactor fuel⁴ have been under development for almost 20 years, and much of this technology is ideally suited for solidification of high-level waste into glass or alternative waste forms.

Sol-gel processes⁵⁻⁷ are being developed for producing glass waste forms and alternative waste forms such as supercalcine⁸ and Synroc.⁹ Microspheres and pellets of various Synroc compositions containing up to 25% simulated defense waste have been prepared by the sol-gel process. Spheres of the Synroc-B waste form have been produced by internal gelation¹⁰ and are shown in Fig. 2. A density¹¹ of up to 95% of theoretical density with 1.3% open porosity has been achieved for these sintered spheres. Dilatometry has shown that most of the densification occurs in the temperature range between 600 and 900°C. This range is 300 to 600°C lower than required for conventionally prepared Synroc-B. Lower sintering temperatures will (1) minimize vaporization during sintering and (2) optimize product throughput. X-ray diffraction has shown that the phases zirconolite ($\text{CaZrTi}_2\text{O}_7$), perovskite (CaTiO_3), and hollandite ($\text{BaAl}_2\text{Ti}_6\text{O}_{16}$) are obtained when sintering is performed in an Ar-4% H_2 atmosphere. Sintering in Ar-4% H_2 saturated with water vapor

*Research sponsored by the Office of Waste Operations and Technology, U.S. Department of Energy, under contract W-7405-eng-26 with Union Carbide Corporation.

†Chemical Technology Division.

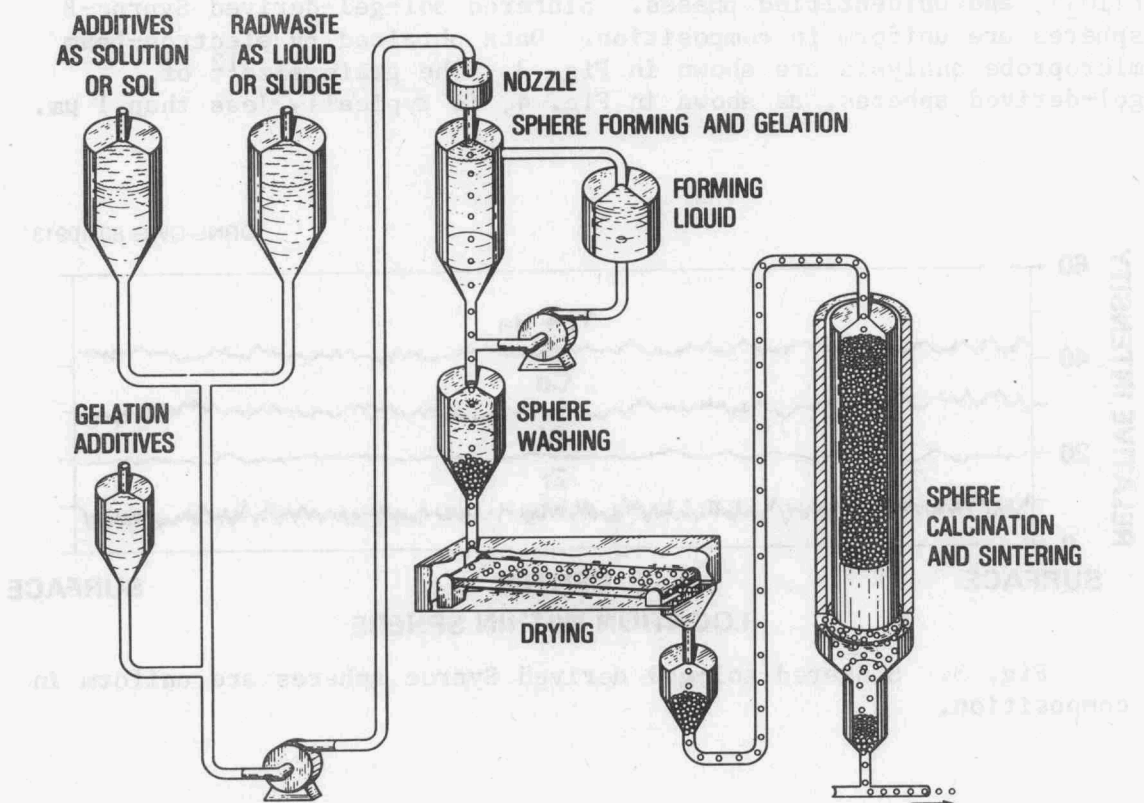
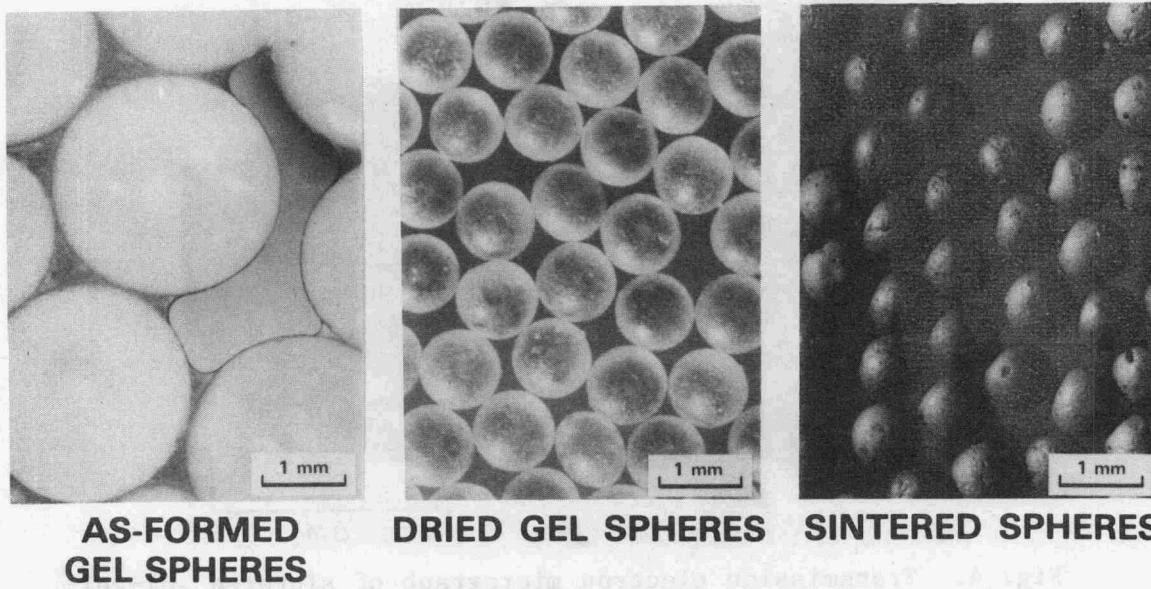


Fig. 1. Sol-gel process flowsheet.

ORNL PHOTO 2758-80



AS-FORMED GEL SPHERES

DRIED GEL SPHERES

SINTERED SPHERES

Fig. 2. Spheres of Synroc-B made by the internal gelation process.

results in a hollandite phase of $\text{BaAl}_2\text{Ti}_5\text{O}_{14}$, zirconolite, rutile (TiO_2), and unidentified phases. Sintered sol-gel-derived Synroc-B spheres are uniform in composition. Data obtained by electron-beam microprobe analysis are shown in Fig. 3. The grain size¹² of gel-derived spheres, as shown in Fig. 4, is typically less than $1\ \mu\text{m}$.

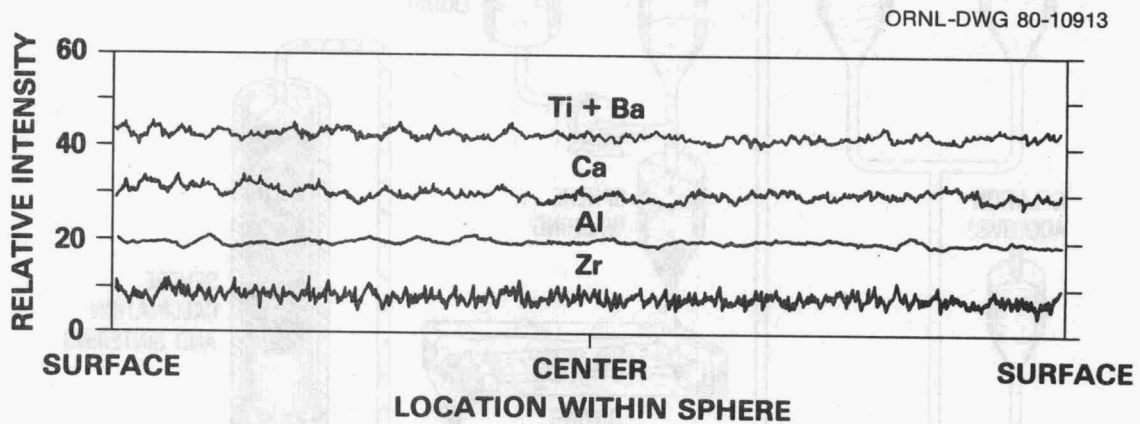


Fig. 3. Sintered sol-gel derived Synroc spheres are uniform in composition.

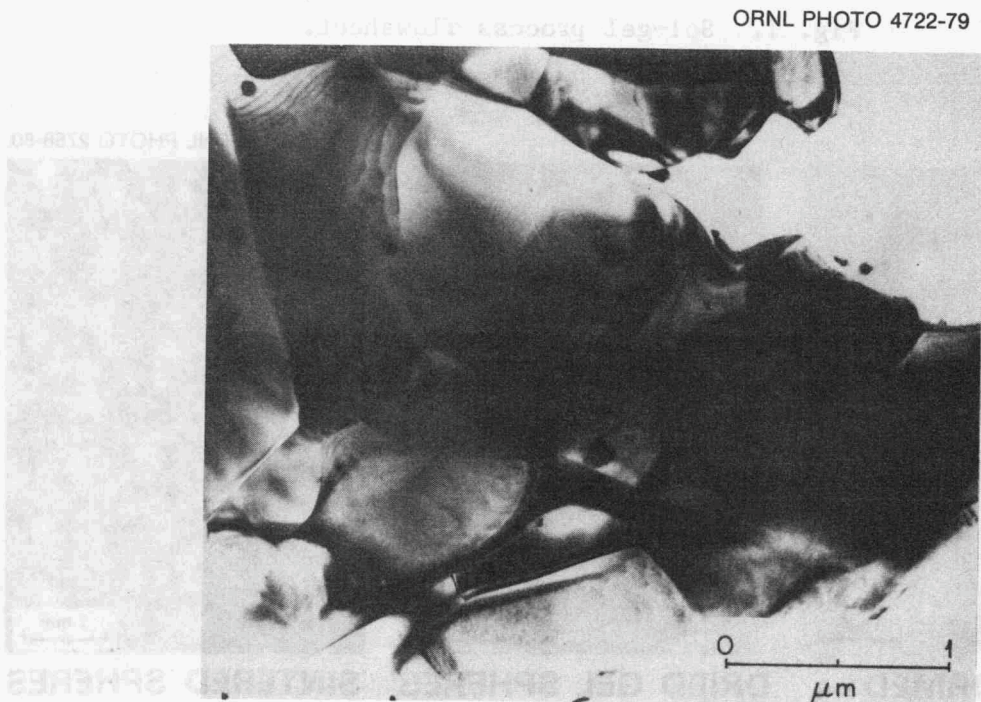


Fig. 4. Transmission electron micrograph of sintered sol-gel-derived Synroc-B. (Grain size is in the vicinity of $1\ \mu\text{m}$.)

These characteristics result in improved mechanical behavior over inhomogeneous large-grained materials. We have produced various physical forms including sintered spheres, sintered pellets, hot-pressed pellets, spheres coated with pyrolytic graphite, and spheres coated with silicon carbide. The partitioning¹³ of the actinides U (natural), ²³⁹Pu, ²⁴¹Am, and ²⁴⁴Cm has been identified in Synroc-B produced from conventional powders and processing. The actinides partitioned mainly into the perovskite (CaTiO₃) phase. They were also found in the zirconolite phase (CaZrTi₂O₇) but to a lesser extent. The actinides were not detected (within background level) in the hollandite (BaAl₂Ti₆O₁₆). Minor amounts of pseudobrookite (Al₂TiO₅) and rutile (TiO₂) phases were found. However, no actinides (within background levels) were detected in these phases.

In summary, sol-gel technology appears applicable to waste solidification. It is attractive for remote operation, and a variety of waste compositions and forms can be produced. Spheres and pellets of gel-derived Synroc waste forms were produced. Spheres of the Synroc-B type were coated with pyrolytic carbon and silicon carbide. Partitioning of actinides in Synroc-B was experimentally determined.

ACKNOWLEDGMENTS

The authors gratefully acknowledge C. E. DeVore, W. H. Elliott, R. Hickey, J. C. McLaughlin, and R. L. White for their technical assistance; A. R. Olsen, T. F. Scanlan, F. J. Homan, W. J. Lackey, R. E. Blanco, and R. G. Donnelly for reviewing the manuscript; S. Peterson for editing the manuscript; and Rhonda Castleberry for preparing the manuscript.

DISCUSSION

HOWITT: The question I have refers to a comment you made very early, in which you noted that the sintering behavior of gel-derived materials was comparable to that of conventionally prepared ceramic powders but that sintering occurred at several hundred degrees lower. Would you amplify on that point?

ANGELINI: In the introduction of this presentation, I referred to our experience in producing reactor fuel spheres and sintered pellets. In those cases, for example, UO₂ spheres could be sintered to nearly theoretical density at 1400°C, ThO₂ produced by the water extraction gelation process has been sintered to nearly theoretical density at 1000°C, and ThO₂ produced by internal gelation has been sintered to nearly theoretical density as pellets or spheres at 1400°C. Our work with waste forms is just beginning, but our dilatometry data indicate that densification is occurring at much lower temperatures than in material produced by conventional ceramic powder processing.

HOWITT: Then the question really is, I suppose, is this for the case of compacted pellets or is it the case for individual spheres? Because if it's the case for individual spheres, it's hardly surprising because you have a very fine particle size.

ANGELINI: The sol-gel process parameters usually depend on whether one produces sintered spheres or pellets. Thus far, in our waste work we have emphasized fabrication of spheres that are suitable for coating. The general shrinkage behavior of spheres and pellets is similar. Thus far, the final density of sintered spheres is greater than the geometric density for sintered pellets.

SHEETZ: You indicated that you put 25 wt % loading of waste into Synroc-B composition. What was the specific waste you put in?

ANGELINI: The waste was simulated Savannah River Plant waste of the composite composition produced by the Southwestern Chemical Company to SRL specifications.

BOATNER: I have one quick question. I think I must have missed something entirely. In one of the slides you showed the gel spheres before sintering and then you showed the spheres after sintering and they seemed to be about the same size. And yet, if I recall correctly, in the graph you showed, the densification of a given sphere seemed like it started out about 30% and went up to 95%. Either I have missed something, or — how does that happen?

ANGELINI: The two main techniques we use for density determination are mercury pycnometry and dilatometry. The slide you refer to is a macrograph showing as-gelled spheres, dried spheres, and sintered spheres. There is a large size reduction upon drying of the gelled spheres. A smaller size reduction takes place upon sintering of dried spheres. Since the final density varies as the inverse of the cube of the diameter, it is difficult to judge density from the photograph.

REFERENCES

1. P. A. Haas, J. M. Begovich, A. D. Ryon, and J. S. Vavruska, Chemical Flowsheet Conditions for Preparing Urania Spheres by Internal Gelation, ORNL/TM-6850 (July 1979).
2. J. E. Mack, R. R. Suchomel, and P. Angelini, Development of Nuclear Fuel Microsphere Handling Techniques and Equipment, ORNL/TM-7143 (January 1980).
3. W. J. Lackey and J. E. Selle, comps., Assessment of Gel-Sphere-Pac Fuel for Fast Breeder Reactors, ORNL-5468 (October 1978).

4. D. P. Stinton and W. J. Lackey, Influence of Process Variables on Permeability and Anisotropy of Biso-Coated HTGR Fuel Particles, ORNL/TM-6087 (November 1977).
5. W. J. Lackey, R. E. Blanco, and A. L. Lotts, "Application of Sol-Gel Technology to Fixation of Nuclear Reactor Waste," Nucl. Technol. 49: 321-24 (July 1980).
6. W. J. Lackey, P. Angelini, F. L. Layton, D. P. Stinton, and J. S. Vavruska, pp. 392-417 in "Sol-Gel Technology Applied to Glass and Crystalline Ceramics," Waste Management '80, Vol. 2, R. G. Post, ed., The University of Arizona, Tucson, 1980.
7. A. M. Platt and J. L. McElory, Management of High-Level Nuclear Wastes, PNL-SA-7072 (December 1978).
8. G. J. McCarthy, "High-Level Waste Ceramics: Materials Considerations, Process Simulation and Product Characterization," Nucl. Technol. 32: 92-105 (1977).
9. A. E. Ringwood, S. E. Kesson, N. G. Ware, W. O. Hibberson, and A. Major, "The Synroc Process. A Geochemical Approach to Nuclear Waste Immobilization," Geochem. J. 13(4): 141-65 (August 1979).
10. J. S. Vavruska, "Gel-Sphere Technology Applied to Synroc Waste Forms," Bull. Am. Ceram. Soc. 59(3): 394 (March 1980).
11. D. P. Stinton, J. S. Vavruska, P. Angelini, and W. J. Lackey, "Sintering Behavior and Characterization of Sol-Gel-Produced Synroc," Bull. Am. Ceram. Soc. 59(3): 394 (March 1980).
12. P. Angelini, R. W. Carpenter, and D. P. Stinton, "High Resolution Analytical Electron Microscopy Analysis of Synroc Nuclear Waste Storage Material," Bull. Am. Ceram. Soc. 58(9): 888 (September 1979).
13. P. Angelini, D. P. Stinton, R. W. Carpenter, J. S. Vavruska, and W. J. Lackey, "Phase Identification and Partitioning of Elements in Sol-Gel-Derived Synroc," Bull. Am. Ceram. Soc. 59(3): 394 (March 1980).

CHEMICALLY VAPOR DEPOSITED COATINGS FOR MULTIBARRIER
CONTAINMENT OF NUCLEAR WASTES*

J. M. Rusin and J. W. Shade

Pacific Northwest Laboratory
Richland, Washington 99352

and

R. W. Kidd and M. F. Browning
Battelle, Columbus Laboratories
Columbus, Ohio 43201

ABSTRACT

The Alternative Waste Forms Program conducted by the Pacific Northwest Laboratory (PNL) for the Department of Energy has as one of its objectives the development of coated waste forms. The coated particle may, upon subsequent encapsulation, become part of the multibarrier concept. The multibarrier concept aims to separate the radionuclide-containing inner core material and the environment by the use of coatings and metal matrices.

Chemical vapor deposition (CVD) was selected as a feasible method to coat ceramic cores, since the technology has previously been demonstrated for high-temperature gas-cooled reactor (HTGR) fuel particles. CVD coatings, including SiC, PyC (pyrolytic carbon), SiO₂, and Al₂O₃ were studied. This paper will discuss the development and characterization of PyC and Al₂O₃ CVD coatings on supercalcine cores.

Supercalcine is a crystalline assemblage of solid solution phases, made by modifying the composition of high-level liquid waste with selected additives prior to calcining. Two formulations, which were developed for a simulated PW-7 commercial waste, were studied: SPC-2 and SPC-4. Pellets of calcined material were formed by disc pelletization and sintered between 1100 and 1200°C for consolidation and crystal formation.

Coatings were applied to ~2 mm particles in either fluidized or vibrating beds. The PyC coating was deposited in a fluidized bed with ZrO₂ diluent from C₂H₂ at temperatures between 1100 and 1200°C. The Al₂O₃ coatings were deposited in a vibrated bed by a two-stage process to minimize loss of PyC during the overcoating operation. This process involved

*Work Supported by the U.S. Department of Energy under Contract DE-AC06-76RLO 1830.

applying $\sim 10 \mu\text{m}$ of Al_2O_3 using water vapor hydrolysis of AlCl_3 and then switching to the more surface-controlled hydrolysis via the $\text{H}_2 + \text{CO}_2$ reaction ($3\text{CO}_2 + 3\text{H}_2 + 2\text{AlCl}_3 = \text{Al}_2\text{O}_3 + 6\text{HCl} + 3\text{CO}$).² Typically, 50 to $80^2 \mu\text{m}$ Al_2O_3 coatings were applied over 30 to 40 μm PyC coatings.

The coatings were evaluated by metallographic examination, PyC oxidation tests, and leach resistance. After air oxidation for ~ 100 hours at 750°C , the duplex PyC/ Al_2O_3 coated particles exhibited a weight loss of 0.01 percent. Leach resistance is being determined for temperatures from 50 to 150°C in various solutions. Typical results are given for selected ions. The leach resistance of supercalcine cores is significantly improved by the application of PyC and/or Al_2O_3 coatings.

Present studies involve the development of low-temperature PyC coatings by the use of catalysts such as $\text{Ni}(\text{CO})_4$ and $\text{Co}(\text{AcAc})_2$. Coating temperatures of $\sim 500^\circ\text{C}$ which would reduce process complexity and allow for coatings of glass marbles are feasible.

Three areas of coating technology are discussed in this paper: First, the preliminary coating survey that was conducted on applying coatings to simulated waste particles; second, more detailed work on the duplex pyrolytic carbon/alumina (PyC/ Al_2O_3) coating applied by chemical vapor deposition (CVD); and third, some new work being conducted on lowering the temperature of the PyC deposition by CVD.

Preliminary Coating Survey

Coated particles are part of a multibarrier concept, initiated at PNL in 1973, for the isolation of high-level nuclear waste.¹ As shown in Figure 1, this concept provides barriers by coatings or matrices, or both, and a canister between the waste form and the environment. The inner waste form core might be ceramic (which includes calcine), glass ceramic, or glass beads. The coating would provide improved leach resistance, mechanical strength, and oxidation resistance. The matrix material may consist of metal alloys, ceramics, graphite, or even glass. The matrix provides an addition leach resistant barrier and may offer improved thermal conductivity and mechanical strength.

In the preliminary coating survey, which was conducted from 1973 to 1975, three sites were involved: General Atomic Company (GAC), Oak Ridge National Laboratory (ORNL), and Battelle Columbus Laboratories (BCL). The chemical vapor deposition, in fluidized beds, of PyC and PyC/SiC coatings on simulated nuclear waste was evaluated. In Figure 2, the micrograph on the left shows a PyC/SiC coating applied at GAC. The core is a fluidized-bed particle of aluminum oxide with simulated

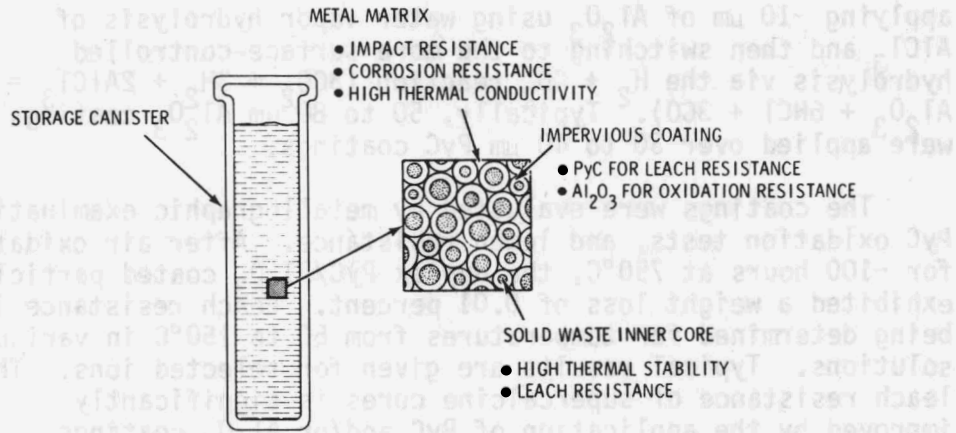


Fig. 1. Multibarrier Concept for Isolating High Level Nuclear Waste.

PyC/SiC ON FLUIDIZED BED SIMULATED WASTE PARTICLES

PyC ON SIMULATED WASTE PARTICLES

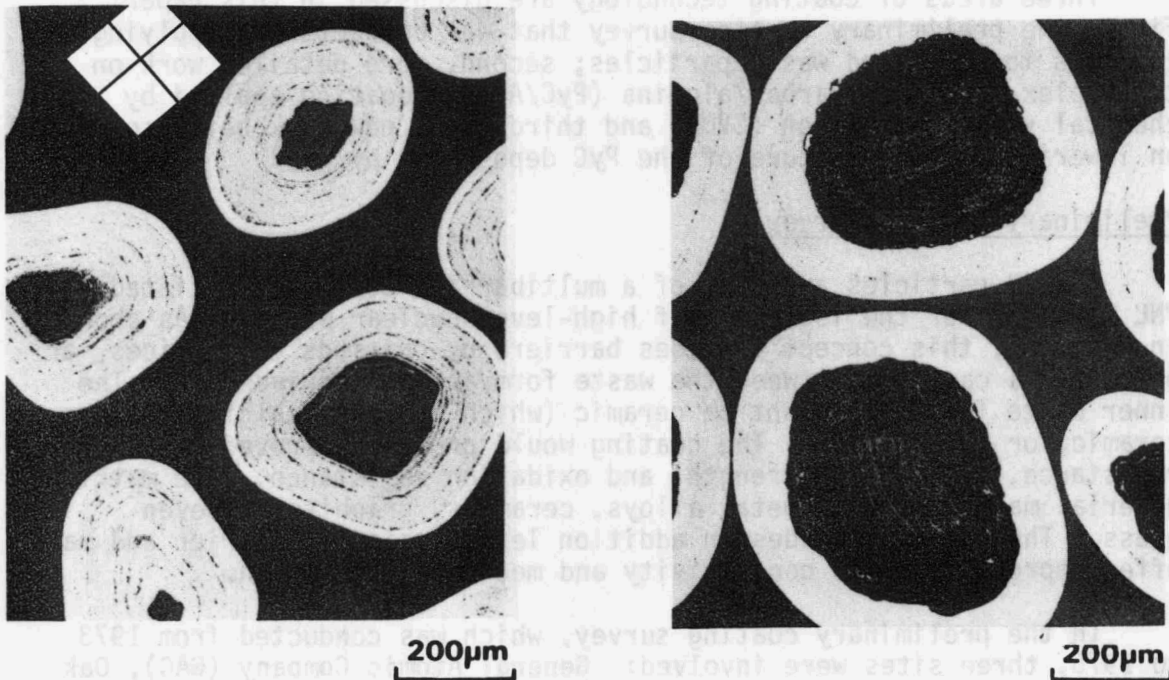


Fig. 2. PyC/SiC and PyC CVD Coated Simulated Nuclear Waste Particles.

waste around it. This was back at the time when the Idaho National Laboratory was producing a fluidized bed material that would be coated with simulated waste. The micrograph on the right shows a PyC coating applied on a calcine particle at ORNL. The thickness of these two coatings ranged from 80 to 100 μm .

At BCL, several single-layer coatings in addition to PyC and SiC were investigated as shown in Table 1, which also lists the reactants and deposition temperatures. Duplex coatings were also investigated at Battelle Columbus. For each of these, the first coating and the overcoating are given in Table 2. Reactants and temperatures are the same as those in Table 1. All of this BCL work was conducted on fluidized-bed particles in the 200 μm range. Two of the BCL coatings are shown in Figures 3 and 4. Figure 3 shows an example of a 4 μm coating of Mo/MoC on an alumina substrate with the simulated waste. Figure 4 shows a duplex coating, initially 4 μm of nickel with an overcoating of 4 μm of Cr_7C_3 . The initial Ni coating was required because the Cr_7C_3 actually reacted with the simulated waste. In addition to CVD coating, plasma spraying was investigated at PNL using Ni/Cr, Al_2O_3 , and Cr_7C_3 coatings.

Table 1. Coatings Applied in a Fluidized Bed to Particles in the 200 μm Range

Coating	Reactants	Deposition Temperature, $^{\circ}\text{C}$
Ni	$\text{Ni}(\text{CO})_4$	170 to 230
Mo/MoC	$\text{Mo}(\text{CO})_6$	350 to 450
C	C_2H_2	800 to 950
Fe	$\text{Fe}(\text{CO})_5$	180 to 200
Si	$\text{SiHCl}_3 + \text{H}_2$	500 to 800
Cr_7C_3	$\text{Cr}(\text{C}_9\text{H}_{12})_2$	500
SiC	$\text{CH}_3\text{SiCl}_3 + \text{H}_2$	1100
Cr_2O_3	$\text{CrO}_2\text{Cl}_2 + \text{H}_2\text{O} + \text{H}_2$	550 to 650
SiO_2	$\text{SiCl}_4 + \text{H}_2\text{O} + \text{H}_2$	700 to 800
Al_2O_3	$\text{AlCl}_3 + \text{H}_2\text{O} + \text{H}_2$	600 to 900

Duplex PyC/ Al_2O_3 Coating

From this initial work, it was decided to pursue Al_2O_3 and PyC coatings. This decision was mainly based upon temperature requirements for the waste form. The 1000 $^{\circ}\text{C}$ temperature specified for fire conditions

Table 2. Duplex Coatings Applied in a Fluidized Bed to Particles in the 200 μm Range

First Coating	Overcoat
Ni	Cr_7C_3
Cr_7C_3	Ni
Al_2O_3	C
Fe	Al_2O_3
Ni	Si
C	SiC
C	Al_2O_3

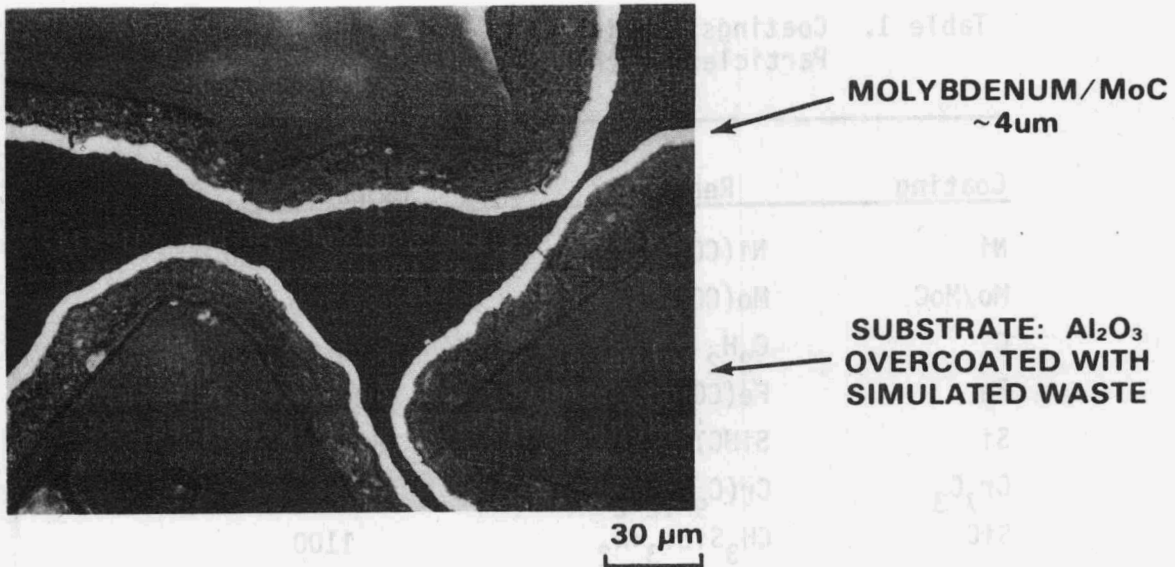


Fig. 3. Molybdenum/MoC CVD Coated Simulated Nuclear Waste Particles.

eliminated many of the coatings that had been investigated. The PyC coating was selected due to its high leach resistance, but PyC will oxidize at the 1000°C temperature. Thus, an overcoat was required for oxidation protection. Candidate overcoat materials were Al_2O_3 , SiO_2 , and SiC. Alumina was selected due to the fact that the leach resistance of Al_2O_3 is higher than that of SiO_2 , and that SiC requires deposition temperatures of 1400°C, which were too high for desired processing conditions.

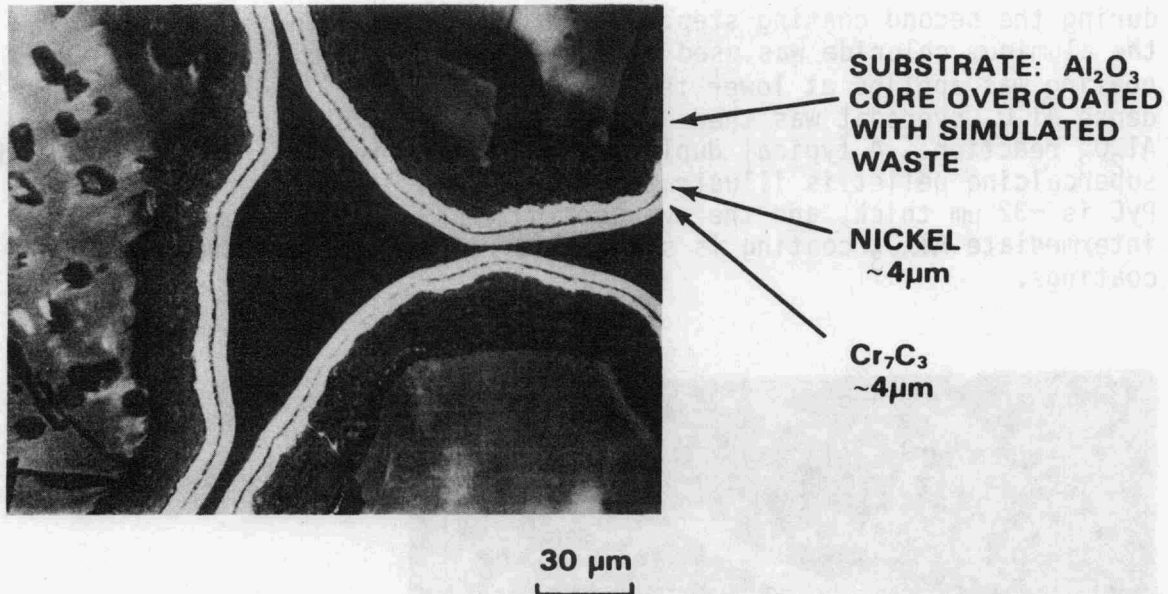


Fig. 4. Ni/Cr₇C₃ Duplex CVD Coated Simulated Nuclear Waste Particles.

The conditions for deposition of PyC and Al₂O₃ on supercalcine are given in Table 3. The PyC coating is applied in a fluidized bed with zirconia (400-700 µm) as a diluent. This technique can handle from 1 to 5 mm diameter. The diluent enables one to use larger diameter particles than normally utilized in a fluidized bed. The reactant was acetylene (C₂H₂) and deposition temperatures ranged from 1100 to 1200°C. Single alumina coatings (not duplex) were applied in a vibrated bed instead of a fluidized bed. Because of different gas nucleation properties, the technique used for PyC coating was not applicable for the particle size range used. Reactants for single Al₂O₃ coatings were aluminum chloride, carbon dioxide, and hydrogen (hydrolysis of AlCl₃ by CO₂ + H₂). Deposition temperatures ranged from 1000 to 1100°C.

With duplex coating the CO₂ from the alumina reaction actually was oxidizing as compared with the PyC, so the CO₂ would react with the PyC

Table 3. Conditions for PyC and Al₂O₃ Coating of Supercalcine

Coating	Core Diameter	Reactor	Temperature	Reactants	Coating Rate
PyC	1-5 mm	Fluidized Bed (ZrO ₂ diluent)	1100° to 1200°C	C ₂ H ₂	1-3 µm/min
Al ₂ O ₃	1-2 mm	Vibrated Bed	1000° to 1100°C	Al+HCl+CO ₂ +H ₂	4 µm/hr
Al ₂ O ₃	3-5 mm	Drum Coater	1100°C	Al+HCl+CO ₂ +H ₂	NA**
Al ₂ O ₃ *	1-2 mm	Vibrated Bed	550° to 1050°C	Al+HCl+H ₂ O	NA

*Applied as intermediate coating between PyC and dense Al₂O₃ duplex coating.

**Not Available

during the second coating step. Therefore, water vapor hydrolysis of the aluminum chloride was used as an intermediate coating step. This coating was applied at lower temperatures of 550 to 1050°C. The final dense Al_2O_3 overcoat was then applied using the previously described Al_2O_3 reaction. A typical duplex PyC/ Al_2O_3 coating on a disc-pelletized supercalcine pellet is illustrated in Figure 5. The inner coating of PyC is $\sim 32 \mu\text{m}$ thick, and the overcoating of Al_2O_3 is $\sim 50 \mu\text{m}$ thick. The intermediate Al_2O_3 coating is shown as a reaction zone between the two coatings.

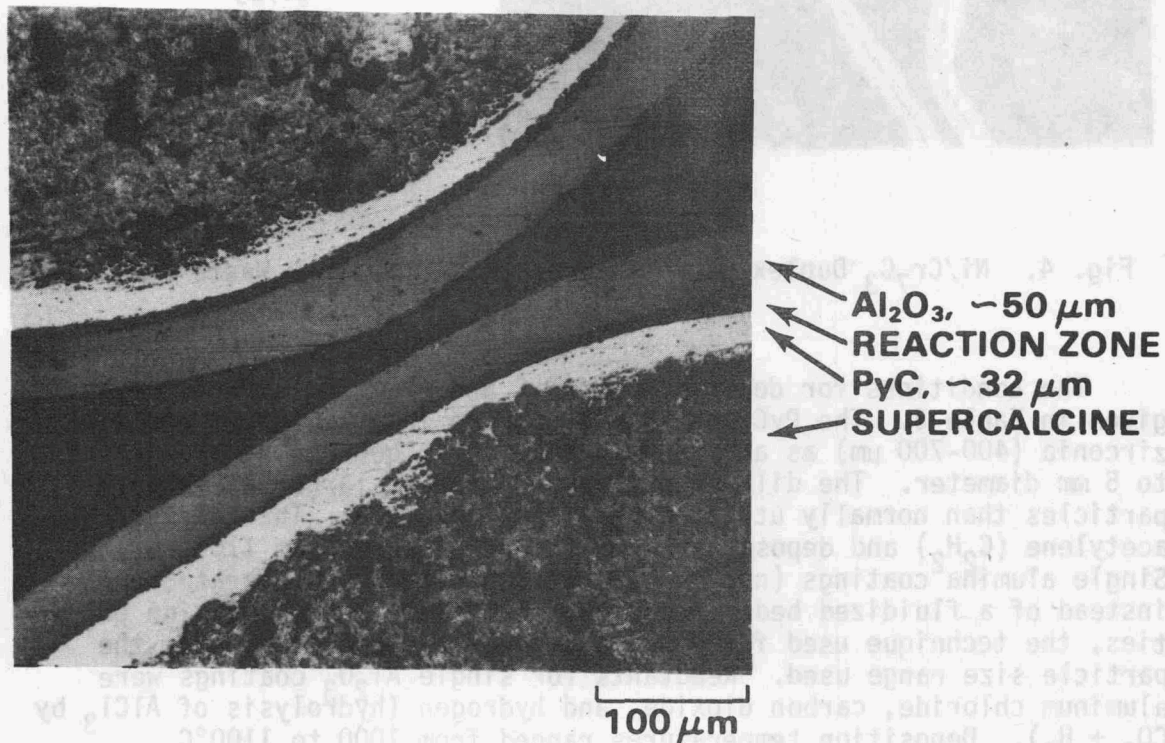


Fig. 5. PyC/ Al_2O_3 Duplex CVD Coated Supercalcine.

The three types of equipment for CVD as listed in Table 3 are shown in Figures 6, 7, and 8. A schematic of a 25 mm ID quartz tube fluidized-bed coater is shown in Figure 6. Particles are fluidized by the reactant and dilutant gases. In the vibrated bed (Figure 7), the process is similar to that of the fluidized bed; the only difference is that the reactor is vibrated mechanically instead of agitated by fluidization. The rest of this equipment (which was omitted for simplicity in Figure 6), shows the complexity of the process. A gas supply and an offgas system are required. For aluminum oxide deposition, a scrubber is required for removal of hydrochloric acid, a process by-product.

For larger particles, a drum coater (Figure 8) was used. It consisted of a glass tube that is rotated to agitate the particles.

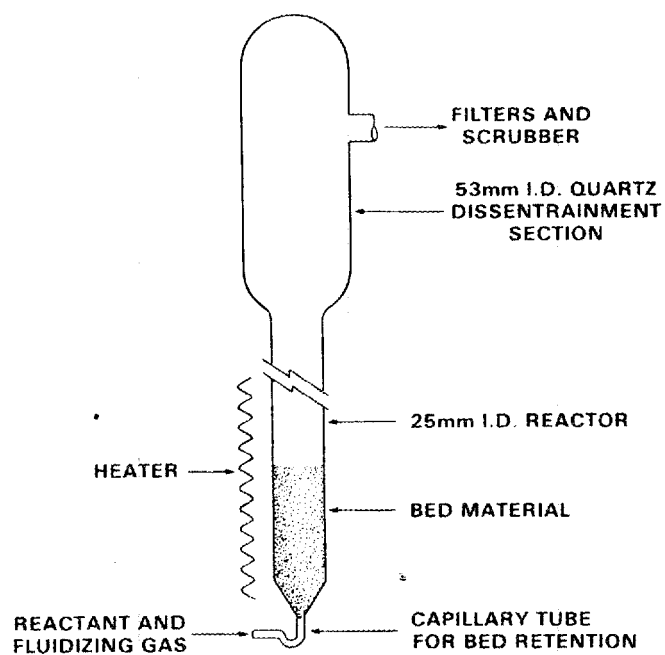


Fig. 6. Schematic Diagram of the Fluidized Bed CVD Process.

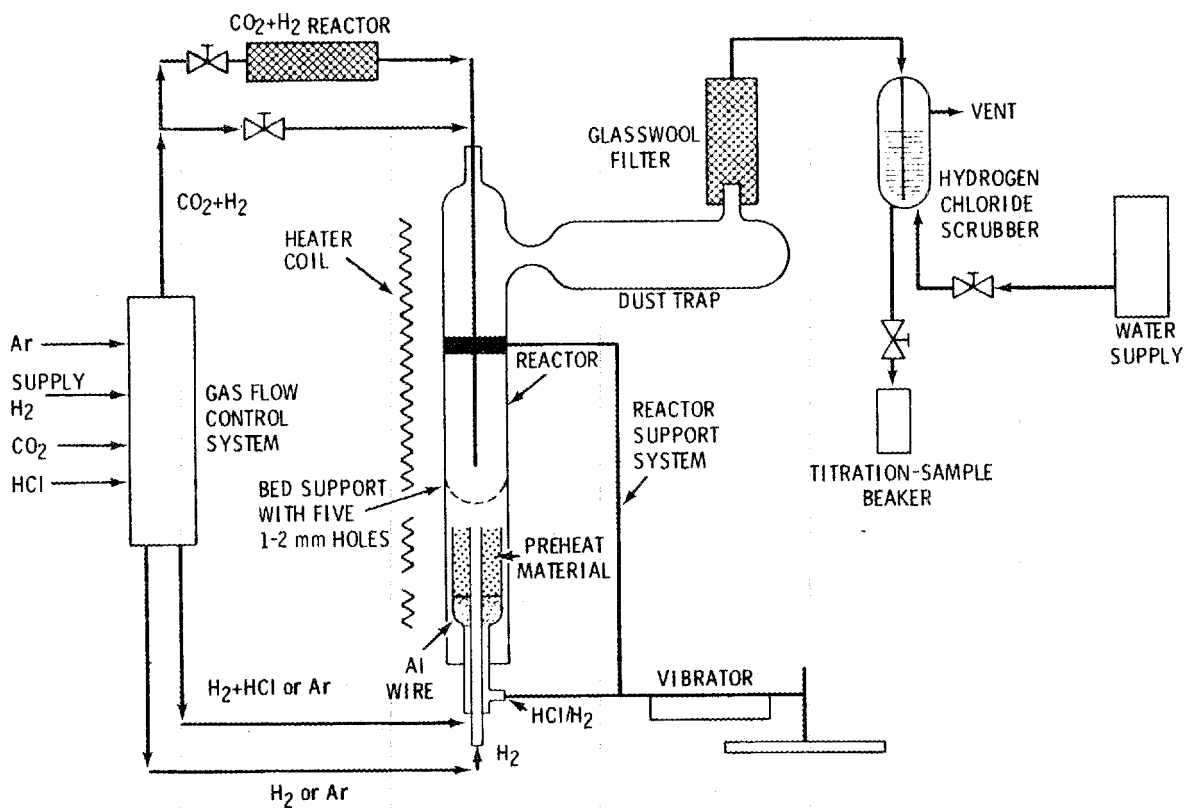


Fig. 7. Schematic of the Vibrating Bed CVD Process.

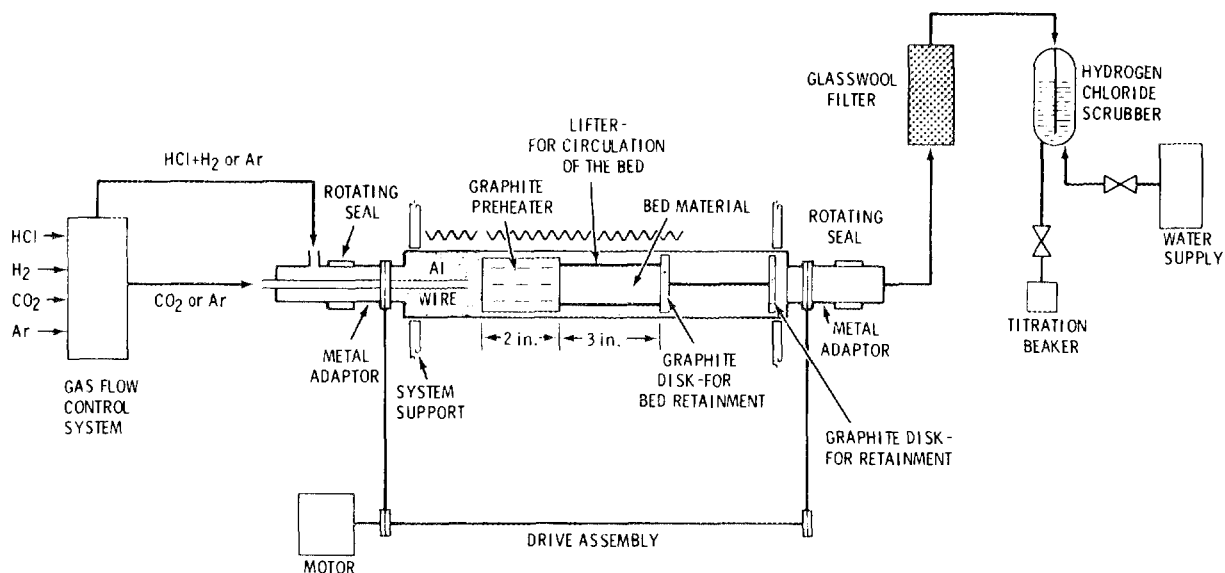


Fig. 8. Schematic of the Rotating Chamber (Drum) Coating CVD Process.

Presently, a screw-agitated bed, which is a vertical tube containing an auger to agitate the particles, is being developed. Coated particles up to 15 mm have been produced in this system.

Coating Characterization

For initial characterization of the CVD coatings, a fairly simple scoping test was used. The duplex coatings were simply heated to 750°C; if there is not a good alumina coating, the PyC will oxidize. A 2 0.01 percent weight loss was observed after 100 hours of heat treatment.

The definitive characterization tests are those that measure the leach resistance of the coatings. Graphite was selected as a coating due to its high leach resistance. The oxidation (reaction rate) of graphite in deionized water and air is shown in Figure 9. Powdered graphite with a surface area of 5.4 m²/g was used to obtain sufficient material for analysis. Even with the high surface area, temperatures of 200°C and higher were required. Extrapolation to the region of 100°C gives a weight loss of 10⁻¹⁰ to 10⁻¹¹ g/cm²·d. This translates into the equivalent that a 40 μm coating on a pellet would last a million years under these conditions, if there were no defects in the coating.

The oxidation tests for graphite powder in water illustrate the potential leach resistance of PyC coatings. However, due to process conditions, PyC CVD coatings may differ in leach resistance as compared to graphite powders. In Table 4, the results are shown for the release of selected elements from uncoated and coated supercalcin pellets which have been leached at 90°C for 28 days in deionized water and 0.5 molar NaCl solution. The results are indicated in normalized elemental

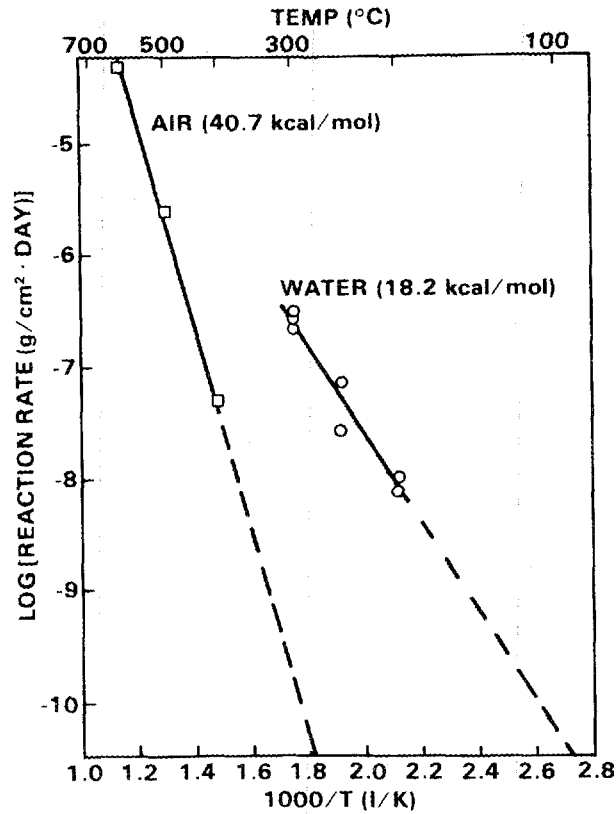


Fig. 9. Reaction Rate of Powdered Graphite in Air and in Water.

Table 4. Leach Resistance of Coated Supercalcine (a)

Core	Coating	Normalized Elemental Loss, g/m ²											
		Si		Ba		Ca		Mo		Sr		Cs	
		DIW	NaCl (b)	DIW	NaCl	DIW	NaCl	DIW	NaCl	DIW	NaCl	DIW	NaCl
SPC-2	None	6.0	6.1	24	33	2.2	3.9	17	20	20	24	3.1	0.9
SPC-2	PyC	0.04	0.14	0.3	0.4	0.3	1.7	0	0.2	0.9	1.0	3.8	1.9
SPC-4	None	6.0	5.5	6.9	18	1.7	5.9	8.9	14	6.0	9.9	4.8	1.2
SPC-4	Al ₂ O ₃	0.09	0.18	0.05	0.05	0.7	3.7	0.02	0.12	0.005	0.05	0.28	0.31
SPC-4	PyC/Al ₂ O ₃	0.09	0.17	0.01	0.05	0.7	4.4	0	0.2	0.01	0.15	0.12	0.28

(a) 90°C-28 days, SA/SV = 10 m⁻¹

(b) 0.5M NaCl

loss, g/m², using geometric surface area. For comparison, a unit of 1.0 g/m² is equivalent to ~3 g/cm²·d. As can be seen by comparison of the uncoated and PyC coated SPC-2 pellets, there is an improvement of 1 to 2 orders of magnitude in leach resistance for the coated waste form except in the case of Cs. Cesium leachability has increased upon coating with PyC. Alumina and PyC/Al₂O₃ coatings on SPC-4 (similar to SPC-2 in formulation) both improve the leach resistance for all elements

detected. Similar results were obtained for samples leached at 50°C for 14 days. The best leach resistance obtained for any element was 1.5×10^{-7} g/cm²·d which is 3 to 4 orders of magnitude below the observed potential for graphite powders.

McCarthy et al⁴ have conducted hydrothermal tests at 400°C on uncoated and PyC/Al₂O₃ duplex coated supercalcine. For duplex-coated supercalcine they show that in both brine and deionized water there was no detectable Cs or Rb in solution. Results for PyC coated supercalcine were not reported.

The increase of Cs leachability for PyC coatings can be explained if one considers the volatility of cesium from supercalcine during the coating process. By energy dispersive x-ray analysis, EDAX, Cs was detected in the PyC coating. The volatility of Cs from supercalcine after 4 hr in dry air at 1200°C ranges from 4 to 11 wt%.⁵ Typical PyC coating temperatures are 1200°C and ~1 hr is required for a 60 μm coating. SEM micrographs of PyC coatings before and after leaching at 90°C show evidence of surface defects or reactions for the leached PyC sample (Figure 10). Thus, in addition to volatile Cs being trapped in the coating, other processing defects may have an influence on the leach resistance of PyC coatings.

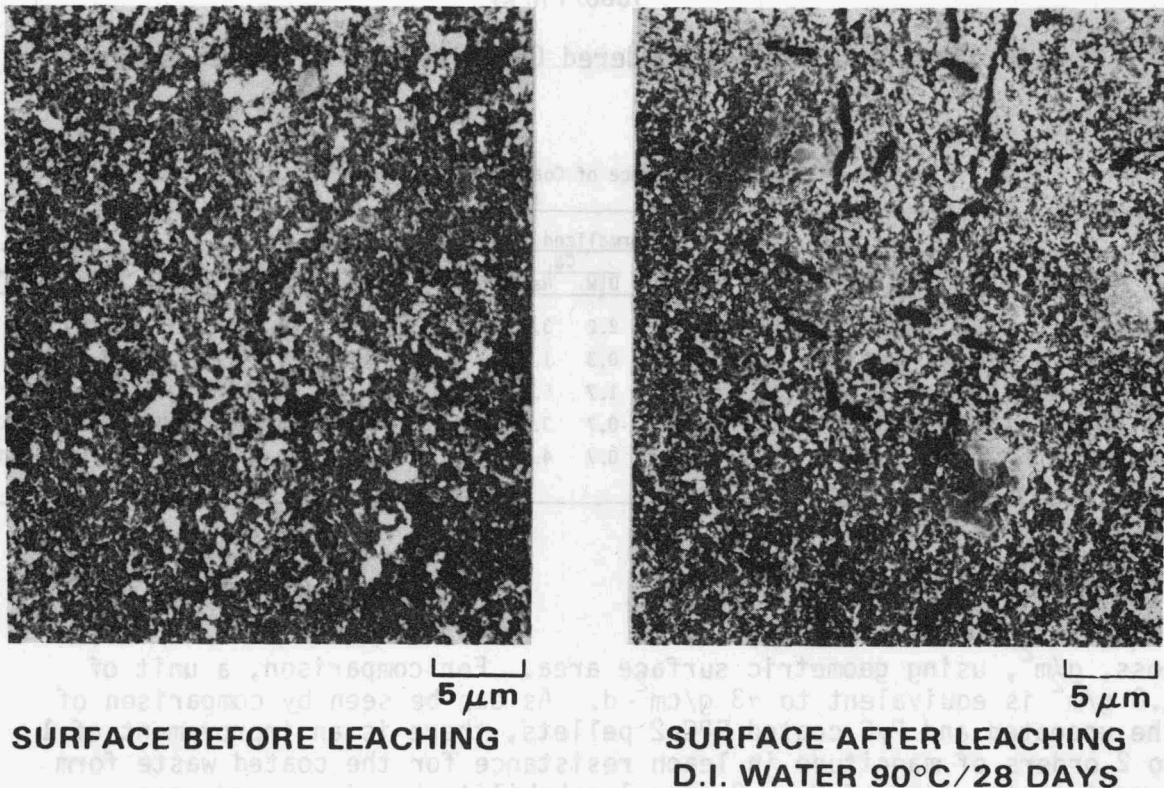


Fig. 10. PyC CVD Coated Supercalcine Before and After Leach Testing.

Cesium was not detected in the single Al_2O_3 coating. This could be due to lower deposition temperatures and different atmospheric conditions. In the case of the duplex $\text{PyC}/\text{Al}_2\text{O}_3$ coating, the Al_2O_3 provided a barrier over the Cs contaminated PyC coating.

Low-Temperature PyC Coating

Because of the volatility of Cs at higher temperatures, low-temperature PyC CVD coating is being pursued. The concept was first demonstrated for nuclear waste immobilization by Neumann.⁶ Nickel tetracarbonyl, $\text{Ni}(\text{CO})_4$, was used to catalyze the decomposition of acetylene, C_2H_2 , at reduced temperatures of 450°C . An example of 6 mm borosilicate glass spheres coated by Neumann are shown in Figure 11. Studies at PNL and BCL have found that optimum coatings are produced from a gas mixture containing ~1.5 m/o C_2H_2 , ~0.006 m/o, $\text{Ni}(\text{CO})_4$ and the balance H_2 . A micrograph of a ceramic substrate coated with PyC at 445°C is shown in Figure 12. Coating rates are $6 \mu\text{m}/\text{hr}$ in fluidized bed CVD coating and 1 to $2 \mu\text{m}/\text{hr}$ in the screw-agitated coater.

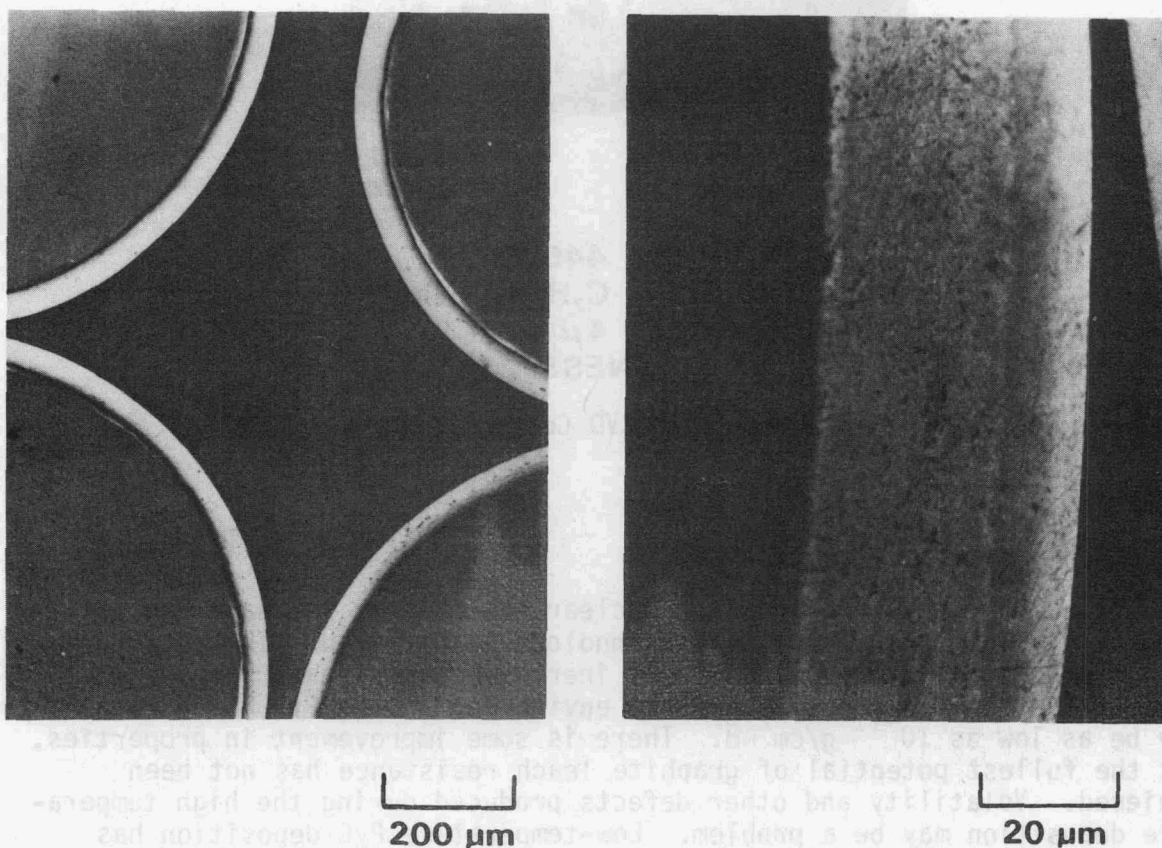
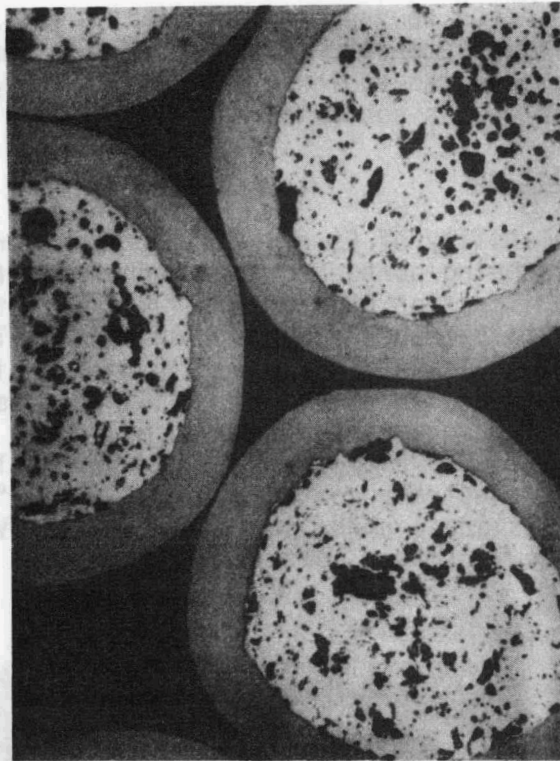


Fig. 11. Low-Temperature PyC CVD Coated Glass Beads.



┌──┐
20um

TEMPERATURE: 445°C
REACTANTS: C₂H₂, H₂, Ni(CO)₄
COATING RATE: 4 μm/hr
COATING THICKNESS: 16 μm

Fig. 12. Low-Temperature PyC CVD Coated Ceramic Substrates.

Summary

In summary, PyC coatings for nuclear waste forms increase process complexity, but established HTGR technology is utilized. The coatings have the potential to provide a very inert leach-resistant barrier between the inner waste form and the environment. The PyC leach rate may be as low as 10^{-11} g/cm²·d. There is some improvement in properties, but the fullest potential of graphite leach resistance has not been achieved. Volatility and other defects produced during the high temperature deposition may be a problem. Low-temperature PyC deposition has been demonstrated but further development is required. Coatings of PyC, Al₂O₃, and PyC/Al₂O₃ have been demonstrated on a laboratory-scale basis for both ceramic pellets and glass beads.

DISCUSSION

Barry Scheetz: To reiterate the statement that John made about the Cincinnati meeting, the solution analyses in both deionized water and the bittern brines up to 400°C did not show any detectable cations in solution, down to the resolution of the atomic emission spectrometer that we were using.

John Rusin: I think, as I said, that we really are looking at a process problem here in the deposition of the PyC, due to the volatility of the components.

REFERENCES

1. J. M. Rusin, R. O. Lokken, J. M. Lukacs, K. R. Sump, M. F. Browning, and G. M. McCarthy, Multibarrier Waste Forms Part I: Development, PNL-2668-1, Pacific Northwest Laboratory, Richland, WA 99352, September 1978.
2. R. W. Kidd, M. F. Browning, and J. M. Rusin, "Chemical Vapor Deposited Coatings for Multibarrier Containment of Nuclear Waste," Proceedings of the Seventh International Conference on Chemical Vapor Deposition, 1979, Los Angeles, CA, October 1979.
3. W. J. Gray, "Reaction of Graphite with Water and its Implications for Radioactive Waste Storage," Radioactive Waste Management, Vol. 1 (1), May 1980, pp. 105-109.
4. G. J. McCarthy, W. B. White, S. Komarneni, B. E. Scheetz, W. P. Freeborn, and D. K. Smith, "Hydrothermal Stability of Spent Fuel and High-Level Waste Ceramics in the Geologic Repository Environment," Ceramics in Nuclear Waste Management, Cincinnati, OH, CONF-790420, April 1979.
5. J. M. Rusin, W. J. Gray, and J. W. Wald, Multibarrier Waste Forms Part II: Characterization and Evaluation, PNL-2668-2, Pacific Northwest Laboratory, Richland, WA 99352, August 1979.
6. W. Neumann and O. Kofler, "Coating of Waste Containing Ceramic Granules," Ceramics in Nuclear Waste Management, Cincinnati, OH, CONF-790420, April 1979.

A REVIEW OF THE SORPTION OF ACTINIDES
ON NATURAL MINERALS

G. W. Beall

Radian Corporation
8500 Shoal Creek Boulevard
Austin, Texas 78766

ABSTRACT

Over the past few years, a large body of data concerning sorption of actinides on geologic media has been built in connection with high-level-waste disposal. The primary aim of the work has been to allow predictions of the migration behavior of these radionuclides in the case of a breach of the repository that allowed groundwater flow through the repository. As a result of this work, some new backfill materials specifically tailored for the actinides have also been designed.

Several major mechanisms of sorption that appear to dominate the sorption of actinides have emerged from these studies. These mechanisms can be divided into solution reactions dominated by hydrolysis, chemisorption reactions, and oxidation-reduction reactions. Each of these mechanisms will be discussed in detail, with experimental examples. Surprisingly, one mechanism, cation exchange, does not play an important role; why it fails to operate in any significant way in the environmental pH region will be discussed.

The implications of the sorption mechanisms for waste forms and backfill materials will be discussed in detail. These discussions will center primarily around the valence state of the actinide in various waste forms and the effect of various anions on leachability from waste forms and backfill materials.

In the first part of my talk, I would like to spend some time identifying some of the principal mechanisms that are important in natural systems for the sorption of the actinides on various geologic media. Later in the talk I would like to slant the discussion toward how these mechanisms can be used to design backfill materials or to choose a rock formation that would be ideal for the site of a repository. The discussion will center primarily around the actinides. The importance of the actinides in the long-term decay of radioactive waste is illustrated in Figure 1. The talk will include some information about technetium, but primarily it will be concerned with the actinides, mainly americium, neptunium, and plutonium, with a brief discussion of technetium.

I will try to discuss four major mechanisms of sorption that appear to be operating in natural systems. The discussions of the first three will include primarily data that has been obtained on pure mineral systems with batch equilibration methods. The discussion of the last

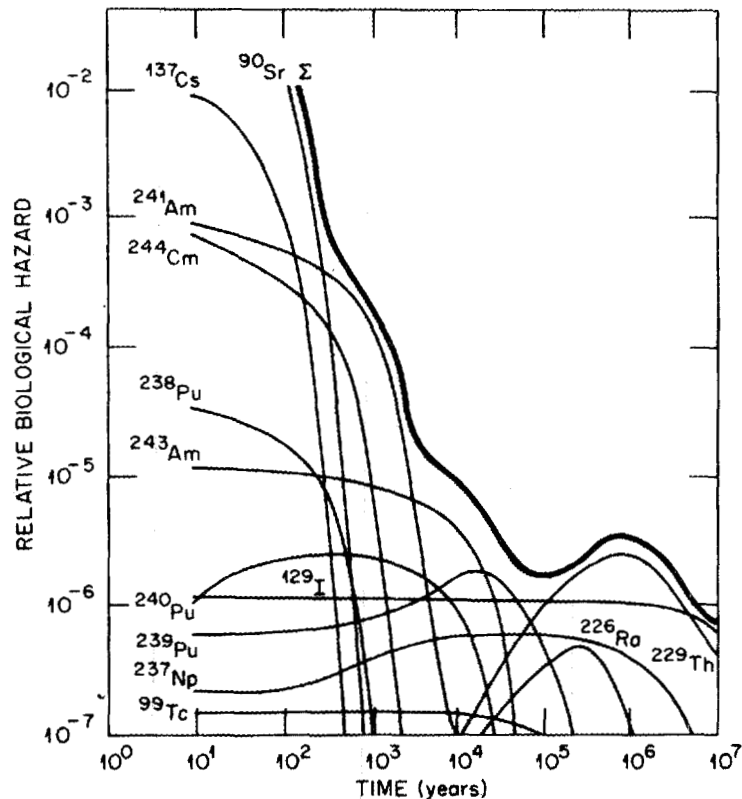


Fig. 1. Relative biological hazard of some radioactive isotopes present in nuclear wastes as a function of time. The dominant long-term hazard is posed by the long-lived α -active actinides.

mechanism will be in terms of data collected on whole granite samples with polished surfaces.

Initially, the thought was that the major mechanisms working in the environment would be simple cation exchange. In fact, the first experiments we conducted were on high-capacity cation exchange minerals, such as montmorillonite, kaolinite, and several other clays. Figure 2 shows the americium distribution coefficient between the liquid and solid phase, as a function of pH, for montmorillonite in a synthetic groundwater and in 4 molar NaCl, and for quartz, a fairly inert material. At low pH, we find a difference of approximately 2-1/2 orders of magnitude between the sorption of americium on montmorillonite and on quartz. This is in good agreement with the relative capacities of the two minerals, indicating that simple cation exchange behavior is occurring. Also, we see that there is a strong salt dependence. We find that sorption on montmorillonite in 4 molar solution is drastically different from sorption in groundwater. This, again, is an indication of simple cation exchange behavior.

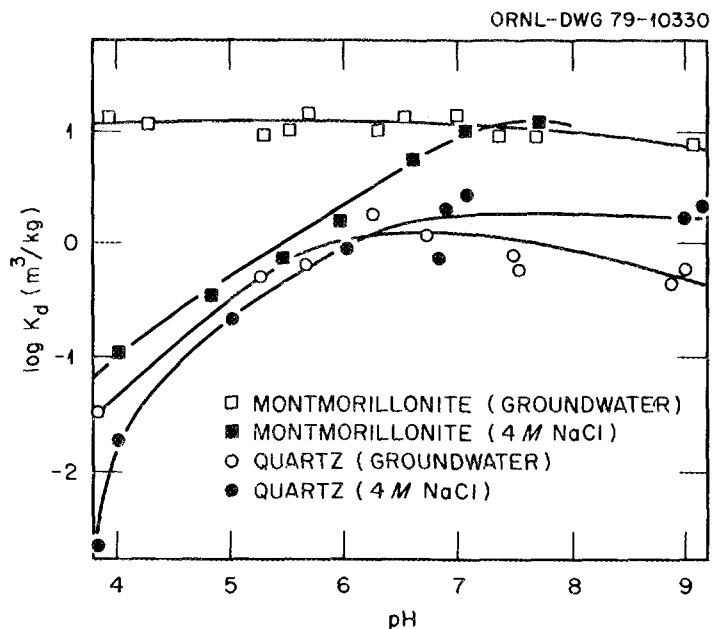


Fig. 2. Americium distribution coefficients between the liquid and solid phases as a function of pH for montmorillonite and quartz.

The relationships get complicated, though, if we change the pH. At a pH of around 6 to 7, we find that quartz and montmorillonite are only about an order of magnitude apart, which is in poor agreement with their relative capacities, but now it correlates fairly well with the surface area of the two minerals. Also, the salt dependence has disappeared. Both of these are very strong indications that simple cation exchange is no longer the dominant mechanism for absorption. We have demonstrated this for several cations: americium in the trivalent state, neptunium in the pentavalent state, plutonium in the tetravalent state, and uranium in the hexavalent state. Of these four, only uranium in the hexavalent state appears to be sorbed through a simple cation exchange mechanism.

Next we turn to trying to explain how we can get these tremendous differences in distribution coefficients just by changing the pH. The only explanation we could deduce was that the solution chemistry of the system was dominating rather than the substrate. So, we decided to look at a whole host of minerals and how they sorbed the actinides such as americium. We did, essentially, thirty-six different minerals. We did the sorption tests and determined the distribution coefficient as a function of pH for all 36. Distribution coefficients for only a few representative minerals are shown in Figure 3 primarily for clarity since the inclusion of all the minerals would be extremely confusing. What we found were some very general trends. At very low pH we observed very low sorption, even down to the point where it was difficult to measure the distribution coefficient. But then, by changing the pH a couple of units, we changed the distribution coefficient by three orders

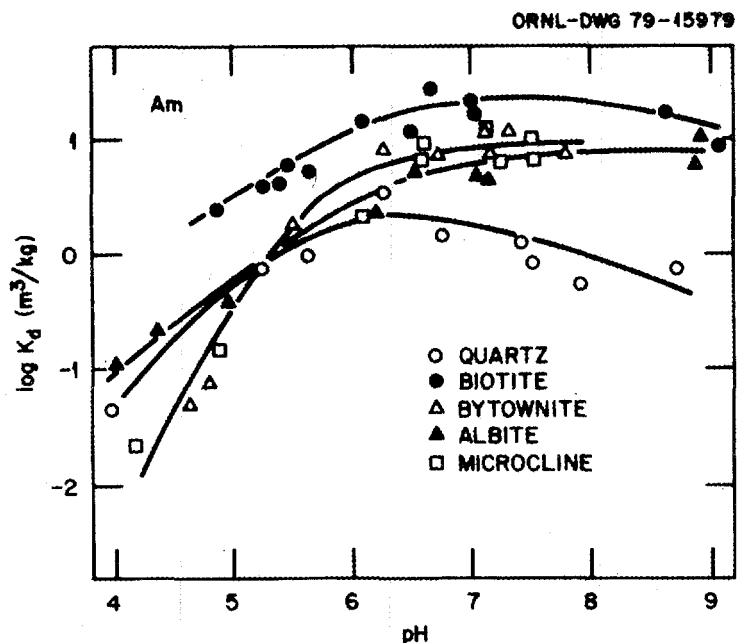


Fig. 3. Americium distribution coefficients as a function of pH for selected minerals.

of magnitude in many cases. One thing that is important to emphasize here is that this is not a precipitation reaction. The K_{sp} for americium trihydroxide would indicate that, at about 10^{-6} to 10^{-7} molar, we should get precipitation. These measurements are done at 10^{-11} and 10^{-12} molar, so this is not a precipitation reaction. It is some sort of reaction that is involved with hydrolysis, but not precipitation in a classical sense. The interesting lack of agreement that I brought up earlier between predictions of sorption based on simple cation exchange theory is also illustrated by biotite vs quartz. Their cation exchange capacities differ by about 2 to 2-1/2 orders of magnitude, yet the approximate difference in sorption is slightly over one order of magnitude. Again, it does not follow simple cation exchange. When we looked at salt dependence data on this, the salt data and the groundwater data all fell essentially on the same line.

We decided to look at the hydrolysis species in solution for a trivalent ion. We found (Figure 4) that the area where we start to see this drastic change in sorption is exactly the area where we would predict the various hydrolysis products for a trivalent rare earth or actinide. And, in fact, if we plot these same species for americium vs loss of americium from solution in our sorption experiments on very inert material like quartz, there is a one-to-one correlation between where these hydrolysis products begin and where we see the sorption occurring (Figure 5).

This was for a trivalent ion. We decided to see whether this would work for other classes of cations with very different hydrolysis

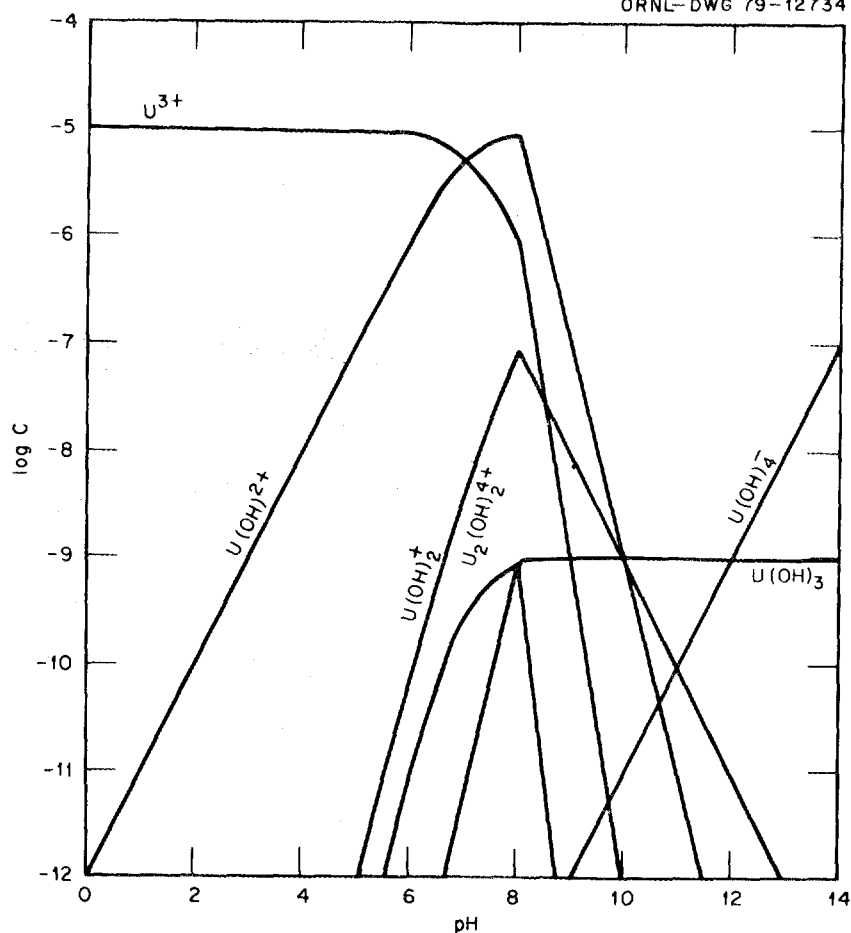


Fig. 4. The log of the concentration of hydrolysis species for trivalent uranium is shown as a function of pH.

behavior. The next one we looked at was neptunium (Figure 6). In this case, neptunium exists in the solution in the pentavalent state as NpO_2^+ . We have different behavior now as a function of pH: very low sorption up to about pH 7 to 7-1/2, but then a very drastic increase with very little change in pH. Thirty minerals fall in a very narrow band about the width of the band between the quartz and biotite curves in Figure 6. So, again, the solution chemistry is apparently dominating rather than the substrate. If we look at the hydrolysis behavior in neptunium (Figure 7), one finds that right in the pH area 7-1/2 to 8 is where hydrolysis begins to occur very strongly for the neptunyl ion. Indeed, the hydrolysis behavior in Figure 8 in the pH area where we see the decrease in neptunium in solution, or sorption onto the quartz, is exactly where hydrolysis becomes dominant.

We also looked at plutonium, which presumably was in the tetravalent state, predominantly, in our aerated solution. The band was somewhat wider, as shown in Figure 9, and we do not yet understand why quartz is so low, but the majority of minerals fell in a band of about

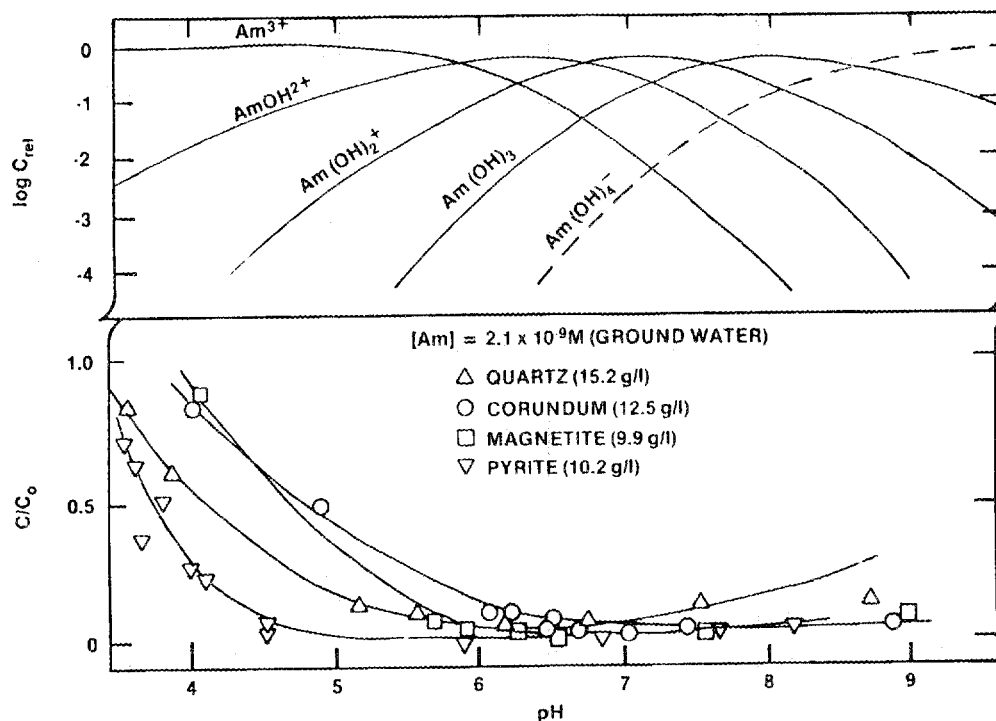


Fig. 5. The log of the concentration of hydrolysis species for trivalent americium is shown as a function of pH in the top graph. The ratio of the americium in solution to the initial concentration C_0 is shown in the bottom graph as a function of pH for sorption on several mineral species.

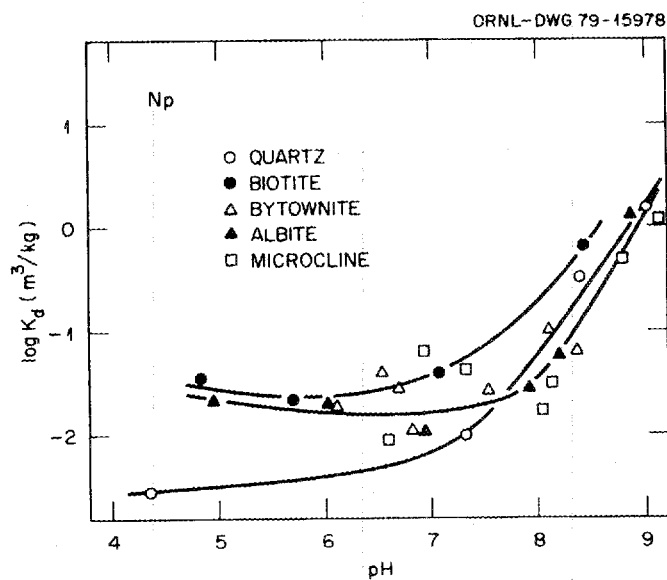


Fig. 6. Distribution coefficients for NpO_2^+ as a function of pH for a representative set of minerals.

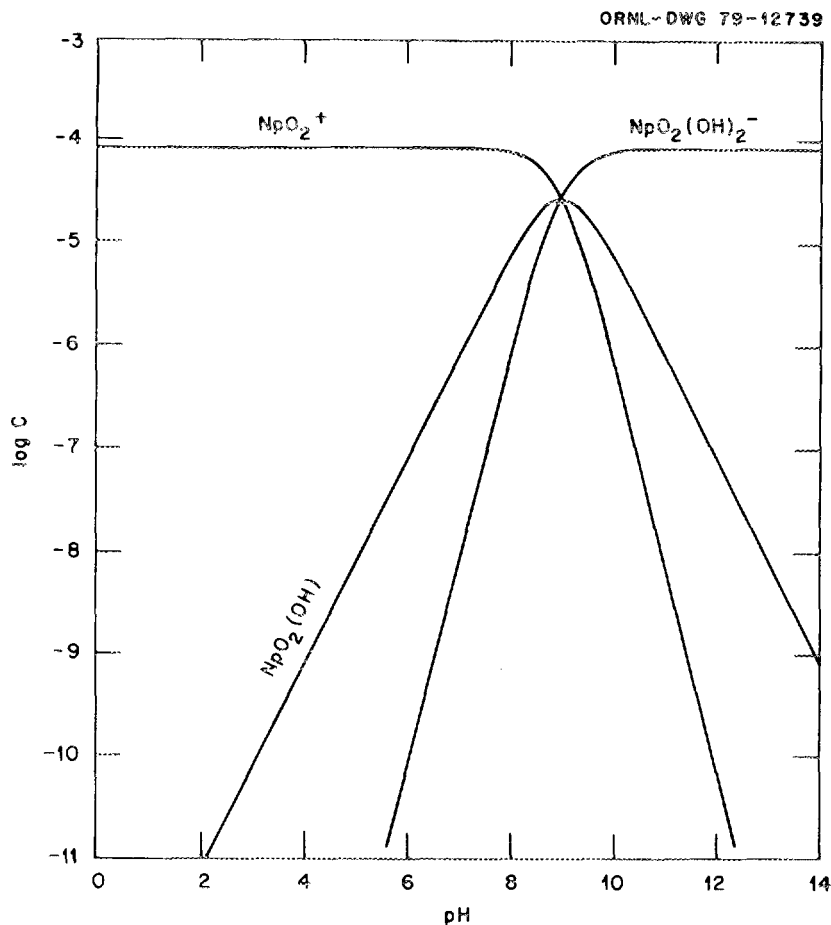


Fig. 7. The log of the concentration of various Np hydrolysis species is shown as a function of pH.

one order of magnitude for plutonium. When we look at the hydrolysis properties of a tetravalent ion (Figure 10), the hydrolysis begins at very low pH. Therefore, if those hydrolysis products are responsible for the sorption, we would expect to get very little pH dependence (Figure 11) and, even at pH 4, very strong sorption.

Most of these measurements, as I said, were done on pure materials; so we wanted to see whether, indeed, we can take our pure mineral measurements and predict what will happen on a whole rock. We took climax stock granite and westerly granite, and measured the distribution coefficients for both of those granites for americium and neptunium as a function of pH, as shown in Figure 12. The dashed lines are the lines that bound the general curves for all 30 minerals we looked at, and we find that the sorption on the whole granites fall within the bounds of what we measured on the pure minerals. In fact, if we look at the mineralogy of an individual granite, and use the distribution coefficients for its pure components, we can come within about a factor of 3 in predicting the sorption on that particular granite. So we feel

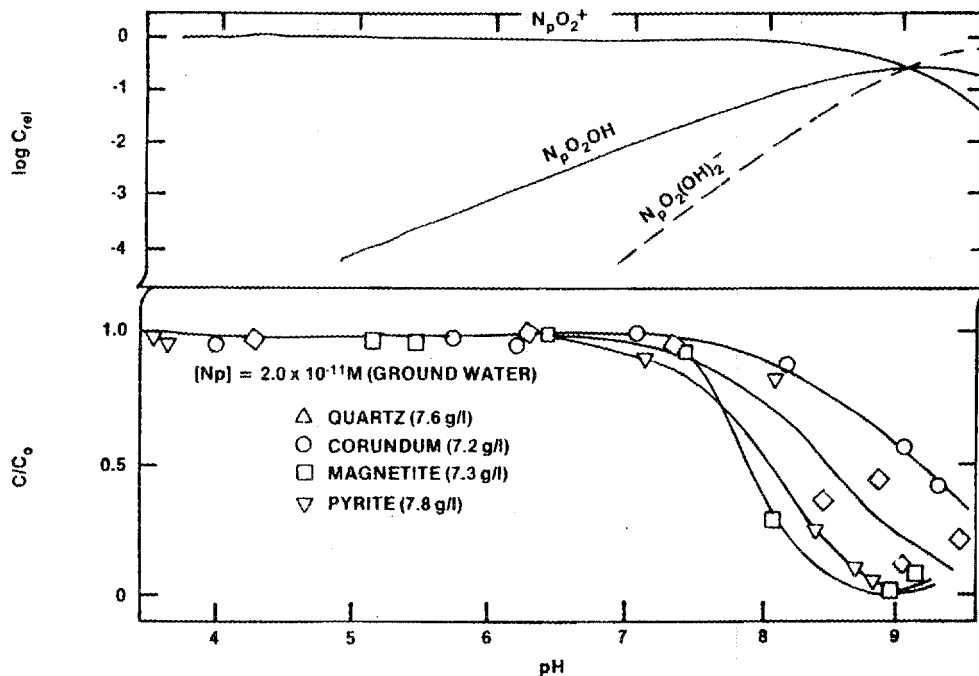


Fig. 8. The log of the relative concentration of Np hydrolysis species is shown as a function of pH in the top graph. The ratio of the concentration of Np in solution to the original concentration C_0 is shown as a function of pH for a representative set of minerals in the bottom graph.

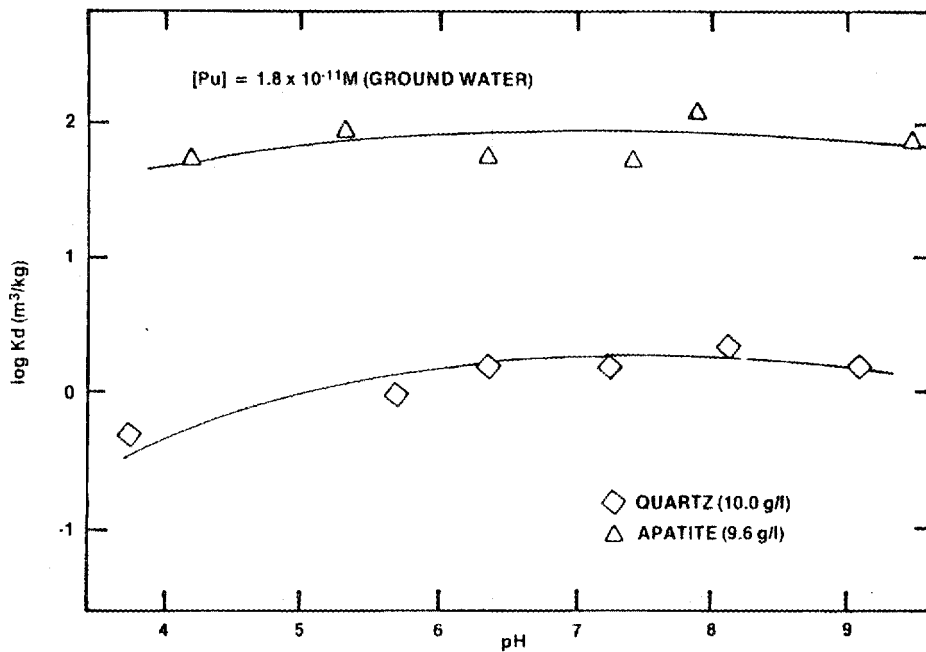


Fig. 9. The distribution coefficient for tetravalent Pu is shown as a function of pH for quartz and apatite.

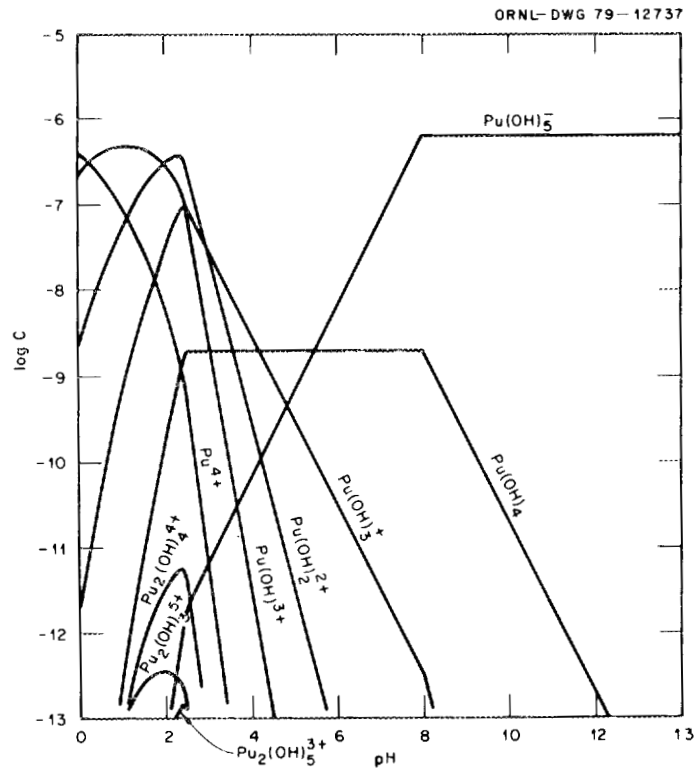


Fig. 10. The log of the concentration of Pu hydrolysis species is shown as a function of pH.

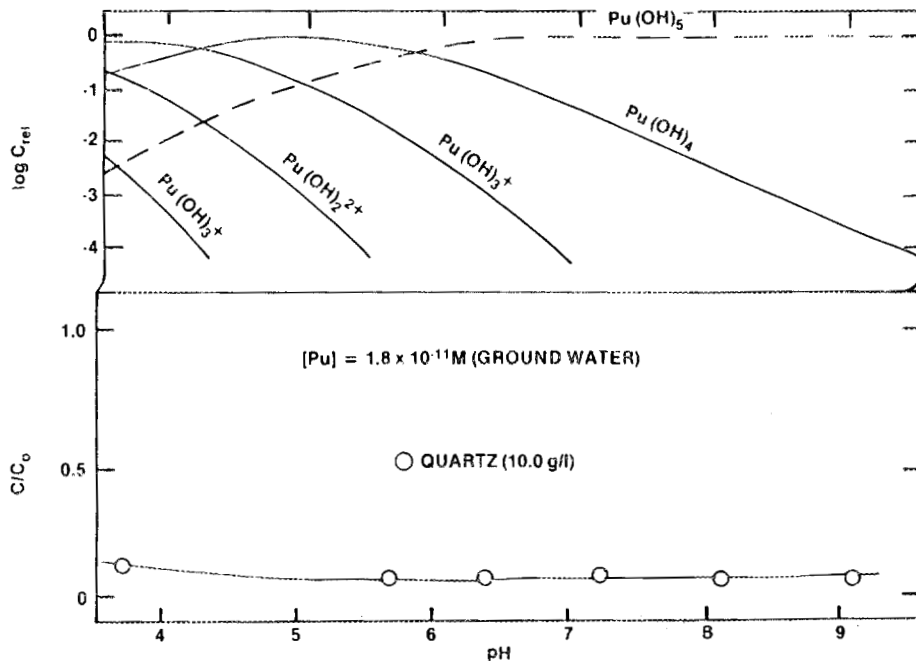


Fig. 11. The log of the relative concentration of plutonium hydrolysis species is shown as a function of pH in the top graph. The ratio of the concentration of Pu remaining in solution to the original concentration C_0 is shown as a function of pH in the bottom graph for sorption on quartz.

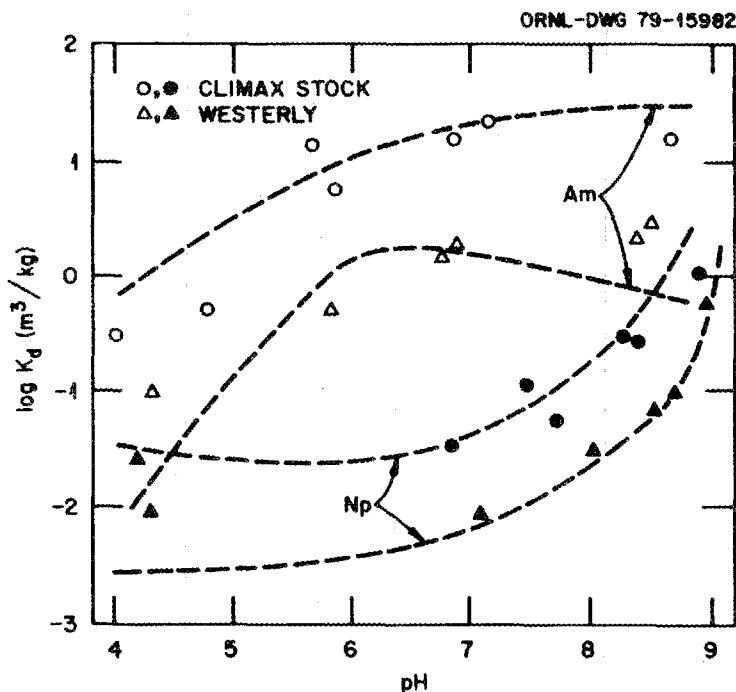


Fig. 12. Distribution coefficients of Am and Np as a function of pH for sorption on climax stock and westerly granite.

that is a fairly adequate prediction for determining retardation factors in a geologic medium.

A somewhat qualitative explanation for what is going on here has been given by James and Healey¹. In Figure 13, they plot the energy of sorption versus the charge Z on the cation. They claim that there are two factors operating against one another: a coulombic term that operates to cause sorption, and a solvation term that tends to keep the ion in solution. It turns out that the coulombic term is less sensitive to the charge on the cation (or the overall charge on the complex) than the solvation term is. Therefore, hydrolysis or complex formation tends to enhance the possibility of sorption. We have done some calculations using their theory, and it gives qualitative agreement with where we see the onset of this strong sorption. So, it looks like a reasonable qualitative theory at this point. This theory would predict then, that, if we increase the amount of various complexing anions in solution, we should see enhancement of sorption. We have sorbed americium onto quartz, which is fairly inert, with increase concentrations of sulfate, fluoride, phosphate, and carbonate, which are all fairly good complexing agents for americium, as shown in Figure 14. Indeed, we do get increased sorption for fluoride, phosphate, and sulphate. We do not see much increase, if any, for chloride or carbonate except, possibly, at lower pH. The chloride is a very weak complexing agent for the americium, so that seems reasonable. On the other hand, the groundwater that we use already has about 200 parts per million carbonate, so I believe that we just have not added enough carbonate to see much effect

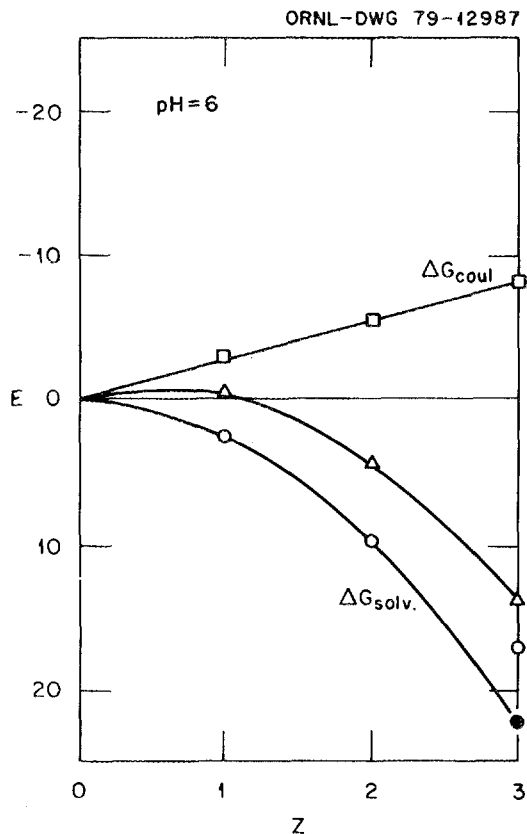


Fig. 13. The energy of sorption as a function of the charge on the cation. The coulombic term produces sorption while the solvation term tends to keep the ion in solution.

here. We did get definite enhancement for phosphate and fluoride, which are very strong complexing agents for americium. So again, we get some fairly good qualitative agreement between the theory of James and Healey¹ and what we have observed experimentally.

One factor that I think has been ignored to a great extent, is the role of CO_2 -water equilibrium in the effect of carbonate on all these systems. Figure 15 shows infrared spectra of plutonium polymer (Toth *et al.*²). The first spectrum has an intense sorption band around 1500. In the past that had been attributed to nitrate. This seemed reasonable since the plutonium polymer was prepared from nitrate solutions and obtained as a very gelatinous precipitate. This seemed straightforward until analysis for nitrate yielded negative results. What was found was about 1/2% carbon in their precipitate. When they did the precipitation with rigorous exclusion of CO_2 , they found that this band all but disappeared and their analysis showed essentially no carbon in the precipitate. So, it is necessary to note that even atmospheric CO_2 equilibrium with water can be very important in the case of actinides such as plutonium and americium, where there are very high complexation constants for those particular cations. In summary, this second mechanism seems to be dominated by the solution chemistry of the ion, and it

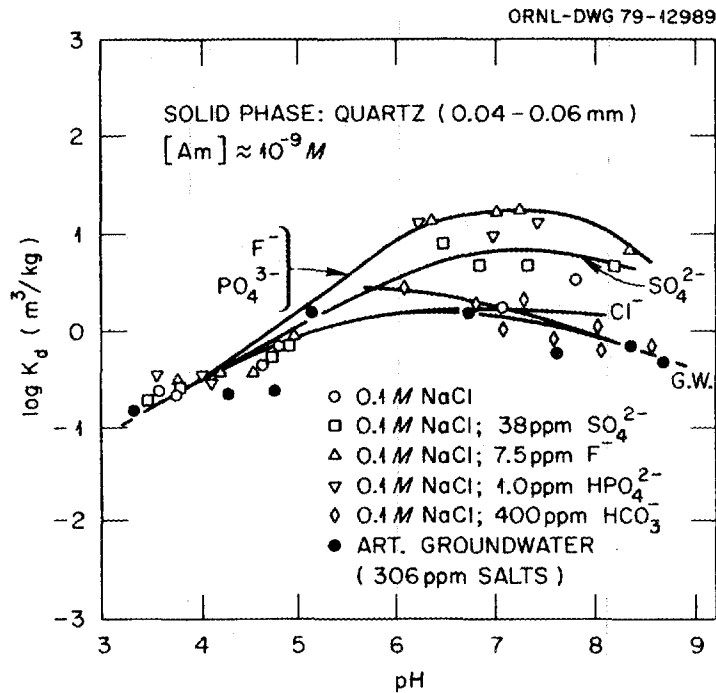


Fig. 14. Distribution coefficients for the sorption of Am on quartz in the presence of various complexing anions as a function of pH.

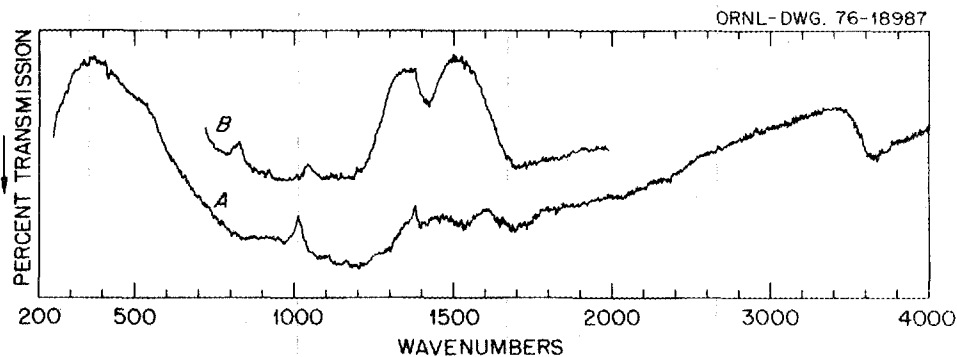


Fig. 15. The infrared spectrum observed for plutonium polymer.

seems to be fairly independent of the mineral, or the of the rock acting as a substrate.

The third mechanism appears to be just the opposite: it is dominated by the substrate. The earlier data for sorption of americium on various minerals is shown in Figure 16. You can see, from the general shape, that there is very low sorption at low pH and reasonably high sorption in the vicinity of pH 6 to 8. There is a class of minerals (apatite is one example, as shown in Figure 16) that has extremely high sorption and is very pH independent. For americium this class includes

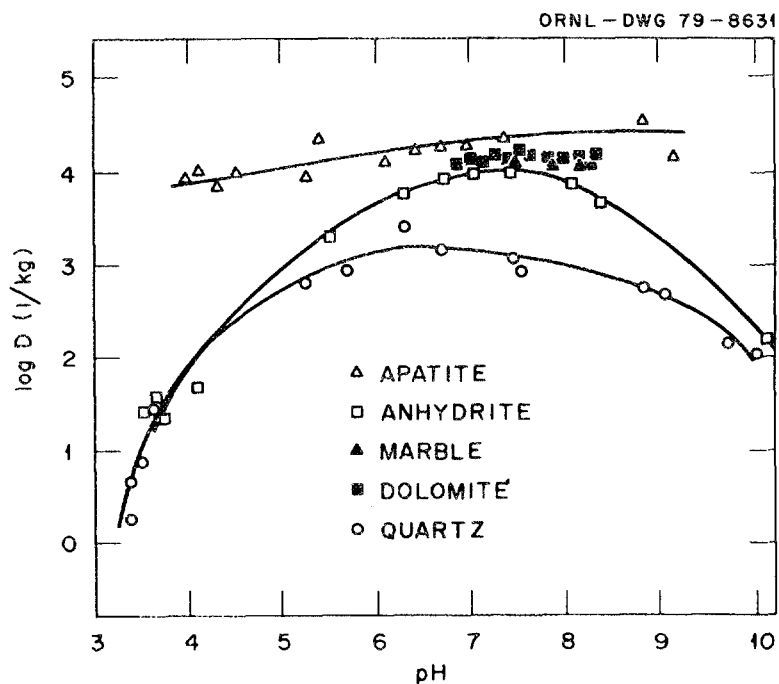


Fig. 16. Log D for the sorption of americium is shown as a function of pH for various accessory minerals.

fluorite, apatite (which is calcium hydroxyfluorophosphate), and carbonate minerals, which are all strong complexing agents for americium. In fact, if you look at the americium distribution coefficients (Table 1) for apatite, which contains phosphate; marble, which contains carbonate; fluorite, which contains fluoride; and anhydrite, which contains sulfate, you find that they exhibit high distribution coefficients. Furthermore, the distribution coefficient correlates well with

TABLE I. ANION EFFECTS IN THE SORPTION OF ^{241}Am AND ^{235}Np ON SELECTED MINERALS

Mineral	^{241}Am D(L/kg)	^{235}Np D(L/kg)
Apatite	20,000	20,000
Marble	10,000	2,000
Fluorite	10,000	3
Anhydrite	5,000	6

the magnitude of the complexation constant for the anions contained in these minerals. The same is true of neptunium. Carbonate and phosphate are the only two that have extremely high complexation constants for neptunium. I want to emphasize that the americium is trivalent, and the neptunium is pentavalent. One thing is very important in general about this mechanism: if you need to absorb a particular cation, one rule of thumb is to look for an anion that complexes that cation very strongly. Once anions in this class are found, a search for a mineral that is fairly insoluble, and which contains that anion, is made; that mineral will probably make an excellent backfill material to absorb the cation. So, this is a third general mechanism that appears to be important, and it appears to be associated with a chemisorption reaction on the surface of the mineral. In the case of apatite, for instance, a phosphate group on the surface apparently actually bonds with the cations on the surface of the mineral. We believe that this is a surface reaction, because we have put those same minerals in our groundwater for three months, and then analyzed to see if there is any contribution of the phosphate, carbonate, or fluoride to the solution. In every case except marble, there was no measurable change in the concentration of the anion in solution. So, we feel that it is strictly a surface phenomenon, a chemisorption reaction.

The fourth mechanism, which appears to be very important (this has been emphasized in earlier talks at this meeting), is the effect of the valence state of the actinide. If you have a hexavalent or pentavalent actinide, you are probably in trouble because that is just going to migrate right through your geologic media and not stick very well at all! So we decided to do some measurements to see if the Fe(II)-Fe(III) redox couple will be able to reduce the hexavalent and pentavalent states of the actinides. We chose climax stock granite as the granite to conduct studies on. Figure 17 gives an idea of the mineralogy of this granite (it is actually a monzonite). In Figure 17a, the streaks of white grains are pyrite (iron(II) sulphide), the black is primarily biotite, the lighter areas are large quartz crystals, and the background matrix is mainly feldspar. The important thing to note is that pyrite is iron sulfide and the biotite structure contains fairly large amounts of Fe(II).

The first element we wanted to look at was neptunium, which will exist primarily in the pentavalent state in aerated solutions (Figure 18). We exposed the granite slab to aerated solutions of neptunium, and we found that there was very strong sorption along the pyrite grains, as shown in Figure 19c. (The white areas indicate where the alpha activity has gone.) There was strong correlation with the streak of pyrite. Also, you can see the very nicely outlined biotite grains. However, the general sorption on the feldspar and the quartz was fairly low. There is one-to-one correlation if you compare the biotite and the pyrite grains with the Np sorption. We then decided to investigate whether that was just specificity for neptunium or actually reduction of the surface, so we oxidized the granite before we exposed it to the neptunium. We found that the sorption was very general, and not specific for any particular mineral (Figure 19d). By eliminating the Fe(II) on the surface of the rock, apparently we eliminated this specificity.

ORNL-DWG 79-19991

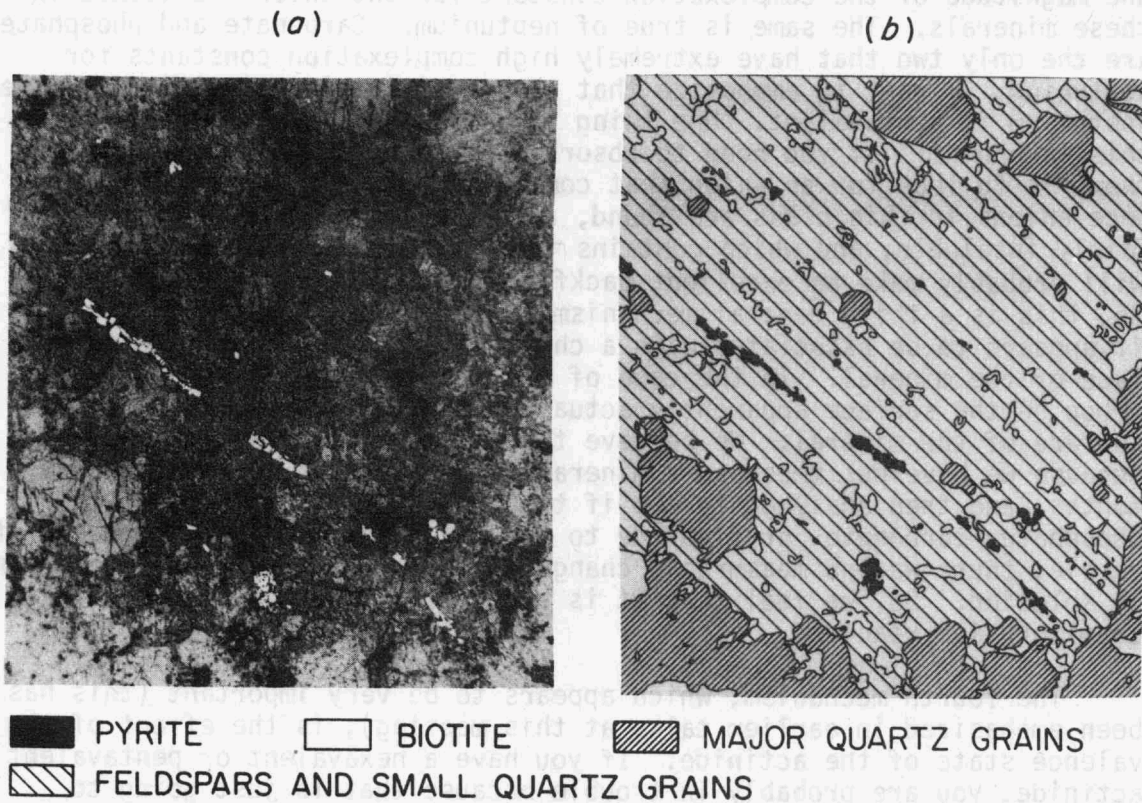


Fig. 17. The mineralogy of climax stock granite. A photograph of a polished section about 2.5 cm on a side is shown in (a) and the composition of the various features is illustrated in (b).

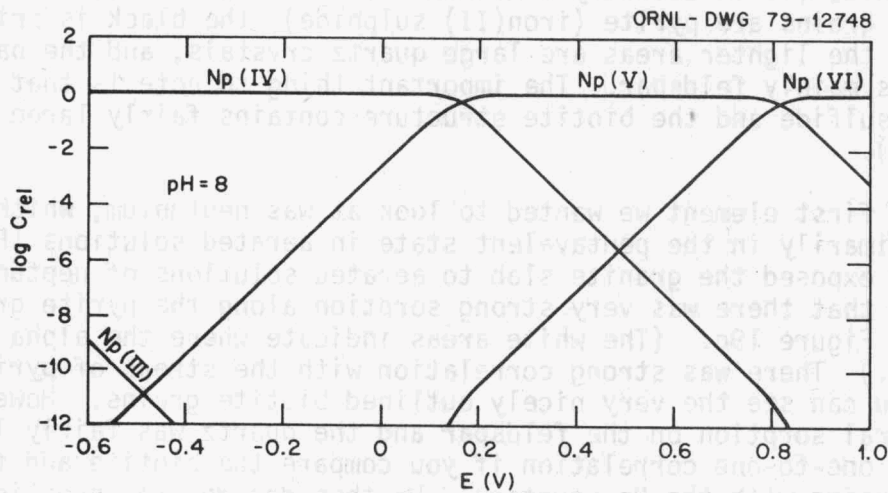
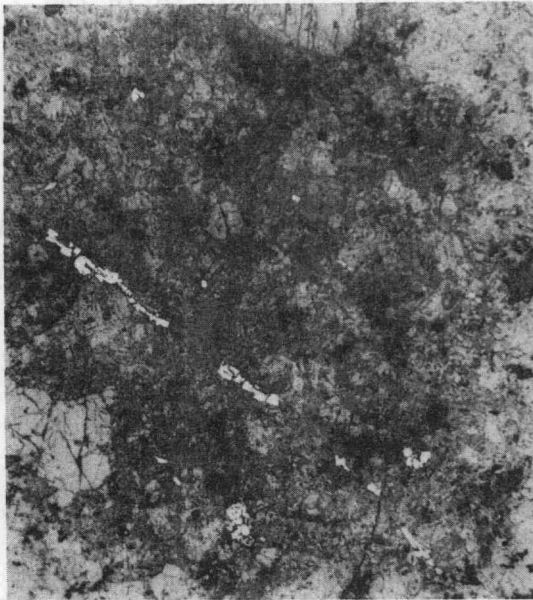


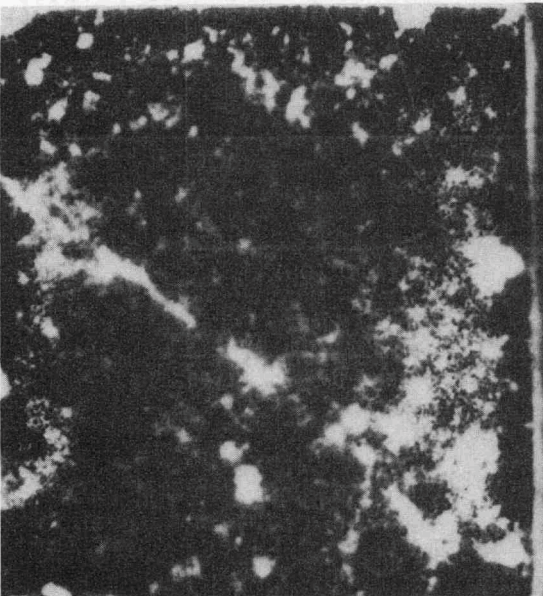
Fig. 18. The log of the relative concentration of Np species at pH = 8 as a function of Eh. Np^{5+} is expected to be the dominant species in aerated solutions.



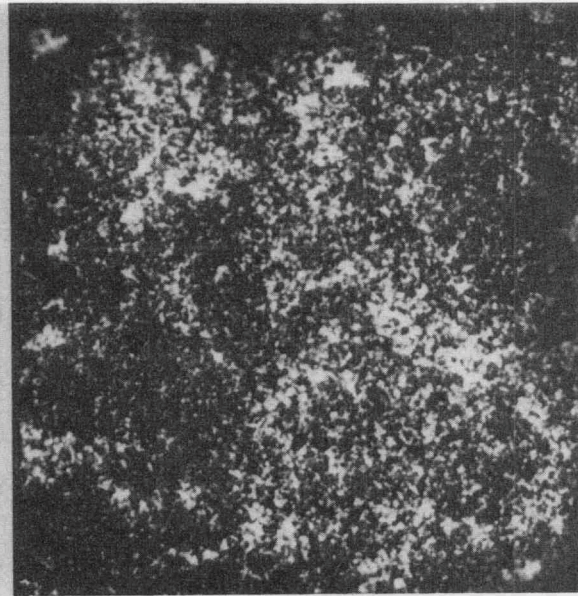
(a) CLIMAX STOCK GRANITE



(b) Np IN NITROGEN PURGED SOLUTION



(c) Np IN AERATED SOLUTION



(d) Np ON OXIDIZED SURFACE

Fig. 19. (a) photograph of a 2.5 x 2.5 cm² climax stock granite slab. Autoradiographs for Np sorbed on the granite slab (b) from a nitrogen-purged solution, (c) from an aerated solution, and (d) on an oxidized surface.

Then we decided to try to get slightly more reducing conditions, so we purged the system with nitrogen for a while before we put the granite in. We found that the sorption on the pyrite and the biotite in the system purged with nitrogen was actually enhanced tremendously vs what was sorbed on the background (Figure 19b). We believe that this is proof that the neptunium is being reduced from Np(V) to Np(IV) at the surface of the minerals containing Fe(II).

The next element we wanted to look at was plutonium. Plutonium predominantly will be Pu(IV) in most aerated solutions (Figure 20). In recent work by Bondiotti³ and others it was found that there is a small component of Pu(VI) or Pu(V). They have not determined which it is in aerated solution, but a small percentage appears to be in these higher valence states. Predominantly, however, it will be tetravalent plutonium. When we did the sorption in aerated solutions, we found fairly heavy general sorption (Figure 21c). (The exposures on these are much shorter than those we saw on neptunium.) In fact, about 99.9% of all the plutonium came out of solution overnight. There seems to be some correlation with the pyrite grain and the biotite, but it is not nearly so strong as the correlation that we saw in the case of neptunium. We feel that this is possible proof that indeed there is a certain amount of plutonium in the higher valence state. Nitrogen purging (Figure 21d) did not seem to affect the system very much. It is much the same kind of sorption; the background is a little bit higher here. However, when we oxidize the plutonium before we expose it to the granite, so that we predominantly get the hexavalent state, we find very strong correlation with the pyrite grain and the biotite (Figure 21b). So it indeed looks like the Pu(VI) can easily be reduced by Fe(II).

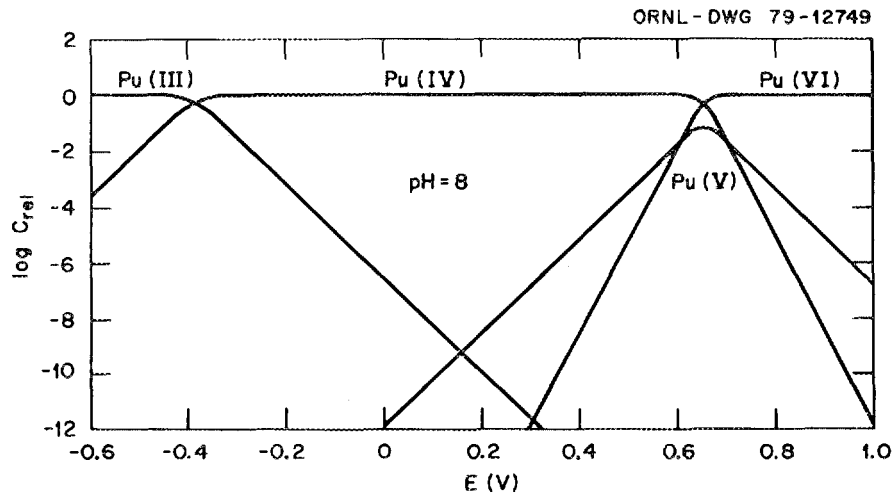


Fig. 20. The log of the relative concentration of plutonium species at pH = 8 as a function of Eh. In aerated solutions Pu(IV) is expected to predominate.

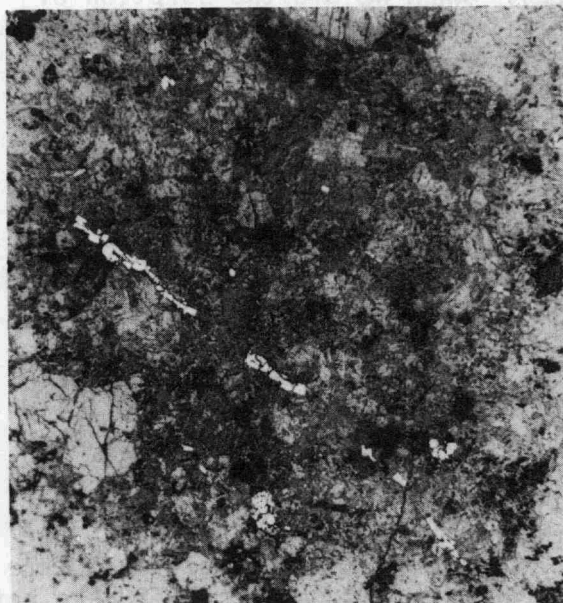
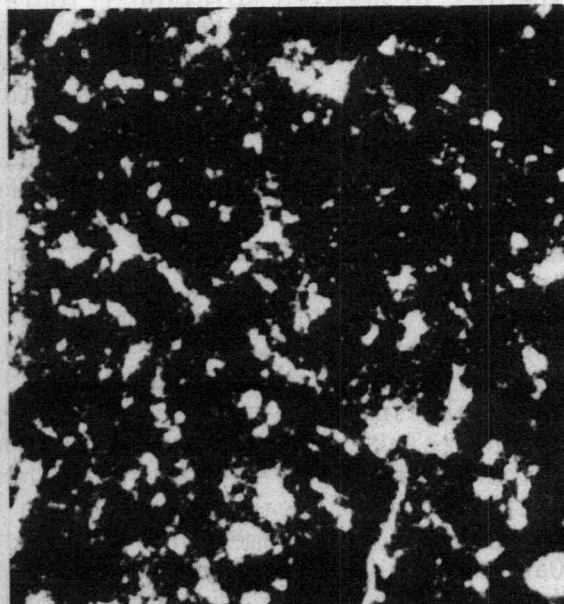
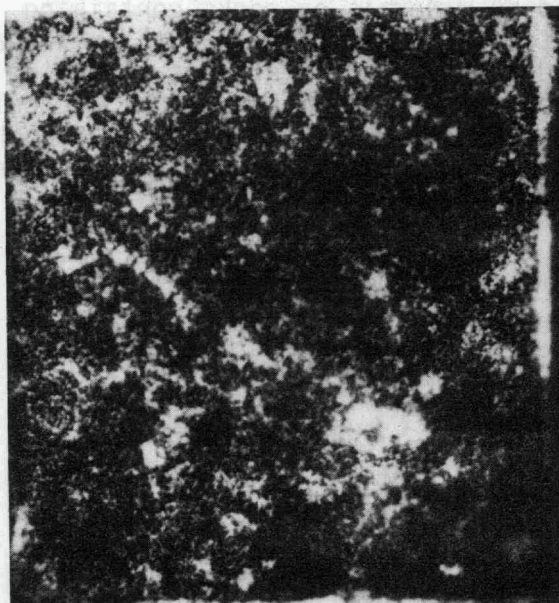
**(a) CLIMAX STOCK GRANITE****(b) Pu OXIDIZED WITH O₃****(c) PU IN AERATED SOLUTION****(d) PU IN NITROGEN PURGED SOLUTION**

Fig. 21. Autoradiograph from Pu sorbed on the climax stock granite slab shown in (a) above and in Figs. 17 and 19(a). The autoradiographs are for Pu sorption for: (b) Pu oxidized with O₃, (c) Pu in an aerated solution, and (d) Pu sorbed from a nitrogen purged solution.

Next we came to U(VI), which will be the predominant uranium species in aerated solution (Figure 22). When we did the sorption of U(VI), we found that it did not matter if we oxidized the surface, or aerated it, or purged it with nitrogen. We got essentially the same autoradiograph (Figure 23). We did find that it correlated somewhat with the biotite grains, but not with the pyrite. These are very long exposures; it is very low sorption, and most of the uranium stayed in solution. Since biotite contains Fe(II), we considered the possibility that it could be a reduction reaction, but the pyrite is completely absent. So we decided that, rather than a reduction reaction, it may be the fact that biotite has a fairly high cation exchange capacity and the U(VI) is acting as a simple cation exchanger. We decided to do an experiment in which we first sorbed the uranium on the granite in a dilute groundwater solution (Figure 24a). Then we reintroduced that same slab into the same solution, except that we adjusted the molarity of the solution to 4 M NaCl and found that indeed the uranium desorbed (Figure 24b). So, we feel that this is evidence that U(VI) is the only actinide that appears to be acting through the simple cation exchange mechanism. This same sort of reduction has been seen by Bondietti³ at Oak Ridge on technetium and neptunium. He found that the pertechnetate ion does tend to be strongly sorbed on granite and basalts that have not been oxidized vs those that have been oxidized. So it looks like, based on this data, that the pertechnetate ion is being reduced to TcO_2 , then sorbed very strongly. He found data on neptunium that agreed fairly well with ours; that Np(V) is reduced by minerals or rocks containing Fe(II). So, this mechanism appears to be very important in the retardation of the actinides in geologic media, but it was very disappointing that U(VI) apparently was not reduced in our experiments. We could only reduce Pu(VI) and Np(V). We conducted all of our experiments in the pH range around 8. So we surmised that our conditions are probably in the

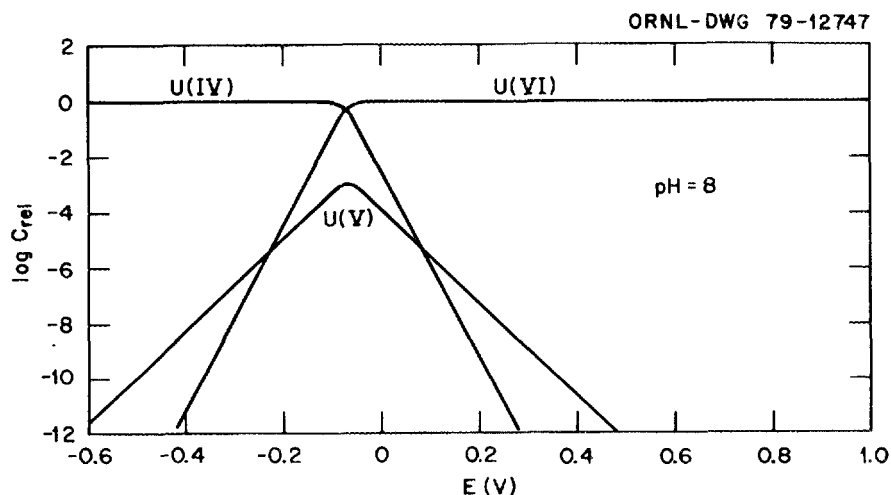


Fig. 22. The log of the relative concentration of uranium species for pH = 8 as a function of Eh. U(VI) is expected to be the predominant species in an aerated solution.

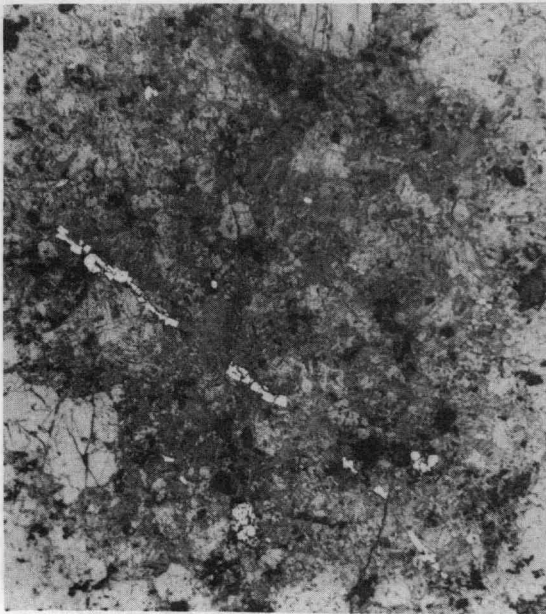
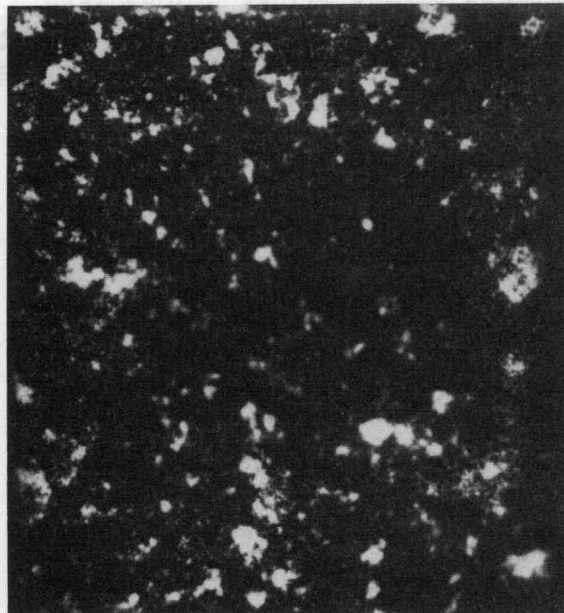
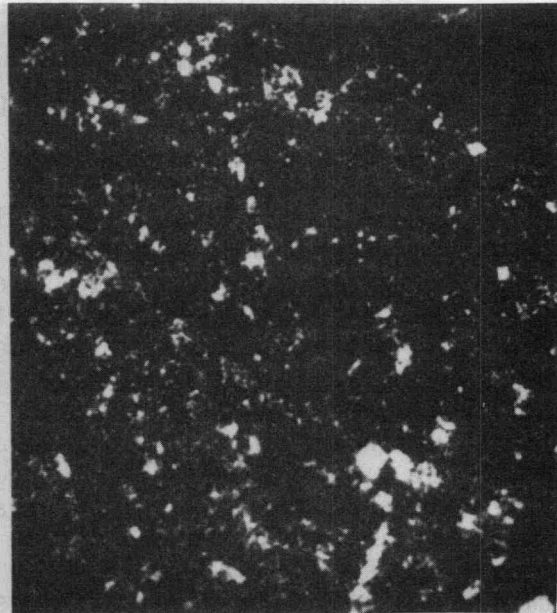
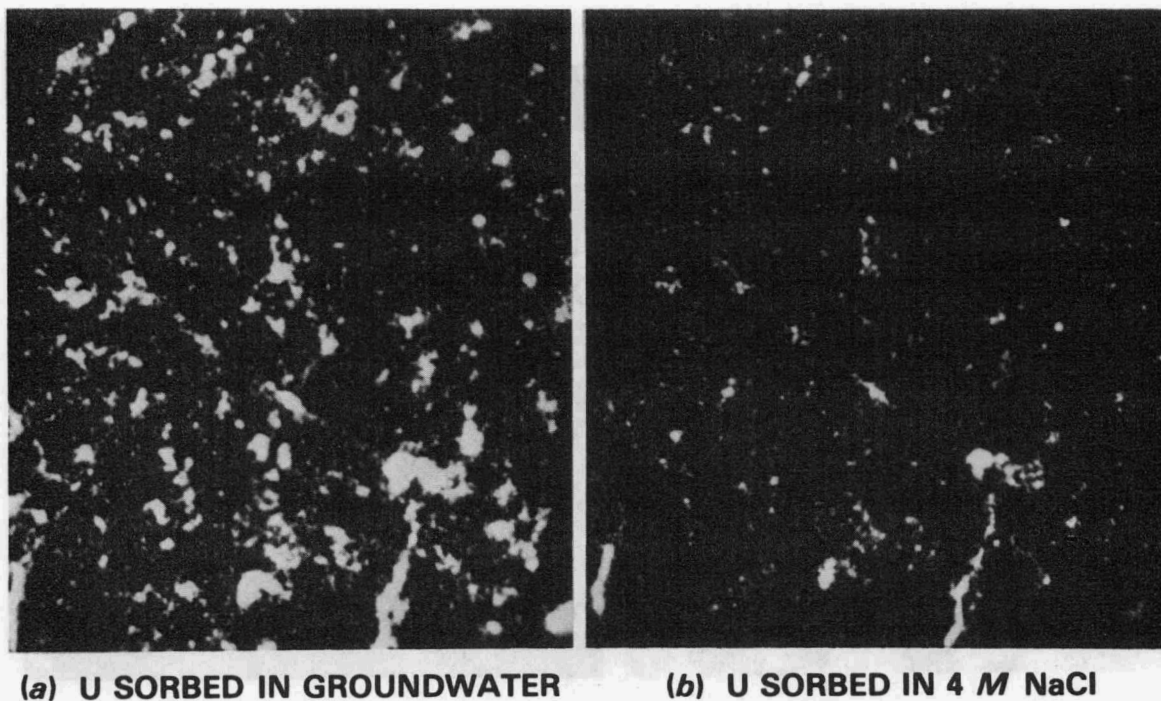
**(a) CLIMAX STOCK GRANITE****(b) U IN NITROGEN PURGED SOLUTION****(c) U IN AERATED SOLUTION****(d) U ON OXIDIZED SURFACE**

Fig. 23. Autoradiographs from uranium sorbed on the climax stock granite slab shown in (a) above and in Figs. 17, 19(a), and 21(a). The autoradiographs are for uranium sorbed: (b) from a nitrogen purged solution, (c) from an aerated solution, and (d) on an oxidized surface.



(a) U SORBED IN GROUNDWATER **(b) U SORBED IN 4 M NaCl**

Fig. 24. Autoradiographs from uranium sorbed on the climax stock granite slab shown in Figs. 17, 19(a), 21(a), and 23(a). In (a) above, the autoradiograph is for U sorbed from a dilute groundwater solution and in (b) following reintroduction of the slab into the same solution after the molarity was adjusted to 4 m NaCl. The evidence for uranium desorption in the NaCl solution is clear.

small blacked-in box in Figure 25. I have plotted Eh-pH data for general groundwaters that you can find in the environment. I have also plotted a smaller box (just below the black box) of Eh-pH data for deep geologic deposits that have no direct contact with air, and apparently their redox potentials may be low enough to reduce U(VI) to U(IV), thus enhancing the absorption. It has been observed in some Swedish studies that, indeed, in nature the U(VI) is reduced under these conditions. So, I think the problem we had with our experiments was that we simply did not get conditions reducing enough to allow the Fe(II) to reduce the U(VI). Nitrogen purging is by no means a rigorous exclusion of oxygen. I think this mechanism is one of the central mechanisms affecting the design of a backfill material or the choice of a rock formation to retard these higher-valence actinides.

In designing a backfill material, we have discussed three major mechanisms that appear to be working. One is dominated by the solution chemistry of the ion. Another appears to be a chemisorption reaction dominated by the substrate. The third is the action of the Fe(II)-Fe(III) oxidation-reduction couple. If we look at what we need to know about designing backfill material, we have some physical requirements such as keeping the cannisters fixed in position and releasing stress.

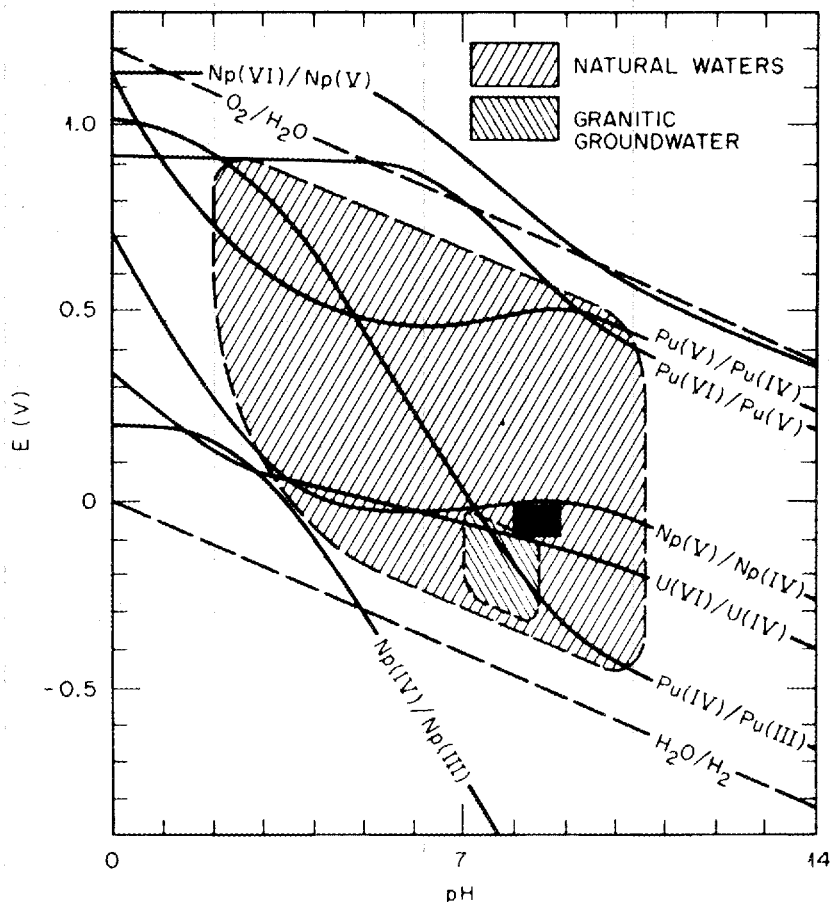


Fig. 25. Eh versus pH for various actinide species. The fields appropriate to natural groundwaters and deep granitic groundwaters are indicated. The conditions appropriate to most of the present experiments are in the field indicated by the small black box.

Those physical properties we have a good handle on, by and large. Under a chemical barrier, though, we need something that is fairly impermeable to water and will not let the water migrate around and away from the cannister very easily. But we also need something that retains nuclides fairly well. The Swedes have proposed a backfill material, which I am sure is quite familiar to everyone, of about 80 to 90% quartz and 10 to 20% montmorillonite. The quartz is there mainly to satisfy the physical properties of the backfill material such as thermal conduction. The montmorillonite forms a nice impermeable barrier to water flow, but also the assumption was that, since it had the high cation exchange capacity, it must absorb ions well. As I presented in this talk, simple cation exchange is not the most important mechanism working to retard ions, so a much better approach to designing backfill material would be to take these three major mechanisms and try to identify minerals that can be included in the backfill material that will specifically sorb the

actinides and technetium, through either chemisorption reactions or the reduction reactions that I presented. Some examples of these are listed in Table II. Apatite is an excellent chemisorption-type mineral that actually will absorb all the actinides, even the hexavalent ones, fairly strongly on the surface. In fact, we have trouble determining the distribution coefficients for apatite because they are so high. There is just so little left in solution to count, and you cannot wash that solid with more groundwater or sodium chloride and get the sorbate back off. It really appears to be irreversible in the time scales that we studied. Marble and dolomite are fairly reasonable; the only problem is that there is enough carbonate contributed from these two minerals that I think you run the risk of forming possible anionic carbonate complexes with, especially, U(VI), and maybe actually mobilizing it rather than demobilizing it. So I think these would not be recommended in general for backfill material. One that might be interesting is iron

TABLE II. POSSIBLE BACKFILL MATERIALS FOR WASTE DEPOSITORY

		<u>Nuclides Sorbed</u>
Apatite	$\text{Ca}_5(\text{OH})(\text{PO}_4)_3$	All actinides
Marble	CaCO_3	All actinides
Vivianite	$\text{Fe}_3(\text{PO}_4)_2 \cdot 8\text{H}_2\text{O}$	All actinides
Olivine	$(\text{Mg}, \text{Fe})_2[\text{SiO}_4]$	All actinides
Montmorillonite	$(\text{Al}, \text{Mg})_8(\text{SiO}_{10})_3$ $(\text{OH})_{10} \cdot 12\text{H}_2\text{O}$	Fission products and lower valent actinides
Monazite	R.E. PO_4	Actinides

phosphate. You could accomplish two goals at once with this compound. You have the phosphate as a chemisorption reactant, and the Fe(II) can act as a reducing agent. Olivine, garnet, and biotite would be types of minerals containing the Fe(II) that can act as a reducing agent for the higher-valence actinides. I still think montmorillonite is very good for forming a coating impermeable to water flow, but it also is reasonably good for absorbing cesium and strontium, the fission products. One that has come up several times this week, monazite, would even be a good material for a backfill. The phosphate group acts very nicely as a chemisorption material, and monazite is very insoluble. So, you make your monazite container and pack monazite around it.

In conclusion, we have about three major mechanisms that we at least qualitatively understand. And, we should be able to utilize those not only to design better backfill material for repositories, but also to choose, in a more intelligent way, the particular site for the repository, and whether it should be of salt, granite, or basalt.

DISCUSSION

SMYTH: How did you determine the purity of the minerals? We found that 1% of a few impurities in feldspars can throw the sorption measurements off by an order of magnitude or more. For instance, the montmorillonite impurities in feldspars will do that. We found, in the climax, that the major phase which was doing the sorption of americium and plutonium was the montmorillonite alteration bands in the plagioclase feldspars. That accounted for more than 90% of the sorbed activity from those actinides.

Also, it would be very nice if you could study the two very abundant minerals in the southern Great Basin in Nevada: clinoptilolite, which is a zeolite, and kaolin, which is the major mineral in the eleana formation.

BEALL: On your first question, we checked the purity by X-ray diffraction and electron microprobe, so we have fairly good data on the composition of the minerals. On the second question, we did look at kaolinite. We did not look at any zeolites. We had so much mineral data that it is a mess when you try to display it all.

SMYTH: There are cubic kilometers of clinoptilolite in southern Nevada.

MACHIELS: Regarding the three mechanisms, I see the second one, the chemisorption one, as being a true mechanism; but as for the solution chemistry and the oxidation-reduction behavior, are those true mechanisms or simply parameters, basically? What they do is change the exact nature of the ions in solution, but can you call those mechanisms in themselves?

BEALL: One of the problems there and part of the problem I am addressing is that the only thing that many modelers want you to do is give them a distribution coefficient. They do not want to know what the pH is. They don't want to know what the eH is. They don't care. So I guess I am trying to battle against that trend. However, I agree with you; to call it a distinct mechanism may be going too far.

MACHIELS: How does the distribution coefficient change the concentration? You are working with very dilute concentrations, and there should be a very strong influence of the concentration, especially on the chemisorption mechanism. It is overwhelming for very low concentration but once you go to higher concentration . . .

BEALL: On the chemisorption reaction, apparently we never reached the point where we used up all the available sites. About 10^{-8} molar was as high as we went because we were afraid of getting into precipitation problems, but at that level we always had more than sufficient surface area on the mineral to sorb. By decreasing, I guess, the amount of solid, you should reach some point at which you can see an effect of using up the sites, but we never reached that point.

SEITZ: I think I have addressed this comment to you at another time when you gave a talk. In looking at the interaction of something in solution with a solid phase in a lot of these systems, especially in considering things like the possibility of americium reacting with carbonates, and so forth, I think we have to consider that precipitation reactions are going to occur. This is particularly probable when we change pH of solutions over a large range of values. You answer, correctly, I think, in saying that the americium concentrations in your solutions are at 10^{-14} molar, which are extremely low concentrations, but I just want to make the point that we should be very sensitive to precipitation reactions, and I think we need to be more specific about concentrations of actinide elements in solutions and about complexes (for example, the carbonate ions) in solution as well.

BEALL: I agree with you. I think carbonate complexing needs a lot of study to enable us to deal with it correctly.

INFLUENCE OF WASTE SOLID ON NUCLIDE DISPERSAL

M. G. Seitz and M. J. Steindler

Chemical Engineering Division, Argonne National Laboratory
Argonne, Illinois 60439

ABSTRACT

The method most often considered for permanent disposal of radioactive waste is to incorporate the waste into a solid, which is then placed in a geologic formation. The solid is made of waste and nonradioactive additives, with the formulation selected to produce a durable solid that will minimize the potential for dispersal of the radionuclides.

Leach rates of radionuclides incorporated in the solid waste indicate the quantity of radioactivity available for dispersal at any time; but leach rates of stable constituents can be just as important to radionuclide dispersal by groundwater. The constituents of the solid will perturb the chemical character of the groundwater and, thereby, profoundly affect the interaction of radionuclides with the geologic medium.

An explicit example of how the solid waste can affect radionuclide dispersal is illustrated by the results of experiments that measure cesium adsorption in the presence of rubidium. The experiments were performed with granulated oolitic limestone that absorbed cesium from groundwater solutions to which various concentrations of stable rubidium chloride had been added. The results are expressed as partition coefficients [the ratio of the concentration of cesium in the rock (as moles cesium per gram rock) to the concentration in solution (as moles cesium per milliliter of solution)]. Large coefficients indicate strong adsorption by the rock and, hence, slow migration. The partition coefficient for cesium decreases as the rubidium concentration in solution is increased. Because the coefficient for cesium depends on the amount of rubidium in solution, it will depend on the leach rate of rubidium from the solid. Rubidium has no radionuclides of concern for long-term isolation of nuclear waste, so its leach rate from a waste solid is rarely ever reported.

The leaching of other stable alkali metals is also likely to affect cesium adsorption by rock. The adsorption and migration of radionuclides other than cesium are

likewise expected to depend on the concentration at trace levels of other stable constituents from the solid. For example, the adsorption of actinide elements is expected to be sensitive to concentration of lanthanide elements with comparable valence states. It is apparent that a solid waste form needs to be evaluated with regard to groundwater interaction not only using the leach rates of individual radionuclides but also by assessing the solid's total effect on groundwaters that can, ultimately, influence the subsequent migration of leached radionuclides. Therefore, migration data for radionuclides obtained for a specific geologic material may not be applicable if the waste form source of the radionuclides is changed.

The method generally considered for the permanent disposal of nuclear waste is to incorporate the waste into a solid, which is then placed in a geologic repository. That has been the predominant assumption in all of the work that has been discussed at this meeting. The few exceptions in some discussions dealt with disposal in deep sea beds. For geologic disposal, the solid is made of waste and nonradioactive additives, with the formulation being developed to produce a durable solid that will minimize the dispersal of radioactivity and, specifically, isolate the radioactivity from man's environment.

Most people believe that the most credible mechanism for the dispersal of radionuclides from such a repository in a well-chosen geologic site is a fissuring or similar disruption of the repository and the contact of groundwaters with the waste. Figure 1 is my schematic of a breached geologic repository for nuclear waste. The repository itself is depicted by the rectangle surrounding the solidified waste. The groundwaters can leach radionuclides from the waste and transmit them to the surrounding bedrock, where the radionuclides can react with the rock or remain in solution and be carried downstream with the ultimate potential of being returned to man's environment. It is this leaching process and the subsequent interaction of the radionuclides with the rock that determine the dispersal characteristics of the solid waste in the particular repository system. Usually the leaching process and the migration process are treated separately often at separate laboratories, by different experimenters, and experiments. In the discussion and evidence I will show today, I want to make the specific point and present the argument that these two processes should be considered collectively in an evaluation of the waste form as a solid for resistance to the dispersal of radionuclides. I will conclude by discussing some of the experimental methods in which these two processes are combined.

Leach rates of radionuclides from the solid waste indicate the important parameter, quantity of radioactivity as a function of time

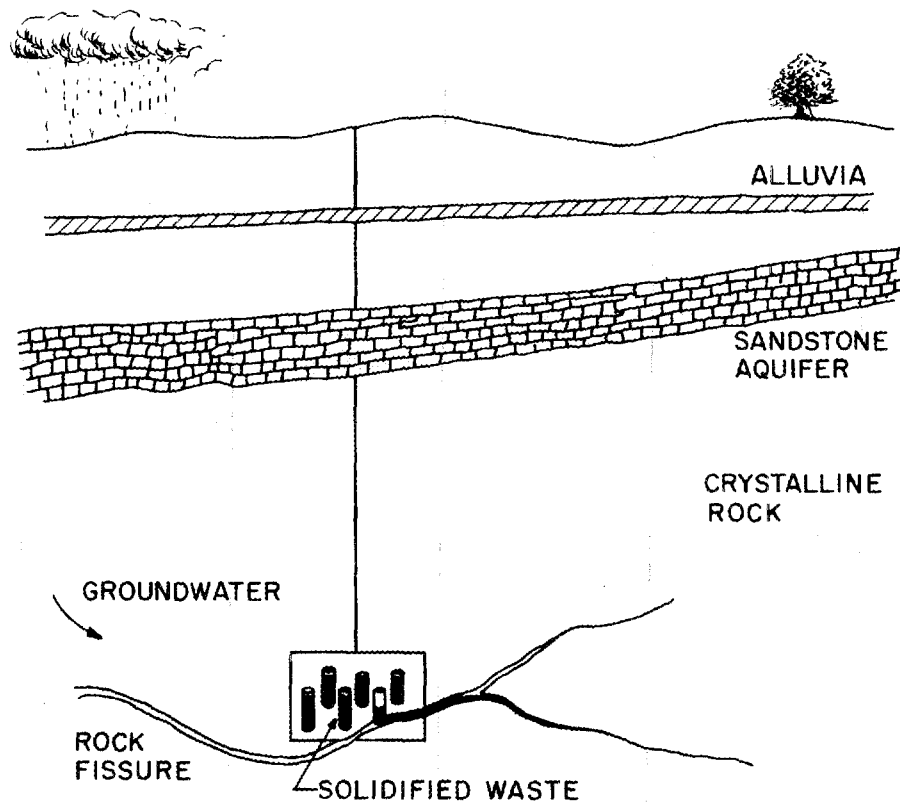


Fig. 1. Schematic of a Breached Repository.

that is available for dispersal. This quantity is the upper limit of radioactivity that is available at any time to an aquifer system and that may be released into man's environment. However, the leach rates of stable constituents of a solid waste can be equally as important to the migration of radionuclides, because of their effect on the composition of the groundwater and thereby on the migration of radionuclides. The dissolved constituents, even though they may be stable and not radioactive elements, can change the chemical character of the groundwater and affect nuclide migration.

I want to give an explicit example of how a potential nonradioactive constituent of a solid waste can affect migration. The evidence comes from experiments in which granulated oolitic limestone adsorbed radioactive cesium from groundwater solutions containing varied concentrations of rubidium that had been added as rubidium chloride. These are very simple batch adsorption experiments of the type shown in Fig. 2; the groundwater solutions are agitated with granulated material (in this case oolitic limestone), for a period of a week or several weeks, after which the solution and the rock solids are separated. The concentration of radio-cesium in the solution and the concentration of radiocesium on the rock are then measured. The results are expressed as partition coefficients in Fig. 3. A partition coefficient is the ratio of the concentration

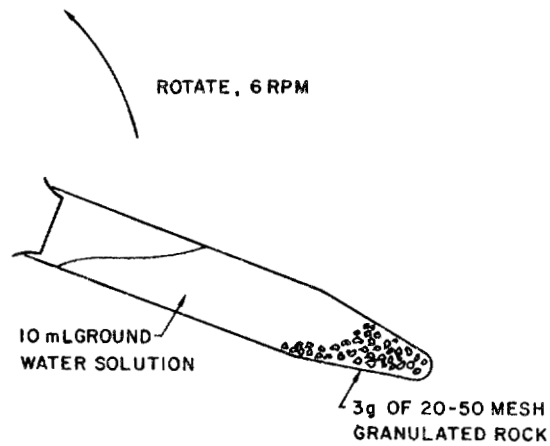


Fig. 2. Schematic of the Arrangement for a Simple Batch Adsorption Experiment.

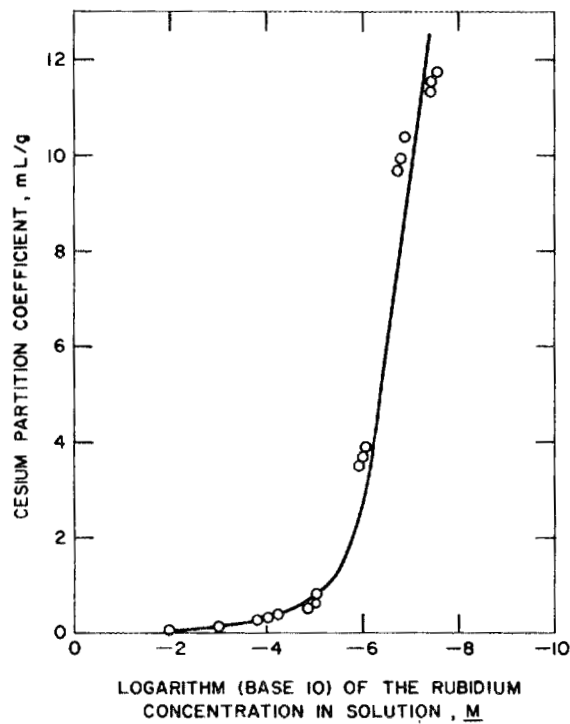


Fig. 3. The adsorption of cesium (and, therefore, the migration of cesium) depends on the concentration of rubidium in solution (which, in turn, depends on the leach rate of rubidium from the waste solid).

of cesium on the limestone to the concentration in solution (moles of cesium for each gram of rock divided by the moles of cesium in each milliliter of solution). In Fig. 3 high partition coefficients mean that most of the radiocesium is adsorbed by the rock, and, therefore, we would predict that the migration rate for cesium would be very low compared with the rate of the groundwater flowing through the geologic material. On the other hand, a low partition coefficient, such as on the left side of Fig. 3, indicates that a lot of the cesium remains in solution and is transported in the groundwater as it moves down stream.

We see a wide variation in Fig. 3, and we also see a very strong dependence of the partition coefficient for cesium as a function of the rubidium concentration at trace levels of rubidium, 10^{-6} to 10^{-8} molar concentrations. I would predict from these results that the cesium migration characteristics would depend on the concentration of rubidium in solution and, therefore, would depend on the leach rate of rubidium from the solid waste form. Rubidium is present in the waste as a fission product and possibly also added during the processing or the solidification of the waste. However, the rubidium does not have radionuclides of concern to safety for long-term geologic disposal. Therefore, the leach rates of rubidium from solid waste forms are rarely ever reported. However, I emphasize that the leach rates for rubidium may be important to the subsequent migration of cesium.

If the rubidium in our waste forms is only a product of fission then we do not have a large concern. The amount of rubidium produced by fission is about one-sixth the amount of fission-product cesium. Therefore, if we assume that the rubidium and cesium have similar leach rates, that they are coming out in proportion to their molar concentrations in the waste form, and that only fission-generated rubidium is present, we would expect relatively small perturbation of the behavior of cesium based on rubidium, and the major behavior of cesium would be dependent on the concentration of cesium itself. In the specific instance, where we are only dealing with fission-produced rubidium, we do not have a concern, but I make the point that we can see very strong effects of a stable element on the adsorption and predicted migration of a radioactive element.

The effect that we see is the result of an exchange process. Cesium is less able to compete for adsorption sites in the presence of higher concentrations of rubidium. In other words, as we increase the rubidium concentration, less of the cesium is absorbed and more cesium moves downstream. This is a fairly typical and easily theorized type of process. In fact, knowing the process, we predict similar behavior for potassium and other alkali metals that may be in higher abundances in wastes than rubidium. Also, we can expect the same process for other radionuclides, in addition to cesium. For example, the actinide elements, which are very strongly adsorbed on materials, are predicted to exhibit adsorption dependent on the concentrations of other elements in solution (particularly lanthanide

ions that have valences and species in solution that are comparable to those of actinide ions). This becomes important, because we see large concentrations of lanthanide ions in waste forms, both as fission products and from processing or formulation of waste solids. Particularly, we are talking this morning about the monazite crystal, which seems to form a very good and durable waste solid; but it is a solid in which the lanthanide ion exceeds the amount of actinide ion generally by a factor of 10. So, if we leach lanthanide and actinide ions in similar proportions, we would get higher concentrations of lanthanides by a factor of 10 and severe interference of the lanthanides with the absorption of the actinides.

We can suggest from this work that important considerations in evaluating waste forms for migration potential of cesium and actinides are the leach rates of alkali metals and of lanthanide elements, even though they are nonradioactive constituents of the waste.

There are ways, other than through competition during adsorption that characteristics of the waste form can affect migration. By the reaction of the solid waste form with the groundwaters, the composition of the waste form may determine the valence of a radionuclide that is leached. The composition of the waste form may determine the chemical species of radionuclides in solution by introducing complexes that may form, perhaps very special, species of radionuclides that are not generally included in adsorption experiments.

Rather than trying to postulate each way that the waste form might affect radionuclide migration and then study each possibility individually, we have taken the approach of actually simulating the leaching and migration processes, and trying to understand the behavior of the leached species in terms of more simple adsorption tests. Figure 4 is a schematic of the apparatus that we have used for what we call leach-migration experiments. Groundwater is made to flow by means of a pump across a solid waste form where radionuclides are leached from the waste these leached radionuclides are transported to geologic material. The material can be either a core of fissured rock or a core of permeable rock. The radionuclides can react with the rock or remain in solution, thereby transported through the rock and collected with the solutions. By analyzing these solutions and cutting up the rock core to analyze where the radionuclides are in the rock, we can determine the migration behavior of solution and waste constituents in the presence of all of the leached species, including all radionuclides and nonradioactive constituents leached from the glass. We then determine if the results indicate behavior that is not represented in results of simple adsorption experiments.

I think you can see the analogy here in the experiment to the breached repository. We are actually simulating the leaching and migration processes. We have elevated temperature of the waste solid to simulate the radioactive heating, and can vary temperature to examine any temperature-dependent migration process. We have

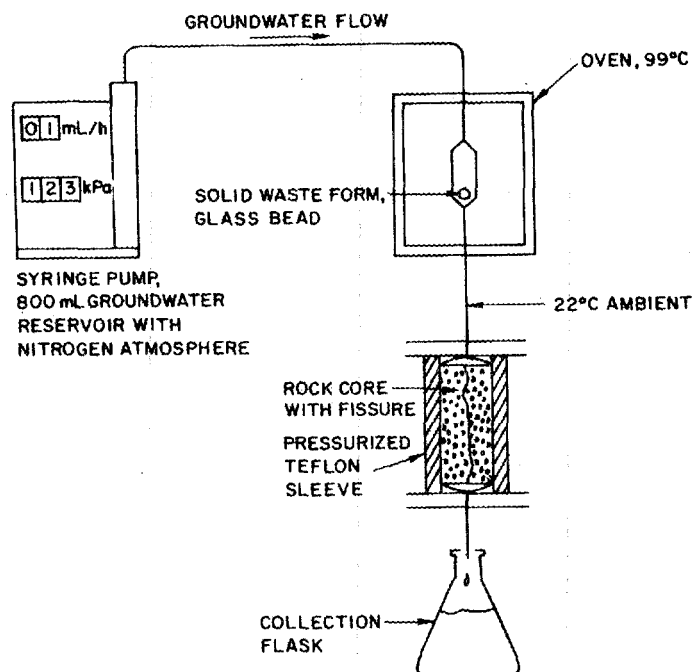


Fig. 4. Schematic of apparatus used in leach-migration experiments. Groundwater stream simulation experiments are of similar design but include more components (engineered back fill, canister, radiation field, etc.) of the repository.

controlled the oxygen, as well as other gases, in the solutions before they are pumped into the apparatus to contact the waste. We are developing the stream-simulation experiment as an elaboration of the leach-migration experiment to include other constituents of the waste repository system: For example, backfill material on each side of the waste solid, a radiation field imposed on the waste solid, etc. are being included in stream simulation experiments. We feel that from these simulations, we can determine if we understand nuclide behavior in terms of basic adsorption or precipitation data. If not, we can then, using simpler experiments, try to understand what reactions have occurred that are important to the subsequent migration of the radionuclides from the solidified waste and through the "surrounding" rock. The experimental simulation approach can be viewed as an evaluation of the waste solid in that the influence of the waste solid on the subsequent migration of leached radionuclides is evaluated as an important property of the waste form.

DISCUSSION

BABAD: Considering that most of the experimentation, due to convenience, is being done at 22 and 90°C, that our repository conditions are going to have an ambient groundwater temper-

ature near 75°C, and that you are going to go into maybe 200 or 250°C in the near field, how are you going to extrapolate the data with the variability of the system that you are working?

SEITZ: I have just shown 99°C as a typical temperature. It is a temperature we can use for experiments without having to pressurize our solutions. We have pressurized solutions, and commonly work at temperatures of 250°C. That is no problem. It is more complicated equipment and so, would have required more description for this talk.

HOWITT: In your final diagram, analysis of your solution following the leaching process seemed to be absent.

SEITZ: That is an integral part of experiments. In contacting solution with waste, we see changes in solution composition that are generated by the waste. For example, when a solution at elevated temperature contacts a waste consisting of borosilicate glass, we expect to find borate, silicate, etc., in solution. Knowing what these changes are is an integral part of these experiments.

HOWITT: So you are measuring all the components?

SEITZ: No, we measure what we can. For example, we see that cesium adsorption is sensitive to cesium concentrations to 10^{-10} molar, and sensitive to rubidium concentrations to as low as 10^{-10} molar. So, we need to measure any concentrations of cesium and rubidium above 10^{-10} molar for a definitive statement about cesium migration. With a radionuclide like cesium-134, for example, we have no problem working in this range. With inert constituents, we do have problems at very low concentrations. We do not routinely measure nonradioactive rubidium, for example, at 10^{-9} molar concentrations. We can do it, but it becomes very time consuming. If we are talking about measuring everything, we obviously have problems. We by no means do everything. We attempt to do what we find is important, and we may certainly be missing things along the way. If we see no unexpected migration behavior in our experiments, we assume that we haven't missed an important constituent.

BOATNER: A point I would like to make is that something like PW-4b contains 35 wt % rare-earth oxides in the waste to begin with, and about 0.35 wt % americium, so it does not really matter what kind of waste form you put this in. If you are looking at dissolution of the waste form, there are going to be approximately 100 times as many rare-earth ions coming out as americium ions, for example. And so, if you put it in something like a rare-earth orthophosphate,

maybe there are three times as many coming out as if you put it in any given waste form.

SEITZ: Right, I think that's true. I was very impressed by what I heard this morning about monazite. I don't know how it behaves and what the subsequent migration characteristics of actinides would be because of its large lanthanide loading. I just merely make the point that these things that are normally considered nonradioactive (such as the nonradioactive lanthanides that are fission products, as you suggest), and that are normally not considered as a problem in long-term geologic storage, might be quite important in evaluating the migration or dispersal characteristics of that waste form.

MACHIELS: You are measuring distribution coefficients and those are ratios of concentration in the liquid and in the solid, basically. When you talk about the water flowing through geologic formations, you have to deal with a tremendous quantity of solid material. I think that what you see now, the effect of the inert materials which are leached from the waste form, will constitute minor perturbations and you will see the effect only very close to the canister. Once your water has traveled some distance away, the amount which is leached from the waste form compared with the ions which are in the soil and so on, will become insignificant.

SEITZ: There are two things to say. One is that we do the simulation experiments I have talked about. For example, results that we got with cesium from these experiments were inconsistent with the results that were reported from simple adsorption experiments of the K_d type. This discrepancy led us to look more specifically at the concentration dependence of cesium absorption and the effect of other alkali metals on the cesium absorption. We were successful at explaining the discrepancy. Therefore, our normal mode of operation at which we have been successful has been to look at very complex systems in these integration experiments and then, when we do not understand something, try to determine what is going on. So we are looking at a complex situation rather than simply at distribution coefficients, as you say.

Secondly, what you say about rock is possibly true; you might say that the buffering capacity of a geologic system is potentially enormous. You are talking about a relatively small package in an enormous body of material, and if you go out 1 or 2 km in distance, you can make an assumption that the buffering of the geologic system has worked and that the groundwater is back in composition to where it used to be. But the radionuclide addition is a perturbation

just like the stable element addition is. Which perturbation dies out first? We agree that the addition of stable elements can affect radionuclide migration close to the repository, maybe within a kilometer or two. But if we do not recognize and understand these effects, experimentally, we have a very difficult time making a valid and substantial argument as to what might happen in a breached repository. We have a difficult time arguing at what distance from the repository the perturbation of radionuclide dies out. So, I consider the entire perturbation of the waste form on the groundwater system. When we deal with elements like technetium, for example, that are totally absent in nature, there must be a prolonged perturbation on the groundwater composition. It may extend out to hundreds of kilometers if it is not strongly adsorbed, so I think you can always find the perturbation; it is a question of whether that perturbation is important or not.

Notice

The work represented in this article was conducted for the Department of Energy under the Battelle Northwest Laboratories, Office of Nuclear Waste Isolation, Subcontract #38139-AK.

HIGH LEVEL WASTE FIXATION IN CERMET FORM

E. H. Kobisk, W. S. Aaron, T. C. Quinby, D. W. Ramey

Solid State Division, Oak Ridge National Laboratory*
Oak Ridge, Tennessee 37830

ABSTRACT

Commercial and defense high level waste fixation in cermet form is being studied by personnel of the Isotopes Research Materials Laboratory, Solid State Division (ORNL). As a corollary to earlier research and development in forming high density ceramic and cermet rods, disks, and other shapes using separated isotopes, similar chemical and physical processing methods have been applied to synthetic and real waste fixation. Generally, experimental products resulting from this approach have shown physical and chemical characteristics which are deemed suitable for long-term storage, shipping, corrosive environments, high temperature environments, high waste loading, decay heat dissipation, and radiation damage. Although leach tests are not conclusive, what little comparative data are available show cermet to withstand hydrothermal conditions in water and brine solutions. The Soxhlet leach test, using radioactive cesium as a tracer, showed that leaching of cermet was about X100 less than that of 78-68 glass. Using essentially uncooled, untreated waste, cermet fixation was found to accommodate up to 75% waste loading and yet, because of its high thermal conductivity, a monolith of 0.6 m diameter and 3.3 m-length would have only a maximum centerline temperature of 29 K above the ambient value.

Processing employed to fix wastes as solid cermet begins with the dissolution of waste and predetermined additives in a mixture of nitric acid and urea or in urea alone. Urea causes nearly every component in the waste to be dissolved with the exception of silica and high-fired actinide oxides (even zeolites are dissolved). Because cermet is a combination of tailored ceramic components (aluminosilicates, titanates, phosphates, etc.) microencapsulated in a continuous, compounded metal alloy matrix, the process makes use of hydrogen-reducible cations

*Research sponsored by the Division of Waste Products, U. S. Department of Energy, under contract W-7405-eng-26 with the Union Carbide Corporation.

in the initial dissolution step to assure correct formulation of the metal matrix. Similarly, additives correctly and quantitatively form the insoluble ceramic (mineral) species with fission products and other radioactive and stable materials.

Spray calcination of the solution (slurry) results in simultaneous destruction of contained nitrate (and urea) to form innocuous gaseous products and metal oxides of approximately 5- μ m diameter or larger (depending upon the urea-to-nitrate ratio). Because urea forms a reducing calcination environment, little or no volatilization of radioactive species occurs, e.g., Ru. Extrusion or other methods of compaction of the subsequent calcine, using water as a binder-lubricant, and liquid phase sintering of the compacted product in a reducing atmosphere produces a high density monolith.

It should be noted that none of the technologies used in the cermet waste fixation process are new and all are comparable to similar processes necessary to achieve the preparation of other candidate HLW forms, e.g., Synroc, tailored ceramics, coated particles. To date, real Thorex waste from Nuclear Fuel Services and real sludge and acid wastes from the Savannah River Plant have been successfully converted to cermets using in-cell batch processing.

INTRODUCTION

The ORNL cermet program is of relatively recent origin (about two years) and has resulted from an adaptation of technology developed for preparing ceramic reactor neutron dosimetry materials. Cermet preparative technology employs urea homogenization of preselected chemical components and waste with subsequent physical forming of the resultant ceramic materials.

In Figure 1 are shown very small capsules of vanadium into which ceramic or metallic "wires" are inserted; the resultant encapsulated materials are used in the core and blanket regions of reactors to determine fluence, neutron energy and other neutronic properties. Such dosimeters were developed in support of FFTF, EBR-2, and other fast reactor characterizations. Whatever waste storage form is considered, it must be compatible with very hostile environments. This is especially true from a radiation damage point of view because high levels of radiation will be present which arise from the contained wastes. The ceramic dosimeter materials, described above, are known to resist degradation in very high level radiation fields for long time periods and therefore a similar waste form should equally resist damage or degradation.

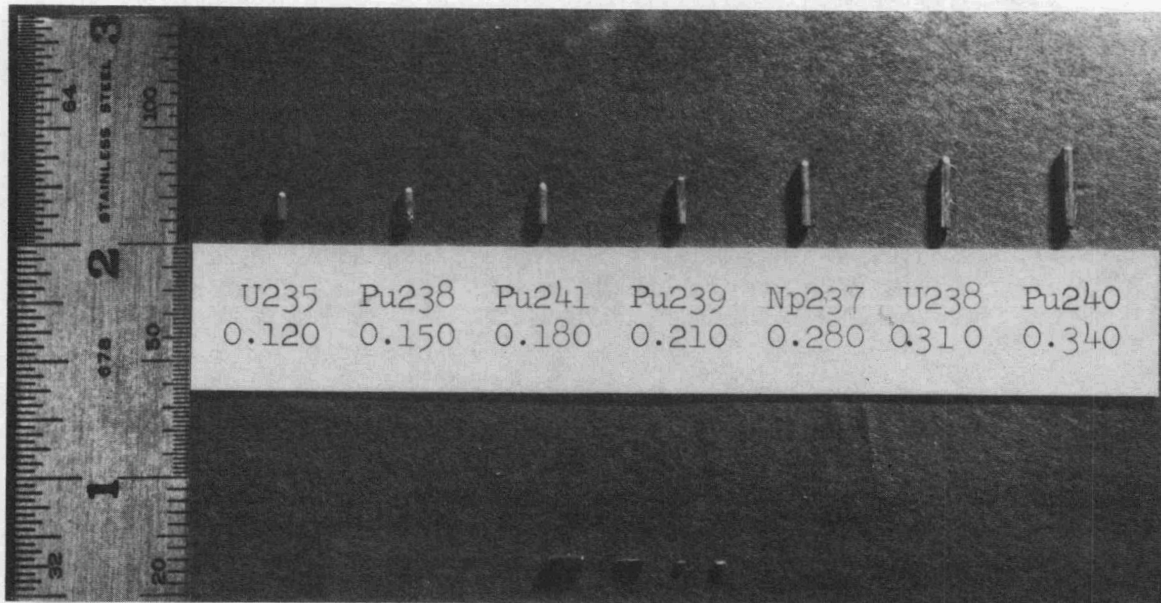


Fig. 1. Neutron dosimeter capsules (1.25-mm diam) containing ceramic "wire" isotope oxides.

Figure 2 illustrates samples of ceramic wires used for reactor dosimetry (inserted in capsules illustrated in Figure 1). These materials are exceedingly homogeneous such that over a length of 10 m the variation in chemical composition is less than 0.05% of the mean value. In Figure 3 is a view (through a glove box window) of an extrusion die; extruded material at the end of the die is pure $^{244}\text{Cm}_2\text{O}_3$ together with a binder material. At the bottom of Figure 3 is shown the extruded sample before and after sintering; it can be seen that shrinkage occurs during sintering by comparison with the physical size of the "green" material (left). In this case the original extrusion was dimensionally formed such that upon sintering shrinkage would result in a dimensional piece exactly fitting into the opening in the illustrated metal holder (center). There is approximately 700 milligrams of material in each $^{244}\text{Cm}_2\text{O}_3$ ribbon. After two years, the sintered material has remained in the same physical form as it was after preparation; this fact illustrates the ceramic's resistance to radiation damage.

With regard to the fixation of waste, the same process as described for dosimetry materials preparation was used as the basis for the preparation of the cermet waste form. Initially all materials are dissolved or slurried in a urea or urea-nitric acid solvent. The urea dissolution process has been used in preparing pure oxide materials, homogeneous oxide mixtures, and metal-ceramic mixtures; this latter combination is the chosen form for the cermet waste form. By urea dissolution, hydrogen-reducible metals can be mixed on an atomically homogenized basis. In addition, simultaneous formation of

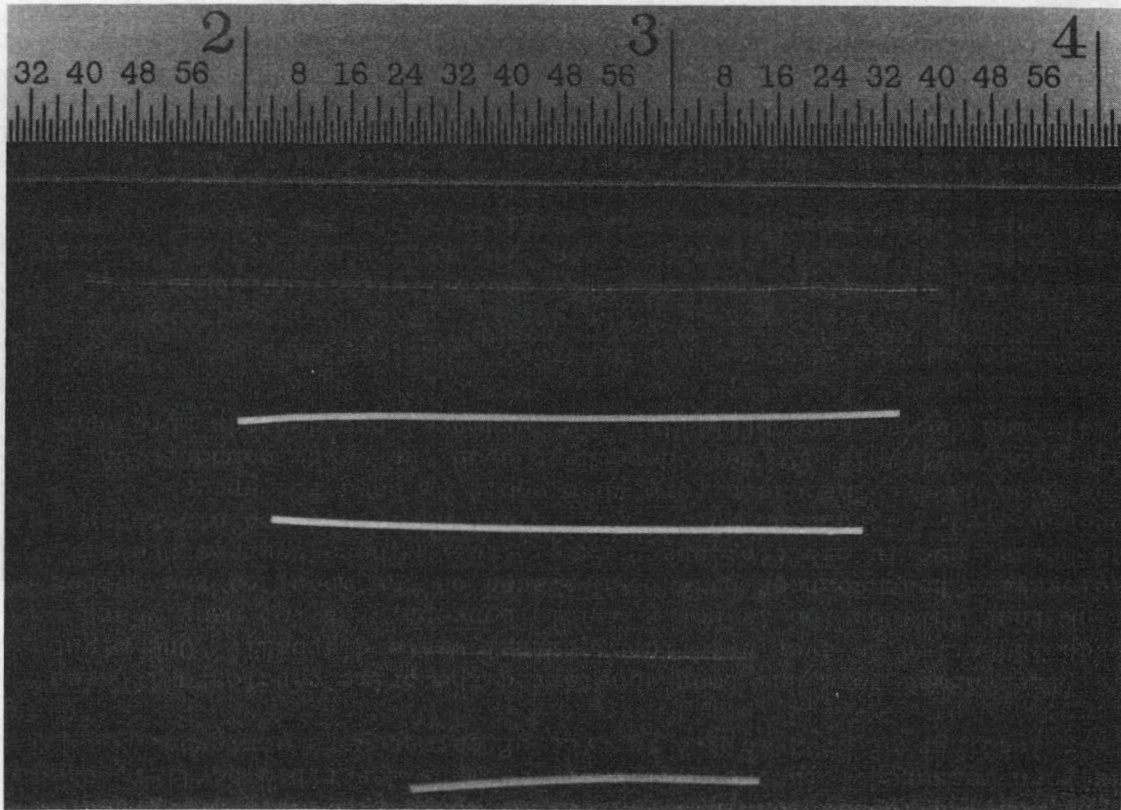


Fig. 2. Ceramic "wires" of dosimeter materials formed by extrusion and sintering of urea-precipitated cations. From top to bottom: Mn, 0.1 wt. % Co in MgO, Sc_2O_3 , UO_2 , 16 wt. % ^{61}Ni in MgO. Wire diameter: ~ 0.5 mm.

ceramic phases occur to make the cermet waste form. Monazite forms, described earlier by Marvin Abraham, and the Synroc forms as described by John Tewhey can and have been made by this process.

The cermet waste form consists of multimicron-size particles of insoluble ceramics distributed uniformly in a metal alloy matrix which is tailored specifically to achieve compatibility of the waste form with storage environments. The metal matrix is derived primarily from waste components, remembering that there is much iron in many of the wastes that now exist. Chemical additions at the head end of the process (dissolution) are designed to optimize both the ceramic and alloy compositions so that highly insoluble ceramic compounds are formed from some waste components and others are eventually converted into the desired composition of the alloy matrix.

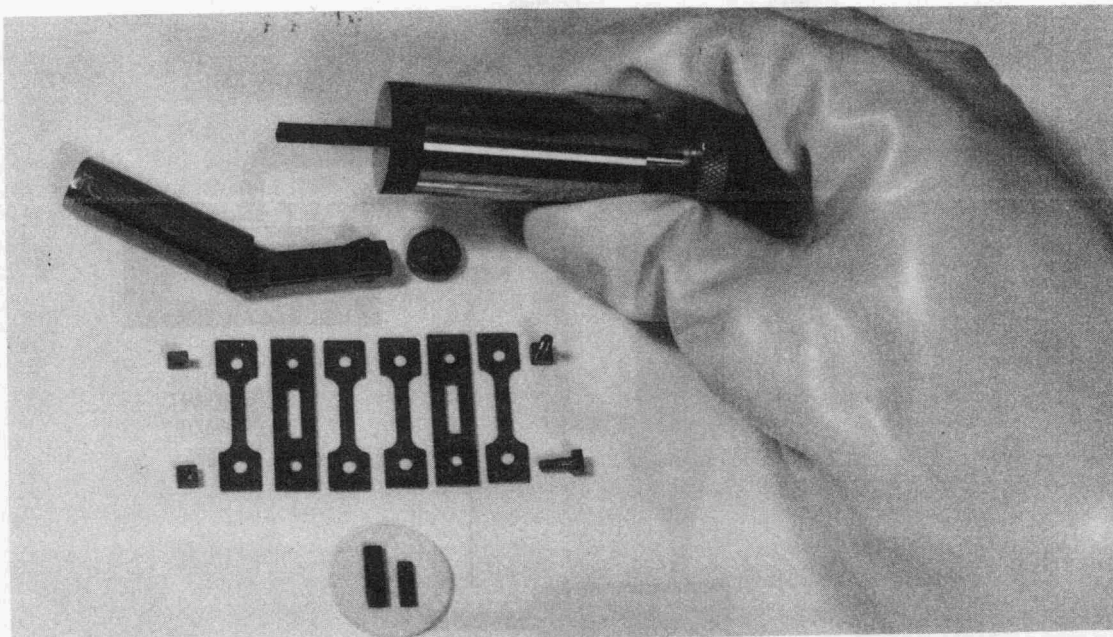


Fig. 3. Extrusion of $^{244}\text{Cm}_2\text{O}_3$ using a wax binder. "Green" and sintered samples are shown at the bottom. Size of sintered material exactly fits the slot in the metal frames (center).

CERMET PREPARATIVE PROCESSES

Generally, the urea process is relatively simple. Waste is added to the urea solvent and is dissolved; if zeolites are present they are totally dissolved, which offers a unique method of homogenization of most waste components. It should be noted that although urea is an excellent solvent, high-fired plutonium oxide and silica are not dissolved by urea treatment. The next step in the cermet process is to spray-calcine the solution or slurry to obtain dry, homogeneous mixed oxides. Finally the mixed oxides are densified by some method. As shown in Figure 4, continuous extrusion is the suggested method of densification where a continuous process (as versus a batch process) is desirable. Also, Figure 4 indicates that the use of liquid-phase sintering in a reducing atmosphere, below the combustion limits of the reductant, is proposed to derive the high density cermet waste form.

Schematically, (Figure 4) the process uses a dissolution vessel into which waste, urea and additives are mixed. This process is not dissimilar to many dissolution processes that are used in other waste form preparations. The resulting solution or slurry is subsequently fed into the spray calciner. This injection step is quite different from standard processes because the urea solutions are more viscous

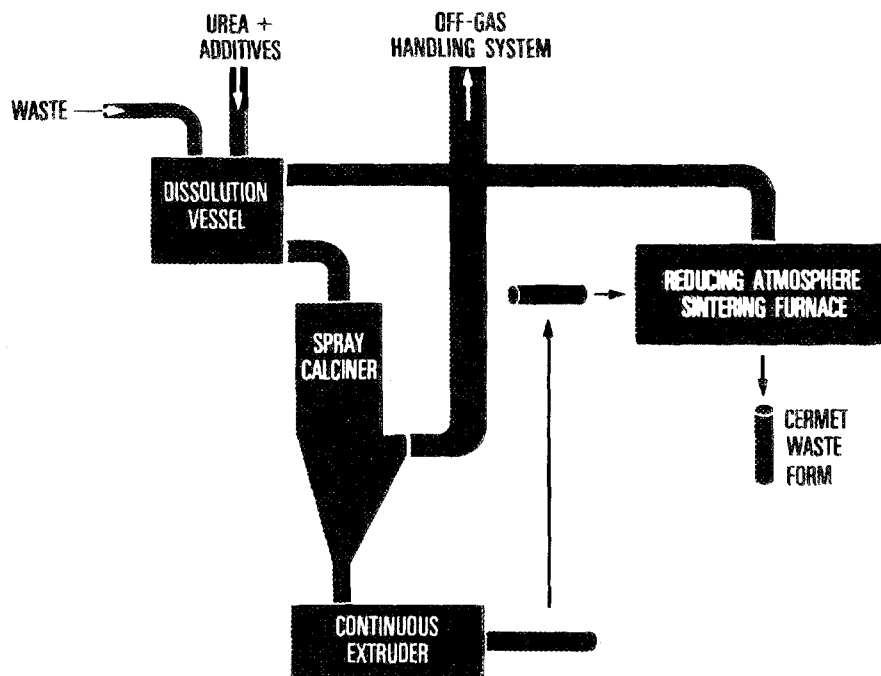


Fig. 4. Flowchart of the continuous cermet waste form process.

than aqueous solutions. In the calciner a chemical reaction takes place such that the centerline temperature of the calciner is maintained nearly the same as the wall temperature. Following calcination, the product is put through a continuous extruder and then into a reducing-atmosphere furnace. To obtain the product monolith, a reducing-atmosphere furnace is required to convert all oxides that are hydrogen reducible to their respective metals so that an alloy is formed in which microencapsulation of the ceramic phases is achieved.

Spray calcination is advantageous because it has inherent high material throughput. In the continuous spray calcination mode, a one-to-one mole ratio of urea-to-nitrate ion is used to obtain a uniform and rapid chemical reaction rate. In the end, innocuous off gases result; volatilization of radioisotope species is very minimal, if it occurs at all, in this process. It has been shown that only 0.0024% of the cesium content of the starting material is lost during calcination and that none of the ruthenium and technetium are lost. Because of the presence of urea, the system is chemically reducing in nature, and it is of interest that after the end of the spray calcination, reduced metals have been observed in the product.

Since urea solutions are more viscous than most aqueous solutions, a special injection nozzle was designed with a geometry to attain uniform atomization of the viscous fluid; this nozzle is called an ultrasonic injector. Illustrated in Figure 5 is the actual subtended solid

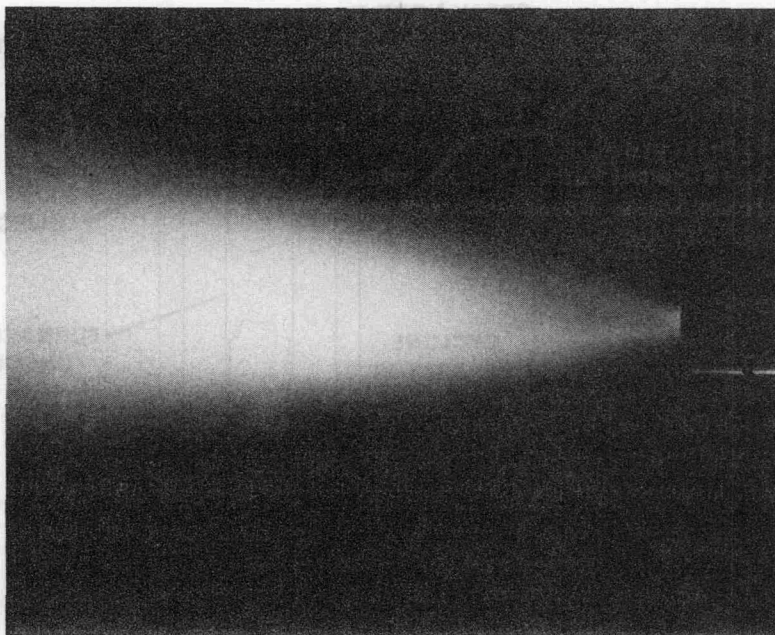


Fig. 5. Injection spray geometry in the continuous calciner.

angle of the spray from the injector nozzle. In practice the cross section of solid injection angle remains less than the diameter of the calciner until calcination is complete. As a result, at a calciner wall temperature of about 800°C , no material buildup occurs on the walls. In the calciner a chemical reaction takes place simultaneous with calcination, and, in this system, the centerline temperature is maintained at the same level as that of the wall because of the exothermic reaction. A centerline temperature of 800°C was measured.

In Figure 6 the entire calcination system is represented. At the top of the 23-cm-diam calciner the spray nozzle is mounted on a flange. Injection air enters the nozzle and forces the urea solution into the inconel-lined furnace. At the exit port of the calciner, a cyclone separator is used to collect the product such that only 0.5% to 1.5% of the total product material passes the separator. Because the resultant calcine is highly magnetic, magnetic collectors for the fines are now being developed. Calcine cooling is necessary preceding magnetic collection so as to remain below the curie points of the magnetic components; such cooling is achieved in the section (Fig. 6) labeled "Baffle Collection Chamber." Continuing development of this portion of the operation can eliminate or at least significantly reduce material collection on the absolute metal filters at the end of the system.

In the spray calciner, no noxious gaseous effluents are generated, as shown in Table 1; in fact, easy disposal of product gases result. The highest oxidation state of nitrogen in the off-gas is the compound NO ,

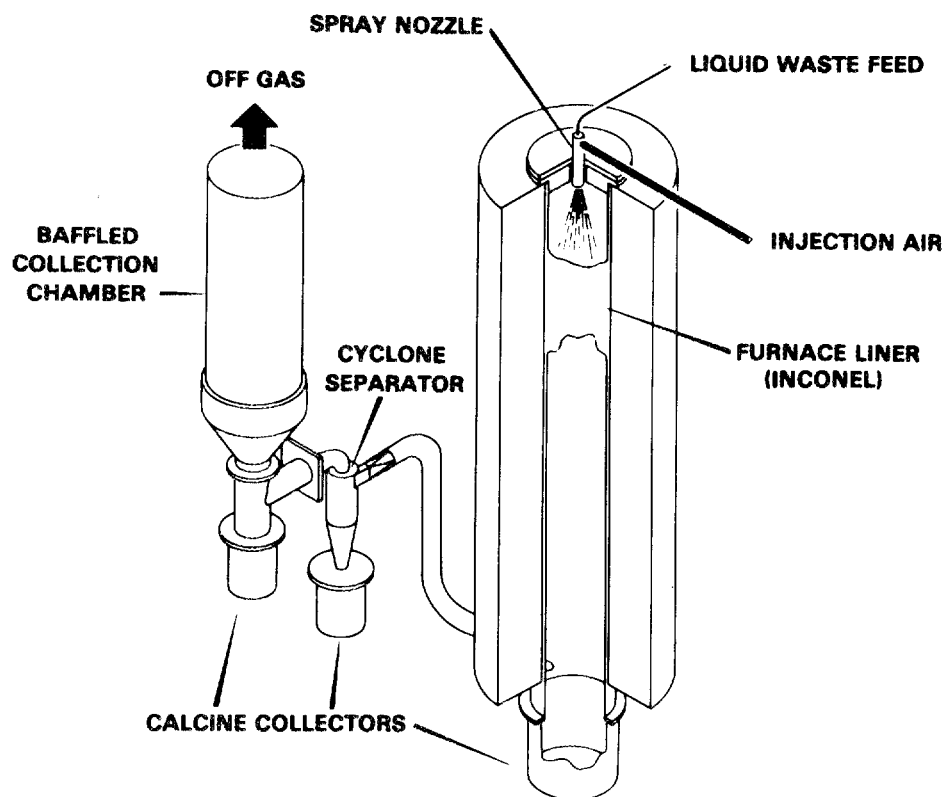


Fig. 6. Schematic representation of the spray calciner and calcine collection systems.

TABLE 1. TYPICAL OFF-GAS COMPOSITION OFFERS NO DISPOSAL PROBLEMS

N_2 and/or CO^*	75.09%
H_2O^*	11.95%
CO_2 and/or N_2O	2.56%
O_2	9.39%
NO	0.77%
H_2	0.17%
NO_2	<0.09%

* CO <0.43%, NH_3 not detectable.

and very little of this species is present. Most important is that ammonia gas is not generated.

With regard to the liquid-phase sintering portion of the cermet process, a simplistic phase diagram, Figure 7, illustrates two possible traverse routes. During normal reduction the temperature is raised and held at about 800°C until reduction is complete. In the subsequent sintering step the temperature is raised to an appropriate level. The total process requires about 24 hours. A preferential traverse route is illustrated in Figure 7 during which rapid heating causes the mixed oxides to cross into the liquidus portion of the phase diagram resulting in some melting of the composite material. By this path, a much improved density of the material results with the void volume being markedly reduced. In Figure 8, using conventional sintering, the time-temperature curve extends over a period of 24 hours. Using liquid-phase sintering, the comparative curve shows not only that the maximum required temperature is decreased, but the process time is reduced to only two hours to form the sintered body. This is not only a significant time improvement, but it represents an even more important reduction in power consumption. In addition, liquid-phase sintering enhances cermet densification even though the maximum temperature is between 1050°C and 1100°C.

A SEM photomicrograph of a conventionally-sintered sample of real Nuclear Fuel Services acid Thorex waste cermet is shown in Figure 9. The ceramic bodies (white) are distributed in the metal matrix and are primarily thorium. The darker portions are voids which result in a poor density body. In contrast, the cermet prepared from fresh acid waste (from Savannah River) using the liquid-phase sintering process for densification is illustrated in Figure 10. As before, the ceramic phases

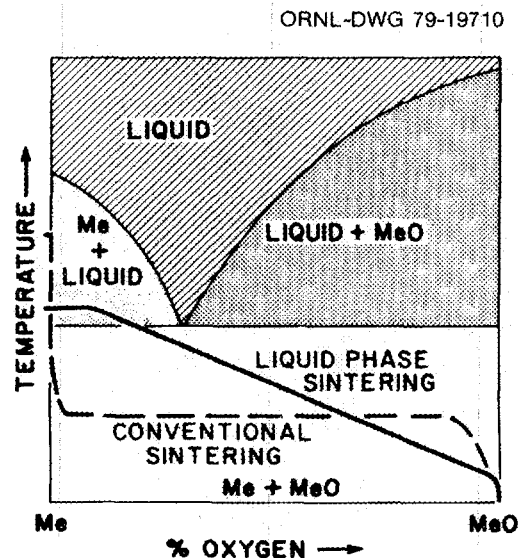


Fig. 7. Liquid phase sintering contrasted with conventional reduction and sintering.

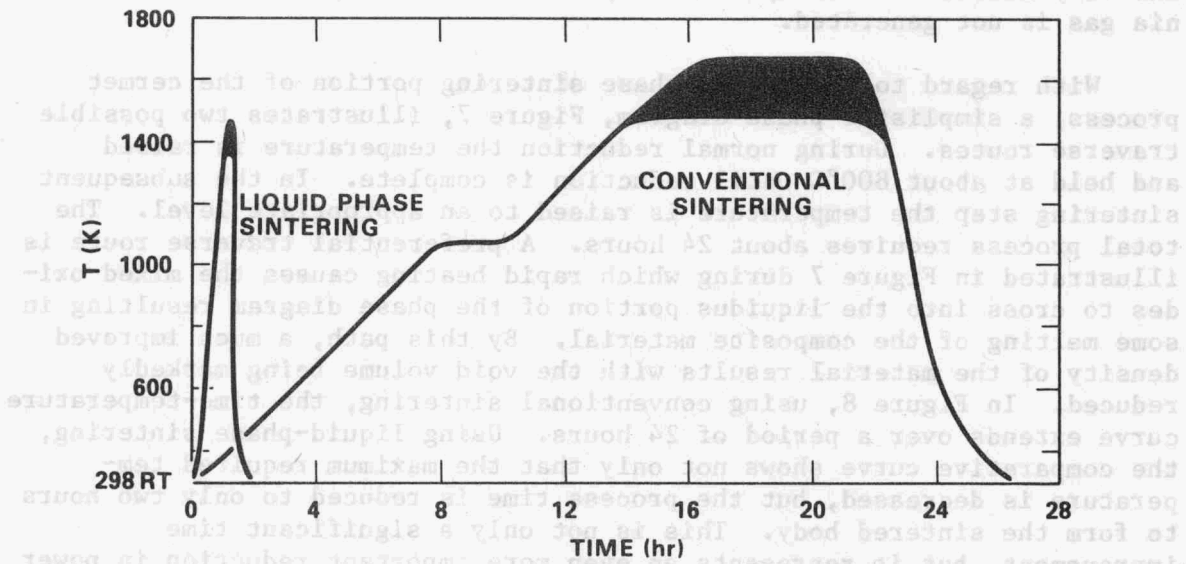


Fig. 8. Comparison of temperature-time relationships between conventional and liquid phase sintering methods.

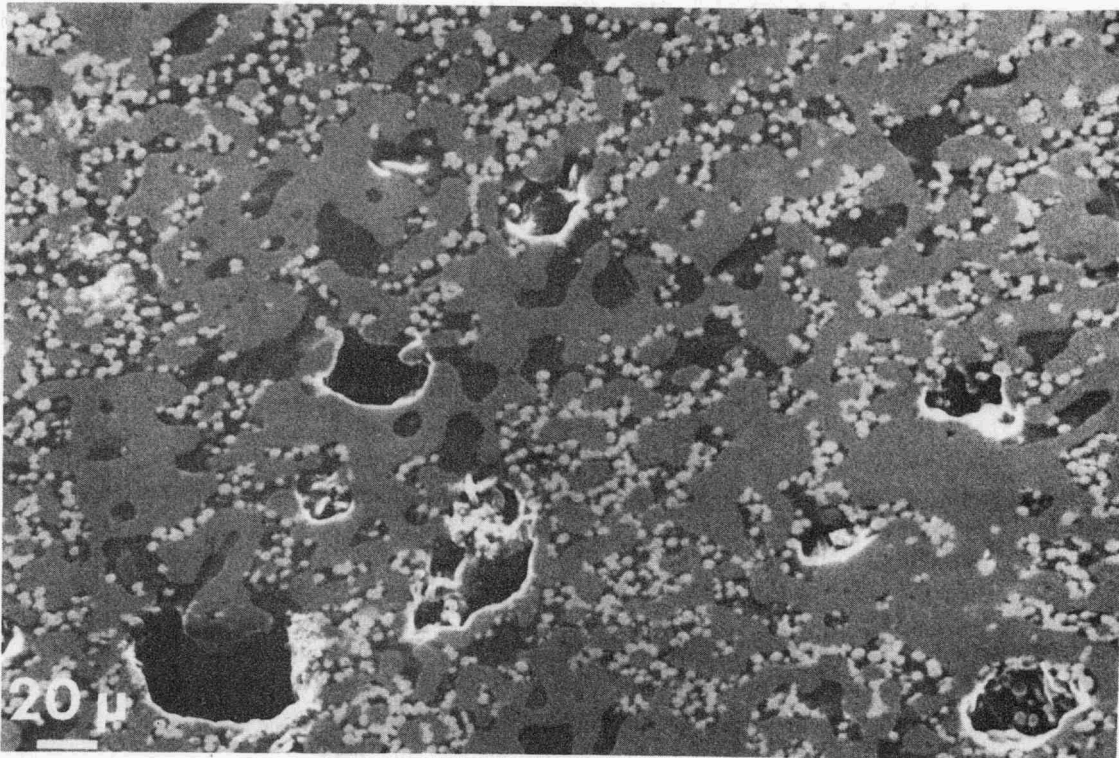


Fig. 9. Real Thorex waste cermet formed using conventional sintering techniques. White particles are mainly ThO_2 ; gray areas are the metal matrix; darker gray areas are voids.

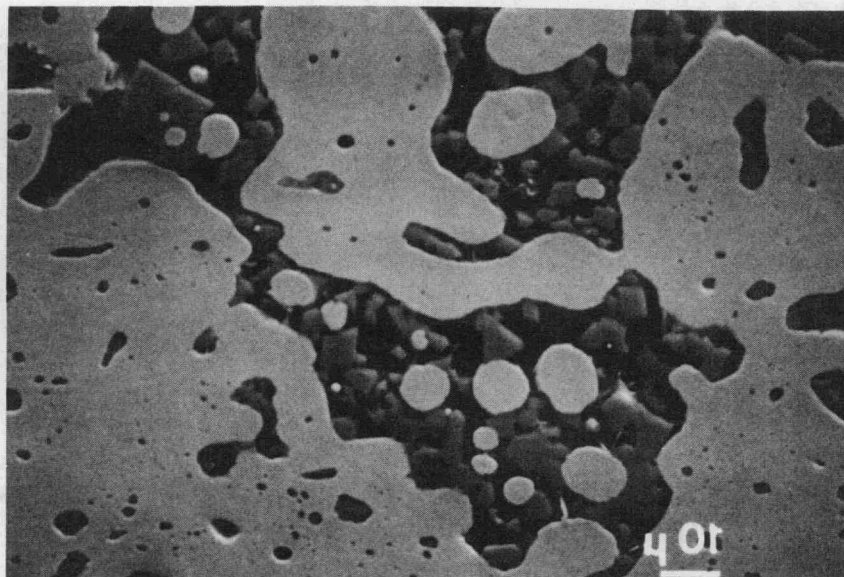


Fig. 10. Real acid, untreated waste (Savannah River Plant) in the cermet form produced by liquid phase sintering.

are uniformly distributed, but in this latter case voids are few in number, and the density of this cermet has increased to levels approaching 95 to 98% of theoretical.

It should be emphasized that both Figures 9 and 10, illustrate cermets prepared from real waste material. These cermet bodies were produced over a year ago, and the samples are still in existence and remain physically unchanged. Generally the worst case of waste fixation would be using fresh commercial waste (with regard to radiation damage).

Examples of cermet materials that have been made are shown in Figure 11; these are not real waste cermets. At the left of the figure is a "green" extruded rod of cermet (black). This extrusion was produced using a wax binder, (which is no longer necessary). After sintering, the extruded rod was converted to the metallic form shown directly below the black extruded rod. To the right of the figure is shown a hot-pressed pellet of cermet. In both cases the cermets contained a 50% waste loading.

The cermet process has significant advantages over other waste fixation methods, inasmuch as the unit processes use existing technology; indeed all unit processes noted have been used in hot cell facilities. The urea treatment offers a very low loss of radionuclides during processing. There is no material buildup on the calciner walls, because the exothermic reaction during calcining causes the centerline temperature to be approximately equivalent to the wall temperature.



Fig. 11. Extruded "green" and sintered cermet (left) and hot-pressed cermet. Wax was used during extrusion.

The maximum process temperature is only about 1100°C, and that value is reached in the sintering system. The process is compatible with many wastes. To date, in addition to wastes already described, INEL calcines (both the high-alumina and high-zirconia calcines) were dissolved in urea with no difficulty and eventually resulted in good cermet bodies. Generally, the cermet process seems to be less complex than the processes designed for Synroc and coated ceramics. If errors in processing were to occur, the resultant calcine or cermet could be dissolved in acid, for example, and returned to the head-end of process. Since less than combustible levels of CO or hydrogen are used in the reduction process, no explosion hazards would be encountered. Finally, the maximum temperature in the entire process is only 1100°C (liquid phase sintering).

CERMET FORMULATION AND CHARACTERIZATION

Cermet formulations have been varied over a range of waste loadings, from 2 to 75 wt. %. Waste volume reductions of 1-to-1 to 100-to-1 have been achieved. It should be noted that volume reduction as quoted is not measured from sludge containing water to the final cermet volume but rather from dried starting material to the cermet form. Ceramic phase loading varies between 20 and 50 wt. %; it can be

increased, but the resultant cermet loses physical strength. The metal phase loading is the reverse of the ceramic phase concentrations: 50 to 80 wt. %; the metal phase composition (by weight) which has been most frequently used is 70 parts iron, 20 parts nickel, 5 parts copper, and 5 parts other reducible metals originating in the waste.

There are many reducible species in the waste that enter the metal phase of the cermet, e.g., technetium and the platinum metals. All hydrogen-reducible species will become part of the metal phase of the cermet. Assuming the waste does contain a large amount of iron, the iron is used to achieve the final metal matrix formulation. Since the nickel concentration in most wastes is low, some nickel must be added. However, the nickel additive could be obtained from DOE contaminated stockpiles of about 1600-2600 metric tons which presently cost the government a considerable expense because of storage fees. For all intents and purposes, this nickel stockpile is free. If all of the waste in the tanks at Savannah River, as of January 1980, was converted to cermet, only one third of all the stored contaminated nickel would be consumed in the process. For the iron component, most any scrap material could be used at low cost (assuming little or no iron is in the waste initially). Copper is very expensive but, again, in the same contaminated metals repository with the contaminated nickel, are large quantities of contaminated copper. Far more copper is in storage than would ever be used if all wastes were converted to cermet.

Cermet, being a metal matrix material, has extremely high density: 6 to 8.2 g per cc. Variation in density results because of the weight loading of the ceramic phase. The alloy composition that has been most frequently used is an iron-nickel base alloy; it is well known that such alloys are very compatible with brine environments at elevated temperatures. Similar alloys are used in commercial salt solution processing at temperatures up to 350°C, e.g., Hastelloy. Basically, the composition of the cermet matrix is 70% Fe - 25% Ni - 5% Cu, a Hastelloy-like formulation without the prescribed molybdenum component.

The thermal conductivity that can be attained using formulations as described above approaches that of Hastelloy, except that some decrease in conductivity occurs because of the occluded ceramic phase. Even at maximum loading, however, the thermal conductivity is extremely high, and, at lesser loadings, values of about 230 watts meter/degree C has been measured. In the real waste cermets described earlier, thermal power loadings of 0.02 to 0.2 watt/cc of cermet were achieved.

The cermet form has been considered the prime candidate if deep space injection is ever used for terminal waste disposal. One might think that this option is not a viable concept, but for many years radioactive heat sources have been placed on the moon, on the bottom of the ocean, and in orbiting space satellites. These sources are all encapsulated. Strontium-90, ^{238}Pu , ^{244}Cm , and other radioisotopes have been used. The waste form that would be used for space injection really is not very dependent upon the waste composition (radiation damage susceptibility, for example) but depends more upon

the physical characteristics necessary should a mission abort and a 10-ton sphere containing the waste returns to earth. To maintain physical integrity under such conditions a very high-strength body would be required. Indeed, cermet meets this requirement. Similarly, minimal oxidation and dispersion upon re-entry is of vital importance. Experimentally, a cermet containing PW-4b waste at temperatures up to 500°C in air for 8 hours was found to only form a 2- μm thick, adherent oxide layer. Another sample taken to 800°C for two hours, formed a 5-7 μm -thick oxide layer. After three thermal cycles to 900°C followed by immediate quenching in water, SEM examination showed no microcracking or dispersion of any kind. The deep space disposal of waste scenario is illustrated in Figure 12.

Cermet samples were sent to Pacific Northwest Laboratories (PNL) for leach evaluation. The results of these tests, on samples that were certainly not of as good a quality as those now being made, showed a leach rate of 7.1×10^{-6} g/cm² day by total weight loss and 7.2×10^{-5} g/cm² day by measured cesium loss. No ruthenium loss was observed. Remembering that ruthenium is in the metal matrix phase of the cermet, this is a particularly interesting result in that ruthenium is uniformly distributed all over the surface and yet does not leach. One would conclude that the metal alloy is not dissolving or dispersing

ORNL PHOTO 3466-80

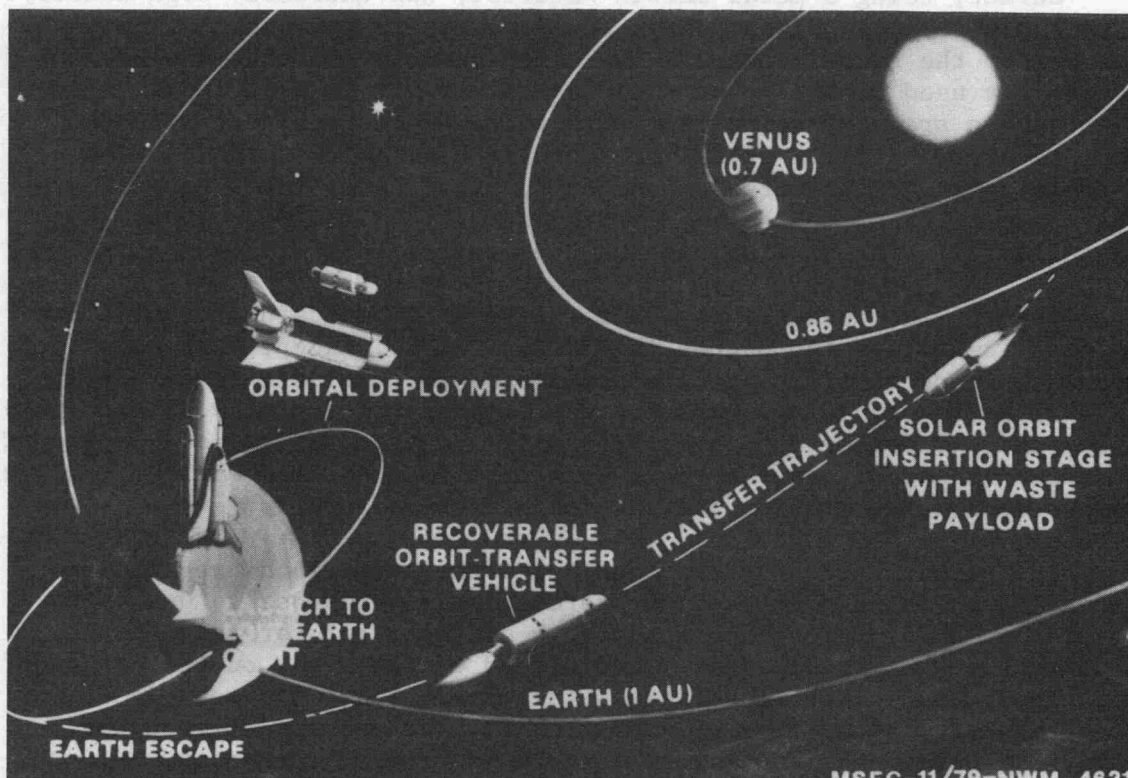


Fig. 12. Space disposal of nuclear waste.

under oxidizing conditions. The test reported above was a Soxhlet test of 72-hour duration. Comparable tests on 76-68 glass, reported earlier by PNL, gave a total weight loss of $90 \times 10^{-4} \text{ g/cm}^2 \text{ day}$.

In Figure 13, a hot-pressed cermet sample is shown after leaching in a 146-day IAEA test at 25°C. Although the appearance of the surface would indicate severe corrosion, this is not the case. The corrosion products resulted from oxidation of the stainless steel basket into which the cermet was placed during the test; the stainless steel dissolved by galvanic action and subsequently deposited on the cermet sample. In Figure 14, a cross sectional view proves that the cermet was not attacked on the surface of the sample. In another case the sample was subjected to the PNL standard hydrothermal test in brine at 350°C and 1550 psi. Figure 15 shows the results of this test. No stainless steel basket was used in this case, but rather a plastic container was used to hold the sample. In the illustration it is evident that a mild

ORNL PHOTO 1265-79

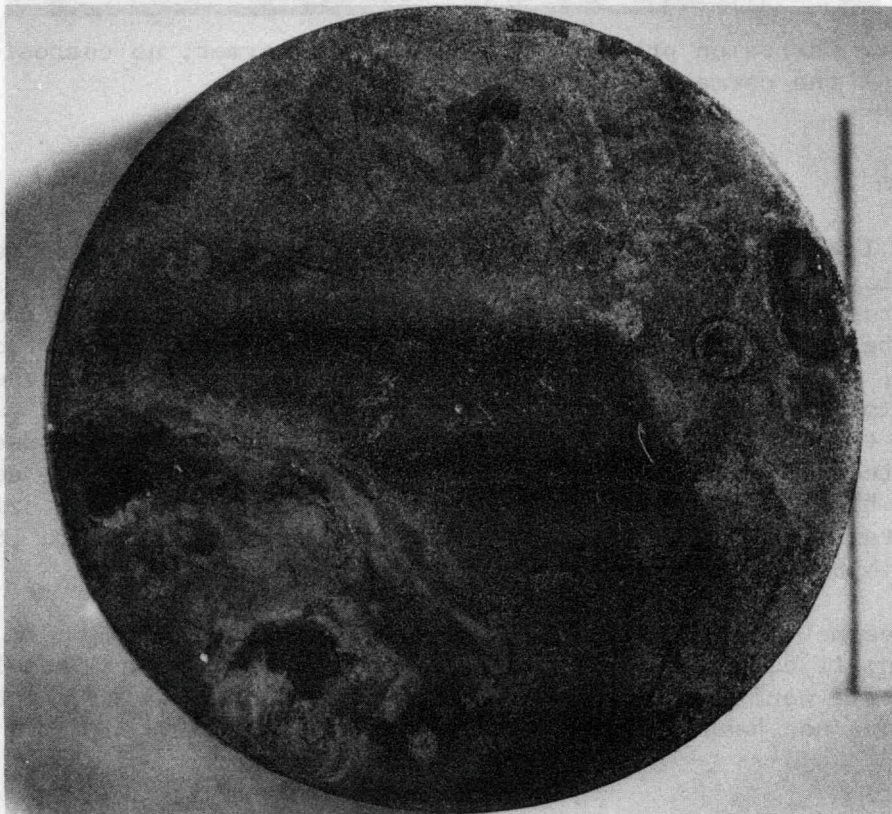


Fig. 13. Hot pressed cermet sample after IAEA leach test at 300 K for 146 days. Corrosion products arose from dissolution and deposition of the stainless steel sample basket.

SURFACE DEPOSITION PNL 146 day

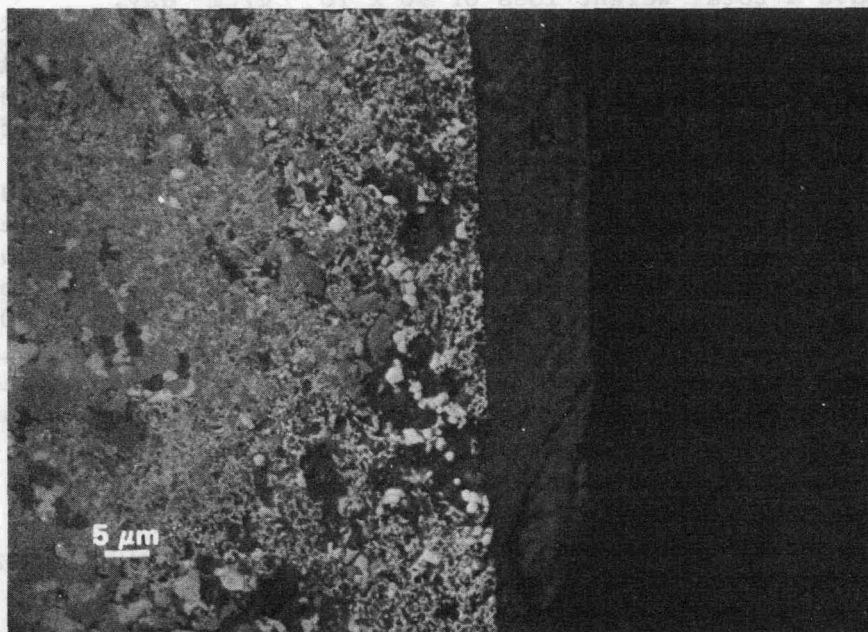


Fig. 14. Corrosion products deposited onto cermet; no corrosion of the cermet is observable.

oxidation layer was formed on the surface of the cermet. This very adherent layer could not be removed except by abrasion. Figure 16 shows a cross section of this sample; the adherent oxide layer was found to be about 5 microns thick. In the interior of the surface artifacts, the thickness of corrosion is observed to be about the same. The most important aspect of these results is that the ceramic particles in the oxidized layer are adherent and have not been caused to disperse because of local oxidation. It would appear that the cermet system is highly resistant to dispersion even after corrosive oxidation of the metal matrix. Incidentally, the sample shown in Figure 16 is of synthetic NFS Thorex waste.

The cermet alloy matrix is highly resistant to corrosion or galvanic action; if coupled with metals like copper or stainless steel, those latter metals would preferentially dissolve. All possible galvanic couples have not been measured as yet, but such measurements are in progress.

SUMMARY

Cermet is not a fully-developed waste form and improvements can be made. Parametric refinements to the unit processes themselves can be

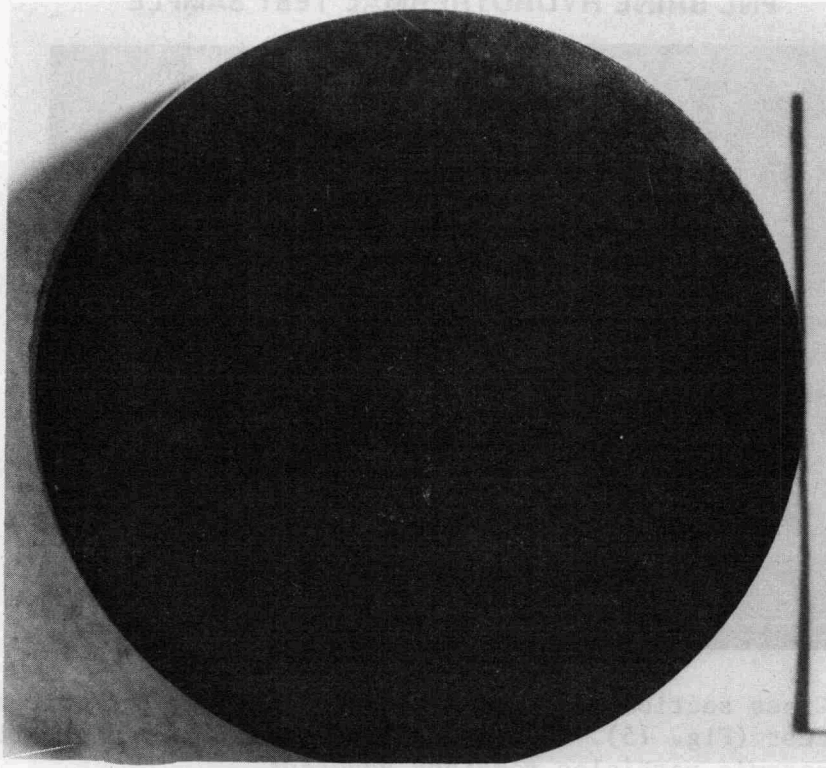


Fig. 15. Corroded film on cermet sample after brine exposure at 620 K and 1550 psi for seven days. Abrasion was required to penetrate corroded surface.

made to make them more adequate for large-scale processing. There is a need to better quantify the product, especially with respect to its leaching characteristics. Leach rates measured and reported by PNL are probably higher than those that would be found for later cermet products.

The cermet waste form has advantages with regard to compatibility in storage, levels of waste loading, density, and minimization of storage volume. High thermal conductivity permits fresh waste to be treated by this method. Physical strength of the cermet body reduces handling and transport hazards. Resistance to corrosion of the metal matrix is very high, and the oxide layer that is formed is not dissolved but is very adherent to the remaining base material. The ceramic phases in the cermet appear to be resistant to dispersion even after corrosion of the matrix takes place, and generally, the overall leach resistance appears acceptable.

PNL BRINE HYDROTHERMAL TEST SAMPLE

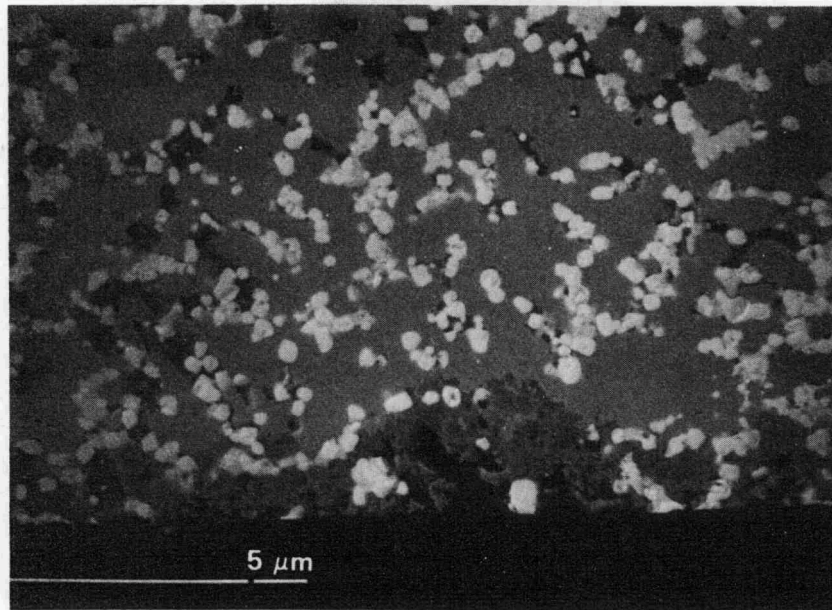


Fig. 16. Cross section of sample subjected to hydrothermal brine test (Fig. 15). Corrosion penetrated about 5 μm , but ceramic particles remained adherent.

One excellent application of this technology would be to put fresh waste into the cermet form and place it in above-ground storage to cool. Such an approach would preclude tank storage in liquid or slurry form with much less attendant volume. At some future time the cermet would be suitable for permanent interment.

DISCUSSION

QUESTION: Could you clarify something on one of your slides? You showed the leaching data from PNL; the value, I think, by weight measurement was something like 7.1×10^{-6} , and your loss by cesium determination was 7.2×10^{-5} .

ANSWER: That represented a 0.026% cesium loss from the total amount of cesium in the sample.

QUESTION: I see. So you mean it was a guess of the total weight loss by measuring the cesium.

ANSWER: A calculation.

QUESTION: Have you characterized the ceramic phases and do you know what they are?

ANSWER: Some of them. I did not go into detail about the head-end chemical additions, which are not too dissimilar from those made in the Synroc process or any other process. Most of the cations end up as oxides. We have begun characterization, but we didn't want to concentrate on that until we could use liquid-phase-sintered material. One other thing is that uranium is present in the cermet material. To date, we have yet to find any uranium in the leach solutions. So I believe the uranium is present as an insoluble oxide.

QUESTION: What's magnetic?

ANSWER: The mixed iron oxide, when it comes from the calciner. This property permits a very handy collection system to be used. You can magnetically collect the fines, if there are any. Fines, at present, are running about 0.5-1.5%. In the end, the cermet itself is, of course, very magnetic, and so, as I pointed out, transport of the cermet between various process steps using magnets could be used, which is very efficient for in-cell movement.

QUESTION: Yes. One question that that brought about. The fact that you're dealing with a metal phase. What do the Ellingham diagrams look like for this kind of material? Are you getting into the stable region of the metallic phase when you get above, say, 600 or 700°C?

ANSWER: I can't answer that. I do not know.

QUESTION: The point is, when you pass those lines, then perhaps it would be more applicable to compare lower-temperature data, since it's unlikely that, if your thermal conductivity is this good, you're going to get very high temperature effects just sitting in a repository unless you cool the cermet.

ANSWER: That's right. If you had a monolith of this material, two feet in diameter and ten feet high, with fresh waste, (six-months-cooled material), the centerline temperature of that monolith would only be only 29° different from the ambient value.

QUESTION: Yes, but the irony of the situation is that you may, in fact, want it to be at high temperature to maintain the stability, if, in fact, you remain below the stability on the Ellingham diagram for that. For the metal part of the cermet, at least.

ANSWER: I just don't know. I'm sorry. Someone asked a question the other day about our metal phase, and I pointed out to them that there are many iron-nickel based meteors in the ocean. Some have been in the oceans for many of years, and apparently are stable to the brine system.

QUESTION: I'm a little worried about differences between the leach rates based on cesium and the leach rate based on weight loss. There is a factor of 10 difference. Does that imply that the ceramic phase is coming out preferentially during a leach test with respect to the metal phase.

ANSWER: Sure. The cesium component.

QUESTION: Is the cesium in the ceramic phase?

ANSWER: Yes. Let me point out that the cermets that were leach-tested contained trace levels of radioactivity. We had cesium-137 in the samples. Leach rate is based on the amount of cesium lost from the total activity present. We are not doing any leaching ourselves right at the moment. We hope to very shortly, and I think the cermet product that we now have is greatly improved and, hopefully, will show a considerably lower leach-rate than that presented here.

QUESTION: In your leach tests?

ANSWER: Not mine.

QUESTION: Using our (PNL) leach tests you compared the values to glass. I was curious if the sample configuration was the same. The reason I ask is that normally the glass tests are run on a crushed sample (40 + 60 mesh) and your samples, I believe were little slugs of the cermet. So there is probably a surface area difference. I think, in a lot of the papers, both in the past and even tomorrow in the glass ceramics paper I'll be presenting, comparisons of leach information do not take the surface area into consideration. It's a difficult problem because of the differences in sample size, the conditions, the amount of, say, cesium you have in there versus one sample and the other and other factors. That's just a general comment and (sort of a question as well).

ANSWER: I believe, and I would have to check it out, that this was a solid sample of that glass. Ours was solid; you're not about to break up cermet into powder.

HIGH-SILICA GLASS MATRIX PROCESS FOR HIGH-LEVEL WASTE SOLIDIFICATION

Joseph H. Simmons and Pedro B. Macedo

Vitreous State Laboratory, Catholic University of America
Washington, D. C. 20064

ABSTRACT

In the development of host materials for the solidification of high-level wastes from nuclear fuel reprocessing plants, it has long been recognized that glasses offer a very attractive solution. Because of their amorphous nature, they receive equally well a wide variety of waste oxides within their structure, and avoid reconcentration of similar isotopes into hot spots, as would be the case for crystals. Glasses have exhibited good chemical durability characteristics and high resistance to radiation damage and thus are likely to show superiority to crystals in these areas. The major weakness of glasses in service as high-level solidification matrices may arise under hydrothermal conditions, where significant deterioration has been reported at 400-500°C. Since the chemical durability of all materials decreases with increasing temperature however, it is not clear at this time that any materials (glass or ceramic) have sufficient resistance to warrant the use of these temperatures. This result simply imposes a restriction on the upper storage temperature under wet conditions, which can be satisfied by proper size selection, loading levels, metal baths, and multibarrier encapsulation.

In the search for an optimum glass matrix composition, we have determined that chemical durability and thermal stability are maximized, and that stress development is minimized for glass compositions containing large concentrations of glass-forming oxides, of which silica is the major component (80 mol %). These properties and characteristics were recently demonstrated to belong to very old geological glasses known as tektites (ages of 750,000 to 34 million years).

The barrier to simulating tektite compositions for the waste glasses was the high melting temperature (1600-1800°C) needed for these glasses. Such temperatures greatly complicate furnace design and maintenance and lead to an intolerable vaporization of many of the radioisotopes into the off-gas system.

Research conducted at our laboratory led to the development of a porous high-silica waste glass material with approximately 80% SiO₂ by mole and 30% waste loading by weight. The process

can handle a wide variety of compositions, and yields long, elliptical, monolithic samples, which consist of a loaded high-silica core completely enveloped in a high-silica glass tube, which has collapsed upon the core and sealed it from the outside. The outer glass layer is totally free of waste isotopes and provides an integral multibarrier protection system.

INTRODUCTION

The suitability of various fixation media for the safe disposal of high-level radioactive wastes is determined by both the chemical and structural stability of each material under consideration. The release of toxic materials from solids by chemical leaching is a function of: (1) the specific dissolution rate per unit area and (2) the surface area exposed to the dissolution media. The former is a factor of the chemical stability of the material. The latter is determined by the initial configuration and the structural stability, which is related to the tendency of a material to shatter or powder in time via internal stresses or external shocks.

High-silica glasses have a fortunate combination of very good mechanical stability and high chemical durability. These conclusions are based on numerous laboratory tests and on strong geological evidence. For example, high-silica glass fibers are desirable for use as optical waveguides because of their high strength; tektite glasses which are as old as several million years have withstood weathering with relatively low leach rates. Their extreme durability appears to result from the high glass-former (silica and alumina) and low modifier content.

This paper describes a glass sintering process which allows the use of a high-silica-base glass to vitrify nuclear defense reprocessing wastes, while maintaining the qualities of high chemical and structural stability characteristic of silica glass.

VITRIFICATION PROCESS

The Porous Glass Matrix (PGM) process presented herein was developed as an outgrowth of research in molecular engineering of glasses. The generic process allows for the selective addition of various chemical elements to develop desired physical and/or chemical properties in high-silica glasses. The glasses produced have very high silica content (greater than 80% by mole) and therefore exhibit excellent chemical durability characteristics. The glass is formed by sintering and therefore avoids the very high melting temperatures of silica glasses (typically 1800°C). The process is relatively insensitive to waste composition. It has been used with both simulated commercial and military high-level wastes (Pw4b, Pw7a, Pw8a, U.K. M22 and SRP wastes) and with wastes with a solids content of 0% to 100%. The process is designed to minimize volatilization of toxic materials, which has been verified in laboratory tests and has the unique feature that the porous glass can be

prepared in a separate, nonradioactive plant including the reaction of selected additives with the glass, thus avoiding handling of the additional materials in the radioactive plant.

The process consists of mixing the high-level liquid wastes and solid precipitates with a dry porous high-silica glass crushed into powder. The pores within each powder grain vary between 0.01 and 0.02 μ , and the grains vary from 10 to 50 μ in diameter. When the porous powder is mixed with a waste stream, the liquid penetrates into the pores of the powder and deposits the dissolved wastes while the solid precipitates are deposited between the grains of the powder (see Fig. 2.1).

Drying, then heating the mixture allows decomposition of the wastes to oxides and combination with the glass to form a silicate glass. The pores are then collapsed to trap the dissolved wastes in the glass matrix of each powder grain. The mixture is then heated inside a high-silica glass tube with a sealed end. After the powder reacts with the intergranular waste solids and forms a solid glass core by liquid-phase sintering, the tube itself is collapsed on the high-silica glass and waste mixture. The collapsing temperature depends upon the specific composition of the high-silica glass and waste mixture and ranges from 900° to 1200°C.

The solid glass composite thus obtained consists of a core which contains the waste element oxides fixed in a solid high-silica glass

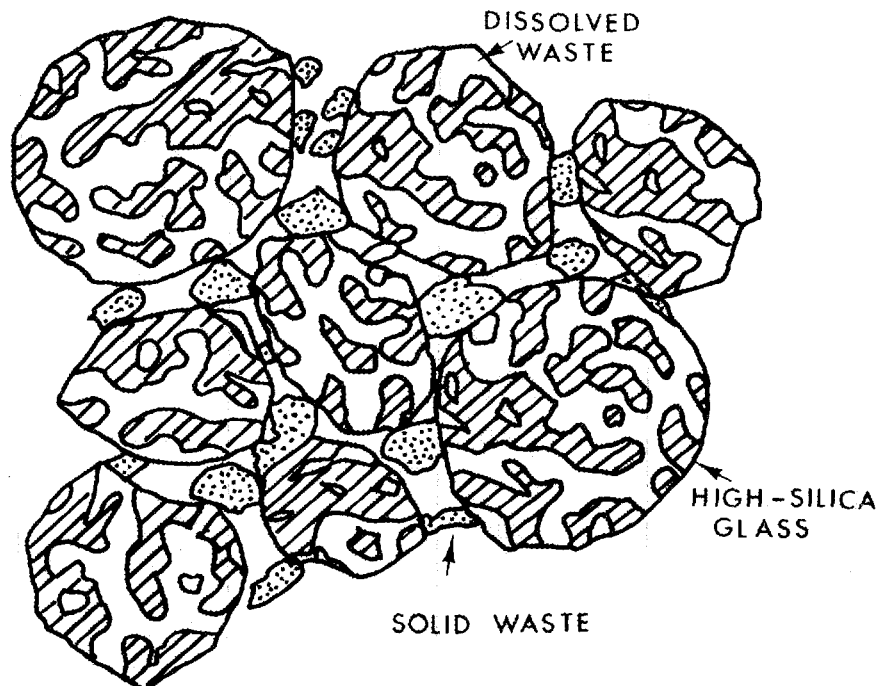


Fig. 1. Powdered porous glass with radioactive wastes. The pore size is 0.01 to 0.02 microns and the grain size is 10 to 300 microns.

matrix and an outer cladding layer which consists of a high-silica glass totally free of waste components. The core has a silica content of above 80 mole percent, thus satisfying very high chemical durability criteria. In addition, the core has a higher coefficient of thermal expansion than does the cladding layer. Therefore, during cooling, pre-determined residual compressive stresses are developed at the surface of the object, and good strengthening may be achieved. The cladding layer also provides multibarrier protection to chemical attack and exhibits a very high chemical durability. This high-level waste solidification process, termed Porous Glass Matrix (PGM) process, has demonstrated good physical and chemical stability for radwaste fixation. To date, we have produced composites 1.5 cm in diameter by 5 cm long containing waste compositions listed in Tables 1, 2, and 3 with 5% to 35% loading levels. We have used some modified outer tubes to form composites with success, and are presently working to optimize their thermomechanical match to the core materials. The process for making modified outer tubes was also developed at this laboratory and involves the use of porous glass

Table 1. West Valley PW-8a Waste Composition

Oxide	Reported wt %	Simulated wt %
Na ₂ O	16.62	16.62
Fe ₂ O ₃	34.29	34.29
Cr ₂ O ₃	1.36	1.36
NiO	1.74	1.74
P ₂ O ₅	1.58	1.58
Rb ₂ O	0.21	0.21
SrO	1.25	1.25
ZrO ₂	5.84	5.84
MoO ₃	7.54	7.54
Rh ₂ O ₃	0.36	0.36
Ag ₂ O	0.104	0.104
TeO ₂	0.86	
Cs ₂ O	1.14	1.14
BaO	1.85	1.85
Y ₂ O ₃	0.05	0.05
La ₂ O ₃	6.05	6.05
CeO ₂	12.09	12.09
Pr ₆ O ₁₁	1.06	1.06
Nd ₂ O ₃	3.62	3.62
Sm ₂ O ₃	0.64	0.64
Eu ₂ O ₃	0.17	0.17
Gd ₂ O ₃	0.43	0.43

Table 2. United Kingdom UKM-22 Waste Composition

Oxide	Reported wt %	Simulated wt %
Al ₂ O ₃	19.89	19.89
Rb ₂ O	0.43	0.43
Cs ₂ O	3.00	3.00
MgO	24.68	24.68
SrO	1.25	1.25
BaO	1.48	1.48
Y ₂ O ₃	0.66	0.66
La ₂ O ₃	1.71	1.71
Pr ₆ O ₁₁	1.67	
Nd ₂ O ₃	7.08	7.08
CeO ₂	3.85	3.85
ZrO ₂	5.57	5.57
P ₂ O ₅	0.93	0.93
Cr ₂ O ₃	2.18	2.18
MoO ₃	6.89	6.89
Fe ₂ O ₃	10.63	10.63
RuO ₂	2.65	2.65
NiO	1.40	1.40
PdO	1.71	1.71
ZnO	1.71	1.71
U ₃ O ₈	0.23	Replaced by CeO ₂
SO ₄	0.39	0.39

tubes. These can be designed to have a wide variety of thermomechanical properties and are expected to give the desired match of coefficient of thermal expansion and glass transition temperature with the loaded core.

CHEMICAL DURABILITY

The chemical durability of high-silica waste glasses prepared via the PGM process for the encapsulation of simulated military and commercial radwastes such as the West Valley PW-8a waste (see Table 1), the United Kingdom UKM-22 waste (see Table 2), and the Savannah River Plant waste (see Table 3), was tested and compared against the chemical durability of waste glass prepared via the borosilicate process. The data reported were taken on the core glass only without the protective outer jacket. The chemical durability test was conducted by immersing powdered glass from the core of prepared composite samples in distilled water at 45 and 70°C for a variety of times up to 10 days. The rate of silica release into the distilled water at 45 and 70°C was measured.

Table 3. Savannah River Plant Waste Composition

Salts	Reported wt %	Simulated wt %	Oxides	Reported wt %	Simulated wt %
NaNO ₃	2.28	2.28	Na ₂ O	2.98	2.98
NaNO ₂	0.20	0.20	Fe ₂ O ₃	36.87	36.87
NaAlO ₂	0.20	0.20	Al ₂ O ₃	7.48	7.48
NaOH	1.02	1.02	MnO ₂	10.41	10.41
Na ₂ CO ₃	0.08	0.08	U ₃ O ₈	3.45	*
Na ₂ SO ₄	1.06	1.06	CaO	2.75	2.75
Na ₂ C ₂ O ₄	0.0013	0.0013	NiO	4.57	4.57
NaCl	1.91	1.91	SiO ₂	3.34	3.34
NaF	0.19	0.19			
NaHHgO ₂	0.0007				
Starch	0.00003	0.00003			
Na-EDTA	5.62	5.62			
NaBO ₂	0.00001	0.00001			
C	2.58	2.58			
Hg	1.27				
HgI ₂	4.00				
Zeolite	7.73	7.73			

*U₃O₈ is replaced by 2.12 wt % CeO₂ in simulation tests.

The rates are summarized in Table 4. The high-silica PGM glass exhibits a much lower dissolution rate than borosilicate glasses and other waste forms at these temperatures.

Calculations may be conducted of the rate of radioisotope release expected from a composite PGM glass consisting of a loaded core completely encased within the protective outer collapsed tube. Leach rate measurements on the outer glass tube material have shown that the time to dissolve 1 mm of material which is the typical thickness of the pro-

Table 4. Dissolution of Glass Matrices at Various Temperatures in g/cm²/Day

PGM Glass	Borosilicate Glass	T(°C)
3 x 10 ⁻¹⁰	8 x 10 ⁻⁸	13
5 x 10 ⁻¹⁰	1 x 10 ⁻⁷	20
1 x 10 ⁻⁷	3 x 10 ⁻⁶	70
1 x 10 ⁻⁶	1 x 10 ⁻⁵	100

protective jacket is longer than 3 million years at 20°C, 30,000 years at 70°C, and 3,000 years at 100°C. Due to the slow dissolution rate of the protective jacket, estimates of the effective radioisotope release rate from PGM glasses may follow either of two alternatives: diffusion of radioisotopes through the outer jacket, or breakage of the composites exposing the loaded core to aqueous dissolution.

Measurements of the alkali ion conductivity of the tube jacket material were conducted and yielded a diffusion coefficient for radioactive cesium of 10^{-29} cm²/s. Other ions are slower by several orders of magnitude. For a 1 mm clad thickness, this diffusion coefficient yields an initial radioactive cesium release rate of 8×10^{-25} g/cm²/day between 20 and 100°C which changes very slowly with time. Therefore, the only effective release of waste isotopes is achievable by fracture of the composite and exposure of the core to aqueous attack. The effect of a cladding material is therefore to reduce the actual exposed surface area and to strengthen the composite to avoid excessive breakage. Calculations are presented below of an effective radioisotope leach rate from borosilicate glasses, from a totally exposed PGM core and from a partially clad PGM composite corresponding to an average breakage rate of 0.2%. A calculation is presented which evaluates the amount of each radioactive isotope released into the surrounding bath as a function of storage time. The amount M_i of radioisotope, i , released into the surrounding medium due to a dissolution of the glass is calculated as a function of storage time, t , and initial concentration in the waste, M_{0i} , by the following expression:

$$\frac{M_i}{M_{0i}} = \alpha_i e^{-t/\tau_i} \left(\frac{2Dt}{\rho r_0} - \frac{D^2 t^2}{\rho^2 r_0^2} \right) + \alpha_j \left(\frac{2Dt}{\rho r_0} - \frac{D^2 t^2}{\rho^2 r_0^2} \right) \left(\frac{\tau_i}{\tau_j - \tau_i} \right) (e^{-t/\tau_j} - e^{-t/\tau_i})$$

where the isotope i is the decay product of the isotope j ; D is the matrix dissolution rate; ρ is the glass density; r_0 is the radius of the waste glass rod; τ_i and τ_j are the mean lifetimes of isotopes i and j , respectively; and α is the ratio of the concentration of each isotope in the dissolved glass to the concentration of each isotope loaded in the glass.

Generally, α is unity unless the glass contains several regions with different waste element concentrations, such as in a multibarrier protection system. Then α becomes the ratio of the concentration of wastes in the outer barrier which is dissolved to the concentration in the bulk. The values of the constants used in the calculations were $r_0 = 1$ cm and $\rho = 2.5$ g/cm³ for both fixation media. Calculations were conducted for a borosilicate glass of composition 76-68 with waste composition Pw8a-2 ($\alpha = 1$) and for the high-silica PGM glass with (a)

complete exposure of the core region ($\alpha = 1$, no protective barrier) and (b) a protective barrier which exposes the core over 0.2% of the total area corresponding to inadvertent breakage ($\alpha = 0.002$).

The calculations are conducted for two specific long-lived isotopes, namely Tc^{99} and Pu^{239} which have half-lives of 212,000 and 24,400 years, respectively. Pu^{239} is a decay product of Am^{243} with a half-life of 7400 years. These calculations also involve various types of thermal conditions during storage which include one scenario with a storage at 20°C for the entire disposal period; and one scenario with a storage at 100°C for the initial 100 years and at 20°C thereafter.

The amounts of Tc^{99} and Pu^{239} released to the bath for storage at 20°C are shown in Figs. 2-2 and 2-3, respectively, for the borosilicate glass, the high-silica glass core totally exposed, and the high-silica glass with a protective barrier and some core surface exposure due to breakage. For a storage condition of 100°C for the first 100 years and 20°C thereafter, the accumulated Tc^{99} and Pu^{239} released are shown in Fig. 2-4 and 2-5, respectively. These results show clearly the effect of the difference in chemical durability between the high-silica and the borosilicate glass (Curve 1) for radwaste fixation. The further reduction in release rate afforded by the protective barrier with a 0.2% surface exposure is seen in the comparison of Curve 3 with Curve 2.

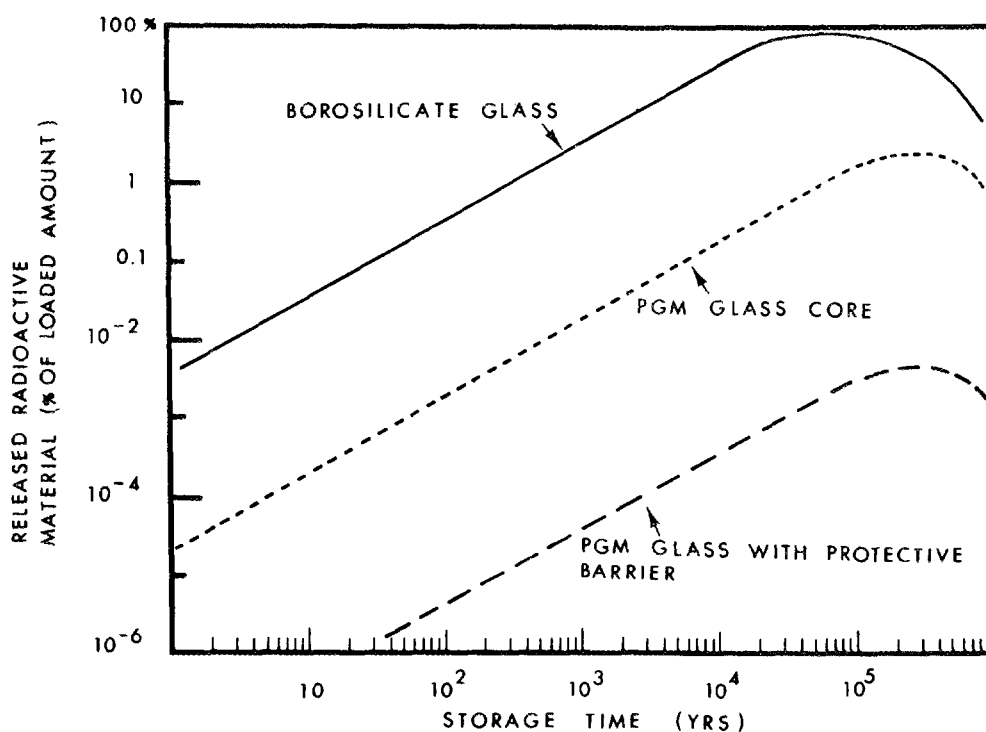


Fig. 2. Percent of ^{99}Tc released at 20°C as a function of storage time.

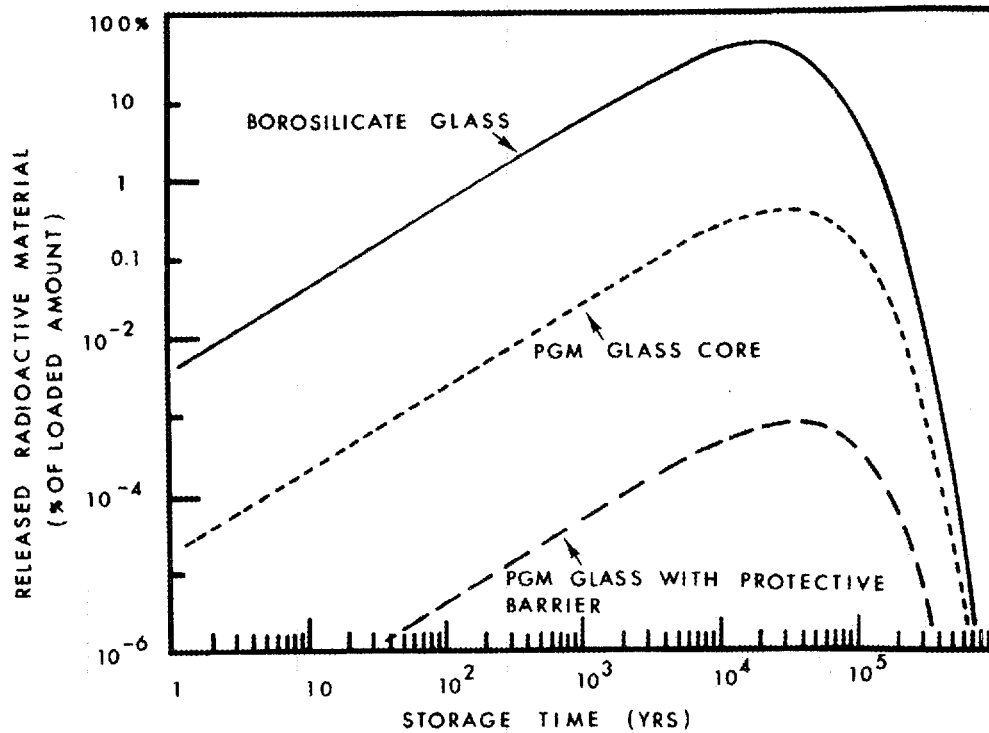


Fig. 3. Percent of ^{239}Pu released at 20°C as a function of storage time.

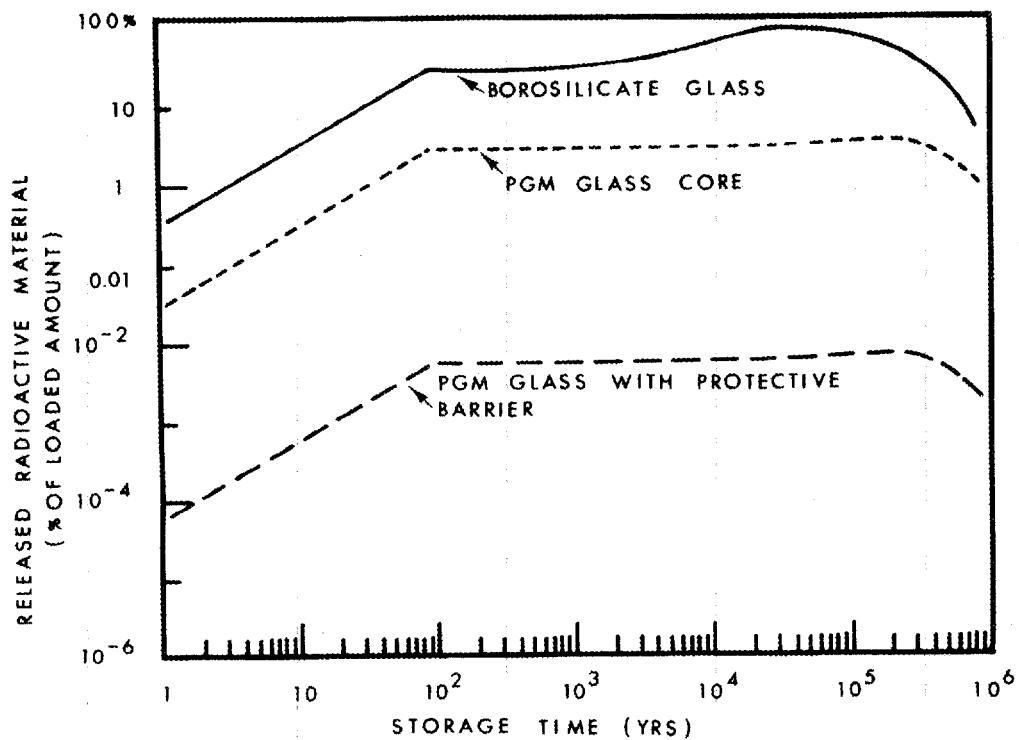


Fig. 4. Percent of ^{99}Tc released at 100°C for the first 100 yr and at 20°C thereafter.

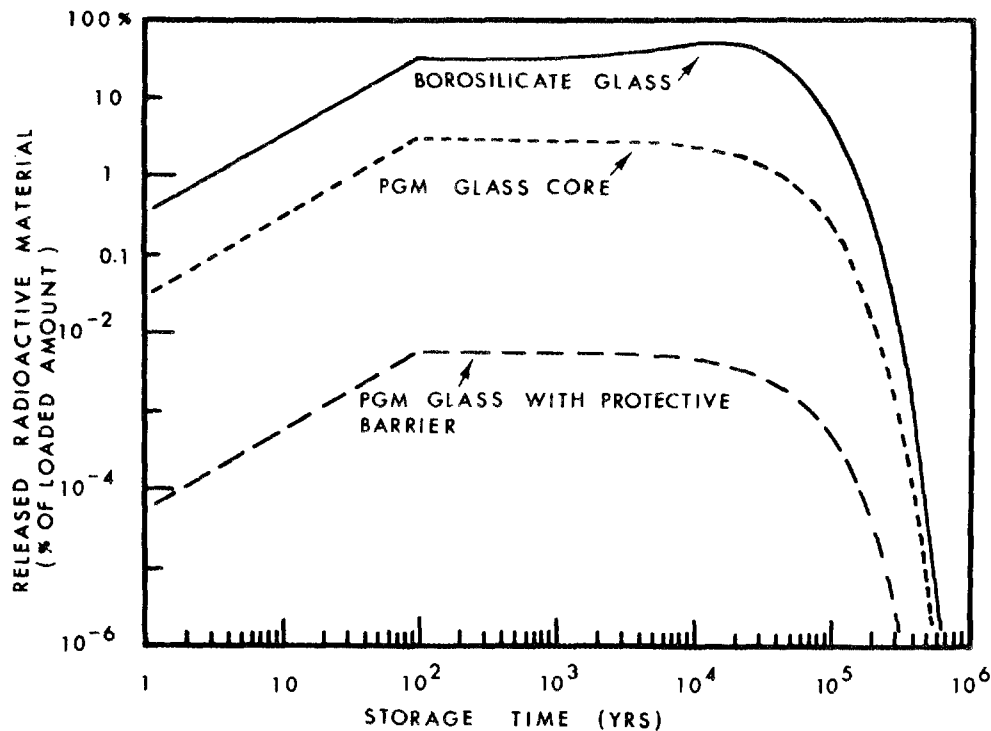


Fig. 5. Percent of ^{239}Pu released at 100°C for 100 yr and at 20°C thereafter.

MECHANICAL STABILITY

Glasses break by brittle fracture which occurs through the catastrophic growth of surface flaws when exposed to high tensile stress. Breakage may be avoided by several mechanisms. First, the stresses in the glass may be reduced. These develop during cooling and are due to the contraction of the glass. If different portions of the glass cool at different rates, then large stresses will develop. This problem may be minimized by reducing cooling rates and by designing glass fixation materials with low coefficients of thermal expansion. Some stresses in the glass occur by external events, such as impact or static stresses during storage. Breakage occurs when the tensile stress at a crack tip is large enough to propagate it. Failure may occur immediately (catastrophic crack propagation) or after a long period of slow crack growth (delayed failure).

The mechanism which may be used to prevent breakage operates by preventing the stresses at the glass surface, where the cracks are present, from becoming high tensile stresses. This is accomplished by designing materials which, upon cooling, develop a large residual compressive stress on the surface. Since the net stress at the crack tip is the sum of all stresses present, this large residual compressive stress avoids breakage and delayed failure as long as the applied tensile stresses are smaller in magnitude. This mechanism is the major mode of strengthening

glass and is used in glass tempering processes. This mechanism also has been applied to composites such as Ventura dinnerware by using a difference in coefficient of thermal expansion between the glaze and the body of the material.

In PGM waste glass composites, the high residual surface compression necessary for strengthening is obtained by developing a layered material with a core and a surface or cladding region. If the core region has a higher coefficient of thermal expansion and a lower glass transition temperature than the cladding region, the composite, during cooling after fabrication, will exhibit a high compressive stress in the surface or cladding region. If the cladding material is made up of a high silica glass, then it will also exhibit a low coefficient of thermal expansion, a very high chemical durability and a high resistance to devitrification. The resulting composite is expected to develop compressive stresses of 30-50,000 psi in the surface layer. These levels have already been achieved in similar systems.

DISCUSSION

POHL: I understand the structure of the small, I believe you called them Vycor, beads that have been filled and then the surface cleaned again and collapsed. You have silicon oxide on the outside, and inside you have something that is probably pretty close to the original phase-separated glass prior to leaching. I wonder if you could tell us a little more about the composition and structure of what you call the core in the case of a large silicon oxide capsule, inside of which you have the Vycor phase beads, together with a liquid that has been partly soaked up and so on. After the heat treatment, what is the shape and composition of that core?

SIMMONS: Before we put in any waste?

POHL: No. After, because if you collapse it before adding the waste, then I think that you have essentially what the Vycor people have. They start out with 50% porous material and collapse it all into a silicon oxide of half the volume and twice the density.

SIMMONS: That is correct.

POHL: But if you stuff these channels with the waste, and then heat treat it, what does the glass look like?

SIMMONS: We have not looked at electron probe traces over the glass, so we are not sure what happens microscopically, but on a larger scale the glass is homogeneous, the material has collapsed into a solid, and the tube actually takes up the volume change. The tube collapses last. In our process, the material begins to collapse; then the tube collapses into it and solidifies. If you cut it you have a piece of glass which has different colors because the inside has a large iron content, but it is a solid piece of glass all the way across.

POHL: So what you are saying is that the water has all disappeared, and the 50% voids, the Vycor voids, just sort of vanish and just a little bit of the dried waste residue has remained.

SIMMONS: That's right. Everything is gone. All the gases, all the water, and all the nitrates are gone by about 650°C. By 800°C we seal up the pores, so the pores do not trap anything. By 1050°C we seal up the tube, so that all the volume has been changed at that point.

UNIDENTIFIED QUESTIONER: When you are treating the Savannah River sludges, and you have the small particles in between your glass spheres, how do you characterize the system after melting? It appears as if you are just occluding these particles of zeolites and sludges, and perhaps some of them diffuse into the glass.

SIMMONS: There is a little bit of liquid-phase sintering. So, as I said, I am not sure what the real structure of the material is on a microscopic scale. What we have done is to take the glass and fracture it, so that we have a solid face which is exposed to water, and we have conducted leach tests on this material. Then we have taken the core itself and crushed it into very fine powder and conducted leach tests on that, and our dissolution rates are pretty close. So, if there is any included material, it is obviously inert; but we are not sure how much there is.

HOWITT: If you pull a barnacle off the side of a ship, you will find that the corrosion is actually under the barnacle and that around the outside of the creature you have erosion. Since you have positively charged ions and electrolytic types of dissolution going on, I think that you are on very unsafe ground when you draw a conclusion between the condition of the glass underneath that creature and the surface condition of the glass and that dissolution rate. As a comment, I do not think that you can do that sort of extrapolation without being very careful about the dissolution rate of the glass and the erosion rate, which you claim to know a great deal about.

SIMMONS: Of course the ships are metallic and there is quite a different problem.

HOWITT: I don't think it is that different, because what you have is an oxygen-deficient or an ion-deficient situation. As you pointed out, we do not know very much about the dissolution rates. You cannot make that drastic conclusion. What you are doing in that conclusion is assuming a mechanism that you do not know.

SIMMONS: I would be the first to agree with that.

MACHIELS: I have a question about the leach test results. You state that in principle we should get a dependence on the square root of time for the cumulative leaching. Why do we usually get a time dependence to a power that is larger than the square root?

SIMMONS: In the initial leach measurements?

MACHIELS: Yes.

SIMMONS: We have made measurements of sodium and silicon leach rates. I think that it is important to remember what is being followed. If you are following the sodium, it does follow a square root dependence initially. If you follow other ions, divalent ions like calcium, for example, then there is a big problem, because what happens in the calcium is that you can have ion exchange on the surface and immediately your square root dependence will die; i.e., something else will happen. If you are following weight loss, it is an integral of all these dependences and becomes even more complicated. It is the sodium that one has to follow. Sodium, potassium, any of the alkali ions.

MACHIELS: Don't you think that, if you have precipitation under the surface, this should lead to a lower time dependence? The initial leach rates would be of the diffusion type, so you would get the square root dependence; however, as soon as you get precipitation, you go to something which is less than the square root. Usually we see the opposite: We get a very drastic change as a function of time at the very beginning; and then it levels off, which makes sense with precipitation. Still, the initial slope does not fit very well in that picture.

SIMMONS: Are you careful to define your exposed surface area? You may have fines on the surface; or, if you have an uneven surface area, you will have accelerated leaching because of the larger exposed area, and then your time dependence will be mixed in with the surface area change. You have to be very careful of that.

MACHIELS: I am referring to a test where it should not be a factor.

SIMMONS: Obviously, what you are saying is that it is very complicated, and I agree with that.

MOORE: You say that you reduce the amount volatilized by a layer of phasal on the top. How much is volatilized? Another question is, when you listed the composition of the simulated waste, you said that you left out a few elements because they were difficult to work with. Would you explain that statement more completely?

SIMMONS: Our problem at the university is hood space. We have only recently been supported to do research in this area. Up to now, we have been doing it pretty much on our own. We left out mercury-containing compounds, because we did not have a hood that could handle mercury.

MOORE: So it will volatilize, completely?

SIMMONS: We did not want to take a chance.

MOORE: How much volatilization did you get even with the layer of phasal on top?

SIMMONS: What you are asking is, have we ever run a test in which we put the powder on top and the material underneath. We have never run a test with Savannah River waste underneath and phasal on top. We have run a test with cesium, which had powder underneath and the layer on top. We have run tests with other coloring agents, such as copper, with no material underneath and evaporated the copper (for example) to see whether it would precipitate within the glass. What we have demonstrated is that that layer does precipitate vapors, though we have never made quantitative measurements. We are planning to do that eventually.

MOORE: But we do not know what would happen to things like ruthenium, mercury, fluoride?

SIMMONS: Conceptually, as I described. I do not know exactly.

MOORE: But have you no data yet?

SIMMONS: No, not yet.

UNIDENTIFIED QUESTIONER: Have you evaluated the types of phases, perhaps crystalline phases, which might remain in this material, by either x-ray diffraction or TEM?

SIMMONS: We have not. We are going to do that with electron diffraction in the coming year. As I said, we just received some support to do that kind of work. We will be looking with electron diffraction and scanning probe studies.

A REVIEW OF GLASS CERAMIC WASTE FORMS*

J. M. Rusin

Pacific Northwest Laboratory
Richland, Washington

ABSTRACT

Glass ceramics are polycrystalline solids prepared by the controlled crystallization of glasses. Crystallization is accomplished by subjecting suitable glasses to a regulated heat-treatment schedule which results in the nucleation and growth of crystal phases within the glass. In many cases, the crystallization process can be taken almost to completion, but a small proportion of residual glass phase is often present.

Many different types of glass ceramics have been developed for commercial applications. A wide variety of crystal types can be developed in glass ceramics, depending upon the composition of the parent glass. Titanium dioxide is commonly used as a nucleating agent, although many other nucleating agents have been discovered. Metallic colloid formation, photosensitive reactions, and phase separation by oxides are typical nucleating methods for controlled crystallization.

The manufacture of glass ceramics is of technological significance, in that the fabrication process involves the preparation first of a glass, which is shaped in its molten or plastic state to produce articles of the required form. The final polycrystalline product is formed during subsequent heat treatment. The advantage of the glass-ceramic process is that a product can be produced with properties similar to that of a ceramic, such as high-strength and low-thermal expansion, by methods which may produce a more homogeneous and dimensionally controlled product than conventional ceramic processes.

Glass ceramics are being considered for the immobilization of nuclear wastes to obtain a waste form with improved properties relative to glasses. Improved impact resistance, decreased thermal expansion, and increased leach resistance are possible. In addition to improved properties, the spontaneous devitrification exhibited in some waste-containing glasses can be avoided by the controlled crystallization after melting in the glass-ceramic process.

*Work Supported by the U.S. Department of Energy under Contract DE-AC06-76RLO 1830.

The majority of the glass-ceramic development for nuclear wastes has been conducted at the Hahn-Meitner Institute (HMI) in Germany. Two of their products, a celsian-based ($\text{BaAl}_3\text{Si}_2\text{O}_8$) and a fresnoite-based ($\text{Ba}_2\text{TiSi}_2\text{O}_8$) glass ceramic, have been studied at Pacific Northwest Laboratory (PNL). A basalt-based glass ceramic primarily containing diopsidic augite ($\text{CaMgSi}_2\text{O}_6$) has been developed at PNL. This glass ceramic is of interest since it would be in near equilibrium with a basalt repository. Studies at the Power Reactor and Nuclear Fuel Development Corporation (PNC) in Japan have favored a glass-ceramic product based upon diopside ($\text{CaMgSi}_2\text{O}_6$).

Compositions, processing conditions, and product characterization of typical commercial and nuclear waste glass ceramics are discussed. In general, glass-ceramic waste forms can offer improved strength and decreased thermal expansion. Due to typically large residual glass phases of up to 50%, there may be little improvement in leach resistance.

Introduction

The current efforts in alternative waste forms at Battelle Pacific Northwest Laboratories involve glass ceramics, coated particles, and matrices. The matrices and coated particles are part of the multi-barrier concept for containment of nuclear wastes. The glass ceramic development resulted from PNL exchanges with the Hahn-Meitner Institute in Berlin. The paper is in four parts: (1) introduction to glass ceramics and their production, (2) commercial glass ceramics, (3) glass-ceramic nuclear waste forms, and (4) a comparison of glass-ceramic waste form properties.

The first and second parts are background information for the discussion of glass-ceramic waste forms. In the first part, glasses, ceramics, and glass ceramics are defined, nucleation and crystallization of glass ceramics are discussed, and examples of various nucleating agents are given. In the second part, potential advantages of glass ceramics for commercial use are discussed, along with a brief history of their development. Typical compositions of commercial glass ceramics are given, and crystalline phases that are obtained are listed. Bulk, thermal, and mechanical properties of commercial glass, glass ceramics, and ceramics are compared. Properties and leach resistance data are presented for a common household glass ceramic.

The third and fourth parts deal with glass ceramic nuclear waste forms per se. In the third part, reasons for considering glass-ceramic waste forms and some property data for studies at HMI, KFK, PNC, and PNL are presented. In the fourth part, residual glass content is discussed, and the dependence of leach resistance upon residual glass content is illustrated. Leach resistance, density, thermal expansion, thermal conductivity, and impact resistance are compared for glass and

glass-ceramic waste forms. Data is presented to illustrate the effect of radiation on glass ceramics (primarily the crystalline component).

Glass Ceramics

Glasses are inorganic products of fusion; they are supercooled, metastable, and have short-range order. Ceramics and inorganic nonmetallic materials; unlike glasses, are thermodynamically stable and have long-range order. Glass ceramics are polycrystalline solids prepared by the controlled crystallization of glasses. They are melted and formed as a glass, using conventional glass techniques. They are converted largely to crystalline form by controlled devitrification (crystallization). Thus, the product will have a large amount of crystals and exhibit crystalline properties. However, glass ceramics often have some residual glass. Thus, the properties of the glass ceramic will be a combination of those of the crystalline and residual glass components.

The kinetics for the nucleation and growth of crystals in the production of glass ceramics can be expressed briefly by two equations. The equation for nucleation is

$$I = K \exp (W^*/RT),$$

where W^* is work of critical nucleus formation. The equation for crystal growth is

$$U = \alpha_0 \nu \exp(-\Delta G^*/RT)[1 - \exp(\Delta G/RT)],$$

where α_0 is interatomic separation, ν is vibrational frequency at the crystal-glass interface, ΔG is bulk free energy of crystallization, and ΔG^* is free energy of activation.

The controlled nucleation and crystallization of a glass ceramic are illustrated schematically in Figures 1 and 2. The process begins with the melting and forming of a glass at high temperatures (e.g., 1300°C). The glass is cooled, then reheated to, say 500°C for nucleation, and finally to perhaps 900°C for crystal growth.

Generally, nucleation is accomplished by separation of metals or by separation of oxides. In nucleation by separation of metals, metallic colloids are formed and serve as sites for nucleation. Nucleating agents for this process are Cu, Ag, Ce, and the Pt group metals. Photosensitive reactions can be used with the first four elements. Nucleation by separation of oxides proceeds by the phase separation of oxide systems. Nucleating agents are TiO_2 (very popular), P_2O_5 , V_2O_5 , Cr_2O_3 , MoO_3 , WO_3 , and Fe_2O_3 . Actually, discussing nucleating agents for waste glass is academic, because nuclear waste streams contain many elements including those mentioned as nucleating agents.

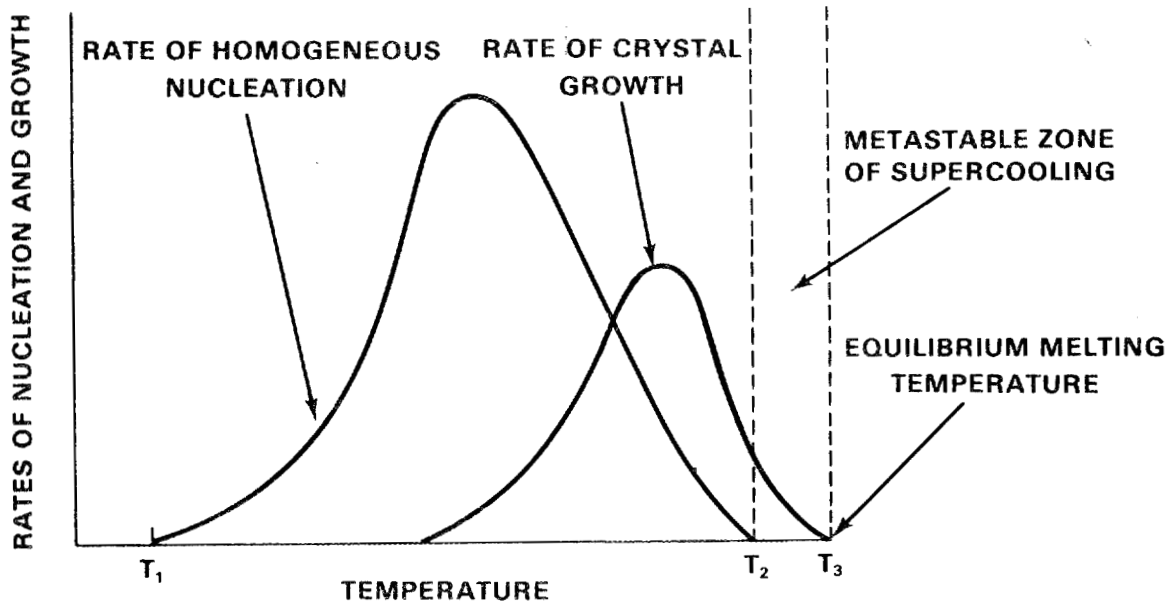


Fig. 1. Rates of Homogeneous Nucleation and Crystal Growth in Viscous Liquids.

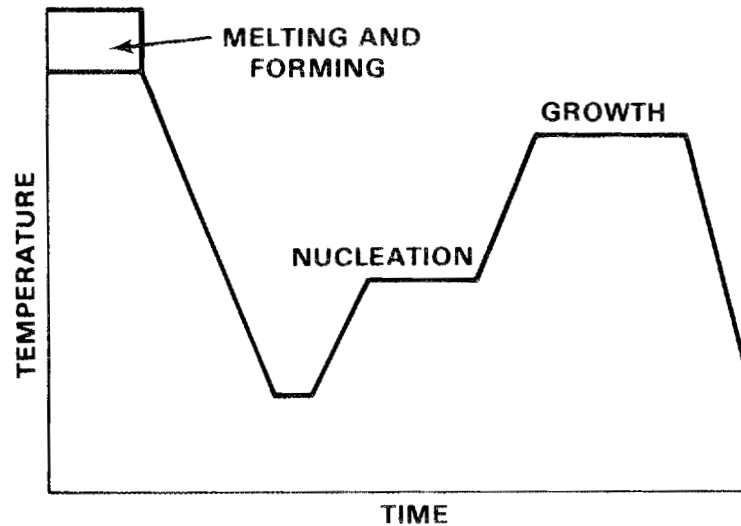


Fig. 2. Schematic Time-Temperature Cycle for the Controlled Crystallization of a Glass-Ceramic Body.

Commercial Glass Ceramics

Glass ceramics have a number of advantages for commercial use. They are easy to fabricate using conventional glass processes. The products are very homogeneous; instead of using a mixture of solid oxides to form a ceramic, the method of production first forms a homogeneous glass and then crystallizes that. Glass ceramics are applicable

to a wide range of compositions. The final dimensions can be controlled easily, because glass can be formed with good tolerances, and there is very little shrinkage during crystallization of the glass. Glass ceramics have high strength and resistance to mechanical shock. Glass ceramics have low thermal expansion and good resistance to thermal shock. Finally, they have high durability.

In one of the most interesting chapters in the history of the development of commercial glass ceramics, S. D. Stookey¹, at Corning Glass Works, was working with photosensitive glass that contained metallic crystals. The glass was allowed to heat up to a temperature higher than usual, and, instead of melting, it opacified. It was found that metallic colloids had formed in the glass and had nucleated the² growth of crystallites, thus forming a glass ceramic. Later, Stookey² used TiO_2 as a nucleating agent; and most of the glass³ ceramics today are nucleated by TiO_2 . In a parallel effort, McMillan³, in the United Kingdom, looked at metallic phosphates as nucleating agents.

Some of the glass ceramics available commercially are shown in Table 1. Probably the most well known, the lithium-aluminosilicate system, has low thermal expansion, due to the formation of β -spodumene and β -eucryptite. Magnesium aluminosilicate is alkali free and produces a glass ceramic with high resistivity. Lithium-magnesium-silicate glass ceramics have a high thermal expansion, which is unusual. Normally a glass ceramic will have a low thermal expansion. Table 1 also lists other systems and characteristics.

TABLE 1. Glass Compositions for Commercial Glass-Ceramic Production

Glass-Ceramic System	Comments
$LiO - SiO_2$	Photosensitively Nucleated
$Li_2O - Al_2O_3 - SiO_2$	Low Thermal Expansion
$Na_2O - Al_2O_3 - SiO_2$	High Thermal Expansion
$MgO - Al_2O_3 - SiO_2$	Alkali Free, High Resistivity Low Dielectric Loss
$Li_2O - MgO - SiO_2$	High Thermal Expansion Coefficients
$Li_2O - ZnO - SiO_2$	High Mechanical Strength Wide Range of Thermal Expansion
$ZnO - Al_2O_3 - SiO_2$	Replace SiO_2 With B_2O_3 To Produce Special Coating and Sealing Compositions
$RO - Al_2O_3 - SiO_2$	R = Ca, Ba, Pb, Cd

It would be useful to compare some of the properties of commercial glass ceramics, glasses, and conventional ceramics. The densities of glass ceramics fall within the same ranges as those of glasses and ceramics. They are a combination, of course, of glass and ceramic, so the density of each glass ceramic depends upon the relative amounts of glass and ceramic in its composition. The thermal conductivities of glass ceramics are slightly higher than those of glasses, as shown in Table 2. They are not as high as thermal conductivities of most ceramics, but approach those of the ceramic systems. In pendulum-type impact tests, a glass ceramic has an impact resistance even higher than that of a 95% alumina ceramic and over twice as high as those of the two soda-lime glasses. Glass ceramics offer a promise of a higher impact resistance and a higher strength in general.

Table 2. Thermal Conductivities of Glass-Ceramics and Other Materials at 100°C

Material	Thermal Conductivity (cal sec ⁻¹ cm ⁻¹ °C ⁻¹)
<u>Glass-ceramics</u>	
Li ₂ O-ZnO-SiO ₂ (c. 5% ZnO)	0.0067
Li ₂ O-ZnO-SiO ₂ (c. 30% ZnO)	0.0052
Li ₂ O-Al ₂ O ₃ -SiO ₂ (c. 20% Li ₂ O)	0.0130
Li ₂ O-ZnO-Al ₂ O ₃ -SiO ₂	0.0070
<u>Glasses</u>	
Fused silica	0.0036
Low expansion borosilicate	0.004
Soda-lime-silica	0.0035-0.004
<u>Ceramics</u>	
Pure alumina	0.072
Pure magnesia	0.090
95 percent alumina ceramic	0.052
Porcelain	0.004

(From McMillan⁴)

In common with a number of other properties, the thermal expansion of glass ceramics is made up of the combination of the thermal expansions of the residual glass and the crystalline phases. Low thermal expansion is mainly obtained from systems that have α -eucryptite, which has a negative coefficient of thermal expansion, and α -spodumene. The coefficient of thermal expansion of a glass ceramic can be higher or lower than that of the corresponding glass, depending upon the crystalline phases or the glass system.

When glass ceramics were first considered for nuclear waste immobilization, thermal shock resistance, ΔT , was of importance because wastes of high heat content were being proposed. Glass ceramics, in general, have a lower coefficient of thermal expansion than glass. Therefore, one would expect them to have a higher thermal shock resistance, in accordance with

$$\sigma = E\alpha\Delta T/2(1-\nu),$$

where σ = surface stress (compressive or tensile), ΔT = temperature difference between faces, α = linear thermal expansion coefficient, and ν = Poisson's ratio. Thermal shock resistance is plotted against coefficient of linear thermal expansion for various glass ceramics, two glasses, and a conventional ceramic (Figure 3). This demonstrates that a material that has low thermal expansion will generally have a high thermal shock resistance.

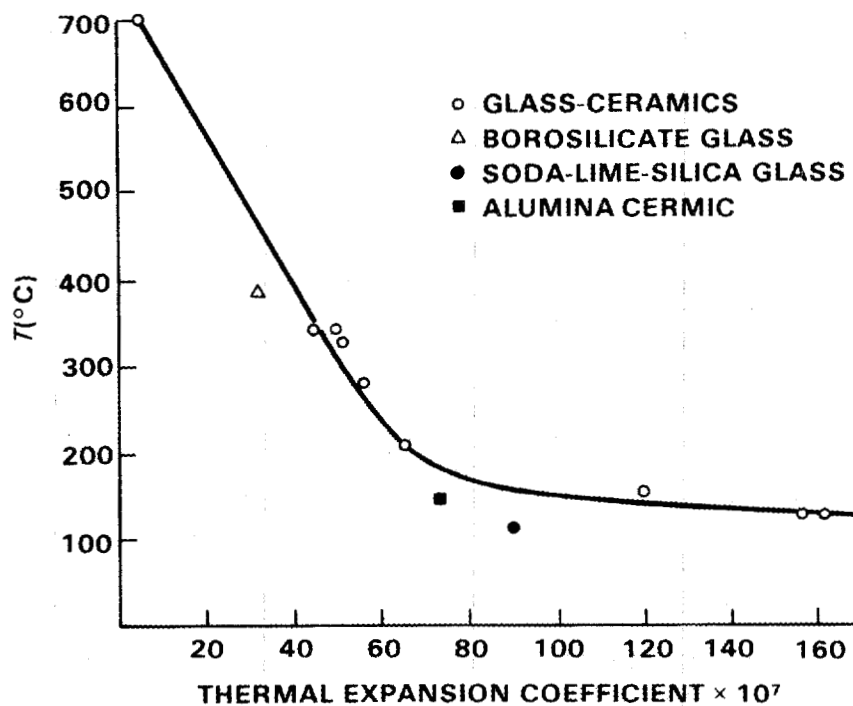


Fig. 3. Relationship Between Thermal Shock Resistance and Linear Coefficient of Thermal Expansion for Glass-Ceramics and Other Materials (From McMillan).

One commercial glass ceramic, Corning Code 9617 (Pyroceram), was used by Sundquist at Corning Glass Works in a study for ASEA to provide a package for spent fuel. Some of the properties of code 9617 are given in Table 3. The phase analysis shows primarily β -spodumene, some rutile or anatase, some spinel, and a residual glass phase of approximately 2 to 5%. The density of 2.51 g/cm³ is in the low range for a glass ceramic. The thermal expansion is very low, $8.4 \times 10^{-7}/^{\circ}\text{C}$. The thermal conductivity is slightly higher than that of a normal glass.

Table 3. Properties of a Commercial Glass Ceramic Code 9617

● Phase Analysis	
- β -spodumene ($\text{Li}_2\text{O} \cdot \text{Al}_2\text{O}_3 \cdot 7\text{SiO}_2$)	85-90%
- Rutile, anatase (TiO_2)	~5%
- Spinel (Mg or ZrAl_2O_4)	~5%
- Residual Glass	2-5%
● Bulk Properties	
- Density: 2.51 g/cm ³	
- Thermal expansion: $8.4 \times 10^{-7}/^{\circ}\text{C}$	
- Thermal conductivity: 0.0049 cal/sec·cm·°C	

Sundquist conducted leaching experiments on the Code 9617 glass ceramic (Figure 4). Depending on temperature (about 90 to 180°C) and ratio of solution volume to surface area (0 to 20), corrosion rates ranged from < 1 to ~ 100 cm/1000 yrs (1 cm/1000 yrs = 10^{-5} g/cm²·day). The resultant leach solution, was very cloudy and when analyzed, the suspended solid particles were found to be β -spodumene. The residual glass, which had acted as a binder for the β -spodumene crystallites, was leaching away. A major portion of the weight loss was due to the glass being leached and the release of crystalline particles, which, in glass ceramics are very fine, less than 1 micron. There is a technique in the glass industry of using sulphur dioxide to increase the strength of glass. This produces a high-silica-content layer on the surface. Sundquist used this SO₂ treatment on the Code 9617 glass ceramic and found that the leach resistance was increased by a factor of 2 to 6, depending upon the temperature.

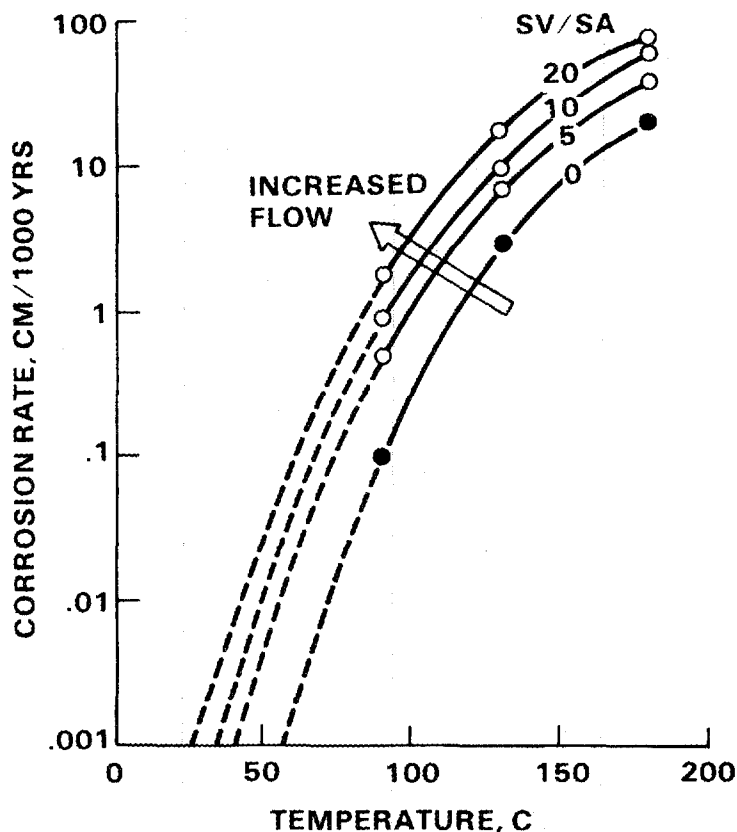


Fig. 4. Corrosion Rate of Glass-Ceramic Code 9617 as a Function of Temperature and Solution Volume to Surface Area Ratio (From Sundquist⁵).

Glass-Ceramic Nuclear Waste Forms

There are several reasons for considering glass ceramics for nuclear waste forms. First, there is promise of improved properties, lower thermal expansion, higher thermal conductivity, improved strength, and possibly even improved durability. Second, there is ease of fabrication, using conventional glass processes which already have been established. Third, with reference to the problem of spontaneous devitrification of some waste glass systems, a glass ceramic is produced by controlled devitrification and then can be used to produce a ceramic or crystalline waste form that would have durable properties.

Most of the work on glass-ceramic nuclear waste forms has been done at Hahn-Meitner Institute (HMI) on glass ceramics based on celsian ($BaAl_2Si_2O_8$) and fresnoite ($Ba_2TiSi_2O_8$). The Kernforschungszentrum Karlsruhe (KFK) has a glass ceramic called VCP-15. The Power Reactor and Nuclear Fuel Development Corporation (PNC) in Japan, looked at several glass ceramics and concluded that the best was a formulation based on diopside ($CaMgSi_2O_6$). At Battelle Pacific Northwest Laboratories (PNL), celsian and fresnoite glass ceramics have been studied, mainly

in collaboration with HMI. Basalt-based glass ceramics are also being developed at PNL.

Table 4 lists compositions of the parent glasses of the four original HMI glass ceramics, based on celsian, diopside, eucryptite, and perovskite.^{6,7} Soxhlet leach rates were from 10^{-4} to 10^{-5} g/cm²·day for all four of these waste forms. In general, the leach resistance of the glass ceramic was equivalent to or worse than the leach resistance of the original glass that was used to form the glass ceramic. Some other properties of these four glass ceramics are given in Table 5. The melt temperature range of 1200 to 1400°C is higher than would be desired for remote facilities. A temperature range of 1050 to 1150°C would be better. Nucleation temperatures range from 500 to 700°C for periods of 3 to 5 hours. The crystallization temperature is higher, generally in the 800 to 900°C range. Notice that for the celsian type there is no nucleation temperature. The celsian type nucleates as it cools during casting; it does not generally require a separate nucleation stage. A nucleation step at 600°C for 3 hrs can be used for improved crystallization. The eucryptite type has a very low thermal expansion. The other three are all in the high thermal expansion range, more equivalent to waste glasses. SEM micrographs of the celsian glass ceramic are shown in Figure 5. The effect of heat treatment, which is very important in the processing of glass ceramics, is illustrated. The sample on the left is more typical of a desirable product. It was nucleated at 600°C for 3 hr and then raised up to 800°C for 12 hours

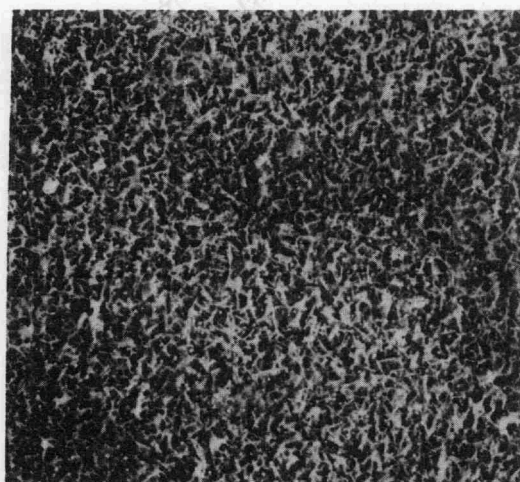
TABLE 4. Compositions of Parent Glasses and Crystal Phases of HMI Glass Ceramics

	Glass Ceramics							
	Celsian		Diopside		Eucryptite		Perovskite	
Glass composition (wt%) (a)	SiO ₂	32-37		45-52		41-60		32-50
	Al ₂ O ₃	10-17		10-18		14-24		12-15
	B ₂ O ₃	5-8		1-5		4-11		5-10
	CaO	6-10		10-15		2-9		12-14
	BaO	18-23	MgO	5-10	BaO	0-5		
	Na ₂ O	2-6		0-10		0-3		5-8
	Li ₂ O	0-2		0-3		5-10		0-3
	TiO ₂	5-11		3-5 (+ZrO)		5-8		10-14
	ZnO	4-6		0-3		4-13		0-5
	Ca ₂ O	0-2	Fe ₂ O ₃	0-5				0-2
Crystal phases	H-celsian (BaAl ₂ Si ₂ O ₈)		diopside CaMg(SiO ₃) ₂		β-eucryptite (LiAlSiO ₄)		perovskite CaMoO ₄ or Mo-nosean	
	perovskite (CaTiO ₃)		CaMoO ₄		CaMoO ₄		Mo-nosean	
	BaMoO ₄		Mo-nosean		(Ce,Zr)O ₂		(Ce,Zr)O ₂	
	pollucite		Na (AlSiO ₄) ₈		Ca ₄ La ₆ (SiO ₄) ₄ (OH) ₂		pollucite	
	(Cs,Na)AlSi ₂ O ₆		(AlSiO ₄) ₆ MoO ₄		Li-Zn-silicates			
					pollucite			

(a) Excluding 20 wt% fission product oxides.

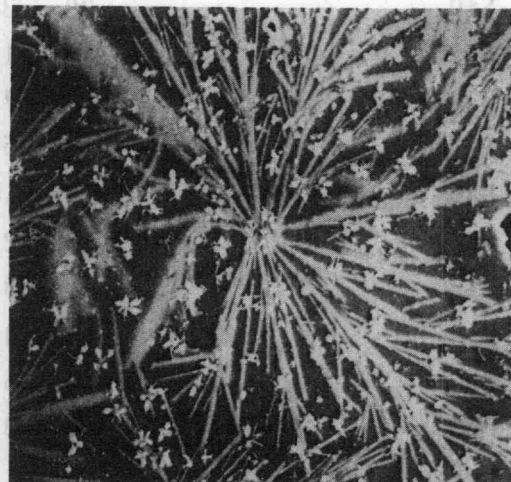
TABLE 5. Conditions for Preparation of HMI Glass Ceramics

Properties	Celsian	Diopside	Eucryptite	Perovskite	
Melting temp. ($^{\circ}\text{C}$)	1200-1300	1200-1297	1100-1400	1250-1350	
Transformation temp. ($^{\circ}\text{C}$)	560-590	610-660	470-560	590-620	
Nucleation temp. ($^{\circ}\text{C}$)		650-700	530-580	630-670	
time (hr)		5	3-5	3-5	
Crystallization temp. ($^{\circ}\text{C}$)	770-860	860-960	630-750	800-870	
time (hr)	6-15	10	10-24	12-24	
Leaching rates ($\text{g}/\text{cm}^2\text{d}$) $\times 10^6$	glass ceramic	8-10 8-12	8-10 11-12	3-6 8-12	6-10 8-11
Thermal expansion $^{\circ}\text{C}^{-1} \times 10^7$		90-110	70-100	50-75	90-110



600 $^{\circ}\text{C}$ FOR 3 HR
800 $^{\circ}\text{C}$ FOR 12 HR

30 μm



1000 $^{\circ}\text{C}$ FOR 1 HR

60 μm

Fig. 5. Effect of Heat Treatment of Celsian Glass Ceramic.

for crystallization. Typically, the crystal sizes are between 0.5 and 1 micron in these glass ceramics. The sample on the right was heated for 1 hr at 1000 $^{\circ}\text{C}$ to purposely grow large crystals to identify where the actinides (^{244}Cm doped) were going. This treatment grew very large crystals, and there is a lot of residual glass in the sample. This illustrates a potential processing problem: one needs to have controlled crystallization to obtain fine crystal sizes and high crystal yield.

Hahn-Meitner Institute developed a fresnoite-based glass ceramic to improve upon their original four glass ceramics. The celsian-based glass ceramic when heat treated for longer periods of time would produce recrystallization of the celsian phase, crystal growth of new phases, and loss of mechanical integrity. Also, the celsian-based glass ceramic has a high boron content. The boron goes into the residual glass phase resulting in a glass of high leachability. The fresnoite-based glass ceramic has a low boron content (Table 6) and upon further heat treatment does not change its crystalline structure. Hahn-Meitner Institute reached the conclusions in their glass ceramic study that there were some improved properties by going to a glass ceramic; these being mechanical and thermal, such as thermal conductivity and thermal stability. But when it came to leach resistance, there was no improvement over the equivalent glass systems.

TABLE 6. Composition of HMI Celsian and Fresnoite Glass Ceramics

	Celsian-Types wt %	Fresnoite-Types wt %
SiO ₂	28 - 38	22 - 28
Al ₂ O ₃	10 - 13	0 - 2
B ₂ O ₃	2 - 7	0 - 3
CaO	0 - 6	0 - 4
BaO	13 - 16	28 - 36
Na ₂ O	0 - 2	-
Li ₂ O	1 - 3	-
TiO ₂	3 - 4	14 - 23
ZnO	3 - 5	0 - 6
PbO	0 - 3	-
Waste Oxides	20	20
Crystal Phases	Crymrit or h-Celsian m-Celsian (Ba) BaAl ₂ Si ₂ O ₈ Re-Titanate (Re, An, Sr) Re ₂ Ti ₂ O ₇ Ba-Molybdate (Mo, Ba) BaMoO ₄ Pollucite (Cs, Rb) (Cs, Na)AlSi ₂ O ₆	Fresnoite (Ba, Sr) Ba ₂ TiSi ₂ O ₈ Priderite (Ba) K ₂ Fe ₂ Ti ₆ O ₁₆ Re-Titanate (Re, An, Sr) Re ₂ Ti ₂ O ₇ Ba-Molybdate (Ba, Mo) BaMoO ₄

The glass ceramic product developed at KFK⁹ is VCP-15. Its composition and some of its properties are shown in Table 7. Titanium is the nucleating agent. This glass ceramic has a fairly high thermal expansion, 12.5 and 11.2 x 10⁻⁶/°C. Thermal conductivity is higher than that of typical glasses. The leach rate for a Soxhlet and a brine test at 100°C was 10⁻⁵ to 10⁻⁶ g/cm²·day. Silicon, sodium, and boron were found in the leach solution and were primarily from the residual glass. A high-level waste containing VCP-15 glass ceramic was produced. The Soxhlet leach rates in this case were 10⁻⁵ g/cm²·day for the bulk loss, but for ¹³⁴Cs and ²⁴¹Am, 10⁻⁸ g/cm²·day was measured. The conclusions of this study were that the VCP-15 has much better thermal stability and slightly better leach resistance than the equivalent KFK waste glass GP98-12.¹⁰

The compositions and crystal phases of several glass ceramics investigated at PNC¹¹ are given in Table 8. In this table D-62 and D-210 are diopside-based, C-27 is celsian-based, P-50 is perovskite-based, E-63 is based on β-spodumene, and P-71 is apparently based on spheen.

Table 7. Composition and Physicochemical Properties of the KFK Glass-Ceramic Product VCP 15

Composition of VC 15 Frit, wt%		
SiO ₂		50.0
TiO ₂		5.0
Al ₂ O ₃		10.0
B ₂ O ₃		5.0
Na ₂ O		5.0
K ₂ O		5.0
Li ₂ O		10.0
CaO		5.0
MgO		5.0
Composition of VCP 15 Product, wt%		
VC 15 Frit	85.0	or 81.0
HAW oxide	15.0	15.0
Gd ₂ O ₃		4.0
Physicochemical Properties		
Density (kg · m ⁻³)	2.9	3.0
Thermal expansion (C ⁻¹ × 10 ⁻⁶)	12.5	11.2
T, transformation point (°C)	440	507
Thermal conductivity (W · m ⁻¹ · K ⁻¹)	2.10	2.00

TABLE 8. Compositions and Crystal Phases of PNC Glass Ceramics

Composition	Sample Number					
	D-62	C-27	P-50	E-63	D-210	P-71
SiO ₂	47.5	35.0	30.0	50.0	41.02	40.0
Al ₂ O ₃	6.8	15.0	10.0	12.5	8.20	6.5
B ₂ O ₃		5.0	5.0		3.50	3.5
Fe ₂ O ₃	9.5				8.70	
TiO ₂	2.7	5.0	10.0	6.0	3.20	10.0
CaO	6.8	4.0	25.0		4.10	10.0
MgO	6.8				1.37	
BaO		13.0				
ZnO		2.7		4.0		
Li ₂ O				7.5		
HLW	20.0	20.0	20.0	20.0	30.0	30.0
Total	100.0	100.0	100.0	100.0	100.0	100.0
Crystal	(a)	(b)	(c)	(d)	(a)	(e)
Phases	Fe ₃ O ₄ CaMoO ₄ CaTiO ₃	CaMoO ₄ CaTiO ₃	CaSiO ₃ CaMoO ₄ Sphene	Li ₂ SiO ₃	CaMoO ₄ Fe ₃ O ₄ CaTiO ₃	CaMoO ₄
Heat	1000°C	850°C	900°C	800°C	900°C	900°C
Treatment	1 hr	1 hr	3 hr	2 hr	1 hr	1 hr

- (a) Diopside (CaO·MgO·2SiO₂)
 (b) hexa-Celsian (BaO·Al₂O₃·2SiO₃)
 (c) Perovskite (CaTiO₃)
 (d) β-Spondumene (Li₂O·Al₂O₃·4SiO₂)
 (e) sphene (CaO·TiO₂·SiO₂)

The coefficients of thermal expansion of all of these glass ceramics were from 80 to 90 x 10⁻⁷/°C. PNC researchers reached a conclusion that the diopside was the best system.

Leach rates of the PNC glass ceramics after immersion at 90°C for 24 hrs in distilled water range from 9 x 10⁻⁴ to 3.6 x 10⁻⁵ g/cm²·day. The investigators at PNC heat-treated these samples at 700°C for 3000 hrs. In the case of the diopside, celsian, and perovskite systems, there was no change, but for the β-spondumene system, there was some crystal growth and the leach rate increased by a factor of 3 during the heat treatment.

The diopside system was demonstrated on a larger scale. A canister, 30 cm in diameter by 35 cm high, was produced. By slow cooling the canister of glass, a glass ceramic was formed without separate nucleation

and crystallization steps. The canister was insulated with asbestos. The glass ceramic from the canister had the same properties that were observed in the small-scale tests (Table 9). Again, there was no change in the crystalline phases after 3000 hrs at 700°C.

In addition to the HMI developed celsian and fresnoite glass ceramics, basalt-based glass ceramics are being developed at PNL. Basalt-based forms have several advantages. Material is readily available; PNL studies use Hanford basalt as the raw material. The basalt glass ceramic would be chemically compatible with the host repository rock. Basalt glass ceramics are not new. Basalt glasses and glass ceramics are common in Europe.¹² Corning has a patent on basalt glass ceramics.¹³ Beall and Ritter¹⁴ state that the durability of basalt glass ceramics are better than that of the original rock. The basalt glass ceramics produced by Beall and Ritter contained 50% to 60% residual glass phase. This is high, but it is the range of that in most of the glass ceramic nuclear waste forms. Basalt glass ceramics also have been shown to have a very high mechanical strength¹⁵ (Modulus of rupture, 16,000 psi and compressive strength, 71,000 psi).

TABLE 9. Properties of D-62 Glass Ceramic Crystallized in Canister During Cooling

Crystal phases	Diopside, Fe_3O_4 , CaTiO_3 , CaMoO_4
Leach rate wt. loss	4.3×10^{-5} g/cm ² -d
Cs_2O	5.6×10^{-5} g/cm ² -d
SiO_2	7.5×10^{-5} g/cm ² -d
Bending Strength	1100 kg/cm ²
Thermal expansion coeff.	$81.8 \times 10^{-7}/^\circ\text{C}$ (30-380°C)
Softening temp.	>1100°C
Thermal conductivity	1.93 w/m-°C
Density	3.00 g/cm ³
Thermal stability	No change after heating at 700°C for 3,000 hrs.

Basalt glass ceramics have been successfully produced using Hanford basalt and 20 wt% PW-9 simulated waste calcine.¹⁶ The basalt glass with calcine was melted at 1400°C and annealed at ~550°C. The annealed glass samples were reheated to 670°C for nucleation and raised to 920°C and held for 8 hr for crystal growth. Nucleation times were varied from 1 to 4 hr with no significant difference in end product. Primary crystalline phases in the glass ceramic as determined by x-ray diffraction are augite [(Ca,Fe,Mg)SiO₃], powellite [(Ca,Sr)MoO₄], and spinel (NiFe₂O₄).

Leach resistance tests have been conducted in deionized water and at temperatures of 90°C and 150°C. Results for tests conducted at 90°C are shown in Table 10. Basalt rock and basalt glass with and without PW-9 calcine are included for reference. It is interesting to note that the basalt glass has better leach resistance, especially at 90°C, than the basalt rock. This is probably due to porosity and glass phases in the basalt rock. The durability is improved upon crystallization by a factor of 2 at 90°C. The results at 150°C are varied as leach resistance of some elements are increased and others decreased by crystallization. In general, one could state that there is no significant difference between the basalt glass and glass ceramic (i.e., not more than an order of magnitude). The residual glass phase is preferentially leached as illustrated in the SEM micrographs in Figure 6.¹⁶

TABLE 10. Leach Resistance of Basalt Glass Ceramics in Deionized Water at 90°C (a)

Waste Form	Element in Solution, g/m ² (b)							
	Al	Ca	Mg	Si	Na	Mo	Sr	Cs
Basalt	-(c)	2.72	2.45	3.73	-	-	-	-
Basalt Glass	-	0.30	0.19	0.22	-	-	-	-
Basalt Glass/PW-9	0.38	2.46	1.89	1.89	-	3.27	2.08	2.84
Basalt Glass Ceramic/PW-9	-	0.75	0.23	1.04	-	1.86	1.91	1.97

(a) 9 days, SA/SV = 14 m⁻¹

(b) normalized g/m²

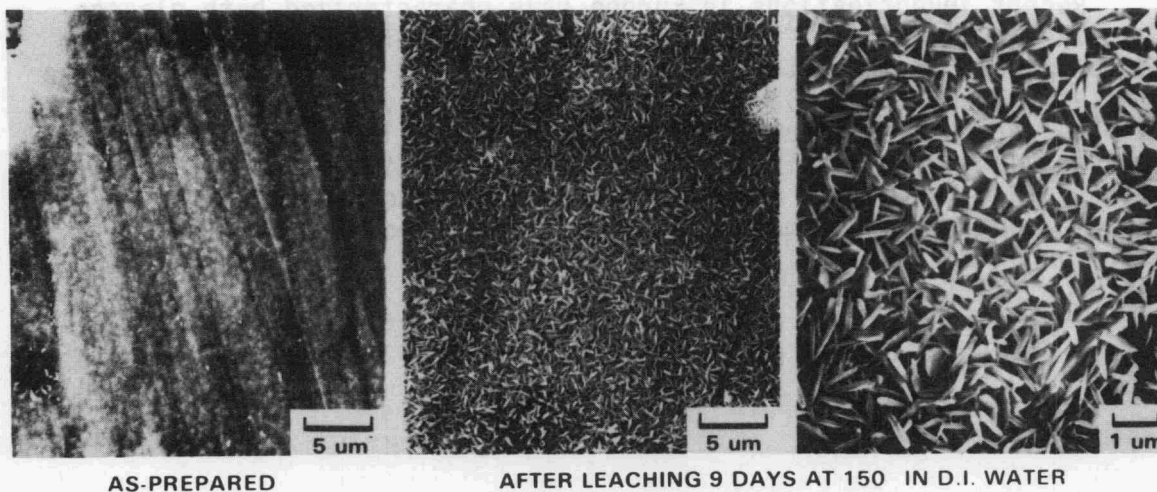
(c) solution concentration below detection limit

Basalt glass ceramics have also been produced containing PW-4b-7 and PW-8a-2 calcines and are presently being characterized. The basalt glass ceramics appear to be able to accept a wide range of waste streams.

Comparison of Waste Form Properties

In this section, comparison between glass waste forms and glass-ceramic waste form is made. First, the effect of residual glass content will be reemphasized. Leach resistance, some general properties, and radiation stability are discussed.

In Table 11, the residual glass contents of representative commercial glass ceramics are compared with the nominal maximum residual glass content of glass-ceramic nuclear waste forms. The commercial glass ceramic with low thermal expansion and 10 vol% residual glass is Corning 7617, a typical lithium aluminosilicate. From the literature



- a. SAMPLE WAS RECRYSTALLIZED BY HEATING FOR 4 HOURS AT 670 C AND 8 HOURS AT 920 C

Fig. 6. SEM Micrographs of Celsian Glass Ceramic Before and After Leaching (From Lokken¹⁶).

Table 11. Residual Glass Content in Commercial Glass Ceramics and in Glass-Ceramic Nuclear Waste Forms

Glass Ceramic	Residual Glass Content (vol %)
Commercial Glass Ceramics*	
Low-thermal-expansion glass ceramic	10
Complex glass ceramics (MgO, B ₂ O ₃ , Li ₂ O, Al ₂ O ₃ and SiO ₂)	30
Mullite containing glass ceramic (BaO·Al ₂ O ₃ ·SiO ₂)	60
Glass-Ceramic Nuclear Waste Forms	As high as 50

*From McMillan⁴

it has been stated for commercial glass ceramics⁴, that high chemical durability requires the volume of residual glass phase to be small. Durability or leach resistance is an important criteria for nuclear waste forms. In glass-ceramic nuclear waste system, the residual glass content can be as high as 50 vol% or higher. Residual glass content is the limiting factor in glass-ceramic waste forms.

Recent investigations in Europe have characterized both glasses and glass ceramics.¹⁸⁻²¹ One program, a joint effort of the European communities²¹ on characterization of waste forms is studying phosphate glasses, borosilicate glasses and glass ceramics. Soxhlet leach rates in water are shown in Table 12 and hydrothermal leaching data from tests conducted in a salt brine saturated in sodium chloride and carnallite ($KClMgCl_2 \cdot 6H_2O$) are shown in Table 13. In both tests the glass ceramic does not offer much improvement over borosilicate glass. In fact, under hydrothermal conditions the leach resistance of the glass ceramic is slightly less than that of the parent glass. The results for a PNL comparative study²² on the leach resistances of a 76-68 glass, a celsian glass ceramic, and supercalcine SPC-5B are given in Table 14.

TABLE 12. Soxhlet Leach Rates for European Glass and Glass Ceramics

Waste form	Number	Soxhlet leach rates ($g\ cm^{-2}\ day^{-1}$)	
		Temperature	
		100°C	50°C
Borosilicate glasses	UK-189	$1.3 \pm 0.2 \times 10^{-3}$	5.0×10^{-5}
	UK-209	$2.6 \pm 0.9 \times 10^{-4}$	1.0×10^{-5}
	VG-98/3	$1.9 \pm 0.3 \times 10^{-3}$	1.1×10^{-4}
Glass ceramic	C-31-3	$6.6 \pm 0.6 \times 10^{-4}$	3.6×10^{-5}
Phosphate glass	78/7	$4.9 \pm 0.5 \times 10^{-5}$	2.5×10^{-6}

TABLE 13. Hydrothermal Leach Rates of European Glass and Glass Ceramics in Brine

Waste form	Number	Leach rate, %wt. loss								
		Temperature/Time								
		120°C		150°C		200°C				
		3d	3d	3d	15d	30d	60d	90d	360d	
	UK-209		0.02		1.5					
Borosilicate glasses	UK-189		0.06		0.8					
	VG-96/3		0.08		2.0					
	C-31-3			0.3	2.3	2.5	2.3	2.3	2.6	1.8
Glass ceramic	C-31-3		0.8		1.5	1.8	1.5	2.5	1.7	2.1
Phosphate glass	78/7		3.0		20				Decomposed	

TABLE 14. Comparative Study Results for Glass,
Glass Ceramic, and Ceramic Waste Forms

Property	Glass 76-68	Celsian Glass Ceramic	Supercalcine(a) SPC-5B
Bulk Density, g/cm ³	3.00	3.1	1.95
Compressive Strength, psi	7465 ± 1945	4969 ± 1206	4155 ± 893
Volatility, mg/mm ²			
3 hr 700°C	5.0 x 10 ⁻⁴	2.9 x 10 ⁻⁴	1.5 x 10 ⁻⁴
3 hr 900°C	4.0 x 10 ⁻³	1.2 x 10 ⁻³	3.0 x 10 ⁻⁴
3 hr 1100°C	2.8 x 10 ⁻²	8.8 x 10 ⁻²	1.3 x 10 ⁻²
3 hr 1300°C	4.1 x 10 ⁻¹	6.2 x 10 ⁻¹	2.6 x 10 ⁻²
Leachability(b), g/m ²			
Ca	2	9	2
Al	-	3	11
B	20	22	-
Na	23	13	75
Mo	19	25	70
Si	15	6	20
Sr	0.5	12	1
Cs	17.8	11	2

(a) Cold pressed and sintered at 1125°C-2 hr

(b) Deionized water, 90°C, 3 days, SA/SV = 6 m⁻¹, normalized units

General properties of glass and glass-ceramic waste forms²³ are compared in Table 15. Glass ceramic waste forms tend to have a slightly higher density than the glass waste forms. Both forms can have low thermal expansion. The thermal expansion of $125 \times 10^{-7}/^{\circ}\text{C}$ is that of the VCP-15 from KFK, a higher-expansion glass ceramic. Thermal conductivity is higher for a glass ceramic than for a glass waste form. Impact resistance was determined by Lutze.⁸ The glass-ceramic waste form demonstrated improved impact resistance over the glass waste form. In a comparative study conducted at PNL,²² a dihedral compression test was used to measure mechanical strength. The celsian glass ceramic had a dihedral compressive strength of 4969 psi as compared to 4155 psi for supercalcine and 7465 psi for 76-68 glass (Table 14).

Some radiation stability data²⁴ is shown in Figure 7. Figure 7 shows percentage volume change as a function of radiation dose in samples doped with ²⁴⁴Cm. In all waste form systems, there is some volume change. Supercalcine and the lead glass 75-LG increase in

TABLE 15. Summary of Generic Glass, Glass-Ceramic and Ceramic Waste Form Properties

Property	Waste Form Type		
	Glass	Glass Ceramic	Ceramic
Density, g/cm ³	2.5 - 4.8	2.9 - 3.7	1.0 - 4.8
Thermal Expansion, °C x 10 ⁷	75 - 180	50 - 125	94 - 160
Thermal Conductivity, W/m°K	0.8 - 1.4	1.2 - 2.2	0.8 - 5.0
Volatility 3 hr @ 900°C, mg/mm ² x 10 ³	4	1.2	3.0
Leach Resistance Soxhlet, g/cm ² d	10 ⁻⁴ - 10 ⁻⁷	10 ⁻⁴ - 10 ⁻⁶	10 ⁻⁴ - 10 ⁻⁷
Impact Resistance % < 1mm	≥ 50	< 30	-
Energy adsorbed, cm ² /J	6.6	6.3	-
Compressive Strength, psi	7465	4699	4155

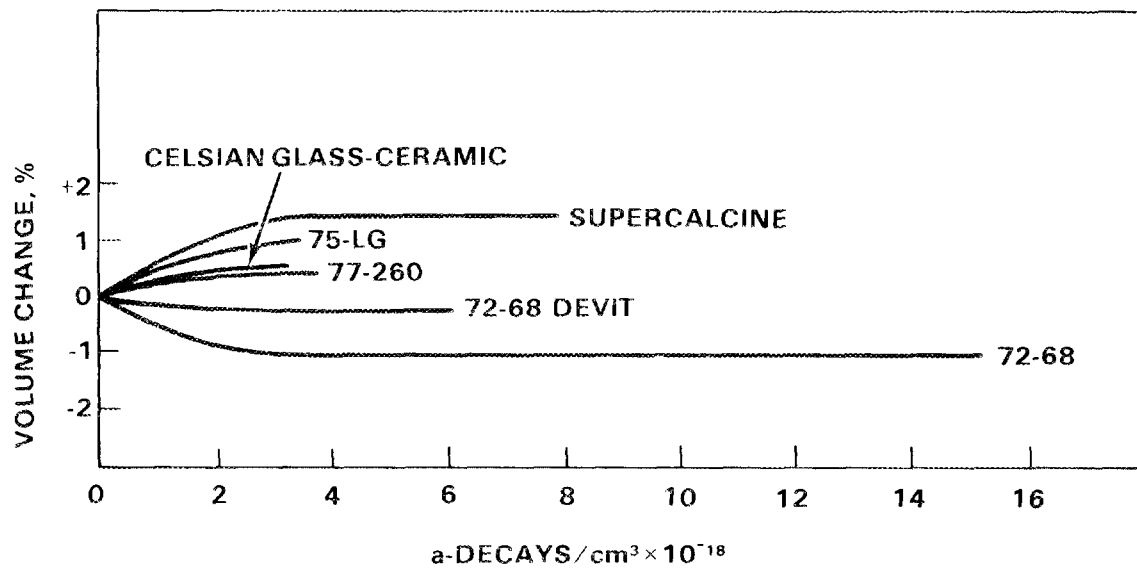


Fig. 7. Effects of Radiation on the Volume of Waste Solids (From Ross et al.²⁴).

volume. The 72-68 glass, one of the earlier glass systems developed at PNL, has a decrease, but the devitrified 72-68 has a much smaller volume increase. In 77-260 glass and the celsian glass ceramic both increase to some extent.

To summarize, there is very little increase in process complexity using conventional glass processes for processing glass ceramics. There might be some increase if it were necessary to nucleate and grow the crystals, but it has been demonstrated one can simply cool the melt and get crystallization without any special heat treatment. Glass ceramics have better thermal stability and higher thermal conductivity than glasses; but, with the low-heat-content wastes, these are not as important as they were in initial waste form studies. Impact strength and compressive strength are higher for glass ceramics; these may be important in the transportation problem. The leach resistance is about the same as that of glass, mainly because there is a high residual glass phase. Radiation stability is the same problem as that with crystalline waste forms, and perhaps there would be a greater problem in radiation stability with glass ceramics than with glass systems. Glass ceramics, other than basalt-type glass ceramics which may be in near equilibrium with the repository rock, in general offer very little advantage over glass.

ACKNOWLEDGMENTS

The SEM micrographs in Figure 5 were provided by W. Lutze (HMI) from unpublished work conducted at PNL.

DISCUSSION

SIMMONS: I think that in the case of the basalt-type glass ceramics, in which you have a large volume fraction of glass content, you are probably making a more durable material than you would if you had a low volume fraction. The reason is that when you crystallize from a variable starting composition, if you have a low volume fraction of residual glass and very little control over the composition of that glass, you could produce a material that is very soluble, and then it dumps all of your little crystals into solution as you said in the β -spodumene.

RUSIN: That is a good point, but what about the Corning glass ceramic that had only 2% residual glass and exhibited excellent durability?

SIMMONS: That is probably true. With most glass ceramics, if you have a well-defined starting composition, then you know what your glass phase is going to be. But, if you do not know what your glass phase is going to be, you should try to aim for a larger volume fraction of glass for better control of composition.

RUSIN: I think that is a good point. One of the problems in glass-ceramic nuclear waste forms is that one really does not have that

control over what that residual glass will be. I think in commercial glass ceramics you can have better control over the residual glass.

ANGELINI: Into which phases, either glass or crystalline, does the curium partition in that one figure?

RUSIN: The curium goes into the rare-earth titanate and the celsian phase.

REFERENCES

1. S. D. Stookey, Brit. Patent No. 752,243 (1956).
2. S. D. Stookey, Brit. Patent No. 829,447 (1960).
3. P. W. McMillan and G. Partridge, Brit. Patent No. 924,996 (1963).
4. P. W. McMillan, Glass Ceramic, 2nd Ed., Academic Press, New York, (1979).
5. J. D. Sundquist, "Preliminary Corrosion Studies of Glass-Ceramic Code 9617 and a Sealing Frit for Nuclear Waste Canisters," Corning Glass Works 78-03-14, KBS Teknisk Rapport 93, Karnbranselsakerhet Order No. 166, Stockholm, Sweden. (1978).
6. A. D. De et al., "Development of Glass Ceramics for the Incorporation of Fission Products," Bull. Am. Ceram. Soc. 55(5), 500 (May 1976).
7. A. K. De, B. Luckscheiter, G. Malow, and E. Schiewer, Fission Products in Glasses Part II: Development of Glass Ceramics, HMI-B218, Hahn-Meitner-Institute, Berlin, West Germany, (1977).
8. W. Lutze, J. Borardt, and A. K. De, "Characterization of Glass and Glass-Ceramic Nuclear Waste Forms, Proceeding of Scientific Basis for Nuclear Waste Management, Vol. 1, G. J. McCarthy (ed), Plenum, NY, (1979).
9. W. Guber, M. Hussain, L. Kahl, W. Muller, and J. Saidl, "Development and Characterization of the Glass Ceramics VCP-15 for Immobilization of High-Level Liquid Radioactive Waste," Proceedings of Ceramics in Nuclear Waste Management, Cincinnati, CONF-790420, Technical Information Center, Oak Ridge, TN, (1979).
10. W. Guber, M. Hussain, L. Kahl, G. Ondracek, and J. Saidl, "Preparation Characterization of an Improved High Level Radioactive Waste (HAW) Boro-silicate Glass," Proceedings of Scientific Basis for Nuclear Waste Management, Vol. 1, G. J. McCarthy (ed), Plenum, NY, (1979).

11. N. Oguino et al., "Solidification of HLLW by Glass-Ceramic Process," in Proceedings of the Conference on Ceramics in Nuclear Waste Management, Cincinnati, CONF-790420, DOE Technical Information Center, Oak Ridge, TN, (1979).
12. A. Portevin, "Molten Basalt" Mem. Soc. Ing. Civil France, 266-330 (1928).
13. G. H. Beall and H. L. Rittler, "Process for Forming a Basaltic Glass Ceramic Product," U.S. Patent 3,557,575 (1971).
14. G. H. Beall and H. L. Rittler, "Basalt Glass Ceramics," Bull. Am. Ceram. Soc. 55(6), 579 (1976).
15. D. Bahl, J. A. Roberts, and J. H. Weymouth, "Basalt Glass-Ceramics" J. Australian. Cer. Soc., 10(2), 25-27 (1974).
16. R. O. Lokken and J. M. Rusin, "Evaluation of Basalt-Based Waste Forms," Am. Ceram. Soc. Bull., 59:392, 1980.
17. A. M. Platt and J. A. Powell, Nuclear Waste Management Quarterly Progress Report January Through March 1980, PNL-3000-5, Pacific Northwest Laboratory, Richland, WA 99352, p. 2.5, June 1980.
18. E. Ewest and H. W. Levi, "Evaluation of Products for the Solidification of High-Level Radioactive Waste From Commercial Reprocessing in the Federal Republic of Germany" IAEA-SM-207/18. Proceedings of a Symposium on the Management of Radioactive Wastes from the Nuclear Fuel Cycle, IAEA, Vienna, (1979).
19. G. Malow, V. Beran, W. Lutze, J. A. C. Marples, J. T. Dalton, A. R. Hall, A. Hough, K. A. Boulton, Testing and Evaluation of the Properties of Various Potential Materials for Immobilizing High Activity Waste, First Annual Report EUR 6213 EN, Commission of the European Communities, (1978).
20. W. Lutze, "Glassy and Crystalline High Level Nuclear Waste Forms: An Attempt of Critical Evaluation," Proceedings of Ceramics in Nuclear Waste Management, Cincinnati, CONF-790420, Technical Information Center, Oak Ridge, TN (1979).
21. J. A. C. Marples, W. Lutze, and C. Sombret "The Leaching of Solidified High Level Waste under Various Conditions" Proceedings of The First European Community Conference on Radioactive Waste Management and Disposal, Luxembourg, (May 1980).
22. J. M. Rusin, J. W. Wald, R. O. Lokken, and J. W. Shade, Comparative Waste Forms Study, PNL-3516, Pacific Northwest Laboratory, Richland, WA 99352, 1980.

23. J. M. Rusin, An Assessment of Glass-Ceramic Waste Forms, PNL-3515, Pacific Northwest Laboratory, Richland, WA 99352, September 1980.
24. W. A. Ross, R. P. Turcotte, J. E. Mendel, and J. M. Rusin, "A Comparison of Glass and Crystalline Waste Materials," Ceramics in Nuclear Waste Management, Cincinnati, OH, CONF-790420, April 1979.

SOLID RADIONUCLIDE WASTE FORM
DEVELOPMENT IN THE UNITED STATES

D. E. Gordon

E. I. du Pont de Nemours & Company
Savannah River Laboratory
Aiken, SC 29808

ABSTRACT

The long-term immobilization of the high level radioactive wastes resulting from chemical processing of nuclear reactor fuels and targets is the responsibility of the Department of Energy (DOE) Office of Nuclear Waste Management. This program is widely assigned through the waste-producing sites, the DOE laboratories, industrial laboratories, and universities. All aspects of the program are being managed through the DOE Savannah River Operations Office, with personnel in the Atomic Energy Division of E. I. du Pont de Nemours and Company acting as technical advisors. Several options for immobilizing high level wastes (HLW) have been identified, and work is progressing to determine the optimum fixation forms and fabrication methods. The candidate waste forms are surveyed. The waste form developers and their specific research areas are given. The waste form requirements and selection process are discussed.

The Department of Energy (DOE) is conducting a comprehensive program to isolate all U.S. nuclear wastes from the human environment¹. The DOE Office of Nuclear Waste Management (NEW) has full responsibility for managing the high level radioactive wastes resulting from chemical processing of nuclear reactor fuels and targets at defense installations and additional responsibility for providing the technology to manage existing commercial high level wastes. The responsibilities of the five offices of DOE-NEW are shown in Figure 1. Lead office assignments for program management of disposal technology development for the variety of nuclear waste categories are shown in Table 1. Responsibility for short-term radioactive waste activities (interim storage) remains with DOE Headquarters in the Office of Waste Operations and Technology.

The existing high level nuclear reprocessing wastes in the United States are those generated in the Nation's defense programs plus those generated in commercial reprocessing at the Nuclear Fuel Services Plant in West Valley, New York, from 1966 to 1971. Quantities of these wastes

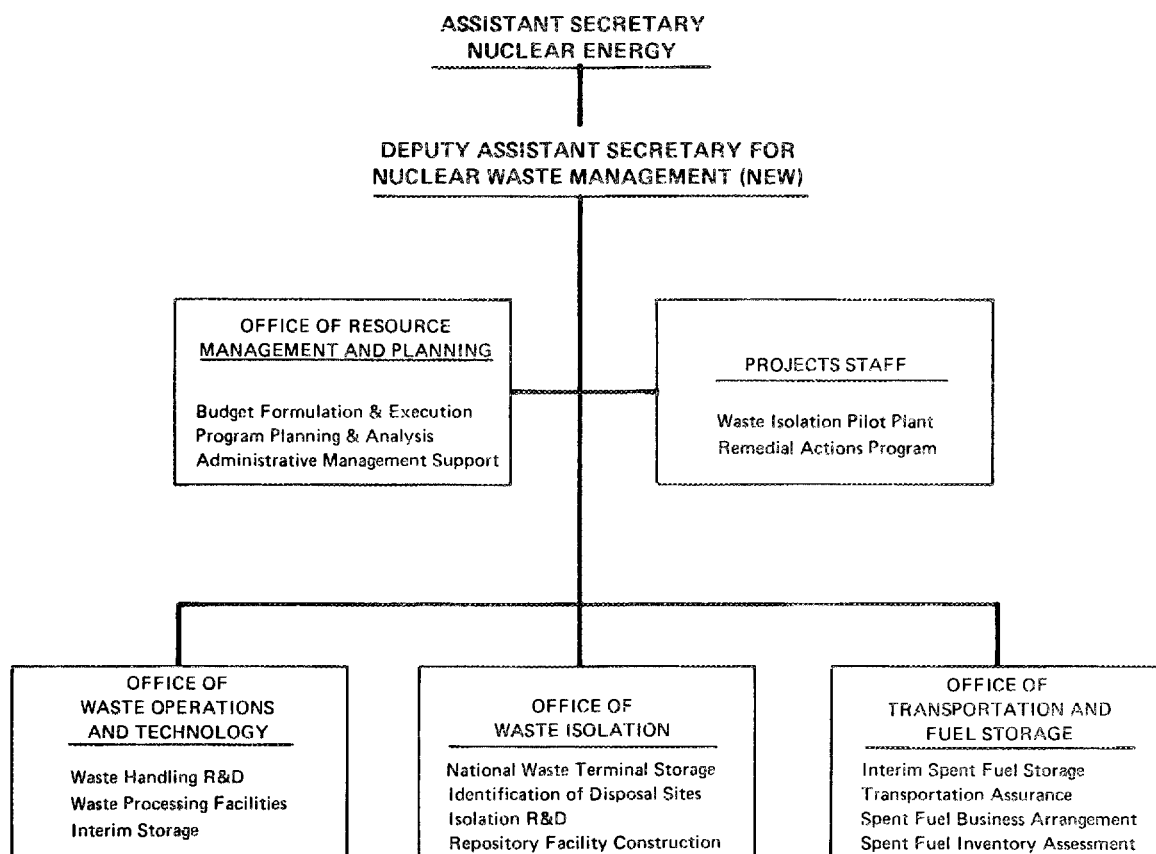


FIGURE 1. NEW ORGANIZATION CHART

TABLE 1. LEAD FIELD OFFICES AND CONTRACTORS

TECHNOLOGY AREA	LEAD FIELD OFFICE	CONTRACTOR
HLW	Savannah River	Du Pont
TRU	Albuquerque	Rockwell
LLW	Idaho	EG&G
Airborne	Idaho	Exxon Nuclear
Decontamination & Decommissioning	Richland	United Nuclear
Waste Isolation	Richland	Battelle Columbus
Spent Fuel	Savannah River	Du Pont
Transportation	Albuquerque	Sandia

are listed in Table 2. They are now stored in underground tanks or bins at the defense sites at Hanford, Savannah River, and Idaho Falls, and at the NFS site at West Valley, New York. The spent fuel elements from commercial power reactors are a potentially much larger source of re-processing waste should fuel recycling be resumed in the United States.

Three options for high level waste (HLW) immobilization are being considered; 1) in-place solidification, 2) interim transport, and 3) terminal disposal. If the risk of removing nuclear wastes from interim storage is greater than leaving those wastes in situ, then in-place solidification may be the appropriate disposal method. A leave or retrieve decision is being considered at both Hanford and Idaho Falls. The interim transport approach has been suggested for the NFS wastes at West Valley, New York. There are assessments underway to determine the feasibility and applicability of incorporating the NFS wastes into an interim waste form for transport to a terminal form production site for further processing. Most of the effort in HLW immobilization is in the development of terminal disposal forms.

The candidate waste forms for fixation of HLW can be grouped into three categories as shown in Table 3. The majority of the waste forms have been under development for one and one-half years or less. Standardized test procedures for determining material properties of chemical durability, radiation stability, thermal stability, and mechanical strength are still being developed by the Materials Characterization Center established at the Pacific Northwest Laboratory. Thus, standard characterization data for the candidate waste forms are not yet available. The waste form product performance information that is available does reveal general strengths and weaknesses. The relative merits and deficiencies of the candidate waste forms are listed in Tables 4, 5, and 6.

Phosphate glass has received considerable attention as a waste form. It does have performance characteristics similar to those of borosilicate glass for waste loading, leachability, and volatility. Phosphate glasses are highly corrosive to almost all container materials and do exhibit a

TABLE 2. U.S. HIGH-LEVEL NUCLEAR WASTES

SOURCE	TYPE	1980 QUANTITIES			1990 QUANTITIES
		10 ⁶ GAL	TANKS	MEGACURIES	MEGACURIES
Hanford Plant	Alkaline	50	156	190	230
	Cs/Sr Sources	—	—	350	425
Idaho Chemical Processing Plant	Acid	2.5	9	20	16
	Calcine	0.45	(3)	35	340
Savannah River Plant	Alkaline	23	33	570	680
Nuclear Fuel Services	Alkaline	0.6	1	64	48
	Acid	0.01	1	2.1	1.6
Spent LWR Fuel	Not Processed	—	—	1,900	14,000

TABLE 3. CANDIDATE WASTE FORM CATEGORIES

TYPE	WASTE FORM
Glass	Phosphate Glass Borosilicate Glass High-Silica Glass Glass Ceramics
Ceramic	Concrete (Special) Clay Ceramics Supercalcine Synroc Titanates
Matrix	Metal Matrices Multibarrier Cermets

TABLE 4. HLW GLASS FORMS**PHOSPHATE GLASS**

- | | |
|----------------------|---|
| Advantages | - Very low leachability and volatility
Accommodate wide range of waste compositions |
| Disadvantages | - Easy devitrification with major increase in leachability
Molten glass highly corrosive |

BOROSILICATE GLASS

- | | |
|----------------------|---|
| Advantages | - Very low leachability and volatility
High radiation stability
Relative insensitivity to composition variation |
| Disadvantages | - Reacts with high temperature water and brines
Devitrifies with a small increase in leachability |

HIGH-SILICA GLASS

- | | |
|----------------------|---|
| Advantages | - Demonstrated long geologic lifetime
Lower leachability than borosilicate glass |
| Disadvantages | - Formation temperature of $\sim 1600^{\circ}\text{C}$ volatilizes some waste radionuclides |

GLASS CERAMICS

- | | |
|----------------------|--|
| Advantages | - Good impact resistance |
| Disadvantages | - Close control required on nucleation process
Higher leach rates than borosilicate glass |

TABLE 5. HLW CERAMICS FORMS

CONCRETE (Special)

- | | |
|----------------------|---|
| Advantages | - Lower leachability and less gas generation from radiolysis than ordinary concrete |
| Disadvantages | - Low impact resistance
Strontium retention capability questionable |

CLAY CERAMICS

- | | |
|----------------------|---|
| Advantages | - Applicable to a variety of waste types |
| Disadvantages | - Higher leachabilities, lower impact resistance, and lower radiation stability than borosilicate glass |

SUPERCALCINE

- | | |
|----------------------|--|
| Advantages | - Excellent leach resistance
High thermal stability
High waste loadings |
| Disadvantages | - Formation of equilibrium assemblage uncertain
Radiation stability unknown |

SYNROC

- | | |
|----------------------|---|
| Advantages | - Excellent leach resistance up to very high temperatures
High thermal stability |
| Disadvantages | - Capability to accommodate wide range of waste compositions uncertain
Radiation stability unknown |

TITANATES

- | | |
|----------------------|--|
| Advantages | - Accommodate wide range of waste compositions
High thermal stability |
| Disadvantages | - Cesium retention capability uncertain
Radiation stability unknown |

TABLE 6. HLW MATRIX FORMS

METAL MATRICES	
Advantages	- Extra barrier layer Excellent heat transfer High impact resistance
Disadvantages	- Low waste loading Loss of low melting metals in fires Corrosion questions on metal
MULTIBARRIER	
Advantages	- Very high leach resistance Volatiles containment Redundant barriers
Disadvantages	- High surface area of waste particles Capability of producing quality product uncertain
CERMET	
Advantages	- High impact resistance High thermal conductivity
Disadvantages	- High surface area of waste particles Leaching resistance may depend primarily on metal integrity

significant increase in leachability at devitrification temperatures of 400 to 500°C. These two major deficiencies have ended development of phosphate glass as a waste form.

Borosilicate glass is currently the best developed waste form for high-integrity radionuclide containment. The merits of this glass form are low leachability, high radiation stability, low volatility, relative insensitivity to waste composition, and good mechanical strength in a canister. The primary concerns about borosilicate glass are chemical attack by leachants at high temperatures and pressures and devitrification. Borosilicate glass does react with water and brines at elevated pressures and temperatures. Devitrification of this glass form at 400 to 500°C does cause an increase in leachability.

High-silica natural glasses (obsidians and tektites) are known to have persisted for long periods in both terrestrial and lunar environments. These glasses are formed at about 1600°C, a temperature high enough to drive off most of the ruthenium and cesium radionuclides from the wastes. Development of low temperature processes for making high-silica glass is being pursued. Initial results show these glasses to have very low leachabilities and good mechanical strength.

Glass ceramics are formed by adding nucleating agents to the glass melt and then cooling the glass in a controlled manner so as to produce an assembly of small crystals held together by a glassy phase. This waste form has good impact resistance and low leach rates, although higher than borosilicate glass. The disadvantages are tied to the close control on the nucleation process required for product formation.

Studies at the Savannah River Laboratory showed that normal concrete is an inferior product to borosilicate glass for immobilizing high level wastes. All current studies, therefore, are directed at advanced forms. Concrete formed under elevated temperatures and pressures (FUETAP) is being developed to improve performance characteristics. The advantages of the FUETAP concrete are lower leachabilities and less gas generation due to radiolysis than ordinary concrete. The deficiencies of this waste form are low impact resistance and undemonstrated ability to retain strontium adequately.

Clay ceramics are aluminosilicate-based crystalline materials made by firing an appropriate mixture of HLW and clay at $\sim 1000^{\circ}\text{C}$. This waste form has higher leachabilities, lower impact resistance, and lower radiation stability than borosilicate glass. Very little development effort is going into clay ceramics except for an assessment of the product's potential as an in-place solidification form for Hanford wastes.

Supercalcines, or tailored ceramics, are formed by calcining the waste with suitable additives such as Ca and Al oxides and then heating the calcines at 900 to 1200°C to produce a polycrystalline form. The supercalcines offer the advantages of very high waste loadings, very good leach resistance, and high thermal stability. Two questions which arise for supercalcine waste forms are the stability of the various crystals under radiation and transmutation stress and the assurance of forming an equilibrium assemblage of the desired species.

SYNROC is a synthetic titanate mineral in which the radioactive elements in the waste are incorporated as solid solutions in the crystal lattice of perovskite, zirconolite, and hollandite phases. SYNROC product performance data have shown very good leach resistance even at high temperatures and high thermal stability. The major concerns about SYNROC are its ability to handle a large variety of waste species and its long-term radiation stability.

Titanate ceramics are formed by using a series of hydrous-oxide inorganic ion exchangers to concentrate waste radionuclides and then sintering at 900 to 1100°C to produce a polycrystalline assemblage. These titanates have high thermal stability and can accommodate a wide range of waste compositions. The disadvantages are the uncertainty in ability to retain cesium and the stability of various crystals under radiation and transmutation stress.

Metal matrix waste forms are produced by casting low-melting alloys around small waste form particles of calcine, concrete, glass or ceramic materials. The major advantages of such a composite arrangement are

improved heat transfer, high impact resistance, and additional leaching barriers. The disadvantages of this waste form are low waste loadings and undesirable features of a low-melting alloy such as poor corrosion resistance and loss of metal in a high temperature environment (fire).

The most complex waste forms are made by coating the waste particles with impervious materials such as carbon, alumina, or silicon carbide before placing the waste particles in a matrix. Such coatings provide additional barriers against waste leaching and allow the use of high-temperature matrix formation processing by reducing radionuclide volatilization. The main questions about the multibarrier waste forms are their high complexity and ability to produce a quality product. The application of an impervious coating to very small particles having very large surface areas requires highly developed technology.

Cermet waste forms are a particular metal matrix form in which very fine waste particles are dispersed in the metal by in situ reduction of the metal from the waste. The cermet form has high impact resistance and high thermal conductivity and can incorporate a wide variety of waste compositions. The disadvantages of this waste form are the high surface area of the waste particles and the dependence of leach resistance on the corrosion rate of the Hastelloy-like metal.

The development of alternative waste forms is widely assigned to the waste producing sites, the DOE national laboratories, industrial laboratories and universities. Table 7 lists the HLW form developers and their specific assignment of waste form technology development. Twelve waste forms are being developed at 14 laboratories.

The waste forms must be considered as one part of a total nuclear waste disposal system. Their primary role within this system is to provide the initial barrier against radionuclide release. Here the overwhelming emphasis has been on reducing the availability of the waste radionuclides to water leaching when the wastes are disposed of in a repository. Current policy on long-term waste isolation is that the waste package (which includes the waste form and any engineered barriers) should provide a complement to the natural geologic barrier until the waste hazard has been greatly reduced by radioactive decay.

The draft criteria from the regulatory agencies (Environmental Protection Agency and Nuclear Regulatory Commission) provide specific requirements for waste disposal system performance (Table 8). Draft criteria from the EPA specify dose-to-man restrictions in terms of health effects. The draft NRC criteria specify zero release from the waste package for the first 1000 years and an annual radionuclide release rate of less than one part in one hundred thousand of the total activity present in HLW 1000 years after repository decommissioning for the next 9000 years.

Selection parameters considered important in judging the relative merits of candidate waste forms are given in Table 9. Waste form leachability is assigned a high weighting factor since radionuclide contain-

TABLE 7. U.S. HIGH-LEVEL WASTE FORM DEVELOPERS

CONTRACTOR	WASTE FORMS
Savannah River Laboratory	Borosilicate Glass
Rockwell Hanford	Glass & Clay Ceramics
Exxon Nuclear Idaho Co.	Glass & Calcines
Pacific Northwest Laboratory	Glass, Glass Ceramics Matrices & Coated Particles
Oak Ridge National Laboratory	Concrete, Cermet, & Sol-Gel
Argonne National Laboratory	Synroc & Metal Matrices
Lawrence Livermore Laboratory	Synroc
Sandia Laboratories	Titanate Ion Exchanger
Rockwell - PSU	Tailored Ceramics
Catholic University	Porous Glass Matrix
NC State University	Synroc
University of Florida	Surface Reaction Studies
NASA	Glass Analog Study

TABLE 8. WASTE FORM REQUIREMENTS

- **DRAFT EPA CRITERIA**
 - Less than 200 health effects in 10,000 years from HLW disposal
 - Health effect risks to be only for unlikely events
 - **DRAFT NRC REGULATIONS (10 CFR 60)**
 - Zero release from waste package for first 1,000 years
 - 10^{-5} release per year for 10,000 years
-

TABLE 9. HLW FORM SELECTION FACTORS

PRODUCT
Leachability
Dispersability and impact resistance
Volatility
Radiation stability
Thermal stability
Waste Loading
PROCESS
Process safety
Licensable product achievable
Remote operation capability
Feed preparation required
Process waste generation

ment is the major objective in waste disposal. Measures of product performance in transportation environments such as mechanical strength and dispersion resistance are also included. Waste form processing parameters are also important and include processing safety, ability to produce a fully licensable product, capability for remote operation, and secondary waste generation.

The selection of a final waste form for an immobilization facility involves the consideration of a number of decision inputs as listed in Table 10. Currently within DOE, representatives from the production, transportation, and isolation programs are developing product performance factors to establish a standard basis for comparison among candidate waste forms based on product performance in a variety of environments. Similarly, waste form process evaluation criteria are being developed by waste form assessment groups now organized at each of the defense sites. A waste form peer review panel has convened twice to evaluate the candidate waste forms on scientific merit and engineering practicality^{2,3}.

TABLE 10. HLW FORM SELECTION

DECISION INPUTS
Waste form product performance
Waste form production process evaluation
Regulatory criteria
Waste site requirements
Waste package and repository criteria
Review panel recommendations
Public response to EIS
DOE recommendation

Future reviews by the peer panel are planned annually until the final forms are selected.

The schedule for HLW form development calls for the continued development of all candidate forms through FY-1981. At that point, a selection will be made of three to four of the most promising forms for intensive development. At the end of FY-1983, the field will be narrowed further by the selection of one or two waste forms for full-scale equipment development. These final forms are expected to be applicable for both defense and commercial high-level wastes. Also scheduled for the end of FY-1983 is the selection of the final form for the Defense Waste Processing Facility (DWPF) at the Savannah River Plant site, planned as the initial U.S. immobilization facility.

DISCUSSION

WITTELS: I would like to clarify a point for the record: The opening statement that I was concerned about diversification. That is a very serious comment on this sensitive subject. I am not concerned about diversification. As a matter of fact, I insist upon it. Is the record clear?

GORDON: I stand corrected.

UNIDENTIFIED COMMENT: One of your factors for selecting waste forms was development status. That is, perhaps, a little unfair if you are really going to pay attention to the regulatory requirements. If you put the kind of money into some of these other forms that you have put into glass, they would all be pretty well developed. I think it is unfair. Speaking as a devil's advocate here, if I were a concerned U.S. citizen, I would say, "why don't you really give me the best waste form?" I am not sure of the weighting that you have used in saying that development status will be used to help come to a decision.

GORDON: Working within the restraints of the budget dollars we have available to us, and the interest in getting on with the program of encapsulating the waste, I guess we have to come to a balance there. However, in regard to the applicable large-scale experience, some of the waste form developers have gone to related industries that use similar kinds of equipment and have applied a number of those techniques. I guess an example is the application of hot pressing to encapsulating high-level waste in the ceramic form. You are right: If we had plenty of time, as much time as has been devoted to glass for the last 20 years, we would all have the best judgment, but we have to make some decisions.

UNIDENTIFIED QUESTIONER: On the coated particle, which is extremely well developed for the HPPR and, I believe, some of the Navy programs, you say that this process is not well developed. That is not true. I think that it is developed.

GORDON: I'm sorry. The fluidized-bed coated particle equipment that I have seen is complex.

JOHNSTON: I would like to make a point on the process and waste form considerations in selection of the waste form. I think there is a step being left out, and that is "what is going to have to be done to put an engineered-barriers package around the waste form in the repository to meet the criteria?" The point is, that for a less durable waste form, you will require a more extensive engineered-barriers package on the whole, and this will also have to be done in a remote type of operation.

GORDON: I guess that may change your rating somewhat. The charter that we see in the high-level waste lead office is to make a waste form that can be placed in some kind of containment suitable for shipment to another site. The application of engineered barriers or a backfill material at the repository has been assigned as the responsibility of ONWI. Correct me if I am wrong about that. Your point is well taken and I can add that to the list. You would not want to make something that would be impossible to put an engineered barrier around. Is that your point?

JOHNSTON: Yes. That is basically the point. I think we need a cradle-to-grave consideration, rather than stopping at the shipment point.

GORDON: There are mechanisms for integrating all these concerns; they are called interfaced working groups. Some of these have been set up to select a national canister design. They are looking at how we can make something that will be applicable in the defense waste processing facility that you can get in the repository with the same grappling hook, the same dimensions, that sort of thing.

UNIDENTIFIED QUESTIONER: On the national canister design, are they certain that their national canister is going to be compatible with more than one rock type? Metallurgists tell me that what may be compatible in one type of rock environment will not survive in another type.

GORDON: I cannot answer that, because the results are not in from the design, but I am sure that they need to make those considerations. I agree with you.

HOWITT: We have been looking at some of the PNL 7668 glass with, I think, a PW-4a waste addition. We have been using the technique of electron microscopy. Unfortunately, I do not have the slides here, but I could get them if it is necessary. But it is the most complex system. It is not simple. It is not homogeneous. It has crystallites all over it. It has composition variations throughout it. I think what we are looking at in the glass is a lot of empirical data. We have a lot of empirical data on concrete, and we do not understand that either. I think when we do a comparison between state-of-the-art technology in glass and in ceramic materials we have to remember that we have been looking at ceramic materials with the technique designed for looking at

the structure of ceramic materials, i.e., x-ray diffraction. We know the crystalline phases; we can identify their behavior. But as far as I know very little work has been done on either borosilicate or phosphate glasses in determining their structure and chemical durability, or the physical properties of the glass in relation to what you have there. We do not understand the structure of those complicated glasses, and I do not think you can say categorically that we have a great deal of knowledge about glass systems. We have a great deal of data, but we do not know very much about them.

GORDON: I cannot disagree with you on that. Other people tell me that the glass is homogeneous, however.

BOATNER: I do not like the concept that you can clothe something in general respectability by saying that it was approved by an independent review panel. In fact, the conclusions reached by an independent review panel can be determined in advance by careful selection of the members who make up the review panel.

UNIDENTIFIED QUESTIONER: If I understand correctly you are giving us the program only for the defense wastes. The title of your paper was just high-level waste in general. But you are really talking about defense wastes only, when you give us the time schedule for the decisions. Is that correct. The reason why I am saying this is that you do not say anything about the spent fuel as a waste form, unless I missed it in your talk. I am sure that had you included civilian waste you would have included that. Perhaps I missed it.

GORDON: Our charter is to look at commercial spent fuel should it ever become a liquid. If it remains in the form of the spent fuel elements, then the disposal of that is under the Division of Waste Isolation program. But, yes, the development of waste forms for defense waste, which is the forefront of the waste we are concerned with now, has been emphasized. The addressing of the commercial waste form has sort of taken a secondary role, but I think that a lot of the things that apply to defense wastes can be applied to the isolation of commercial fuel should it be reprocessed. I meant to make that point early in my talk, but most of my words were about the defense waste because that is what we are concerned with right now. Our charter is high-level waste: both current and future defense waste, and also any reprocessed spent fuel.

REFERENCES

1. "Nuclear Waste Management Program Summary Document, FY-1981," DOE/NE-0008 (March 1980).
2. "The Evaluation and Review of Alternative Waste Forms for Immobilization of High Level Radioactive Wastes," USDOE Report DOE/TIC 10228, Alternative Waste Form Peer Review Panel (August 1979).

3. "The Evaluation and Review of Alternative Waste Forms for Immobilization of High Level Radioactive Wastes, Report Number 2," USDOE Report DOE/TIC 11219, Alternative Waste Form Peer Review Panel (June 1980).

THE IDENTIFICATION OF BASIC AND APPLIED RESEARCH NEEDS IN THE
DEVELOPMENT OF RADIOACTIVE WASTE FORMS - A COMBINED
PRESENTATION AND OPEN GROUP DISCUSSION

L. A. Boatner, Chairman

BOATNER: The final item on the agenda is a general discussion session. I have prepared some questions that have occurred to me based on presentations at this workshop and on some preconceived ideas. I would like to present these thoughts and ideas, and then invite people to attack them if they so desire, or to add to or subtract from them.

To put things in perspective, my own simplistic way of looking at this problem is to divide the subject into three general areas: The actual solid - or what I like to call the primary waste form - it can be a glass, a polycrystalline substance, a cermet, or any of the different materials that we have heard about for the last two and one-half days. In general, it is some kind of solid that entrains in one way or another the radionuclides. Then there is some kind of interface, and I like to view that interface as being either the surface of the actual primary waste form which has interacted with its environment, a passivated surface, or something similar, or a canister, a cask, or some kind of enclosure. In any event, it is one or more things that separates this solid from a geologic environment in which we can have a liquid. This liquid, depending on any one of a number of given scenarios, can be brine, a groundwater, and so on. I view the primary waste form area as belonging in the domain of people who have training in solid state physics, solid state chemistry, ceramists, and materials scientists. This is where they can really come into play. Not much has been said in this workshop about the problems associated with interfaces and the interactions at surfaces between the solid and the canister, or the canister and the environment, but, in any event, certainly surface physicists and chemists and corrosion specialists have a big role to play here and could probably play a larger role. Finally, we have the liquid and geological environment. If water breaches the system, then, of course, this problem is being dealt with by chemists, radiochemists, and geochemists. The overall problem actually involves many different specialists and it is fair to say that the eventual satisfactory solution of this problem, if there is one, is going to involve a lot of interplay between these people. As we have seen, based on the paper "Waste Form Characterization and its Relationship to Transportation Accident Analysis" by Wilmot and McClure, all kinds of factors can also come into play in the design of waste forms for transportation. Different criteria are obviously being applied to different waste forms, and not all of these criteria apply just to the waste form in place in a geologic repository.

When we are considering the primary waste form and the solid phase, the experiments should be performed using radioactive material whenever

possible. At this point in time, simulations are of limited and questionable value, and there is no viable reason why the experiments cannot be performed using radioactive material. This is particularly true in the case of the actinides and alpha-active isotopes. There is no reason not to use the actual radioactive material, and there are a lot of reasons for using it, because when we use the radioactive materials in our experiments we have automatically built into the experiments radiation damage effects, and solid-state chemical effects, such as valence changes, etc. This is particularly important for the actinides, because their solid state chemistry is not analogous to the solid state chemistry of their rare-earth analogs. In fact, for the second half of the actinide series, berkelium, einsteinium, and so on, the rare earths that fall above actinides in the periodic table are relatively good analogs, but we are not interested in einsteinium or berkelium in dealing with nuclear waste. The actinides in the first half of the transition series are frequently not good analogs of the rare earths. This information is in the literature and has been there for years and was apparently not taken into consideration when the Synroc concept was put forth. That does not mean that the Synroc concept is bad just because it was based on some faulty assumptions, but, nevertheless, we should keep this in mind. One can see americium-4+ in the solid state (e.g., in cerium dioxide). One can see americium-2+ in strontium chloride. With the actinides, as well as other elements in the solid state, one can see valence states that you do not normally think you would find, and might not find in solution chemistry.

UNIDENTIFIED QUESTIONER: Aren't experiments using radioactive material going to be too expensive?

BOATNER: I think that it is more expensive not to do them, because if you do not do a meaningful experiment and try to save money by using simulations that are not valid, you spend the money and do not get the right answer. So it is better to do the radioactive experiments with the proper facilities; and we do have the proper facilities, certainly at the National Laboratories, as well as at other laboratories. It is important at this point in time to stop relying on simulations that may be unreliable.

HOWITT: One important problem that you did not discuss is that you get interference from radioactivity in attempts to get the data - for example, in x-ray fluorescence analysis. There are reports that, in fact, you cannot do these composition analyses using such techniques.

BOATNER: If you are looking only at general phase properties, and that sort of thing, then you are probably all right. If you are looking at leaching effects and the solid state chemistry of these systems, however, then I think that it is important to use "real-world" material. I see no reason not to, other than that it may be an added inconvenience, and it cannot be done everywhere. I was very much impressed by and enjoyed the paper by Rong Wang, in which he discussed leaching experiments on spent fuel waste forms. He made a very valid and

important point. Leaching experiments in this area, if they are really going to be meaningful, are going to have to be done in an environment where there is a radiation field, if, indeed, the leachant - the water, or the brine, or whatever comes in contact with the waste form - is going to be subjected to radiation. As Wang has shown, and as people have known for years, one can have radiolysis of water; you can get the formation of hydrogen peroxide and other radiochemical effects that result in the production of highly corrosive and reactive chemicals. Once this occurs, then any experiment that was performed in the absence of radiation in distilled water, or brine, or groundwater, really does not have much meaning. Mark Wittels made a very good point, I thought, in his introductory remarks. You cannot just put in distilled water and do leaching experiments. These experiments have to be done under the kinds of conditions that the waste form is actually going to experience.

UNIDENTIFIED SPEAKER: How you conduct the test is probably going to have a large effect on what you measure. So if you do not know what mechanisms you are looking at, how are you going to be able to extrapolate that to the mechanics in a canister in a mine two thousand years from now. You see our approach has been to take deionized water in as simple as possible a system, with simple glasses and more complex glasses and see what happens when you go step by step all the way through.

BOATNER: I do not think that one can ignore the actual conditions that will exist, and, as Wang showed in his results, the leach rates that you get can change by three orders of magnitude if radiation effects come into play. Three orders of magnitude is a lot, and I think this can affect whether a waste canister - let's talk about the whole package - canister and primary waste form - whether it maintains its chemical and physical integrity for 100 years, 1000 years, or 10,000 years. This brings up the question of "what do we really want?" Do we want fundamental parameters or do we want to know how the waste form behaves? If the waste form package is sitting in a flowing stream with water going by, then these fundamental parameters may apply, but if it is sitting where there is ground water seepage, then the porosity of the surrounding medium dictates how fast the water comes in, and you may have time to reach some kind of equilibrium condition. In that case, these are the conditions that are going to determine what leaches out, and how fast it leaches out.

HOWITT: I think the point is that a lot more thought has to go into the experiment before we do it. A classic example was pointed out yesterday in the environmentalists' study with crashing the truck against the wall. They did not put any strain gauges on the material. They came out with a lot of data that may not be so useful. They spent a million and a half dollars and destroyed a good truck. We are doing the same thing with our leaching experiments.

MOORE: As we all know, probably the biggest thing that has to be done is to determine the leachability, and I would remind you that we hope

in the fall of this year to get most of the people together that have been working on leaching experiments. We cannot even agree among ourselves how to report the data, so how can you possibly agree on anything else. There will be a workshop where we hope to get a consensus opinion. I've seen data that has been taken for 72 hours with gigantic conclusions drawn from it. I have taken leach data from experiments that have run from two to three years and have found that everything goes fine for the first couple of years, and then all of a sudden things start changing. It is a long-term thing. It is an expensive thing, and there is no way to accelerate it. You can work at advanced temperatures, but you cannot convince me that you can back-track and say that this is what is going to happen. I do not agree with you that we should start off by doing it in a radioactive environment. If we did that, our great-great grandchildren might not see nuclear energy, but we do have to eventually do it in a radioactive environment.

BOATNER: But John, are we really starting off at this point? People have been doing leaching experiments on various waste forms for a long, long time and...

MOORE: You will find that there are very few experiments that have been going on for a long time that are meaningful. The Canadians have a beautiful natural experiment. They are the only people who really had foresight. Hahn-Meitner has some very nice experiments that have been going along for a long time. Ours are probably the longest on concrete. Most people are doing them for short-time periods and are drawing big conclusions from the results. I disagree with you about deionized water. It is probably the worst leachant you could ever find.

BOATNER: I never meant to imply that deionized water was not one of the most corrosive substances known in the sense that it wants to take up every available ion, but is it really a realistic measurement? It is a realistic experiment in terms of predicting the long-term chemical and physical stability of a waste form that is going to see some type of groundwater or brine.

UNIDENTIFIED SPEAKER: Obviously the ultimate simulation is to make the waste form and put it into a repository and observe that for 20 years or 1000 years. Anything less than that is going to be a compromise. In designing that repository, we need to do approximations and rough simulations. I think everybody would agree that we need to focus on how to better represent the real situation - the situation we envision. I just want to comment that we need to go back and look at what we are doing - that is the disposal of radioactive waste with the geologic environment as an integral part of that waste disposal. We not only consider the leachant, but we consider the interaction with the geologic environment. We need to know not only what leaches out but how the leachants interact with the environment. Our approach is to combine the leaching and migration experiments in an attempt to combine a total systems approach, as approximate as it is, to the envisioned situation.

BOATNER: It would be nice to do experiments for 20 to 1000 years, but it is extremely tough to keep graduate students for that length of time - as well as funding.

WITTELS: We could discuss the leaching problem for the next three weeks - if we could last that long. John Moore says the problem is insoluble. Well, it is a case of public credibility again, and I am speaking as an ombudsman. If the waste people tell the United States that the scientists involved in this area cannot agree on the design of tests and standardization, then where are we? I think that in the leaching situation - people have to sit down in a closed room - and not get out of that room until they design a standard for these tests. That is the crux of this problem.

MOORE: I did not say it was an insoluble problem. I said that people have been doing it in their own little way for years and years - and have been doing it for very short times. We live in a different era right now. Years ago when the tests were done they answered the questions in a manner people thought was satisfactory. Now we are engaged in developing a standard leach test. The ISO (The International Standards Organization) is putting forth a standard leach test, and the Committee 16 is working on a standard which should be out before the end of the year. This will be used as a basis for fundamental research, as well as a basis for quality assurance for reactor people that are putting away their waste materials. At the end of this year, I believe it is going to be either in early October or in December, we hope to bring together most of the people in the US (and some from abroad) that are working on leach tests, in order to determine the best way to proceed. My point was that this is not done in a short length of time.

RAPPAZ: It is one thing to standardize the leach tests - this is a problem of experimental work; but we have only heard one paper that was primarily concerned with the theoretical aspects of the problem, i.e., to extrapolate the results (because, of course, as Lynn Boatner says, it's difficult to keep graduate students and funding for more than a thousand years). Machiels has presented some calculations concerning the leaching rate, and I think that if you really want to have more information and to know how these elements are going into a liquid, it is a very complicated problem. If you knew the microstructure, where the impurities are going in the solid, and in which valence state, then maybe you could do some modeling, calculate something, and extrapolate the short-term leaching data to very long terms.

UNIDENTIFIED COMMENT: There is a need for standard leaching tests which can be used as quality control, basically, where one obtains quick information about the quality of the product. If you want to extrapolate the behavior, then you have to try to determine what the fundamental processes are - to design specific experiments which will test a particular aspect of the process. These can be done without radiation, but, obviously, they will have to eventually also include radiation. I think there is room for a variety of leaching tests.

WITTELS: I did not want to oversimplify my comments about leaching. The gentleman from Rockwell mentioned his concern about whether any consideration was given to the total system, including canisters. This also has to be included in any leaching experiment, the whole system, all the way through the overpack, and into the geologic media. I'm not suggesting it is an easy system to understand and, in fact, I know from last year's studies of canisters in various environments, that experts in the United States have come to the conclusion that you must be very specific about that environment. It is absolutely essential, and this just multiplies the complexities. So in terms of the end point of depositing radioactive material in a safe place, the whole system has to be considered. Unfortunately, decisions regarding a site, and the environmental factors surrounding that site have not been made. I think that as scientists we must look into all possibilities, all reasonable possibilities - whether it's a completely dry environment - whether the chemistry of the rock has a certain nature, etc. I think they all have to be considered, because we do not know where it is going to be placed.

UNIDENTIFIED COMMENT: For the material that is in storage - in the waste repository environment - one has to separate the condition of this system into near-field and far-field effects. In the near-field effect, one looks at a situation that is much more static than the so-called once-through leaching tests. This follows more closely the thermodynamic equilibrium conditions, because I hope the engineer is smart enough to choose a repository which does not have a river running through it. If one looks at the Canadian leach results, it can be concluded that we do not need to do anything now. (These are the Chalk River experiments in Canada.) If you tell the American people that you are going to put a waste glass in running water, no matter how good you tell them it is and that it will not leach - they will not believe it, and they will not take that for granted. I think that the factor of major importance is the licensing process, because there are some very sincere fanatics who will choose the most ridiculous scenarios and conditions. That means that we had better have some answers for them.

About leaching. On September 3rd and 4th, at Argonne, we will have a workshop - the Second Argonne Workshop. We are trying to discuss leaching conditions and leaching mechanisms for different types of waste forms, and to see if we can have some basic understanding of leaching mechanisms for glass, ceramics, metal matrices, and spent fuel. The purpose is to try to see whether we can get any general consensus - whether we can understand the mechanism. As everyone points out time and time again, this is a very complex problem. You just get data. You systematically vary the conditions. You can get a completely different set of data, and you just keep on doing tests in a complete cycle and you never get any improvement. So one must find some basic understanding and see whether this mechanism can apply to different waste forms. If we do not understand the basic mechanism, then there are too many variables in the situation.

DOWNS: We are talking about two different problems. One problem is the sequestering of kinetic data, and the second is the thermodynamic data. We are going to do the "hot" experiments that have been referred to - tests that should be run with fully loaded glasses and fully loaded waste forms. We are going to be running these under hydrothermal conditions, up to 300°C, totally saturated with water. In addition, we will build circulating systems which will allow one pass experiments to be conducted. We are starting out with the thermodynamic experiments - just the equilibrium solubilities of the waste form and of the basalt surroundings. We will use the same basalt that will be in the waste repository. Of course, this all goes toward, or is designed to point toward the "worst possible case" scenario that occurs when the repository is breached and is breached at the time the thermal regime is at its highest - i.e., when the water comes through in large quantities. In effect, we have turned the Columbia River down through the basalt, and it heads right on through and out the other side. Our first experiments will probably start around June of 1981. We will be running the initial leaching experiment just as hydrothermal alteration experiments with the cold basalt and the cold waste forms. We will begin the hot work approximately the first part of Fiscal 84, if all goes well. The reason for this is that our safety people want to know how long our hydrothermal reaction vessels and our hydrothermal system will last without breaking down. They have to make a safety analysis for the hot systems in a radioactive hot cell. Needless to say, these data are not available because if something breaks down now with our hydrothermal system, we simply walk in and fix it. So, for the first two to two and one-half years we are going to be evaluating the cold waste forms, or cold surrogate waste forms, and the cold basalt. Once we have that data we will be moving on to the fully loaded waste form.

LEVY: I would like to say something that really enforces Mark Wittels' comments, but I would like to put it in a slightly different way. I think it is well to address the question as to what sort of things one does to gain acceptance for the waste disposal concept from a very skeptical public. My own skeptical public in the last year or so has been people at Brookhaven who are not in any way involved in this program. They are people like mathematicians, high energy physicists, and so on. It probably doesn't come as any surprise to most of you to know that these people have a very low opinion of us - the people in the waste disposal community. I have tried to use these people as a sounding block or a test group, and to find out what sort of questions we have to ask that would convince them. My concensus at the moment is - and I point out again that this is a reasonably technically competent group, who are maybe a little more reasonable than the general public - that they will accept what I would like to refer to as a multiple risk analysis of the waste disposal situation. They would like to see in every aspect, for example, what is the probability of a canister rupture? What is the probability that a presumably dry geological location will be breached by water? You can make a whole list of these probabilities. What they will accept, I believe, is the idea that there are multiple risks. They fully expect that we are going to be

off in our assessment of one or more of these risks. But, they will accept from us the idea that if we have eight or ten separate risks and if we err on a couple of them, we still have a viable repository. Then they will go along with the concept of underground waste disposal. In other words, it is well to look at things from the point of view of making, for example, leach measurements under the worst possible conditions but to try to establish these in such a way that they are clearly the worst possible conditions. Then, if a compounding of these worst possible conditions still produces a negligible interaction with the biosphere, the general public, and more particularly these skeptical scientists, will accept it.

MARK WITTELS: One of the factors in the apparent demise of the nuclear reactor program in this country was a scientific factor. In the fuel elements, you have fast neutrons and fission fragments creating damaging events that produce displacements and integrated fluxes at a level such that all the atoms are displaced as many as a hundred times. If you can picture a solid in which every atom has been moved from its position a hundred times, then you can imagine that this is a very disruptive affair. For twenty years radiation effects measurements had been made under controlled temperature conditions, and predictions were made on the integrity of the fuel elements because the migration rates were known along with the activation energies, and the science at that time gave a very simple explanation. If one went to higher temperatures the worries were over, because things would move around so fast that they would annihilate. Unfortunately, this was not the case, because over a very narrow temperature range, for example, the range at which the breeder reactors at that time were scheduled to operate, the vacancies that were created in the solid combined to form voids. Then there was a synergistic effect, because as this nuclear fission process is going on helium is created in the material. So one has helium, large vacancies, and hydrogen. This was a great surprise because the integrity of the cladding was broken, and this caused a tremendous disruption in the reactor program. I am not suggesting that such a surprise is in store for the people that are working on solids for waste disposal - but, I do not assume that such surprises may not be there. I suspect that in materials with high loadings, that over very long periods a large gas buildup could occur, and this cannot be overlooked.

BOATNER: The statement was made earlier that the public perception and possibly the perception in some parts of the scientific community, of people working in the waste management area is not very good. If that statement is true, I think we certainly should ask ourselves - each of us - why it is true. Perhaps it is easy to understand this perception, because if one has experiments that have continued for such long periods of time - like the leaching experiments - and still so little is understood, and when we argue extensively among ourselves, then it is easy to see why there is a confidence gap. I am not suggesting that we do things like some organizations, i.e., sweep everything unpleasant under the rug, but probably we are frequently ill-served by a lot of premature public exposure of really deep scientific rifts and disagreements in the interpretation of some of the experimental data in this area.

APPENDIX A

PROGRAM

MONDAY, MAY 12

4:00 PM - 9:00 PM Workshop registration in the Lobby of the
Glenstone Lodge

6:00 PM - 8:00 PM Reception in the Highlander Room

TUESDAY, MAY 13

8:00 AM - 5:00 PM Workshop registration in the Lobby of the
Glenstone Lodge

8:30 AM Convene in the Dogwood I and II Rooms

8:30 AM - 8:45 AM "Welcoming Remarks"

Alex Zucker
Oak Ridge National Laboratory

8:45 AM - 9:00 AM "Workshop Purpose and Objectives"

Mark C. Wittels
The Division of Materials Sciences
USDOE

9:00 AM - 9:50 AM "The Application of Synroc Waste Forms
to U.S. Defense Wastes"

John Tewey
Lawrence Livermore Laboratory
(Invited)

9:50 AM - 10:10 AM "On the Thermodynamic and Kinetic Stability
of Perovskite in Natural Waters"

H. W. Nesbitt, G. M. Bancroft, W. S. Fyfe,
S. Karkhanis, P. Melling, and A. Nishijima
University of Western Ontario, Canada

10:10 AM - 10:30 AM COFFEE BREAK

- 10:30 AM - 11:20 AM "A Review of Ceramic Nuclear Waste Forms"
Gregory J. McCarthy
North Dakota State University
and
Rustum Roy
The Pennsylvania State University
(Invited)
- 11:20 AM - 11:40 AM "Hydrothermal Interaction of a Ceramic
Waste Form with Basalt"
S. Komarneni, B. E. Scheetz, D. K. Smith,
and C. A. F. Anderson
The Pennsylvania State University
- 11:40 AM - 12:00 Noon "Probable leaching Mechanisms for Spent Fuel"
R. Wang and Y. B. Katayama
Pacific Northwest Laboratories
- 12:00 Noon - 2:00 PM LUNCH
- 2:00 PM - 2:20 PM "Short-Term Leaching Behavior of Waste
Forms - A Potential Area for Improvement"
Albert J. Machiels
University of Illinois
- 2:20 PM - 3:10 PM "Radiation Damage in Natural Materials:
Implications for Radioactive Waste Forms"
R. C. Ewing
The University of New Mexico
(Invited)
- 3:10 PM - 3:30 PM "Radiation Damage Studies on Natural and
Synthetic Rock Salt"
P. W. Levy and K. J. Swyler
Brookhaven National Laboratory
- 3:30 PM - 3:50 PM COFFEE BREAK

3:50 PM - 4:40 PM "A Review of Heat Dissipation in Geologic Media"

Robert Pohl
Cornell University
(Invited)

4:40 PM - 5:00 PM

"Spent Fuel Resistance to Internally
Produced Cladding Degradation"

R. E. Einziger, D. A. Cantley, and
J. C. Krogness
Hanford Engineering Development Laboratory
and
D. Stellrecht and V. Pasupathi
Battelle Columbus Laboratories

WEDNESDAY, MAY 14

8:30 AM

Convene in the Dogwood I and II Rooms

8:30 AM - 9:20 AM

"A Review of research on Analogs of
Monazite for the Isolation of Actinide
Wastes"

M. M. Abraham, L. A. Boatner, G. W. Beall,
C. B. Finch, R. J. Floran, P. G. Huray,
and M. Rappaz
Oak Ridge National Laboratory
(Invited)

9:20 AM - 9:40 AM

"The Application of EPR Spectroscopy to
the Characterization of Crystalline Nuclear
Waste Forms"

M. Rappaz, L. A. Boatner, and M. M. Abraham
Oak Ridge National Laboratory

9:40 AM - 10:00 AM

"Hot and Cold Pressing of LaPO_4 -Based
High-Level Waste Forms"

R. J. Floran, M. Rappaz, M. M. Abraham,
and L. A. Boatner
Oak Ridge National Laboratory

10:00 AM - 10:20 AM

COFFEE BREAK

- 10:20 AM - 11:10 AM "A Survey of Concrete Waste Forms:
J. G. Moore
Oak Ridge National Laboratory
(Invited)
- 11:10 AM - 11:30 AM "Solidification of Nuclear Waste in
Concrete"
Hans Christensen
ASEA-ATOM, Vasteras, Sweden
- 11:30 AM - 11:50 AM "Waste Form Characterization and Its
Relationship to Transportation Accident
Analysis"
E. L. Wilmot and J. D. McClure
Transportation and Technology Center
Sandia National Laboratories
- 11:50 AM - 2:00 PM LUNCH
- 2:00 PM - 2:50 PM "Sol-Gel Technology Applied to Alternative
High-Level Waste Forms Development:
P. Angelini, D. P. Stinton, J. S. Vavruska,
A. J. Caputo, and W. J. Lackey
Oak Ridge National Laboratory
(Invited)
- 2:50 PM - 3:10 PM "Chemically Vapor Deposited Coatings for
Multibarrier Containment of Nuclear Wastes"
J. M. Rusin and J. W. Shade
Pacific Northwest Laboratory
and
R. W. Kidd and M. F. Browning
Battelle Columbus Laboratories
- 3:10 PM - 3:30 PM COFFEE BREAK
- 3:30 PM - 4:20 PM "A Review of the Sorption of Actinides
on Natural Minerals"
G. W. Beall
The Radian Corporation
(Invited)

4:20 PM - 4:40 PM

"Influence of Waste Solid on Nuclide
Dispersal"

M. G. Seitz and M. J. Steindler
Argonne National Laboratory

4:40 PM - 5:30 PM

"High Level Waste Fixation in Cermet Form"

E. H. Kobisk, W. S. Aaron, T. C. Quinby,
and D. W. Ramey
Oak Ridge National Laboratory
(Invited)

6:30 PM

Buses begin leaving the Glenstone Lodge
for the Cookout site. Extra tickets for
wives and guests are available at the
Workshop registration desk.

THURSDAY, MAY 15

8:30 AM

Convene in the Dogwood I and II Rooms

8:30 AM - 9:20 AM

"High-Silica Glass Matrix Process for
High-Level Waste Solidification:

J. H. Simmons and P. B. Macedo
Catholic University
(Invited)

9:20 AM - 10:10 AM

"A Review of Glass Ceramic Waste Forms"

J. M. Rusin
Pacific Northwest Laboratory
(Invited)

10:10 AM - 10:30 AM

COFFEE BREAK

10:30 AM - 10:50 AM

"Solid Radionuclide Waste Form Development
in the United States"

Donald E. Gordon
Waste Management Planning Division
Savannah River Laboratories

10:50 AM - 12:00 Noon

"The Identificatin of Basic and Applied
Research Needs in the Development of Radio-
active Waste Forms - A combined presentation
and open group discussion"

L. A. Boatner, Chairman

APPENDIX B

LIST OF ATTENDEES AT THE WORKSHOP ON ALTERNATE NUCLEAR WASTE
FORMS AND INTERACTIONS IN GEOLOGIC MEDIAGatlinburg, Tennessee
May 13-15, 1980

Marvin M. Abraham
Solid State Division
Oak Ridge National Laboratory
P. O. Box X
Oak Ridge, TN 37830

G. M. Bancroft
Department of Chemistry
The University of Western Ontario
London N6A5B7, Ontario
CANADA

T.-M. Ahn
Brookhaven National Laboratory
Upton, NY 11973

Gary W. Beall
Radian Corporation
8500 Shoal Creek Boulevard
Austin, TX 78766

Anthony T. Aldred
Argonne National Laboratory
9700 South Cass Avenue
Argonne, IL 60439

Gerald T. Bida
Brookhaven National Laboratory
Upton, NY 11973

Peter Angelini
Metals and Ceramics Division
Oak Ridge National Laboratory
P. O. Box X
Oak Ridge, TN 37830

J. J. Blakeslee
Nuclear Waste Processing
ESG - Rockwell International
P. O. Box 464
Golden, CO 80401

Harry Babad
Rockwell Hanford Operations
P. O. Box 800
Richland, WA 99352

Raymond E. Blanco
Chemical Technology Division
Oak Ridge National Laboratory
P. O. Box X
Oak Ridge, TN 37830

Carlos Bamberger
Chemistry Division
Oak Ridge National Laboratory
P. O. Box X
Oak Ridge, TN 37830

L. A. Boatner
Solid State Division
Oak Ridge National Laboratory
P. O. Box X
Oak Ridge, TN 37830

Harvey Burkholder
Ames Laboratory
Iowa State University
Ames, IA 50011

Neil A. Chapman
Institute of Geological Sciences
Harwell Laboratory
Building 151
Didcot, Oxfordshire
ENGLAND OX11 0RA

Robert W. Charles
Los Alamos Scientific Laboratory
CNC-11, MS 514
P. O. Box 1663
Los Alamos, NM 87545

Hans Christensen
Chemical Process Engineering
ASEA-ATOM
Box 53
Vasteras
SWEDEN 72104

Donald E. Clark
Hanford Engineering Development
Laboratory
W/C-35
P. O. Box 1970
Richland, WA 99352

W. F. Downs
EG&G Idaho/INEL
P. O. Box 1625
Idaho Falls, ID 83415

Robert E. Einziger
Westinghouse Hanford
P. O. Box 1970
Richland, WA 99352

P. Gary Eller
Los Alamos Scientific Laboratory
MS 346
P. O. Box 1663
Los Alamos, NM 87545

R. C. Ewing
Department of Geology
University of New Mexico
Albuquerque, NM 87131

C. B. Finch
Metals and Ceramics Division
Oak Ridge National Laboratory
P. O. Box X
Oak Ridge, TN 37830

John E. Flinn
EG&G Idaho Inc.
Route 4, Box 461A
Idaho Falls, ID 83401

Robert J. Floran
Environmental Sciences Division
Oak Ridge National Laboratory
P. O. Box X
Oak Ridge, TN 37830

William H. Goldthwaite
Battelle-Columbus Laboratories
505 King Avenue
Columbus, OH 43201

Donald E. Gordon
E. I. du Pont de Nemours
Savannah River Laboratory
Aiken, SC 29801

Joseph Halperin
Chemistry Division
Oak Ridge National Laboratory
P. O. Box X
Oak Ridge, TN 37830

Frank Hetzler, Sr.
ASEA-ATOM
4 New King Street
White Plains, NY 10604

D. G. Howitt
Department of Mechanical Engineering
University of California - Davis
Davis, CA 95616

Matthew B. Hoyt
Physics Department
The University of Tennessee
Knoxville, TN 37916

Paul Huray
Chemistry Division
Oak Ridge National Laboratory
P. O. Box X
Oak Ridge, TN 37830

Joseph Indusi
Building 830
Brookhaven National Laboratory
Upton, NY 11973

L. H. Jenkins
Solid State Division
Oak Ridge National Laboratory
P. O. Box X
Oak Ridge, TN 37830

Richard G. Johnston
Rockwell Hanford Operations
P. O. Box 800
Richland, WA 99352

Joe M. Keeton
Science Applications, Inc.
800 Oak Ridge Turnpike
Oak Ridge, TN 37830

John F. Kircher
Battelle Columbus Laboratories
ONWI
505 King Avenue
Columbus, OH 43201

E. H. Kobisk
Solid State Division
Oak Ridge National Laboratory
P. O. Box X
Oak Ridge, TN 37830

Kenneth D. Kok
Battelle Columbus Laboratories
505 King Avenue
Columbus, OH 43201

Daniel J. Lam
Materials Science Division
Argonne National Laboratory
9700 South Cass Avenue
Argonne, IL 60439

A. R. Lappin
Sandia Laboratories
P. O. Box 5800
Albuquerque, NM 87185

Francine O. Lawrence
Los Alamos Scientific Laboratory
MS 514
Los Alamos, NM 87545

J. Mark Legan
Physics Department
The University of Tennessee
Knoxville, TN 37916

Paul W. Levy
Department of Physics
Brookhaven National Laboratory
Upton, NY 11973

Gregory J. McCarthy
Departments of Chemistry and Geology
North Dakota State University
Fargo, ND 58105

Albert J. Machiels
Department of Nuclear Engineering
University of California
Berkeley, CA 94720

Neil E. Miller
Battelle Columbus Laboratories
505 King Avenue
Columbus, OH 43201

Donald P. Moak
Battelle Columbus Laboratories
505 King Avenue
Columbus, OH 43201

J. G. Moore
Chemical Technology Division
Oak Ridge National Laboratory
P. O. Box X
Oak Ridge, TN 37830

Mary Anne Moore
Physics Department
The University of Tennessee
Knoxville, TN 37916

Stanley E. Nave
Department of Chemistry
The University of Tennessee
Knoxville, TN 37916

H. W. Nesbitt
Centre for Chemical Physics and
Department of Geology
University of Western Ontario
London, Ontario
CANADA

G. D. O'Kelley
Chemistry Division
Oak Ridge National Laboratory
P. O. Box X
Oak Ridge, TN 37830

Gerhard Ondracek
Kernforschungszentrum Karlsruhe
Institut für Material- und
Festkörperforschung
Postfach 3640
D-7500 Karlsruhe
WEST GERMANY

Steven G. Oston
The Analytic Sciences Corporation
Six Jacob Way
Reading, MA 08167

Calvin R. Palmer
Battelle Memorial Institute
P. O. Box 999
Richland, WA 99352

Donald A. Palmer
Chemistry Division
Oak Ridge National Laboratory
P. O. Box X
Oak Ridge, TN 37830

V. Pasupathi
Battelle Columbus Laboratories
505 King Avenue
Columbus, OH 43201

F. J. Pearson, Jr.
INTERA Environmental Consultants, Inc.
11999 Katy Freeway, Suite 610
Houston, TX 77079

Robert O. Pohl
Physics Department
Cornell University
Clark Hall
Ithaca, NY 14853

Jack E. Powell
Ames Laboratory
Iowa State University
211A Met. Dev. Bldg.
Ames, IA 50011

Dan W. Ramey
Solid State Division
Oak Ridge National Laboratory
P. O. Box X
Oak Ridge, TN 37830

Michel Rappaz
Solid State Division
Oak Ridge National Laboratory
P. O. Box X
Oak Ridge, TN 37830

J. M. Rusin
Battelle Pacific Northwest Laboratories
PSL/1150
P. O. Box 999
Richland, WA 99352

B. E. Scheetz
Materials Research Laboratory
Pennsylvania State University
University Park, PA 16802

Klaus Schwitzgebel
Radian Corporation
8500 Shoal Creek Boulevard
Austin, TX 78758

Martin G. Seitz
Chemical Engineering
Argonne National Laboratory
9700 South Cass Avenue
Argonne, IL 60439

George V. Shalimoff
Lawrence Berkeley Laboratory
1 Cyclotron Road, 1159-70A
Berkeley, CA 94720

John J. Shefcik
General Atomic
P. O. Box 81608
San Diego, CA 92138

S.-Y. Shiao
Chemistry Division
Oak Ridge National Laboratory
P. O. Box X
Oak Ridge, TN 37830

Catherine J. Simmons
Physics Department
Catholic University of America
4th and Michigan Avenue
Washington, DC 20064

Joseph H. Simmons
Physics Department
Catholic University of America
4th and Michigan Avenue
Washington, DC 20064

Joseph R. Smyth
Los Alamos National Laboratory
P. O. Box 1663
Los Alamos, NM 87545

Paul N. Stevens
Science Applications, Inc.
800 Oak Ridge Turnpike
Oak Ridge, TN 37830

John A. Stone
E. I. du Pont de Nemours & Company, Inc.
Savannah River Laboratory
773-A
Aiken, SC 29801

J. L. Swanson
Battelle Pacific Northwest Laboratories
Bldg. 325, 300 Area
P. O. Box 999
Richland, WA 99352

T. Tamura
Environmental Sciences Division
Oak Ridge National Laboratory
P. O. Box X
Oak Ridge, TN 37830

John D. Tewhey
Lawrence Livermore Laboratory
University of California
P. O. Box 808
Livermore, CA 94550

Emil Veakis
Brookhaven National Laboratory
Bldg. 830
Upton, NY 11973

Rong Wang
Battelle Pacific Northwest Laboratories
P. O. Box 999
Richland, WA 99352

John L. Warren
Division of Materials Sciences
U.S. Department of Energy
MS 309
Washington, DC 20545

D. W. Wester
Argonne National Laboratory
9700 South Cass Avenue
Argonne, IL 60439

Bob Wielems
Science Applications, Inc.
800 Oak Ridge Turnpike
Oak Ridge, TN 37830

M. K. Wilkinson
Solid State Division
Oak Ridge National Laboratory
P. O. Box X
Oak Ridge, TN 37830

Edwin L. Wilmot
Transportation Analysis and
Information Division - 4551
Transportation Technology Center
Sandia Laboratories
Albuquerque, NM 87185

Mark C. Wittels
Division of Materials Sciences
Office of Basic Energy Sciences
U.S. Department of Energy
Mail Station J-309
Washington, DC 20545

Gary Wolf
Rockwell Hanford Operations
MO-037, 200 West Area
P. O. Box 800
Richland, WA 99352

Alex Zucker
Central Management Offices
Oak Ridge National Laboratory
P. O. Box X
Oak Ridge, TN 37830